

UNIVERSITY
OF COLOGNE

Isotopic and archaeo-informatic perspectives on ecological and economic change in late Holocene coastal eastern Africa

Inaugural dissertation

to complete the doctorate from the Faculty of Arts and Humanities

of the University of Cologne

in the subject Archaeological Science

presented by

Victor Iminjili

5th June 1976
Kakamega, Kenya

2026

First Examiner: Prof. Dr. Patrick Roberts

Second Examiner: Prof. Dr. Michael Bollig

External Examiner: Prof. Dr. Paul Lane

Examination Committee Chair: Prof. Dr. Anne Haour

Date of the oral defense: 28th September 2026

Abstract

Isotopic and archaeo-informatic perspectives on ecological and economic change in late Holocene coastal eastern Africa

Victor Iminjili
Institute for Prehistory and Early History, University of Cologne
Thesis submitted for the degree of Doctor of Philosophy in Archaeological Science
Summer 2026

Insights from isotopic and archaeo-informatic perspectives can complement those from other archaeological sciences, providing a holistic understanding of human–environment interactions in coastal eastern Africa during the late Holocene. These perspectives offer high-resolution, context-specific insights and broader views, respectively, providing information on diachronic ecological fluctuations and their relationship to the emergence of complex adaptive strategies for subsistence. Combining these methodologies and perspectives also enables exploration of spatiotemporal patterns in the emergence and dispersal of food production and highlights key research gaps.

This thesis takes an interdisciplinary approach, combining isotopic and archaeo-informatic perspectives to provide in-depth insights into ecological fluctuations, emergence and dispersal of intricate subsistence strategies, and food-producing communities in the coastal region and the interior of eastern Africa. The first case study presents stable carbon and oxygen isotope analyses of zooarchaeological remains recovered from Kuumbi Cave on Unguja Island, spanning the late Pleistocene to the late Holocene. The second case applies a multi-isotope approach to Iron Age caprines, associated wild fauna and human remains from Unguja Ukuu and Fukuchani on Unguja Island and Panga ya Saidi in coastal mainland Kenya. The third case study analyses maps generated from the *Wanyika* dataset, which contains scientific dates and associated assemblages from archaeological sites in eastern Africa.

The first case study reveals the persistence of foragers and their coexistence with food producers at Kuumbi Cave during the Iron Age in the face of ecological stability. The second study indicates the long-term settlement of immigrant agropastoralists at UU, who were involved in raising caprines in a setting rich in farmland and marine manure, away from wild animals. The third case study highlights patterns indicating that migration played a core role in the emergence and dispersal of food-producing communities to the coastal region. Overall, this thesis emphasizes the importance of new site-specific and larger informatics approaches for studying human socioeconomic relationships to the environment on different scales, providing a reference for assessing ongoing questions in sub-Saharan African archaeology.

Preface and acknowledgments

Although this thesis project was shaped by the COVID-19 pandemic, it has been highly rewarding from a scientific perspective, aligning with my interests in isotope ecology and human–environment interactions in eastern Africa. When it became clear that the lockdown was going to last longer than expected, my primary supervisor, Nicole Boivin, suggested switching to a study focusing on literature and laboratory work for my PhD thesis instead of the original field-based study. She recommended an archaeo-informatics project focusing on eastern Africa and helped me assemble a team of scientists to guide me through the process. Through frequent meetings and discussions with an advisory team — including Andrea Kay, Steve Goldstein, Patrick Roberts, Alison Crowther and Nicole Boivin — I constructed the basic dataset. Ricardo Fernandes joined us partway through, playing a pivotal role in redesigning the dataset to focus on scientific dates and teaching me how to calibrate scientific dates, particularly radiocarbon dates, online via Oxcal. Alison Crowther provided critical feedback that helped refine the dataset and downloaded all the Azania articles for me. The result was the production of the *Wanyika* dataset, comprising scientific dates and associated artefacts from archaeological sites in eastern Africa dating to the late Holocene. Before the other team members, Ricardo Fernandes and Patrick Roberts read the *Wanyika* dataset paper multiple times. This dataset was subsequently published in *Nature Scientific Data*. Chapter seven of this thesis is formed by this *Wanyika* dataset publication.

Ongoing research by the Sealinks project (directed by Nicole Boivin and Alison Crowther) at several sites along the eastern African coast has revealed that the zooarchaeological collections across multiple sequences are dominated by small, forest-adapted species and marine resources, with limited evidence of food production. By contrast, others are dominated by assemblages that suggest complex subsistence strategies, including caprine husbandry during the Iron Age. My other supervisor, Patrick Roberts, suggested that I analyse the Kuumbi Cave isotopes from the faunal and human remains in order to reconstruct the palaeoecology and human foraging at this site on Unguja Island. He recommended that I consult the 2020 Roberts et al. paper on the palaeoecology of Panga ya Saidi, the first isotope study of coastal sites in eastern Africa. Further discussions with Patrick Roberts and Steve Goldstein helped me to develop the project's basic outline. I later conducted carbon and oxygen isotope analyses of faunal and human enamel to gain a more detailed understanding of the late Pleistocene to late Holocene palaeoecology and human foraging at Kuumbi Cave on Unguja Island. Sean Hixon helped with the statistics and taught me how to produce figures in GG plots. Chapter five discusses the Kuumbi Cave faunal and human isotope dataset, published as Iminjili et al. (2023) in Frontiers in Environmental Archaeology.

Finally, discussions with Nicole Boivin, Alison Crowther, and Patrick Roberts inspired me to start working on the Unguja Ukuu caprine project. Alison Crowther and Patrick Roberts played a pivotal role in designing the study and outlining the paper. She also directed me towards the work of Fenner et al. (2018) on the early domestication of goats and their subsequent translocation in Bali. This formed the basis for my analysis of caprine husbandry and translocation on the eastern African coast. Frequent discussions with Patrick Roberts, Nicole Boivin and Alison Crowther were instrumental in shaping my ideas and drafting the paper. Sean Hixon also played a pivotal role in advising on the statistical analysis. The Unguja Ukuu project produced the Unguja Ukuu caprine husbandry dataset, forming the basis of chapter six. I am looking forward to submitting the Unguja

Ukuu results in the Proceedings of the National Academy of Sciences (PNAS) before the end of the year.

All four of my Max Planck supervisors played a pivotal role in ensuring the success of this project. From conception to completion, they offered the academic support required in the form of mentorship, advice, guidance, inspiration, patience, understanding, and networking opportunities. I would like to express my personal gratitude to Nicole Boivin and Alison Crowther for agreeing to supervise me and for allowing me to work on the Sealinks archaeological assemblage from the eastern African coast. Special thanks go to Ricardo Fernandes for his invaluable help with the dataset project. Thanks also to Patrick Roberts for his unwavering support in developing all three case studies. In particular, Patrick read the three case studies and the thesis multiple times. Thanks also go to Michael Bollig, Paul Lane and Patrick Roberts for supervising me at the University of Cologne and supporting me through its requirements.

The Max Planck Institute of Geoanthropology has consistently provided me with exemplary support in the form of a network of colleagues and friends. Hans Sell (Graphic Design) played a significant role in helping to create elegant and highly informative figures for my thesis. Kristin Starkloff (Library) helped me access articles and books for my projects, especially for the dataset project. The IT team solved my IT problems and made sure my laptop worked properly. Anja Hannawald and Anja Schatz helped me to navigate the administrative processes of the institute. Bettina Bock, Inna Malyshevska and the entire IMPRS team were instrumental in helping me successfully navigate the German administrative requirements. Special thanks also go to Jana Ilgner, Mary Lucas, Erin Scott and Stefanie Schirmer in the laboratory for their technical assistance during my laboratory work. Thanks also to Ulrike Thüring for granting me access to the stored archaeological material. Finally, I would like to thank my fellow researchers at the MPI who helped me in various ways: Victor Andrade, Michael Ziegler, Veronica Zuccarelli, Mariya Antonosyan and Laura Furquim in particular. I would also like to thank the Max Planck Society and the German government for providing me with this once-in-a-lifetime opportunity to fulfil one of my greatest dreams.

Finally, I would like to thank my family for their unwavering support throughout my academic career. Special thanks go to my mother and late father, who inspired me to pursue an academic career. I would also like to thank my wife, Irene Mwongeli, for her patience during my studies and during the long periods I have spent away from home. Thank you to my elder sister for taking care of family responsibilities in my absence. It's been almost twenty years since I started my PhD journey in America in 2007, but it was cut short due to unavoidable circumstances. Finally, it has come to fruition. THANK YOU ALL!

Table of Contents

Abstract ..... **i**

Preface and acknowledgements ..... **ii**

Table of contents ..... **iv**

List of figures ..... **viii**

List of tables ..... **xv**

Chapter 1: Introduction **1**

1.1 Isotope ecology in the archaeology of food production in eastern Africa 9

1.2 Archaeo-informatics and the late Holocene archaeology of eastern Africa 12

1.3 Isotopic and archaeo-informatic perspectives in ancient coastal archaeology of eastern Africa 14

1.4 Thesis structure 17

Chapter 2: The migration and indigenous continuity hypotheses of late Holocene socioeconomic change in eastern Africa **21**

2.1 History of theory in the archaeology of food production in eastern Africa 22

2.2 The normative approach and monolithic migrations in eastern Africa 26

2.3 The idiographic approach and indigenous continuity in eastern Africa 43

2.4 Integrating the normative and idiographic approaches 54

2.5 Archaeological sciences in the late Holocene archaeology of coastal and interior eastern Africa 64

2.6 Case studies 66

Chapter 3: Climatic and environmental change in eastern Africa during the last 20, 000 years and its relevance to socioeconomic change **75**

3.1 Environmental changes in the interior of eastern Africa over the last 20,000 years 76

3.2 High-resolution environmental records from marine sedimentary cores in the coastal region of eastern Africa 82

3.3 The potential of isotopes and archaeo-informatics in the late Holocene archaeology of coastal eastern Africa …. 88

Chapter 4: Methodological background in isotopes and archaeo-informatics 92

4.1 Isotope systematics 93

4.2 Isotopes in the biosphere 96

4.3 Application of isotopes in human palaeoecological reconstruction and animal husbandry 104

4.4 Archaeo-informatics in eastern Africa and beyond 115

4.5 Limitations in the isotopic and archaeo-informatic perspectives 124

Chapter 5: Materials, methods, and results for the Kuumbi Cave isotopic case study 134

5.1 Zooarchaeology background, identification, and carbon and oxygen sampling and analysis 135

5.2 Statistical analysis 137

5.3 Variation in taxa and dietary groups at Kuumbi Cave 138

5.4 Variation over time at Kuumbi Cave 143

5.5 Human values 147

5.6 Comparison of Kuumbi Cave and published mainland eastern African sites 147

Chapter 6: Materials, methods and results for the Unguja Ukuu isotopic case study 151

6.1 Unguja Ukuu, Fukuchani and Panga ya Saidi contexts and faunal assemblages 152

6.2 Samples and sample identification 153

6.3 Stable isotope analysis 155

6.4 Indicators of collagen preservation and direct dates 159

6.5 Variation in taxa at Unguja Ukuu 160

6.6 Caprine bone collagen from Unguja Ukuu, Fukuchani, Panga ya Saidi, and Enkapune ya Muto 165

6.7 Caprines, wild fauna, and human enamel from Unguja Ukuu, Kuumbi Cave, and Panga ya Saidi 169

6.8 Caprine enamel from Unguja Ukuu, and the interior of eastern Africa 172

Chapter 7: Methods, quality control and results for the *Wanyika* scientific dates case study 176

7.1 The *Wanyika* Dataset 176

7.2 Sampling strategy 177

7.3 Demarcation of country regions and vegetation cover 180

7.4 Data collection and deposition 183

7.5 Scientific dates and calibration 185

7.6 Quality control 189

7.7 Data records 201

Chapter 8: Insights from isotopic and archaeo-informatic perspectives on the emergence and dispersal of food production and food-producing communities in coastal eastern Africa during the late Holocene ……..... 211

8.1 Ecological stability and forager persistence at Kuumbi Cave during the late Pleistocene and late Holocene 212

8.2 Caprine husbandry and complex subsistence strategies at Unguja Ukuu, Zanzibar, during the Iron Age 224

8.3 *Wanyika* dataset and migrations in eastern Africa 235

8.4 The ‘Bantu package’ dilemma 265

8.5 A synthesis of the multi-isotopes and archaeo-informatic perspectives in the late-Holocene archaeology of coastal eastern Africa 269

Chapter 9: Conclusions, limitations and future work 276

9.1 Conclusions 276
9.2 Milestones of this thesis in the late Holocene archaeology of eastern Africa 282

9.3 Limitations and future work 285

References 290

Appendix 1 - Tables and statistical analysis associated with "Chapter 5: The Kuumbi Cave isotopic case study" 356

Tables A1:1 - A1:2 356
Statistical analysis 393

Appendix 2 - Tables associated with "Chapter 6: The Unguja Ukuu isotopic case study" 408

Tables A2:1 - A2:7 408

Appendix 3 – Table associated with "Chapter 7 – The *Wanyika* scientific dates case study" 420

Table A3:1 420

List of Figures

Chapter 1

Figure 1.1. Map of Africa highlighting eastern Africa and the four countries that provided most of the data for this thesis: Kenya, Tanzania, the Comoros Islands, and Madagascar. Rwanda is also highlighted. Unguja Island is also highlighted because it provided the primary data for this thesis. The figure was created for this study by Hans Sell (Graphic Designer for the Max Planck Institute of Geoanthropology, Jena, Germany). 8

Chapter 2

Figure 2.1. A visual representation of the migration hypothesis in eastern Africa, showing the following: (A) the pre-food production period (before 3000 BCE), when indigenous people relied solely on hunting and gathering; (B) the onset of Neolithic pastoralist immigration (3000-500 BCE), which gradually displaced and replaced foragers; (C) the onset of immigration by iron-using pastoralists (800 CE-1800 CE), which continued to displace the remaining indigenous foragers; and (D) the onset of agropastoralist immigration (500 BCE-1800 CE), which also displaced indigenous foragers. Ultimately, the remaining foragers were marginalized. Note: Independent invention and diffusion are negligible in the migration hypothesis. The figure was created for this study by Hans Sell (Graphic Designer for the Max Planck Institute of Geoanthropology, Jena, Germany). 27

Figure 2.2. Map of Africa showing hypothesized Neolithic pastoralist migrations into eastern Africa's interior from the Sudan, Ethiopia, and Somalia regions: (A) Elmenteitan Pastoral Neolithic migration from Sudan following the Nile River to the Lake Victoria region, and (B) Savannah Pastoral Neolithic migration from the Ethiopia-Somalia region into the interior of eastern Africa to the southern region of Tanzania. The figure was created for this study by Hans Sell (Graphic Designer for the Max Planck Institute of Geoanthropology, Jena, Germany). ... 29

Figure 2.3. Map of Africa highlighting the two hypotheses of western agropastoralist migration: (A) the early-split, and (B) the late-split. Note the solid arrows representing rapid migration from western to eastern Africa. The figure was created for this study by Hans Sell (Graphic Designer for the Max Planck Institute of Geoanthropology, Jena, Germany). 33

Figure 2.4. Visual representation depicting the differences in recovered artifacts from different sites representing the following subsistence strategies: (A) Foragers (hunter-gatherers) with Kansyore ceramic ware featuring punctate decorations, stone tools, and a high concentration of wild animal remains; (B) Neolithic pastoralists with elongated Nderit ceramic ware, stone bowls and platters, and tools, as well as a high concentration of livestock remains; (C) Iron Age pastoralists with iron weapons, elongated Lanet ware ceramics, and a high concentration of livestock remains; (D) Agropastoralists/farmers with iron weapons, Urewe ceramic ware featuring wavy triangular decorations, and a mixture of livestock and farmland crops. The figure was created for this study by Hans Sell (Graphic Designer for the Max Planck Institute of Geoanthropology, Jena, Germany). 36

Figure 2.5. Visual representation of the indigenous continuity hypothesis in eastern Africa showing: (A) The pre-food production period (before 3000 BCE), during which indigenous peoples engaged in hunting and gathering as their sole subsistence strategy; (B) Through independent invention and diffusion, indigenous foragers transitioned to Neolithic pastoralism (migrations were negligible) (3000 – 500 BCE); (C) Through independent invention and diffusion, indigenous foragers transitioned from Neolithic to Iron Age pastoralism, incorporating metallurgy and complex ceramic technology (800 CE – 1800 CE); (D) Through independent invention and diffusion, some indigenous foragers continued to transition to agropastoralism, incorporating African domesticated crops such as sorghum, millet, cowpeas, and lablab beans (500 BCE – 1800 CE). Note: Migration is negligible in the indigenous continuity hypothesis meaning a stable genetic pool. The figure was created for this study by Hans Sell (Graphic Designer for the Max Planck Institute of Geoanthropology, Jena, Germany). 44

Figure 2.6. Map of Africa highlighting the recently revised western African agropastoralist migrations to eastern Africa, known as the riverine migration hypothesis, with two proposed routes: (A) the riverine route, which is backed by archaeological evidence, and (B) the northern Congo forest route, which lacks archaeological and other evidence. Note the small continuous arrows representing gradual, periodic migrations. The figure was created for this study by Hans Sell (Graphic Designer for the Max Planck Institute of Geoanthropology, Jena, Germany). 57

Figure 2.7. Map of Africa depicting a second version of the revised western African agropastoralist migration to eastern Africa, known as the 'late-split savannah peeling-off' hypothesis. Note the arrows 1-13 showing the peeling-off patterns towards the forested northern and southern savannah regions of the main migration route. The figure was created for this study by Hans Sell (Graphic Designer for the Max Planck Institute of Geoanthropology, Jena, Germany). 59

Figure 2.8. Map of the Indian Ocean rim showing the commerce networks to eastern Africa. The figure was created for this study by Hans Sell (Graphic Designer for the Max Planck Institute of Geoanthropology, Jena, Germany). 63

Figure 2.9. A schematic representation of the geographical area of eastern Africa, highlighting the locations of sites with stable isotope data referenced in this thesis. (1) Porc Epic; (2) FxJj12; (3) GaJj11; (4) GaJj2; (5) Dongodien; (6) Ele Bor; (7) 'AW'; (8) 'Equid site'; (9) '514'; (10) Lothagam Lokam; (11) Kakapel; (12) Wadh Lang'o; (13) Kanam East; (14) Luanda; (15) Gogo Falls; (16) Lukenya Hill; (17) PYS; and (18) Kalemba Rockshelter. Figure 2.9(B) shows the location of KC on Unguja (Zanzibar) Island. The modern vegetation classification is based on (A) White (1983) and (B) Hardy et al. (2015) and was developed using regional base maps and validated through ground surveys. Photos of KC: (C) facing the entrance from outside; (D) facing outside from inside; (E) a view of the Trench 10 excavation; and (F) a Trench 10 cross-section (Iminjili et al., 2023). 69

Figure 2.10. Map of eastern Africa highlighting sites where isotope studies have been performed on caprines, namely UU, FK, and KC (wild fauna only) in Unguja Island and PYS along the Kenyan coast, and Dongodien, EYM, Gogo Falls, Wadh lang'o and Luxmanda in the

interior eastern Africa. Modern vegetation based on (A) White (1983) and (B) Hardy et al. (2015): classification of vegetation biomes developed from regional base maps validated through ground surveys. Aerial view of UU (Ua-Uc), and Trenches excavated at UU by the Sealinks Project 2011-2012 (Ta-Td). 71

Figure 2.11. Map of eastern Africa showing the spatial distribution of: a) scientific dates by country (5000 BCE to 1800 CE), highlighting specific sites with archaeobotanical finds in Rwanda; b) dated archaeological sites (5000 BCE to 1800 CE) with finds relating to archaeobotany, zooarchaeology, and metallurgy; c) identified ceramic traditions associated with pastoralists, farmers, hunter-gatherers, and Indian Ocean commerce (5000 BCE to 1800 CE) (Iminjili et al., 2025a; Iminjili et al., 2025b). 73

Chapter 3

Figure 3.1. Timeline of the KC stratigraphic succession alongside regional climate conditions and the formation of Unguja Island (Iminjili et al., 2023). The various shades of brown represent different stages of island formation, while blue signifies the ocean and the white diamond indicates the location of KC. The island's formation occurred between 12,000- and 10,000-years BP. This represents H. Rouby's reconstructions of Unguja Island in Prendergast et al. (2016), modified to include an illustration of stratigraphic integrity and regional climatic change. 84

Chapter 5

Figure 5.1. Two different formats are used to show the scatterplots of the KC $\delta^{13}C$ and $\delta^{18}O$ values. The first format (A) shows the information sorted by family. The color of each data point indicates the family: forest (dark and light green for closed and open canopy, respectively), mosaic grassland (light brown), extirpated fauna (squares), and two *Homo sapiens* specimens (red triangles). The second arrangement (B) displays the information categorized by taxa. The sample sizes for each taxon are given in brackets. Symbols and colors are used to represent the different faunal groups mentioned in A and B. These groups comprise primates, bovids, other large mammals, and small mammals. However, the five large animals that are no longer found in the area are shown using square symbols. These are *O. oreotragus, S. grimmia, R. redunca, T. scriptus* and *E. quagga*. The error bars in (A) represent standard deviations (Iminjili et al., 2023). 140

Figure 5.2. Box and jitter plots of (A) $\delta^{13}C$ and (B) $\delta^{18}O$ values. The values have been classified by faunal dietary category. Outliers are represented by dots and Xs along the midline of the graphs. The sample sizes are indicated in brackets above the plot labels on the x-axis (Iminjili et al., 2023). 142

Figure 5.3. Taxon-specific regression analysis of the relationship between $\delta^{13}C$ and $\delta^{18}O$ data for the three families with the widest range of $\delta^{13}C$ values shows a significant correlation within each family. These families are the Bovidae (ranging from -20.4 to -1.9 ‰), the Equidae (ranging from -8.2 to -2.0 ‰), and the Procaviidae (ranging from -18.4 to -2.5 ‰). The grey bands represent the 95% confidence intervals linked to each regression line. The sample sizes for each taxon are given in brackets (Iminjili et al., 2023). 143

Figure 5.4. Scatterplots of $\delta^{13}C$ and $\delta^{18}O$ values by taxa in Phases I–IV. Different groups of animals are represented by different symbols and colors: primates, bovids, other large mammals and small mammals. Nevertheless, there is an exception to this rule. Five extinct large animals

are shown as square symbols: *O. oreotragus, S. grimmia, R. redunca, T. scriptus,* and *E. quagga*. The two *Homo sapiens* specimens are denoted by red triangles. The quantity of specimens for each taxon is indicated in brackets (Iminjili et al., 2023). 145

Figure 5.5. Box and jitter plots showing the $\delta^{13}C$ values of taxa present at most sites in eastern Africa. The distribution of KC is largely distinct from that of the inland sites (Iminjili et al., 2023). 149

Figure 5.6. Box and jitter plots showing the $\delta^{13}C$ values of the feeding groups in different regions and sites in eastern Africa. Outliers are indicated by dots and Xs along the midline of the plots. The sample sizes for each site or region are shown in brackets (Iminjili et al., 2023). 150

Chapter 6

Figure 6.1. Stratigraphy of UU Trench 14 highlighting the Early Phase contexts where high numbers of samples that failed to produce isotope results originated. 155

Figure 6.2. Scatterplots of $\delta^{13}C_{coll}$ and $\delta^{15}N$ values by species highlighting the distinctions between wild herbivores (Small Forest adapted antelopes and other browsers have $\delta^{13}C$ values less than −18‰ and $\delta^{15}N$ values less than 9‰) and caprines (almost all of the $\delta^{13}C$ values are above −14‰ and most of the $\delta^{15}N$ values above 10‰) from the UU site. 162

Figure 6.3. Scatterplots of enamel values from UU caprines and human by (A) $\delta^{13}C$ and $\delta^{18}O$ values (caprines $\delta^{13}C_{enamel}$ values are higher than −7‰ and almost all $\delta^{18}O$ values are lower than 1‰) highlighting the similarity in the caprines $\delta^{13}C_{enamel}$ and $\delta^{13}C_{coll}$ patterns; (B) Variation in the $^{87}Sr/^{86}Sr$ and $\delta^{18}O$ values from UU caprines and human highlighting the sheep value from a deciduous tooth, and the low $^{87}Sr/^{86}Sr$ value with the highest $\delta^{18}O$ value in the UU dataset and five values higher than 0.710. 164

Figure 6.4. Scatterplots of $\delta^{13}C_{coll}$ and $\delta^{15}N$ values of caprines from three coastal (UU, FK, and PYS) and one interior eastern African (EYM) sites highlighting the similarity between UU and EYM, and the distinctions between them and PYS. 167

Figure 6.5. Scatterplots of $\delta^{13}C_{coll}$ and $\delta^{15}N$ values of wild herbivores and caprines from FK and PYS highlighting the distinctions between forest adapted herbivores ($\delta^{13}C_{coll}$ values concentrated below -18 and $\delta^{15}N$ values below 10 and caprines (PYS sheep unusually low $\delta^{13}C_{coll}$ value, and unusually high $\delta^{15}N$ values for sheep, common duiker (*S, grimmia*), and eland (Tragelaphini)). 168

Figure 6.6. Scatterplots of enamel values by (A) $\delta^{13}C_{enamel}$ and $\delta^{18}O$ values from KC small forest adapted antelopes ($\delta^{13}C$ values lower than −10‰ and $\delta^{18}O$ values lower than 0‰) and wild grazers ($\delta^{13}C$ values higher than −10‰ and $\delta^{18}O$ values below 0‰) and caprines from UU ($\delta^{13}C$ values higher than −7‰ and almost all $\delta^{18}O$ values are lower than 1‰) highlighting the distinctions between the small forest adapted antelopes and UU caprines similar to the patterns in the collagen $\delta^{13}C$ values; (B) Variation in the $^{87}Sr/^{86}Sr$ and $\delta^{18}O$ values from UU caprines and

humans from UU, KC and PYS highlighting the five caprine and PYS $^{87}Sr/^{86}Sr$ values higher than 0.710. 171
Figure 6.7. Scatterplots of $\delta^{13}C_{enamel}$ and $\delta^{15}N$ values of caprines from UU and three sites (Dongodien, Gogo Falls, and Wadh Lang'o) from the interior eastern Africa (caprines from these three sites have not been identified to species level via ZooMS). The plot highlights the distinctions between UU values ($\delta^{13}C_{enamel}$ values packed between −8‰ and −2‰ and $\delta^{18}O$ values between −3‰ and 1‰) and interior eastern African sites with Wadh Lang'o and Gogo Falls $\delta^{13}C$ values falling above −2‰ and $\delta^{18}O$ values concentrated between 1‰ and 6‰) and the Dongodien $\delta^{13}C_{enamel}$ values falling between −8‰ and 1‰ and $\delta^{18}O$ values between 1‰ and 7‰). The plot also highlights the bimodal distribution of the Dongodien values with values lower than −4‰ representing goats and values above −4‰ representing sheep. 174

Chapter 7

Figure 7.1. Flow chart summarizing the construction of the *Wanyika* dataset (Iminjili et al., 2025a; Iminjili et al., 2025b). The flow chart was created for this study by Hans Sell (Graphic Designer for the Max Planck Institute of Geoanthropology, Jena, Germany). 184

Figure 7.2. Map of eastern Africa showing the differences in the spatial distribution of scientific dates by dating technique (^{14}C, OSL and IRSL, TL, and OH) (Iminjili et al., 2025a; Iminjili et al., 2025b). 186

Figure 7.3. Map of eastern Africa showing the differences in the spatial distribution of scientific dates according to their stratigraphic integrity and reliability. Note: Class A dates are the most reliable (Iminjili et al., 2025a; Iminjili et al., 2025b). 191

Figure 7.4. Map of eastern Africa showing the spatial variation in the distribution of ^{14}C dates obtained from plant material. Note: Class A dates are considered to be the most reliable (Iminjili et al., 2025a; Iminjili et al., 2025b). 196

Figure 7.5. Map of eastern Africa showing differences in the spatial distribution of ^{14}C dates from faunal material due to the aquatic reservoir effect. Note: Class A dates are considered to be the most reliable (Iminjili et al., 2025a; Iminjili et al., 2025b)**.** 198

Figure 7.6: Map of eastern Africa showing differences in the spatial distribution of scientific dates, based on the accuracy of the pre-treatment procedure for ^{14}C dates. Note: Class A dates are the most reliable (Iminjili et al., 2025a; Iminjili et al., 2025b). 200

Chapter 8

Figure 8.1. Scatter plot showing the distribution of arboreal fauna (primates and hyraxes) at KC. The values mirror the exploitation of resources by animals within each given taxon along a gradient between the forest floor and upper canopy (Iminjili et al., 2023). 216

Figure 8.2. Graphic representation of regional caprine husbandry strategies in eastern Africa, showing differences in herding practices. (A) Interior: Pastoralist wildland herding, where caprines are herded in close proximity to wild animals and feed similarly. (B) Coast and Islands:

Agropastoralist farmland herding, where caprines are herded in manured farmlands, including penning and paddocking, far from wild animals. They feed predominantly on cultivated crops, such as sorghum and millet. Note that the interior is dominated by large, open, wild animals, while the islands are dominated by small, forest-adapted animals. Agropastoralist communities on the islands are also involved in foraging, fishing, ironworking, and Indian Ocean trade. The figure was created for this study by Hans Sell (Graphic Designer for the Max Planck Institute of Geoanthropology, Jena, Germany). 231

Figure 8.3. Maps showing 3-time windows highlighting change in land use patterns in eastern Africa between 5000 BCE to 1800 CE: (a) the north-south dispersal of domesticated animals from the Lake Turkana region beginning 3000 BCE, (b) the west-east dispersal of African domesticated crops and iron technology from the Lake Victoria region, (c) convergence of domesticated animals and local crops, and exotic crops along the eastern Africa hinterland coast, islands and Madagascar (Iminjili et al., 2025a; Iminjili et al., 2025b). The figure was created for this study by Michael Fisher (Digital archaeologist, Max Planck Institute of Geoanthropology, Jena, Germany). 238

Figure 8.4. Maps showing two-time windows that highlight general patterns in the spatial and temporal distribution of ceramics related to pastoralists originating from the Lake Turkana region and circulating in the interior of eastern Africa: (A) the Pastoral Neolithic (3000–500 BCE) and (B) the Pastoral Iron Age (800 CE–1800 CE) (Iminjili et al., 2025a; Iminjili et al., 2025b). 241

Figure 8.5. Maps showing three-time windows that highlight general patterns in the spatial and temporal distribution of farmer-related ceramics originating from the Lake Victoria region and circulating in eastern Africa's interior. (A) Urewe ceramic ware, found around Lake Victoria, has the earliest dates (earlier than 100 BCE). This is followed by Kwale, found in the coastal region, with the earliest dates around 1-200 CE. Next is Tana ware, with the earliest dates around 300-500 CE. (B) Kwale and Tana ware dominate the coast and become prevalent in the islands during the Middle Iron Age (700-1000 CE). (C) Tana ware spreads to Madagascar, where Rezoky, Andaro, Beropitika, and Tranovato become prevalent in southern Madagascar. (Iminjili et al., 2025a; Iminjili et al., 2025b). 243

Figure 8.6. Maps showing 3-time windows highlighting dates from extinct megafauna taxa tracking their late persistence and appearance of introduced species and humans in Madagascar (a-c). Map (c) shows that humans, introduced species and extinct megafauna coexisted between 601 to 1800 CE (Iminjili et al., 2025a; Iminjili et al., 2025b). 246

Figure 8.7. a) Distribution of *Wanyika* archaeological sites located in Kenya, Tanzania, Comoros, and Madagascar, organized into k-means groups (Hartigan–Wong algorithm) (Hartigan and Wong, 1979). The groups are numbered 1-19. The larger symbols represent group centroids. b) Distribution of group dates (vertical tick marks with median value as a dot) within the 5000 BCE to 1800 CE time period (Iminjili et al., 2025a; Iminjili et al., 2025b). The figure was created for this study by Ricardo Fernandes (Archaeo-informatics expert, Max Planck Institute of Geoanthropology, Jena, Germany). 249

Figure 8.8. Map of eastern Africa highlighting the disparities in the distribution of direct dates from domesticated crops: four African and three exotic breeds. n = total number of dates and number of sites in brackets (Iminjili et al., 2025a; Iminjili et al., 2025b). 251
Figure 8.9. Map of eastern Africa highlighting the disparities in the distribution of the number of direct zooarchaeological dates from three livestock, three commensals. n = total number of dates and number of sites in brackets (Iminjili et al., 2025a; Iminjili et al., 2025b). 254

Figure 8.10. Map of eastern Africa highlighting the disparities in the distribution of direct iron and ceramic dates according to the stratigraphic integrity and reliability of date quality control classes. n = total number of dates and number of sites in brackets (Iminjili et al., 2025a; Iminjili et al., 2025b). 257

Figure 8.11. Map of eastern Africa highlighting the disparities in the distribution of direct human dates. n = total number of dates and number of sites in brackets (Iminjili et al., 2025a; Iminjili et al., 2025b). 264

List of Tables

Chapter 3

Table 3.1. Chronology of climate-driven ecological transformations in eastern Africa from the late Pleistocene to the late Holocene collated from in text citations (Talbot and Lærdal, 2000; Kiage and Liu, 2006; Foerster et al., 2015; Revel et al., 2015; Schaebitz et al., 2021). Years recorded in uncalibrated years before present (BP). 77

Chapter 5

Table 5.1. Summary statistics for $\delta^{13}C$ and $\delta^{18}O$ values at coastal and inland sites in eastern Africa. 148

Chapter 7

Table 7.1. Delineation of regions based on country boundaries and citations from the bibliography. The main vegetation cover is taken into account, as well as the approximate boundaries, which are defined by geographical coordinates of a delimiting rectangle (Iminjili et al., 2025a; Iminjili et al., 2025b). 182

Table 7.2. Qualities of dates used to define classes in the stratigraphic integrity and reliability quality control measure. 193

Table 7.3. Synopses of dating methods and quality control measures (chronometric hygiene founded on stratigraphic integrity and the reliability of the dates) are proffered, accentuating the paucity of Class A dates in the *Wanyika* dataset (Iminjili et al., 2025a) See Table 1 for information on the demarcation of country regions. 194

Table 7.4. Scheme for grading ^{14}C dates for botanical and aquatic materials, and the accuracy of chronological determination. 197

Table 7.5. Data categories and field details. For definitions of column fields, see the section below. 201

Table 7.6. Period and ceramic tradition associated with regional cultural phases. 205

Chapter 8

Table 8.1. List of extinct faunal species including megafauna, introduced species and human with direct dates from Madagascar tracking their coexistence. Note the disparity in direct human dates. 247

Table 8.2. Highlighting the disparities in the distribution of the number of direct archaeobotanical dates from four African and three exotic crops, n = Total number of dates and number of sites in brackets. 252

Table 8.3. Highlighting the disparities in the distribution of the number of direct zooarchaeological dates from three livestock, three commensals, humans and megafauna per country, n = total number of dates and number of sites in brackets. 255

Table 8.4. Chronology of 24 major ceramic traditions from the interior eastern Africa, the coast, and islands limited to the period spanning 5000 BCE to 1800 CE, based on class A dates and all class dates in Figure 7.3. Some ceramic traditions do not have class A, B, and D dates. $\mathbf{n^1}$ = total number of dates and $\mathbf{n^2}$ = number of direct ceramic dates (from identified ceramic tradition). 259

A people without knowledge of their history, origin, and culture are like a tree without roots (Marcus Garvey, 1887-1940).

Chapter 1 – Introduction

The complex ecological setting related to the unique geography of eastern Africa, coupled with flexible human adaptive strategies, played a significant role in shaping the emergence and diversification of food production and the dispersal of food-producing communities in the region during the late Holocene (White, 1983; Ambrose, 1984a; Clark and Brandt, 1984; Marshall, 1986; Chami, 1994; Ambrose, 1998; Marshall and Hildebrand, 2002; Ambrose, 2003; Lane, 2004; Kusimba and Kusimba, 2005; Chami, 2009; Lane, 2013b; a; Crowther et al., 2018; Marchant et al., 2018; Chami and Silayo, 2023). This resulted in a unique and diverse blend of adaptive subsistence trajectories compared with other regions of the world (Lemmen, 2011; Lemmen et al., 2011; Mulrooney et al., 2011; Bocquet-Appel et al., 2012; Crombé and Robinson, 2014; Hofmanová et al., 2016; Kay et al., 2019; Long et al., 2022). However, eastern Africa has not received adequate scholarly attention from archaeologists studying human-environment interactions during the late Holocene. Major hypotheses developed about the emergence of food production and dispersal of food-producing communities have not been adequately tested due to a lack of adequate archaeological data and the lack of a synthesis of the existing archaeological data within an archaeo-informatic-oriented dataset.

Two major philosophical approaches have guided late Holocene archaeology in eastern Africa: the normative approach and the idiographic approach (Ambrose, 1982; Ehret and Posnansky, 1982; Vansina, 1995; Ehret, 1998; 2001; Kusimba and Kusimba, 2005; Crowther et al., 2018). The normative approach provides a broad, general perspective on the archaeological record, while the idiographic approach provides the particularities, or site-context-specifics, that shape practical

human–environment interactions. The normative approach presents the archaeology of eastern Africa as being broadly shaped by monolithic migration events involving pastoralists from the north-eastern region of Africa and agropastoralists from the western region of Africa, who interacted with indigenous foragers during the late Holocene (Ambrose, 1982; Ehret and Posnansky, 1982; Ambrose, 1984b; 1998; Ehret, 1998; 2001; Ambrose, 2003). In contrast, the idiographic approach presents a nuanced, mostly synchronic, and site-context-specific perspective of the archaeological record (Kusimba et al., 2005; Kusimba and Kusimba, 2005; Crowther et al., 2018). The normative approach's monolithic migration hypotheses have been criticized for being overly general and promoting unilinear evolution in archaeology (Kusimba and Kusimba, 2005; Crowther et al., 2018). Conversely, the idiographic approach is criticized for focusing too much on site-specific details at the expense of the diachronic background of human-environment interaction (Binford, 1968; Harris, 2001; Erickson and Murphy, 2003; Trigger, 2007). Monolithic migration hypotheses have now been refined into more detailed gradual processes that are worthy of reconsideration in the archaeology of eastern Africa (Pakendorf et al., 2011; Russell et al., 2014; Grollemund et al., 2015; Seidensticker et al., 2021; Koile et al., 2022; Grollemund et al., 2023). I integrate these philosophical approaches, contextualizing my thesis around broader debates relating to migration and indigenous continuity hypotheses in the particular context of human subsistence.

Central Africa, which is believed to have played a significant role in the migration of western African agropastoralists to eastern Africa, has been a particular area of focus for multidisciplinary studies of Holocene subsistence in Africa (Pakendorf et al., 2011; de Filippo et al., 2012; Russell et al., 2014; Grollemund et al., 2015; Bostoen, 2018; Seidensticker et al., 2021; Koile et al., 2022; Grollemund et al., 2023; Coutros et al., 2024; Fortes-Lima et al., 2024; Bostoen and Coutros, 2025). Scholars working in central Africa have developed new hypotheses based on computer-generated

models that shed light on these migration events (Russell et al., 2014; Grollemund et al., 2015; Seidensticker et al., 2021; Koile et al., 2022; Grollemund et al., 2023). Rather than adopting the monolithic, rapid Bantu expansion perspective, the new Bantu migration hypotheses propose a gradual, multi-wave process. The number of new archaeological publications and hypotheses developed by scholars working in eastern Africa has also increased substantially over the last sixty years (Ambrose, 2003; Lane, 2004; Kusimba and Kusimba, 2005; Crowther et al., 2018; Chami and Silayo, 2023). One of the most recently published hypotheses for eastern Africa is the subsistence mosaic hypothesis (Crowther et al., 2018). This hypothesis provides an idiographic view of the archaeology of coastal eastern Africa. It posits that complex interactions between different subsistence groups led to the blurring of dichotomies such as foragers versus food producers in Iron Age coastal site assemblages in eastern Africa. A similar argument has been made for densely populated areas in the interior of eastern Africa (Kusimba et al., 2005; Kusimba and Kusimba, 2005). In other words, it is impossible to distinguish the contributions of pastoralists from north-eastern Africa and agropastoralists from western Africa in the archaeological assemblage (Crowther et al., 2018). The intricate subsistence patterns that cause this effect can be better understood through undertaking multi-scalar diachronic study incorporating multiple isotopes and archaeo-informatics (Schoeninger and DeNiro, 1984; Balasse, 2014; Russell et al., 2014; Ventresca Miller and Makarewicz, 2017; Kay et al., 2019; Bird et al., 2022; Kinaston, 2023). This approach also has the potential to provide in-depth insights into the emergence and dispersal of food production and food-producing communities in the coastal region and eastern Africa more broadly.

Growing multi-isotope archaeological data from new finds in the coastal region and the recently created archaeo-informatics-oriented dataset of scientific dates and archaeological remains from

archaeological sites in eastern Africa (see Appendix 3 and Case Study Three of this thesis) mean that there is significant potential to undertake such a study (Crowther et al., 2016a; Crowther et al., 2016b; Prendergast et al., 2016; Shipton et al., 2016; Prendergast et al., 2017b; Crowther et al., 2018; Roberts et al., 2020; Wang et al., 2020; Culley et al., 2021a; Culley et al., 2021b; Kotarba-Morley et al., 2022). These methods can be used to address the use of wild resources by communities practicing different subsistence strategies, intricate subsistence adaptive strategies that incorporate crop and livestock production, and the complex herding strategies applied by livestock keepers. This, in turn, provides an opening to revisit the emergence and diversification of food production and dispersal of food-producing communities in the archaeology of the coastal and interior regions of eastern Africa based on a complementary, systematic perspective of the migration and indigenous continuity hypotheses. This synthesized analysis, based on a multidisciplinary, consistent methodological approach and theoretical complementarity, provides a more insightful way of interpreting the archaeological data from the coastal and interior of eastern Africa on the same level.

Although isotopic and archaeo-informatic perspectives, as well as other approaches from the field of archaeological science, are now fully assimilated into projects around the world, they have yet to be widely adopted in eastern Africa (Steele, 2010; Buchanan et al., 2011; Russell et al., 2014; Chaput et al., 2015; Williams et al., 2015; Shennan, 2018; Bird et al., 2021; Seidensticker et al., 2021; Bird et al., 2022; Koile et al., 2022; Billings et al., 2025). These approaches offer new, previously inaccessible, in-depth insights into complex human-environment interaction scenarios. They provide information on the nature of subsistence in different ecosystems and regional approaches to plant cultivation, livestock herd management, and the exploitation of wild species around the world. These approaches have been successfully applied within a few projects in eastern

Africa, including the Sealinks Project and the Archaeology of the Movement of People, Plants, and Animals in Holocene Southeastern Africa Project—publishing a high number of papers (Crowther et al., 2014; Crowther et al., 2016a; Prendergast et al., 2016; Shipton et al., 2016; Prendergast et al., 2017a; Prendergast et al., 2017b; Crowther et al., 2018; Shipton et al., 2018; Faulkner et al., 2019; Prendergast et al., 2019a; Roberts et al., 2020; Culley et al., 2021a; Culley et al., 2021b; Faulkner et al., 2021; Faulkner et al., 2022; Kotarba-Morley et al., 2022; Goldstein et al., 2024; Goldstein et al., 2025). These approaches include context-specific excavations, high-tech recording, the mass production of radiocarbon dates from multi-stratified sites, isotopic and ancient DNA (aDNA) analysis, zooarchaeology by mass spectrometry (ZooMS), proteomics, advanced flotation and microscopy, species identification, and in-depth analyses of zooarchaeological and archaeobotanical remains.

Globally, scientific dates and the results of multidisciplinary approaches to archaeological studies have been synthesized into regional, archaeo-informatics-oriented datasets (Gkiasta et al., 2004; Oslisly et al., 2013; Russell et al., 2014; Chaput et al., 2015; Kay et al., 2019; Bird et al., 2021; Seidensticker et al., 2021; Bird et al., 2022; Koile et al., 2022; Billings et al., 2025). These datasets have been analyzed using Bayesian modeling, summed probability distributions (SPDs), and geospatial-temporal analysis with software such as QGIS. These approaches have provided in-depth insights into regional human-environment interactions during the late Holocene. The use of multiple methodologies in similar ways to central Africa and other parts of the world could be used to produce an archaeo-informatics-oriented meta-database in eastern Africa. Applying modeling and other computer-aided methodologies to this meta-database could greatly enhance testing hypotheses and developing theories about complex subsistence adaptive strategies and the

emergence of food production and the dispersal of food-producing communities in eastern Africa during the late Holocene.

This thesis employs multidisciplinary analyses of archaeological assemblages, integrating multi-isotope and archaeo-informatics perspectives to examine human-environment interactions in coastal and inland eastern Africa during the late Holocene (Figure 1.1). This includes connections between ecological fluctuations and complex subsistence strategies, such as utilizing wild resources, managing caprine herds, and cultivating plants, in coastal and inland eastern Africa during the late Holocene. Furthermore, I explore the emergence of food production and the dispersal of food-producing communities in coastal and inland regions. I examine these phenomena within the theoretical contexts of migration and indigenous continuity. This approach provides valuable insights into human-environment interaction trends in coastal eastern Africa from the late Pleistocene to the late Holocene that were previously inaccessible. It also provides information on the complex adaptive strategies of subsistence and the interactions between foragers and food producers during the Iron Age. Lastly, this approach enables a comparative evaluation of site-specific paleoecological and economic trends in coastal areas and the interior of eastern Africa using maps generated from an archaeo-informatics dataset. This unravels broad, in-depth, diachronic insights into human-environment interactions in the region.

My work is presented through three closely related case studies. The first two are based on multi-isotopic data from Kuumbi Cave (KC) and Unguja Ukuu (UU), which are located on Unguja Island in the Zanzibar archipelago. The first case study provides palaeocological insights from four time periods spanning the late Pleistocene to the late Holocene at KC, with climatically diverse conditions. The second case study provides insights into caprine husbandry in a coastal island

environment within the context of agropastoralism and Indian Ocean commerce at UU. The third case study examines the diachronic ecological patterns driving the emergence and dispersal of complex subsistence strategies and food-producing communities in coastal and inland areas of eastern Africa. This study is based on maps generated from an archaeo-informatics-oriented dataset of scientific dates and associated archaeological assemblages from eastern African sites spanning nearly seven millennia. Similarly, I use the maps to identify spatial-temporal research gaps in eastern African archaeology that limit the testing of existing hypotheses and highlight areas of significant potential for future research.

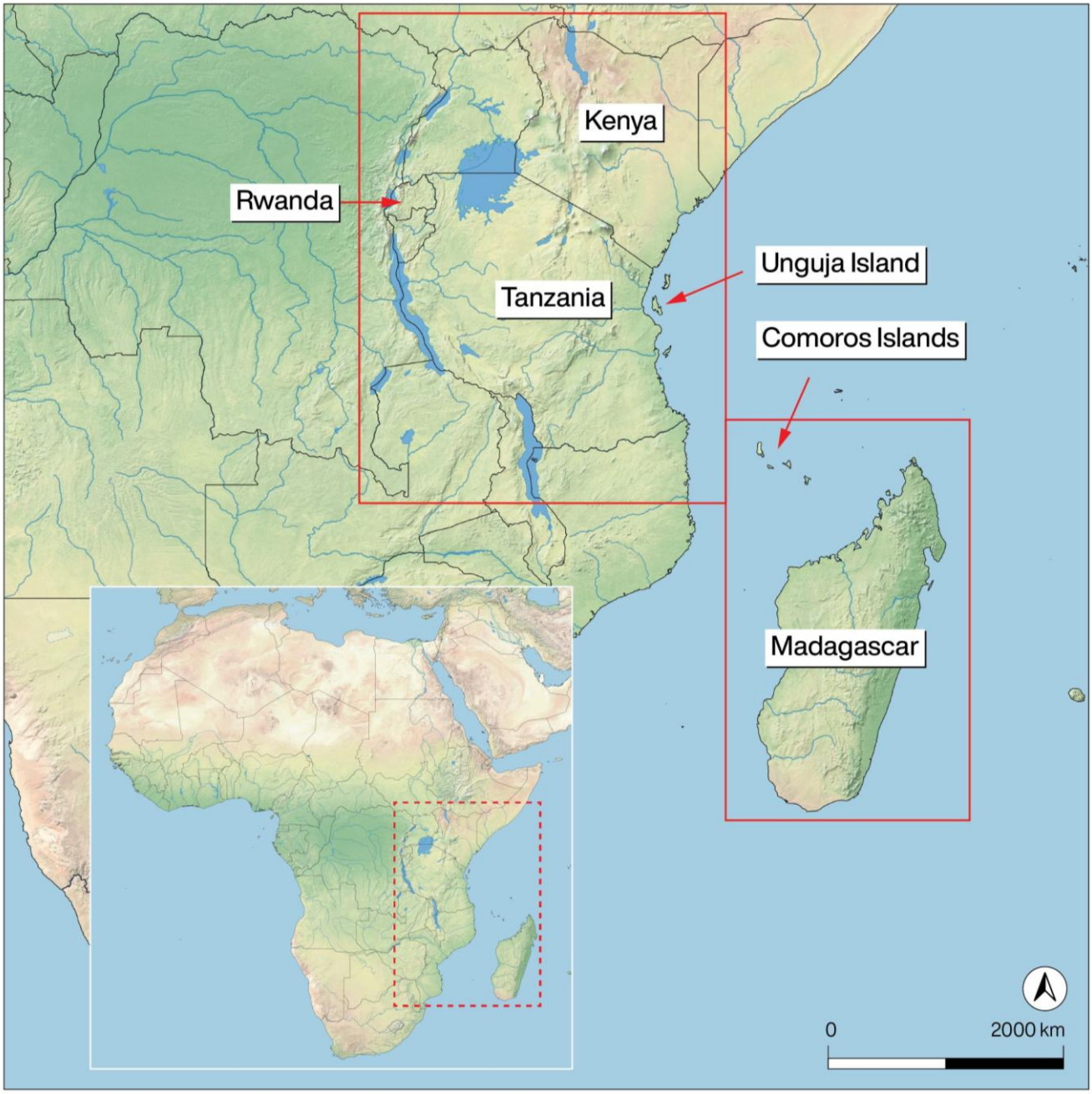


Figure 1.1. *Map of Africa highlighting eastern Africa and the four countries that provided most of the data for this thesis: Kenya, Tanzania, the Comoros Islands, and Madagascar. Rwanda is also highlighted. Unguja Island is also highlighted because it provided the primary data for this thesis. The figure was created for this study by Hans Sell (Graphic Designer for the Max Planck Institute of Geoanthropology, Jena, Germany).*

1.1 – Isotope ecology in the archaeology of food production in eastern Africa

Isotope dynamics, diet, ecology, and mobility

The ratios of the lighter and heavier isotopes of carbon ($\delta^{13}C$), oxygen ($\delta^{18}O$), nitrogen ($\delta^{15}N$), and strontium ($^{87}Sr/^{86}Sr$) change in unique, systematic patterns as they circulate through the geosphere, hydrosphere, and biosphere (Schoeninger and DeNiro, 1984; Ambrose et al., 2000; Limburg, 2004; Ramachandran et al., 2008; Janzen et al., 2020a; Janzen et al., 2020b; Janzen, 2022). Analyzing these element-specific patterns using samples from biological tissues (e.g., collagen and tooth enamel) can help reconstruct the diet, ecology, and mobility patterns of biological forms (Schoeninger and DeNiro, 1984; Cerling et al., 2004; Levin et al., 2006; Sponheimer et al., 2009; Lee-Thorp et al., 2010; Sponheimer, 2013; Cerling et al., 2015; Schulting et al., 2017; Chritz et al., 2019; Blanz et al., 2020; Janzen et al., 2020a; Janzen et al., 2020b; Roberts et al., 2020; Janzen, 2022; Kinaston, 2023; Prendergast et al., 2023). In general, browsers and grazers that are raised in arid, open grassland regions with older geological deposits will have distinct $\delta^{13}C$, $\delta^{18}O$, $\delta^{15}N$, and $^{87}Sr/^{86}Sr$ value patterns compared to similar herbivores that are raised in densely forested regions with younger geological deposits. Animals that utilize marine resources will also have different $\delta^{13}C$, $\delta^{18}O$, $\delta^{15}N$, and $^{87}Sr/^{86}Sr$ value patterns than terrestrial feeders. Similarly, animals raised in arid, open grasslands with older geological deposits who then migrate to densely forested regions with distinct geological deposits, which are both chemically and chronologically different (e.g. volcanic, metamorphic or sedimentary), will exhibit different $\delta^{13}C$, $\delta^{18}O$, $\delta^{15}N$, and $^{87}Sr/^{86}Sr$ isotopic values compared to resident animals.

Stable isotopes in human palaeoecology in eastern Africa

Although researchers have extensively applied stable isotope analysis of faunal and human enamel $^{13}C/^{12}C$ and $^{18}O/^{16}O$ values to reconstruct Plio-Pleistocene dietary patterns and paleoecology in the interior of eastern Africa (Cerling et al., 1977; Cerling et al., 1999; Cerling et al., 2003a; Cerling et al., 2003b; Levin et al., 2008; Cerling et al., 2010; Uno et al., 2011; Cerling et al., 2013; Cerling et al., 2015; Iminjili and Fernandes, 2023), there have been fewer studies on Pleistocene and late Holocene time periods, particularly in the coastal region (Robinson, 2017; Chritz et al., 2019; Roberts et al., 2020; Robinson, 2022). This time period is defined by significant climate variations caused by gravitational forces and further influenced by orogenic landmarks (such as the Rift Valley, lakes and rivers, and volcanic mountains and highlands) (Bonnefille et al., 1990; Kiage and Liu, 2006; Stager and Johnson, 2008). The wide range of ecological diversity supported various subsistence systems (Marean, 1992a; Ambrose, 1998; Kusimba, 1999; Prendergast, 2009). Intense periods of aridity during glacial and interglacial periods are reflected in lake core records from the interior of eastern Africa (Stager and Johnson, 2000; Kiage and Liu, 2006; Stager and Johnson, 2008; De Cort et al., 2013; Gelorini and Verschuren, 2013; Stager et al., 2017). During these periods, human populations would have faced impacts of frequent water shortages in different parts of eastern Africa (Marean, 1992b; Kusimba, 2013; Tryon and Faith, 2016). However, more subtle changes in precipitation and forest extent along the coast have been suggested by recent $^{13}C/^{12}C$ and $^{18}O/^{16}O$ isotopes in coastal contexts, suggesting different trajectories of human-environment interactions between the interior and the coast (Shipton et al., 2018; Roberts et al., 2020). Eastern Africa's insular territories have remained largely unexamined from the standpoint of this interdisciplinary approach.

Multi-isotopes analysis and caprine husbandry

The emerging archaeological evidence in eastern Africa, which demonstrates a multifaceted interaction between pastoral practices, other forms of livelihood, environmental conditions, and sociopolitical forces, underscores the necessity of direct studies of caprine herding strategies across diverse regions and time periods (Davies et al., 2014; Russell et al., 2014; Crowther et al., 2016a; Petek and Lane, 2017; Prendergast et al., 2017b; Skoglund et al., 2017; Marshall et al., 2018; Sawchuk et al., 2018; Chritz et al., 2019; Janzen et al., 2020a; Roberts et al., 2020; Culley et al., 2021b; Goldstein et al., 2024). The complex terrain of eastern Africa, with its mosaic of grass-dominated vegetation and widely dispersed patches of dense forests, as well as its fluctuating climate patterns over the last five millennia, would have shaped spatiotemporal caprine herding strategies in diverse ways (White, 1983; Kingdon, 1984b; Marshall, 1990; Burgess and Clarke, 2000; Kingdon, 2001; Marshall and Hildebrand, 2002; Russell et al., 2014; Crowther et al., 2018; Culley et al., 2021a; Culley et al., 2021b). Eastern Africa's islands provide a key part of the above-mentioned diversity, though remain particularly understudied from the perspective of long-term animal management.

Multi-isotope analysis is a powerful approach for exploring past caprine herd management dynamics within complex and fluid eastern African ecological settings (Marshall, 1990; Janzen, 2015; Hildebrand et al., 2018; Marchant et al., 2018; Sawchuk et al., 2018; Chritz et al., 2019; Janzen et al., 2020a; Janzen et al., 2020b; Roberts et al., 2020; Janzen, 2022). In tropical eastern Africa, stable carbon isotope analysis of herd animals has mainly been used to distinguish between browsing and grazing animals, with C_3 plants dominating tropical forest and shrubland areas and C_4 plants dominating in open settings (Ambrose and DeNiro, 1986a; 1989). Stable nitrogen isotope

values can provide insights into caprine habitats, with lower values associated with closed forests and high rainfall areas and high values associated with open/dry habitats (Ambrose and DeNiro, 1986a; 1989). Simultaneously high $\delta^{13}C_{coll}$ and $\delta^{15}N$ can be linked to marine foodstuffs which, while rare in herd animal diets, have been observed in caprine herding contexts elsewhere (Schoeninger and DeNiro, 1984; di Lernia and Tafuri, 2013; Schulting et al., 2017; Blanz et al., 2020). Tooth enamel $\delta^{18}O$ provides insights into local precipitation and hydrological conditions, with higher values linked to greater aridity (Kohn et al., 1996; Buchmann and Ehleringer, 1998; Kohn et al., 1998; Levin et al., 2006; Carter and Bradbury, 2015; Roberts et al., 2020). Finally, strontium isotope values ($^{87}Sr/^{86}Sr$) are indicative of the geological deposits present within a particular region (Bentley, 2006a; Tafuri et al., 2006; Slovak and Paytan, 2011; Janzen et al., 2020b; Stewart et al., 2020).

1.2 – Archaeo-informatics and the late Holocene archaeology of eastern Africa

Notwithstanding its significance in seminal models of human demographic and linguistic expansion, dispersal of food production, and Indian Ocean trade, the Holocene archaeological corpus of eastern Africa remains predominantly unsynthesized and a wellspring of considerable contention (Marshall, 1990; Chami, 1992; Ambrose, 1998; Chami, 1998; Kusimba, 1999; Chami, 2001a; Chami, 2001b; Chami and Chami, 2001; Marshall and Hildebrand, 2002; Chami and Kwekason, 2003; Peregrine and Ember, 2003; Lane, 2004; Sinclair et al., 2006; Chami, 2007; 2009; Pearson et al., 2010; Crowther et al., 2014; Ashley and Grillo, 2015; Crowther et al., 2016a; Crowther et al., 2016b; Prendergast et al., 2016; Crowley et al., 2017; Crowther et al., 2018; Marchant et al., 2018; Wynne-Jones and LaViolette, 2018; Douglass et al., 2019; Godfrey et al.,

2019; Hixon et al., 2021a; Kusimba and Walz, 2021; Chami and Silayo, 2023). Addressing significant archaeological questions, such as whether late Holocene changes in the archaeological record reflect climate-driven migrations of human populations, requires compiling existing data on past human-environment interactions (Courtney Mustaphi and Marchant, 2016; Marchant et al., 2018; Courtney Mustaphi et al., 2019; Kay et al., 2019; Goldstein et al., 2022a). At present, a significant portion of the archaeological data from sites in eastern Africa is disseminated across a variety of publications that vary in terms of accessibility. This distribution hinders the types of analyses that are currently being employed in other regions and that have the potential to illuminate pivotal research inquiries and debates (Djindjian; Kintigh, 2006; Oslisly et al., 2013; Russell et al., 2014; Chaput et al., 2015; Gattiglia, 2015; Kay et al., 2019; Loftus et al., 2019; Huggett, 2020; VanValkenburgh and Dufton, 2020; Bird et al., 2021; Seidensticker et al., 2021; Bird et al., 2022; Koile et al., 2022). Archaeological data concerning the mid-to-late Holocene in eastern Africa has seen significant growth since the early 20th century (Leakey, 1943; Odner, 1972; Gramly, 1975; Clark and Brandt, 1984; Lane, 2004; Pearson et al., 2010; Giblin and Fuller, 2011; Lane, 2011; Helm et al., 2012; Lane, 2013b; Mitchell and Lane, 2013; Skoglund et al., 2017; Crowther et al., 2018; Prendergast et al., 2019b; Wang et al., 2020; Culley et al., 2021a; Culley et al., 2021b; Robertshaw, 2021). Nevertheless, the existing documentation has yet to be consolidated into a standardized archaeo-informatic-oriented dataset format.

1.3 – Isotopic and archaeo-informatic perspectives in ancient coastal archaeology of eastern Africa

In this thesis, I use multi-isotopic and archaeo-informatic approaches to study patterns of continuity and change in ecological settings and complex subsistence adaptive strategies, including foraging, caprine herding and agropastoralism, within the context of migration and indigenous continuity in a coastal, forest-dominated eastern African environment. I address three main research areas and hypotheses presented in three case studies using a multi-proxy approach led by primary multiple isotope data (carbon, nitrogen, oxygen, and strontium) from coastal sites, as well as an informatics-oriented dataset of scientific dates and associated archaeological assemblages from across eastern Africa. This approach aims to provide a comprehensive understanding of the late Holocene archaeological record of eastern Africa by offering both a worm's-eye and a bird's-eye view. Note: I use uncalibrated years before present (BP) and uncalibrated BCE/CE throughout the thesis.

The first case study is entitled "*Late Pleistocene to Late Holocene Paleoecology and Human Foraging at Kuumbi Cave, Unguja Island*." This case study is published in the journal *Frontiers in Environmental Archaeology* (Iminjili et al., 2023). Using faunal and human enamel $\delta^{13}C$ and $\delta^{18}O$ values from KC, I test the stability of coastal forests and the persistence of foragers after the introduction of food production to the coastal strip and offshore islands of eastern Africa during the Iron Age. KC is a multi-stratified site with deposits dating from the late Pleistocene to the late Holocene. Sampling wild fauna and humans from four stratified deposits spanning the late Pleistocene and late Holocene time periods allows me to characterize coastal forest dynamics and human foraging across global dry and wet climatic periods. These results are then compared to published faunal and human enamel $\delta^{13}C$ and $\delta^{18}O$ values from PYS, a multi-stratified site in the

coastal strip of eastern Africa with deposits spanning the late Pleistocene to the late Holocene. Lastly, I compare the $\delta^{13}C$ and $\delta^{18}O$ values from the coastal sites (KC and PYS) with published values from late Pleistocene and late Holocene sites in the interior of eastern Africa. The use of this comparative methodology facilitates testing the hypothesis that:

1. *The stability of forests along the coastal strip and on offshore islands in eastern Africa may have played a significant role in the endurance of indigenous foraging communities at Kuumbi Cave when interacting with immigrating agropastoral groups during the Iron Age.*

The second case study is entitled "*Isotopic Insights into Iron Age Caprine Management at the Indian Ocean Trading Port of Unguja Ukuu, Zanzibar*." Using a multi-isotopic approach that includes collagen carbon and nitrogen, as well as enamel carbon, oxygen, and strontium isotope data, I test for differences in caprine and wild animal herding strategies, as well as human dietary and mobility patterns, during the Iron Age in the coastal region. I used primary data from the Unguja Ukuu (UU), Fukuchani (FK), and Panga ya Saidi (PYS) sites. I compare UU collagen $\delta^{13}C$ and $\delta^{15}N$ and enamel $\delta^{13}C$ and $\delta^{18}O$ values from caprines, wild animals, and humans to differentiate their herding strategies and dietary patterns. I also analyze $^{87}Sr/^{86}Sr$ and $\delta^{18}O$ values from caprines and humans to investigate mobility patterns in the UU and PYS datasets. I also conduct an inter-site comparison analysis on caprine and wild animal collagen $\delta^{13}C$ and $\delta^{15}N$ values from UU, FK, PYS, and Enkapune Ya Muto (EYM). Finally, I conducted a comparative analysis of the $\delta^{13}C$ and $\delta^{18}O$ values of caprine enamel from UU and four Pastoral Neolithic and Pastoral Iron Age sites (two from each period) in eastern Africa, in order to test for regional, spatial and temporal

differences in herding strategies. The use of this multi-isotope approach enables testing of the hypothesis that:

2. *The Unguja Ukuu forest and marine ecosystem, along with its archaeological assemblage, portrays a complex caprine herding strategy intertwined with an economic livelihood that originates from the forested coastal region of eastern Africa. This coastal herding strategy differs greatly from those in the predominantly arid interior of eastern Africa.*

Finally, the third case study is entitled "*Wanyika: A dataset of scientific dates from archaeological sites in eastern Africa that spans from approximately 5000 BCE to 1800 CE*." This case study is published in the journal Nature *Scientific Data* (Iminjili et al., 2025a; Iminjili et al., 2025b). I synthesized scientific dates and associated archaeological finds from sites in eastern Africa dating from 5000 BCE to 1800 CE, creating an archaeo-informatics-oriented dataset. I then used maps generated from this dataset to highlight the basic spatio-temporal dispersal patterns of food production and food-producing communities and major research gaps limiting in-depth hypothesis testing in eastern Africa. More than 500 scientific publications were consulted as data sources. The dataset covers sites in Kenya, Tanzania, the Comoros Islands, and Madagascar, and selected sites in Rwanda. It provides details on scientific dates and associated crop, faunal, iron, and ceramic finds. The scientific dates were calibrated to calendar years and subjected to four chronometric quality control criteria, which graded them into four classes (Classes A–D). Class A is the most secure and reliable, while Class D is the least. This archaeo-informatics-oriented dataset is used to generate maps that facilitate testing the hypothesis that:

3. *Taking an archaeo-informatics approach to the archaeological record of eastern Africa from 5000 BCE to 1800 CE provides broad and in-depth diachronic insights into human–environment interactions. These insights include connections between the ecology and the complex subsistence strategies employed by coastal and inland communities. This perspective should also reveal significant research gaps and biases that hinder rigorous hypothesis testing.*

1.4 – Thesis structure

This thesis is divided into nine chapters. Chapter two provides a review of the major hypotheses on food production and human-environment interactions in eastern Africa, divided into three phases: thesis, antithesis, and synthesis. The first section of the chapter provides an overview of the historical development of theory in the archaeology of food production in eastern Africa. The second section is about the thesis phase, which emphasizes monolithic migration hypotheses. The third section is about the antithesis phase, which includes the indigenous continuity, mosaic interactions, and subsistence mosaics hypotheses, among others. The fourth section is based on the synthesis phase and focuses mainly on the late-split riverine and late-split savannah peeling-off hypotheses from central Africa. Sections five and six cover scientific advancements in late Holocene archaeology in eastern Africa and the inadequacies of the archaeological record from the region's coasts and islands in hypothesis testing. Ultimately, section seven narrows in on the three case studies that comprise this Ph.D. thesis.

Chapter three evaluates records of climatic and environmental changes in eastern Africa over the past 20,000 years BP and highlights recently published, high-resolution marine records on

mangrove dynamics and tidal inundation in the coastal region. It provides a broad overview of climatic and ecological changes in eastern Africa over the past 20,000 years, as recorded in lake sediments and sand dunes, and their impact on human behavior. The chapter culminates in a discourse on high-resolution environmental records obtained from marine sedimentary cores extracted at four pivotal coastal locations. These records offer perspicacity into the dynamics of mangroves and tidal inundation in the coastal strip and on Unguja Island in eastern Africa during the preceding 20,000 years. The final section of the chapter summarizes the limited isotope ecology studies in eastern Africa, highlighting the absence of such studies on offshore islands, and exploring what isotope ecology and archaeo-informatic studies could reveal about the coastal region.

Chapter four provides a review of the methodological background of isotopes and archaeo-informatic perspectives. The first section summarizes the fundamental principles of isotope ecology and the four isotopes examined in this thesis: carbon, nitrogen, oxygen, and strontium. The second section discusses the composition of these isotopes in the biosphere. The third section discusses the application of $\delta^{13}C$ and $\delta^{18}O$ values in paleoecological studies and multi-isotope approaches to herd management in eastern Africa and beyond. This is followed by a review of the dispersal of caprines in coastal eastern Africa and the available archaeological record. The primary sites used in this study (UU, FK, and PYS) are also described. Next, in section four, there is an overview of archaeo-informatics in archaeology at the global and regional scales, followed by a discussion of its applicability in eastern Africa. The final section of this chapter provides an overview of limitations in isotopic and archaeo-informatic perspectives.

Chapter five outlines the materials and methods employed in the first case study of Kuumbi Cave, alongside the isotope results. The materials and methods section provides background information

on zooarchaeology and isotope analysis, as well as sampling procedures, laboratory analysis standards, and statistical analysis methods. The results section presents the faunal $\delta^{13}C$ and $\delta^{18}O$ values, followed by the variation in taxa and dietary groups and the variation over time. Finally, the human values are presented. The final part of this section presents the results of the comparative study between KC and mainland eastern African sites.

Chapter six summarizes the materials and methods used in the second case study on Unguja Ukuu, alongside the results. The materials and methods section begins with an overview of caprines and the archaeological assemblage from the UU, FK, and PYS sites. This is followed by presentations on the stable isotope laboratory preparation and analysis procedures, as well as the statistical analysis. The results section presents UU collagen $\delta^{13}C$ and $\delta^{15}N$, and enamel $\delta^{13}C$ and $\delta^{18}O$ and $^{87}Sr/^{86}Sr$ analyses. First, a summary of the results on indicators of preservation in bone collagen is presented. Next are the results on variation in taxa, beginning with collagen $\delta^{13}C$ and $\delta^{15}N$, and enamel $\delta^{13}C$ and $\delta^{18}O$ and $^{87}Sr/^{86}Sr$. Lastly, the results of the inter-site comparison between data from coastal and interior eastern African sites, based on collagen and enamel values from caprines, wild animals, and humans, are presented.

Chapter seven outlines the methods and results of the third case study, which is based on the *Wanyika* dataset. The methodology section describes the sampling strategy, data collection and deposition, scientific data and calibration, and quality control. The results section provides a description of the *Wanyika* dataset. It begins with a description of the data records, including the total number of scientific dates, data categories, and column organization. It also defines the column fields. Lastly, it describes the technical validation procedures, usage notes, and code availability.

Chapter eight presents major insights into complex subsistence adaptive strategies, emergence and dispersal of food production and food-producing communities in the coastal strip and offshore islands of eastern Africa, as revealed by multi-isotopic and archaeo-informatic perspectives. The first section discusses the isotopic findings of the first case study, which is based on data from KC in Zanzibar. The second section focuses on isotopic insights from the second case study, which is based on data from UU in Zanzibar. The third section discusses archaeo-informatic insights from the third case study, which is based on data from across eastern Africa. Section four provides an overview of the enigmatic 'Bantu package' dilemma in late Holocene archaeology in eastern Africa. Section five concludes the chapter by summarizing insights from multi-isotopic and archaeo-informatic analyses, highlighting the complementarity of the two perspectives.

Chapter nine concludes the thesis by synthesizing the results of the isotope and archaeo-informatics case studies, which tested the overarching hypotheses on the emergence of complex subsistence strategies and the dispersal of food production and food-producing communities in eastern Africa. The first section of this chapter presents a synthesis of the results testing the hypotheses set out in each of the three case studies. These include results on the hypothesis of the role of coastal forest stability and the persistence of foragers after the introduction of food production at KC. Next are the results on the hypothesis of the farmland caprine herding strategy and agropastoralism at UU. Finally, the results on the hypothesis of the emergence and dispersal of food production and food-producing communities in coastal and interior eastern Africa based on the archaeo-informatic oriented dataset are presented, along with the major research gaps.

Chapter 2 – The migration and indigenous continuity hypotheses of late Holocene socioeconomic change in eastern Africa

This chapter reviews the major hypotheses concerning the emergence and dispersal of food production, food-producing communities, and the associated complex adaptive strategies in eastern Africa, and it provides supporting archaeological evidence. It also provides a critique of these hypotheses. The chapter is divided into six sections. The first section provides a brief history of theory in the archaeology of food production in eastern Africa. This history is divided into three phases: the thesis, antithesis, and synthesis. The second section focuses on the thesis phase. This section reviews the monolithic migration hypotheses in eastern African archaeology. These include the Cushitic- and Nilotic-speaking pastoralist migration hypothesis, which has been further expanded by the 'trickle-and-splash' hypothesis and the Bantu expansion hypotheses (western African agropastoralists). The cultural-historical archaeological theoretical framework is also covered. Archaeological evidence supporting the migration hypotheses is provided, and a critique of these hypotheses is presented at the end of the section. The third section presents the antithesis phase, covering indigenous continuity, forager immediate and delayed return, moving frontier, and mosaic interactions and subsistence mosaics. This section also covers the archaeological evidence supporting these hypotheses. Lastly, a critique of the antithesis hypotheses is provided. The fourth section covers the synthesis phase, presenting the late-split riverine and late-split savannah peeling-off hypotheses from central Africa. The spread-over-spread hypothesis is discussed here, followed by hypotheses concerning the environmental impact of the Bantu expansion. This is followed by the fifth section, which covers archaeological science in late Holocene archaeology in coastal and inland eastern Africa. The sixth section addresses the inadequacies of the archaeological record

from coastal and island eastern Africa in hypothesis testing. Finally, the seventh section presents the three case studies on which this PhD thesis is based, relating them to the broader framework.

2.1 – History of theory in the archaeology of food production in eastern Africa

Due to the limited scholarly attention, theoretical frameworks in the late Holocene archaeology of eastern Africa and Africa have often echoed ongoing global archaeological and anthropological debates (Binford, 1962; 1968; Trigger, 1989; Harris, 2001; Erickson and Murphy, 2003; McGee and Warms, 2008). In these discussions, theoretical frameworks are seen as going through three major phases as we gain more knowledge about human-environment interaction (Harris, 2001; Erickson and Murphy, 2003; McGee and Warms, 2008). This includes the thesis phase, which is associated with the normative approach. In this phase, a theory is proposed in a basic manner with limited evidence. The antithesis phase, associated with the idiographic approach, follows. A critique of the thesis is made, and new theoretical frameworks are proposed. Lastly, a synthesis phase associated with integrating the thesis and antithesis hypotheses emerges. In this thesis, I view the archaeology of eastern Africa as following these phases, with it currently being at the synthesis phase. This thesis presents an integrated approach of the thesis and antithesis phases in the archaeology of the coastal and interior eastern Africa. The thesis phase is represented by the grand migration hypotheses formulated in the 1960s to '90s (Greenberg, 1963; Ehret and Posnansky, 1968; Ehret, 1974; Ambrose, 1982; Ehret and Posnansky, 1982; Bower, 1991; Vansina, 1995; Ambrose, 1998; Ehret, 1998; 2001). These include the Cushitic-speaking and Nilotic-speaking migration hypotheses that postulated that these communities migrated from the northeastern region into the interior of eastern Africa (Ehret, 1974; Bower, 1991). Additionally, the thesis phase also

includes the rapid Bantu expansion hypotheses that postulated that the Bantu-speaking populations migrated from western Africa to eastern Africa in a single massive migration wave through either the northern Congo forest-savannah corridor or the southern Congo forest-savannah corridor (Oliver, 1966; Ehret and Posnansky, 1982; Vansina, 1995; Ehret, 1998; 2001; 2002). These hypotheses were mainly formulated based on historical linguistics, oral history, and ethnography. Archaeology was patchy across the region and contributed less to the development of these hypotheses. The later part of the thesis phase included building the archaeological evidence and organizing the assemblages into scientific categories (Bower and Nelson, 1978; Ambrose, 1982; Nelson and Kimengich, 1984; Clist, 1987b; Bower, 1991; Van Grunderbeek, 1992; Stewart, 1993; Ambrose, 1998; 2003; Lane, 2013a; Ashley and Grillo, 2015). Material culture remains, including ceramics, were organized based on function and associated with modern cultural communities that share similar material culture. Ceramics became the *fossile directouer* in defining the major cultural groups and was used to reinforce the migration hypothesis (Ambrose, 1984b; 1998; 2003; Pakendorf et al., 2011).

The antithesis stage is marked by a shift from the grand regional perspective of migrations to focusing on the interactions between foragers and immigrating food producers within the eastern African region (Ambrose, 1998; Lane, 2004; Kusimba and Kusimba, 2005; Dale, 2007; Prendergast, 2009; Prendergast, 2011; Lane, 2013a; b; Crowther et al., 2018). This antithesis phase can be seen in the critique of the monolithic migration hypotheses in the archaeology of eastern Africa (Chami, 2001b; Chami and Chami, 2001; Kusimba and Kusimba, 2005; Crowther et al., 2018; Chami and Silayo, 2023). This is marked by the rise of two branches in explaining the archaeology of eastern Africa – normatively oriented and idiographically oriented perspectives (Lane, 2004; Kusimba and Kusimba, 2005; Dale, 2007; Dale and Ashley, 2010; Lane, 2013a;

Crowther et al., 2018; Chami and Silayo, 2023). The normative approach mainly took a specific focus on eastern Africa. This is represented by the indigenous continuity, moving frontier, and the foragers' immediate and delayed return hypotheses (Chami, 2001b; Lane, 2004; Dale, 2007; Lane et al., 2007; Dale and Ashley, 2010; Chami and Silayo, 2023). The indigenous continuity hypothesis provides a diametrically different perspective of the dispersal of food production in eastern Africa (Chami, 2001b; Chami and Kwekason, 2003; Chami, 2007; Chami and Silayo, 2023). Instead of migrations, it postulates independent invention by indigenous foragers as the main force in the dispersal of food production and food-producing communities in eastern Africa. The moving frontier hypothesis is more focused on specifics of the interactions between foragers and food producers (Lane, 2004). The immediate and delayed return foragers hypothesis also provides specifics on how foragers interact with food producers (Dale et al., 2004; Dale, 2007).

The idiographic perspective of the archaeology of eastern Africa is represented by the mosaic interactions and subsistence mosaic interaction hypotheses (Kusimba and Kusimba, 2005; Crowther et al., 2018). These hypotheses have critiqued the monolithic migration hypotheses as being too general and missing the specifics of human-environment interactions, which are more theoretically intriguing. Currently, I would argue that we are now in the synthesis phase supported by the success in the application of archaeological sciences in the archaeology of eastern Africa and the sub-Saharan Africa region in general (Pakendorf et al., 2011; de Filippo et al., 2012; Russell et al., 2014; Bostoen et al., 2015; Grollemund et al., 2015; Prendergast et al., 2016; Skoglund et al., 2017; Chritz et al., 2019; Godfrey et al., 2019; Prendergast et al., 2019b; Grillo et al., 2020b; Roberts et al., 2020; Culley et al., 2021a; Culley et al., 2021b; Koile et al., 2022; Lipson et al., 2022; Grollemund et al., 2023; Fortes-Lima et al., 2024). Recent multidisciplinary approaches applied in the central African region leading to the revision of the grand migration hypotheses have

inspired the integration of the normative and idiographic approaches in the archaeology of eastern Africa (Pakendorf et al., 2011; de Filippo et al., 2012; Russell et al., 2014; Bostoen et al., 2015; Grollemund et al., 2015; Seidensticker et al., 2021; Koile et al., 2022; Grollemund et al., 2023). The latest publications from the central African region present the Bantu migration as being a multi-wave, gradual process (Russell et al., 2014; Grollemund et al., 2015; Grollemund et al., 2023). These refined approaches are based on multiple datasets from archaeology, aDNA, language, and ethnographic records of the central African region. These datasets have also been synthesized into archaeo-informatics-oriented formats that allow high tech-computer analysis of the datasets.

In this thesis, I take an integrated approach that synthesizes the normative and idiographic approaches in a way that helps unravel novel insights into the complex adaptive subsistence strategies, emergence of food production, and the dispersal of food-producing communities in eastern Africa during the late Holocene. This approach also includes applying multi-isotope and archaeo-informatic perspectives to analyze the archaeological record. I provide a systematic overview of these major hypotheses based on the thesis, antithesis, and synthesis phases below; a critique of these epistemological perspectives and the archaeological datasets used to support them is also provided.

2.2 – The normative approach and monolithic migrations in eastern Africa

The monolithic migration hypotheses

In eastern Africa, the thesis phase of archaeology is primarily dominated by the normative perspective, an anthropological framework that analyzes cultures by focusing on behaviors that are guided by shared cultural norms (Ambrose, 1982; Ehret and Posnansky, 1982; Ambrose, 1984b; Clark and Brandt, 1984; Ambrose, 1998; 2003). Material remains, such as pottery, tools, and structures, are considered expressions of these shared norms (Ambrose, 1982; Ambrose, 1998; 2003). This leads to equating specific material remains with cultural groups. This theoretical framework is represented by monolithic migration hypotheses, including the pastoralist migration hypothesis (Ambrose, 1982; Bower, 1991; Ambrose, 1998; 2003; Lane, 2013a), and the early and late Bantu expansion hypotheses (Ehret and Posnansky, 1982; Ehret, 1998; 2001; 2002). The monolithic migration hypotheses applied in eastern Africa are based on the universal migration theoretical framework (Trigger, 1989; Harris, 2001; Erickson and Murphy, 2003). Tenets of this framework include migration, single-origin independent invention, and demic diffusion. (Figure 2.1) (Adams et al., 1978; Trigger, 1989; Burmeister, 2000; Harris, 2001; Erickson and Murphy, 2003; Trigger, 2006; Bentley and Maschner, 2007; van Dommelen, 2014; Burmeister, 2019; McSparron et al., 2020; Pluckhahn et al., 2020; Anthony, 2023; Högberg et al., 2025). In this context, the term "migration" refers to the movement and settlement of a population in a different area. The single-origin, independent invention principle asserts that only societies in strategic locations possess the ability to create new, sophisticated technologies (Trigger, 1989; Harris, 2001; Erickson and Murphy, 2003; Trigger, 2006). The single-origin diffusion (demic diffusion) tenet holds that only the material culture and biological elements from the single-origin point are

dispersed in all directions (Figure 2.1). This displaces the indigenous cultures and biology. This hypothesis has been used to explain the migration of Cushitic- and Nilotic-speaking pastoralists, as well as Bantu-speaking agropastoralists, from northeastern and western Africa to eastern Africa, and the subsequent displacement and assimilation of indigenous foragers (Ambrose, 1982; Ehret and Posnansky, 1982; Ambrose, 1998; Ehret, 1998; 2001; Ambrose, 2003; Lane, 2004; 2013a; Russell et al., 2014).

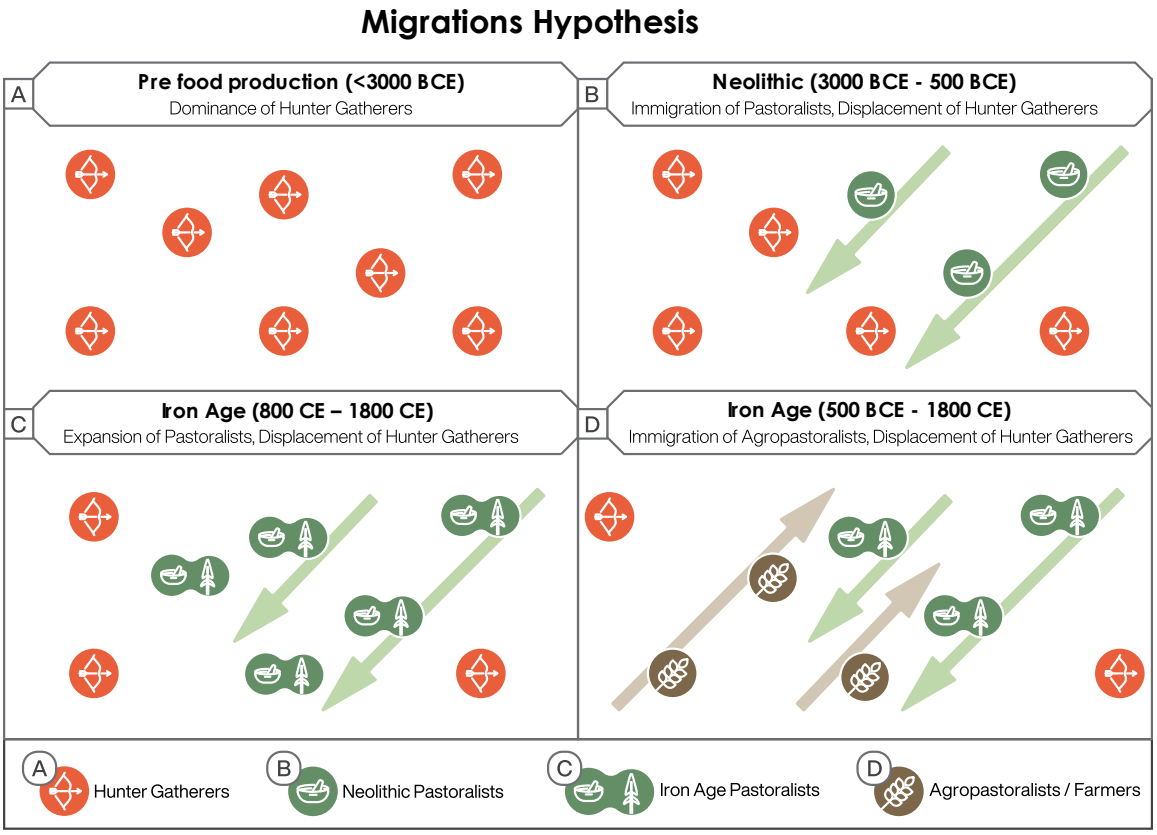


Figure 2.1. *A visual representation of the migration hypothesis in eastern Africa, showing the following: (A) the pre-food production period (before 3000 BCE), when indigenous people relied solely on hunting and gathering; (B) the onset of Neolithic pastoralist immigration (3000-500 BCE), which gradually displaced and replaced foragers; (C) the onset of immigration by iron-using pastoralists (800 CE-1800 CE), which continued to displace the remaining indigenous foragers; and (D) the onset of agropastoralist immigration (500 BCE-1800 CE), which also displaced indigenous foragers. Ultimately, the remaining foragers were marginalized. Note: Independent invention and diffusion are negligible in the migration hypothesis. The figure was created for this study by Hans Sell (Graphic Designer for the Max Planck Institute of Geoanthropology, Jena, Germany).*

Pastoralist migrations and the 'trickle-and-splash' hypothesis

The pastoralist migration hypothesis postulates a series of climate-induced migrations of pastoralists from north-eastern Africa to the interior of eastern Africa between 3000 BCE and 1850 CE, after the end of the African Humid Period (AHP) (Figure 2.2) (Ambrose, 1982; Ambrose, 1984b; Marshall, 1986; Ambrose, 1998; Marshall and Hildebrand, 2002; Ambrose, 2003). These migrations have been correlated with typological distinctions and periodization of archaeological data, which are used to divide the migration process into two periods: the Pastoral Neolithic and the Pastoral Iron Age (Figure 2.2) (Ambrose, 1982; Ehret and Posnansky, 1982; Ambrose, 1984b; 1998; Ehret, 1998; 2002; Ambrose, 2003; Lane, 2013a). The Pastoral Neolithic expansion is hypothesized to have involved two major cultural entities (Ambrose, 1984b; 1998; 2003; Lane, 2013b; a). One is the Savanna Pastoral Neolithic (Ambrose, 2003; Lane, 2013a) linked to Cushitic-speaking people. The other is the Elmenteitan Pastoral Neolithic (Ambrose, 2003; Lane, 2013a), linked to Nilotic-speaking people. Pastoral Iron Age migrations involved the Sirikwa (proto-Nilotic-Kalenjin speakers) and multiple groups associated with modern pastoralist ethnic groups (Figure 2.2) (Sutton, 1965; Chapman, 1966; Sutton, 1973; 1987; 1993b; 1998c). Both Neolithic and Iron Age pastoralists are thought to have dispersed predominantly in open savannah grasslands, avoiding dense forests.

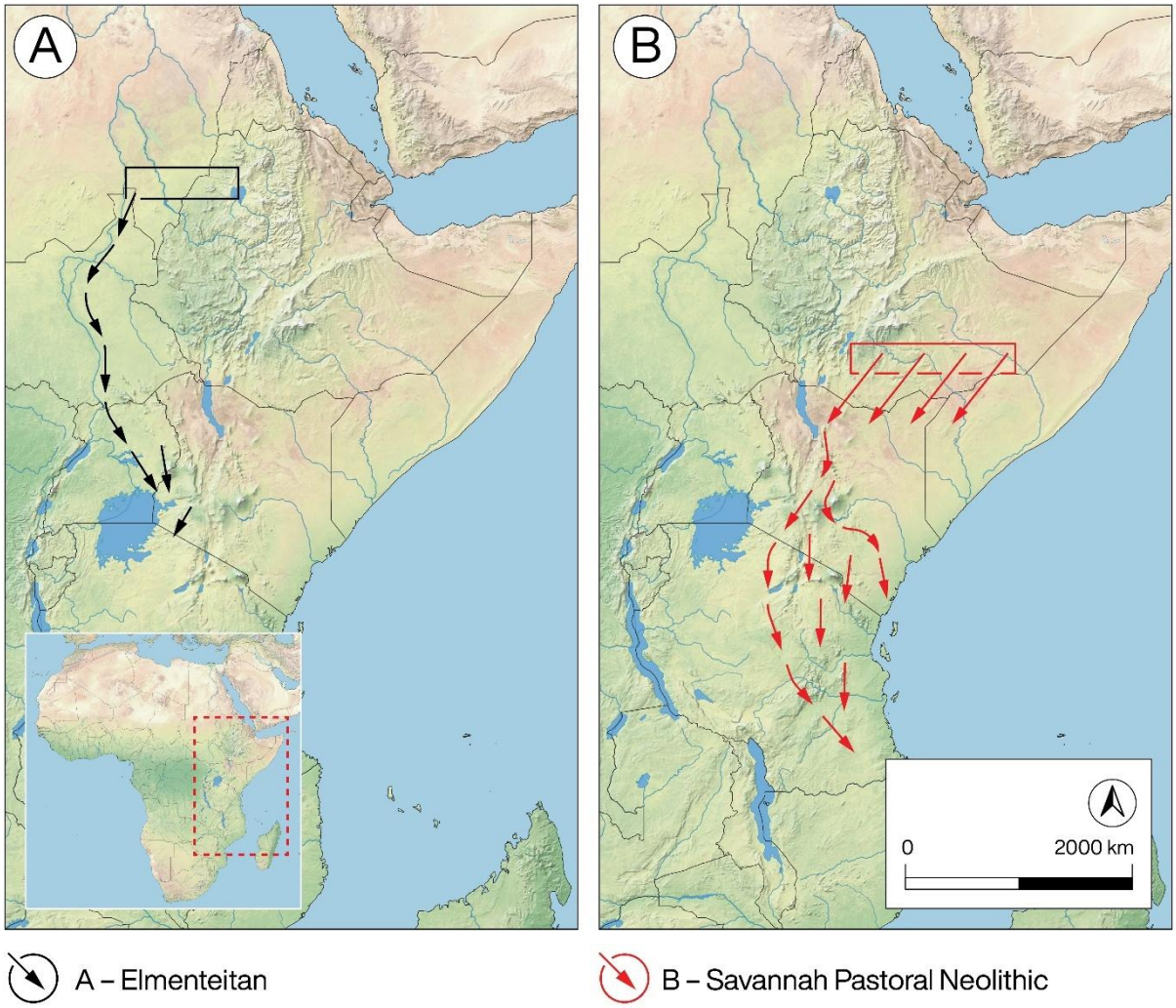


Figure 2.2. *Map of Africa showing hypothesized Neolithic pastoralist migrations into eastern Africa's interior from the Sudan, Ethiopia, and Somalia regions: (A) Elmenteitan Pastoral Neolithic migration from Sudan following the Nile River to the Lake Victoria region, and (B) Savannah Pastoral Neolithic migration from the Ethiopia-Somalia region into the interior of eastern Africa to the southern region of Tanzania. The figure was created for this study by Hans Sell (Graphic Designer for the Max Planck Institute of Geoanthropology, Jena, Germany).*

It has been hypothesized that the spread of pastoral Neolithic cultures occurred in a 'trickle-and-splash' pattern rather than a 'bow wave' (Bower, 1991). This pattern occurred in three stages: the early stage (4000–3000 BP), the evolved stage (3000–1900 BP) and the late stage (1900–1300 BP). The diversity of PN ceramics is said to reflect this pattern (Bower, 1991). In the early stage, small

groups of herders trickled into the interior of eastern Africa from the north, where indigenous foragers acquired domestic livestock and became the region's first pastoralists (Bower, 1991). The presence of domestic animal bones is also noted as being low on these sites. This scenario is characterized by the presence of continuity in lithics with autochthonous pastoral Neolithic ceramic wares, which are represented by a broad diversity of wares, including two well-established ones: Kansyore and Nderit. These two types of pottery may have originated in eastern Africa, as they do not resemble any other known pottery outside the region. In the evolved stage (3000–1900 BP), larger groups than in the early stage migrated from the north (Bower, 1991). Allochthonous ceramics, including Narosura and Elmenteitan types, dominated this period and possibly Maringishu too. The Narosura ware is linked to the ceramic wares from northwestern Ethiopia. A different set of stone tools was also present. Changes in subsistence strategies and settlements are also evident. This includes a greater number of domestic than wild animals, basic nomadism and specialised dairying. There is also evidence of shelter construction and other complex settlement patterns. The late stage (1900–1300 BP) is the least well documented, with only one ceramic tradition: the Akira ware (Bower, 1991). This stage of the PN was characterized by another shift in subsistence practices. While these were dominated by wild fauna and fish, there was no clear cultural discontinuity from the preceding stage. This suggests that immigration may have been minimal, if any. The Pastoral Iron period began at around 1300 BP, following the end of the late Neolithic stage, with evidence of iron and livestock emerging at Deloraine in the central Rift Valley. However, no follow-up studies have been conducted to test this hypothesis.

One group of archaeologists has hypothesized that, due to extreme arid conditions during migration periods, these pastoralists practiced limited crop farming (Marshall and Hildebrand, 2002) (the ‘cattle before crops’ hypothesis), while another group of scholars (historical linguists and

ethnographers) has hypothesized that these pastoralists could have practiced crop farming and dispersed it into the interior of eastern Africa as early as the Neolithic period (Ehret and Posnansky, 1968; Ehret and Posnansky, 1982; Ehret, 1998; 2002). Although pastoralists from north-eastern Africa likely pioneered the spread of domesticated crops to the interior of eastern Africa, there is currently no concrete archaeological evidence to support this claim (Phillipson, 1984; Sutton, 1998c; Ambrose, 2003; Bostoen, 2018; Grollemund et al., 2023). Recent studies indicate that a wetter ecological setting existed in the Turkana Basin during Neolithic times (Chritz et al., 2019; Chritz and Kinyanjui, 2025; Kinyanjui et al., 2026). Other studies also show that sorghum, pearl millet, finger millet, cowpea, and lablab beans were circulating in the Upper Nile region of Sudan and Ethiopia and spread across the Sahara and the Red Sea to India as early as 1000 BCE (Fuller, 2003; Arthur et al., 2019; Fuller et al., 2019; Barron et al., 2020b; Fuller et al., 2021). In addition, modern Dassanetch pastoralists inhabiting the Ileret region of Lake Turkana are known to source sorghum, coffee, and livestock from the Omo Delta region in Ethiopia (Kiura, 2005; Kiura, 2008a). Long-distance obsidian trade networks (Ndiema, 2011; Ndiema et al., 2011) that could have also included cereals are also known to have existed in the Turkana Basin during the late Holocene. These observations suggest that pastoralists may have dispersed crops in eastern Africa from as early as the Neolithic, though direct evidence remains elusive to archaeologists.

Early-split and the late-split Bantu expansion hypotheses

Discussions relating to the expansion of Bantu-speaking agropastoralists from their homeland in western Africa (Nigeria and Cameroon) to eastern Africa have been shaped by two major opposing hypotheses: the early-split hypothesis and the late-split hypothesis (Figure 2.3) (Ehret and

Posnansky, 1982; Vansina, 1995; Ehret, 1998; 2001; Pakendorf et al., 2011; de Maret, 2013; Koile et al., 2022; Grollemund et al., 2023; de Maret, 2025). Based on the less challenging physical terrain, which is characterized by fewer rivers and an extensive west-east woodland-forest corridor, as well as the ongoing circulation of African domesticated crops across the Sahelian region, the early-split Bantu expansion hypothesis provides the most logical migration route for the Bantu-speaking agropastoralists (Fuller, 2003; Fuller and Stevens, 2018; Winchell et al., 2018; Barron et al., 2020b). This would have enabled them to pioneer the quick and easy dispersal of the five major African crops and additional livestock to the interior of eastern Africa, the coast and the islands. This assumes that Nilotic and Cushitic pastoralists were not involved in dispersing these crops. However, most historical linguists now feel that the early-split hypothesis is not supported by the available data (Vansina, 1995; Russell et al., 2014; Grollemund et al., 2023). This also includes a lack of archaeological evidence. Although the Congo Basin terrain is highly challenging due to its multiple large rivers and dense forest cover, which makes migration difficult, the late-split hypothesis is favoured by scholars because there is reasonable linguistic, archaeological and genetic evidence to support it (Vansina, 1995; Ehret, 2001; 2002; Pakendorf et al., 2011; de Filippo et al., 2012; Bostoen, 2018; Koile et al., 2022; Coutros et al., 2024; Fortes-Lima et al., 2024; Bostoen and Coutros, 2025).

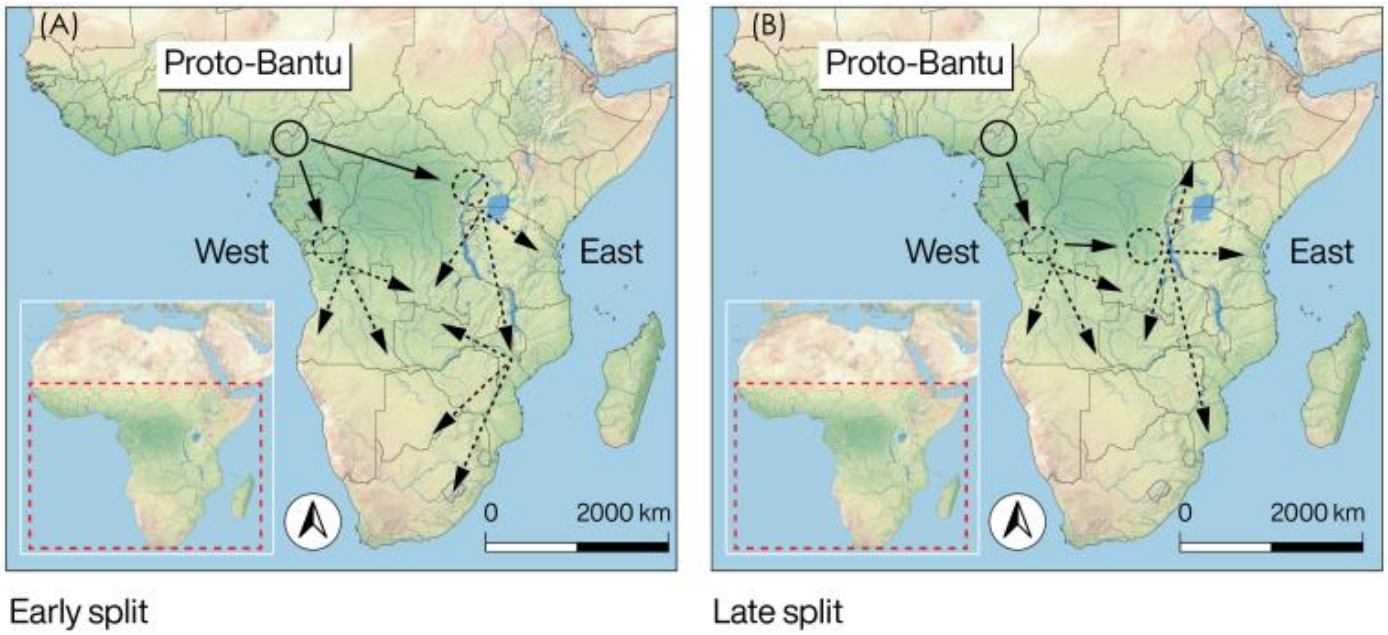


Figure 2.3. *Map of Africa highlighting the two hypotheses of western African agropastoralist migration: (A) the early-split, and (B) the late-split. Note the solid arrows representing rapid migration from western to eastern Africa. The figure was created for this study by Hans Sell (Graphic Designer for the Max Planck Institute of Geoanthropology, Jena, Germany).*

It is hypothesized that Bantu-speaking agropastoralist communities migrated from their original homeland around the Nigeria-Cameroon border to eastern and southern Africa from around 3000 BCE (Figure 2.3) (Vansina, 1995; Ehret, 1998; 2001; Pakendorf et al., 2011). They dispersed through regions south of the Sahara, reaching eastern and southern Africa, as well as the islands, in two major waves: the eastern and western waves. One group of scholars has postulated that the eastern and western waves split in the Bantu homeland region of Nigeria and Cameroon (Vansina, 1995; Ehret, 1998; 2001; Pakendorf et al., 2011). This is called the "early-split" or "deep-split" Bantu expansion hypothesis. Another group of scholars has postulated that the Bantu expansion began as a single wave that moved southwest from Cameroon towards Congo-Kinshasa. The eastern wave is thought to have split around the Congo River and followed the savannah

woodlands-forest margin to the Great Lakes region of eastern Africa (Pakendorf et al., 2011; Koile et al., 2022). This is called the "late-split" Bantu expansion hypothesis.

According to the early-split hypothesis, following the initial branching, Bantu speakers dispersed along the northern margins of the shrinking Congo Forest. They ultimately reached the Nile River in northern Uganda and Sudan, where they encountered Nilotic agropastoralists (Pakendorf et al., 2011; Whiteley et al., 2019). These Bantu-speaking agropastoralists migrated with their livestock, including cattle, goats and sheep, as well as western African domesticated crops such as pearl millet and cowpeas. They may also have adopted sorghum, finger millet and lablab beans from Nilotic pastoralists. They brought these crops with them as they migrated southward along the Nile River to the Lake Victoria region. Some scholars have suggested that the Bantu agropastoralists adopted iron technology from Nilotic speakers (Grollemund et al., 2015; Grollemund et al., 2023; Bostoen and Coutros, 2025). According to the early-split hypothesis, Bantu-speaking agropastoralists dispersed domesticated crops, such as pearl millet, sorghum, finger millet, cowpeas, and lablab beans, as well as iron technology and Urewe-related ceramic wares, from the Great Lakes region to southern Africa, including the interior, coastal regions, and islands (Ehret and Posnansky, 1982; Ehret, 1998; 2001; Bostoen and Coutros, 2025). The early-split hypothesis was primarily supported by language classification studies and limited archaeological work. These days, however, it is not so widely accepted (Russell et al., 2014; Bostoen, 2018).

The late-split Bantu expansion hypothesis posits that the Bantu expansion originated as a single wave that traveled southwest from the Nigeria-Cameroon homeland along the Atlantic Ocean coast (Vansina, 1995; Pakendorf et al., 2011; Currie et al., 2013). It is theorized that the Bantu speakers followed the savannah-woodland forest margin ecotone, which expanded due to an increase in

global aridity. After migrating southwest to the Congo-Kinshasa region, the eastern Bantu wave emerged from the western Bantu wave. The eastern wave is believed to have followed the savannah woodland ecotone along the southern edge of the Congo Forest to the Great Lakes region of eastern Africa, around Lake Tanganyika (Vansina, 1995; Ehret, 2001; Pakendorf et al., 2011). The eastern wave then split, with one group heading north to the Lake Victoria region and another group heading east and southeast to the eastern African coast, southern Africa, and the islands. It is hypothesized that this wave immigrated to eastern Africa with only livestock, pearl millet, and cowpeas, and that the immigrants adopted Urewe ceramics, iron technology, sorghum, finger millet, and lablab beans from the Nilotic and Cushitic-speaking pastoralists along the Nile and the Great Lakes region of eastern Africa (Vansina, 1995; Ehret, 2001; Pakendorf et al., 2011).

Cultural-historical archaeology

The cultural-historical archaeological theoretical framework is normative and serves as the foundation for explaining the diachronic distribution of late Holocene archaeological assemblages in eastern Africa (Ambrose, 1982; Ambrose, 1998; Harris, 2001; Ambrose, 2003; Erickson and Murphy, 2003; Trigger, 2006; Trigger, 2007). This theoretical perspective classifies material culture assemblages into distinct, diachronically defined cultural groups (Figure 2.4). This theoretical perspective has been used to define the resident communities and immigrants in eastern Africa during the late Holocene of eastern Africa (Ambrose, 1998; Lane, 2004). The four major cultural groups that inhabited eastern Africa from the late Holocene era (beginning 5,000 years before present) are defined by their archaeological assemblages (Ambrose, 1982; Ambrose, 1984b; a; Clark and Brandt, 1984; Ambrose, 1997; Ambrose, 1998; 2003; Lane, 2004; Dale, 2007; Prendergast, 2010a; 2011; Lane, 2013a; Prendergast et al., 2014). The groups include foragers

(hunter-gatherers and fishers), Cushitic- and Nilotic-speaking pastoralists, and Bantu-speaking agropastoralists (farmers) (Figure 2.4) (Ambrose, 1998; 2003; Lane, 2004; Lane et al., 2006; Lane et al., 2007; Prendergast, 2009; 2010b; Prendergast, 2011; Lane, 2013a).



Figure 2.4. *Visual representation depicting the differences in recovered artifacts from different sites representing the following subsistence strategies: (A) Foragers (hunter-gatherers) with Kansyore ceramic ware featuring punctate decorations, stone tools, and a high concentration of wild animal remains; (B) Neolithic pastoralists with elongated Nderit ceramic ware, stone bowls and platters, and tools, as well as a high concentration of livestock remains; (C) Iron Age pastoralists with iron weapons, elongated Lanet ware ceramics, and a high concentration of livestock remains; (D) Agropastoralists/farmers with iron weapons, Urewe ceramic ware featuring wavy triangular decorations, and a mixture of livestock and farmland crops. The figure was created for this study by Hans Sell (Graphic Designer for the Max Planck Institute of Geoanthropology, Jena, Germany).*

In general, the presence of wild animals and/or marine resources, stone tools, and Kansyore ceramics at an archaeological site indicates foraging, whereas the presence of livestock, Nderit and Elmenteitan ceramics (plus stone tools and platters), and Lanet ceramics (plus iron weapons) suggests pastoralism (Ambrose, 1998; 2003; Lane, 2004; 2013a). Pastoral sites are characterized by a high concentration of assemblages, which typically indicates large, interdependent communities of more than ten families living together (Figure 2.4). The presence of a combination of livestock, African crops, Urewe-related ceramics, and iron production and use suggests agropastoralism, or farming. Agropastoral sites are characterized by a low concentration of assemblages, indicating small, independent communities of fewer than five families. The presence of a mix of domestic animals, crops, wild and marine animals, and several types of ceramics suggests there is greater complexity underlying these assumptions.

More than twenty-four spatio-temporally distributed ceramic traditions have been used to define the cultural groups in eastern Africa (Soper, 1967b; a; Soper, 1969; Soper, 1976; Collett and Robertshaw, 1980; Ambrose, 1982; Collett and Robertshaw, 1983; Robertshaw, 1990b; Sinclair, 1991; Robertshaw, 1994; Ambrose, 1998; 2003; Pearson et al., 2010). Three major ceramic traditions are associated with foragers: the Lowasera and Eburran, which are distributed in the northern and central Rift Valley; and the Kansyore ceramic tradition, which is mainly distributed around Lake Victoria, the Rift Valley, and other regions of eastern Africa's interior, all the way to South Africa (Munene, 2002; Kusimba and Sibel, 2004; Dale and Ashley, 2010). The Cushitic-speaking pastoralists are linked to the Savanna Pastoral Neolithic ceramic tradition. This tradition is made up of four major spatiotemporal wares: the Nderit and Ileret, Maringishu, Narosura, and Akira (Ambrose, 1998; Munene, 2002; Ambrose, 2003; Lane, 2013a; Grillo et al., 2022). These wares are found between Lake Turkana and the Great Lakes region. They also extend to the interior

of eastern Africa, reaching as far as Lake Eyasi and southern Tanzania. The Elmenteitan ceramic tradition, which is distributed between the Lake Victoria region and parts of the central, western, and eastern Rift Valley highlands, is associated with Nilotic-speaking pastoralists (Lynch and Robbins, 1979; Ambrose, 1998; 2003; Peregrine and Ember, 2003; Lane, 2013a). The Pastoral Iron Age comprises five major ceramic traditions: Turkwell, Lanet, Kisima, and Oldorotua (Ambrose, 2003; Lane, 2013a; Petek-Sargeant, 2025).

A series of more than ten spatiotemporal ceramic traditions are associated with Bantu-speaking farmers (Odner, 1971c; b; a; Chami, 1992; Stewart, 1993; Chami, 1994; Horton, 1996; Chami, 1999; Helm, 2000; Chami, 2003b; Kwekason, 2007; Ashley, 2010; Pearson et al., 2010; Horton, 2017; Crowther et al., 2018; Horton et al., 2022). These include Urewe, Kwale, Maore, Lelesu, Kilimanjaro, Tana (including the triangular incised ware (TIW), Rezoky, Beropitika, Andaro, and Tranovato (Soper, 1967b; Soper, 1969; Odner, 1971c; b; Soper, 1971; 1976; Clist, 1987a; Van Grunderbeek, 1988; Sinclair, 1991; Chami, 1992; Chami, 1994; Chami and Msemwa, 1997a; Lane et al., 2006; Pearson et al., 2010; Giblin and Fuller, 2011; Ashley and Grillo, 2015). These traditions are systematically distributed from the Great Lakes region, the western and eastern Rift Valley highlands, the coastal strip, and offshore islands all the way to Madagascar and southern Africa (Soper, 1967b; a; Soper, 1969; Huffman, 1970; Odner, 1971c; b; Soper, 1976; 1979; Collett and Robertshaw, 1980; Huffman and Vogel, 1991; Sinclair, 1991; Huffman and Herbert, 1994; Robertshaw, 1994; Pearson et al., 2010). The diachronic distribution of these ceramics and their associated assemblages were used to validate migration hypotheses in eastern Africa developed based on oral histories, linguistics, historical records, and ethnography (Ehret and Posnansky, 1968; Ambrose, 1982; Ambrose, 1984b; Ehret, 1997; Ambrose, 1998; Ehret, 1998; 2000; Chami, 2001a; Chami, 2001b; Chami and Chami, 2001; Ehret, 2001; Ambrose, 2003; Chami and Kwekason, 2003;

Lane, 2004; Kusimba and Kusimba, 2005; Chami, 2007; 2009; Lane, 2013a; Chami and Silayo, 2023).

Archaeological evidence in support of the migration hypotheses

The archaeological record suggests that Nilotic and Cushitic-speaking pastoralists largely pioneered the dispersal of livestock in the interior of eastern Africa, while Bantu-speaking agropastoralists largely pioneered the dispersal of African crops from the interior to the coast and islands (Marshall, 1990; Ambrose, 1998; Marshall and Hildebrand, 2002; Ambrose, 2003; Lane, 2004; 2013a; Russell et al., 2014). Earlier than 3000 BCE, sites in eastern Africa were occupied by foragers and contain only wild fauna and plants, as well as the Kansyore-Eburran-Lowasera ceramic tradition (Munene, 2002; Kusimba and Sibel, 2004; Dale and Ashley, 2010). The earliest evidence of cattle, goats, and sheep is found in Pastoral Neolithic sites, alongside Nderit and Ileret ceramics from northern Kenyan sites, dating to around 3000 BCE (Barthelme, 1977; Owen et al., 1982; Marshall et al., 1984; Barthelme, 1985; Hildebrand et al., 2011; Hildebrand and Grillo, 2012; Grillo and Hildebrand, 2013; Hildebrand et al., 2018; Sawchuk et al., 2018; Grillo et al., 2022; Sawchuk et al., 2022). This is followed by sites in the central Rift Valley, Lake Victoria, Lukenya, Tsavo, Serengeti, and the Lake Eyasi region, dating to around 2000-1000 BCE (Marean, 1992a; Marean et al., 1994; Ambrose, 1998; Peregrine and Ember, 2003; Wright, 2003; Wright, 2005a; Prendergast et al., 2007; Prendergast, 2010a; 2011; Mitchell and Lane, 2013; Prendergast et al., 2013; Prendergast et al., 2014; Grillo et al., 2018; Grillo et al., 2022). There are different patterns in the distribution of the four major Savannah Pastoral Neolithic and Elmeteitan Neolithic ceramics (Ambrose, 1998; Munene, 2002; Ambrose, 2003; Peregrine and Ember, 2003; Lane, 2013a; Mitchell and Lane, 2013; Grillo et al., 2022). Pastoral Iron Age sites, dating from around 800 CE

to 1800 CE, are defined by the presence of iron, as well as Lanet, Oldorotua, Kisima, and Turkwell ceramics, alongside cattle, goats, and sheep (Ambrose, 1998; 2003; Lane, 2013a). Although nine ceramic traditions have been identified as being associated with the migration of pastoralists, no further attempts have been made to test and develop the 'trickle and splash' hypothesis of pastoralist migration.

Agropastoralism is estimated to have originated from the Great Lakes region, around 500 BCE, but the earliest archaeological evidence at Kakapel dates to 300 BCE and Rwandan sites date to around 200 CE (Giblin and Fuller, 2011; Goldstein et al., 2024; Goldstein et al., 2025). This record includes several domesticated African crops and animals as well as wild fauna and Urewe ceramics (Giblin and Fuller, 2011; Goldstein et al., 2024; Goldstein et al., 2025). The Kilimanjaro region has also produced Kwale, Maore, and Kilimanjaro ceramic wares associated with agropastoralists dating from 100 CE (Odner, 1971c; b; Crowther et al., 2018). The earliest sites with evidence of farming along the coastal strip date to 200 CE, followed by offshore islands dating to 600 CE (Helm et al., 2012; Crowther et al., 2014; Crowther et al., 2016a; Crowther et al., 2016b; Prendergast et al., 2016; Prendergast et al., 2017b; Crowther et al., 2018; Culley et al., 2021a; Culley et al., 2021b). These sites contain various domesticated African and Asian crops and animals, as well as Bantu (Kwale and Tana) and Asian ceramics. Lastly, similar assemblages became dominant in the Comoros and Madagascar between 800 and 1500 CE, featuring four versions of the Tana tradition (Radimilahy, 1998; Pearson et al., 2010; Crowther et al., 2016a; Crowther et al., 2018). The subsistence shift hypothesis is supported by direct scientific dates from megafauna remains and bones with cut marks from stone and iron tools. Other evidence includes associated ratite ostrich eggshell fragments, an increase in domesticated crops and animals, and human activities such as

ironworking, clearing forests, and establishing farmlands (Pearson et al., 2010; Godfrey et al., 2019).

A critique of the monolithic migration hypotheses

Scholars who favor the idiographic approach—a framework of archaeology that emphasizes the in-depth, synchronous study of particular cultures, prioritizing context-rich, unique observations over broad generalizations—have criticized the monolithic migration hypotheses (Lane, 2004; Kusimba and Kusimba, 2005; Crowther et al., 2018). Using ecology-based evidence, it has been argued that migrations through the Congo Forest and other sub-Saharan African ecosystems by Bantu-, Nilotic-, and Cushitic-speakers were practically impossible (Robertson and Bradley, 2000). These contexts would have included dense equatorial forests full of wild animals and disease-causing pathogens, as well as uncrossable and unnavigable rivers. The migration hypotheses were criticized for being monolithic and for assuming that pots equaled people/linguistic communities (Kusimba and Kusimba, 2005; Crowther et al., 2018). They were also criticized for focusing on generalities at the expense of the variabilities and particularities of everyday life, which are more theoretically informative. The normative approach in archaeology was criticized as colonial because it aimed to promote unilinear evolution through dichotomies that defined subsistence patterns. Classifying subsistence patterns in the archaeological record as either immediate- or delayed-return foragers, fishers, pastoralists, or agropastoralists using dichotomies borrowed from ethnohistorical studies was seen as a means of legitimizing unilinear evolution (Kusimba and Kusimba, 2005; Layton and Rowley-Conwy, 2013). It was noted that the ethnographic present does not always reflect the past because ecological and human adaptive patterns, including cultural changes, evolve over time. Using ceramics to identify linguistic groups was also criticized, as

ethnic boundaries are fluid, as evidenced by ethnic alliances and trade networks (Lane, 2015a; Lane, 2017). Additionally, the use of linguistic-related terminology to describe these migrations was criticized as unreasonable because languages diversify over time and space. The Neolithic linguistic groups differed from those in the present.

The antithesis phase is marked by the rise of the idiographic approach to explain eastern African archaeology, which presented an alternative way of studying the field (Kusimba and Kusimba, 2005; Crowther et al., 2018). Rather than focusing on the emergence of food production and the dispersal of food-producing communities, as well as complex adaptive strategies in human-environment interactions from a diachronic, normative perspective, this approach provides a synchronic, idiographic perspective. The mosaic interaction and subsistence mosaic interaction hypotheses are major idiographic-oriented studies in eastern Africa (Kusimba and Kusimba, 2005; Crowther et al., 2018). The other hypotheses—indigenous continuity, moving frontier, and immediate and delayed return—remained normative but became more focused on eastern Africa (Chami, 2001b; Chami and Chami, 2001; Chami and Kwekason, 2003; Dale et al., 2004; Lane, 2004; Chami, 2007; Dale, 2007; Chami and Silayo, 2023). Below, I provide an overview of these major antithesis hypotheses and the archaeological evidence used to support them. First, I discuss the normative approaches, followed by the idiographic approaches.

2.3 –The idiographic approach and indigenous continuity in eastern Africa

The indigenous continuity hypothesis

The indigenous continuity hypothesis contrasts with the migration hypothesis. It is based on three principles: continuous indigeneity and independent invention from multiple origins, as well as cultural diffusion (Figure 2.5) (Adams et al., 1978; Trigger, 1989; Harris, 2001; Erickson and Murphy, 2003; Bentley and Maschner, 2007). In the context of eastern Africa, continuous indigeneity refers to the cultural and genetic continuity of a society's presence in a region from the late Pleistocene era to the present day (Chami, 2001b; Chami and Chami, 2001; Chami and Kwekason, 2003; Chami, 2007; Chami and Silayo, 2023). The multi-origin independent invention hypotheses view each society as having the innate capacity to invent novel and complex technological advancements. Finally, multi-origin diffusion signifies the dispersal of tangible and intangible material culture from diverse neighboring communities in all directions, while each community maintains its primary genetic continuity (Figure 2.5). This hypothesis has been used to argue that Bantu-speaking people have inhabited eastern Africa from as early as the late Pleistocene (Later Stone Age (LSA) >10000 years BP) and that these people invented their own form of food production, including livestock and crop farming (Chami, 2001a; Chami, 2001b; Chami and Chami, 2001; Chami and Kwekason, 2003; Chami, 2006; Chami, 2007; 2009; Chami and Silayo, 2023). They also had their own technological inventions, such as stone tools, ceramics, and iron. Neighboring indigenous Bantu-speaking people primarily circulated beveled and fluted pottery, iron technology, and diverse domesticated livestock and crops among themselves through multi-origin diffusion rather than immigration.

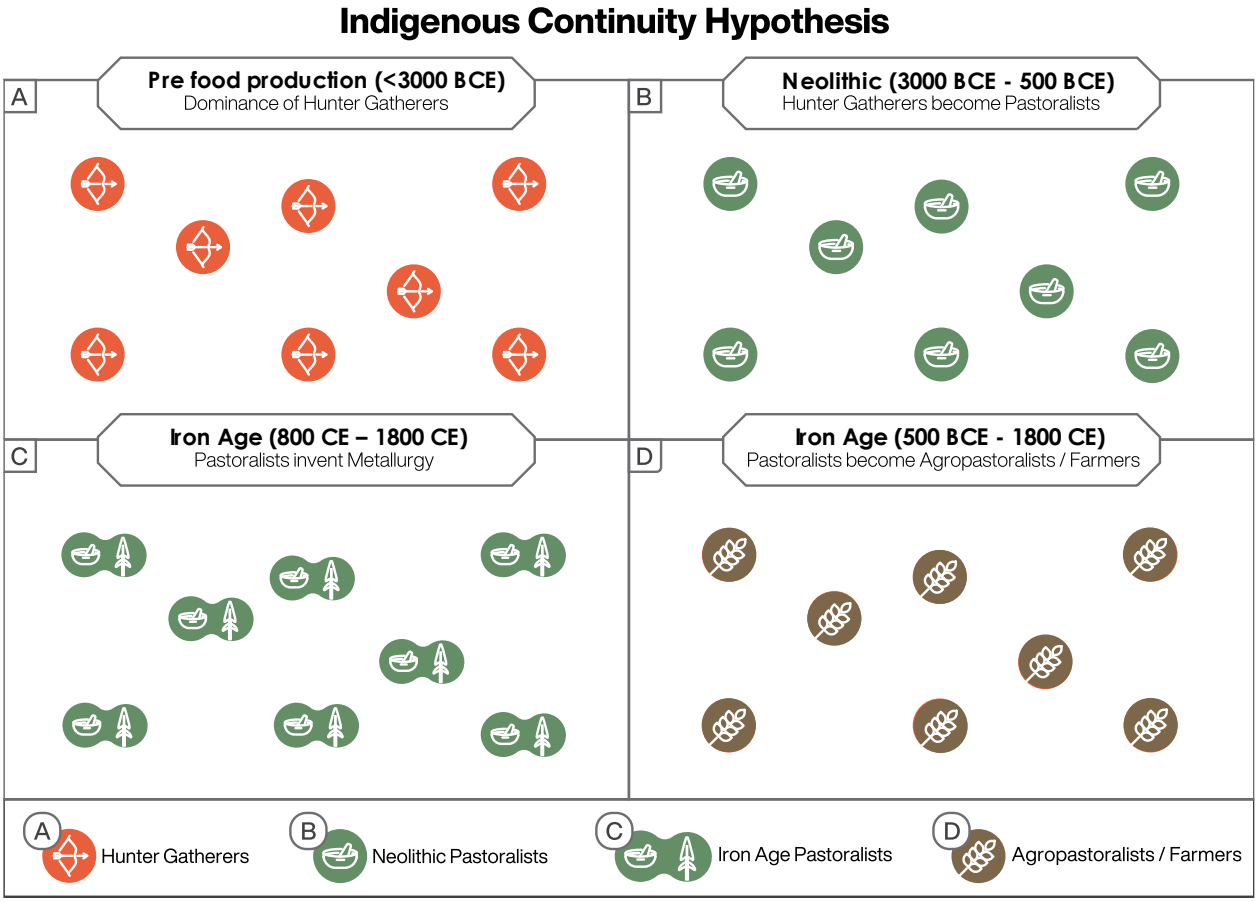


Figure 2.5. *Visual representation of the indigenous continuity hypothesis in eastern Africa showing: (A) The pre-food production period (before 3000 BCE), during which indigenous peoples engaged in hunting and gathering as their sole subsistence strategy; (B) Through independent invention and diffusion, indigenous foragers transitioned to Neolithic pastoralism (migrations were negligible) (3000 – 500 BCE); (C) Through independent invention and diffusion, indigenous foragers transitioned from Neolithic to Iron Age pastoralism, incorporating metallurgy and complex ceramic technology (800 CE – 1800 CE); (D) Through independent invention and diffusion, some indigenous foragers continued to transition to agropastoralism, incorporating African domesticated crops such as sorghum, millet, cowpeas, and lablab beans (500 BCE – 1800 CE). Note: Migration is negligible in the indigenous continuity hypothesis, meaning a stable genetic pool. The figure was created for this study by Hans Sell (Graphic Designer for the Max Planck Institute of Geoanthropology, Jena, Germany).*

Archaeological evidence in support of the indigenous continuity hypothesis

Proponents claim that archaeological evidence from several sites in eastern Africa supports the indigenous continuity hypothesis (Gramly and Rightmire, 1973; Chami, 2001a; Chami, 2001b;

Chami and Chami, 2001; Chami and Kwekason, 2003; Chami, 2007; 2009; Chami and Silayo, 2023). The similarity in cranium features in the Lukenya partial cranium dated to the late Pleistocene (LSA 17700 years BP) with Elmenteitan skulls and other Rift Valley Pastoral Neolithic crania (PN <5000 years BP) which through multivariate statistical analysis are well within the range of the modern Taita people (modern Bantu speakers) has been used to argue for the persistence of the Bantu speaking people in eastern Africa since the late Pleistocene to the present (Gramly and Rightmire, 1973). These proponents have also used archaeological evidence from the Mount Kilimanjaro region to argue for the continuity of Chagga settlements (a modern Bantu-speaking ethnic group) in the area earlier than 1000 BCE (Chami and Silayo, 2023). Chami and Silayo (2023) have also argued that the multi-stratified Machame Kisiki Trench 2 site reveals the succession and simultaneous appearance of early Iron Age (EIA) ceramics (linked to Urewe ware), Neolithic ceramics (linked to Kansyore and Narosura), and Middle to Late Iron Age (MIA to LIA) ceramics (linked to Maore and plain ware). Chami and Silayo (2023) also argue that evidence from neighboring sites confirms the simultaneous appearance of Kansyore, Narosura, Maore, and plain wares. Furthermore, according to Chami and Silayo (2023), changes in ceramic traditions over time represent the Chagga people's adoption of new traditions through independent invention and diffusion, primarily among neighboring Bantu-speaking residents, rather than immigration.

Additionally, Chami and Silayo (2023) have posited that similar patterns of ceramic tradition succession and co-appearance at Gogo Falls and Wadh Lang'o represent continuity among Bantu-speaking peoples in the Lake Victoria region. Chami et al. also argue that the ceramic traditions associated with pastoral Neolithic herders (Narosura), found by Chami et al. at KC, Machage Cave on Unguja Island, and other sites in mainland Tanzania, represent continuity of the Bantu-speaking peoples (Chami, 2001a; Chami, 2001b; Chami and Chami, 2001; Chami and Kwekason, 2003;

Chami, 2006; Chami, 2007; 2009; Chami and Silayo, 2023). These researchers have also claimed that the zooarchaeological assemblages at KC and Machage Cave include chickens and livestock associated with Bantu-speaking peoples (Chami, 2001a; Chami, 2009). They also argue that the Kilimanjaro region's stable rainfall, balanced seasonal variability, fertile land, and lack of tsetse flies made long-term habitation and farming possible for the Chagga, and that similar ecological settings across eastern Africa support the Chagga continuity scenario (Chami, 2001a; Chami, 2001b; Chami and Chami, 2001; Chami and Kwekason, 2003; Chami, 2006; Chami, 2007; 2009; Chami and Silayo, 2023).

Forager immediate and delayed return hypotheses

The immediate return and delayed return hypotheses are used to predict the adoption of food production by foragers in eastern Africa (Dale, 2000; Dale et al., 2004; Dale, 2007; Prendergast et al., 2007; Prendergast, 2009; Dale and Ashley, 2010; Prendergast, 2010a; Prendergast, 2010b; Prendergast, 2011; Prendergast et al., 2014). It has been postulated that foragers who practice the delayed-return model are more likely to adopt pastoralism more quickly than those who practice the immediate-return model (Dale et al., 2004; Dale, 2007). Those who practice the immediate-return model are defined by economic activities focused on the present. They consume food as soon as it is secured. Private property ownership is nonexistent, and high labor investment is unnecessary (Dale et al., 2004). In contrast, the delayed-return model focuses on the past, present, and future (Dale et al., 2004). It involves investing in the preservation of food through drying, smoking, salting, or freezing for future consumption. Wild food resources are protected for future production. Archaeological data from sites around Lake Victoria show that Kansyore foragers practiced a moderately delayed-return foraging model and easily shifted to farming and herding

(Dale, 2000; Dale et al., 2004; Dale, 2007; Dale and Ashley, 2010). In contrast, data from the Eyasi sites do not suggest a delayed-return foraging economy and provide mixed signals regarding foraging and herding economies (Prendergast et al., 2007; Prendergast, 2009; Prendergast and Mutundu, 2009; Prendergast et al., 2013; Prendergast et al., 2014).

The moving frontier hypothesis

The moving frontier hypothesis (Lane, 2004) explains the interaction patterns between foragers, pastoralists, and agropastoralists in eastern Africa over the past 4500 years. It attempts to reconcile the indigenous and migration hypotheses by emphasizing the role of each subsistence group in disseminating novel cultures and food production throughout the region. According to the hypothesis, the coalescence of these communities occurred through a three-phase process involving a moving frontier. This process involved the reduction and disappearance of the material culture and genetic signature of foragers from the archaeological record. The three phases are the Pioneer Phase, the Substitution Phase, and the Consolidation Phase (the end of the moving frontier) (Lane, 2004). During the Pioneer Phase, the sites of food producers indicate pioneers exploiting environments like those of foragers. These sites are archaeologically represented by technologies and temporary settlements of foragers, as well as occasional traces of domesticates and material culture of food producers (Lane, 2004). Meanwhile, interaction between foragers and pioneer food producers is indicated in the archaeological record by occasional traces of domesticated animals and plants and the dominance of indigenous material culture (Lane, 2004).

In the Substitution Phase, food producers begin to modify the land by creating pastures and farmlands, accessing water, and building permanent homes (Lane, 2004). Genetic and sociocultural

networks are also established, leading to changes in genetic makeup and sociocultural organization. Among foragers, the intrusion of food producers' lifeways increases, leading to absorption and assimilation, while others retreat to the margins (Lane, 2004). Finally, in the Consolidation Phase (the end of the frontier), food producers' sites are transformed by new technologies, such as irrigation, stall grazing, and manuring (Lane, 2004). In forager sites, evidence of foraging disappears from the archaeological record as a result of their biological and sociocultural absorption into food producers' settlements. Eventually, the "static frontier" forms when "either all currently usable land is taken up" or "the limits of the climatic tolerance of currently domesticated plants and animals are reached (Lane, 2004)." A "static frontier" also results from biological and sociocultural avoidance among some foragers and food producers, leading to their persistence as distinct groups and hence socio-ethnic mosaics (Lane, 2004).

The moving frontier hypothesis has been argued to be supported by archaeological evidence from the central Rift Valley and Lake Victoria regions (Lane, 2004). At multi-stratified pastoralist sites such as EYM, older contexts with high proportions of wild animals, occasional domesticates, and Pastoral Neolithic ceramics (Savanna Pastoral Neolithic and Elmenteitan) are said to denote the pioneer phase of the moving frontier (Lane, 2004). Younger contexts with high proportions of domesticated animals, Pastoral Neolithic or Pastoral Iron Age ceramics, and occasional wild animals are said to indicate the consolidation phase (Lane, 2004). At Gogo Falls and Wadh Lang'o, the simultaneous appearance of Kansyore, Elmenteitan, and/or Urewe ware represents the Substitution Phase. In foraging settings where Kansyore, Urewe, and domesticated animals co-appear, this indicates a transition to agropastoralism (Lane, 2004). For example, at Usenge 3, the ceramics resemble classic Urewe ceramics in terms of form and decoration, but the manufacturing processes are more characteristic of LSA Kansyore (Lane et al., 2006; Ashley, 2010). It has

therefore been suggested that, at this site where the Urewe culture overlaps with the Kansyore culture, hunter-gatherers are in the process of becoming agropastoralists. The fauna also supports this interpretation.

Mosaic interactions and subsistence mosaics hypotheses

The mosaic interactions hypothesis, based on the idiographic approach, postulates that the convergence of migrating Cushitic- and Nilotic-speaking pastoralists and Bantu-speaking farmers with indigenous foragers in eastern Africa led to the formation of complex, multi-ethnic, multi-economic regions (Kusimba et al., 2005; Kusimba and Kusimba, 2005). These regions are referred to as "mosaics" and cannot be captured by the normative approach. These mosaics were bound together by friendships, client-ship alliances, knowledge, and concepts of personal and social identity. Over the past 2,500 years, as food production spread, foraging persisted, and diverse farming and pastoral strategies were practiced (Kusimba and Kusimba, 2005). Complex interactions included degrees of fluidity between linguistic, social, and economic entities. The mosaic interactions hypothesis argues that finer details of human environment interaction are overshadowed by the "boundaries" created by cultural-historical categories of subsistence strategies, such as foragers, fishers, pastoralists, and agropastoralists, as well as technological inventions, such as the Stone Age, Kansyore, Savannah, Elmenteita, Pastoral Neolithic, Urewe, and Tana ceramic wares (Kusimba and Kusimba, 2005). Some of these divisions actually overlapped in space and time. These boundaries indicate an ethnically and economically diverse frontier where groups interacted at different spatial and temporal scales in relationships involving competition, conflict, exchange, symbiosis, and assimilation (Kusimba and Walz, 2018). The subsistence mosaics hypothesis argues that the dichotomies between foragers, pastoralists, and

agropastoralists, as well as the correlations between material culture and economic strategies, become increasingly blurred in light of higher-resolution archaeobotanical and zooarchaeological datasets from the coast (Crowther et al., 2018). It is argued that food production rarely, if ever, spreads as a single, coherent package.

The mosaic interactions hypothesis has been supported by archaeological evidence from the Great Lakes region, the central Rift Valley, the Taita-Tsavo region of southern Kenya, and the coastal strip and offshore islands of eastern Africa (Kusimba et al., 2005; Kusimba and Kusimba, 2005; Crowther et al., 2018). Inter-site differences in archaeological assemblages are believed to result from mosaic interactions. In ceramic assemblages, this is indicated by the co-appearance of two or three different traditions in the same context or site, and the dominance of one tradition in other contexts or sites (Kusimba et al., 2005; Kusimba and Kusimba, 2005; Crowther et al., 2018). For example, the co-presence of the Kansyore, Elmenteitan and Urewe ceramic traditions has been observed at Gogo Falls and Wadh Lang'o (Kusimba and Kusimba, 2005). Although both sites are stratified, there is well-attested stratigraphic mixing at Gogo Falls, whereas there was much greater stratigraphic integrity at Wadh Lang'o. In zooarchaeological assemblages, mosaic interactions are indicated by the dominance of wild fauna in some sites, domesticated fauna in others, and an almost equal representation of domesticated and wild fauna in others (Kusimba and Kusimba, 2005). In archaeobotanical assemblages, some sites have domesticated crops, while others do not (Crowther et al., 2018). Some sites have iron, while others do not.

A critique of the idiographic hypotheses

The ethnographic present is still the most intelligible template for interpreting human-environment interactions in eastern Africa during the late Holocene, and continues to be employed (Dale et al., 2004; Kiura, 2008b; Marlowe, 2010; Mutundu, 2010). The normative subsistence and ceramic categories are the most effective means of organizing the region's archaeological record, and they continue to be used (Ashley and Grillo, 2015; Grillo et al., 2020a; Goldstein et al., 2025). The focus on particularities shaped by human agency in a specific time period and space, without acknowledging that these particularities are part of a larger process that has unfolded over time in different ecological settings, is a significant limitation (Kusimba et al., 2005; Kusimba and Kusimba, 2005; Crowther et al., 2018). This makes it impossible to discern the diachronic patterns that shaped context-specific assemblages at an archaeological site. Multidisciplinary data from central and eastern Africa indicate that the Iron Age was marked by periods of climate-driven aridity (Verschuren et al., 2000; Lamb et al., 2003; Verschuren, 2004b; Verschuren, 2004a; Kiage and Liu, 2006; De Cort et al., 2013; Gelorini and Verschuren, 2013; Bostoen et al., 2015; Grollemund et al., 2015; Marchant et al., 2018; Bostoen and Coutros, 2025). The archaeological data used by the mosaic interaction and subsistence mosaic hypotheses are from the Iron Age and from specific high-resource ecological settings that could have served as refugia for diverse groups during climate-driven arid periods (Kusimba et al., 2005; Kusimba and Kusimba, 2005; Crowther et al., 2018). These high population convergence zones would have been different in wet periods. Interaction patterns outside the specified convergence regions were also different.

Although most zooarchaeological assemblages at late Holocene archaeological sites in eastern Africa indicate the mixing of wild and domesticated animals, multidisciplinary approaches that

combine isotopic and aDNA and proteomics perspectives can differentiate indigenous foragers and pastoralists from northeastern Africa from agropastoralists from western Africa (Ambrose and DeNiro, 1986b; Kiura, 2008b; Skoglund et al., 2017; Wang et al., 2020; Bleasdale et al., 2021; Lipson et al., 2022). For instance, the hair carbon and nitrogen isotope values of the El Molo hunter-gatherers of Lake Turkana differ significantly from those of the neighboring Gabra pastoralists and Dassanach agropastoralists (Kiura, 2008a). The El Molo's isotope values also differ from those of the Luo fishing community of Lake Victoria. These differences reflect regional ecological variations between the Lake Turkana and Lake Victoria regions. However, another study in the Turkana region has shown that herders' reliance on livestock and crops varies depending on the season, and there is limited difference in isotope values between herders and cultivators (Bleasdale et al., 2026). A site- and context-specific approach cannot capture these broader patterns and comparisons. Ancient DNA evidence indicates that foragers, pastoralists, and agropastoralist communities are distinct based on region of origin (Wang et al., 2020; Lipson et al., 2022). Material culture assemblages differ as well, with pastoralist sites dominated by round, elongated ceramic containers designed for dairying (Ambrose, 2003). In the Great Lakes region, the ceramics found at farmers' sites have a globular shape with a narrow mouth, and are designed for cooking and storing cereals (Phillipson, 1975; 1977). The ceramics used by foragers differ in that they have a wide mouth for storing honey, wild vegetables and meat (Dale et al., 2004). This explains why pastoralist ceramics and other associated artefacts are only found in arid grasslands (the optimal region for pastoralism), and why Urewe, Kwale and Tana ceramics are only found in agropastoralist sites in equatorial regions with high rainfall (the optimal region for agropastoralism). Forager ceramics (e.g. Kansyore and Lowasera) and associated artefacts, meanwhile, are found across the region in settings that are optimal for hunting and gathering. An idiographic approach cannot reveal these background ecological and functional patterns. Combining data from diverse sources, such

as zooarchaeology, archaeobotany, and material culture, with molecular data can help distinguish these subsistence groups and track their fluidity more precisely.

The indigenous continuity hypothesis is limited in terms of multidisciplinary data and breadth of hypothesis (Chami, 2001b; Chami and Chami, 2001; Chami and Kwekason, 2003; Chami, 2007; Chami and Silayo, 2023). The data used to support the hypothesis lack crucial information from zooarchaeology (e.g., ancient DNA and isotope ratios), archaeobotany (e.g., domesticated crops), and metallurgy (e.g., ironworking). Only ceramics data are emphasized, which is insufficient to validate the hypothesis. The hypothesis is limited in breadth because it only presents one version of the hypothesis. Apart from the version involving cultural and genetic continuity, where foragers invent and switch to pastoralism and agropastoralism (Chami and Silayo, 2023), there are scenarios in which foragers retain their long-term cultural and genetic continuity (Marlowe, 2010; Skoglund et al., 2017; Roberts et al., 2020). For instance, the Hadza and Sandawe of Tanzania exemplify a foraging lifestyle and genetic continuity, as evidenced by genetic and ethnographic studies (Tishkoff et al., 2007; Marlowe, 2010; Skoglund et al., 2017). The indigenous continuity hypothesis continues to use the Bantu linguistic group to argue that it has existed since the late Pleistocene era. However, no cultural group called the ‘Bantu’ existed during the late Pleistocene. Additionally, the study used ceramics alone to argue for the cultural and genetic continuity of the Chagga community in the Kilimanjaro region (Chami and Silayo, 2023). The lack of ancient human DNA evidence to support the hypothesis makes it weak.

The limitations of the idiographic approach in the archaeology of eastern Africa warrant an integrated approach combining idiographic and normative methods. Since the 1970s, the archaeological record in this region has improved substantially and can be used for the normative

approach. Additionally, scientific methods of analysis have multiplied and become more accurate. These methods include isotopic, archaeo-informatics, and aDNA perspectives that have provided in-depth insights in archaeological studies worldwide (Skoglund et al., 2017; Prendergast et al., 2019b; Bird et al., 2021; Bird et al., 2022; Lipson et al., 2022; Sirak et al., 2022). These approaches have been applied in western and central Africa, providing significant background information that is valuable for understanding the archaeological record in eastern Africa (Pakendorf et al., 2011; de Filippo et al., 2012; Bostoen et al., 2015; Grollemund et al., 2015; Kay and Kaplan, 2015; Patin et al., 2017; Kay et al., 2019; Seidensticker et al., 2021; Grollemund et al., 2023; Coutros et al., 2024; Fortes-Lima et al., 2024). Archaeologists are also more aware of the colonial legacies of archaeology in eastern Africa and have refined their approaches. These developments provide an opportunity to reevaluate monolithic migration hypotheses using an integrated approach with archaeological data from eastern Africa.

2.4 – Integrating the normative and idiographic approaches

There are multiple justifications for the integrative application of normative and idiographic approaches to archaeological investigations in eastern Africa. Using the normative approach alone leads to missing the specific details that shape a phenomenon. Similarly, using only the idiographic approach leads to missing the historical and ecological background patterns that shape the site- and context-specific cultural phenomenon, resulting in a blurred or narrow view of the studied phenomenon. Integrating these approaches provides a more insightful perspective of a phenomenon. The lack of archaeological data in the postulated migration routes in western, central, and eastern Africa was a major impediment to testing monolithic hypotheses. Currently, however,

the archaeological record in these regions is substantial enough to test these hypotheses. The methodological issues raised in ethnohistorical and linguistic studies have been addressed, and more data have been collected. Advancements in archaeological science have made it possible to apply archaeo-informatics and other multidisciplinary perspectives to the archaeological record of these regions. Despite the use of normative subsistence categories, the application of archaeo-informatics in western Africa has revealed that the dispersal of food production in this region occurred along multilinear rather than unilinear pathways (Kay et al., 2019).

The application of the archaeo-informatic or 'big data' comparative approach to archaeological, aDNA, and historical linguistic datasets in central Africa has produced novel insights that warrant revisiting migration hypotheses using an integrated perspective of the archaeological record in eastern Africa (Pakendorf et al., 2011; de Filippo et al., 2012; Bostoen et al., 2015; Grollemund et al., 2015; Koile et al., 2022; Grollemund et al., 2023; Fortes-Lima et al., 2024). This approach has led to the revision of monolithic migration hypotheses, proposing late-split riverine and late-split savannah peeling-off hypotheses (Russell et al., 2014; Grollemund et al., 2023). These migrations are now presented as gradual and occurring via three major routes. These studies have also produced new insights on the ecological changes and complex human adaptive strategies involved in these dispersals that shaped the archaeological record in eastern Africa. Advancements in human-environment interaction studies in Madagascar have also led to a large number of dates from megafauna species and associated archaeological information, leading to the subsistence shift hypothesis (Godfrey et al., 2019). Below, I present an overview of these hypotheses and highlight important insights significant for understanding the archaeology of eastern Africa.

Late-split riverine and late-split savannah peeling-off hypotheses

The conversation about the Bantu expansion is currently dominated by two versions of the late-split hypothesis: the late-split riverine hypothesis and the late-split savannah peeling-off hypothesis (Russell et al., 2014; Grollemund et al., 2015; Bostoen, 2018; Grollemund et al., 2023). The late-split riverine hypothesis views the Bantu-speakers as a people primarily adapted to rainforest environments (Russell et al., 2014). According to this hypothesis, the eastern Bantu wave split from the western branch after moving southwest and migrating deep into the riparian Congo River system (Figure 2.6). This group then headed east through the Congo Forest to the Great Lakes region, using riparian habitats that had become more open due to a global drying trend that had led to the fragmentation of the forest. Apart from livestock, this wave of Bantu-speakers dispersed western African crops, such as pearl millet and cowpeas, to eastern Africa (Seidensticker et al., 2021). There, they adopted sorghum, finger millet, and lablab beans from Nilotic and Cushitic-speaking agropastoralists in the Great Lakes region.

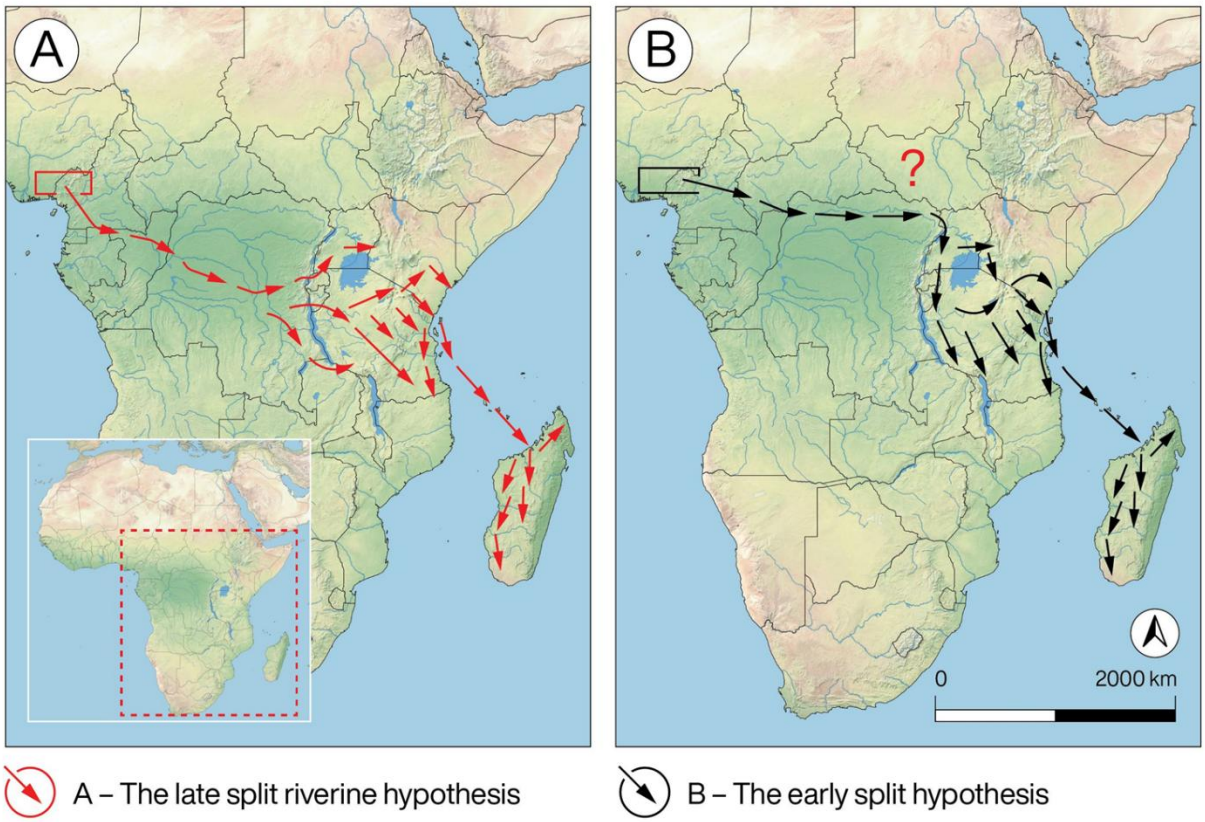


Figure 2.6. *Map of Africa highlighting the recently revised western African agropastoralist migrations to eastern Africa, known as the riverine migration hypothesis, with two proposed routes: (A) the riverine route, which is backed by archaeological evidence, and (B) the northern Congo forest route, which lacks archaeological and other evidence. Note the small continuous arrows representing gradual, periodic migrations. The figure was created for this study by Hans Sell (Graphic Designer for the Max Planck Institute of Geoanthropology, Jena, Germany).*

According to this late-split riverine hypothesis, the Bantu expansion through the forests occurred in a "spread-over-spread" pattern. This pattern consisted of multiple overlapping migrations rather than one massive event (Seidensticker et al., 2021). These multiple migrations are supported by evidence for two periods of intense human activity in the Congo Forest and adjacent areas: one from 800 BCE to 1 CE, and another from 1400 to 1900 CE (Seidensticker et al., 2021). These periods are defined by two distinctive phases. The first phase is marked by widespread pottery style exchange. The second phase is characterized by the regionalization of pottery styles, with many local styles emerging and becoming distinct. Lastly, the late-split riverine hypothesis argues for the

possibility of the early-split occurring along the northern margin of the Congo forest (Russell et al., 2014). These creates the possibility of Bantu-speaking people migrating eastwards via the northern forest margin along the Sahelian region acquiring and dispersing the major African domesticated crops as a package in the Great Lakes region. It also creates the possibility of the early-split wave and the late-split wave to merge in different patterns involving exchange of material culture and crops around the Great Lakes region and disperse in the interior, coast and islands with different combinations of material culture and crops. This hypothesis is supported by linguistic phylogeography, genetics, and archaeology.

The late-split savannah peeling-off hypothesis (Figure 2.7) posits that the original Bantu speakers were adapted to the savannah woodlands of the Nigeria-Cameroon homeland (Grollemund et al., 2015; Grollemund et al., 2023). It is hypothesized that the Bantu-speaking people followed the savannah corridor, which developed due to climate change, from southwest Cameroon to Angola. According to this hypothesis, a massive, trunk-like wave dispersed the Bantu speakers to eastern Africa in peeling-off patterns or small branches from the main trunk of a tree. This involved the formation of smaller branches heading north into the forests and south into the woodlands of southern Africa (Grollemund et al., 2023). This led to the formation of many branching waves rather than one massive wave from western Africa splitting into two (western and eastern), as postulated by the original late-split hypothesis.

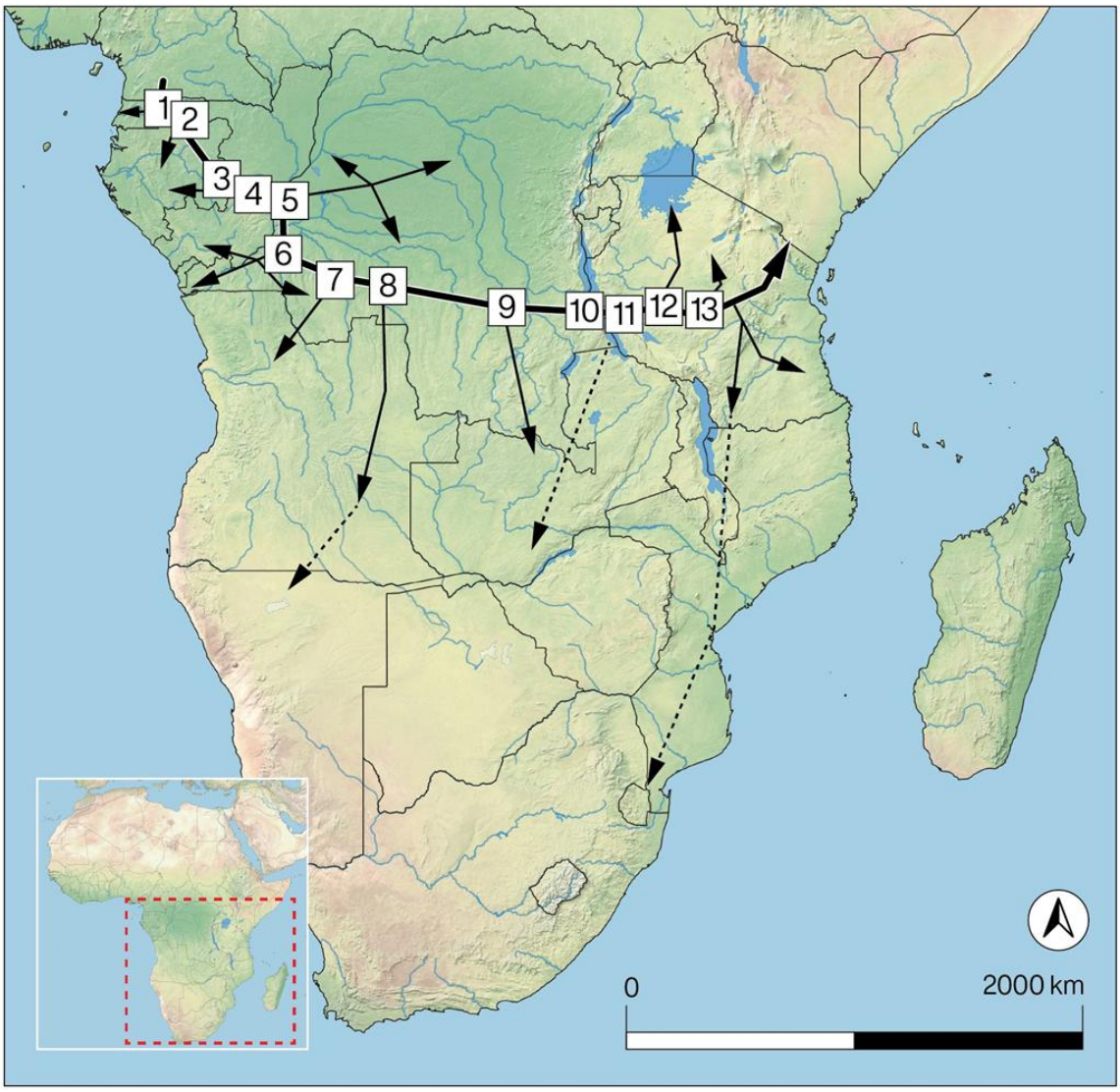


Figure 2.7. *Map of Africa depicting a second version of the revised western African agropastoralist migration to eastern Africa, known as the 'late-split savannah peeling-off' hypothesis. Note the arrows 1-13 showing the peeling-off patterns towards the forested northern and southern savannah regions of the main migration route. The figure was created for this study by Hans Sell (Graphic Designer for the Max Planck Institute of Geoanthropology, Jena, Germany).*

This savannah peeling-off hypothesis postulates that the Bantu speakers were highly adaptive; some stuck to agropastoralism, while others shifted to foraging depending on ecological settings. Those who shifted to foraging are thought to have moved faster through the savannah woodlands

to the Great Lakes region. It is also hypothesized that this wave of immigrants consciously left behind livestock, crop farming, and iron technology and relearned these practices from Nilotic and Cushitic-speaking agropastoralists in the Great Lakes region (Grollemund et al., 2023). Then, they dispersed this package to the interior and coast of eastern Africa, offshore islands, reaching as far as Comoros and Madagascar (Soper, 1967b; a; Soper, 1969; Soper, 1971; 1976; 1979; Sinclair, 1991; Pearson et al., 2010; Crowther et al., 2014; Crowther et al., 2016a; Crowther et al., 2016b; Crowther et al., 2018). Other waves dispersed to southern Africa (Huffman, 1970; Huffman and Vogel, 1991; Huffman and Herbert, 1994). The hypothesis also states that Urewe ceramic ware existed in the Great Lakes region before the Bantu speakers immigrated to the area. The Bantu are said to have adopted the ware and dispersed it to other regions of eastern Africa. Proponents of the late-split savannah hypothesis strongly reject the early-split Bantu expansion hypothesis, claiming that it lacks sufficient linguistic, archaeological, and genetic evidence (Grollemund et al., 2023).

In addition to hypotheses concerning the emergence and dispersal of intricate subsistence patterns and food-producing communities, there are also hypotheses regarding the environmental impact of migrations by agropastoralists of western African descent (Pearson et al., 2010; Bayon et al., 2012b; Bayon et al., 2012a; Bostoen et al., 2015; Grollemund et al., 2015; Godfrey et al., 2019; Kay et al., 2019). These hypotheses can be categorized into two perspectives. One perspective focuses on human agency as the main cause of deforestation in the Congo forest (the 'forest crisis' hypothesis) (Bayon et al., 2012b; Bayon et al., 2012a) and megafaunal extinctions in Madagascar (the 'subsistence shift' hypothesis) during the late Holocene (Godfrey et al., 2019). The other perspective argues that these ecological changes were primarily caused by climate change (Pearson et al., 2010; Bostoen et al., 2015; Grollemund et al., 2015; Maley et al., 2018; Kay et al., 2019). These hypotheses are of critical importance as they provide valuable insights into past human-

environment interactions, which are highly relevant in the contemporary context of sustainable resource management and wildlife conservation. Significant progress has been made in addressing these hypotheses through approaches from archaeological science. Below, I provide an overview of the forest crisis in the Congo Basin, as well as the subsistence shift hypothesis and megafaunal extinctions in Madagascar.

Forest crisis hypothesis

The forest crisis hypothesis suggests that deforestation in the Congo and other forests across sub-Saharan Africa was significantly caused by slash-and-burn agricultural practices and the demand for wood used for iron smelting by immigrating agropastoralists (Bayon et al., 2012b; Bayon et al., 2012a). It is hypothesized that agropastoralists of western African descent played an active role in deforestation by clearing large swathes of land for settlements, farming, and fuel for iron smelting and cooking (Bayon et al., 2012b; Bayon et al., 2012a). Iron tools in particular made it easier to clear forests. Anomalies in the geochemical signatures of marine sediments sourced from the mouth of the Congo River in the central African forest have been used to support this hypothesis (Bayon et al., 2012b; Bayon et al., 2012a). These marine records indicate an intense chemical weathering event in the 3rd millennium BP, which departs from long-term weathering fluctuations related to climate changes over the past 40,000 years. This geochemical signature anomaly coincides with agropastoral migration across the central African forest landscape. This suggests that land use intensification by immigrating agropastoralist populations was the driver of the ecological changes that led to these anomalies (Bayon et al., 2012b; Bayon et al., 2012a). Conversely, the climate crisis hypothesis posits regional climate change and natural drying trends as the main cause of deforestation in the Congo forest (Maley J. et al., 2012; Neumann K. et al., 2012; Bostoen et al.,

2015; Grollemund et al., 2015; Maley et al., 2018; Kay et al., 2019). It also argues that agropastoral migration had a limited and small-scale environmental impact. It views the agropastoralists from western Africa as opportunistic users of existing savannah corridors, rather than destroyers of the forest (Bostoen et al., 2015; Grollemund et al., 2015; Grollemund et al., 2023). Pollen analyses, paleoclimate models, and population density analyses of data from the central African region have been used to support this hypothesis (Bostoen et al., 2015; Maley et al., 2018).

Subsistence shift hypothesis and megafauna extinctions in Madagascar

Lastly, the "subsistence shift hypothesis," an extension of the migration hypothesis, was developed to answer the question: Was human predation or climate-induced aridity the cause of megafaunal extinctions in Madagascar? According to the hypothesis (Godfrey et al., 2019), the extinction of megafauna in Madagascar was triggered by the expansion of Indian Ocean commerce and the shift from a foraging-based economy to one that increasingly relied on agropastoralism, trade, and urbanism (Figure 2.8). The megafauna population declined as more settlers, including agropastoralists from eastern Africa, arrived from across the Indian Ocean and introduced new crops and animals. The hypothesis emphasizes the long overlap between humans and megafauna. However, the negative impacts associated with the shift from a foraging economy (pre-700 CE) to a pastoral economy (post-700 CE), triggered by the immigrant population (predominantly from eastern Africa), hastened the collapse of megafaunal populations (peaking between 750 and 850 CE, with complete collapse by 1050 CE) (Godfrey et al., 2019). The hypothesis also acknowledges hunting, settlement by new immigrants, and the rapid increase in the human population (including Bantu-speaking and Asian immigrants) as significant drivers of megafaunal extinctions in Madagascar (Godfrey et al., 2019). Conversely, other hypotheses explain the major trigger of

megafaunal extinctions in Madagascar differently. One set cites complex anthropogenic factors, such as hunting, introduced animals, and pathogens, while the other cites ongoing aridity cycles, not humans. The last set cites both anthropogenic and climate factors as major drivers of megafaunal extinctions in Madagascar (Pearson et al., 2010).

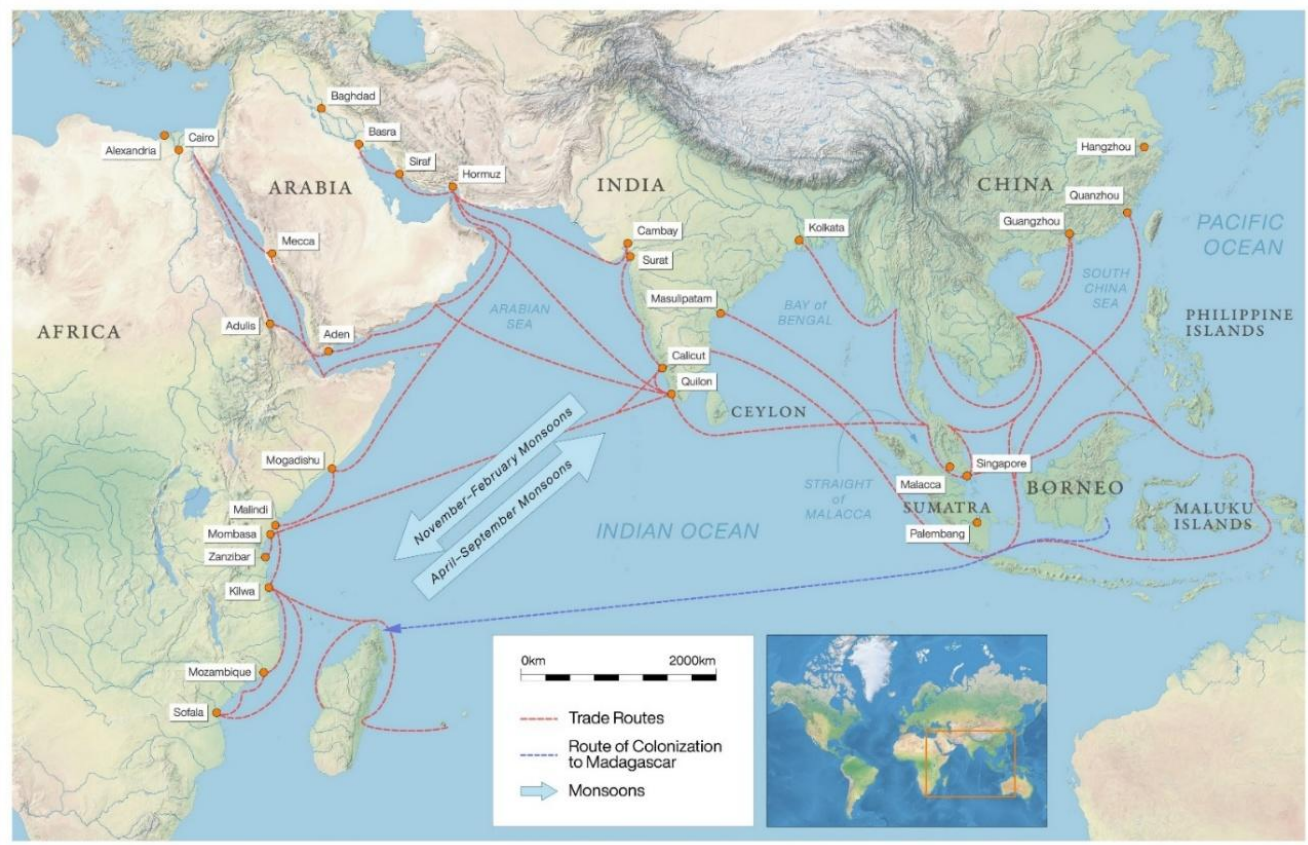


Figure 2.8. *Map of the Indian Ocean rim showing the commerce networks to eastern Africa. The figure was created for this study by Hans Sell (Graphic Designer for the Max Planck Institute of Geoanthropology, Jena, Germany).*

2.5 – Archaeological sciences in the late Holocene archaeology of coastal and interior eastern Africa

Due to the challenges, limitations, and gaps involved in testing the different hypotheses outlined above, diverse multidisciplinary approaches are necessary to examine archaeological assemblages at various sites in eastern Africa. These approaches can help identify relations between indigenous foragers and immigrants, such as agropastoralists from western Africa and pastoralists from the Sudan-Nile and Ethiopia-Somali regions. They can also help explain the diverse subsistence patterns and changes visible in the archaeological record. Multidisciplinary analyses grounded in archaeological science represent an important means to more directly test the principles of the indigenous continuity and migrations hypotheses (Binford, 1968; Harris, 2001; Erickson and Murphy, 2003; Killick, 2006; Martinón-Torres and Killick, 2015; Bird et al., 2021; Bird et al., 2022). By highlighting the similarities and differences in the biomolecular composition of assemblages (e.g., isotopes, ancient DNA and proteomics) at site and regional levels, visible patterns are expected to reveal whether an assemblage is the result of indigenous population persistence or migration. Biomolecular methods, such as isotopic analysis, ZooMS, aDNA, high-resolution radiocarbon dating, and archaeo-informatic perspectives, applied to multiple sites evenly distributed across different ecological regions and countries in eastern Africa, could greatly increase the region's contribution to theory building at the regional and global scales. These approaches are now commonly used to improve chronological accuracy and produce insightful data critical to answering major research questions, testing hypotheses, and building theories. Examples from around the world show that insights from studies led by isotopic and archaeo-informatic approaches, supported by other archaeological science methods, enrich hypothesis testing and theory development (Bird et al., 2021; Bird et al., 2022).

Over the last twenty years, a significant number of archaeological projects in eastern Africa have employed multiple archaeological science approaches, yielding refined and novel insights (Crowther et al., 2014; Crowther et al., 2016a; Crowther et al., 2016b; Crowther et al., 2018; Roberts et al., 2020; Culley et al., 2021a; Culley et al., 2021b; Kotarba-Morley et al., 2022; Goldstein et al., 2024; Goldstein et al., 2025). Context-specific excavation, recording, and direct dating have boosted chronological accuracy (Prendergast et al., 2016; Shipton et al., 2016; Goldstein et al., 2024; Goldstein et al., 2025). Flotation and microscopy have led to the recovery and identification of species of large samples of archaeobotanical remains, which are dominated by domesticated African and Asian crops (Crowther et al., 2014; Crowther et al., 2016a; Crowther et al., 2016b; Crowther et al., 2018; Mueller et al., 2022; Goldstein et al., 2024; Goldstein et al., 2025). Advanced zooarchaeology has also led to the recovery and identification of species of large numbers of domesticated and wild animals (Prendergast, 2009; Prendergast, 2010a; Prendergast, 2010b; Prendergast et al., 2016; Prendergast et al., 2017a; Prendergast et al., 2017b; Prendergast and Beyin, 2018; Prendergast et al., 2019a; Roberts et al., 2020; Prendergast et al., 2023). ZooMS has boosted the identification of goats, sheep, and other antelope species (Prendergast et al., 2019a; Culley et al., 2021a; Culley et al., 2021b). Proteomics and aDNA have been used to highlight differences and admixture among pastoralist, farming, and foraging populations of diverse origins in eastern Africa (Skoglund et al., 2017; Prendergast et al., 2019b; Wang et al., 2020; Bleasdale et al., 2021; Lipson et al., 2022; Sirak et al., 2022). Isotope analysis has provided insights into paleoenvironmental, dietary, and mobility patterns over time (Chritz et al., 2019; Prendergast et al., 2019a; Roberts et al., 2020). Studies oriented toward archaeo-informatics have also produced significant insights (Causey and Lane, 2005; Russell et al., 2014).

Insights from applying these multidisciplinary archaeological perspectives to recent studies of the coastal region are just the tip of the iceberg. Major gaps in our understanding of human-environment interactions in this region during the late Holocene remain, including the lack of isotopic data from wild animals and livestock for paleoecological and herding strategy reconstructions. These data are necessary to systematically capture change in the vegetation over time and its causes, and the earliest anthropogenic introductions and subsequent developments in order to test the indigenous continuity, migrations, and subsistence shift hypotheses and others. Comparing the patterns in the isotopic values and associated archaeological assemblages at the context-site-specific scale with patterns in values from similar assemblages at multiple sites across the eastern African region could provide valuable insights for testing these hypotheses. I present three case studies that demonstrate how multidisciplinary projects with multi-isotopic and archaeo-informatic perspectives can reveal valuable insights that can be used to test the tenets of the indigenous continuity and migration hypotheses.

2.6 – Case studies

In this section, I will introduce the three case studies of this thesis and explain why they were chosen and how they address the identified hypotheses, questions, and gaps. The three case studies were selected for a variety of reasons relating to the study of ecological fluctuations, intricate subsistence strategies, and the emergence and dispersal of food production and communities that produce food in eastern Africa. The two case studies based on isotope analyses were selected because the sites are located in the coastal and offshore island region of eastern Africa, where only one isotope study has been previously published. These sites were recently excavated by the

Sealinks Project, which is a multidisciplinary study of the earliest maritime networks that connected and transformed societies across the Indian Ocean (Boivin et al., 2013; Shipton et al., 2013; Boivin et al., 2014; Crowther et al., 2014; Crowther et al., 2016a; Crowther et al., 2016b; Langley et al., 2016; Prendergast et al., 2016; Shipton et al., 2016; Prendergast et al., 2017a; Crowther et al., 2018; Faulkner et al., 2018; Shipton et al., 2018; Faulkner et al., 2019; Roberts et al., 2020; Wang et al., 2020; Culley et al., 2021a; Culley et al., 2021b; Faulkner et al., 2021; Faulkner et al., 2022; Kotarba-Morley et al., 2022). The project focused primarily on excavations and sampling at coastal strip and offshore island sites in eastern Africa. A new suite of diverse, cutting-edge methodologies was applied, including zooarchaeological, archaeobotanical, genetic, artefactual and palaeoenvironmental studies, to understand the interplay between cultural and biological factors shaping societies, species and environments in the region. The Sealinks Project produced high-resolution archaeological assemblages for the region which have been studied using multiple archaeological science approaches. The sites were excavated and recorded using context-specific methodologies. The sites were also studied using archaeobotanical flotation, in-depth zooarchaeological studies, and ZooMS. These studies included the identification of samples to the species level, aDNA studies, and geological studies, among others. The zooarchaeological and archaeobotanical assemblages have been identified down to the species level. The ceramic assemblages are also well identified. The sites have also been well radiocarbon dated using multiple direct dates from domesticated animals and short-lived crops (e.g., sorghum, pearl millet, and cowpea). The third case study on archaeo-informatics was chosen to synthesize scientific dates and associated zooarchaeological, archaeobotanical, ceramic, and metal finds in an archaeo-informatics-oriented dataset. This dataset is used to generate maps that offer spatial-temporal insights on human-environment interactions in eastern Africa.

Case study one: Paleoecology and human foraging from the late Pleistocene to the late Holocene at Kuumbi Cave, Unguja Island.

In case study one, stable carbon ($\delta^{13}C$) and oxygen ($\delta^{18}O$) isotope analyses were performed on human and faunal tooth enamel from KC on Unguja Island in Tanzania. These analyses are used to track dietary and ecological changes that occurred from the late Pleistocene to the late Holocene. The site contains evidence of human occupation from the late Pleistocene to the late Holocene (20,000 to 500 cal. BP), covering periods of glacial-to-interglacial climate change, as well as the island's connection to and subsequent isolation from the mainland (Figure 2.9) (Prendergast et al., 2016; Shipton et al., 2016). The sequence is divided into four phases, with a gap in human occupation between phases II and I (Shipton et al., 2016). The pre-food production phases (IV, III, and II) are characterized by a lack of domesticates and associated material culture (e.g., iron and pottery). The site also documents the extirpation of at least six medium-to-large mammals on the island following the Pleistocene: Thomson's gazelle (*Eudorcas thomsonii*, reported by Prendergast et al., 2016, as *Gazella thomsoni*); buffalo (*Syncerus caffer*); waterbuck (*Kobus ellipsiprymnus*, reported by Prendergast et al., 2016, as *K. defassa*); reedbuck (*Redunca redunca*); zebra (*Equus quagga*); and bushbuck (*Tragelaphus scriptus*). Additionally, two small bovids became extirpated: klipspringer (*Oreotragus oreotragus*) and bush duiker (*Sylvicapra grimmia*) (Prendergast et al., 2016). Enamel $\delta^{13}C$ and $\delta^{18}O$ values are a reliable reflection of the diets and environments of consumers in the region (Roberts et al., 2020). This study integrates stable isotope data (n = 229; see Table A1:1) and complementary archaeological data to elucidate the significant role that the stability of forests along the coastal strip and on offshore islands in eastern Africa may have played in enabling indigenous foraging communities to endure when interacting with immigrating agropastoral groups during the Iron Age. Regional context is provided by comparing the study data

with published stable isotope records (n = 756, Table A1:2) from the Pleistocene-Holocene coastal cave site of PYS in Kenya and a series of sites in eastern Africa's interior.

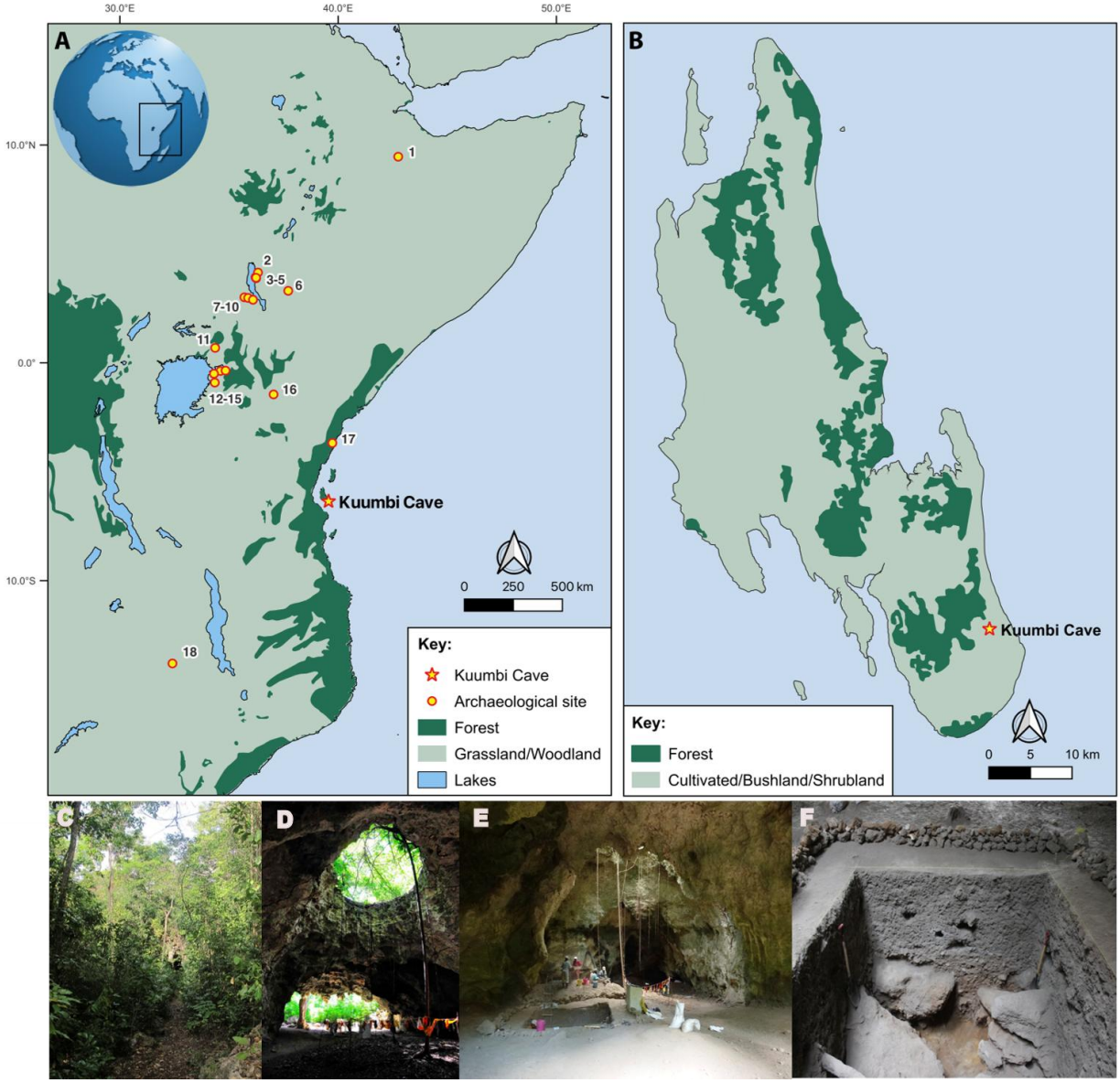


Figure 2.9. *A schematic representation of the geographical area of eastern Africa, highlighting the locations of sites with stable isotope data referenced in this thesis. (1) Porc Epic; (2) FxJj12; (3) GaJj11; (4) GaJj2; (5) Dongodien; (6) Ele Bor; (7) 'AW'; (8) 'Equid site'; (9) '514'; (10) Lothagam Lokam; (11) Kakapel; (12) Wadh Lang'o; (13) Kanam East; (14) Luanda; (15) Gogo Falls; (16) Lukenya Hill; (17) PYS; and (18) Kalemba Rockshelter. Figure 2.9(B) shows the location of KC on Unguja (Zanzibar) Island. The modern vegetation classification is based on (A) White (1983) and (B) Hardy et al. (2015) and was developed using regional base maps and validated through ground surveys. Photos of KC: (C) facing the entrance from outside; (D) facing outside from inside; (E) a view of the Trench 10 excavation; and (F) a Trench 10 cross-section.*

Case study two: Intricate caprine herding strategies in Unguja Ukuu, Unguja Island

Case study two analyzes the collagen carbon ($\delta^{13}C_{coll}$) and nitrogen ($\delta^{15}N$), as well as the enamel carbon ($\delta^{13}C_{enamel}$), oxygen ($\delta^{18}O$), and strontium ($^{87}Sr/^{86}Sr$) isotopes, of caprine and wild herbivores (n=62, Table A2:1 and A2:2) from three sites in coastal forest mosaic habitats in eastern Africa (Figure 2.10). The sites are UU and FK on Unguja Island in Tanzania, as well as PYS on the coast of mainland Kenya. $\delta^{13}C_{coll}$ and $\delta^{15}N$, as well as $\delta^{13}C_{enamel}$, $\delta^{18}O$, and $^{87}Sr/^{86}Sr$ values reliably reflect the diets, environments, climates, and mobility patterns of consumers in the region. The application of ZooMs to identify taxa to species in the fragmented assemblage from these sites enabled the analysis of more samples for isotopic reconstruction (Culley et al., 2021a; Culley et al., 2021b). Using multi-isotope analysis and complementary archaeological datasets, I explore caprine management at these sites. I contextualize the data by comparing it with published data from three Pastoral Neolithic contexts: EYM, Dongodien, and Luxmanda (Ambrose and DeNiro, 1989; Chritz et al., 2019; Prendergast et al., 2019a) (Table A2:5 and A2:6). I also compare the results to data from three Iron Age contexts: KC (Table A2:4) on Unguja Island and Gogo Falls and Wadh Lang'o in eastern Africa's interior (Figure 2.10, Table A2:6) to provide a wider understanding of herding variability during the Iron Age across diverse eastern African environments (Chritz et al., 2019). I also include unpublished human $^{87}Sr/^{86}Sr$ and published $\delta^{13}C_{enamel}$ and $\delta^{18}O$ values from UU, KC, and PYS (values from four individuals, Table A2:3) (Roberts et al., 2020). I also use the associated archaeological assemblages to aid in interpreting the isotope data (Prendergast et al., 2017; Roberts et al., 2020). Specifically, I employ multi-isotope approaches to ascertain whether the Unguja Ukuu forest and marine ecosystem, along with its associated archaeological assemblages, exhibits a sophisticated caprine herding strategy embedded within an economic livelihood originating from the forested coastal region of eastern Africa. This

coastal herding strategy differs greatly from those in the predominantly arid interior of eastern Africa.

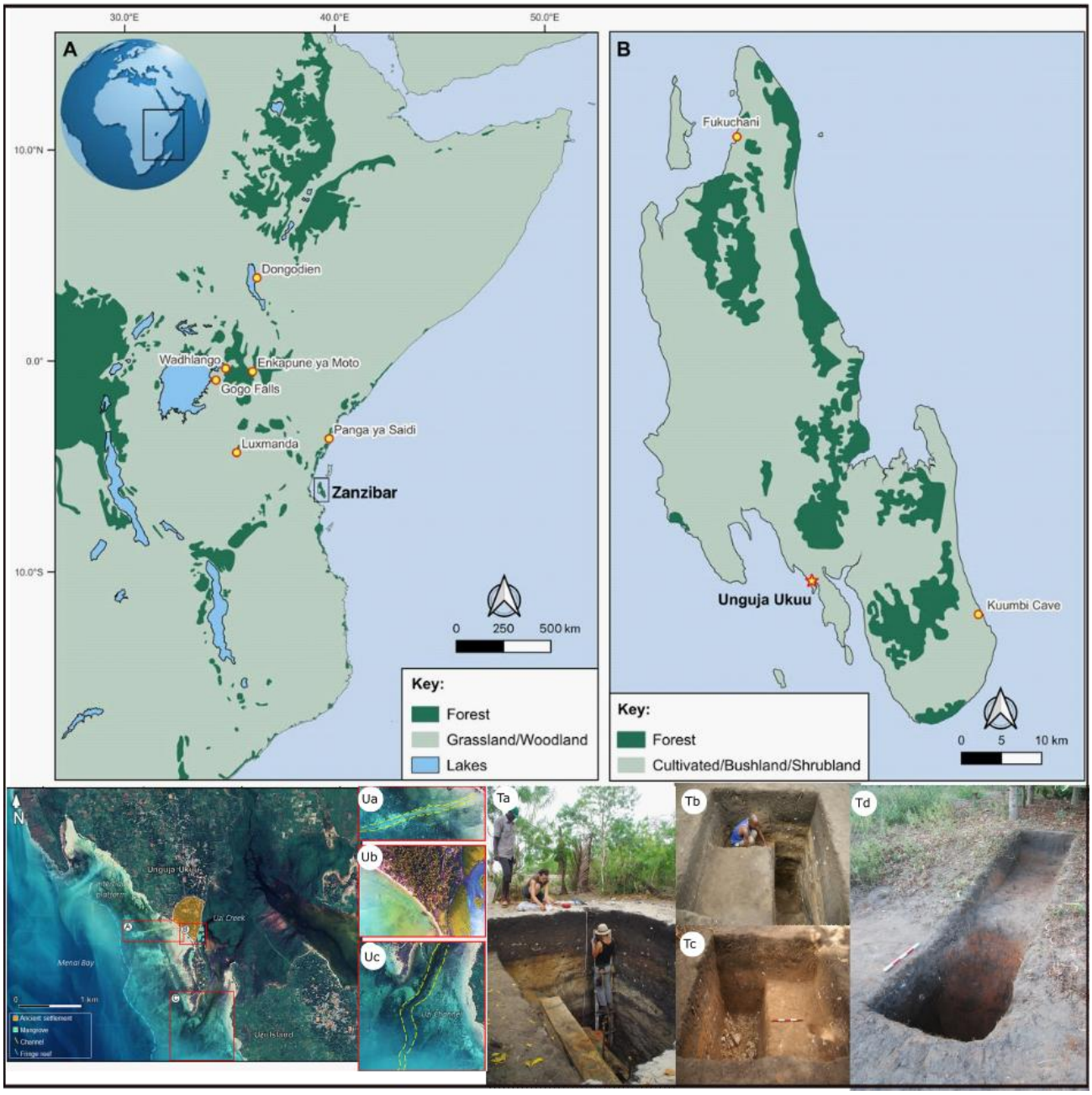


Figure 2.10. *Map of eastern Africa highlighting sites where isotope studies have been performed on caprines, namely UU, FK, and KC (wild fauna only) in Unguja Island and PYS along the Kenyan coast, and Dongodien, EYM, Gogo Falls, Wadh Lang'o and Luxmanda in the interior eastern Africa. Modern vegetation based on (A) White (1983) and (B) Hardy et al. (2015): classification of vegetation biomes developed from regional base maps validated through ground surveys. Aerial view of UU (Ua-Uc), and Trenches excavated at UU by the Sealinks Project 2011-2012 (Ta-Td).*

Case study three: The Wanyika dataset and the dispersal of food production and food-producing communities in late Holocene eastern Africa

In case study three, I present the extensive *Wanyika* dataset, which comprises scientific dates and associated archaeological records from mid-to-late Holocene sites spanning four countries in eastern Africa, in addition to a selection of sites in Rwanda (Figure 2.11, see Table A3:1 for an abridged version of the *Wanyika* dataset). The collection emphasizes these four countries because they contain some of the most thoroughly recorded archaeological evidence in eastern Africa for this time frame, especially because of the use of radiocarbon dating. *Wanyika* is an informatics-oriented dataset in which data spanning almost seven millennia, from 5000 BCE to 1800 CE, has been drawn together. The Bantu word "*Wanyika*" means "people of the wilderness." It refers to all ethnic groups in eastern Africa, including those who migrated to offshore islands and Madagascar (Werner, 1915; Hamilton, 1920; Morton, 1972).

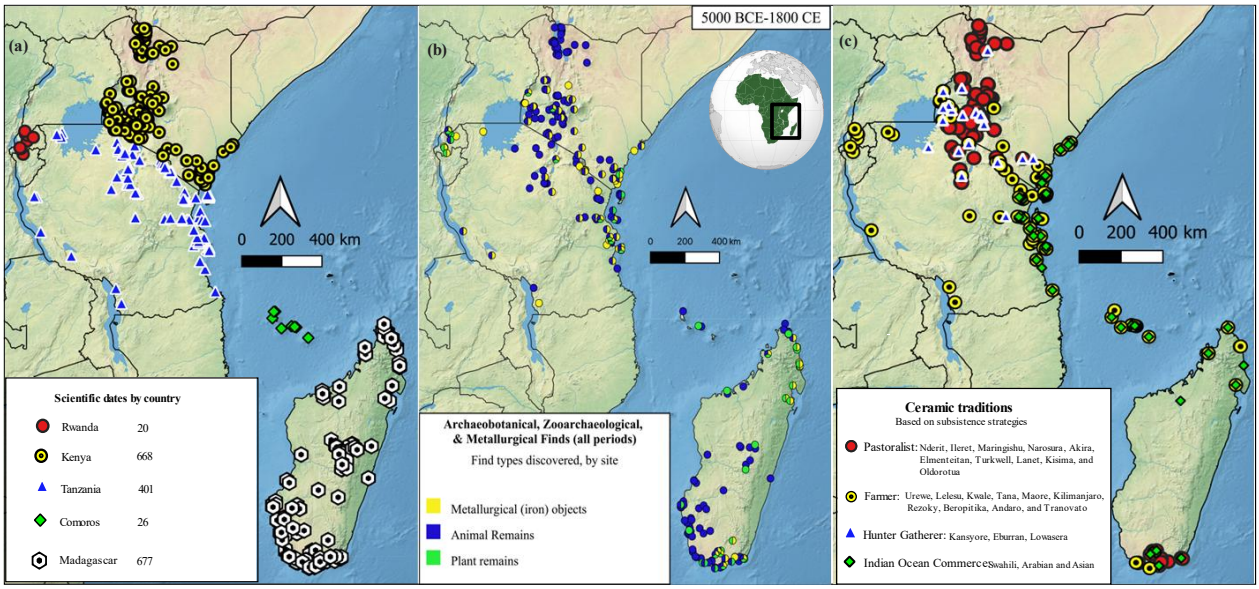


Figure 2.11. *Map of eastern Africa showing the spatial distribution of: a) scientific dates by country (5000 BCE to 1800 CE), highlighting specific sites with archaeobotanical finds in Rwanda; b) dated archaeological sites (5000 BCE to 1800 CE) with finds relating to archaeobotany, zooarchaeology, and metallurgy; c) identified ceramic traditions associated with pastoralists, farmers, hunter-gatherers, and Indian Ocean commerce (5000 BCE to 1800 CE).*

The archaeological records associated with this project include spatial-temporal data on various finds from published archaeological sites, as well as several unpublished sites, across key regions of mainland and island eastern Africa. These finds include plants, animals, iron, and ceramic materials. I included iron and ceramic finds because they are closely (although not exclusively) associated with the spread of new cultures and food production from the interior to the coastal regions of eastern Africa. These finds are valuable for analyzing patterns of dispersal to the coast and islands, as well as for identifying existing research gaps that have hindered hypothesis testing and theory building in eastern African archaeology (Phillipson, 1975; Van Noten, 1979; Collett and Robertshaw, 1980; Collett and Robertshaw, 1983; Ambrose, 1984a; Collett, 1985; Robertshaw, 1990b; Robertshaw, 1991; Sinclair, 1991; Ambrose, 1998; 2003; Lane et al., 2006; Lane et al., 2007; Giblin and Fuller, 2011; Crowther et al., 2018). Ceramic finds are important because ceramic styles differ among hunter-gatherers, pastoralists, and farmers (Bower et al., 1977; Onyango-

Abuje, 1977a; Bower and Nelson, 1978; Collett and Robertshaw, 1980; Collett and Robertshaw, 1983; Mturi, 1986; Bower, 1991; Sinclair, 1991; Ambrose, 1998; Munene, 2002; Dale, 2007; Prendergast, 2009; Giblin and Humphris, 2010; Prendergast, 2010a; Prendergast et al., 2014; Wynne-Jones and LaViolette, 2018; Grillo et al., 2022; Goldstein et al., 2024). Moreover, records on megafaunal persistence and coexistence with humans in Madagascar are also included (MacPhee et al., 1985; MacPhee, 1986; MacPhee and Burney, 1991; Wright and Fanony, 1992; Burney, 1997; Goodman and Rakotozafy, 1997; Simons, 1997; Burney, 1999; Goodman, 1999; Burney et al., 2004; Karanth et al., 2005; Rakotozafy and Goodman, 2005; Crowley, 2010; Pearson et al., 2010; Goodman et al., 2013; Crowley et al., 2017; Anderson et al., 2018; Hansford et al., 2018; Lawler, 2018; Douglass et al., 2019; Mitchell, 2020; Hixon et al., 2021a; Hixon et al., 2021b; Hixon et al., 2021c). Instead of offering a thorough summary, the *Wanyika* dataset is a preliminary study that paves the way for future research. Finally, I use maps generated from the *Wanyika* dataset in QGIS to test the hypothesis that an archaeo-informatics approach to the archaeological record of eastern Africa from 5000 BCE to 1800 CE could provide broad, in-depth, diachronic insights into human–environment interactions associated with the emergence and dispersal of food production and food-producing communities across eastern Africa. These insights include connections between ecology and the complex subsistence strategies employed by indigenous and immigrating coastal and inland communities. This perspective should also reveal significant research gaps and biases that hinder rigorous hypothesis testing.

Chapter 3 – Climatic and environmental change in eastern Africa during the last 20,000 years and its relevance to socioeconomic change

The climatic and environmental changes in eastern Africa over the past 20,000 years BP are reviewed in this chapter, with high-resolution mangrove dynamics and tidal inundation paleoenvironmental records from marine sedimentary deposits in the coastal region highlighted, which are of value to this thesis. First, it provides a broad chronological overview of global glacial and interglacial climatic patterns over this time period, as well as how these patterns are reflected in the African context. Next is a review of sedimentary records spanning from the late Pleistocene to the late Holocene. It begins with lacustrine deposits from major lakes in eastern Africa's interior, followed by sand dune data from the Congo Basin in central Africa. Lastly, it reviews ecological changes and their shaping of human-environment interactions in eastern Africa's interior over the past 20,000 years BP. The second section discusses high-resolution environmental records obtained from marine sedimentary cores taken at four key sites, which provide insights into tidal inundation and mangrove dynamics in the coastal strip and on Unguja Island in eastern Africa from the late Pleistocene to the late Holocene. It begins with a review of the geographical history of Unguja Island from the late Pleistocene, when it was part of mainland Africa, to the Holocene, after it formed as an island. The marine sedimentary records from the Rufiji Delta and the Pangani River (on the coastal mainland) and Unguja Ukuu and Makoba Bay (on Unguja Island) are then discussed, with a particular focus on the Unguja Ukuu records, which are valuable for interpreting the archaeology of Unguja Island. The third section summarizes isotope ecology studies of sites in eastern Africa's interior, including the PYS site on the coastal strip, and highlights the insights that can be gained from isotope ecology and archaeo-informatic studies of offshore islands, the coast, and the interior in general.

3.1 – Environmental changes in the interior of eastern Africa over the last 20,000 years

Lacustrine records indicate that interior eastern Africa experienced dramatic, climate-driven ecological transformations during the late Pleistocene to the late Holocene, which were linked to changes in the Earth's orbit (Figure 2.9-10 and Table 3.1) (Talbot and Lærdal, 2000; Kiage and Liu, 2006; Foerster et al., 2015; Revel et al., 2015; Schaebitz et al., 2021). Paleoclimatic discussions of eastern Africa focus on precipitation as the major climatic parameter (Bonnefille et al., 1990; Stager and Johnson, 2000). However, the majority of these discussions and the aforementioned climatic changes are based almost entirely on eastern African lacustrine and marine records from the arid interior and the Indian Ocean coast (Talbot and Lærdal, 2000; Kiage and Liu, 2006; Foerster et al., 2015; Revel et al., 2015; Schaebitz et al., 2021). Global patterns indicate that the Last Glacial Maximum (24,500 to 18,000 BP) was dominated by dry conditions that continue to 14,670 BP followed by a wet period during the Late Glacial Interstadial (14,670 to 12,890 BP) (Gasse, 2000; Talbot and Lærdal, 2000; Kiage and Liu, 2006; Foerster et al., 2015; Revel et al., 2015; Schaebitz et al., 2021). The terminal Pleistocene (Younger Dryas (YD) 13,000 to 10,000 BP) was cooler and drier than the later periods. The African Humid Period (AHP: 11-6,000 BP) was wetter and warmer, but punctuated by a brief drying event around 8700 to 8200 BP. The post-AHP was cooler and drier than the AHP (Talbot and Lærdal, 2000; Kiage and Liu, 2006; Foerster et al., 2015; Revel et al., 2015; Schaebitz et al., 2021). An increase in climatic fluctuations with a dominance of cooler and drier conditions during the post-AHP (last 6000 years BP) is noted. In general, the beginning of the post-AHP phase (6000 to 3000 BP) was drier, but still wetter and warmer than today. Two drying phases: 5200 BP and 4000 BP punctuate this period.

The modern climatic regime conditioned by the Intertropical Convergence Zone (ITCZ), and less wet than the post-AHP, was established around 3000 to 2500 BP (Talbot and Lærdal, 2000; Kiage and Liu, 2006; Foerster et al., 2015; Revel et al., 2015; Schaebitz et al., 2021). Sedimentary records indicate variability in the way regions in mainland eastern Africa (lakes in the Rift Valley and sand dunes in the Congo basin) responded to these climatic fluctuations (Hastenrath and Kutzbach, 1983; Gasse, 2000; Verschuren, 2004b; Verschuren, 2004a; Robakiewicz et al., 2019; Fischer et al., 2020; Robakiewicz et al., 2025). The coast and islands may have been more marine influenced and more humid (Crowther et al., 2016a; Crowther et al., 2016b; Prendergast et al., 2016; Shipton et al., 2016; Crowther et al., 2018; Shipton et al., 2018; Roberts et al., 2020; Faulkner et al., 2021; Faulkner et al., 2022; Kotarba-Morley et al., 2022; Prendergast et al., 2023).

Table 3.1. *Chronology of climate-driven ecological transformations in eastern Africa from the late Pleistocene to the late Holocene collated from in-text citations (Talbot and Lærdal, 2000; Kiage and Liu, 2006; Foerster et al., 2015; Revel et al., 2015; Schaebitz et al., 2021). Years recorded in uncalibrated years before present (BP).*

Climate Phase	**Time in BP**	**Ecological Conditions**
Last Glacial Maximum (LGM)	24,500 to 18,000	Extremely dry
Post LGM	18,000 to 14,670	Dry
Last Glacial Interstadial	14,670 to 12,890	Wet
Younger Dryas (YD)	13,000 to 10,000	Cooler and drier than later periods
African Humid Period (AHP)	10,000 to 6,000	Wetter and warmer
	8,700 to 8,200	Brief drying event
Post AHP	6,000 to 3,000	Drier than early Holocene, but wetter and warmer than today
	5,200 and 4,000	Two dry phases
Modern Climatic Regime	3,000 to present 2,000 to 1,600 800 to 600 200 to 150	Increase in aridity and climatic fluctuations Three notable dry episodes

Lacustrine deposits from Lake Victoria and other major lakes in eastern Africa capture dramatic climatic changes that occurred between the Last Glacial Maximum (LGM) and the late Holocene (Hastenrath and Kutzbach, 1983; Stager et al., 1997; Gasse, 2000; Stager and Johnson, 2000; Verschuren et al., 2000; Stager et al., 2003; Verschuren, 2004a; Stager et al., 2005a; Stager et al., 2005b; Stager and Johnson, 2008; Robakiewicz et al., 2019; Fischer et al., 2020; Robakiewicz et al., 2025). These lacustrine records show that Lake Victoria disappeared once and has contracted and expanded in sync with global climate patterns from the late Pleistocene to the present. During the late Pleistocene epoch, approximately 18,000 to 15,000 years BP, the lake completely dried up. It then refilled rapidly around 14,600 years BP, in sync with global climate cycles. The rising lake level caused a brief overflow event into the White Nile around 14,200 to 13,600 years BP. The lake was dominated by closed-basin conditions until approximately 11,200 years BP, when the Nile River became permanently established and provided an outlet. During the early and mid-Holocene epoch (approximately 11,500–5,500 years BP), particularly during the AHP, the region experienced elevated humidity. This resulted in forests encircling the lake. The lake experienced several brief periods of aridity during the Holocene, with reduced water levels and closed-basin conditions at times (for example, around 10.5, 9, 7.8–7.2, 4, and 3.2–3.0 thousand years BP). However, the lake did not completely dry up during these intervals. Over the past three millennia, the lake's size has fluctuated significantly due to variations in regional rainfall and evaporation rates (Stager et al., 2005a; Stager et al., 2005b). There have been at least six large, century-scale droughts in the Lake Victoria region over the last 2,700 years. These droughts have significantly impacted the region's ecosystems and economies. These events caused substantial drops in lake levels. For instance, during two of the most significant droughts of the past 1,000 years, the lake level dropped by approximately 81 feet (25 meters) and 97 feet (30 meters), respectively (Verschuren et al., 2000; Stager et al., 2003; Stager et al., 2005a; Stager and Johnson, 2008).

Lacustrine records also indicate that throughout most of the late Pleistocene era, the size of the lakes in Kenya's Great Rift Valley fluctuated significantly (Hastenrath and Kutzbach, 1983; Gasse, 2000). However, during the AHP, these lakes expanded to more than twice their current size (Hastenrath and Kutzbach, 1983; Fischer et al., 2020). Lake Turkana rose 80 metres higher and received 20% more water (Hastenrath and Kutzbach, 1983). Mega Lake Nakuru-Elmenteita rose 180 metres higher and received 23-45% more water (Dühnforth et al., 2006). Lake Naivasha rose 110 metres higher and received 29-33% more water (Richardson and Richardson, 1972; Hastenrath and Kutzbach, 1983; Bergner et al., 2003). Following the AHP, dramatic changes occurred, shifting from warm, wet periods to predominantly cool, dry periods. During this time, the lakes in the Great Rift Valley, including Lake Turkana, Lake Nakuru, Lake Elmenteita, and Lake Naivasha, were reduced to their current sizes (Hastenrath and Kutzbach, 1983; Dühnforth et al., 2006; Fischer et al., 2020). Several lake level fluctuations, from a freshwater to a saline lake, are noted (Hastenrath and Kutzbach, 1983; Dühnforth et al., 2006; Robakiewicz et al., 2025). Some lakes, such as Lake Naivasha, disappeared and reappeared during the post-AHP period (Bergner et al., 2003). Pollen records from various sites in eastern Africa also reflect these fluctuating patterns, which are dominated by dry phases.

Rainfall patterns obtained from a 25,000-year-old sediment core taken from Lake Challa — a deep (90 m), 4.2 km² crater lake located on the eastern slope of Mount Kilimanjaro, in the easternmost area of the African tropics (3° S, 38° E) — indicate an increase in climatic fluctuations and aridity during the late Holocene (Verschuren et al., 2009; Tierney et al., 2011). The records suggest that after the mid-Holocene drought, rainfall in equatorial eastern Africa increased again from 6.8 thousand years BP (peaking between 4.5 and 2 thousand years BP), with distinct multi-century droughts in between (Verschuren et al., 2009). Moreover, the Challa records document the three

most notable dry episodes of the past two millennia (2.0–1.6, 0.8–0.6, and 0.2–0.15 thousand years BP) (Verschuren et al., 2009).

Sand dune records from the Congo Basin in central Africa (which borders eastern Africa and was likely a route for Iron Age Bantu agropastoralist migrations) suggest that the Sahara belt and the Congo rainforest experienced the "Green Sahara and Desert Congo Switch" in synchrony with climatic shifts caused by orbital forcing from the late Pleistocene to the late Holocene (White, 1983; Kingdon, 1984b; Russell et al., 2007; Werdelin and Sanders, 2010; Russell et al., 2014; Seidensticker et al., 2021; Olaka and Ebinger, 2023; Coutros et al., 2024). This switch occurred as a result of the expansion and contraction of forests and grasslands, respectively. The presence of large, active sand dunes in the Congo Basin suggests that there were periods in the past when the rainforest retreated due to extreme aridity. Along with other evidence, the records show that the forest expanded significantly during the AHP in the early to mid-Holocene (10,000 to 6,000 years BP), covering areas that are now savanna, as well as parts of the Sahara (White, 1983; Kingdon, 1984b; Russell et al., 2007; Seidensticker et al., 2021; Olaka and Ebinger, 2023; Coutros et al., 2024). Around 4,000 years BP, drier conditions led to forest contraction at its edges and savanna encroachment. Between 2,500- and 2,000-years BP, major forest fragmentation and disturbance occurred.

Climatic shifts and fluctuations in eastern Africa from the late Pleistocene to the late Holocene would have been translated through its rugged terrain and its proximity to the Indian Ocean, resulting in the dominance of mosaic woody grasslands in the region as opposed to a continuation of the tropical Congo forest type habitats across interior eastern Africa (Figure 2.9-10 and Table

3.1) (White, 1983; Kingdon, 1984c; a; Bonnefille et al., 1990; Kingdon, 1997; 2001; Black, 2005; Bonnefille, 2010; Patridge, 2010; Werdelin and Sanders, 2010; Garcin et al., 2012; Foerster et al., 2015; Camberlin, 2018; Ring, 2018; O'Malley et al., 2021; Schaebitz et al., 2021; Olaka and Ebinger, 2023). These factors resulted in a complex mosaic of forests, woodlands, and arid grasslands that were periodically disconnected and reconnected in low-lying regions of eastern Africa. During glacial periods, open grasslands dominated the interior of eastern Africa, forming a corridor that connected the arid lands of northern and southern Africa while partly disconnecting the equatorial Congo forest and the coastal forests of eastern Africa (White, 1983; Kingdon, 1984b; Bonnefille et al., 1990; Bonnefille, 1995; Burgess and Clarke, 2000; Bonnefille, 2010). During interglacial periods, a thin corridor of closed woodlands and forests partially connects the equatorial Congo forest and the coastal forests. Riparian habitats around major rivers and lakes, such as the Nile and Omo rivers and Lakes Victoria and Turkana, have also fluctuated in response to climate change (Butzer et al., 1972; Hastenrath and Kutzbach, 1983; Bonnefille et al., 1990; Talbot and Lærdal, 2000). The montane vegetation in the highlands, including Mount Kilimanjaro, Mount Kenya, the Rift Valley, and the Ethiopian Highlands, have also been expanding and contracting over time (Figure 2.9-10) (White, 1983; Kingdon, 1984c; a; Mahaney, 1988; Kingdon, 1997; Thompson et al., 2002; Sinninghe Damsté et al., 2011; Githumbi et al., 2018; van der Plas et al., 2020; Courtney Mustaphi et al., 2021). These climate- and terrain-driven, mosaic ecological patterns have shaped human-environment interactions in eastern Africa in complex ways. The dispersal of different elements, including domesticated animals and plants (arid- vs. wetland-adapted) across the eastern African region was shaped by these ecological conditions. These ecological conditions also shaped the migration trajectories and interaction patterns of forest- and grassland-adapted foragers and food producers in eastern Africa.

3.2 – High-resolution environmental records from marine sedimentary cores in the coastal region of eastern Africa

Marine sedimentary records from four strategic locations along the Indian Ocean coastal strip and Unguja Island have provided high-resolution records on tidal inundation and mangrove dynamics during the late Pleistocene to the late Holocene, which are of great value for paleoenvironmental reconstructions in this thesis (Punwong et al., 2012; 2013; Bouimetarhan et al., 2015; Liu et al., 2017; Punwong et al., 2018; Sefton et al., 2021; Englong et al., 2023). These high-resolution sedimentary cores were recovered from the Rufiji Delta and the Pangani River in the coastal strip, and Unguja Ukuu and Makoba Bay on the coast of Unguja Island. Unguja Ukuu is also one of the key archaeological sites covered by this thesis, and Makoba Bay is close to Fukuchani, which is another key site (Punwong et al., 2012; 2013; Bouimetarhan et al., 2015; Liu et al., 2017; Punwong et al., 2018; Sefton et al., 2021; Englong et al., 2023). Apart from high-resolution chronology by radiocarbon dates, multiple analyses, including palynological, geochemical and geomorphological studies, were carried out on these sedimentary cores. The results suggest that a wet and humid AHP was followed by an increase in climatic variability and fluctuations during the late Holocene in this coastal region of eastern Africa. I will discuss the main findings from the high-resolution marine sedimentary cores regarding climate-induced ecological fluctuations at these sites, focusing on Unguja Ukuu, which provides in-depth insights into human-environment interactions during the Iron Age. First, however, I will provide some background on the formation of Unguja Island during the late Pleistocene to Holocene period.

Unguja Island (also called Zanzibar Island) of the Zanzibar Archipelago was connected to the mainland of eastern Africa during the last glacial period (see Figure 3.1), when sea levels were

lower than they are now (For information about the topography of Zanzibar between 20–7 thousand years BP, see Prendergast et al. 2016: Figure 4-5) (Moreau and Pakenham, 1940; 1941; Burgess and Clarke, 2000; Prendergast et al., 2016). During this epoch, vast grasslands seemingly prevailed in the heart of eastern Africa. This established a connection between the arid regions of northern and southern Africa while severing the connection between the Congo forest in the equatorial region and the coastal woodlands of eastern Africa (Kingdon, 1984b; 2001). Sea-level rise during the Holocene led to the formation of Unguja Island, while increased precipitation resulted in the expansion of closed woodlands and forests in the coastal and interior regions of eastern Africa (Burgess and Clarke, 2000; Prendergast et al., 2016). These ecological dynamics may have influenced human-environment interactions differently in interior and coastal regions, particularly concerning the emergence of complex subsistence strategies and the dispersal of food production and food-producing communities (Ambrose, 1984a; 1998; Marshall and Hildebrand, 2002; Lane, 2004; Kusimba and Kusimba, 2005; Crowther et al., 2014; Crowther et al., 2016a; Prendergast et al., 2016; Prendergast et al., 2017b; Crowther et al., 2018; Culley et al., 2021a; Kotarba-Morley et al., 2022).

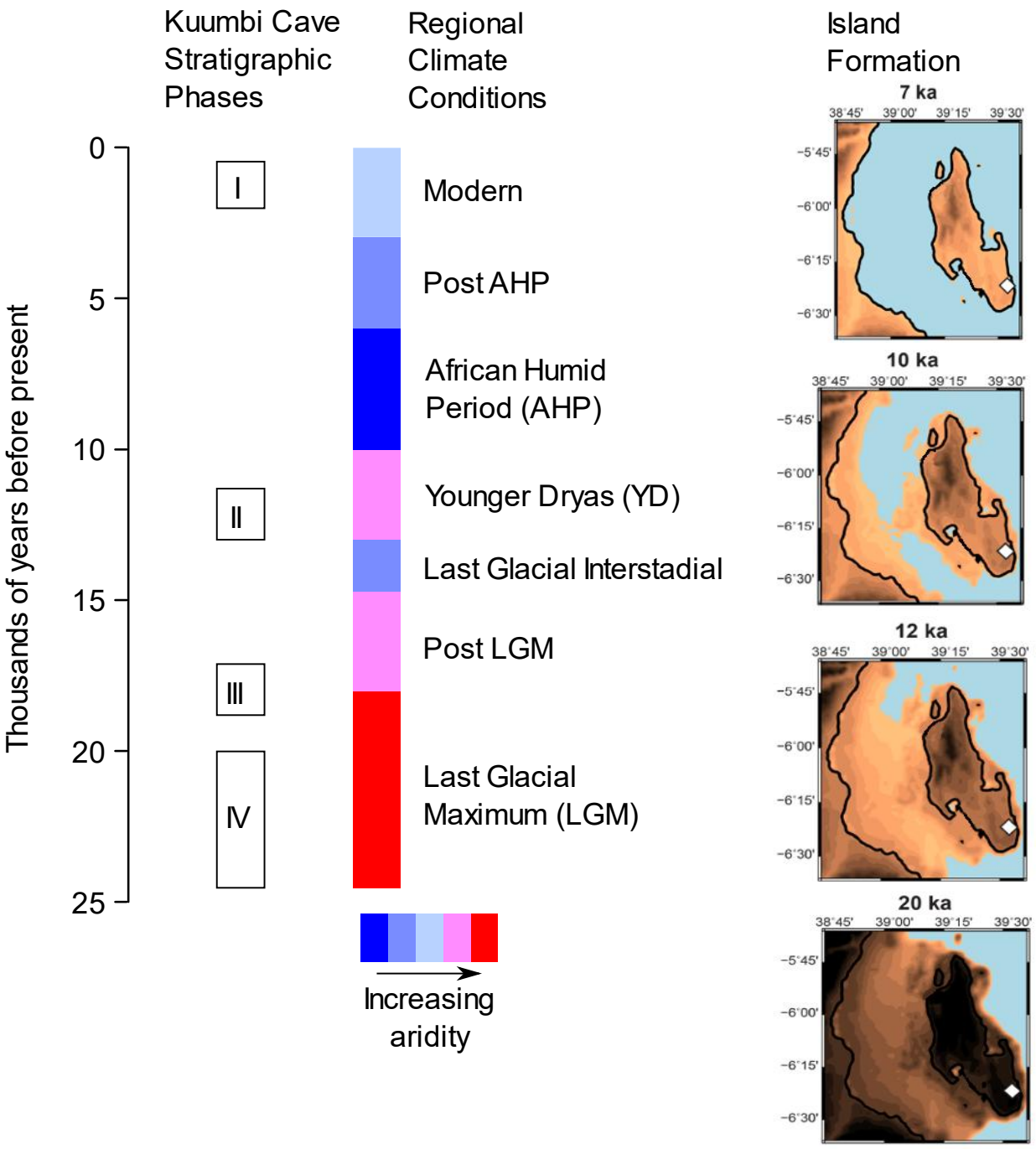


Figure 3.1. *Timeline of the KC stratigraphic succession alongside regional climate conditions and the formation of Unguja Island. The various shades of brown represent different stages of island formation, while blue signifies the ocean and the white diamond indicates the location of KC. The island's formation occurred between 12,000- and 10,000-years BP. This represents H. Rouby's reconstructions of Unguja Island in Prendergast et al. (2016), modified to include an illustration of stratigraphic integrity and regional climatic change.*

The high-resolution pollen records from a marine sediment core recovered off the coast of the Rufiji River delta have provided valuable data on ecological fluctuations during the late Pleistocene and late Holocene (Bouimetarhan et al., 2015). The records show important changes in pollen groups during the last ice age, and highlight how plant communities reacted to changes in rain, sea levels and coastal movements, as well as changes in plants in uplands and lowlands. The pollen records suggest that the upland Rufiji region was drier between 16.6 and 14.8 thousand years BP, with a transition to more humid conditions around 14.8 thousand years BP, as demonstrated by the growth of forests and humid woodlands (Bouimetarhan et al., 2015). In contrast, the lowland vegetation shows the presence of well-established salt marshes and mangroves throughout the entire record, with a substantial expansion of mangroves after 14.8 thousand years BP in response to increased moisture availability in the coastal area (Bouimetarhan et al., 2015). Mosaic forests, humid woodlands, dry woods and shrubs dominated the period between 12.8 and 11.5 thousand years BP. This period is followed by increased precipitation, as suggested by the sharply rising aluminium/calcium (Al/Ca) ratios and high sedimentation rates, as well as the presence of pollen from forests and humid woodlands, around 11.6 thousand years BP (Bouimetarhan et al., 2015). In contrast, the decline in nearly all pollen taxon percentages, Al/Ca ratios, and sedimentation rates at the end of the record, around 10.6 thousand years BP, suggests a return to drier conditions or the cessation of active terrestrial input (Bouimetarhan et al., 2015). The geochemical record from the Pangani sediment core at the mouth of the Pangani River on the mainland coast of Tanzania shows an increase in the elemental ratios of biogenic elements compared to aluminium (Al) during the mid-late Holocene transition, specifically the calcium/aluminium (Al/Ca) and strontium/aluminium (Al/Sr) ratios (Liu et al., 2017). Significant increases in these elemental ratios were seen at the end of the mid-Holocene, between 5 and 3.5 thousand years BP, indicating a

gradual shift from the humid early and mid-Holocene to the arid late Holocene in eastern Africa (Liu et al., 2017).

A more structured analysis of sedimentary deposits from three sites — the northern Rufiji Delta (Tanzanian mainland), Makoba Bay, and Unguja Ukuu — which involved taking three sediment cores at different distances from the ocean at each site, provides finer details on climate-driven ecological changes based on evidence from tidal inundation and mangrove dynamics (Punwong et al., 2012; 2013; Woodroffe et al., 2015; Englong et al., 2023). Pollen records from these three sites show that the sea level in coastal Tanzania has been changing a lot over the last 10,000 years. The sediment cores from each site show variations in mangrove taxa ratios, indicating that mangrove development occurred at different periods during the Holocene from around 7,900 years BP. Records show that the sea level rose from around 7,900 years BP to somewhere between 4,700 and 4,600 years BP, possibly reaching a higher level than it does today. This happened during the early-to-mid Holocene period. This period is followed by a lower relative sea level (RSL) until 4,400 years BP, after which RSL rises until ~2,000 years BP. After that, the RSL levels of the last few thousand years were marked by an increase at around 700–500 years BP, before dropping below the current level at around 100 years BP. Evidence suggests that the RSL has risen more recently over the past few hundred years.

The high-resolution, multiproxy analysis of the sedimentary record from the Unguja Ukuu site, which included pollen, charcoal, geochemistry and geomorphology, has revealed in-depth insights into environmental changes in the mangrove and sea-level ecosystems over the past 5,000 years (Punwong et al., 2013; Englong et al., 2023). The record also provides significant evidence of human-environment interactions during the Iron Age, associated with migrations of western

African-related agropastoralists to offshore islands. The Unguja Ukuu region was defined by a combination of mangrove forests and beaches, suggesting a minimal level of tidal inundation dating back to at least 3300 BCE (Englong et al., 2023). Coconut remains found in deposits from this time are thought to have been spread by natural processes, such as floating. The area experienced a rise in sea level, which caused mangrove forests to expand from 2750 BCE. This inundation is also extensively reported as the mid-Holocene sea-level rise in Tanzania from around 5950 to 2650 BCE. The sea level was stable at around 2650 BCE, but then it started to drop until around 1800 BCE. The record indicates that there was an accumulation of charcoal around 2650 BCE, as well as the presence of grasses, as demonstrated by the presence of poaceae pollen grains. Coconuts are also present. This combined evidence has been interpreted as indicating an increase in aridity during this period, which is consistent with other records indicating aridity around 2550–2150 BCE (Englong et al., 2023). A rise in sea levels was recorded from 1800 BCE. The pollen record, particle size analysis and the presence of shell fragments all indicate further sea-level rise between 600 and 1100 CE. This sea-level rise is consistent with other records from mainland Tanzania (Rufiji) and Zanzibar (Makoba Bay), which cite a rise between 750 and 1450 CE (Punwong et al., 2012; 2013; Woodroffe et al., 2015; Punwong et al., 2018; Englong et al., 2023). High charcoal content is also evident in all three cores at this site during this period. This high charcoal content could be a result of burning wood for iron smelting and slash-and-burn agriculture by agropastoral communities who immigrated to the island. After 1100 CE, the area of mangrove forest decreased, indicating a fall in sea level. These findings suggest the sea level dropped from 1300 to 1900 CE, a phenomenon that aligns with a sea-level regression along the Tanzanian coast from 1450 to 1850 CE (Åse, 1981; Punwong et al., 2018; Englong et al., 2023). However, researchers have not explored the extent to which these paleoenvironmental fluctuations influenced the emergence of complex subsistence

strategies and the dispersal of food production and food-producing communities on islands such as Unguja using isotopic and archaeo-informatic perspectives.

3.3 – The potential of isotopes and archaeo-informatics in the late Holocene archaeology of coastal eastern Africa

Rich insights into the responses of faunal and human communities to climatic change have been provided by paleontological and zooarchaeological records from eastern African sites (Marean, 1992a; b; Dale, 2007; Tryon and Faith, 2016; Prendergast and Beyin, 2018). Fossils have documented major turnover of grazing fauna as arid grasslands expanded in the interior during glacial periods in the late Pleistocene (Marean, 1992b; Kusimba, 2013; Tryon and Faith, 2016; Robinson, 2017; 2022). Conversely, the 78,000-year-long zooarchaeological record from PYS, located on the coast, demonstrates the presence of fauna adapted to both forests and grasslands throughout its period of occupation (Shipton et al., 2018; Roberts et al., 2020; Prendergast et al., 2023). Available faunal carbon and oxygen isotope records from the interior and coastal regions of mainland eastern Africa also indicate regional variability in ecological change synchronous with orbital forcing timescale climatic shifts during the last 20,000 years BP (Robinson, 2017; Chritz et al., 2019; Roberts et al., 2020; Robinson, 2022). These records from eastern Africa's interior suggest fluctuations over time between the expansion and contraction of closed woodlands and open wooded grasslands, accompanied by increased aridity. Faunal carbon and oxygen isotope values from sites in the Turkana and Lake Victoria regions, meanwhile, suggest that these regions were dominated by arid, open grasslands (Chritz et al., 2019). However, Ele Bor and Dongodien in the Turkana region had significant patches of closed woodlands from the early to late Holocene

(8,000 to 1,000 years BP) (Chritz et al., 2019). Faunal isotope values from the Lake Victoria region suggest that open grasslands existed at certain sites during the early and late Holocene. At PYS on the coastal strip of Kenya, carbon and oxygen isotope data demonstrate changes through eight strata from MIS 5 to the Iron Age (Roberts et al., 2020). These isotope data suggest a forest-dominated mosaic habitat existed in the early period, followed by a shift to open woodlands and grasslands with significant forest patches. Lastly, there was a switch back to forest-dominated mosaic habitats from the Middle Holocene to the Iron Age (Roberts et al., 2020).

Regional ecological differences between the interior and the coast appear to have influenced human-environment interactions differently in eastern Africa from the late Pleistocene to the late Holocene (White, 1983; Kingdon, 1984b; Burgess and Clarke, 2000; Olson et al., 2001). For example, foragers in the interior focused on large, arid-adapted grassland species, whereas coastal foragers focused on small, forest-adapted species (Marean, 1992b; a; Marean et al., 1994; Prendergast, 2010b; Prendergast et al., 2016; Shipton et al., 2016; Prendergast et al., 2017b; Robinson, 2017; Chritz et al., 2019; Roberts et al., 2020; Culley et al., 2021b; Robinson, 2022). From the middle to the late Holocene, food production emerged in the form of domesticated animals and plants. Interior zooarchaeological records show complex variations in the use of wild and domesticated resources and the gradual, nonlinear adoption of cattle, sheep, goats, and crops (Gifford-Gonzalez, 1998; Marshall et al., 2011; Prendergast, 2011; Robertshaw, 2021). However, before this thesis, isotope palaeoecological studies on the offshore islands of eastern Africa were absent. This is despite the global fascination with the impact of foragers on island environments and species extinction or extirpation, as well as the expansion of food production (Rick et al., 2013; Fitzpatrick et al., 2015; Braje et al., 2017).

Sedimentary, carbon and oxygen isotope data from the interior of eastern Africa and the coastal site of PYS suggest that regional vegetation changed in response to global wet and arid cycles from the late Pleistocene to the late Holocene (Robinson, 2017; Chritz et al., 2019; Robinson, 2019; Roberts et al., 2020; Chritz and Kinyanjui, 2025). While the interior of eastern Africa was characterized by the expansion of arid grasslands and the reduction of closed woodlands during arid periods, the Congo Basin and the eastern African coast were dominated by the fragmentation of dense forest mosaics, with forests sometimes disappearing entirely, as evidenced at PYS. Due to its marine ecological setting and high humidity, Unguja Island's ecological setting may have been shaped differently during wet and dry climatic cycles, with stable tropical forest-dominated mosaic habitats and mangrove forests along the coastline. The rich, well-defined and dated zooarchaeological record from the multi-stratified KC site, particularly the faunal and human data, provides an opportunity to use carbon and oxygen isotopes to gain in-depth, previously inaccessible insights into the paleoecology of the island and its impact on human-environment interactions from the late Pleistocene, when humans relied solely on foraging, to the late Holocene, when food production emerged, and food-producing communities began to disperse. The stability of forests along the coastal strip and on offshore islands in eastern Africa likely played a significant role in the endurance of indigenous foraging communities in the coastal region, even when interacting with immigrating agropastoral groups of western African descent in the Iron Age and to the present day.

The affluent, well-defined and dated caprine-dominated zooarchaeological record from the Iron Age deposits of Unguja Ukuu, Fukuchani and Panga ya Saidi, which also includes wild fauna and humans, provides an opportunity to take a multi-isotopic approach involving four major isotopes (carbon, oxygen, nitrogen and strontium) to gain in-depth, previously inaccessible insights into

caprine herding strategies and translocation at coastal sites. As Kuumbi Cave, Unguja Ukuu, and the other coastal sites are in proximity to mangrove and tropical forests, it is expected that the wild fauna would have consumed forest resources, and that the goat-dominated herds at UU would similarly have been herded on these resources. As the archaeological assemblage at UU depicts an agropastoral lifestyle, it is also likely that the herding of caprines differed from that of wild animals. Additionally, as UU was a trade port with a high population, a significant percentage of the livestock consumed there were probably translocated from mainland eastern Africa. Lastly, due to the differences in subsistence strategies at KC and UU, the human populations from these sites probably had different dietary patterns, which should be evident in the isotope records.

Although there are temporal and spatial gaps in the archaeological record of eastern Africa, an archaeo-informatics analysis and chronological representation of synthesized archaeological data from the region could provide valuable insights into the generalities and particularities evident at coastal, offshore island, and interior sites. This would help us to understand how climate-induced ecological conditions shaped complex subsistence strategies and the dispersal of food production and food-producing communities in coastal and interior regions. This synthesized dataset could also highlight major research gaps in Holocene archaeology in the region and inform strategies for addressing these gaps.

Chapter 4 – Methodological background in isotope analysis and archaeo-informatics

This chapter provides an overview of the methodological background to isotope ecology and archaeo-informatic perspectives. The first section begins with an introduction to the fundamental concepts of isotope systematics. This includes a definition of an isotope, followed by explanations of stable carbon, nitrogen, and oxygen isotope systematics, and of how isotope values are measured as ratios of heavy to light isotopes. It also covers how calculations are performed using standard reference materials and reported in delta notation (δ). It also provides a synthesis of stable carbon, oxygen, and nitrogen isotopes and their natural ratios, as well as the different standard reference materials applied per element. Lastly, the section discusses strontium isotope systematics. The second section summarizes the changes that these four isotopes undergo from the atmosphere or geosphere to the biosphere and explains how this knowledge can be used to reconstruct human–environment interactions. The third section presents the application of carbon and oxygen isotopes in palaeoecological studies, as well as multi-isotope approaches to herd management in eastern Africa and beyond. This is followed by a review of current information on the dispersal of caprines in coastal eastern Africa, along with site descriptions of Unguja Ukuu (UU), Fukuchani (FK) and Panga ya Saidi (PYS), as well as related archaeological assemblages. The fourth section reviews archaeo-informatics in archaeology on a global scale and discusses its applicability in eastern Africa. This section provides an overview of published archaeo-informatics projects, beginning with the global radiocarbon database and moving on to selected regional datasets from around the world, particularly western and central Africa. This is followed by a highlight of the late Holocene archaeology of eastern Africa, as well as the major research gaps and unresolved issues that justify

the development of the *Wanyika* dataset. The fifth section provides a summary of the key limitations and challenges in isotopic and archaeo-informatic studies, offering insights into how these were addressed in this thesis.

4.1 – Isotope systematics

Isotopes are defined as atoms of the same element that have the same number of protons and electrons but different numbers of neutrons (Aston, 1922; Thoennessen, 2016). Therefore, isotopes have the same atomic number and identity but differ in atomic mass. Isotopes can be grouped into three categories: radioactive, radiogenic, and stable. Radioactive isotopes undergo radioactive decay at a constant rate. For instance, ^{14}C is a radioactive isotope that decays into the stable isotope ^{14}N (Whitehouse and Putman, 1953; Schuur et al., 2016). Radiogenic isotopes are stable isotopes produced from the decay of radioactive isotopes (Dickin, 2018a). For instance, ^{87}Sr is a product of ^{87}Rb decay (Faure and Powel, 1972; Dickin, 2018b). Stable isotopes do not undergo decay (Craig, 1953; van der Merwe, 1992; Dawson et al., 2002; Tykot, 2004; Schwarcz and Schoeninger, 2012; Thoennessen, 2016).

Stable carbon, nitrogen, and oxygen isotope systematics

Because of their mass differences, isotopes experience separation, or fractionation, during chemical, physical, and biological processes, such as photosynthesis in the case of stable carbon isotopes (DeNiro and Epstein, 1978; Schoeninger, 1995; Cerling and Harris, 1999). This variation in reaction speed can lead to substantial discrepancies in the isotopic ratio of the substrate/reactant

(e.g., diet) and product (e.g., tissue) of a reaction. Heavier isotopes are usually less favored because their larger mass and bond strength cause chemical bonds to break and form less quickly than those involving light isotopes (Faure and Mensing, 2005; Schwarcz and Schoeninger, 2012; Thoennessen, 2016).

Stable isotope ratios are measured as the ratio R, where R is the heavy-to-light isotope ratio for a specific element (Aston, 1922; Hoefs, 2009; Thoennessen, 2016). Since the isotopic differences between materials are usually very small, the ratio is expressed as parts per thousand (‰). This notation system is used for three of the four isotopes applied in this study: carbon (C), nitrogen, and oxygen (O). The calculation of the C, N, and O ratios is performed using standard reference materials and reported in delta (δ) notation as follows:

$$\delta\ (‰) = ((R_{sample}/R_{standard}) - 1)\ X\ 1000$$

$$\delta^{13}C_{(PDB)} = (({}^{13}C/{}^{12}C)_{sample}/{}^{13}C/{}^{12}C)_{PDB} - 1)\ X\ 1000$$

$$\delta^{15}N_{(AIR)} = (({}^{15}N/{}^{14}N)_{sample}/{}^{15}N/{}^{14}N)_{AIR} - 1)\ X\ 1000$$

$$\delta^{18}O_{(PDB)} = (({}^{18}O/{}^{16}O)_{sample}/{}^{18}O/{}^{16}O)_{PDB} - 1)\ X\ 1000$$

A δ value represents the ratio of the sample to the standard (Aston, 1922; Hoefs, 2009; Thoennessen, 2016). A negative δ value means that the sample has fewer heavy isotopes compared to the standard, while a positive value means that the sample has more heavy isotopes compared to the standard. The mass difference is substantial for isotopes of lower-mass elements (e.g., ^{18}O and ^{16}O), with a 12% difference in mass (Aston, 1922; Hoefs, 2009; Thoennessen, 2016). Thus, they have very different reaction rates. Consequently, the degree of fractionation is significant.

There are three common isotopes of carbon: ^{12}C and ^{13}C are stable, while ^{14}C is radioactive (Hoefs, 2009; Schuur et al., 2016). The stable isotopes occur at a ratio of 98.9% to 1.1%, respectively (Aston, 1922; Thoennessen, 2016). Stable carbon isotope ratios are expressed in normalized form as $\delta^{13}C$. These values are relative to an international standard. Originally, the standard was Pee Dee Belemnite (PDB), but it has since been depleted. The new standard is Vienna-PDB. The ^{13}C standards have a higher value than most biological materials, so the $\delta^{13}C$ value of samples is generally negative.

Three common stable oxygen isotopes are known: ^{16}O, ^{17}O, and ^{18}O. Of these, ^{16}O is the most abundant, occurring at 99.755% (Aston, 1922; Hoefs, 2009; Thoennessen, 2016). In contrast, ^{17}O and ^{18}O are found at much lower abundances of 0.039% and 0.206%, respectively. Oxygen isotope ratios are measured as ^{18}O:^{16}O and expressed as $\delta^{18}O$. The Vienna-PDB standard is commonly used in many studies, including this one; initially, the now-exhausted Standard Mean Ocean Water (SMOW) standard was prevalent, followed by the recalibrated Vienna-Standard Mean Ocean Water (V-SMOW) standard. Differences in oxygen isotope ratios in water arise through equilibrium fractionation associated with evaporation and condensation. During these processes, isotopes are sorted due to their different vibrational energies.

There are two stable nitrogen isotopes: ^{14}N and ^{15}N (Aston, 1922; Hoefs, 2009; Thoennessen, 2016). ^{14}N occurs at a frequency of 99.6%, while ^{15}N occurs at a frequency of 0.4%. The stable nitrogen isotope ratio is expressed in normalized form as $\delta^{15}N$. These values are relative to the constant ratio of ^{15}N in atmospheric nitrogen, which is used as the reference standard. This standard, called "AIR," is used to express the isotopic composition of other nitrogen sources in terms of $\delta^{15}N$ values, which represent deviations from the atmospheric ratio.

Strontium isotope systematics

Isotopic variation in heavier isotope systems, such as strontium (Sr), is mostly reported as a ratio (e.g., $^{87}Sr/^{86}Sr$). The mass difference between isotopes of heavy elements is negligible (e.g., ^{87}Sr and ^{86}Sr have a mass difference of 1%), and this results in identical reaction rates. As a consequence, there is minimal fractionation during reactions. Strontium is an alkaline metal with four naturally occurring stable isotopes: ^{84}Sr, ^{86}Sr, ^{87}Sr, and ^{88}Sr (Faure and Powel, 1972). These isotopes are present at abundances of 0.56%, 9.87%, 7.04%, and 82.53%, respectively. Only strontium-87 (^{87}Sr) is radiogenic and is formed by the radioactive decay of rubidium-87 (^{87}Rb), which has a half-life of approximately 4.88×10^{10} years. In many studies, the $^{87}Sr/^{86}Sr$ ratio is recorded without normalization to a standard.

4.2 – Isotopes in the biosphere

Carbon

Plants that use the C_3 and C_4 photosynthetic pathways have tissues with distinct $\delta^{13}C$ values due to differences in fractionation during the fixation of CO_2. C_3 values range from about −36 to −24‰ (global mean −26.5‰) while C_4 values range from approximately −17 to −9‰ (global mean −12‰) (Craig, 1953; Smith and Epstein, 1971; Farquhar et al., 1989). This distinction is transmitted through the food chain and recorded in the tissues of consumers, including durable tissues (e.g., bones, tooth enamel) that are preserved in the archaeological record (DeNiro and Epstein, 1978; van der Merwe, 1982; Cerling and Harris, 1999). Based on the non-overlapping

distinction between C_3 and C_4 resources, animal consumer tissues have been isotopically analyzed to highlight ecological change through time in eastern Africa (Ambrose and DeNiro, 1986a; Cerling et al., 2003c; Cerling et al., 2010). Due to distinctive patterning of C_3 and C_4 between different tropical environments, a dominance of C_3 consumption has been considered indicative of forest/woodland dominance, while C_4 consumption is seen as representative of an abundance of tropical grassland (Codron et al., 2012; Crowley, 2012; Roberts et al., 2020). Within tropical forest settings, C_3 vegetation growing beneath a closed forest canopy typically has lower $\delta^{13}C$ values due to low light and recycled CO_2 (van der Merwe and Medina, 1989; 1991; Carter, 2001; Cerling et al., 2004; Garten et al., 2008; Smith et al., 2010; Iminjili, 2012; Krigbaum et al., 2013; Oelze et al., 2014; Blumenthal et al., 2016). This 'canopy effect' also influences forest consumers, notably primates, and helps distinguish canopy and under-canopy feeders.

The carbon in enamel bioapatite is derived from the bulk diet (Lee-Thorp et al., 1989; Cerling and Sharp, 1996; Cerling et al., 1997; Cerling et al., 1999; Passey and Cerling, 2002; Cerling et al., 2010), including proteins, carbohydrates, and fats, while the carbon in bone or dentin collagen is sourced from the protein component of the diet (Ambrose, 1986; Ambrose and DeNiro, 1986b; a; 1989; Lee-Thorp et al., 1989; Ambrose, 1990; Ambrose and Norr, 1993; Balasse et al., 2001). In mammals, enamel $\delta^{13}C$ values are generally enriched by +11 to +14‰ relative to the bulk diet (Cerling and Harris, 1999; Cerling et al., 2004; Lee-Thorp, 2008; Sponheimer et al., 2009; Cerling et al., 2010; Iminjili, 2012; Blumenthal et al., 2016), while collagen is enriched by around +5‰ (Ambrose, 1986; Ambrose and DeNiro, 1986b; a; Lee-Thorp et al., 1989; Ambrose et al., 1993; Ambrose et al., 2000). Before the Industrial Revolution and the subsequent impact of fossil fuel emissions on atmospheric CO_2, enamel $\delta^{13}C$ values of less than or equal to −14‰ are thought to indicate reliance on closed-canopy forest vegetation (Francey et al., 1999; Sponheimer and Lee-

Thorp, 2003; Cerling et al., 2004; Sponheimer et al., 2009; Cerling et al., 2010; Keeling et al., 2010; Lee-Thorp et al., 2010; Sponheimer, 2013). On the other hand, average values for C_3 and C_4 reliance are around −12‰ and 0‰, respectively (Lee-Thorp et al., 1989; Levin et al., 2008; Cerling et al., 2010; Cerling et al., 2015). A mean of -10 ‰ for C_3 is anticipated to signify reliance on open-canopy wood/shrub vegetation, while values between -8 ‰ and -1 ‰ indicate a combination of C_3 and C_4 vegetation (Cerling et al., 1999; Cerling et al., 2015).

Conversely, collagen $\delta^{13}C$ values of less than or equal to −20 ‰ are thought to indicate reliance on closed-canopy forest vegetation (Ambrose, 1986; Ambrose and DeNiro, 1986b; a; 1989; Lee-Thorp et al., 1989; Ambrose, 1990), while average values for C_3 and C_4 reliance are approximately −18 and −8, respectively. An average of −15‰ for C_3 is expected to indicate reliance on open-canopy wood/shrub vegetation, and values between −14‰ and −11‰ indicate a mixture of C_3 and C_4 vegetation (Ambrose, 1986; Ambrose and DeNiro, 1986b; a; 1989; Lee-Thorp et al., 1989; Ambrose, 1990). Marine and freshwater feeders are intermediate, with values between those of terrestrial C_3 and C_4 feeders (-17‰ to -12‰) (Schoeninger and DeNiro, 1984; Jim et al., 2004; Laffranchi et al., 2016; Rey-Iglesia et al., 2022). However, freshwater feeders often reflect C_3-based systems and can be enriched by C_4 plants or mixed with marine inputs (Kirkels et al., 2022; Yang et al., 2025). This makes them difficult to distinguish from terrestrial sources without nitrogen isotope analysis. These cited baseline values are treated as a working baseline for eastern Africa, as they are currently being debated in other regions of the world (Tejada et al., 2020).

Oxygen

Measuring the stable oxygen isotope values ($\delta^{18}O$) of mammalian enamel provides additional paleoecological information about feeding and drinking contexts. The $\delta^{18}O$ of vegetation in tropical ecosystems indicates either evaporative potential or the source effect of rainfall (Buchmann et al., 1997; Buchmann and Ehleringer, 1998; Giraldo et al., 2022). The relationship between the oxygen isotope of plants ($\delta^{18}O$) and their ability to evaporate can be used to estimate the density of the forest canopy. Previous studies have shown that vegetation $\delta^{18}O$ differs depending on height within the canopy and among different plant parts (da Silveira, 1989; Buchmann et al., 1997). On the other hand, animals that get most of their water from plants will be the best at recording these environmental factors (Kohn et al., 1996; 1998; Levin et al., 2006; Carter and Bradbury, 2015). Precipitation patterns vary geographically, resulting in different $\delta^{18}O$ values in animal tissues (Chritz et al., 2019; Roberts et al., 2020). The average value of fauna from the arid interior of eastern Africa is higher than 1‰, while the average value of those from the high rainfall coastal region is lower than 1‰ (Chritz et al., 2019; Roberts et al., 2020). However, climate change may have altered this difference in $\delta^{18}O$ values over time. The region's climate, vegetation, and geological deposits, as well as its $\delta^{18}O$ values, have been shaped by past orogenic events and the Intertropical Convergence Zone (ITCZ). This creates an ideal setting for a multi-isotope study of caprine husbandry (White, 1983; Janzen, 2015; Janzen et al., 2020a; Janzen et al., 2020b; Janzen, 2022). The interior of eastern Africa is characterized by vast expanses of open wooded grassland mosaics, punctuated by sporadic patches of highland and montane forests that grace the central Rift Valley. In contrast, the coastal strip and offshore islands are dominated by dense forests (White, 1983; Kingdon, 1984c; a; Burgess and Clarke, 2000; Olson et al., 2001).

A recent emphasis has been placed on the necessity of incorporating taxonomic representation bias into stable isotope approaches to African fauna (Cerling et al., 2015; Robinson, 2017; Roberts et al., 2020). This bias must be taken into account when conducting isotopic comparisons, and recent studies have been careful to do so, taking into account feeding behaviors such as browsing, grazing, mixed feeding, and omnivorous diets (Cerling et al., 2015; Robinson, 2017; Roberts et al., 2020).

Nitrogen

Nitrogen isotope ($\delta^{15}N$) measurement of mammalian bone and dentine collagen provides information on whether the source of the protein content is terrestrial, marine or freshwater resources (Schoeninger and DeNiro, 1984; Ambrose, 1986; Ambrose and DeNiro, 1986b; Tykot et al., 1996; Iacumin et al., 1998; Ostrom and Ostrom, 1998; D'Andrea et al., 2011; Schwarcz and Schoeninger, 2012; Schoeninger, 2014; Cartigny and Busigny, 2018; Dyvart et al., 2018; Moore et al., 2020; Leggett et al., 2021; Leichliter et al., 2022; Leichliter et al., 2023). $\delta^{15}N$ values can also distinguish dense forest feeders and arid open woody grasslands (Ambrose, 1986; Ambrose and DeNiro, 1986b; Sealy et al., 1987; Ambrose and DeNiro, 1989; Evans, 2001; Garten et al., 2008; Murphy and Bowman, 2009; Hartman, 2011; de Freitas et al., 2015). Nitrogen isotope values distinguish between plants with nitrogen-fixing bacteria, such as legumes, and those without (Hogberg, 1997; Dawson et al., 2001; Dawson et al., 2002; Liao et al., 2006; Schwarcz and Schoeninger, 2012; Szpak, 2014; Craine et al., 2015a; Craine et al., 2015b).

On average, legumes have $\delta^{15}N$ values of 0‰, while other plants have higher $\delta^{15}N$ values. The highest $\delta^{15}N$ values in plants are associated with arid environments and saline soils (Ambrose, 1986; Ambrose and DeNiro, 1986a; 1989; Ostrom and Ostrom, 1998; Gerschlauer et al., 2019).

Plants growing in marine environments also have high nitrogen isotope values due to the sea spray effect (Ostrom and Ostrom, 1998; Cartigny and Busigny, 2018). The lowest $\delta^{15}N$ values in leguminous plants are found in moist forests and montane areas (Ambrose, 1986; Ambrose and DeNiro, 1986a; 1989). Variations in plant $\delta^{15}N$ values are predominantly dictated by soil $\delta^{15}N$ values (Mudge et al., 2014; de Freitas et al., 2015; Gerschlauer et al., 2019). Nitrogen fixation adds $\delta^{15}N$-depleted nitrogen to the soil, while denitrification increases soil nitrogen values (Ambrose and DeNiro, 1989; Ostrom and Ostrom, 1998; Dawson et al., 2001; Dawson et al., 2002). The cumulative effect of these processes is an increase in soil nitrogen isotope values (Hopkins et al., 2020). However, soil dryness and high temperatures inhibit nitrogen fixation. Overall, cool, moist forest soils have higher rates of nitrogen fixation and mineralization and lower $\delta^{15}N$ values than hot, dry savanna and desert soils (Dawson et al., 2002; de Freitas et al., 2015).

There is a 3-4‰ increase in collagen $\delta^{15}N$ values between animals and their diets, as well as a similar stepwise enrichment in $\delta^{15}N$ values in each trophic level, from plants to herbivores to carnivores (Deniro and Epstein, 1981; Schoeninger and DeNiro, 1984). In tropical mosaic habitats, such as those in eastern Africa, the dominant open grasslands generally have higher $\delta^{15}N$ values than sparsely distributed large, dense forests (Ambrose, 1986; Ambrose and DeNiro, 1986a; 1989). This difference in $\delta^{15}N$ value baselines is also reflected in animals that feed in these environments. Typically, wild animals that feed on grasses in arid, open lands have higher $\delta^{15}N$ values (6-10‰), while those that feed in dense, forested habitats have values below 5‰ (Ambrose and DeNiro, 1986a; 1989). Animals feeding on marine resources have higher $\delta^{15}N$ and also $\delta^{13}C$ values than animals feeding on terrestrial resources (Schoeninger and DeNiro, 1984). Freshwater feeders have highly variable $\delta^{15}N$ values (6-16‰), but on average lower than marine (14-18‰) but higher than

pristine terrestrial feeders (0-10‰) (Schoeninger and DeNiro, 1984; Tykot et al., 1996; Iacumin et al., 1998; Ostrom and Ostrom, 1998; Carter, 2001; Anderson and Cabana, 2006; Kiura, 2008a; D'Andrea et al., 2011; Schwarcz and Schoeninger, 2012; Makarewicz, 2014; Cartigny and Busigny, 2018; Kochi et al., 2018; Marchenko et al., 2021).

Strontium

The $^{87}Sr/^{86}Sr$ ratios fluctuate geologically, contingent on the composition of the rock and its geologic age (Faure and Powel, 1972; Sealy et al., 1991; Blum et al., 1993; Capo et al., 1998; Holt et al., 2021; Guiserix et al., 2022). The decay of ^{87}Rb in minerals is what causes radiogenic ^{87}Sr variations (Faure and Powel, 1972; Capo et al., 1998; Bentley, 2006b; Holt et al., 2021). Soils with older minerals therefore have relatively high amounts of ^{87}Sr, with $^{87}Sr/^{86}Sr$ ratios up to 0.716. Conversely, rocks formed within the last 10 million years have low $^{87}Sr/^{86}Sr$ ratios, generally below 0.704. Strontium is relatively abundant in marine waters, with a concentration of 8 ppm (Faure and Powel, 1972; Sealy et al., 1991; Alonzi et al., 2020). The modern $^{87}Sr/^{86}Sr$ ratio in seawater is uniform (0.709) and is often higher than the ratio in freshwater (Åberg et al., 1989; Capo et al., 1998; Alonzi et al., 2020). However, the $^{87}Sr/^{86}Sr$ ratio of precipitation is similar to that of ocean water, yet the strontium concentration is much lower (Åberg et al., 1989). Through the effects of precipitation and sea spray, a small amount of marine strontium ends up on continents (Capo et al., 1998; Blum et al., 2000).

The $^{87}Sr/^{86}Sr$ ratios of terrestrial water bodies are also affected by weathering, which is basically the chemical breakdown of bedrock. In rivers, this occurs in the catchment area through which the river flows. Lakes reflect the strontium concentrations and $^{87}Sr/^{86}Sr$ ratios of inflowing rivers and

groundwater (Ojiambo et al., 2003). The mass discrepancy between ^{87}Sr and ^{86}Sr is so minuscule (less than 1%) that mass-dependent fractionation is unremarkable when strontium is absorbed up the food chain. However, it is important to note that weathering and ash can also affect strontium levels. Additionally, plants sample different parts of the soil for bioavailable strontium, and animals have different ranges (Faure and Powel, 1972; Åberg et al., 1989; Capo et al., 1998; Ojiambo et al., 2003; Bentley, 2006a; Szostek et al., 2015; Snoeck et al., 2019; Janzen et al., 2020b; Plomp et al., 2020; Tarrant et al., 2024). The isotopic signal of a source is transmitted without significant change to organisms. This makes strontium a useful indicator of animal and human migration among areas with different geologies (Sealy et al., 1991; Koch et al., 1995; Schoeninger, 1995; Capo et al., 1998; Bentley, 2006b; Evans et al., 2006; Evans and Chenery, 2006; Szostek et al., 2015; Fenner et al., 2016; Henton et al., 2017; Janzen et al., 2020b; Moore et al., 2020; Plomp et al., 2020; Lazzerini et al., 2021; Leggett et al., 2021; Valenzuela-Suau et al., 2022).

For in-depth background information on $\delta^{13}C_{coll}$ and $\delta^{15}N$, and $\delta^{13}C_{enamel}$ and $\delta^{18}O$ and $^{87}Sr/^{86}Sr$ values in eastern Africa, systematics, and instrumentation, refer to earlier publications (Ambrose, 1986; Ambrose and DeNiro, 1986b; a; 1989; Ambrose, 1993; Cerling et al., 1997; Balasse et al., 2001; Balasse and Ambrose, 2005; Janzen, 2015; Janzen et al., 2020b; Roberts et al., 2020).

4.3 – Application of isotopes in human palaeoecological reconstruction and animal husbandry

Stable isotope analysis and human palaeoecology in eastern Africa

Stable carbon and oxygen isotope values have been widely used to reconstruct the diets and paleoenvironments of hominins and herbivores dating from 6 million to 100 thousand years ago in eastern Africa and other regions of the continent, including South Africa and North Africa (Lee-Thorp et al., 2003; Cerling et al., 2011a; Lee-Thorp et al., 2012; Cerling et al., 2013; Lee-Thorp and Sponheimer, 2013; Sponheimer, 2013; Sponheimer et al., 2013; Wynn et al., 2013; Wynn et al., 2020; Iminjili and Fernandes, 2023). These values have provided revolutionary insights into paleoanthropology (Cerling et al., 1999; Sponheimer et al., 2006b; Levin et al., 2008; Lee-Thorp et al., 2010; White et al., 2010; Cerling et al., 2011b; Cerling et al., 2013). The results of these studies, for example, suggest that early hominins did not evolve bipedalism in savanna grasslands but rather in mosaic habitats (Wynn, 2004; Levin et al., 2008; White et al., 2009; Cerling et al., 2011b; Wynn et al., 2013; Wynn et al., 2020). Isotope values also show that, overall, in eastern Africa, Pliocene hominins and wild fauna consumed more C_3 than C_4 foods, whereas Plio-Pleistocene hominins and wild fauna consumed more C_4 than C_3 foods (Cerling et al., 1999; Cerling et al., 2003a; Cerling et al., 2003b; Cerling et al., 2005; Levin et al., 2008; Sponheimer et al., 2009; Cerling et al., 2010; Cerling et al., 2013; Cerling et al., 2015). It is noted that many browsing taxa were replaced by grazing taxa due to dramatic climatic shifts during the Pliocene–Pleistocene era (Bobe and Eck, 2001; Bobe et al., 2002; Bobe and Behrensmeyer, 2004; Bobe, 2006; Bobe, 2011; Bobe and Carvalho, 2019). The results also demonstrate that different hominin species had distinct

dietary patterns, with some specializing in C_3 or C_4 diets, while others consumed a mixture of both (Malone et al., 2021; Iminjili and Fernandes, 2023).

In contrast to these earlier periods, only a few isotopic studies have been conducted to reconstruct the palaeoenvironments in eastern Africa during the late Pleistocene to late Holocene, and most of these studies have focused on the interior (Figure 2.6-7 and Table A1:2) (Robinson, 2017; Chritz et al., 2019; Robinson, 2019). Before the KC study, only one study had been conducted at the coastal site of PYS (Roberts et al., 2020). Despite their limited number, these studies have provided valuable palaeoecological insights. Faunal isotope records from sites in the interior of eastern Africa from the late Pleistocene to the late Holocene suggest that, over time, there were fluctuations between the expansion and contraction of closed woodlands and open woody grasslands (Robinson, 2017; Chritz et al., 2019; Prendergast et al., 2019a; Robinson, 2019; Chritz and Kinyanjui, 2025). These fluctuations occurred in synchrony with orbital forcing timescale climatic shifts and an increase in aridity. Grazers, particularly Alcelaphini from Lukenya, show an increase in $\delta^{13}C$ values over time, as depicted by the median values: 0‰ for the Late Pleistocene (9,000 years BP), 1‰ for the Early-Mid Holocene (5,000 years BP), and 3‰ for the Late Holocene (2,000 years BP) (Robinson, 2017; 2019). These $\delta^{13}C$ values differ from those of neighboring modern Athi ecosystem grazers, which have a median value of 4‰ (Robinson, 2019). Faunal $\delta^{13}C$ and $\delta^{18}O$ values from four occupational units at Kalemba in Zambia, dated by material culture, also show shifts in patterns (Robinson, 2017). The $\delta^{13}C$ values of grazers, fresh grass grazers, and mixed feeders have shifted from high values (0‰) toward low values (−10‰). However, the $\delta^{18}O$ values have shifted from low values (−6‰) toward high values (0‰) throughout the MSA, MSA-LSA

transition, and the early and late LSA. The shift in $\delta^{18}O$ values has been used to argue for an increase in aridity (Robinson, 2017).

Faunal $\delta^{13}C$ and $\delta^{18}O$ enamel values from the Turkana and Lake Victoria regions of eastern Africa suggest that arid, open grasslands dominated these areas during certain periods of the Holocene (Chritz et al., 2019). However, the Ele Bor and Dongodien sites in the Turkana region had significant patches of closed woodlands during certain times of the early to late Holocene (10,000 to 1000 years BP) (Chritz et al., 2019). Wild animal isotope data from Ele Bor, particularly the decrease in $\delta^{13}C$ values between the early and late Holocene, suggest a significant expansion of woodlands. Contexts dated to 7500 BP have higher and less variable $\delta^{13}C$ values (mean −3.4‰, range −8.9 to 2.4‰) than contexts dated to 4600 BP (mean −3.9‰, range −12.4 to 4‰) and 1300 BP (mean −4.6‰, range −12.6 to 3.3‰). A significant fraction of woodlands in the Turkana region is suggested by the presence of several $\delta^{13}C$ and $\delta^{18}O$ values lower than the mean of wild animals (n = 13, mean −2.1‰, range −6 to 0.3‰ and mean 2.8‰, range 0.4 to 5.3‰, respectively) and caprines (n = 20, mean −3.9‰, range −7.9 to 0.1‰ and mean 4.5‰, range 1.5 to 6.7‰, respectively) from Dongodien (3950 BP) (Chritz et al., 2019). Conversely, the $\delta^{13}C$ and $\delta^{18}O$ values of wild animals (n = 24, mean 0.1‰, range −6.9 to 3.1‰ and mean 0.6‰, range −2.4 to 4.9‰, respectively) from Lothagam Lokaam (8300 BP) suggest the dominance of arid, open grasslands at this site during the early Holocene (Chritz et al., 2019).

Faunal $\delta^{13}C$ and $\delta^{18}O$ values from the Lake Victoria region indicate the presence of open grasslands in certain areas during the early and late Holocene (Chritz et al., 2019). Isotope data from wild fauna indicate the dominance of open grasslands at the Luanda site (8400 BP). The dominance of

higher (>−2‰) $\delta^{13}C$ (n = 53, mean 0.8‰, range −11.8 to 3.9‰) and $\delta^{18}O$ values (mean −1.4‰, range −5.5 to 2.3‰) suggest this (Chritz et al., 2019). A similar pattern is reflected in the $\delta^{13}C$ (n = 14, mean −1.5‰, range −8.7 to 3.3‰) and $\delta^{18}O$ values (mean −1.6‰, range −3.7 to 0.4‰) of wild fauna from Kanam (8200 BP). These patterns, characterized by high values, also recur during the late Holocene, as evidenced by the wild fauna $\delta^{13}C$ (n = 17, mean = 1.0‰, range = −3.3 to 3.0‰) and $\delta^{18}O$ values (mean = 2.5‰, range = −1.6 to 5.7‰) and caprine $\delta^{13}C$ (n = 19, mean = 1.1‰, range = −2.2 to 4.1‰) and $\delta^{18}O$ values (mean = 2.5‰, range = −2.4 to 5.4‰) from Wadh Lang'o (1300 to 1800 BP) (Chritz et al., 2019). Similar patterns are evident in wild animal $\delta^{13}C$ (n = 59, mean = 0.1‰, range = −9.6 to 3.2‰) and $\delta^{18}O$ values (mean = 0.5‰, range = −3 to 2.4‰) and in caprine $\delta^{13}C$ (n = 14, mean = 0.3‰, range = −2.1 to 2.6‰) and $\delta^{18}O$ values (mean = 1.9‰, range = −2.7 to 4.3‰) from Gogo Falls (1700 BP) (Chritz et al., 2019).

PYS is a multi-stratified site with deposits that document several time periods from the late Pleistocene to the Iron Age (Roberts et al., 2020; Culley et al., 2021a; Faulkner et al., 2021; Prendergast et al., 2023). The PYS $\delta^{13}C$ and $\delta^{18}O$ values demonstrate a change across eight strata, from MIS 5 to the Iron Age (Shipton et al., 2018; Roberts et al., 2020; Faulkner et al., 2021). MIS 5 (>75,000 years BP) is marked by low median $\delta^{13}C$ and $\delta^{18}O$ values of −13‰ and −3.5‰, respectively. However, these values increased to −3‰ and −2.5‰ in MIS 4 (65,000–55,000 years BP). From MIS 3 (60,000–30,000 years BP) to the Terminal Pleistocene (15,000–14,000 years BP), the $\delta^{13}C$ and $\delta^{18}O$ values remained above −3‰ and −2.5‰, respectively (Roberts et al., 2020). Conversely, during the Middle Holocene (7,600–7,700 years BP), the $\delta^{13}C$ and $\delta^{18}O$ values decreased to −6‰ and −3.5‰, respectively. There was another drop in $\delta^{13}C$ and $\delta^{18}O$ values, reaching −10‰ and −3.5‰, during the Iron Age (1200–300 years BP) (Roberts et al., 2020). These

trends are evident when the isotope values are analyzed according to taxonomic categories split by feeding groups. These isotope value patterns suggest a transition from a dense forest-dominated habitat in the early period, to an increase in the dominance of open woodlands and grasslands, and finally, to a switch to forest-dominant mosaic habitats from the Middle Holocene to the Iron Age (Roberts et al., 2020).

To attain a comprehensive understanding of the similarities and differences in ecological settings and transformations over time in coastal and island settings versus the interior of eastern Africa from the late Pleistocene to the late Holocene, isotopic studies must expand to include the offshore islands of eastern Africa. In the first case study, I use zooarchaeological data to interpret and analyze isotopic data from a faunal assemblage and two human samples. This allows me to explore human paleoecology at KC and the degree to which forest cover changed near the site from the late Pleistocene to the Holocene (see Figures 2.6-7 and Table A1:1). Kuumbi Cave (KC) provides a rare opportunity to study zooarchaeological and other archaeological assemblages ranging from the late Pleistocene to the late Holocene in an eastern African island setting (Prendergast et al., 2016; Shipton et al., 2016). The site is located on the south-eastern coast of Unguja Island (see Figures 2.6–7). A stratigraphic sequence in Trench 10 that captures significant time periods during the last 20,000 years BP was exposed by investigations by the Sealinks Project at KC. These include periods of major climate change and island formation (Prendergast et al., 2016; Shipton et al., 2016). The sequence is divided into four phases (IV-I) (see Figure 3.1), with a gap in human occupation between phases II and I (Shipton et al., 2016). The phases before food production (IV, III and II) are defined by the absence of domesticated plants and animals, as well as the material culture associated with them (for example, iron and pottery). Stone artefacts manufactured using the bipolar technique dominate these phases, as do bone artefacts used as projectile points or awls

(Langley et al., 2016). The faunal remains are dominated by small forest-adapted bovids, monkeys, hyrax, and giant rats, with a smaller percentage of larger animals that fluctuate over time (Prendergast et al., 2016). Fish bones, land snails, and marine shells are also present in these phases. A range of domesticates were identified in earlier projects (Sinclair et al., 2006; Chami, 2007, 2009). However, to date, the Sealinks project has only identified one goat specimen from Phase I (Iron Age; Figure 3.1) (Prendergast et al., 2016; Shipton et al., 2016; Culley et al., 2021b).

Multi-isotope approaches to herd management in eastern Africa and beyond

$\delta^{13}C_{coll\ and\ enamel}$ and $\delta^{15}N$ values from livestock have yielded important insights into management of herds in eastern Africa and other parts of the world (Schoeninger and DeNiro, 1984; Ambrose, 1986; Ambrose and DeNiro, 1986a; b; 1989; Balasse and Ambrose, 2005; Finucane et al., 2006; Balasse, 2014; Samec et al., 2018; Kinaston, 2023; Eerkens et al., 2024). In the tropical eastern Africa region, it is expected that livestock raised in wildlands using a pseudo-wild (relaxed) herding strategy in surrounding forest, woodland, and grassland habitats will have $\delta^{13}C$ and $\delta^{15}N$ value patterns similar to those of wild herbivores. Typically, grazers have higher $\delta^{13}C$ values, while browsers have lower ones (Ambrose and DeNiro, 1986a; 1989). Mixed feeders have intermediate values. In the event of climate change leading to a switch in vegetation (e.g., forest to grasslands), herbivores will also reflect a switch in their $\delta^{13}C$ values from serial samples (Janzen, 2015; Makarewicz and Pederzani, 2017; Ventresca Miller and Makarewicz, 2017; Janzen et al., 2020a; Janzen, 2022).

$\delta^{13}C_{coll}$ and $\delta^{15}N$ values can also be used to study specific differences in livestock diets (Schoeninger and DeNiro, 1984; Makarewicz and Tuross, 2006; 2012; Marciniak et al., 2017;

Pickard et al., 2017; Ventresca Miller and Makarewicz, 2017; Kinaston, 2023). For example, when introduced to C_4 crops and grasses raised on manured farms (through free-ranging or foddering), browsing livestock in C_3-dominated wild habitats exhibit a shift to high $\delta^{13}C_{coll}$ and $\delta^{15}N$ values (Bateman and Kelly, 2007; Fraser et al., 2011; Gillis et al., 2020; Kinaston, 2023). Grazing livestock also exhibit a shift to low values when fed on C_3 resources. Similarly, high $\delta^{13}C_{coll}$ and $\delta^{15}N$ have even documented contributions of seaweed to livestock diets in Neolithic Scotland (Schulting et al., 2017; Blanz et al., 2020). Plants growing in abandoned pastoralist settlements have higher $\delta^{15}N$ values than surrounding regions due to inputs of waste into the soil (Shahack-Gross et al., 2008; Macharia et al., 2012; Marshall et al., 2018), while plants growing in marine waste middens have high $\delta^{13}C_{coll}$ and $\delta^{15}N$ values (Blanz et al., 2019). These patterns are transmitted to herbivores that feed on these sites and are detectable in the $\delta^{13}C_{coll}$ and $\delta^{15}N$ isotopes of modern and archaeological skeletal remains.

Oxygen ($\delta^{18}O$) and strontium ($^{87}Sr/^{86}Sr$) values have provided insights into water use and climate change and mobility patterns in eastern Africa, respectively (Levin et al., 2006; Janzen, 2015; Chritz et al., 2019; Janzen et al., 2020b; Roberts et al., 2020). Regional differences in precipitation patterns lead to variations in the $\delta^{18}O$ values of tissues from animals (Chritz et al., 2019; Roberts et al., 2020). Fauna from the arid interior of eastern Africa, on average, have values higher than 1‰, and those from the high rainfall coastal region have values lower than 1‰ (Chritz et al., 2019; Roberts et al., 2020). Past orogenic events and the Intertropical Convergence Zone (ITCZ) have shaped the regional differences in climate, vegetation, and geological deposits in eastern Africa, creating an ideal setting for a multi-isotope study of caprine husbandry (White, 1983; Janzen, 2015; Janzen et al., 2020b). The interior of eastern Africa is dominated by open wooded grassland mosaics with patches of highland and montane forests along the central Rift Valley, while the

coastal strip and offshore islands are dominated by dense forests (Kingdon, 1984a; Burgess and Clarke, 2000; Kingdon, 2001).

Strontium isotope values have also provided insights into mobility patterns across regions with geological deposits of different ages (Janzen, 2015; Janzen et al., 2020b). Older deposits have higher $^{87}Sr/^{86}Sr$ values, while younger deposits have lower values. A baseline $^{87}Sr/^{86}Sr$ map for the eastern African region is now available (Janzen et al., 2020b). The interior of eastern Africa bordering the coast and offshore islands is characterized by ancient deposits, including the Neoproterozoic Mozambique Belt (1.000–541 million years ago), which has an average $^{87}Sr/^{86}Sr$ value of 0.710–0.712, and the Carboniferous Karoo rocks (359–299 million years ago), which have an average $^{87}Sr/^{86}Sr$ value of 0.708, as found in the Tanga/Duruma Basin in southeastern Kenya. Unguja Island is dominated by Pliocene-Pleistocene and Holocene deposits with an average predicted $^{87}Sr/^{86}Sr$ value of ~0.704 (Janzen et al., 2020b). The presence of fauna and human remains with $\delta^{18}O$ and $^{87}Sr/^{86}Sr$ values in bulk enamel samples that differ from those of the local meteoric water line and geological deposits has been interpreted as indicating immigration (Capo et al., 1998; Price et al., 2000; Wright, 2005b; Bentley, 2006b; Evans et al., 2006; Evans and Chenery, 2006; Buzon et al., 2007; Julien et al., 2012; Janzen, 2015; Szostek et al., 2015; Janzen et al., 2020a; Janzen et al., 2020b; Moore et al., 2020; Plomp et al., 2020; Lazzerini et al., 2021; Leggett et al., 2021; Janzen, 2022). A shift in these values in sequential enamel samples indicates migration to different regions with different rainfall patterns and geological deposits of different ages (Janzen, 2015; Janzen et al., 2020a; Janzen et al., 2020b; Janzen, 2022). These mobility patterns may be associated with pastoral nomadism or the agropastoral search for fertile land and iron ore.

In eastern Africa, modern caprine herding falls into two categories: wildland (extensive/rangeland) and farmland (intensified/crop-linked) (Kenyatta, 1968; Galaty, 1982; Galaty, 1993; Bollig and Wotzka, 2013; Galaty, 2016; Liu, 2019; De Glanville et al., 2020; Galaty, 2021; Greiner et al., 2021). The difference is primarily shaped by the herders' subsistence strategy: pastoralists, who rely solely on livestock, versus agropastoralists, who engage in mixed livestock and crop farming. Wildland caprine herding is a pseudo-nature management strategy involving pseudo-free-range mobility patterns dictated by the herders (Galaty, 1982; Galaty, 1993; Bollig and Wotzka, 2013; Galaty, 2021). In this type of herding, the livestock are released from the kraal in the morning to graze in the wildlands, while the herders keep watch for attacks by wild animals. The animals graze on wild vegetation in patterns similar to wild animals before returning to the kraals in the evening. Wildland herding also involves nomadic and transhumance mobility patterns. In contrast, farmland herding involves herding caprines on family farms (Kenyatta, 1968; Sutton, 1994–95; Sutton, 1998b; Liu, 2019). They feed mostly on crop residues grown using manure from various sources, including marine sources in coastal areas. However, in many cases, livestock are confined to farmland by fences, tethers, or pens. Free-range feeding in farmland herding is minimal. Cushitic- and Nilotic-speaking pastoralists predominantly practice wildland herding, while Bantu-speaking agropastoralists practice farmland herding (Kenyatta, 1968; Galaty, 1982; Galaty, 1993; Sutton, 1993a; Galaty, 2016; Liu, 2019; Galaty, 2021).

The patterns observed in the zooarchaeological record of livestock remains suggest that wildland caprine herd management was the dominant herding strategy adopted during the Neolithic period in the interior of eastern Africa (Bower et al., 1977; Gifford-Gonzalez and Kimengich, 1984; Ambrose and DeNiro, 1989; Robertshaw, 1990a; Ambrose, 1998; Gifford-Gonzalez, 1998; Le Meillour et al., 2023). Sheep husbandry seems to have been preferred in vast grasslands and grew

more rapidly than goat husbandry in the interior of eastern Africa. However, during the Iron Age, immigrating agropastoralists introduced farmland herding, emphasizing feeding and foddering with C_4 crops (mainly sorghum and millet) and grasses (Ambrose et al., 1984; Lane, 2004; Giblin, 2008; Giblin and Fuller, 2011; Crowther et al., 2016a; Crowther et al., 2016b; Crowther et al., 2018; Goldstein et al., 2024).

The trajectory of caprine husbandry at the coast was shaped differently to that in the interior of eastern Africa by a complex interplay of immigrating agropastoralists interacting with foraging communities engaged in specialized forms of hunting and gathering, the intensification of marine resource exploitation and Indian Ocean commerce (Fitton and Wynne-Jones, 2017; Prendergast et al., 2017b; Wynne-Jones and LaViolette, 2018; Roberts et al., 2020; Wynne-Jones et al., 2021). Goats appeared earlier than sheep on the islands of eastern Africa and became dominant perhaps as a result of the woody and forested habitats on these islands that provide abundant browse (Culley et al., 2021b). Indeed, mosaic coastal forests would have favoured wild caprine herding with goats browsing in the dense forests and sheep grazing in the open grasslands. By contrast, agropastoralism and the marine lifestyle on the coastal strip and islands could have led to farmland herding and foddering on nitrogen-enriched C_4 crop residues and grasses and marine resources such as seaweed (Crowther et al., 2016a; Fitton and Wynne-Jones, 2017; Prendergast et al., 2017b; Schulting et al., 2017; Crowther et al., 2018; Faulkner et al., 2018; Blanz et al., 2019; Faulkner et al., 2019; Kotarba-Morley et al., 2022).

Coastal sheep herding communities elsewhere have been shown to have diverse practices, including use of seaweed as animal feed (Schulting et al., 2017; Blanz et al., 2019; Blanz et al., 2020). Trade networks and large urban populations at coastal trade ports could have also ensured

a regular supply of livestock, including caprines, as food from eastern Africa's mainland (Horton and Middleton, 2000; Horton, 2017; Wood et al., 2017; Wynne-Jones and LaViolette, 2018). Only a few isotope studies of caprine husbandry have been conducted in eastern Africa, and they are mainly from the interior and have used bulk samples (Ambrose and DeNiro, 1986a; 1989; Chritz et al., 2019; Prendergast et al., 2019a). The results indicate high variability in the caprine isotope values. Caprines from Pastoral Neolithic sites show a dominance of wildland caprine herding strategy and highlight the effect of aridity on $\delta^{13}C_{coll}$, $\delta^{13}C_{enamel}$, $\delta^{15}N$, and $\delta^{18}O$ values (Ambrose and DeNiro, 1989; Chritz et al., 2019; Prendergast et al., 2019a).

In the second case study, I use a multi-isotope study on wild fauna, caprines, and human remains from UU, FK, and PYS to study caprine husbandry at the coast (Table A2:1 to A2:3) (Prendergast et al., 2017b; Faulkner et al., 2018; Roberts et al., 2020; Culley et al., 2021a; Culley et al., 2021b). I also include the associated archaeological assemblages to aid in interpreting the isotope data (Prendergast et al., 2017b; Roberts et al., 2020). Unguja Ukuu, a prominent commercial hub during the Middle Iron Age, is situated along the southwestern shore of Unguja Island, which is part of the Zanzibar Archipelago (Juma, 2004; Horton, 2017; Wynne-Jones et al., 2021). It has two well-dated phases. The Early Phase dates between 650 to 800 CE and the Late Phase between 800 to 1050 CE (Crowther et al., 2016b; Crowther et al., 2018; Faulkner et al., 2018; Kotarba-Morley et al., 2022). Fukuchani is a Middle Iron Age agropastoralists site located on the northwestern coast of Unguja Island and dates between 601 to 800 CE (Crowther et al., 2016a; Crowther et al., 2016b; Prendergast et al., 2017b; Faulkner et al., 2018). Panga ya Saidi located on the southern Kenya coastal strip, has a Late Iron Age foragers stratum that dates between 1300 to 1600 CE (Roberts et al., 2020; Culley et al., 2021a; Faulkner et al., 2021). It is a multi-stratified site with deposits dating between the late Pleistocene to the late Holocene (Roberts et al., 2020; Faulkner et al., 2021).

Comparative caprine and faunal isotope datasets from KC (Table A2:4), a Pleistocene-Holocene multi-stratified foragers site, and Neolithic and Iron Age (Table A2:5 and A2:6) sites in the interior of eastern Africa provide the basic datasets to interpret the UU, FK and PYS datasets (Ambrose and DeNiro, 1989; Chritz et al., 2019; Prendergast et al., 2019a). I also include unpublished and published human isotopes data from UU, KC, and PYS (values from four individuals, Table A2:3) (Roberts et al., 2020).

4.4 – Archaeo-informatics in eastern Africa and beyond

Archaeo-informatics is an interdisciplinary field that bridges archaeology and computer science (Fischer-Ausserer et al., 2003; Marwick, 2017; LeFebvre et al., 2019; Fisher, 2020; Anderson, 2024; Schmidt and Hageneuer, 2024). It uses computational tools, databases, and data management systems, such as geographic information systems (GIS), artificial intelligence (AI), and web platforms like Pandora, to integrate, analyze, and visualize vast amounts of archaeological data (Russell et al., 2014; Kay et al., 2019; LeFebvre et al., 2019; Fisher, 2020; Bird et al., 2022; Goldstein et al., 2022a; Billings et al., 2025). These data include scientific dates, which are used to build complex chronologies, test hypotheses about past human-environment interactions, expose research gaps, and create accessible digital archives (Russell et al., 2014; Kay et al., 2019; Bird et al., 2022; Anderson, 2024). Archaeo-informatics helps researchers manage thousands of dates, contextualize them with site data (location, context, and materials), convert them to calendar dates using calibration curves, and apply statistical methods to build robust timelines (Fisher, 2020; Moullou et al., 2024). This allows researchers to move beyond single dates and understand broader prehistoric periods.

Scientific dates and other archaeological records from around the world are being synthesized and used for archaeo-informatic modeling and other types of analysis at regional, continental, and global scales (Hamilton and Buchanan, 2007; Steele, 2010; Buchanan et al., 2011; Russell et al., 2014; Chaput et al., 2015; Williams et al., 2015; Shennan, 2018; Kay et al., 2019; Bird et al., 2022). However, this had yet to be done for the eastern African region before my publication. These archaeo-informatics-oriented datasets have helped systematically identify existing research gaps and novel insights on human-environment interactions at regional to global scales (Crombé and Robinson, 2014; Russell et al., 2014; Kay et al., 2019; Loftus et al., 2019; Bird et al., 2022). Synthesizing archaeological data into an archaeo-informatics-oriented dataset will highlight major research gaps in eastern African archaeology and open doors to modeling and other insightful analyses. These analyses will provide in-depth insights into the dispersal of novel cultures and food production, which are useful for testing indigenous continuity and migration hypotheses and for building theories at the global scale.

The Global Archaeological Radiocarbon Database is being assembled to serve noble archaeo-informatic objectives (Bird et al., 2022). The database currently contains 180,070 radiocarbon dates from various regions worldwide. The database increases the reusability of these dates, opening new avenues for comparative research on human-environment interactions and the evolution of social-ecological systems worldwide. The database will be useful for paleodemographic research, Bayesian modeling, summed probability distribution (SPDs) methodologies, and more (Bird et al., 2022). This global database is a product of multiple projects that have worked over the past decade to develop regional databases (Bird et al., 2022). However, eastern Africa was not included in these projects and is inadequately represented in the global database (Bird et al., 2022). The regional studies discussed below provide an overview of what to expect from these methodologies if applied

in eastern Africa and also on a global scale, especially with regard to hypothesis testing and theory development.

Analyses of regional radiocarbon databases from Europe, north America, and western and central Africa provide valuable insights into the usefulness of archaeological radiocarbon dates in archaeo-informatics studies (Gkiasta et al., 2004; Davison et al., 2006; Russell et al., 2014; Chaput et al., 2015; Kay et al., 2019; Bird et al., 2020). The updated European radiocarbon database contains 26,000 dates and has been used for statistical analyses, such as Bayesian modeling and summed probability distributions (SPDs), to study the Neolithic transition (c. 7000–4000 BCE) (Gkiasta et al., 2004; Williams, 2012). Previous analyses of this database indicated the widespread movement of farmers from the Near East. However, the latest analyses, which include large quantities of radiocarbon dates and aDNA, suggest a complex interplay of rapid demographic changes related to immigrating farmers and indigenous population continuity (Gkiasta et al., 2004). In north America, the Canadian Archaeological Radiocarbon Database, which contains over 35,000 radiocarbon dates, was analyzed using the kernel method (Chaput et al., 2015). The spatial distribution of the dates was used to estimate population density at 500-year intervals. Spatial and temporal differences associated with paleodemographic trends that align with genetic, archaeological, and ethnohistoric evidence of human occupation in the region are revealed by the resulting maps. These results have implications for hypothesizing and testing migration routes into and across north America. They also have implications for the relative influence of north American populations on the evolution of the north American ecosystem (Chaput et al., 2015).

An atlas of land use practices from nine time periods spanning from 1800 BCE to 1500 CE was developed using a radiocarbon database in western Africa (Kay and Kaplan, 2015; Kay et al.,

2019). The database synthesizes archaeological, archaeobotanical, archaeozoological, historical, linguistic, genetic, and ethnographic data and classifies current land use into 12 categories. Maps generated from the database illustrate the irregular and nonlinear trajectory of land use changes in prehistoric western Africa (Kay et al., 2019). It also reveals significant spatial and temporal data gaps that may inform future field studies (Kay et al., 2019). This atlas will be valuable for future studies of human-environment interactions.

The Congo forest region in central Africa is notable for its numerous archaeo-informatic oriented studies based on radiocarbon dates and related archaeological assemblages (Currie et al., 2013; Oslisly et al., 2013; Shennan et al., 2013; Li et al., 2014; Russell et al., 2014; Grollemund et al., 2015; Patin et al., 2017; Seidensticker et al., 2021; Koile et al., 2022; Clist et al., 2023). These studies lay the groundwork for eastern African archaeologists to develop an archaeo-informatics infrastructure that connects western, central, and eastern African regions. These studies have consulted extensive ceramic studies (Wotzka, 1995; Seidensticker et al., 2021), in-depth genetic analyses (Pakendorf et al., 2011; de Filippo et al., 2012; Ansari Pour et al., 2013; Li et al., 2014), insightful language phylogenies (Koile et al., 2022), and detailed palaeoecological records (Oslisly et al., 2013; Bostoen et al., 2015; Grollemund et al., 2015; McIntosh et al., 2015; Maley et al., 2018), including isotopic records (Bleasdale et al., 2020), to provide in-depth insights on Bantu-speaking agropastoral migrations from western Africa through the Congo forest in central Africa. I use insights from three major archaeo-informatics studies based on ^{14}C dates from central Africa to demonstrate the value of establishing basic archaeo-informatics infrastructure in eastern Africa.

The first study employed a novel suite of spatial modeling techniques to analyze a radiocarbon database and reconstruct the dispersal of farming from central Africa to eastern Africa (Russell et

al., 2014). This method estimates phylogeographic relationships from archaeologically modeled dispersal maps. The results are reported in a format that allows comparison with linguistic and genetic phylogenies. These results were then used to analyze the "deep-split" and riverine/littoral hypotheses regarding the migration of farmers from western Africa through central Africa to eastern Africa. The results suggest that migrating farmers used rivers through the Congo rainforest as conduits to reach eastern Africa around 3,000–2,500 years BP, when a grassland corridor developed through the rainforest (Russell et al., 2014).

A recent investigation that employed the Bayesian phylogeographic approach with integrated geographical data connecting linguistic, archaeological, and genetic data suggests that farmers moved through the Congo forest as early as 4400 BP (Koile et al., 2022). While this study supports the riverine hypothesis, it suggests that these migrations occurred before the forest opened up. This approach is based on a recently developed "break-away" geographical diffusion model specifically designed for modeling migrations with geographic information included (Koile et al., 2022). Another recent study based on a ^{14}C dataset from the Congo forest used an integrated, multiproxy approach (Seidensticker et al., 2021). This approach integrates a comprehensive analysis of ^{14}C dates using summed probability distributions (SPDs) as a proxy for human activity and potential demographic fluctuations, as well as a comprehensive analysis of pottery style diversity and distribution and genetic data. The results indicate two periods of more intense human activity (Seidensticker et al., 2021). The first one is between 800 BCE to 400 CE. The second one is between 1000 and 1900 CE. These periods are defined by two phases. The first phase is marked by a widespread use of diverse pottery styles. The second phase is characterized by the emergence of numerous local styles, separated by a period of significant population decline between 400 and 600 CE. This decline is followed by a major resettlement that took place centuries later. These

results support the hypothesis of spread-over-spread migration patterns for the dispersal of farmers through the Congo forest (Seidensticker et al., 2021). However, not all scholars agree that a decline occurred; see especially Clist et al. (2021), who argue that there is no evidence of a population collapse in the Congo rainforest between 400 and 600 CE based on pottery style evidence.

Significant transformations in economic organization, food production, trade, social connections, and climatic conditions have marked eastern Africa's past (Davidson et al., 1967; Ogot, 1976; Ehret and Posnansky, 1982; Wright, 1992; Ambrose, 1998; Peregrine and Ember, 2003; Kiage and Liu, 2006; Kiage and Liu, 2009; Maxon, 2009; Wright et al., 2015; Hannaford, 2023). Pastoral communities entered eastern Africa from the north by 3,000 BCE (Marshall et al., 1984; Barthelme, 1985; Ndiema, 2011). However, pastoralism spread gradually and unevenly across the region over the next few thousand years (Ambrose, 1984b; Marshall et al., 1984; Marshall, 1990; Bower, 1991; Marshall and Hildebrand, 2002; Ambrose, 2003; Lane, 2004; Marshall et al., 2011; Lane, 2013a; b; Robertshaw, 2021). The beginnings of crop farming are not as well understood (Young and Thompson, 1999). While scholars debate the timing of the dissemination of farming into eastern Africa, with some positing a date as early as 500 BCE, the first evidence for domesticated crops does not emerge until the period 300 BCE - 250 CE (Giblin and Fuller, 2011; Goldstein et al., 2024; Goldstein et al., 2025). Early farmers and herders also relied on hunting and gathering. They also traded with Indigenous forager populations (Clark and Brandt, 1984; Krzyzaniak and Kobusiewicz, 1984; Ambrose, 1998; Peregrine and Ember, 2003; Prendergast, 2009; Mutundu, 2010; Prendergast, 2010b; Mitchell and Lane, 2013; Courtney Mustaphi and Marchant, 2016; Crowther et al., 2018).

Eventually, diverse indigenous crops and exogenous livestock were incorporated into various forms of food production in eastern Africa, which then spread to other parts of the continent (Huffman, 1970; Robertshaw, 1984; Huffman and Vogel, 1991; Sinclair, 1991; Pawlowicz, 2011; Helm et al., 2012; Crowther et al., 2016a; Crowther et al., 2018). However, there are still major debates about the roles that the migration of different cultural groups played (Marshall, 1990; Radimilahy, 1998; Marshall and Hildebrand, 2002; Lane, 2004; Stahl, 2005; Lane et al., 2007; Maxon, 2009; Pearson et al., 2010; Mitchell and Lane, 2013; Marshall et al., 2018; Prendergast et al., 2019b; Wang et al., 2020) and the influence of major changes in climatic and environmental conditions (Hassan, 1981; Fraedrich et al., 1997; Robertshaw and Taylor, 2000; Jiang et al., 2002) including diseases (Gifford-Gonzalez, 1998; 2017) in these processes. From the first to the second millennium CE, eastern Africa was part of growing proto-global exchange networks across the Indian Ocean. These networks brought crops, animals, spices, material culture, and ideas from Southwest Asia, South Asia, and Southeast Asia (Chami, 1998; Horton and Middleton, 2000; Pouwels, 2002; Boivin et al., 2012; Helm et al., 2012; Boivin et al., 2013; Boivin et al., 2014; Crowther et al., 2016a; Crowther et al., 2016b; Wynne-Jones and LaViolette, 2018; Alders, 2026).

Significant research gaps and unresolved issues remain in eastern African archaeology (Robertshaw, 1984; Sinclair, 1991). For instance, archaeological research is unevenly distributed across the region (Robertshaw, 1984; Sinclair, 1991), and researchers have selectively applied archaeological science methods. Extensive areas of eastern Africa have received little research attention. Large areas of the interior lack evidence of the origin and dispersal of crops, while coastal and island zones have only recently and sporadically been investigated (Odner, 1971a; b; c; 1972; Mehlman, 1989; Robertshaw, 1991; Ambrose, 1998; Young and Thompson, 1999; Peregrine and Ember, 2003; Wright, 2005a). Moreover, a notable proportion of excavated sites are devoid of

scientific dates (Chapman, 1966; Sutton, 1966; Taylor, 1966; Lofgren, 1967; Soper, 1967a; Odner, 1971b; c; Soper, 1975; Soper, 1976; Phillipson, 1979; Wandibba, 1985; Abungu, 1989; Wandibba, 1990; Mosley and Davison, 1992; Abungu and Mutoro, 1993; Davison, 1993; Willis, 1996; Chami and Msemwa, 1997b; Wilson and Omar, 1997; Chami and Kwekason, 2003; Onjala, 2003; Walshaw, 2005; Odede, 2008; Pearson et al., 2010; Pawlowicz, 2011; Helm et al., 2012; Nkirote, 2012; Morales, 2013; Wynne-Jones and LaViolette, 2018; Lyaya, 2020). Additionally, identification to the species level is lacking for almost half of the faunal remains recovered from eastern African archaeological sites (Gifford-Gonzalez and Kimengich, 1984; Gifford-Gonzalez, 2003; Dale, 2007; Prendergast, 2009; Kusimba et al., 2013; Prendergast et al., 2016; Petek and Lane, 2017; Shoemaker, 2018; Goldstein et al., 2024; Goldstein et al., forthcoming). Finally, the potential of residue analysis, micro-CT scanning, and digital archaeology in general has yet to be fully realized (Causey and Lane, 2005; Causey, 2009; Kabiru, 2017; Petek and Lane, 2017; Amy, 2020; Barron et al., 2020a; Barron et al., 2020b; Grillo et al., 2020b).

The involvement of pastoralists in the dissemination of sorghum and finger millet to the interior of eastern Africa remains an open question (Ehret and Posnansky, 1982; Ambrose, 1984a; Ambrose et al., 1984; Clark and Brandt, 1984; Ambrose, 1998; Young and Thompson, 1999; Marshall and Hildebrand, 2002; Maxon, 2009). There is also contention surrounding the spread of livestock, early farming, iron production, and pottery manufacturing, particularly to the coast and islands (Young and Thompson, 1999; Sinclair et al., 2006; Chami, 2009; Nkirote, 2012; Shipton et al., 2016; M'Mbogori, 2017; Crowther et al., 2018; Serneels et al., 2018; Wynne-Jones and LaViolette, 2018; Serneels et al., 2019; Serneels et al., 2020; Culley et al., 2021a; Culley et al., 2021b; Nitsche et al., 2023). Additionally, there is debate about the role of human colonization in extinctions. This is particularly evident in the case of megafaunal extinctions in Madagascar (Pearson et al., 2010;

Anderson et al., 2018; Godfrey et al., 2019; Mitchell, 2020; Hixon et al., 2021a; Hixon et al., 2021c). This debate stems, in part, from unresolved regional chronologies, which would otherwise improve our understanding of the origin and dispersal of food production in eastern Africa, as well as the spread of ironworking and ceramic traditions. These warrants revisiting and reanalyzing existing datasets (Chami et al., 2001; Sinclair et al., 2006; Chami, 2009; Pearson et al., 2010; Ekblom et al., 2016; Douglass et al., 2019).

Many research questions in eastern African archaeology cannot currently be adequately addressed due to these deficiencies. These include questions surrounding the role of diverse populations in the different stages of eastern Africa's deep-time history, as well as the spread of diverse languages, species, and technologies. Additionally, improved datasets are necessary to comprehend the effects of changing land use on local and regional environments, as well as the impact of human activities on biodiversity (Burney et al., 2004; Pearson et al., 2010; Douglass et al., 2019; Hixon et al., 2021a). Improved data are also necessary to understand the complex interactions between fishermen, foragers, pastoralists, and farmers in various geographical settings (Robertshaw et al., 1983; Robertshaw, 1991; Chami and Chami, 2001; Munene, 2002; Chami and Kwekason, 2003; Kusimba and Kusimba, 2005; Lane et al., 2006; Chami, 2007; Lane et al., 2007; Chami, 2009; Prendergast, 2010c; M'Mbogori, 2017; Chami and Silayo, 2023). For the third case study, I compiled the first archaeological dataset of absolute dates, along with associated botanical and faunal remains, as well as iron and ceramic artifacts (Figure 2.8; see Table A3:1 for an abridged version of the *Wanyika* dataset) to begin to more systematically address these critical lacunae at the regional scale. This archaeo-informatics-oriented dataset is publicly available. My goal is threefold. First, I aim to reveal patterns in human-environment interactions in eastern Africa. Second, I intend to highlight existing data gaps. Third, I hope to pave the way for the assembly of large, regional-

scale datasets. By doing so, I aim to facilitate initiatives that address major research questions in eastern Africa. Additionally, I aim to apply past data to current and future challenges.

4.5 – Limitations in the isotopic and archaeo-informatic perspectives

This study employs isotopic and archaeo-informatic approaches, both of which present significant limitations and challenges. Here, I summarize these limitations and challenges and explain how I addressed them in this study. More detailed discussions on how I addressed these limitations and challenges can be found in chapters five, six, and seven.

Isotopes

The primary limitations of applying isotope ecology to the archaeology of eastern Africa can be summarized in two points: sample preservation and evaluation, and interpretation difficulty (Ambrose and DeNiro, 1986b; Ambrose, 1990; Ambrose, 1993; Ambrose et al., 1993; Hakenbeck, 2013; Loftus et al., 2016; Loftus, 2021; Madgwick et al., 2021; Britton et al., 2022; O'Connell, 2025; Simonetti and Buzon, 2025). These limitations underscore the necessity of a meticulous methodology, substantial statistical analysis, and integration with conventional archaeological evidence to ensure precise and reliable ecological reconstructions. In eastern African archaeology, limitations in preservation and sample evaluation manifest in three ways (Ambrose and DeNiro, 1986b; Ambrose, 1990; Ambrose, 1993; Sponheimer et al., 2005b; Sponheimer and Lee-Thorp, 2007; Lee-Thorp, 2008; Lee-Thorp and Sponheimer, 2013; Loftus et al., 2016; Holt et al., 2021; Loftus, 2021; Madgwick et al., 2021; O'Connell, 2025). First, chemical changes (diagenesis) in the

burial environment after death can alter the original isotopic signal of organic materials, such as bone collagen, leading to inaccurate results. Second, the quantity of preserved material from an excavation site can vary significantly due to burial customs, preservation circumstances, and fragmentation. This can lead to flawed statistical analyses and broader interpretations due to small sample sizes. Third, isotopic analysis usually destroys the archaeological material, raising ethical concerns, especially for rare or culturally significant artifacts.

I address the limitations of preservation and sample evaluation through several steps discussed in Chapters five and six. First, I tested all collagen samples using the established indicators of bone collagen preservation standards: the C/N ratio, %C, and %N. Samples that failed these tests were excluded from the study. Enamel samples undergo negligible diagenesis that affects ecological interpretations. Second, the primary sites KC and UU are limited by the adequate representation of certain species in specific chronological phases. This made it impossible to carry out certain statistical analyses; however, this does not affect the thesis's major findings. Compared to other isotope studies in eastern Africa, the KC, UU, and PYS isotope datasets that form the basis of this thesis have some of the best species' identification and representation. All sites have more than thirty samples, which is a high number of total samples. Third, the zooarchaeological collections used in this study are not classified as endangered or rare. Most of the collagen and enamel samples came from fragmented bones and isolated teeth, which are abundant at these sites.

The limitations of interpreting the archaeological record in eastern Africa are expressed in three dimensions (Ambrose, 1986; Ambrose, 1990; Ambrose, 1993; Loftus, 2021; Madgwick et al., 2021; O'Connell, 2025; Simonetti and Buzon, 2025). First, overlapping isotopic signatures from different ecological or dietary sources mean that a specific isotopic value cannot always be linked

unambiguously to a particular food or water source. Second, different body tissues (e.g., bone, hair, and teeth) incorporate isotopic signals at different rates. For instance, interpreting bone collagen values as a representation of the final years of life is an oversimplification. Third, accurate interpretation requires establishing a "local" isotopic baseline (isoscape); however, proper comparison can be hindered by a lack of reference materials from the specific time and place. Furthermore, factors such as the Suess effect (anthropogenic changes to atmospheric CO_2) and modern agricultural practices may make modern environmental data inaccurate.

I have ensured that the limitations associated with equifinality and multifinality are factored into my discussions. For example, I consider the possibility of including C_4 grasses, as well as cereal crops such as sorghum and millet, in my discussions of C_4 presence and use. I also use multi-isotopes and multidisciplinary perspectives to overcome the equifinality challenge. This approach enables the synthesis of interpretations from zooarchaeological, archaeobotanical, material culture, geomorphological, and other assemblages. Archaeological isotope ecology work (C, O, N, and Sr) from the interior of eastern Africa provides a baseline framework for coastal sites (KC and UU). Isotope values from wild fauna in the coastal region are also included to interpret caprine data in the UU study. This thesis uses only archaeological isotope data; no modern data are included.

Limitations and challenges in scientific dates and archaeo-informatics in eastern Africa

Scientific dates

Most limitations in scientific dating in eastern African archaeology are associated with technical aspects of dating procedures, especially radiocarbon dating, and the movement of the Intertropical Convergence Zone (ITCZ) (Reimer and Reimer, 2001; Wright, 2017; Hare and Loftus, 2018;

Marsh et al., 2018; Heaton et al., 2020; Reimer et al., 2020; Pearson et al., 2021). The ITCZ affects the circulation of carbon-14 in complex and fluctuating patterns over time. In general, radiocarbon dating is applied to organic materials or in vivo formed inorganic materials, albeit with some exceptions. Organic materials include plants, animals, wood, charcoal, and bone. Inorganic materials that can be dated include mortar and iron. *In vivo* formed inorganics include the shells of different animals, which are composite materials. However, inorganic materials such as stone and metal cannot generally be dated directly, though apatite can (Schwarcz, 2000; Wright, 2017). Alternative approaches that can date inorganic matter, such as optically stimulated luminescence (OSL) (Bluszcz, 2005; Preusser et al., 2008), thermoluminescence (TL) (Tite and Waine, 1962; Preusser et al., 2008), and infrared stimulated luminescence (IRSL) (Taylor and Aitken, 1997; Wright, 2005a; Duller, 2008; Liritzis et al., 2013), are primarily limited by the need for a "zeroing" event, such as exposure to heat or sunlight. Fortunately, when radiocarbon dating was not applicable due to a lack of organic material, luminescence dating techniques were successfully used. In other cases, both radiocarbon and luminescence dating were applied. Since radiocarbon dating is the dominant scientific dating technique in eastern Africa, with complex limitations related to the Intertropical Convergence Zone (ITCZ) and calibrations, this thesis focuses more on radiocarbon dating and how the limitations were addressed.

The major limitations and challenges of radiocarbon dating in eastern Africa fall into three categories: preservation, precision, sample integrity and context, and calibration (Schwarcz, 2000; Wright, 2017; Hare and Loftus, 2018). The complex tropical ecology of eastern Africa, caused by historically fluctuating climate and vegetation, as well as varying soil and terrain, directly affects the preservation of organic materials needed for accurate dating (Wright, 2017; Hare and Loftus, 2018). Diagenesis occurs during burial, excavation, transport, and even museum curation. Bone,

teeth, and charcoal frequently undergo diagenetic changes, or the chemical alteration of materials after burial. These changes are mainly caused by high temperatures, humidity, and varying pH levels. High heat and humidity often lead to the poor preservation of organic matter and accelerate the degradation of collagen in bones. Diagenesis can introduce "younger" or "older" carbon into samples, making accurate calibration difficult. For example, dolomitization and recrystallization (the replacement of calcium (Ca) ions with magnesium (Mg) ions in calcite and aragonite, which affects carbonate nodules by recrystallizing the outer surfaces while leaving the inner surface intact) in avian eggshells can lead to diagenesis that results in dates older or younger than the expected timeframe. This has been noted in megafauna eggshells in mainland eastern Africa and Madagascar (Pearson et al., 2010). The absence of diagenetic effects must be proven before dating any organic material. Leaching of carbon and microbial attack on collagen can be acute in tropical ecosystems. Post-depositional diagenetic changes affect plant artifacts, especially the outer portions of stalks and seeds. Laboratories that work on carbon isotopes now control many of these effects by performing alternating acid and alkali washes to remove diagenetic contaminants. In arid regions, biological apatite dating has been demonstrated to be successful due to the lower presence of diagenesis-inducing microbes compared to humid ecosystems. Evaluating the ratio of carbon to nitrogen (C/N) in bone can accurately determine whether collagen in samples has undergone postmortem degradation. For plant samples, materials such as charcoal and cellulose are generally more resistant to diagenetic alteration and are preferred for dating purposes.

There is a high degree of imprecision resulting from uncertainty in the dates from eastern Africa (Fagan, 1966; Schmidt, 1975; Michels et al., 1983; Ambrose, 1984b; a; Clist, 1987b; Robertshaw, 1990a; Wright, 2017). This is evident from the high percentage of dates with a standard deviation greater than 25, which is a rough reference point for the Holocene period (Bower et al., 1977;

Maggs, 1977; Onyango-Abuje, 1977a; Gifford et al., 1980; Michels et al., 1983; Ambrose, 1984a; Robertshaw, 1991; Pearson et al., 2010; Kusimba et al., 2013). This is partly because many of these dates were generated earlier than the 1990s, when the ^{14}C dating technique was less precise. While values higher than 25 are possible for AMS measurements, samples dated using modern technology are more precise than those dated before the 1990s. Uncertainty also depends on the age of the sample; samples with lower ^{14}C content have larger uncertainties. Five important limitations fall under the category of sample integrity and context. First, samples are susceptible to contamination from modern and older carbon sources during excavation, handling, and laboratory processing. Modern carbon can make an old sample appear younger, while older carbon can make a young sample appear older. Second, the "Old Wood" effect occurs when old organic material is used in a younger archaeological context. Although the measurement itself may be accurate, the potential inaccuracy arises from the sample chosen for dating. For example, if the charcoal sample used for dating originates from the centre of a three-hundred-year-old tree, it will yield an erroneously old age for the structure. However, if it came from the outer rings, it would provide a more accurate date close to the date of felling, unless the timber was stored for years before use. Third, poor preservation (diagenesis) in certain environments (e.g., hot, humid, or acidic soils) can degrade the target carbon fraction (e.g., bone collagen), resulting in insufficient material for accurate dating or rendering the sample unusable. Fourth, dated material may not directly relate to the desired human activity or event (e.g., using bulk sediment dates rather than specific, short-lived plant remains), which can lead to misinterpretations of the archaeological record.

To navigate the limitations and challenges associated with the preservation, date precision, integrity, and context of the samples, I developed three quality control criteria for ^{14}C dates. These criteria include "short-vs.-long-lived" plant material, aquatic reservoir effects, and the accuracy of

chronological determinations (pretreatment protocol). Using these criteria, I graded the dates into classes A through C, with class A being the highest quality. Currently, different teams are redating, reanalyzing, and re-excavating sites with questionable dates, dates from before the 1990s, and SDs higher than 25. Several sites have been redated using legacy collections and AMS technology. For sites that have been redated, I included both pre- and post-1990 dates in the dataset. Any issues related to range, integrity, or context raised regarding questionable radiocarbon dates are noted in the dataset's notes section.

The amount of carbon-14 (C-14) in the atmosphere fluctuates over time due to solar cycles, the Industrial Age, and nuclear testing (Schwarcz, 2000; Wright, 2017). In eastern Africa, the Intertropical Convergence Zone (ITCZ) complicates C-14 circulation, necessitating complex calibration curves to convert radiocarbon years to calendar years (Hogg et al., 2020; Reimer et al., 2020). The major limitations in calibration and interpretation can be broken down into five points. First, the relationship between carbon years and calendar years is not linear (Wright, 2017). This causes different calendar periods to have different carbon age intervals. This can lead to "clustering" of ^{14}C dates in intervals unrelated to the actual rate of events. Second, marine organisms have different carbon levels than the atmosphere due to the delayed mixing of surface and deep ocean carbon (Reimer and Reimer, 2001; Wright, 2017; Heaton et al., 2020). Thus, separate calibration curves are required for marine samples. Third, local effects, such as regional winds, upwelling, and sea ice, can affect carbon levels; however, these effects are not accounted for in global calibration curves. Finally, global calibration curves are created using data from many laboratories (Reimer and Reimer, 2001; Heaton et al., 2020; Hogg et al., 2020; Reimer et al., 2020). Historical differences in laboratory standards require systematic intercomparisons and quality control to ensure accuracy.

I address the limitations and challenges associated with ^{14}C fluctuations in the atmosphere over time by undertaking multiple calibration procedures. Because the ITCZ's movement causes ^{14}C fluctuations, I use a sophisticated method to calibrate dates in eastern Africa. This method employs the most recent calibration curves, such as IntCal20 and SHCal20. Dates from sites south of latitude -17° are calibrated using SHCal20, while a mixed IntCal20 and SHCal20 curve is used for sites north of latitude -17°. Aquatic samples were calibrated using a localized calibration curve. I used the Bayesian chronological software OxCal v4.4 to convert the ^{14}C dates to calendar years. The calibration process for OSL, IRLS, and TL dates was different. For these dates, I subtracted the reported BP date from the publication year. For optically stimulated luminescence (OSL) dates, the reported BP date was subtracted from 1950 to convert the dates to calendar years.

Archaeo-informatics and the archaeological record in eastern Africa

The archaeological record in eastern Africa is rife with significant limitations and challenges that I had to navigate in this archaeo-informatic study. These limitations affect the distribution of scientific dates, archaeological sites, and archaeological site assemblages in the region. These limitations and challenges can be summarized into five major points. First, more than half of the archaeological sites in eastern Africa lack stratigraphic integrity and reliability due to bioturbation (Mehlman, 1989; Robertshaw, 1991; Pearson et al., 2010; Wilson, 2019). This is particularly evident in contexts with evidence of food production dispersal earlier than predicted (Mehlman, 1989; Chami, 2001a; Chami and Chami, 2001; Munene, 2002; Chami and Kwekason, 2003; Chami, 2009; Mueller et al., 2022; Goldstein et al., 2024; Goldstein et al., 2025). More than half of the dates have an SD above 25. Second, most scientific dates lack crucial contextual information (e.g., sample type, origin, location, and species identification), or this information is reported

inconsistently. This information is vital for "chronometric hygiene" (e.g., correcting for reservoir effects) and data quality control. Third, there are inconsistencies in the format of records, which are duplicated and spread across diverse publications and site datasets with different, often non-standardized, formats (Bird et al., 2022). Linking contextual data to a date requires significant effort to clean the data before analysis can occur. Fourth, spatial-temporal biases affect the reliability of analyses such as paleo-demography. Large swaths of eastern Africa remain unexplored, and there is an uneven distribution of similar chronological contexts. Two additional limitations and challenges in informatics worth mentioning are the "black box" effect of unknown software algorithms and the reproducibility of data and code (Wilkinson et al., 2016; Marwick, 2017; Ziemann et al., 2023; Longo et al., 2024; Turakhujaev, 2025).

I overcame the limitations and challenges I faced by taking a systematic approach to ensure that I produced a dataset that adhered to the basic global standards for developing an archaeo-informatics-oriented database. To address limitations and challenges related to stratigraphic integrity and reliability, I developed a quality control measure that graded dates based on assemblage, context alignment, and standard deviation. Dates with high stratigraphic integrity and reliability received a grade of A, while those with the lowest integrity received a grade of D, and dates lacking crucial contextual information received low grades. I devoted special attention to reviewing multiple publications, including the earliest and latest articles in Azania: Archaeological Research in Africa, the authoritative journal for archaeology in eastern Africa. I also ensured that the dates and assemblages were recorded in a consistent, standardized format that aligned with global standards. I deleted duplicate records from the dataset and linked dates to contextual data wherever possible. Additionally, I highlighted the spatial-temporal gaps in scientific dates and archaeological sites in eastern Africa. I cautioned against using the data for paleo-demographic and

other modeling studies due to its inadequacies. To make the data more interoperable, I adopted the FAIR principles (findable, accessible, interoperable, and reusable) for data management. Information on all the software algorithms used in this study is provided to allow for re-testing. The *Wanyika* dataset is available online through open-source software, and an abridged version is provided in Appendix 3 of this thesis.

Chapter 5 – Materials, methods, and results for the Kuumbi Cave isotopic case study

This chapter presents the materials and methods used in the first case study, as well as the carbon and oxygen isotope results. The study uses primary carbon and oxygen isotope values from faunal and human remains excavated from the Kuumbi Cave site (KC) — spanning the late Pleistocene to the late Holocene — to reconstruct the ecology and human foraging dynamics during periods of global climate fluctuation shaped by glacial and interglacial events. I also perform a comparative analysis of the KC dataset with published datasets from the coastal cave site of Panga ya Saidi (PYS) and other sites in the interior of eastern Africa that also represent the late Pleistocene to late Holocene periods. The first section of the chapter presents the materials and methods. This begins with background information on zooarchaeology and identification for isotope analysis, the total number of faunal and human enamel samples, the number of fauna identified to species and other taxonomic categories, and the four broad feeding groups and five major habitat categories defined for this region and used for isotope ecology interpretations. This section also presents the sampling procedures, laboratory analysis, and methods of statistical analysis. The second section of the chapter presents the carbon and oxygen isotope results from KC (this work is published as Iminjili et al., 2023). Scatterplots and box plots are used to visualize the results. The section begins with a presentation of the findings relating to variation in taxa and dietary groups. This is followed by an examination of variation over time and human values. Finally, the results of the comparative study between KC and mainland eastern African sites are presented.

5.1 – Zooarchaeology background, identification, and carbon and oxygen sampling and analysis

The materials presented in this study are sourced from the faunal assemblage of KC Trench 10, which includes 6,667 individual specimens (Prendergast et al., 2016; Shipton et al., 2016). The remains of most vertebrates were introduced to the site as a result of human activity, as evidenced by cutmarks and burning, which demonstrates the long-lasting impact of humans on the assemblage. Teeth from both animals and humans were selected for isotopic analysis based on the archaeological context, how complete the teeth were, and their availability for study. A total of 229 samples of enamel from both human and non-human subjects were included in the analysis of the isotopes carbon ($\delta^{13}C$) and oxygen ($\delta^{18}O$). The tooth specimens were methodically chosen from the four Phases depicted in the stratigraphic sequence. The analysis included only tooth samples that could be taxonomically identified. The vast majority of the samples came from species-identified fauna (142), while the rest could be identified to the genus (6), family (7), subfamily (63), tribe (7), or order (4) (Prendergast et al., 2016; Shipton et al., 2016). The two human molars examined date from the Iron Age and the terminal Pleistocene. The terminal Pleistocene molar is the earliest human remains found on the littoral islands of eastern Africa, and its discovery will provide insight into the region's ancient human history. It is also notable that the sample set for stable isotope analysis included five extirpated large taxa: reedbuck, zebra, bushbuck, klipspringer, and bush duiker (Prendergast et al., 2016).

I use the basic ecological categories applied by Roberts et al (2020) to categorize taxonomic groups into four broad feeding groups (browsers, grazers, mixed feeders, and omnivores) and five major habitat categories (open and closed forests, open and closed woodlands, and grasslands) (Fleagle,

1999; Gagnon and Chew, 2000; Kingdon, 2001; Cerling et al., 2003c; Cerling et al., 2004; Campbell et al., 2006; Cerling et al., 2010; Cerling et al., 2015). These categories are based on collating ecological observations and isotope studies. "Open habitat" refers to a mixture of open woodlands and grasslands. The term "browsers" in this context refers to mammals that feed on plant material such as leaves, fruits, soft shoots, and roots. The browser category includes the frugivorous taxa blue duiker and Ader's duiker and vervet/blue monkeys, as well as the folivorous Zanzibar red colobus, according to the isotope analysis.

Before analysis, all teeth were meticulously photographed, and after all project studies, they were repatriated back to Tanzania through the British Institute in Eastern Africa (BIEA). Sampling occurred at two locations: the National Museums of Kenya (NMK) and the Max Planck Institute of Geoanthropology (MPI-GEA). Teeth or tooth fragments were cleaned using air-abrasion to remove any external material adhering to them. A bulk sample of enamel powder, representative of the tooth's formation period, was obtained by gently abrading the buccal surface of the tooth with a diamond-tipped drill. This method was used to comprehensively capture the diet and other behavioral aspects during the tooth formation period. The removal of organic or secondary carbonate contaminants was achieved through the pre-treatment of enamel powders. The procedure involved a 60-minute wash with 1.5% sodium hypochlorite, followed by three rinses in purified H_2O and centrifugation. Then, 0.1 M acetic acid was added for 10 minutes, after which three more rinses in purified H_2O ensued (Sponheimer et al., 2005a; Lee-Thorp et al., 2012; Roberts et al., 2017). The samples were then reacted with 100% phosphoric acid, and the resulting gases were analyzed for their stable carbon and oxygen isotope measurements. This analysis was performed using a Thermo Gas Bench 2 connected to a Thermo Delta V Advantage Mass Spectrometer at MPI-GEA.

Isotopic values are expressed as the ratio of the heavier isotope to the lighter isotope ($^{13}C/^{12}C$ or $^{18}O/^{16}O$) as δ values in parts per mill (‰) relative to international standards, VPDB for $\delta^{13}C$ and $\delta^{18}O$. To normalize the $\delta^{13}C$ and $\delta^{18}O$ values, a three-point calibration against international standards was used (IAEA-603 ($\delta^{13}C = 2.5‰$; $\delta^{18}O = -2.4‰$); IAEA–CO–8 ($\delta^{13}C = -5.8‰$; $\delta^{18}O = -22.7‰$); and IAEA NBS 18 ($\delta^{13}C = -5.014‰$; δ18O = −23.2‰)). USGS44 ($\delta^{13}C = -42.2‰$) was incorporated as an in-house standard. A replication of the investigation of USGS44 standards indicates that equipment measurement inaccuracy is around ± 0.1‰ for $\delta^{13}C$ and ± 0.2‰ for $\delta^{18}O$. The study of overall measurement precision involved the measurement of repeat extracts from a bovid tooth enamel standard (n=20, with a margin of error of ± 0.2‰ for $\delta^{13}C$ and ± 0.3‰ for $\delta^{18}O$).

5.2 – Statistical analysis

All statistical analyses were performed using the free R statistical software (R Core Team, 2013). Two-way ANOVAs were performed to examine the impact of phase and family on enamel $\delta^{13}C$ and $\delta^{18}O$ values, given the limited species-specific data available. The quality of the models was checked using Levene's test and the Shapiro-Wilk test. Tukey's method was used to perform post-hoc comparisons, the purpose of which was to ascertain which taxa or stratigraphic layers were distinct from each other. A different set of two-way ANOVAs was used to examine the impact of Phase and dietary category (with each category comprising multiple families) on both $\delta^{13}C$ and $\delta^{18}O$ values. The classification of dietary categories herein encompasses "browsers" (comprising folivores and frugivores), "grazers," "mixed feeders," and "omnivores," a categorization system that draws upon extant ecological publications (Kingdon, 1984b; Gagnon and Chew, 2000;

Kingdon, 2001; Cerling et al., 2003c; Cerling et al., 2004; Cerling et al., 2015). Taxon-specific regression was performed on the three families that include the largest ranges of $\delta^{13}C$ values (Bovidae, Equidae, and Procaviidae) to determine whether a positive association existed between $\delta^{13}C$ and $\delta^{18}O$ values. Except for equids, the taxa that were analyzed at KC are not often found in abundance at sites in mainland eastern Africa. The samples that were specific to particular taxa and that were taken from specific time periods are too small to be able to be statistically analyzed. Nevertheless, Kruskal–Wallis tests (and associated Wilcoxon tests with p-values adjusted according to Bonferroni) were employed to examine the impact of site on regional equid and browser $\delta^{13}C$ data. The details of all statistical analyses are presented in Appendix 1.

5.3 – Variation in taxa and dietary groups at Kuumbi Cave

The results suggest that the patterns of variation in KC's faunal isotopic values, categorized by species and dietary group, resemble those of modern replicate species in dense forest mosaic habitats. The patterns of variation evident in the $\delta^{13}C$ and $\delta^{18}O$ values associated with browsing and forested habitats at KC (e.g., colobus monkeys, forest duikers, and hyrax) resemble those published for modern replicate species in equatorial African forests (Ambrose and DeNiro, 1986a; Cerling et al., 2003c; Cerling et al., 2004). Please note that modern $\delta^{13}C$ values must be corrected for the Suess effect. Similarly, the patterns of variation associated with species that graze or feed in mixed habitats in open grasslands and woodlands at KC (e.g., zebras, reedbucks, and oribis) resemble those reflected in modern replicate species in the wooded grasslands of eastern Africa (Ambrose and DeNiro, 1986a; Cerling et al., 2003c; Cerling et al., 2004). The statistical analyses, particularly ANOVA, tease out the variance of these species and dietary groups at KC. The KC

human $\delta^{13}C$ and $\delta^{18}O$ values are consistent with those of modern foragers in forest ecosystems in eastern and central Africa.

The comprehensive dataset (n = 229) of $\delta^{13}C$ and $\delta^{18}O$ values of faunal teeth is displayed in Table A1:1. Summary statistics, two-way ANOVAs, and post hoc comparisons of the taxa and dietary groups show similar $\delta^{13}C$ and $\delta^{18}O$ patterns (Appendix 1). Faunal $\delta^{13}C$ values at the site varied from −20.4 to −1.9 ‰ (mean = −11.9 ‰, median = −12.3 ‰). These values suggest that the animals that the foragers hunted at the site inhabited different habitats (Figure 5.1, Appendix 1). Approximately 70% of the mammalian faunal remains are made up of small, forest-adapted mammals weighing less than 25 kilograms. This includes five non-human primates, tree hyraxes, giant pouched rats, and small bovids, principally from the forest-adapted Cephalophini and Neotragini tribes. The primates identified as vervet/blue monkeys (*Cercopithecus or Chlorocebus spp*.), Zanzibar red colobus (*Piliocolobus kirkii*), Zanzibar bush baby (*Galago zanzibaricus*), and greater galago (*Otolemur crassicaudatus*) have exhibited a consistent tendency to manifest low $\delta^{13}C$ values (−15.3 to −10.6‰). Tree hyrax (*Dendrohyrax validus*) and bovids blue duiker (*Philantomba monticola*, reported by Prendergast et al., 2016, as *Cephalophus monticola*), suni (*Neotragus moschatus*), klipspringer (*Oreotragus oreotragus*), and bush duiker (*Sylvicapra grimmia*) show the lowest values, ranging from −20.4 to −15‰. The highest values in the dataset are from oribi (*Ourebia ourebi*), reedbuck (*Redunca redunca*), and zebra (*Equus quagga*) (from −5.5 to −1.9‰). The other taxa (suids and diminutive mammals) have intermediate values (−13.2 to −9.2 ‰). Two-way ANOVAs show that family significantly affects $\delta^{13}C$ values (model 1, $p < 0.0001$; see Appendix 1). Further analysis reveals that Equidae samples are significantly enriched in $\delta^{13}C$ relative to samples from all other taxa (model 1, $p < 0.0001$).

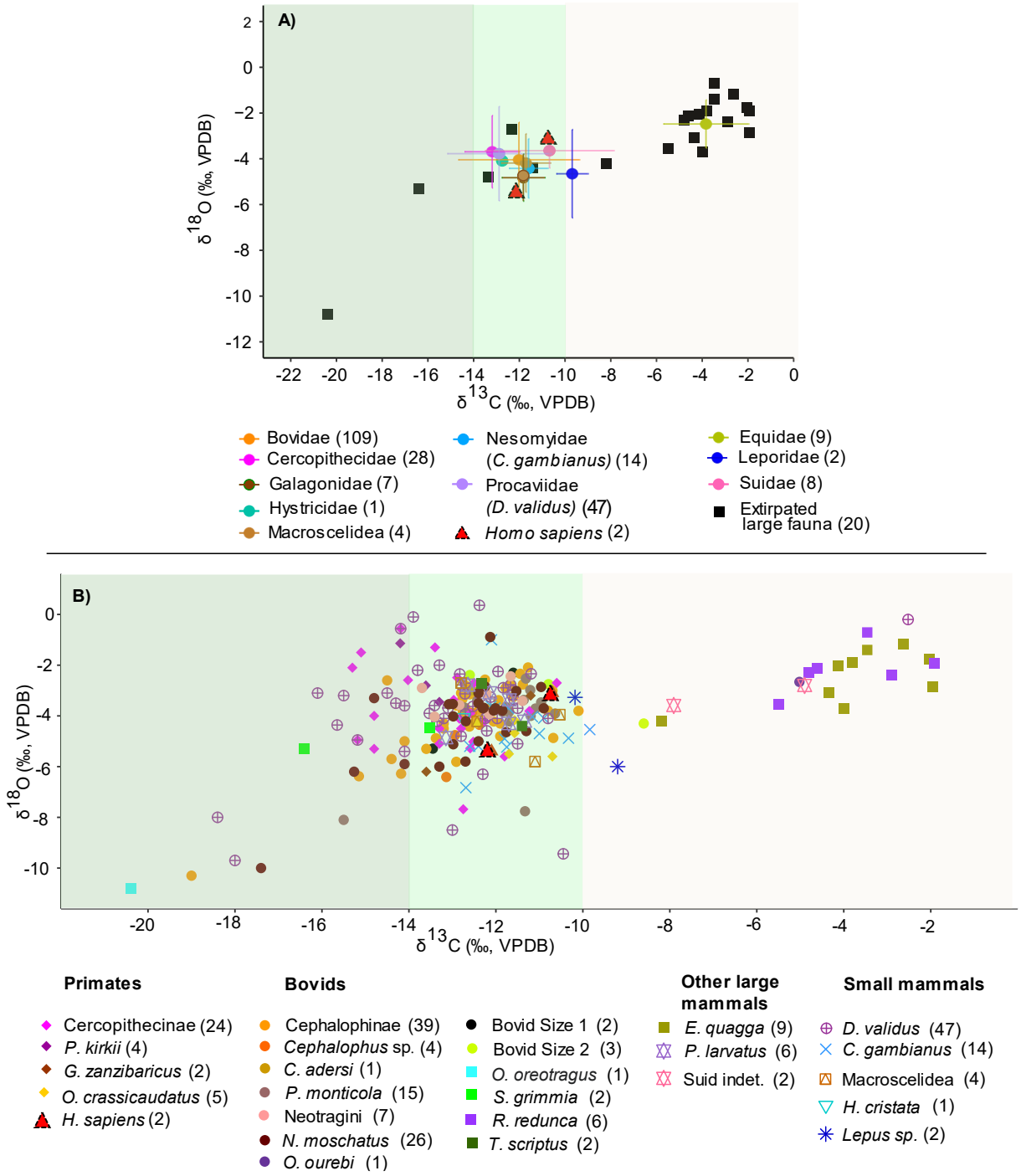


Figure 5.1. *Two different formats are used to show the scatterplots of the KC* $\delta^{13}C$ *and* $\delta^{18}O$ *values. The first format (A) shows the information sorted by family. The color of each data point indicates the family: forest (dark and light green for closed and open canopy, respectively), mosaic grassland (light brown), extirpated fauna (squares), and two* Homo sapiens *specimens (red triangles). The second arrangement (B) displays the information categorized by taxa. The sample sizes for each taxon are given in brackets. Symbols and colors are used to represent the different faunal groups mentioned in A and B. These groups comprise primates, bovids, other large mammals, and small mammals. However, the five large animals that are no longer found in the area are shown using square symbols. These are* O. oreotragus, S. grimmia, R. redunca, T. scriptus and E. quagga. *The error bars in (A) represent standard deviations (Iminjili et al., 2023).*

The KC fauna also exhibit a wide range of $\delta^{18}O$ values (from −10.8 to 0.4 ‰, with a mean of −3.9 ‰; see Figure 5.1 and Appendix 1). The klipspringer has the lowest value of −10.8‰, while the tree hyrax has the widest range and highest values of −9.7 to 0.36‰ (mean of −3.8‰). Relatively low values are possessed by most of the arboreal and bovid taxa. The red colobus has the highest mean among the arboreal taxa (range −18.4 to −2.5‰), followed by the tree hyrax, cercopithecines, Zanzibar bush baby, and greater galago. Similar values to the arboreal taxa are possessed by the forest-adapted terrestrial small mammals, the giant pouched rat and the elephant shrew. Among the ungulates, zebra and reedbuck exhibited the highest values, ranging from −8.2 to −1.9‰. Two-way ANOVAs indicate that family has a substantial impact on $\delta^{18}O$ values ($p = 0.03$). However, subsequent post-hoc comparisons reveal that there are no statistically significant differences in $\delta^{18}O$ values among families (model 2, $p > 0.05$) (Appendix 1).

Significant distinctions were observed in the $\delta^{13}C$ values when the KC faunal dataset was divided into dietary groups (Figure 5.2). The lowest values are found in browsers (mean −12.8‰), and the highest values are found in grazers (mean −3.9‰) (Figure 5.2). As anticipated, the values for mixed feeders (mean −8.1‰) and omnivores (mean −11.7‰) fall between those of browsers and grazers. The $\delta^{18}O$ values are analogous to the $\delta^{13}C$ value patterns, with browsers exhibiting the lowest values (mean −4.0‰) and grazers demonstrating the highest values (mean −2.3‰) (Figure 5.2). Two-way ANOVAs revealed a significant effect of diet groups on $\delta^{13}C$ values (model 3, $p < 0.0001$) and $\delta^{18}O$ values (model 4, $p = 0.02$) (Appendix 1). Subsequent comparisons indicate that grazers, browsers, and omnivores generally exhibit substantially distinct $\delta^{13}C$ values, with grazers displaying the greatest enrichment in ^{13}C, browsers exhibiting the most depletion in ^{13}C, and omnivores occupying a median position between these two extremes (model 3, $p < 0.0001$). The

results of the post-hoc comparisons indicate that grazers are enriched in ^{18}O compared to browsers (model 4, $p = 0.03$).

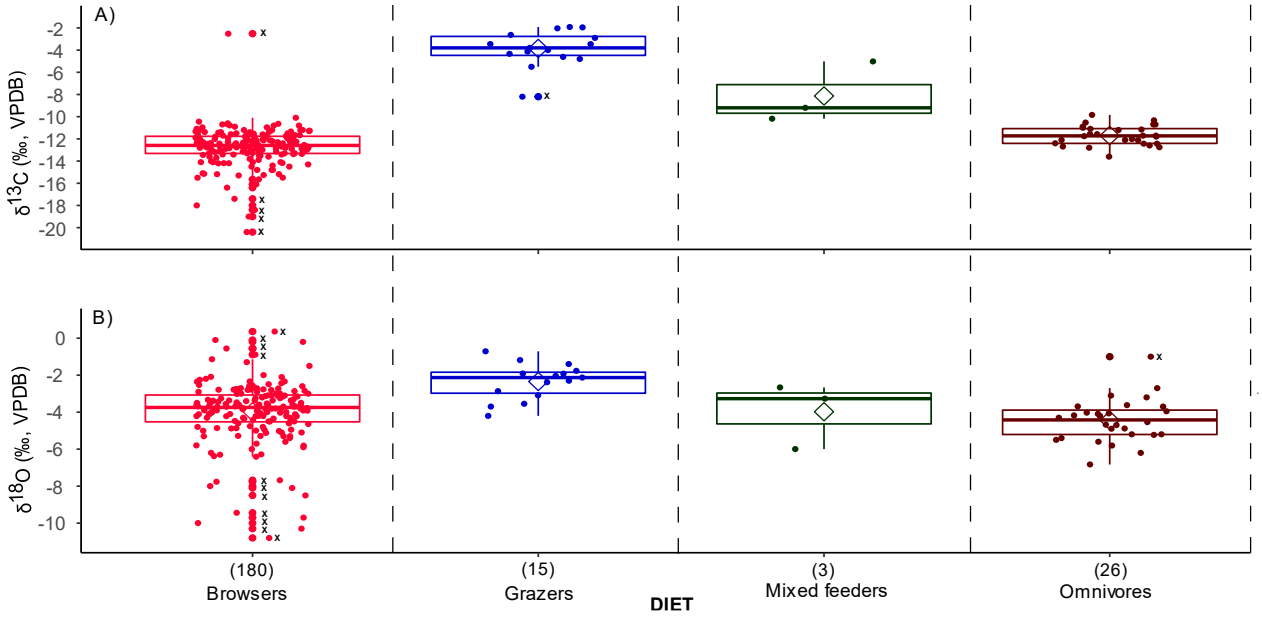


Figure 5.2. *Box and jitter plots of (A) $\delta^{13}C$ and (B) $\delta^{18}O$ values. The values have been classified by faunal dietary category. Outliers are represented by dots and Xs along the midline of the graphs. The sample sizes are indicated in brackets above the plot labels on the x-axis (Iminjili et al., 2023).*

The general linear model (GLM) reveals the overall relationship between the $\delta^{13}C$ and $\delta^{18}O$ values ($p < 0.0001$) (Appendix 1), as illustrated by the regression between the $\delta^{13}C$ and $\delta^{18}O$ values within the Bovidae and Procaviidae groups (Figure 5.3). The data used for the taxon-specific regression (Figure 5.3) came from families with the largest ranges of $\delta^{13}C$ values: Bovidae from −20.4 to −1.9 ‰, Equidae from −8.2 to −2.0 ‰, and Procaviidae from −18.4 to −2.5 ‰. While the variation in $\delta^{18}O$ data is only slightly explained by $\delta^{13}C$ values, a 3‰ increase in $\delta^{13}C$ values is usually accompanied by a ~1‰ increase in $\delta^{18}O$ values.

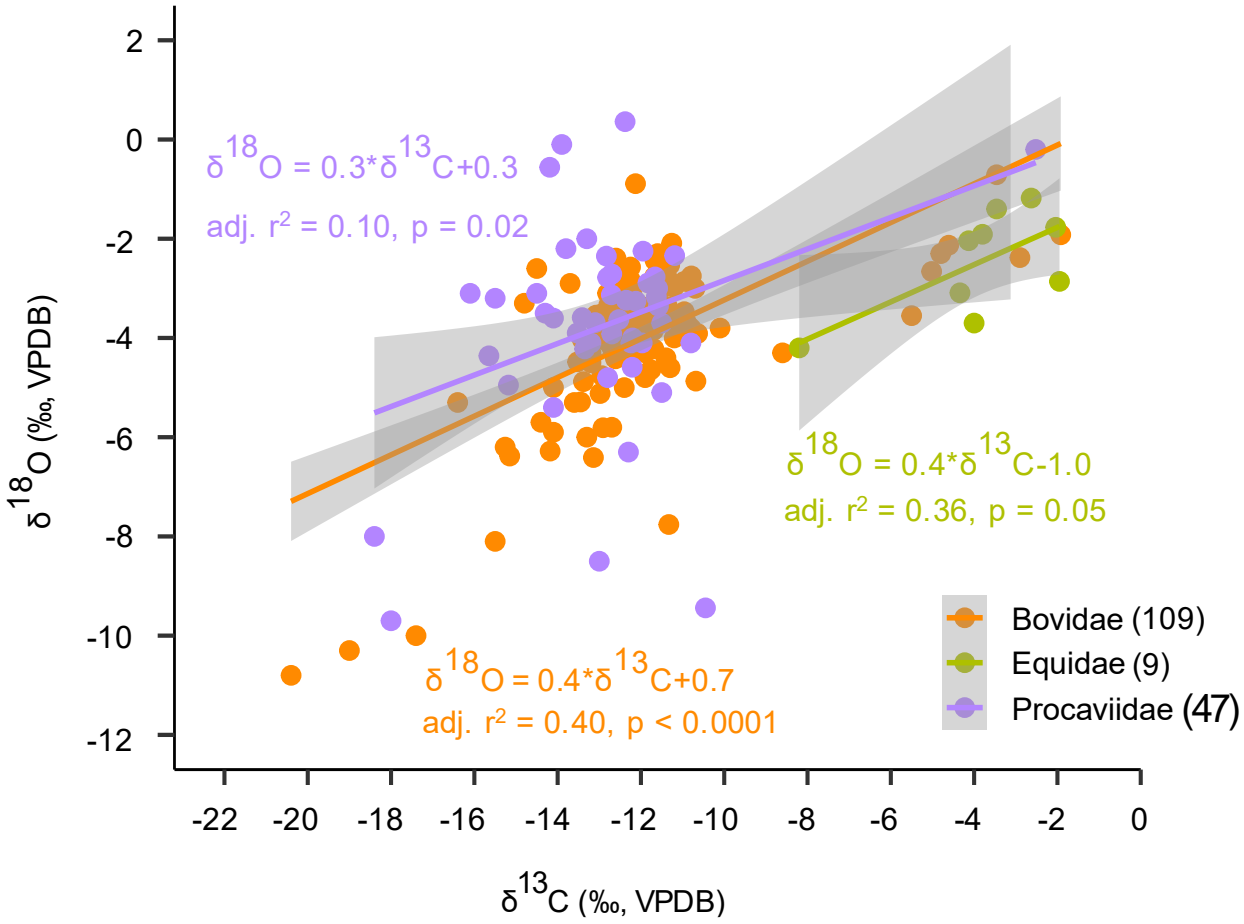


Figure 5.3. *Taxon-specific regression analysis of the relationship between $\delta^{13}C$ and $\delta^{18}O$ data for the three families with the widest range of $\delta^{13}C$ values shows a significant correlation within each family. These families are the Bovidae (ranging from -20.4 to -1.9 ‰), the Equidae (ranging from -8.2 to -2.0 ‰), and the Procaviidae (ranging from -18.4 to -2.5 ‰). The grey bands represent the 95% confidence intervals linked to each regression line. The sample sizes for each taxon are given in brackets (Iminjili et al., 2023).*

5.4 – Variation over time at Kuumbi Cave

The lack of sharp variation in KC's faunal and human isotopic values, when analyzed by phase, suggests that the area surrounding KC had a stable, dense forest mosaic through which foragers hunted wild fauna during the four phases captured in the archaeological deposits. The absence of significant changes in isotope value patterns (e.g., low to high values in all species) throughout the four phases indicates the persistence of dense forests and the continuity of similar foraging patterns,

even during periods of aridity induced by global climate change. The archaeological records of the interior of eastern Africa are marked by drastic changes in isotopic values (from low to high) during periods of climate-induced aridity. The statistical analyses in this section reveal this persistence of similar patterns in isotopic values throughout the four phases represented at KC.

Summary statistics of $\delta^{13}C$ and $\delta^{18}O$, a two-way analysis of variance (ANOVA), and post hoc comparisons demonstrate temporal variability with contrasting patterns between taxa in Phases I and II, and Phases III and IV (Figure 5.4 and Appendix 1). The $\delta^{13}C$ values indicate that taxa within Phases III and IV have higher values than Phase II. Taxa in Phase III have a mean value of −10.8‰, Phase IV have a mean value of −10.0‰, and Phase II have a mean value of −13.3‰ (Figure 5.4 and Appendix 1). Taxa in Phase I have $\delta^{13}C$ values (mean = −12.5 ‰) slightly higher than taxa in Phase II, but taxa in Phase I have the lowest $\delta^{18}O$ values (mean = −4.6 ‰) of the four phases. Significant effects of Phase on $\delta^{13}C$ values ($p < 0.0001$) and $\delta^{18}O$ values ($p < 0.0001$) have been shown by two-way ANOVAs (Appendix 1). Subsequent post-hoc comparisons demonstrate that samples from Phases III and IV exhibit a marked tendency to be considerably elevated in ^{13}C relative to samples from Phases I and II ($p < 0.0004$). The ^{18}O levels in the Phase III samples are consistently higher than those in the Phase I and Phase II samples ($p \leq 0.01$) (Appendix 1).

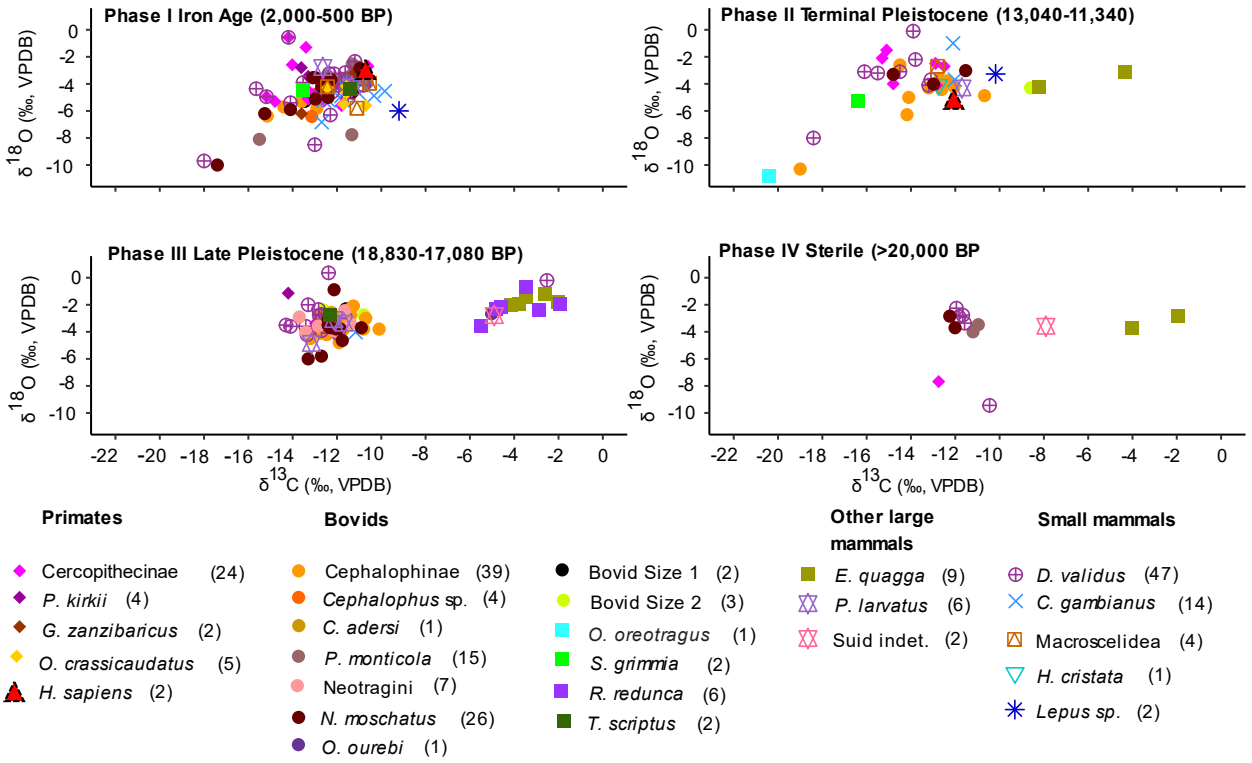


Figure 5.4. *Scatterplots of $\delta^{13}C$ and $\delta^{18}O$ values by taxa in Phases I–IV. Different groups of animals are represented by different symbols and colors: primates, bovids, other large mammals and small mammals. Nevertheless, there is an exception to this rule. Five extinct large animals are shown as square symbols:* O. oreotragus, S. grimmia, R. redunca, T. scriptus, and E. quagga. *The two* Homo sapiens *specimens are denoted by red triangles. The quantity of specimens for each taxon is indicated in brackets (Iminjili et al., 2023).*

The study looked at the $\delta^{13}C$ and $\delta^{18}O$ values of the taxa over time. This showed a tendency for lower values and more variation (see Figure 5.4 and Appendix 1). This tendency is especially evident in arboreal fauna depicted in all four phases. Cercopithecines and tree hyrax exhibit lower values and less variation in Phases I and II than in Phases III and IV. Lower values and increased variability through time are indicated by the values for forest-adapted terrestrial fauna (Figure 5.4 and Appendix 1). The observation is illustrated by the bovid tribes represented in the four Phases (Cephalophini and Neotragini). This variation is amplified by the values for other bovid categories. These categories include the other named tribes and species that are not represented in all four

phases. Some examples of this are klipspringer (Phase II), bush duiker (Phase I and II), bushbuck (Phase III and I), oribi (Phase III), bovid size 1 (Phase I and III), and bovid size 2 (Phase II and III).

Both $\delta^{13}C$ and $\delta^{18}O$ values reveal significant differences when dietary groups are examined over time (Appendix 1). Two-way ANOVAs indicate that the interaction between the effects of phase and family has an insignificant effect on both $\delta^{13}C$ values (model 1, $F(13,199) = 0.49$, $p = 0.93$) and on $\delta^{18}O$ values (model 2, $F(13,199) = 1.51$, $p = 0.11$). This phenomenon persists when taxa are grouped according to dietary category ($\delta^{13}C$ model 3, $F(4,213) = 0.35$, $p = 0.84$, $\delta^{18}O$ model 4, $F(4,213) = 0.62$, $p = 0.65$) (Appendix 1). The values for Phase I and II $\delta^{13}C$ are the lowest for most of the dietary groups. Consistently low $\delta^{13}C$ values are also shown by browsers through the four phases, and lower values are shown by grazers in Phase II, but consistently high values are shown in Phase III and Phase IV (no values are shown for Phase I). The lowest values and the widest ranges are shown to be in Phases I and II by the $\delta^{18}O$ values for browsers (Figure 5.4 and Appendix 1). In Phase II, grazers have relatively low values, but in Phases III and IV, they have high values. Omnivores exhibit comparatively diminished values in Phases I and III, yet elevated values in Phase II. Mixed feeders possess a diminutive sample size. Each of the first three phases has one sample, while Phase IV has no samples. Contrasting variability patterns between browsers, grazers, and omnivores in the different phases have also been highlighted by two-way ANOVAs and post-hoc comparisons for $\delta^{13}C$ and $\delta^{18}O$ values (Appendix 1). Two-way ANOVAs show that phase significantly affects the $\delta^{13}C$ ($p < 0.0001$) and $\delta^{18}O$ ($p < 0.0001$) values of dietary groups (Appendix 1). The findings remain consistent across different grouping methods, whether taxa are organized by family (models 1-2) or dietary category (models 3-4). In Phase III, the value pattern is

characterized by the presence of relatively high numbers of equids and reduncines, as illustrated in Figure 5.4.

5.5 – Human values

The $\delta^{13}C$ and $\delta^{18}O$ values of the two measured human individuals are within the range of other omnivorous taxa: The values are −12.1‰ and −5.4‰ for the Terminal Pleistocene and −10.7‰ and −3.1‰ for the Iron Age.

5.6 – Comparison of Kuumbi Cave and published mainland eastern African sites

The lowest values for $\delta^{13}C$ and $\delta^{18}O$ are shown in eastern Africa to be from KC, followed by PYS and Kalemba (see Table 5.1 and Figure 5.5). High values are associated with the other mainland sites. Statistical comparisons of $\delta^{13}C$ values between sites are possible for equids and browsers because there are sufficient sample sizes (see Figures 5.5 and Appendix 1). Sufficient representation of equids is found in six regional sites (KC, Lake Victoria, Lake Turkana, Kalemba, Lukenya, and Porc Epic). Significant differences in equid values among these sites are indicated by a one-way ANOVA ($F(4,216) = 115.4$, $p < 0.0001$) (Appendix 1). Although the $\delta^{13}C$ model fails Levene's test for equal variance ($F = 7.75$, $p = 0.007$), a Kruskal–Wallis test still supports significant differences in $\delta^{13}C$ values among sites ($H(4) = 180.14$, $p < 0.0001$). The results of the post-hoc Wilcoxon test indicate a significant difference between the KC equid $\delta^{13}C$ values and those at all other sites ($p < 0.0001$, according to the Bonferroni correction). Significant differences

in median equid $\delta^{13}C$ values are evident between samples from Lake Victoria and Lukenya and Kalemba ($p < 0.02$). Additionally, a substantial variation in median $\delta^{13}C$ values is observed between samples from Kalemba and Lake Turkana ($p = 0.006$; refer to Appendix 1 for comprehensive information).

Table 5.1. *Summary statistics for $\delta^{13}C$ and $\delta^{18}O$ values at coastal and inland sites in eastern Africa.*

		$\delta^{13}C$ Values			**$\delta^{18}O$ Values**		
Site	**Sample Size**	**Range**	**Mean**	**SD**	**Range**	**Mean**	**SD**
KC	229	−20.4 to −1.9	−11.9	2.8	−10.8 to 0.4	−4.0	1.7
PYS	129	−16.6 to 3.4	−4.8	5.4	−10.7 to 0.8	−2.7	2.0
Lukenya Hill	111	−14.4 to 3.6	−1.2	3.4	−7.5 to 1.9	−2.3	1.8
L. Victoria	194	−11.8 to 4	0.5	2.7	−5.5 to 5.7	0.3	2.2
L. Turkana	125	−7.9 to 3.2	−1.0	2.5	−2.5 to 6.7	2.0	2.4
Ele Bor	49	−12.6 to 4	−4.0	5.1	−4.3 to 7	2.3	2.2
Porc Epic	60	−11.2 to 2	−3.5	3.3	−3.7 to 7.4	1.9	2.4
Kalemba	88	−15.0 to 1.8	−4.2	4.7	−7.5 to −0.1	−4.0	1.8

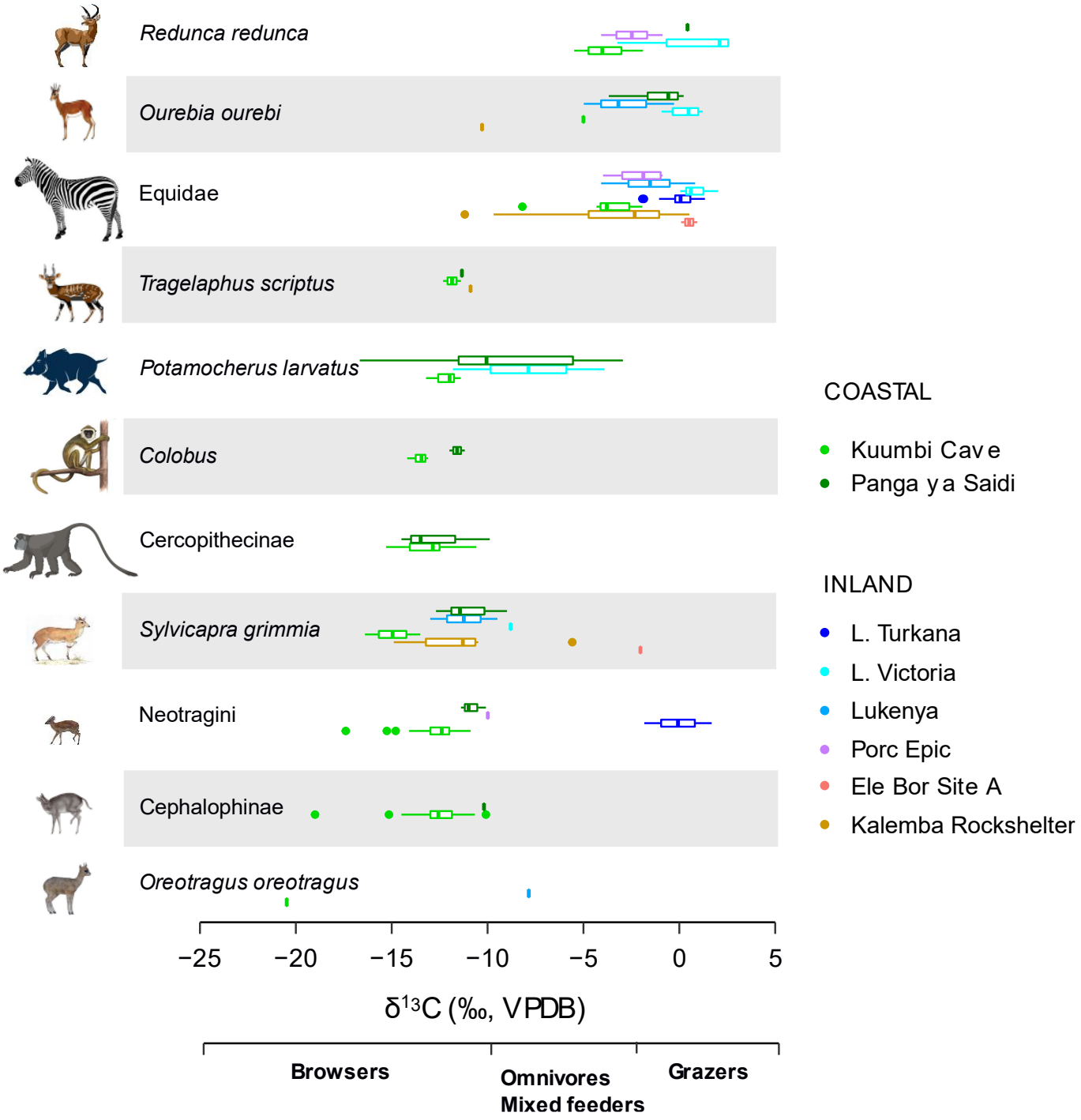


Figure 5.5. *Box and jitter plots showing the $\delta^{13}C$ values of taxa present at most sites in eastern Africa. The distribution of KC is largely distinct from that of the inland sites (Iminjili et al., 2023).*

Except in the Turkana region, statistical comparisons can be made due to the adequate representation of browsers across all sites (see Figure 5.6 and Table A1:2). Significant differences in browser $\delta^{13}C$ values among these sites are suggested by a one-way analysis of variance ($F(6,853) = 221.6$, $p < 0.0001$). Although the $\delta^{13}C$ model fails Levene's test for equal variance ($F = 28.24$, $p < 0.0001$), a Kruskal–Wallis test still supports significant differences in $\delta^{13}C$ values among sites ($H(6) = 509.4$, $p < 0.0001$). Subsequent Wilcoxon tests indicate that browser $\delta^{13}C$ values from KC, Lake Victoria, and Lukenya differ from each other and from those of all other locations ($p < 0.03$ according to the Bonferroni correction; see the R output for more information). Subsequent post hoc tests imply that the Kalemba Rockshelter median browser $\delta^{13}C$ value is distinct from those at KC, Lake Victoria, and Lukenya (see Appendix 1 for more information).

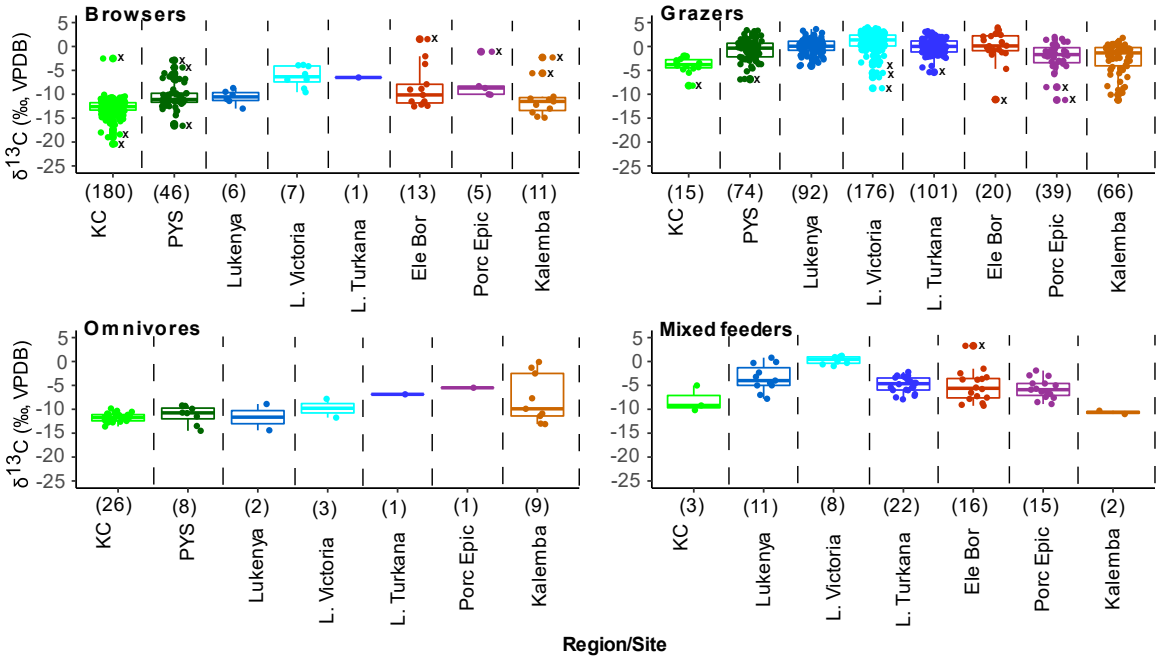


Figure 5.6. *Box and jitter plots showing the $\delta^{13}C$ values of the feeding groups in different regions and sites in eastern Africa. Outliers are indicated by dots and Xs along the midline of the plots. The sample sizes for each site or region are shown in brackets (Iminjili et al., 2023).*

Chapter 6 – Materials, methods and results for the Unguja Ukuu isotopic case study

This chapter presents the materials and methods used in the second case study, as well as the results. The study uses a multi-isotope approach based on primary data from Unguja Ukuu (UU), Fukuchani (FK) and Panga ya Saidi (PYS) to reconstruct the complex, adaptive, caprine-focused herding strategies and subsistence and mobility patterns of coastal communities during the late Holocene. The study also utilizes published data from the interior of eastern Africa for comparative analysis with the coastal datasets. The first section of the chapter presents the materials and methods, including background information on the caprines and zooarchaeological assemblages from the UU, FK and PYS sites, as well as a description of the samples and sample identifications. This section also presents the stable isotope laboratory analysis procedures and statistical analysis. The second section presents the results of collagen carbon and nitrogen from UU, FK and PYS, as well as enamel carbon, oxygen and strontium from UU. The results of the inter-site comparisons begin with a comparison of caprine collagen values from UU, FK, PYS and EYM. This is followed by the results of a comparative study of caprine, wild and human enamel carbon, oxygen and strontium values from UU, KC and PYS. Finally, the results of a comparative study of caprine enamel values from UU and sites in eastern Africa are presented.

6.1 – Unguja Ukuu, Fukuchani and Panga ya Saidi contexts and faunal assemblages

From 2011 to 2012, the Sealinks Project conducted excavations at UU, FK, and PYS as part of a broader study examining early agriculture, trade and biological exchange in coastal eastern Africa (Crowther et al., 2016a; Crowther et al., 2016b; Shipton et al., 2016; Prendergast et al., 2017b; Crowther et al., 2018; Faulkner et al., 2018; Faulkner et al., 2021; Kotarba-Morley et al., 2022). Zooarchaeological and archaeobotanical remains were collected and morphologically identified to species level, when possible (Crowther et al., 2016a; Crowther et al., 2016b; Prendergast et al., 2017b; Crowther et al., 2018). Large numbers of ambiguous caprine and wild fauna skeletal remains from fragmented assemblages were also identified to species or other taxonomic levels using ZooMS (Culley et al., 2021a; Culley et al., 2021b). The material culture from the sites was identified and studied, and more precise radiocarbon dates were produced (Crowther et al., 2016a; Crowther et al., 2018; Kotarba-Morley et al., 2022). For some sites, these were the first radiocarbon dates. This allowed for multifaceted interpretations of the archaeological assemblages.

These three sites have produced rich zooarchaeological assemblages that mostly include remains of caprines and small forest-adapted antelopes, as well as marine fauna (Prendergast et al., 2017b; Faulkner et al., 2018; Roberts et al., 2020; Culley et al., 2021a; Culley et al., 2021b; Faulkner et al., 2021). UU is represented in this study by goat (*Capra hircus*, n=14), sheep (*Ovis aries*, n=4), two small forest adapted antelopes: suni (*Neotragus moschatus*, n=2), and blue duiker (*Philantomba monticola*, n=3), hartebeest (Alcelaphini, n=1), monkey (Cercopithecidae, n=2), and hyrax (Dendrohyrax, n=1). FK is represented by a goat and suni (n=6). PYS is represented by a sheep and three species of small and large forest-adapted antelopes: klipspringer (*Oreotragus oreotragus*, n = 8), common duiker *(Sylvicapra grimmia*, n = 5*)*, and bushbuck (Tragelaphini, n =

2), as well as monkey (n = 2). These three sites have also yielded nearly identical archaeobotanical assemblages, composed primarily of *Sorghum bicolor* (sorghum), *Pennisetum glaucum* (pearl millet), *Eleusine coracana* (finger millet), and *Oryza sativa* (Asian rice) (Crowther et al., 2016a; Crowther et al., 2016b; Crowther et al., 2018). They have also produced material culture remains, including African ceramics of the Tana Tradition/Triangular Incised Ware (TT/TIW), iron, Middle Eastern and Chinese trade wares, glass, shell beads, and bead grinders (Juma, 2004; Wood et al., 2017).

6.2 –Samples and sample identification

This study examined a total of 205 bulk bone and enamel samples, of which 62 are primary, newly-analyzed samples from coastal sites (UU, FK, and PYS), and 143 are published samples from the interior and also coastal regions of eastern Africa (Table A2:1 - A2:7) (Ambrose and DeNiro, 1986a; 1989; Chritz et al., 2019; Prendergast et al., 2019a; Roberts et al., 2020; Iminjili et al., 2023). The primary dataset comprises 62 collagen and enamel samples from caprine and wild animals, including 27 collagen and ten enamel samples from UU, seven from FK, and 18 from PYS, as well as a human enamel sample from UU (Table A2:1 - A2:3). The UU collagen dataset also includes hartebeest (Alcelaphini), a locally extirpated species of large, grazing antelope. The published dataset comprises 137 samples from fauna (wild and domesticates) and six samples from three humans (Tables A2:3 - A2:7). These include collagen samples from EYM (6) and enamel samples from KC (57), Dongodien (21), Luxmanda (20), Gogo Falls (14), and Wadh Lang'o (19), and human enamel samples from KC (from two individuals), and PYS (one individual, four

samples from different teeth). The PYS samples from four teeth were taken from the same Iron Age individual to gain insight into the life history of foragers in this region.

For the primary dataset, we selected collagen and enamel samples for isotopic analysis from the residue samples available from the previous ZooMS study (Culley et al., 2021a; Culley et al., 2021b). This selection was made based on the availability of samples, species, archaeological context, and phase. This was necessary because a significant percentage of the ZooMS study samples were depleted. For Trench 14, which has 46 contexts and is divided into early and late phases, we targeted the Early Phase contexts for the earliest caprine isotope and dating samples (Figure 6.1) (Kotarba-Morley et al., 2022). However, this proved to be a challenge due to the small sample size and poor bone preservation. To minimize the chances of double sampling the same individual in the UU dataset, samples from different contexts were prioritized. These contexts included 1428, 1423, 1420, 1412, 1404, 1414, and 1408. However, in certain cases where a large number of collagen samples were available from the previous ZooMS study and the sample sizes were small enough to fail the standards of collagen preservation, more than one sample from the same context and species was analyzed: 1423 (three samples from three species), 1412 (eight samples from three species), 1414 (four samples from two species), and 1404 (two samples from two species). Some samples from UU likely came from the same individual. Of the ZooMS study samples, ten of the largest caprine enamel samples were selected and divided into three subsets (~10 mg per sample). The first subset was used for carbon and oxygen isotope analysis, the second subset was used for strontium isotope analysis, and the third subset was to be used for radiocarbon dating but failed to produce a large enough sample size per individual. Additionally, enamel samples from wild animals could not be obtained for the UU $^{87}Sr/^{86}Sr$ baseline.

In some cases, the collagen and bone samples were too small or depleted. In other cases, the samples failed to produce collagen or the results failed to meet standards of bone collagen preservation (C/N ratio, %C, and %N) (noted in the results section). These challenges resulted in the loss of 20 samples from UU, FK, and PYS, eight of these samples came from strategic contexts in Trench 14 (seven in the Early Phase) that would have provided intriguing insights into caprine husbandry and translocation in the Early Phase (Figure 6.1).

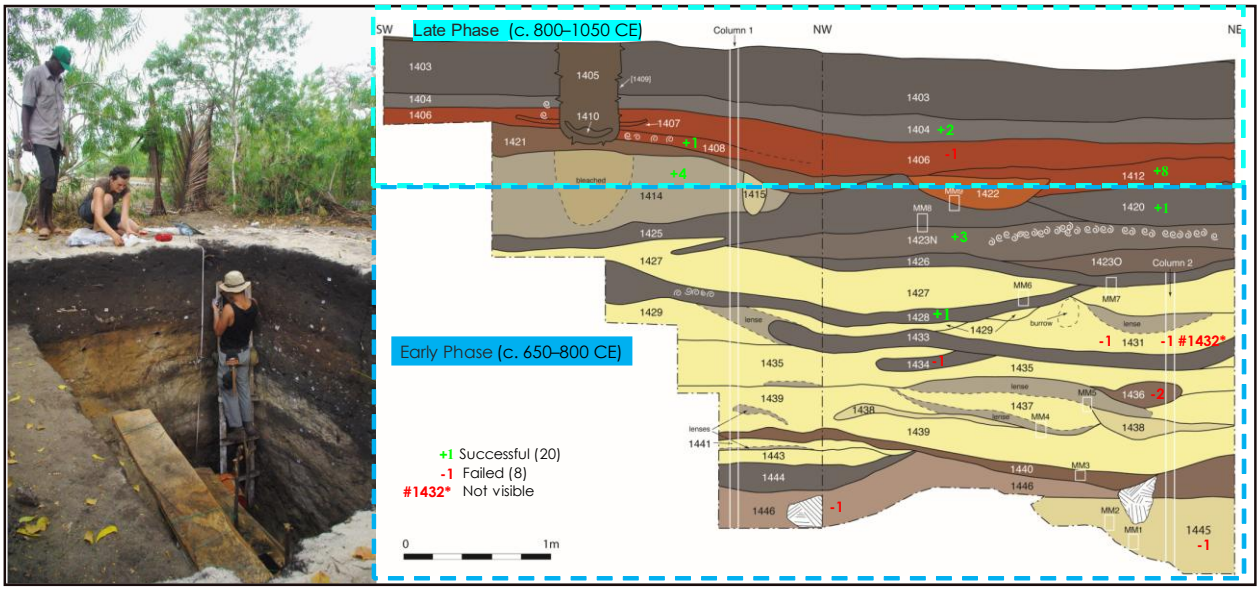


Figure 6.1. *Stratigraphy of UU Trench 14 highlighting the Early Phase contexts where high numbers of samples that failed to produce isotope results originated.*

6.3 – Stable isotope analysis

Collagen samples were taken from residue samples from the ZooMS project, and additional samples were sourced from bone and tooth enamel samples at the Max Planck Institute of Geoanthropology (MPI-GEA). Prior to the isotope study, the original bones and teeth from which these samples were extracted had been repatriated to Zanzibar. Caprine and wild fauna collagen

stable carbon and nitrogen, as well as enamel carbon and oxygen, were analyzed at the Stable Isotope Laboratory at the Max Planck Institute of Geoanthropology in Jena, Germany. Strontium ($^{87}Sr/^{86}Sr$) isotope analysis was performed in the Department of Geosciences at the University of Cape Town in South Africa. The radiocarbon dating samples were sent to the Center for Applied Isotope Studies (CAIS) at the University of Georgia, but they failed to produce enough collagen for analysis. The extraction methods for collagen and enamel, as well as the standards used for stable carbon and nitrogen (collagen) and stable carbon and oxygen analyses, and strontium (enamel) analyses are all described below.

Stable carbon and nitrogen isotope analysis

Bone collagen was extracted using a modified Longin (Longin, 1971) method. Bone samples were placed in 12 mL glass test tubes and underwent standard pretreatment according to in-house protocols. Bone samples were cleaned by abrasion using a sandblaster and approximately 1g bone sample was broken into small pieces and demineralised by immersion in 0.5M HCl for 1-7 days. Once demineralisation was complete, samples were rinsed three times with ultra-pure H2O. The residue was gelatinized in 10 mL of pH3 HCl solution at 70°C for 48 h. The soluble collagen solution was Ezee-filtered to remove insoluble residues, frozen, and lyophilized (Brock et al., 2013). Where sufficient material was available approximately 1mg of the resulting purified collagen was weighed in duplicates into tin capsules for analyses. Samples were analysed together with an in-house standard and international standards using a Thermo Scientific Flash 2000 Elemental Analyser coupled to a Thermo Delta V Advantage mass spectrometer. Isotopic values are reported as the ratio of the heavier isotope to the lighter isotope ($^{13}C/^{12}C$ or $^{15}N/^{14}N$) as δ values in parts per mill (‰) relative to international standards, VPDB for $\delta^{13}C$ and atmospheric N2 (AIR)

for $\delta^{15}N$. Results were calibrated against international standards IAEA-CH-6: δ13C = −10.80 ± 0.47‰, IAEA-N-2: $\delta^{15}N$ = 20.3 ± 0.2‰, and USGS40: $\delta^{13}C$ = −26.38 ± 0.042‰, $\delta^{15}N$ = 4.5 ± 0.1‰. Based on replicate analyses, the machine error is ±0.2‰ for $\delta^{13}C$ and ±0.2‰ for $\delta^{15}N$. Overall measurement precision was studied through the measurement of repeats of fish collagen (n = 20, ±0.2‰ for $\delta^{13}C$ and ±0.2‰ for $\delta^{15}N$).

Stable carbon and oxygen isotope analysis

All teeth were photographed before analysis. Teeth and tooth fragments were cleaned using air-abrasion to remove any adhering external material. Enamel powder was obtained using gentle abrasion with a diamond-tipped drill along the full length of the buccal surface in order to maximize the period of formation represented by the bulk sample. Powdered enamel samples underwent a wet chemistry pre-treatment to remove organic or secondary carbonate contaminants. 1 mL of 0.1M acetic acid was added to each sample for 10 min, followed by three rinses in ultra-pure H_2O and centrifugation (Sponheimer et al., 2005a; Lee-Thorp et al., 2012; Roberts et al., 2017). Samples were freeze-dried for 4 h before 3–3.5mg was weighed out into borosilicate glass vials for analysis. Following the reaction with 100% phosphoric acid at 70°C, sample CO_2 evolved and was analysed for stable carbon ($^{13}C/^{12}C$) and oxygen isotopic ($^{18}O/^{16}O$) composition using a Thermo GasBench 2 connected to a Thermo Delta V Advantage Mass Spectrometer (Thermo Fisher Scientific). Stable carbon and oxygen isotope values are reported as delta (δ) values as parts per thousand (per mil, ‰) relative to the international standard Vienna Pee Dee Belemnite for $^{13}C/^{12}C$ and $^{18}O/^{16}O$, and were calibrated against international standards IAEA NBS 18 ($\delta^{13}C$−5.014 ± 0.032‰, $\delta^{18}O$−23.2 ± 0.1‰), IAEA 603 ($\delta^{13}C$ +2.46 ± 0.01‰, $\delta^{18}O$−2.37 ± 0.04‰) and IAEA CO8 ($\delta^{13}C$−5.764 ± 0.032‰, $\delta^{18}O$−22.7 ± 0.2‰) registered by the International Atomic Energy Agency. The in-house

standard was USGS44($\delta^{13}C$= ~−42.1‰). Machine error based on the analyses of standards is ±0.2‰ for $\delta^{13}C$ and ±0.2‰ for $\delta^{18}O$. Replicate analysis of the standard USGS44 indicates that overall measurement precision was c. ±0.2‰ for $\delta^{13}C$ and ±0.2‰ for $\delta^{18}O$.

Strontium isotope analysis

Processing of the enamel samples before analysis followed the established procedure (Pin et al., 1994). Powdered enamel samples were weighed into 7ml Teflon beakers, 2–3 ml of 65% HNO_3 was added, and the beakers were closed and kept at 140 °C for 1 h. Following complete sample dissolution, the samples were dried and taken up in 1.5 ml of 2M HNO_3. The strontium fraction was then isolated following the procedure in Pin et al. (Pin et al., 1994) using Eichrom Sr. Spec resin, dried down, before being redissolved in 0.2% HNO (Pin et al., 1994). Isolated Sr fractions were subsequently analysed as 200 ppb Sr solutions using the NuPlasma HR MC-ICP-MS. Repeat analysis of an in-house plant reference material Namiso 316 processed in parallel with the plant samples yielded a result of 0.720508 ± 0.000043 (n = 3) which is in good agreement with the average for the facility (0.720508 ± 0.000043; n = 21). The enamel samples were processed alongside repeats of the in-house carbonate reference material (NM95) and gave an average $^{87}Sr/^{86}Sr$ value of 0.7089015 ± 0.000028 (n = 24). This was in good agreement with the long-term average of this reference material at the facility of 0.708911 ± 0.000040 [2σ]; n = 414. All $^{87}Sr/^{86}Sr$ data presented are referenced to bracketing analyses of the international strontium isotope standard NIST SRM987 ($^{87}Sr/^{86}Sr$ reference value of 0.710255). Sample values were corrected for instrumental mass fractionation using the exponential law and an $^{86}Sr/^{88}Sr$ of 0.1194 and isobaric ^{87}Rb interferences were corrected using the measured ^{85}Rb signal and the natural $^{85}Rb/^{87}Rb$. Total

procedural blanks processed with samples in this facility yielded background Sr levels <250 pg and were therefore negligible.

Statistical analysis

All statistical analyses were performed using the free R statistical software (R Core Team, 2013). A series of analyses were performed on $\delta^{13}C_{coll}$ and $\delta^{15}N$, and $\delta^{13}C_{enamel}$ and $\delta^{18}O$ values to reveal differences between the caprine and wild herbivores taxonomic groups. We also compared stable isotope values from herbivore bone collected at coastal and island sites with those from bone collected in the interior of eastern Africa. This set of analyses included the Shapiro-Wilk test for normality, the Brown-Forsythe test for equal variance, and one-way ANOVA. Pairwise multiple comparisons were performed using the Holm-Sidak method, t-test, and Mann-Whitney rank sum test where appropriate. Apart from comparing means and medians, these statistical analyses also compare them relative to the range of variance.

6.4 – Indicators of collagen preservation and direct dates

The summary statistics for the isotope results are shown in Table A2:1. We evaluated the bone collagen results using established indicators of preservation, including a C/N ratio of 2.9-3.6, %C of approximately 15-48%, and %N of approximately 5-17% (DeNiro, 1985; Ambrose, 1990; van Klinken, 1999; Sealy et al., 2014). Almost 85% of the collagen samples passed these tests and are the only values used in the statistical analysis. Twenty-seven samples from UU, seven from FK, and eighteen from PYS demonstrated a successful outcome in these tests, while two from UU and

seven from PYS failed to meet the criteria. Despite failing to obtain direct dates from caprines or sufficient sample sizes for the Early Phase in Trench 14, eight published C_{14} dates from domesticated crops of the Early Phase (650-800 CE) and a relative date from a Chinese Yue pottery of the Late Phase (800-1050 CE) were used to reconstruct the chronology of caprines at the UU site (Crowther et al., 2016a; Crowther et al., 2018; Kotarba-Morley et al., 2022). Further direct dates and additional caprine samples from all contexts in Trench 14 have the potential to offer a clearer view of the ecological changes at the UU site in the future, from the initial sparse settlements of the Early Phase to the dense settlements, established farmlands, and large-scale marine resource exploitation of the Late Phase.

6.5 – Variation in taxa at Unguja Ukuu

Since Unguja Ukuu is within the coastal forests and goats are predominantly browsers, it was anticipated that the collagen and enamel isotope values of the caprines and small, forest-adapted bovids would be similar. Such a finding would suggest that the introduction of goats to the island during the Iron Age led to increased browsing, deforestation, and other negative ecological impacts. Culley et al. (2021b) alluded to such a state at UU. However, the isotope results suggest otherwise. The isotope results indicate that the goats at UU fed on a diet that was completely different from that of the small, forest-adapted mammals, particularly the bovids that are taxonomically most closely related to goats, such as suni and blue duiker. In general, goats and sheep have high $\delta^{13}C_{coll}$ and $\delta^{15}N$ values ($\delta^{13}C_{coll}$ values above –16‰ and $\delta^{15}N$ values above 8‰), whereas small forest-adapted mammals have low $\delta^{13}C_{coll}$ and $\delta^{15}N$ values ($\delta^{13}C_{col}$ values below –18‰ and $\delta^{15}N$ values below 8‰). The high values, which reflect a diet different from that of browsing in dense forests,

are also reflected in the enamel $\delta^{13}C$ and $\delta^{18}O$ values of caprines. These values are likely the result of human intervention through feeding on restricted farmlands fertilized with livestock, crops, and marine fish refuse. As expected for a trade port involved in transoceanic commerce, variability in strontium values indicates that some caprines were translocated from the mainland eastern Africa hinterland-coastal strip. Some of these caprines may have been among the first domesticated animals brought to the islands from mainland eastern Africa.

Collagen $\delta^{13}C$ and $\delta^{15}N$

The UU goats (n=14) and sheep (n=4) are the only taxa with n>3 that could allow statistical significance testing (Figure 6.2). The three antelope species represented in the UU dataset seem to have similar values: blue duiker (*Philantomba monticola*, n=3), suni (*Neotragus moschatus*, n=2), and hartebeest (Alcelaphini, n=1). Accordingly, we boosted the group sample sizes by assuming that all three species of antelope have similar isotopic niches and creating a general "antelope" group (n=6, from 3 taxa).

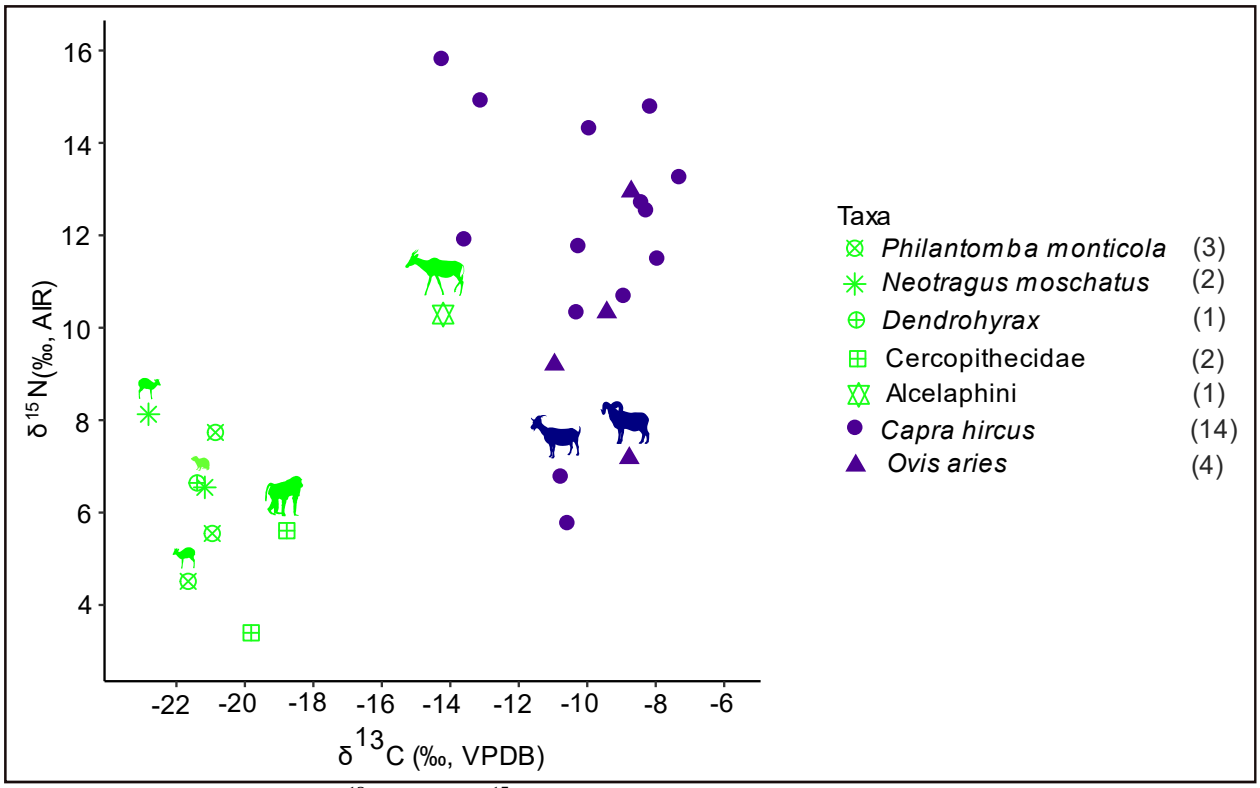


Figure 6.2. *Scatterplots of $\delta^{13}C_{coll}$ and $\delta^{15}N$ values by species highlighting the distinctions between wild herbivores (Small Forest-adapted antelopes and other browsers have $\delta^{13}C$ values less than −18‰ and $\delta^{15}N$ values less than 9‰) and caprines (almost all of the $\delta^{13}C$ values are above −14‰ and most of the $\delta^{15}N$ values above 10‰) from the UU site.*

The $\delta^{13}C_{coll}$ data distributions pass the Shapiro-Wilk test for normality (p=0.56) and Brown-Forsythe test of equal variance (p=0.60), so a one-way ANOVA was applied. This test suggests that there are significant differences in mean $\delta^{13}C_{coll}$ values among these three groups ($F(2,23)=44.313$, $p<0.001$). Pairwise multiple comparisons through the Holm-Sidak method suggest that the mean $\delta^{13}C_{coll}$ value of antelope (n=6, $\bar{x}\pm SD=-20.3\pm3.1$‰) is different from that of both goats (n=14, $\bar{x}\pm SD=-10.2\pm2.2$‰, $p<0.001$) and sheep (n=4, $\bar{x}\pm SD=-9.5\pm1.1$‰, $p<0.001$).

The $\delta^{15}N$ data distributions pass the Shapiro-Wilk test for normality (p=0.28) and Brown-Forsythe test of equal variance (p=0.79), so we can apply a one-way ANOVA. This test suggests that there are significant differences in mean $\delta^{15}N$ values among sheep, goats, and antelopes ($F(2,23)=7.12$,

p=0.004). Pairwise multiple comparisons through the Holm-Sidak method suggest that the only significant pairwise difference is between the mean $\delta^{15}N$ value of goats (n=14, $\bar{x}$±SD=11.9±2.9‰) and that of antelopes (n=6, $\bar{x}$±SD=7.1±2.1‰, =0.004).

Enamel $\delta^{13}C$, $\delta^{18}O$ and $^{87}Sr/^{86}Sr$ values

The UU enamel values are represented by nine caprines: eight goats and one sheep (deciduous) (Figure 6.3A). The UU caprines consistently have $\delta^{13}C_{enamel}$ values higher than −7‰ (−6.5 to −2.2‰, mean −4.9‰). The sheep's value (−4.4‰) falls within the goat values' range (−6.5 to −2.2‰). The UU caprines also show $\delta^{18}O$ values consistently lower than 1‰ (−4.6 to 4.4‰, mean −0.4‰), except one value (4.4‰), which is the highest value in the dataset.

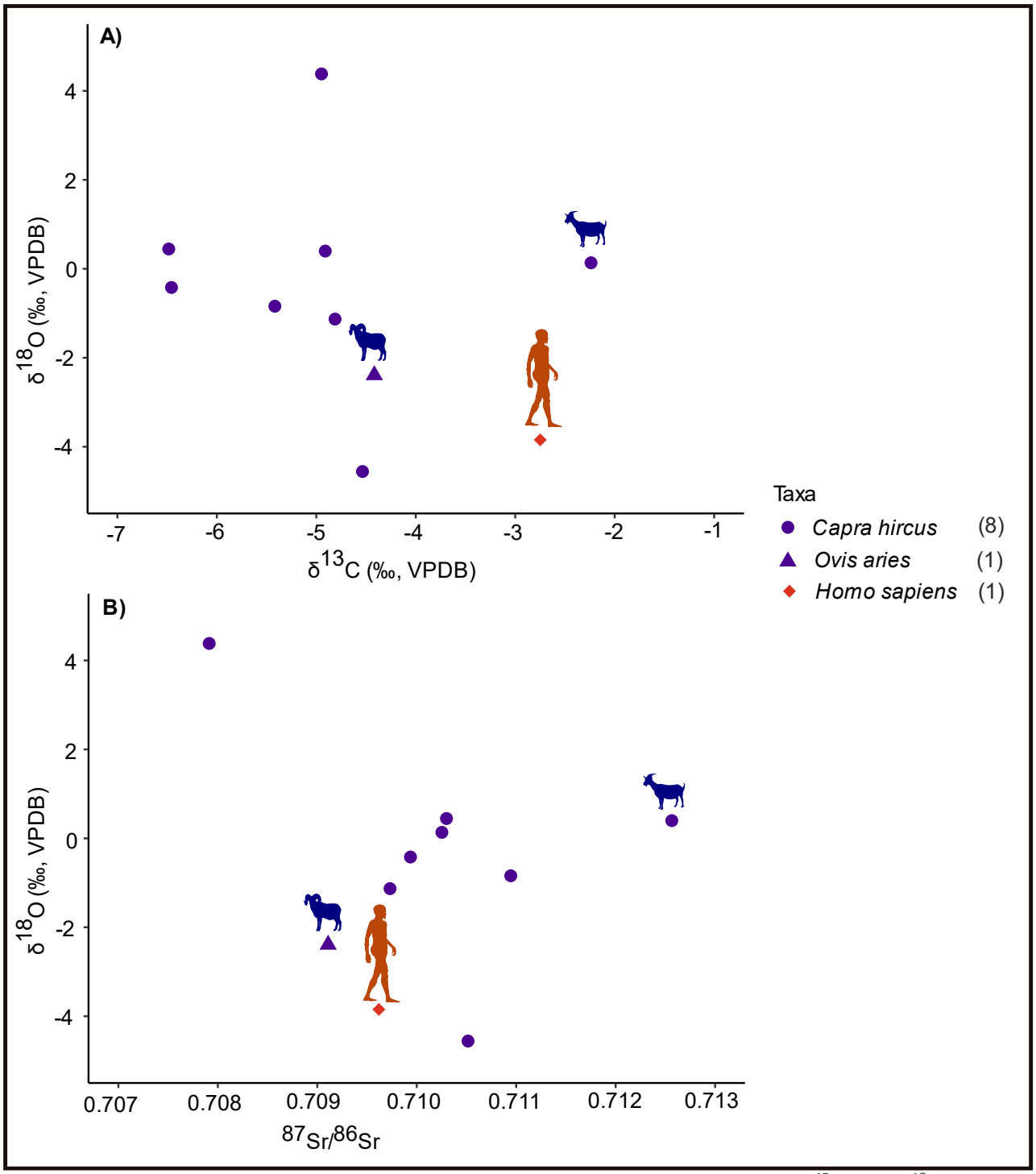


Figure 6.3. *Scatterplots of enamel values from UU caprines and human by (A) $\delta^{13}C$ and $\delta^{18}O$ values (caprines $\delta^{13}C_{enamel}$ values are higher than −7‰ and almost all $\delta^{18}O$ values are lower than 1‰) highlighting the similarity in the caprines $\delta^{13}C_{enamel}$ and $\delta^{13}C_{coll}$ patterns; (B) Variation in the $^{87}Sr/^{86}Sr$ and $\delta^{18}O$ values from UU caprines and human highlighting the sheep value from a deciduous tooth, and the low $^{87}Sr/^{86}Sr$ value with the highest $\delta^{18}O$ value in the UU dataset and five values higher than 0.710.*

The $^{87}Sr/^{86}Sr$ values for the nine UU caprines and one human show patterns that suggest different origins (Figure 6.3B). The nine caprine $^{87}Sr/^{86}Sr$ values are 0.71095, 0.71052, 0.71256, 0.71030, 0.70973, 0.70791, 0.70994, 0.70911, and 0.71025. The low goat value (0.70791) is also associated with the highest $\delta^{18}O$ value (4.4‰) in the dataset. Except for 4.4‰, the other eight $\delta^{18}O$ values are consistently lower than 1‰ (−4.6 to 4.4‰, mean −0.4‰), similar to KC faunal values (Iminjili et al., 2023). The UU human sample has $^{87}Sr/^{86}Sr$ value of 0.709620, $\delta^{13}C_{enamel}$ value of -2.7‰ and $\delta^{18}O$ value of -3.8‰.

6.6 – Caprine bone collagen from Unguja Ukuu, Fukuchani, Panga ya Saidi, and Enkapune ya Muto

This comparative study of collagen values from the coastal sites and the interior eastern African site of Enkapune ya Moto also confirms anthropogenic influences on dietary patterns among caprines at FK and PYS and UU. The FK goat values fall within the dietary range of UU goats. However, the PYS sheep are an unexpected finding for sheep in eastern Africa, with a $\delta^{13}C_{coll}$ value lower than −8‰ and an $\delta^{15}N$ value higher than 12‰. The $\delta^{13}C_{coll}$ and $\delta^{15}N$ values of the Enkapune ya Moto sheep are consistent with those of sheep in a wild grazing setting, free from farmland crop residue, livestock, and marine manure. Similar to the UU caprine collagen values discussed in Section 6.5, the FK and PYS caprine $\delta^{13}C_{coll}$ and $\delta^{15}N$ values differ greatly from those of wild animals from these sites, again suggesting the inclusion of an anthropogenically instigated, marine fodder or C_4 grasses in dry environment.

There is not enough taxonomic coverage at each site to statistically evaluate the effects of both taxon and site on $\delta^{13}C_{coll}$ and $\delta^{15}N$ values (Figure 6.4 and Table A2:1 and A2:5). The strongest comparison that can be made in this regard is between sheep at UU (n=4) and EYM (n=6). The $\delta^{13}C_{coll}$ data distributions for sheep at these sites pass the Shapiro-Wilk test for normality (p=0.31) and Brown-Forsythe test of equal variance (p=0.52). A subsequent t-test suggests that there is no significant difference in mean $\delta^{13}C_{coll}$ value between UU (n=4, $\bar{x}$±SD=−9.5±1.1‰) and EYM (n=6, $\bar{x}$±SD=−7.5±1.7‰, t(8)= −2.08, p=0.07). The $\delta^{15}N$ data distributions for sheep from these sites similarly pass the Shapiro-Wilk test for normality (p=0.83) and Brown-Forsythe test of equal variance (p=0.91), so we can apply a t-test. This test suggests that there is no significant difference in mean $\delta^{15}N$ value between UU (n=4, $\bar{x}$±SD=9.9±2.4‰) and EYM (n=6, $\bar{x}$±SD=8.9±2.0‰, t(8)=0.76, p=0.47).

Unlike UU, which has goats with $\delta^{13}C_{coll}$ values higher than −11.0‰, the FK goat has a lower value (−13.8‰), but it is within the UU range (Figure 6.4 and Table A2:1 and A2:5). The FK goat $\delta^{15}N$ value (10.1‰) is also within the range of UU caprine values. The PYS sheep has a lower $\delta^{13}C_{coll}$ value (−15.4‰) than the UU and EYM sheep. All the EYM sheep $\delta^{15}N$ values are lower than 11‰ (5.8 to 11‰, mean 8.9‰), and UU has a similar pattern, but with one higher value (13‰). The PYS sheep $\delta^{15}N$ value (13.4‰) is higher than all of those of the EYM sheep, but within the range of the UU sheep.

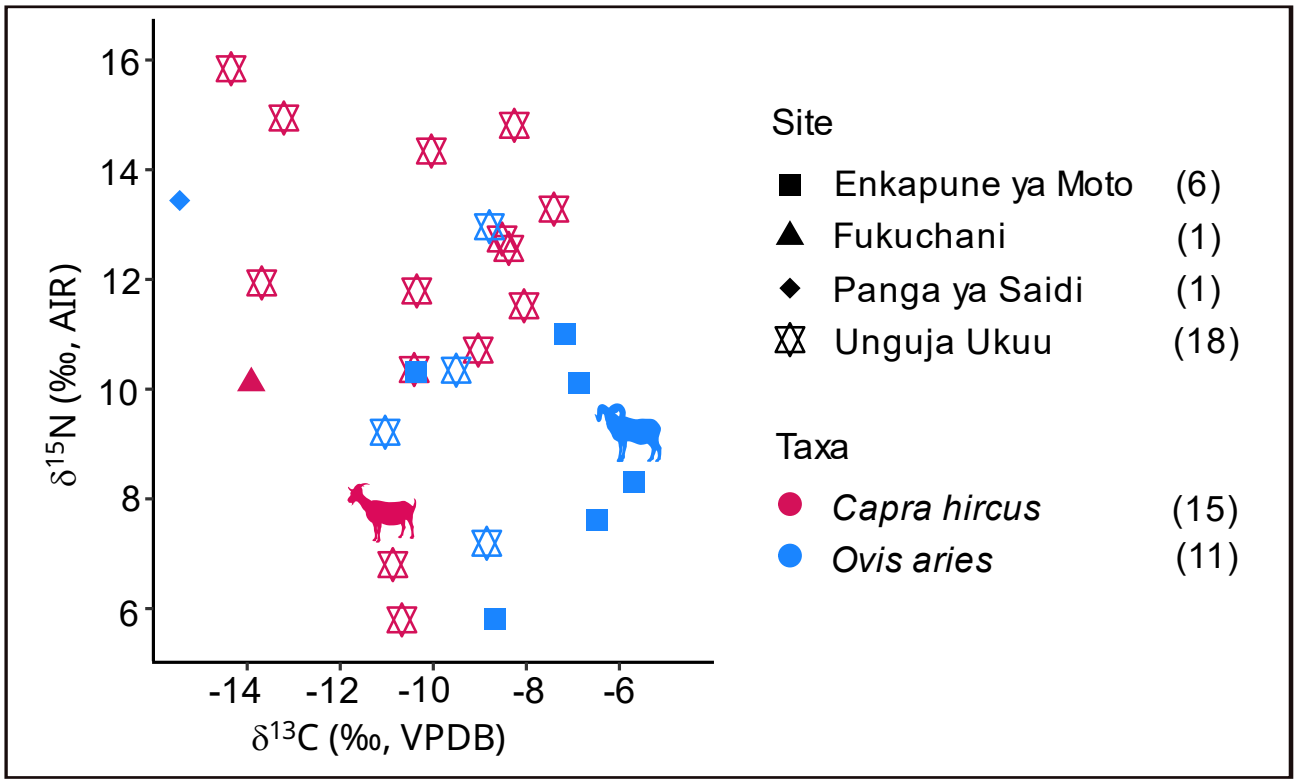


Figure 6.4. *Scatterplots of $\delta^{13}C_{coll}$ and $\delta^{15}N$ values of caprines from three coastal (UU, FK, and PYS) and one interior eastern African (EYM) site highlighting the similarity between UU and EYM, and the distinction between sheep from these sites and PYS.*

Apart from the goat values discussed above, FK is also represented by a set of wild fauna consisting of six suni (Figure 6.5 and Table A2:1). Whereas these suni consistently show $\delta^{13}C$ values lower than −20‰ (−21.2 to −20.2‰; mean −20.7‰) and $\delta^{15}N$ values lower than 10‰ (7.1 to 10.2‰; mean 8.8‰), the goat has a $\delta^{13}C$ value higher than −15‰ (−13.8‰) and an $\delta^{15}N$ value of 10.1‰. The PYS sample also includes forest mosaic adapted wild fauna, including klipspringer (*Oreotragus oreotragus*), bush duiker (*Sylvicapra grimmia*), bushbuck (Tragelaphini), and monkey (Cercopithecidae) (Figure 6.5 and Table A2:1). The wild fauna $\delta^{13}C$ values (n = 17) show consistently low variation, dominated by values lower than −20‰ (−21.9 to −15.3‰; mean −20.1‰). The PYS sheep (n = 1) has a higher value than most wild fauna (−15.4‰), but lower than the expected value for grazers. The PYS $\delta^{15}N$ values (n = 18) demonstrate significant variation

(4.6 to 13.4‰; mean 7.9‰). All wild animals have $\delta^{15}N$ values lower than 12‰. The sheep (n = 1) has the highest $\delta^{15}N$ value (13.4‰).

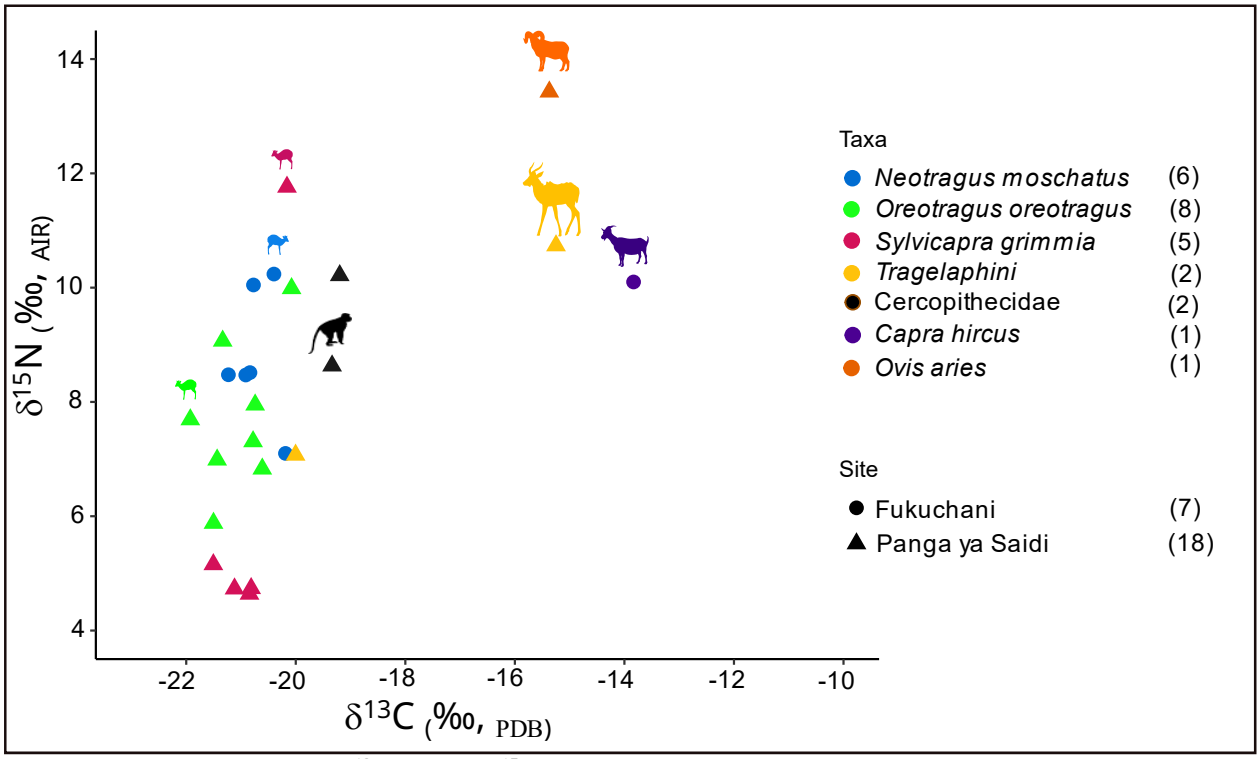


Figure 6.5. *Scatterplots of $\delta^{13}C_{coll}$ and $\delta^{15}N$ values of wild herbivores and caprines from FK and PYS highlighting the distinctions between forest-adapted herbivores ($\delta^{13}C_{coll}$ values concentrated below −18‰ and $\delta^{15}N$ values below 10‰) and caprines (PYS sheep unusually low $\delta^{13}C_{coll}$ value, and unusually high $\delta^{15}N$ values for sheep, common duiker (S, grimmia), and bushbuck (Tragelaphini)).*

6.7 – Caprines, wild fauna, and human enamel from Unguja Ukuu, Kuumbi Cave, and Panga ya Saidi

The results of the comparative study, which analyzed the enamel $\delta^{13}C$, $\delta^{18}O$ and $^{87}Sr/^{86}Sr$ values of caprines from UU, wild fauna from KC, and humans from UU, KC, and PYS, continue to highlight the anthropogenically instigated dietary and mobility patterns of the UU caprines. Similar to the collagen values, the enamel values indicate that these caprines (with $\delta^{13}C$ values above −8‰) had different dietary patterns than small, forest-adapted mammals (with $\delta^{13}C$ values below −8‰). The similarity between the values of the UU caprines and the wild grazers from KC indicates that these caprines fed on some C_4 crops (mainly sorghum and millet) recovered at the site and supplemented with additional wild grazing. The human values highlight the expected distinctions of an agropastoral versus foraging lifestyle. The UU human agropastoral lifestyle is indicated by a distinct $\delta^{13}C$ value of −8‰, which is higher than the PYS and KC forager values (below −8‰). Human $^{87}Sr/^{86}Sr$ values suggest that the UU and KC individuals are consistent with growing up local to the island, and the same is the case for the PYS individual on the coastal forested strip. The diversity in $^{87}Sr/^{86}Sr$ and $\delta^{18}O$ values among caprines suggests the translocation of animals from the mainland. Multiple statistical analyses of the isotopic values confirm these observations (Kruskal Wallis and Dunn's Method).

The UU caprines and KC grazer and browser $\delta^{13}C_{enamel}$ and $\delta^{18}O$ values show high variation (Figure 6.6A). The $\delta^{13}C_{enamel}$ and $\delta^{18}O$ data distributions for UU caprines, KC grazers, and KC browsers fail the Shapiro-Wilk test for normality ($P<0.05$), so we applied a Kruskal Wallis test to compare central tendencies (Figure 6.6A). This test applied to the $\delta^{13}C$ data suggests that there are significant differences in median values between groups ($H(2)=45.82$, $p<0.001$). Pairwise multiple

comparisons following Dunn's Method suggest that UU caprines and KC grazers have statistically indistinguishable $\delta^{13}C_{enamel}$ values but that the median of both groups is significantly greater than that of KC browsers ($p<0.001$). The Kruskal Wallis test applied to the enamel $\delta^{18}O$ data suggests that there are significant differences in median values between groups ($H(2)=28.01$, $p<0.001$). Pairwise multiple comparisons following Dunn's Method suggest that UU caprines and KC grazers have statistically indistinguishable enamel $\delta^{18}O$ values but that the median of both groups is significantly higher than that of KC browsers ($p<0.001$).

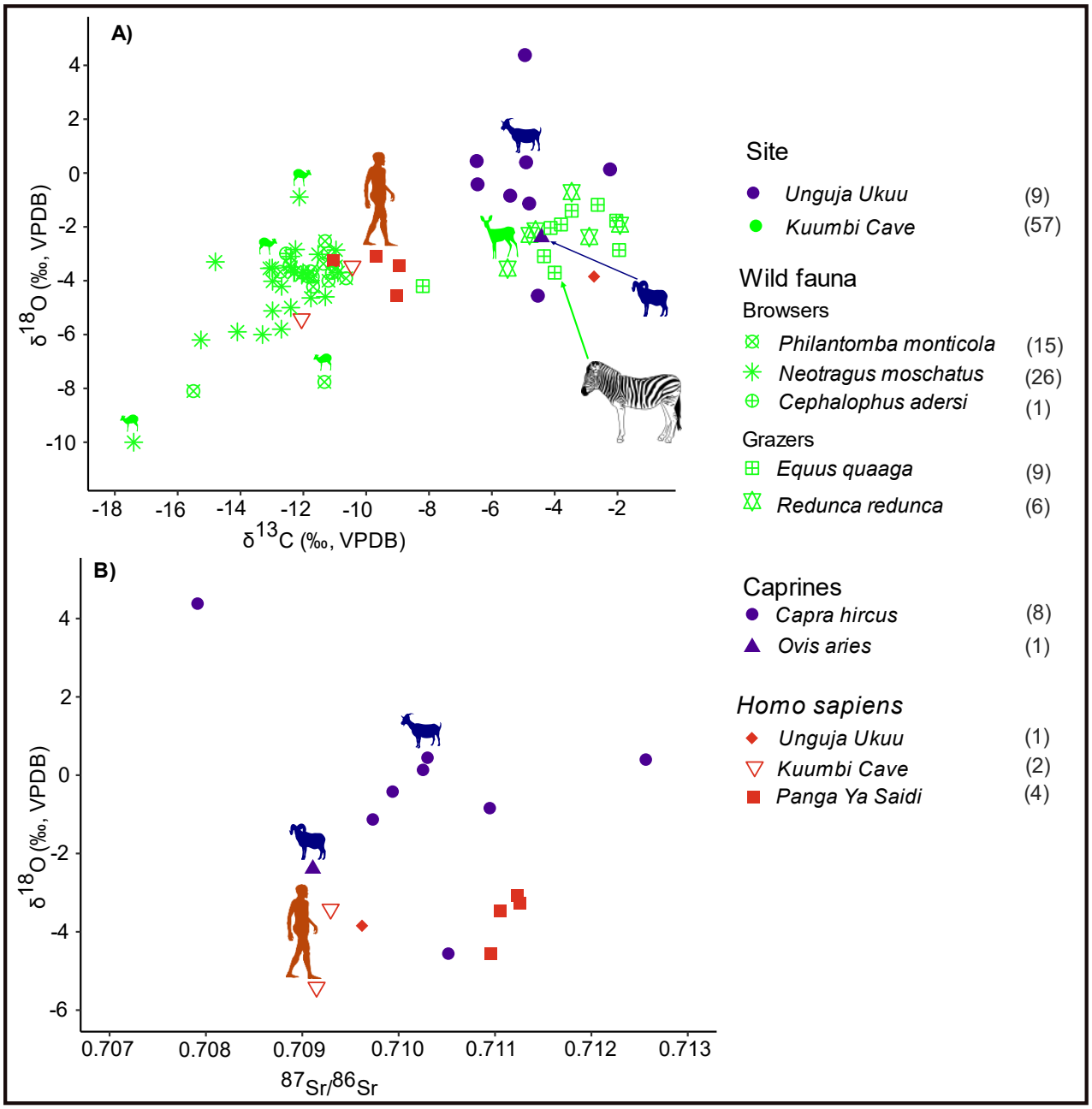


Figure 6.6 *Scatterplots of enamel values by (A) $\delta^{13}C_{enamel}$ and $\delta^{18}O$ values from KC small forest adapted antelopes ($\delta^{13}C$ values lower than −10‰ and $\delta^{18}O$ values lower than 0‰) and wild grazers ($\delta^{13}C$ values higher than −10‰ and $\delta^{18}O$ values below 0‰) and caprines from UU ($\delta^{13}C$ values higher than −7‰ and almost all $\delta^{18}O$ values are lower than 1‰) highlighting the distinctions between the small forest adapted antelopes and UU caprines similar to the patterns in the collagen $\delta^{13}C$ values; (B) Variation in the $^{87}Sr/^{86}Sr$ and $\delta^{18}O$ values from UU caprines and humans from UU, KC and PYS highlighting the five caprine and PYS $^{87}Sr/^{86}Sr$ values higher than 0.710.*

Two KC humans have $^{87}Sr/^{86}Sr$ values of 0.709148 and 0.709298 (Figure 6.6B), with published $\delta^{13}C$ values of −12.1‰ and −10.4‰, and $\delta^{18}O$ values of −3.1‰ and −4.5‰ (Iminjili et al., 2023).

The PYS human has four $^{87}Sr/^{86}Sr$, with published $\delta^{13}C_{enamel}$, and $\delta^{18}O$ values from different teeth that are almost similar (Roberts et al., 2020). The four $^{87}Sr/^{86}Sr$ values are 0.711257, 0.711040, 0.711231, and 0.710954 from the 2nd/3rd molar, 1st molar, incisor, and premolar respectively. These teeth have $\delta^{13}C$ values of −11.1‰, −8.9‰, −9.7‰, and −9‰, and $\delta^{18}O$ values of −3.8‰, −3.2‰, −3.4‰, and −4.5‰ respectively.

6.8 – Caprine enamel from Unguja Ukuu, and the interior of eastern Africa

The results of the comparative study of caprine enamel values from Unguja Ukuu and other sites in the arid interior of eastern Africa highlight the effects of humidity and aridity on the values of these sites. Nearly all UU caprine values have $\delta^{18}O$ values below 1‰, whereas over 70% of caprine values from the arid interior have values above 1‰. The anthropogenic effect on caprine diets constrains $\delta^{13}C$ values between −8‰ and −2‰, whereas wild-herded caprines in the arid interior have a wide dietary breadth, with values ranging from −8‰ to 4‰. Similarly, the $\delta^{18}O$ values of these caprines in the interior range from −2‰ to 6‰, indicating the effects of aridity on imbibed water.

We compared the UU caprine $\delta^{13}C_{enamel}$ and $\delta^{18}O$ values to published caprines and wild animals from four sites (Dongodien, Luxmanda, Gogo Falls, and Wadh Lang'o) in interior eastern Africa (Figure 6.7 and Tables A2:2 and A2:6) (Chritz et al., 2019; Prendergast et al., 2019a). These sites have contexts that span two major time periods: from the Pastoral Neolithic we have Dongodien (2500 BCE) and Luxmanda (1050 BCE), and from the Iron Age we have Gogo Falls (250 CE) and Wadh Lang'o (with two contexts 650 CE and 50 CE). The samples from UU and Luxmanda have

been identified to species level using ZooMS (Prendergast et al., 2019a; Culley et al., 2021b). Samples from Dongodien, Gogo Falls, and Wadh Lang'o have not been identified to species level and are recorded simply as 'caprines' (Chritz et al., 2019). We can conduct multiple statistical comparisons of the mean and median caprine values of $\delta^{13}C_{enamel}$ and $\delta^{18}O$, as well as their relative variance across the four sites (UU, Dongodien, Wadh Lang'o and Gogo Falls), given the relatively large sample sizes at each site (Figure 6.7 and Tables A2:2 and A2:6). As only caprine $\delta^{13}C_{enamel}$ values have been published from Luxmanda, I will only compare these values with those from the other sites and will not include $\delta^{18}O$ values (Table A2:7).

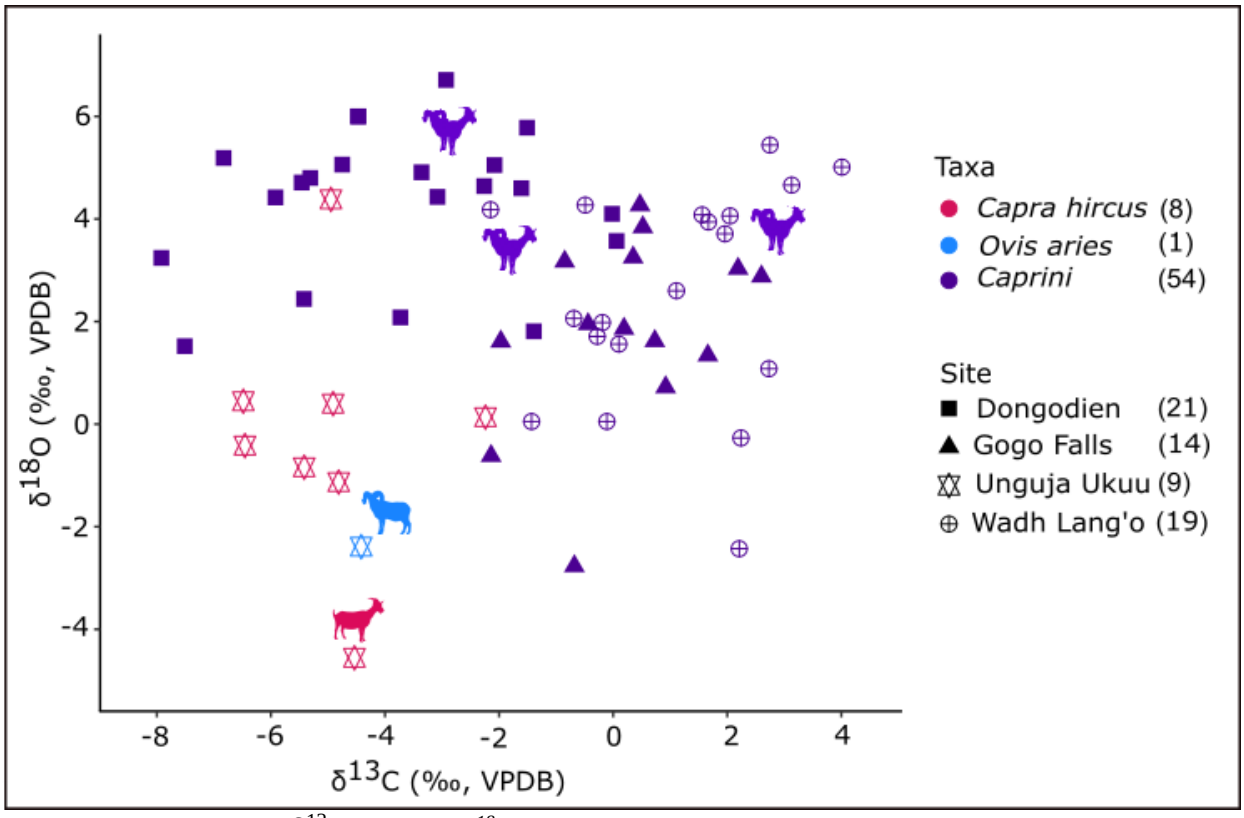


Figure 6.7. *Scatterplots of* $\delta^{13}C_{enamel}$ *and* $\delta^{18}O$ *values of caprines from UU and three sites (Dongodien, Gogo Falls, and Wadh Lang'o) from the interior eastern Africa (caprines from these three sites have not been identified to species level via ZooMS). The plot highlights the distinctions between UU values (*$\delta^{13}C_{enamel}$ *values packed between −8‰ and −2‰ and* $\delta^{18}O$ *values between −3‰ and 1‰) and interior eastern African sites, with Wadh Lang'o and Gogo Falls* $\delta^{13}C$ *values falling above −2‰ and* $\delta^{18}O$ *values concentrated between 1‰ and 6‰, and the Dongodien* $\delta^{13}C_{enamel}$ *values falling between −8‰ and 1‰ and* $\delta^{18}O$ *values between 1‰ and 7‰. The plot also highlights the bimodal distribution of the Dongodien values, with values lower than −4‰ representing goats and values above −4‰ representing sheep.*

The $\delta^{13}C_{enamel}$ data distributions pass the Shapiro-Wilk test for normality (p=0.95) and Brown-Forsythe test of equal variance (p=0.05), so a one-way ANOVA was applied. This test suggests that there are significant differences in mean $\delta^{13}C$ values among these four groups ($F(3,62)=38.7$, $p<0.001$). Pairwise multiple comparisons through the Holm-Sidak method suggest that the group means are all different from each other ($p<0.001$) except in the case of Wadh Lang'o and Gogo Falls (p=0.21) and Dongodien and UU (p=0.25). The $\delta^{18}O$ data distributions pass the Shapiro-Wilk test for normality (p=0.13) and Brown-Forsythe test of equal variance (p=0.16), so we can apply a

one-way ANOVA. This test suggests that there are significant differences in mean $\delta^{18}O$ values among these four groups ($F(3,62)=14.1$, $p<0.001$). Pairwise multiple comparisons through the Holm-Sidak method suggest that the group means are all different from each other ($p\leq0.01$) except in the case of Wadh Lang'o and Gogo Falls ($p=0.34$).

The Luxmanda caprine samples with published $\delta^{13}C$ values indicate significant variation (n = 20, mean = 0.5, range = -5.2 to 3.1), with a dominance of higher values. Most of the high values belong to sheep (n = 15, mean = 1.4, range = -0.2 to 3.1), while the lower values belong to goats (n = 5, mean = -2.1, range = -5.2 to 1.9). These Luxmanda values fall within the range of other published caprine values from interior eastern African sites.

Chapter 7 – Methods, quality control, and results for the *Wanyika* scientific dates case study

This chapter presents the methods and results of the third case study. It uses maps generated from the *Wanyika* dataset of scientific dates from archaeological sites in eastern Africa, spanning from 5000 BCE to 1800 CE, to examine basic chronological dispersal patterns of food production and food-producing communities. It also identifies major research gaps that hinder in-depth hypothesis testing. The first section outlines the methods employed in the study. These include the sampling strategy, the demarcation of country regions, the collection and deposition of data, the scientific dates covered, and the quality control measures applied to these dates. The second section presents the results of the case study in the form of the *Wanyika* dataset of scientific dates (this work is published as Iminjili et al., 2025a and Iminjili et al., 2025b). This section includes a description of the data records, as well as instructions for accessing the online version of the *Wanyika* dataset. Other details include the definition of the column fields, technical validation and usage notes declaring adherence to the FAIR data principles. It also includes the four codes used to calibrate the ^{14}C dates in OxCal.

7.1 – The *Wanyika* Dataset

The production of the *Wanyika* dataset is a significant step towards making the late Holocene archaeological record of eastern Africa compatible with modern, technology-aided studies, such as archaeo-informatics and artificial intelligence. As an archaeo-informatics-oriented dataset,

Wanyika is structured in a systematic, science-friendly manner that is adaptable to future innovations. It provides an inventory of the region's archaeological record, highlighting areas that are relatively well covered and those that are not. The *Wanyika* dataset indicates that almost half of eastern Africa has not been archaeologically explored, and that more than half of the dates in the dataset have a questionable background. Once these issues have been resolved, multiple spatiotemporal archaeoinformatics analyses could be conducted to provide in-depth insights into human–environment interaction using this dataset. Topics such as the emergence of complex subsistence strategies and the dispersal of food-producing communities could be explored. Even as it is, however, it provides valuable basic insights into these topics, which I explore below.

7.2 – Sampling strategy

The *Wanyika* dataset includes sites in Kenya, Tanzania, Comoros, and Madagascar (Iminjili et al., 2025a). These sites span from approximately 5,000 BCE to 1,800 CE (see Figure 2.7 and Table A3:1 for a condensed version of the dataset). The collection of information covers all scientifically dated locations in these countries, offering specifics on available dates, along with details regarding associated plant and animal remains, iron, and ceramic discoveries. Additionally, certain Rwandan locations that contain early indications of domesticated crops and iron tools are incorporated into the study due to their significance in understanding the dissemination of farming practices in eastern Africa (Ambrose et al., 1984; Young and Thompson, 1999; Giblin and Humphris, 2010; Giblin and Fuller, 2011; Goldstein et al., 2024). At present, the database includes four countries, which represent an initial sample of the 18 countries that define eastern Africa (United Nations Statistics Division, 2011; Pandora, 2024). These countries were chosen because of their substantial

contributions to our understanding of past human-environment interactions in the region, as well as the accessibility of published archaeological data. Unlike the northern and southern regions of eastern Africa, the coastal countries (Kenya and Tanzania) and island countries (Comoros and Madagascar) have well-documented Holocene archaeological records (Marshall, 1990; Karega, 1996; Ambrose, 1998; Chami, 2001b; Ehret, 2001; Marshall and Hildebrand, 2002; Munene, 2002; Chami and Kwekason, 2003; Lane, 2004; Kusimba and Kusimba, 2005; Beaujard, 2007; Chami, 2007; Dale, 2007; Prendergast, 2009; Pearson et al., 2010; Russell et al., 2014; Crowther et al., 2018; Douglass et al., 2019; Godfrey et al., 2019; Chami and Silayo, 2023; Goldstein et al., 2024). They are also at the heart of key debates about the dispersal of early farming and biological exchange, mediated by long-distance mobility and cross-cultural interaction.

Over the last 25 years, the application of archaeological science approaches in these countries has bolstered the production of basic and in-depth scientific information about critical assemblages in the application of archaeo-informatics-oriented perspectives (Pearson et al., 2010; Kusimba et al., 2013; Prendergast et al., 2014; Crowther et al., 2018; Hildebrand et al., 2018; Serneels et al., 2018; Shipton et al., 2018; Douglass et al., 2019; Godfrey et al., 2019; Prendergast et al., 2019a; Prendergast et al., 2019b; Sawchuk, 2019; Grillo et al., 2020a; Roberts et al., 2020; Hixon et al., 2021a; Wynne-Jones et al., 2021; Grillo et al., 2022; Horton et al., 2022; Sawchuk et al., 2022; Chami and Silayo, 2023; Goldstein et al., 2023; Le Meillour et al., 2023; Goldstein et al., 2024). This information can be synthesized into two key points. Firstly, a greater number of archaeobotanical and zooarchaeological finds have been recovered and identified to genus or species level. Secondly, significant numbers of chronometric dates have been produced, as well as well-identified material culture. The production of these basic and in-depth scientific insights, made possible through the application of archaeological science approaches, has greatly improved

the quality of archaeological data from this region of eastern Africa, making it conducive to primary experiments in computer-aided methodologies.

Rwandan sites were incorporated into the dataset because they contain some of the earliest recorded evidence of the domestication of crops in eastern Africa. They also lie within the hypothesized dispersal route of farmers into eastern Africa's interior (Huffman, 1970; Were and Wilson, 1970; Maxon, 1986; Clist, 1987b; Huffman and Herbert, 1994; Nurse, 1994; Ehret, 2001; Giblin, 2008; Giblin and Humphris, 2010; Currie et al., 2013; Russell et al., 2014). Unlike in Rwanda, evidence of crop dispersal across eastern Africa's interior is scarce. While Rwanda boasts eight sites with archaeobotanical records, only two sites in the interior have such records: Kakapel and Deloraine in Kenya (Ambrose et al., 1984; Young and Thompson, 1999; Goldstein et al., 2024). Urewe ceramics and iron, critical to interpreting archaeological assemblages in the region, have been found with archaeobotanical remains at the eight Rwandan sites (Giblin and Humphris, 2010; Giblin and Fuller, 2011). These findings have led experts to theorize that the Rwandan region may have served as a gateway and distribution center for agricultural communities that migrated to the interior of eastern Africa. These communities may have traveled through the Mount Elgon or Lake Tanganyika regions.

The *Wanyika* dataset does not cover all of eastern Africa. However, I suggest its use as a basic research resource that has dramatic potential to be further developed. It will cover more countries as time and resources allow. It provides a step-by-step methodology for adding more archaeological data from eastern Africa in the future. A caveat to users of the dataset is that we have incorporated a modest set of sites (exclusively those with scientific dates), which exerts a bias on the estimates of effect sizes in the extant eastern African archaeological data. Restriction to sites with scientific

dates might lead to incorrect conclusions about the complex interactions of farmers, pastoralists, and foragers in different places in eastern Africa, as well as other archaeological phenomena.

7.3 – Demarcation of country regions and vegetation cover

The analysis of geographical patterns in the data (e.g., Table 7.1) was facilitated by the subdivision of Kenya, Tanzania, and Madagascar into smaller sub-regions ('Country Regions'), e.g., southwestern, northwestern. These divisions are frequently cited in archaeological literature (Sutton, 1966; Ambrose, 1984a; b; Barthelme, 1985; Robertshaw, 1990a; Chami, 1992; Chami, 1994; Mapunda, 1995; Chami and Msemwa, 1997a; Sutton, 1998a; Sutton, 1998d; Håland and Msuya, 2000; Chami and Chami, 2001; Ambrose, 2003; Chami, 2003a; Chami and Kwekason, 2003; Chami, 2004; Kwekason, 2007; Davies, 2008; Chami, 2009; Seitsonen, 2012; Wynne-Jones and Fleisher, 2015; Wynne-Jones and LaViolette, 2018; Morel, 2023). However, they had not previously been formally constrained using geographical coordinates. Approximate straight vertical and horizontal lines were used to divide Kenya, Tanzania and Madagascar into four roughly equal parts to identify the geographical coordinates. The coordinates for the hinterland, coast and islands were also estimated based on the demarcation of coastal forests on Google Maps. The boundaries of this study are defined as follows: Mainland Kenya is demarcated by a latitude of 0.5° and a longitude of 37.7°. The hinterland, coast, and islands constitute a fifth region (see Table 7.1, for example). In a similar way, the mainland of Tanzania is split into four regions based on latitude −6° and longitude 35°, and the hinterland, coast, and islands are considered the fifth region. The island of Madagascar is likewise partitioned into four nearly equivalent-sized zones according to latitude −19° and longitude 47°. The vegetation cover that is predominant for each

site and region has also been included (White, 1983; Kingdon, 1984b; 2001; Bonnefille, 2010; Iminjili, 2012; Iminjili et al., 2023). These are separated into six groupings, such as forest/wood/grassland patchwork, mountain forest, coastal forest patchwork, dry coastal wooded grassland, dry northern wooded grassland, and dry southern wooded grassland (e.g., Table 7.1).

Table 7.1. *Delineation of regions based on country boundaries and citations from the bibliography. The main vegetation cover is taken into account, as well as the approximate boundaries, which are defined by geographical coordinates of a delimiting rectangle (Iminjili et al., 2025a; Iminjili et al., 2025b).*

Regions and site bibliographic reference citations	**Predominant vegetation cover**	**Latitude**	**Longitude**
Rwanda (No regions)	Forest/wood/grassland mosaic	-1.1°, -1.1° -2.8°, -2.6°	29.2°, 30.7° 28.8°, 30.9°
Comoros (No regions)	Coastal forest mosaic	-11.3°, -12.8° -11.9°, -13.2°	43.2°, 45.4° 43.0°, 45.3°
Northeastern Kenya	Dry northern wooded grassland	5.4°, 4.1° 0.5°, 0.5°	37.7°, 41.9° 37.7°, 41.1°
Northwestern Kenya	Dry northern wooded grassland Forest/wood/grassland mosaic	5.7°, 5.4° 0.5, 0.5°	33.4°, 37.7° 33.8°, 37.7°
Southeastern Kenya	Dry northern wooded grassland	0.5°, 0.5° -3.2°, -5.0°	37.7°, 41.1° 37.7°, 39.4°
Southwestern Kenya	Dry northern wooded grassland Montane forest Forest/wood/grassland mosaic	0.5°, 0.5° -1.1°, -3.2°	33.8°, 37.7° 33.8°, 37.7°
Hinterland, Coastal and Island Kenya	Coastal forest mosaic	-1.4°, -2.0° -4.7°, -5.0°	41.4°, 41.8° 39.1°, 39.6°
Northeastern Tanzania	Forest/wood/grassland mosaic Dry northern wooded grassland	-1.8°, -4.7° -6°, -5.8°	35.0°, 39.1° 35.0°, 38.4°
Northwestern Tanzania	Forest/wood/grassland mosaic Dry northern wooded grassland	-0.8°, -0.9° -5.6°, -6.0°	29.5°, 34.1° 29.4°, 35.0°
Southeastern Tanzania	Dry southern wooded grassland	-6.0°, -5.7° -11.6°, -10.9°	35.0°, 38.3° 35.0°, 39.8°
Southwestern Tanzania	Dry southern wooded grassland	-5.8°, -6° -8.2°, -11.6°	29.6°, 35.0° 30.7°, 35.0°
Hinterland, Coastal and Island Tanzania	Coastal forest mosaic	-4.9°, -4.9° -10.9°, -10.9°	38.8°, 40.1° 39.8°, 41.1°
Northeastern Madagascar	Coastal forest mosaic	-11.8°, -12.8° -19.0°, -19.0°	47.0°, 51.9° 47.0°, 49.1°
Northwestern Madagascar	Dry coastal wooded grassland	-15.3°, -12.0° -19.0°, -19.0°	44.7°, 47.0° 43.7°, 47.0°
Southeastern Madagascar	Coastal forest mosaic	-19.0°, -19.0° -25.2°, -25.6°	47.0°, 49.2° 47.0°, 47.2°
Southwestern Madagascar	Dry coastal wooded grassland	-19.0°, -19.0° -24.7°, -25.2°	43.7°, 47.0° 43.2°, 47.0°

7.4 – Data collection and deposition

The data collection process followed the workflow depicted in Figure 7.1. I used over 500 scientific publications as data sources. I focused on citations in major review articles and other important works on the study regions (Ehret and Posnansky, 1982; Clark and Brandt, 1984; Robertshaw, 1984; Sinclair, 1991; Ambrose, 1998; Marshall and Hildebrand, 2002; Burney et al., 2004; Pearson et al., 2010; Boivin et al., 2013; Crowther et al., 2016a; Crowther et al., 2016b; Crowther et al., 2018; Wynne-Jones and LaViolette, 2018; Douglass et al., 2019; Hixon et al., 2021a). Using a combination of keywords such as specific country/region names, "archaeology," "scientific dates," "archaeobotany," "zooarchaeology," "iron," and "ceramics," I used the academic search engine Google Scholar to locate further articles. All available volumes of *Azania: Archaeological Research in Africa* (1967 to 2023) were also screened by me to collect additional scientific dates and information about associated archaeological finds. Of the published dates, I obtained the associated assemblage evidence (i.e., archaeobotanical, zooarchaeological, and artifact evidence) from separately published specialist articles for just over half of them. To clarify data issues and locate missing publication data, I consulted the original publication authors or expert archaeologists working in eastern Africa. To obtain additional information on the dates and the material, radiocarbon dating laboratories were also contacted. In accordance with the references enumerated in review articles and other seminal publications, as well as in discussions with researchers versed in the study region, I estimate that a minimum of 90% of the extant scientific dates and associated archaeological records from the sampled eastern African countries are encompassed within the *Wanyika* dataset (Iminjili et al., 2025a).

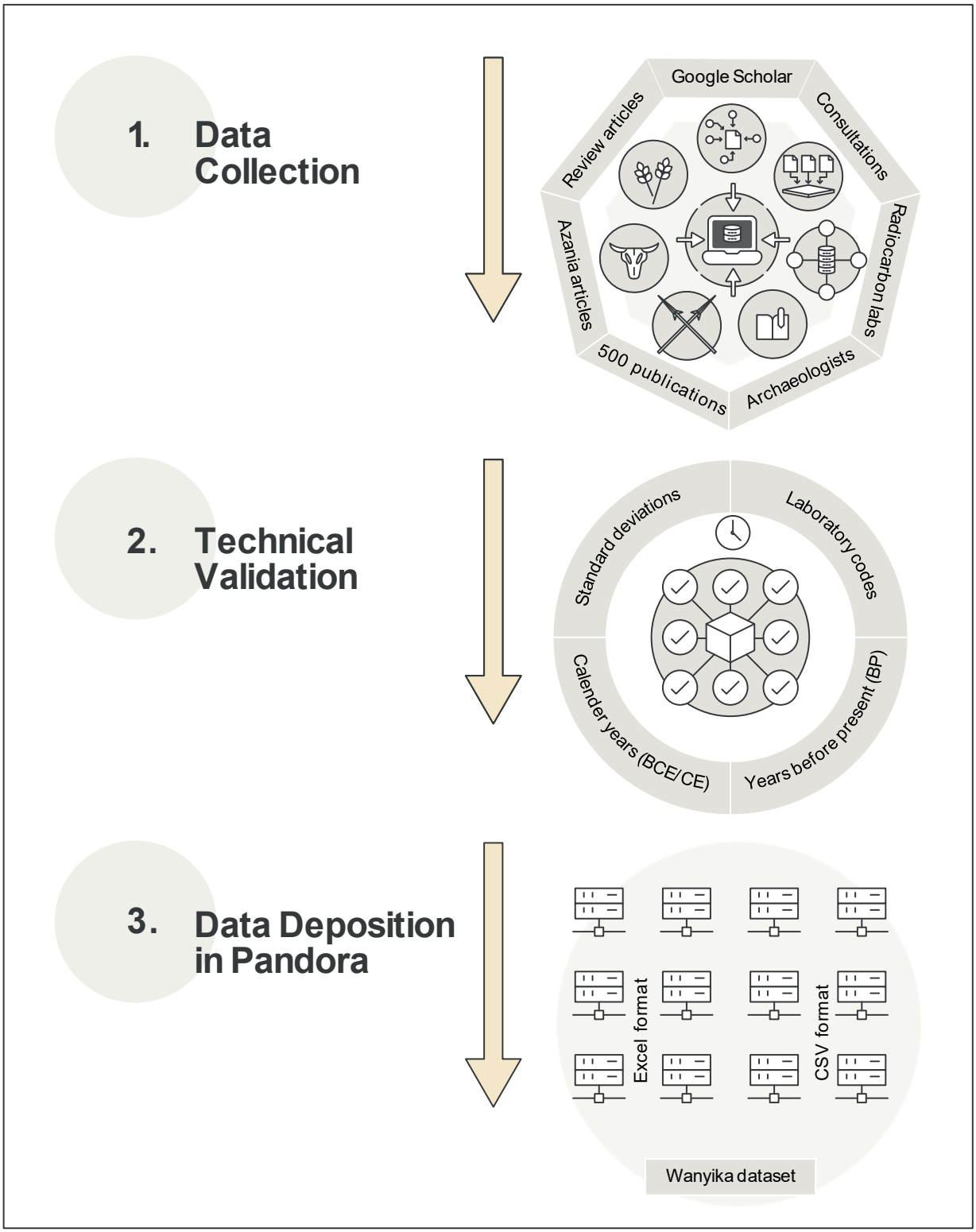


Figure 7.1. *Flow chart summarizing the construction of the Wanyika dataset (Iminjili et al., 2025a; Iminjili et al., 2025b). The flow chart was created for this study by Hans Sell (Graphic Designer for the Max Planck Institute of Geoanthropology, Jena, Germany).*

After completing the data collection and screening, I uploaded the *Wanyika* dataset (Iminjili et al., 2025a) to the Pandora data platform. Pandora is an internet-based, cross-language data management platform where data communities independently oversee membership and self-curate data in various formats (Pandora, 2024).

7.5 – Scientific dates and calibration

The term "scientific date" is my way of referring to a date that is established using scientific dating methods to determine the age of an artifact, feature, and/or site. A quantifiable measure of time with an associated margin of error is provided by these methods. The publications I consulted to compile the *Wanyika* dataset (Figure 7.2) reported five types of scientific dating techniques: radiocarbon dating (^{14}C), optically stimulated luminescence (OSL), infrared stimulated luminescence (IRSL), thermoluminescence (TL), and obsidian hydration (OH) (Figure 7.2) (Robertshaw, 1990a; Wright et al., 1992; Taylor and Aitken, 1997; Wright, 2005a; Hajdas et al., 2006; Hajdas, 2008; Bajaj and Palan, 2022). The calculation of radiocarbon dates is based on the abundance of the ^{14}C isotope in samples. Examples of such samples include archaeobotanical remains or collagen extracted from zooarchaeological remains (Taylor and Aitken, 1997; Schuur et al., 2016). Luminescence dating methodologies, including OSL, IRSL, and TL, ascertain the final instance of mineral grains being exposed to sunlight or elevated temperatures (Taylor and Aitken, 1997; Wright, 2005a; Bajaj and Palan, 2022). Lastly, obsidian hydration (OH) dating uses the amount of water absorbed by obsidian to determine an object's age. Obsidian hydration dating can be used to determine absolute and relative dates. However, the *Wanyika* dataset only documents absolute dates (which can be summarized in calendar year intervals as opposed to merely being

older or younger (Robertshaw, 1990a; Taylor and Aitken, 1997)). This dataset excludes relative dates based on material culture typologies such as ceramics and beads (Huffman, 1970; Huffman and Herbert, 1994; Wynne-Jones and LaViolette, 2018).

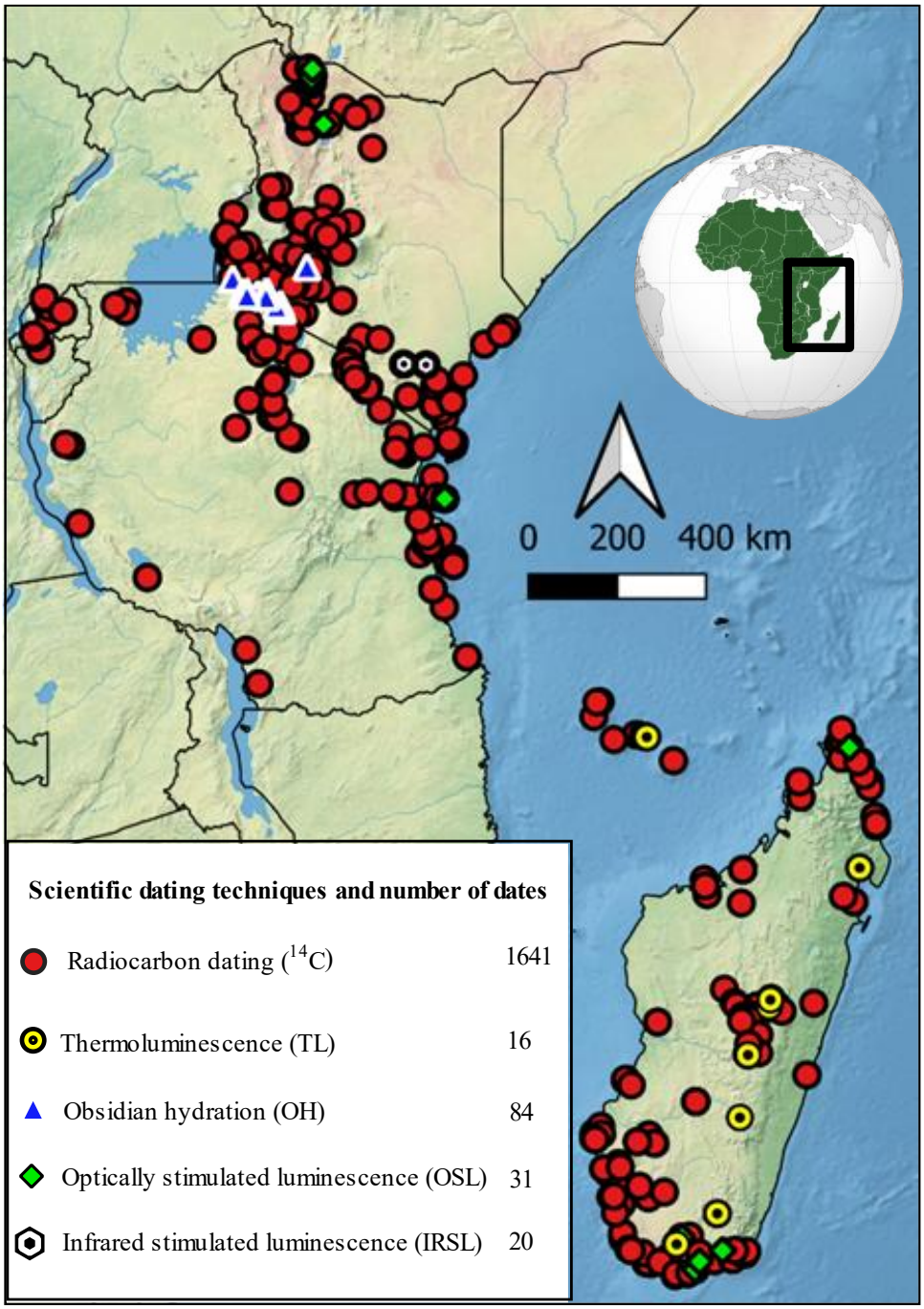


Figure 7.2. *Map of eastern Africa showing the differences in the spatial distribution of scientific dates by dating technique (^{14}C, OSL and IRSL, TL, and OH) (Iminjili et al., 2025a; Iminjili et al., 2025b).*

The scientific date of each sample is shown in three formats. One shows the uncalibrated years before present (BP) in two fields, expressing the date BP and standard deviation (SD). Another shows the calibrated calendar years (BCE and CE) in three fields, expressing a 95% probability range plus a mean. Finally, the calibrated years BP are shown in three fields, expressing a 95% probability range plus a mean. The reference year for uncalibrated ^{14}C and OH dates is 1950. The uncalibrated or conventional ^{14}C dates are reported to facilitate revisions once calibration curves are updated. Here, BP is presented relative to the year of publication instead of the standard BP (Before Present, or 1950) for OSL, IRLS, and TL dates. It is important to note that this may not be the same as the sample recovery or analysis date, which may actually represent the reference year. Nevertheless, this option is seldom documented, and I do not foresee a substantial discrepancy between the reference year and the publication date. Luminescence dating techniques were first introduced in the 1960s. These techniques set a highly conservative upper bound for a potential offset between publication year and the unknown reference year of c. 50 years (Tite and Waine, 1962; Taylor and Aitken, 1997; Feathers, 2003; Wright, 2005a; Liritzis et al., 2013; Bajaj and Palan, 2022; Mahan et al., 2022).

To calibrate the ^{14}C dates, I used the latest calibration curves at the time (IntCal20 and SHCal20) and the Bayesian chronological software OxCal v.4.4 (Bronk Ramsey, 2009; Hogg et al., 2020; Reimer et al., 2020). The calibration process used SHCal20 for samples located south of latitude -17°, which marks the southernmost limit of the Intertropical Convergence Zone (ITCZ). For samples north of the ITCZ, it was necessary to account for the mixing of northern and southern curves (Ziegler et al., 2013; Wright, 2017). For these samples, I calibrated the radiocarbon measurements using a mixed IntCal20 and SHCal20 curve with an unknown level of mixing (flat prior between 0 and 100 in OxCal). A protocol similar to that described in Goldstein et al.

(Goldstein et al., 2022a) was followed for radiocarbon calibrations of aquatic samples. In summary, the marine radiocarbon offset, or ΔR, was ascertained in the vicinity of each maritime burial site (with a radius of 100 km) for a smoothed surface generated using data from the Marine Reservoir Correction dataset (Reimer and Reimer, 2001) and the Bayesian model AverageR (Cubas et al., 2020; Wilkin et al., 2020). Calendar dates were obtained by calibrating radiocarbon dates using the Bayesian chronological software OxCal v4.4 (Bronk Ramsey, 2009). To calibrate a solitary inland shell, discovered in the proximity of the Turkana salt lake, an inland ΔR mean value of 250 ^{14}C years relative to the IntCal20 calibration curve was utilized, as outlined by Beck et al. (Beck et al., 2019), with an assigned uncertainty of ±100 ^{14}C years.

As mentioned earlier, the calibration process for OSL, IRLS, and TL involved subtracting the reported BP date from the publication year. For OH, however, the reported BP date was subtracted from 1950 (Michels et al., 1983; Clist, 1987a; Robertshaw, 1991; Wright, 2005a; Ndiema, 2011; Dewar et al., 2013; Shipton et al., 2016). The dates were changed into calendar years and written as a 95% chance range of calendar years (BCE/CE). The dataset includes a description of the dated sample type and the taxonomic identification for all methods and, when available. The system flags questionable measurements in the notes section of dataset records (e.g., when there are inconsistencies among different measurements or methodologies, or when dates do not align with established chronological boundaries for a cultural layer). Frequently, problematic dates emanate from jumbled, mixed, or unclear contexts (Mehlman, 1989; Robertshaw, 1991; Chami et al., 2001; Munene, 2002; Sinclair et al., 2006; Chami, 2009; Goldstein et al., 2024).

7.6 – Quality control

Four chronometric quality control criteria for the scientific dates were developed, and they were used to grade the dates in the dataset into classes. The first criterion is based on a combination of stratigraphic integrity and reliability. It is applied to all dates in the dataset. The dates were then graded into four classes (Class A–D). Class A is the most secure and reliable. Class D is the least secure and reliable. The other three criteria were only applied to ^{14}C dates. They are based on three variables (i) whether the date was obtained on short- or long-lived plant material (i.e., the potential presence of an old wood effect) (Wright, 2017), (ii) the possible presence of an aquatic radiocarbon reservoir effect (Fernandes et al., 2016), and (iii) the accuracy of the chronometric determination. In each instance, dates were divided into three categories (Class A–C), once more with A being the most trustworthy and C being the least trustworthy. Below, I provide a description of how I applied the quality control criteria.

Stratigraphic integrity and reliability grading

The evaluation of the stratigraphic integrity for each date involved the assignment of points to dates based on the following system (Column BI) (Figure 7.3, Tables 7.2 and 7.3, and *Wanyika* dataset (Iminjili et al., 2025a)). The awarding of six points to a date is dependent on the authors of the original publication indicating that it is reasonably well associated with its archaeological context (i.e., the stratigraphic integrity is not questioned). A date that was questioned by either the original authors or in a subsequent publication was given three points. This could be because the date is more recent than that of the overlying context, or older than that of the underlying context, possibly due to bioturbation. Zero points were allotted to dates devoid of contextual information and

documented as "unreported" in column J. Radiocarbon dating of ratite eggshells and obsidian hydration dating have been shown to be unreliable (Michels et al., 1983; Robertshaw, 1990a; Robertshaw, 1991; Pearson et al., 2010; Wright, 2017). These dates were treated as questioned and awarded three points unless they lacked contextual details, in which case they were awarded zero points. An annotation regarding the stratigraphic integrity of a date is located in Column BH of the dataset. I did not evaluate the stratigraphic integrity of individual dates beyond what has been reported in the published literature.

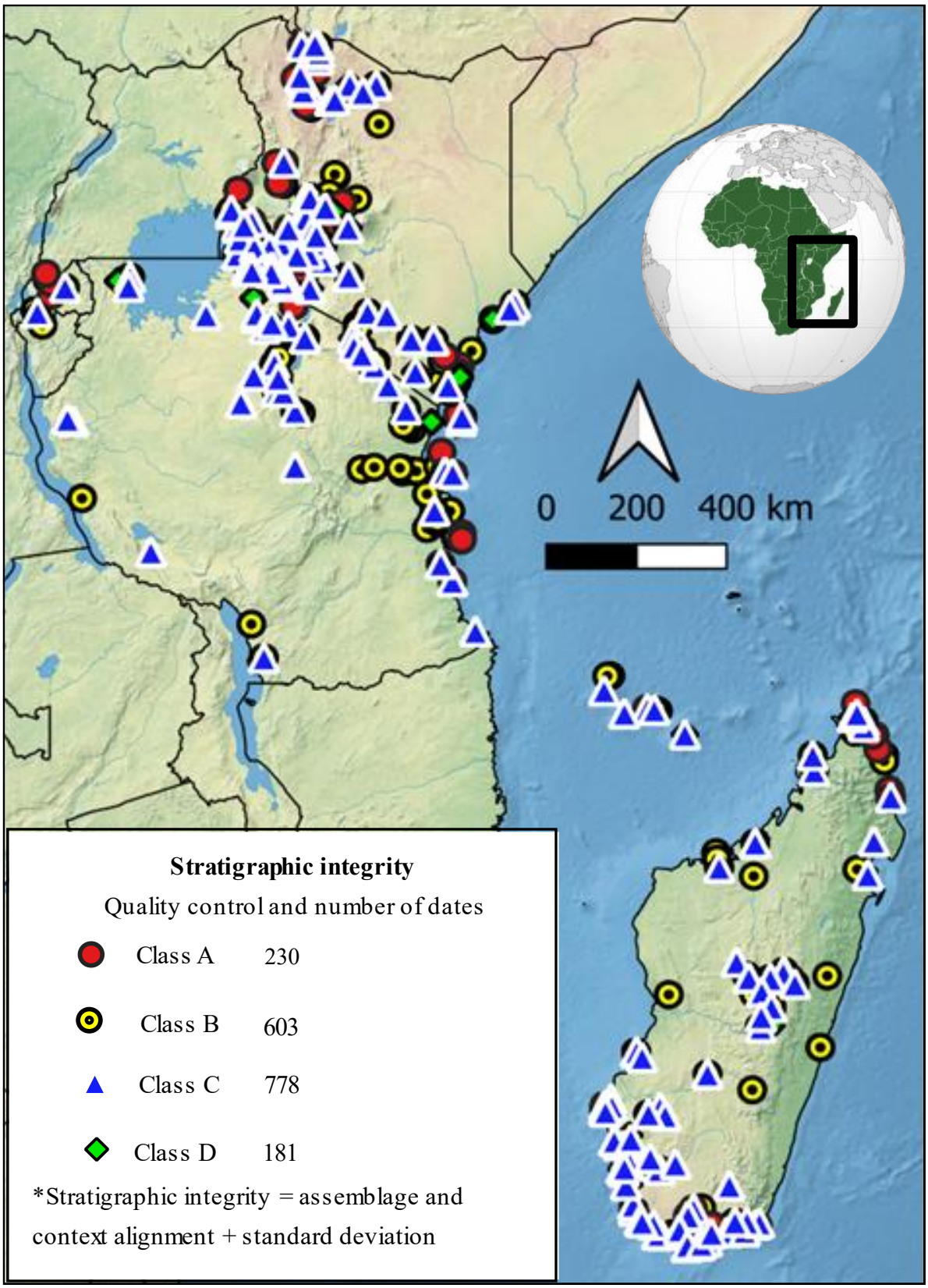


Figure 7.3. *Map of eastern Africa showing the differences in the spatial distribution of scientific dates according to their stratigraphic integrity and reliability. Note: Class A dates are the most reliable (Iminjili et al., 2025a; Iminjili et al., 2025b).*

The standard deviation (column N) of the scientific date was utilized to ascertain its dependability. Dates with standard deviations between 0 and 25, 26 and 50, 51 and 100, and 101 and 650 were assigned point values of six, four, two, and zero, respectively.

Next, the points allotted for stratigraphic integrity and reliability were added together for each date, and then the sum was divided by two to calculate the mean score. This score was then used to generate Class A-D dates, which have respective mean scores of 6, 4-5.5, 2-3.5, and 0-1.5. The application of the grading system produced comparable class qualities (see Table 7.2). A synopsis of the quantity of dates according to country and region, dating methodology, and stratigraphic integrity and reliability quality control grades is provided in Table 7.3.

Good examples of the grading system are provided by the dataset (Iminjili et al., 2025a) records from Kakapel (Entry IDs 217 to 244) and Gogo Falls (Entry IDs 203 to 216). Of the 28 dates from Kakapel, 23 are Class A, and five are Class B; the Class B dates differ in that they have SDs between 25 and 50. All 14 of Gogo Falls' dates have SDs above 60, so none are Class A; it has eight Class B, four Class C, and two Class D dates. Examples of bioturbation and OH dating challenges are also provided by Gogo Falls (e.g., Entry ID 204, which is an OH date with an SD of 115 and therefore classified as Class D). Examples from Andakatomena and Tony-Velondriake in Madagascar illustrate the process by which ratite eggshell dates were classified. The utilization of a questionable dating technique resulted in the categorization of a radiocarbon date from Andakatomena on Aepyornis eggshell (Entry ID 1124) as Class B, with an SD of 25 or less. A comparable specimen from Tony-Velondriake, likewise on Aepyornis eggshell (Entry ID 1120) and with an SD of 25 or less, was designated as Class C owing to its paucity of contextual information.

Table 7.2. *Qualities of dates used to define classes in the stratigraphic integrity and reliability quality control measure.*

Class	**Qualities**
Class A	Dates have a secure stratigraphic association and an SD of 25 or less.
Class B	Dates either: 1) have a secure stratigraphic association and an SD between 26-100; or 2) have a questionable stratigraphic association and an SD of 25 or less.
Class C	Dates either: 1) have a secure stratigraphic association and an SD of 101 or above; 2) have a questionable stratigraphic association and an SD between 26-100; or 3) have unreported context details and an SD of 50 or less.
Class D	Dates either: 1) have a questionable stratigraphic association and an SD of 101 or above; or 2) have unreported context details and an SD of 51 or above.

Table 7.3. *Synopses of dating methods and quality control measures (chronometric hygiene founded on stratigraphic integrity and the reliability of the dates) are proffered, accentuating the paucity of Class A dates in the Wanyika dataset (Iminjili et al., 2025a). See Table 1 for information on the demarcation of country regions.*

		Dating Method					**Quality Control (Chronometric Hygiene)**			
		Number of dates					**Class A-D**			
	Total Number of dates	**Radiocarbon**	**OSL**	**OH**	**TL**	**IRSL**	**A**	**B**	**C**	**D**
COUNTRY TOTALS										
Rwanda	20	20	0	0	0	0	**3**	14	2	1
Comoros	26	25	0	0	1	0	**7**	10	8	1
Kenya	668	556	8	84	0	20	**99**	161	279	129
Tanzania	401	397	4	0	0	0	**61**	224	94	22
Madagascar	677	643	19	0	15	0	**74**	190	387	26
GRAND TOTAL	**1792**	**1641**	**31**	**84**	**16**	**20**	**244**	**599**	**770**	**179**
REGIONAL TOTALS										
Northeastern Kenya	5	5	0	0	0	0	**0**	3	2	0
Northwestern Kenya	135	127	8	0	0	0	**55**	29	44	7
Southeastern Kenya	59	39	0	0	0	20	**0**	9	15	35
Southwestern Kenya	394	310	0	84	0	0	**39**	89	211	55
Hinterland, Coastal and Island Kenya	75	75	0	0	0	0	**5**	31	7	32
Northeastern Tanzania	140	140	0	0	0	0	**12**	82	39	7
Northwestern Tanzania	51	51	0	0	0	0	**0**	16	24	11
Southeastern Tanzania	6	6	0	0	0	0	**0**	6	0	0
Southwestern Tanzania	9	9	0	0	0	0	**0**	4	5	0
Hinterland, Coastal and Island Tanzania	195	191	4	0	0	0	**49**	116	26	4
Comoros	26	25	0	0	1	0	**7**	10	8	1
Northeastern Madagascar	142	127	6	0	9	0	**46**	46	45	5
Northwestern Madagascar	28	28	0	0	0	0	**0**	11	14	3
Southeastern Madagascar	26	24	0	0	2	0	**0**	20	4	2
Southwestern Madagascar	481	464	13	0	4	0	**28**	113	324	16
GRAND TOTAL	**1772**	**1621**	**31**	**84**	**16**	**20**	**241**	**585**	**768**	**178**

Radiocarbon (^{14}C) date grading

Three different criteria were used to perform additional chronometric hygiene on radiocarbon dates (see Table 7.4). The initial two criteria take into account the inherent age of the specimen at the time of its demise, which is contingent upon the nature of the material employed for the purpose of dating. For plant materials, age offsets may be present due to the selection of long-lived wood. This phenomenon is often referred to as the "old wood effect" (Figure 7.4) (Schiffer, 1986; Wright, 2017). Dates obtained from short-lived plant parts that were taxonomically identified (e.g., annual seeds, leaves, and twigs) were graded as Class A. Dates obtained from long-lived plant parts that were taxonomically identified were graded as Class B. Dates where the taxonomic identification of the plant parts was not reported were graded as Class C (see Column BJ in the dataset).

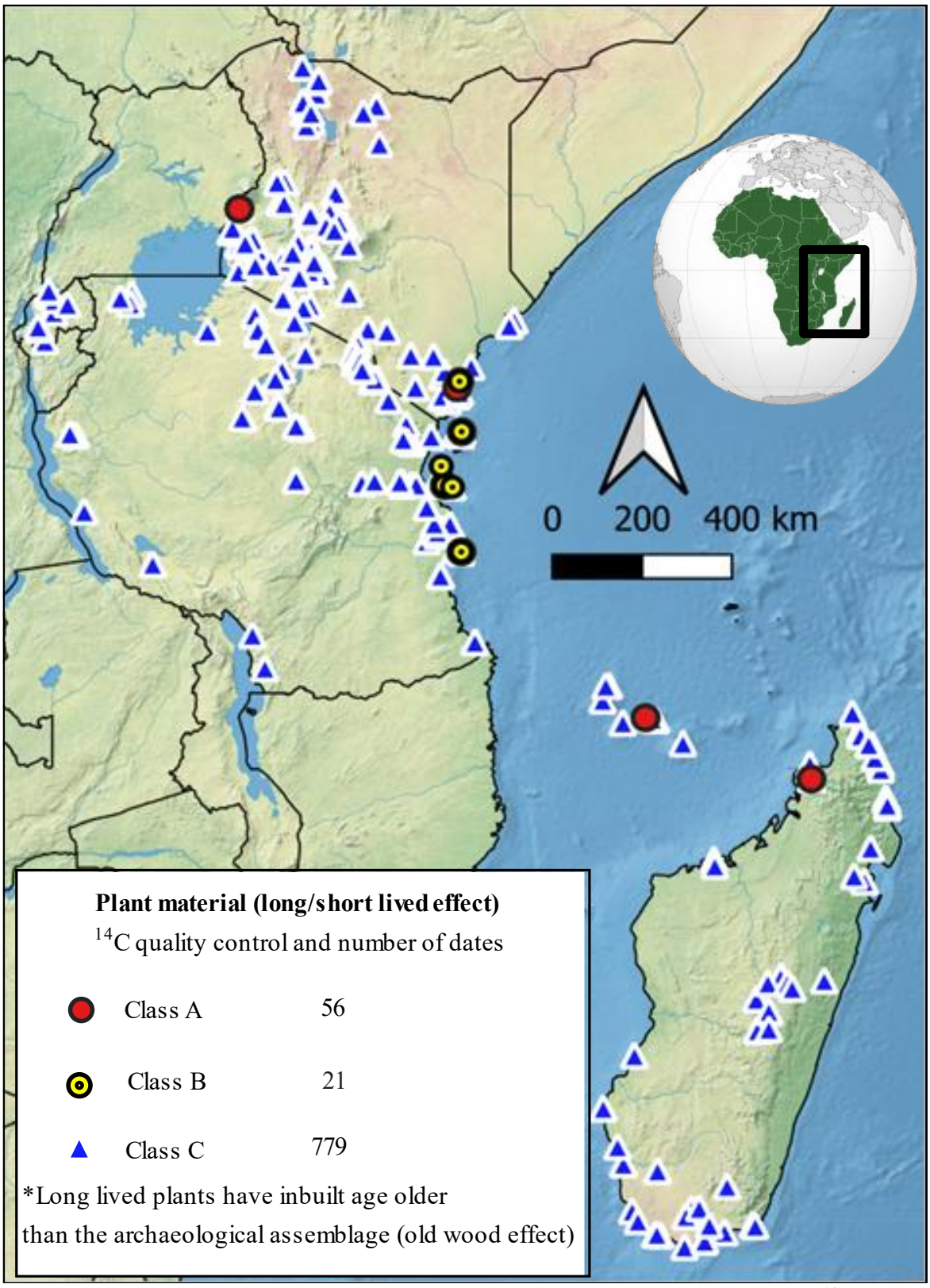


Figure 7.4. *Map of eastern Africa showing the spatial variation in the distribution of ^{14}C dates obtained from plant material. Note: Class A dates are considered to be the most reliable (Iminjili et al., 2025a; Iminjili et al., 2025b).*

Table 7.4. *Scheme for grading ^{14}C dates for botanical and aquatic materials, and the accuracy of chronological determination.*

Short- vs long-lived plant material	Grade
Sample from taxonomically identified short-lived plant parts: Annual seeds, leaves and twigs	**A**
Sample from taxonomically identified long-lived plant parts: Perennial seeds, leaves and twigs	**B**
Unknown/unreported: Taxonomically unidentified plant parts: Charcoal	**C**
Aquatic radiocarbon reservoir effects	
Fully terrestrial sample	**A**
Aquatic sample	**B**
Unknown/humans or other animals that may have consumed aquatic foods	**C**
Accuracy of chronological determinations (Pre-treatment protocol)	
Published after 1988. The ultrafiltration method and AMS were introduced around 1988.	**A**
Published between 1972 and 1988. The Longin method was introduced in 1971.	**B**
Samples published prior to 1972	**C**

The second criterion took into account the possibility of an age offset resulting from the aquatic radiocarbon reservoir effect (Fernandes et al., 2016) (see Figures 7.5 and Table 7.4). This effect arises from the uptake of ^{14}C-depleted carbon by a marine or freshwater organism, or from the inclusion of such organisms in human or animal diets (Fernandes, 2013; Fernandes et al., 2015; Fernandes, 2016; Fernandes et al., 2016) (Column BK). The effect of aquatic radiocarbon reservoirs on radiocarbon dates depends on local environmental conditions (which can also change over time) and variations between species due to their habitat and dietary preferences (Petchey et al., 2012). I straightforwardly tackled the problem, classifying samples with a terrestrial diet as Class A, samples from aquatic sources as Class B, and samples with an origin that wasn't reported or samples derived from humans or animals that might have consumed aquatic foods as Class C. I did not, however, conduct a more thorough review of the original publications to evaluate, for instance, whether local radiocarbon reservoir offsets were calculated for dates or the probability of aquatic diets using stable isotope data.

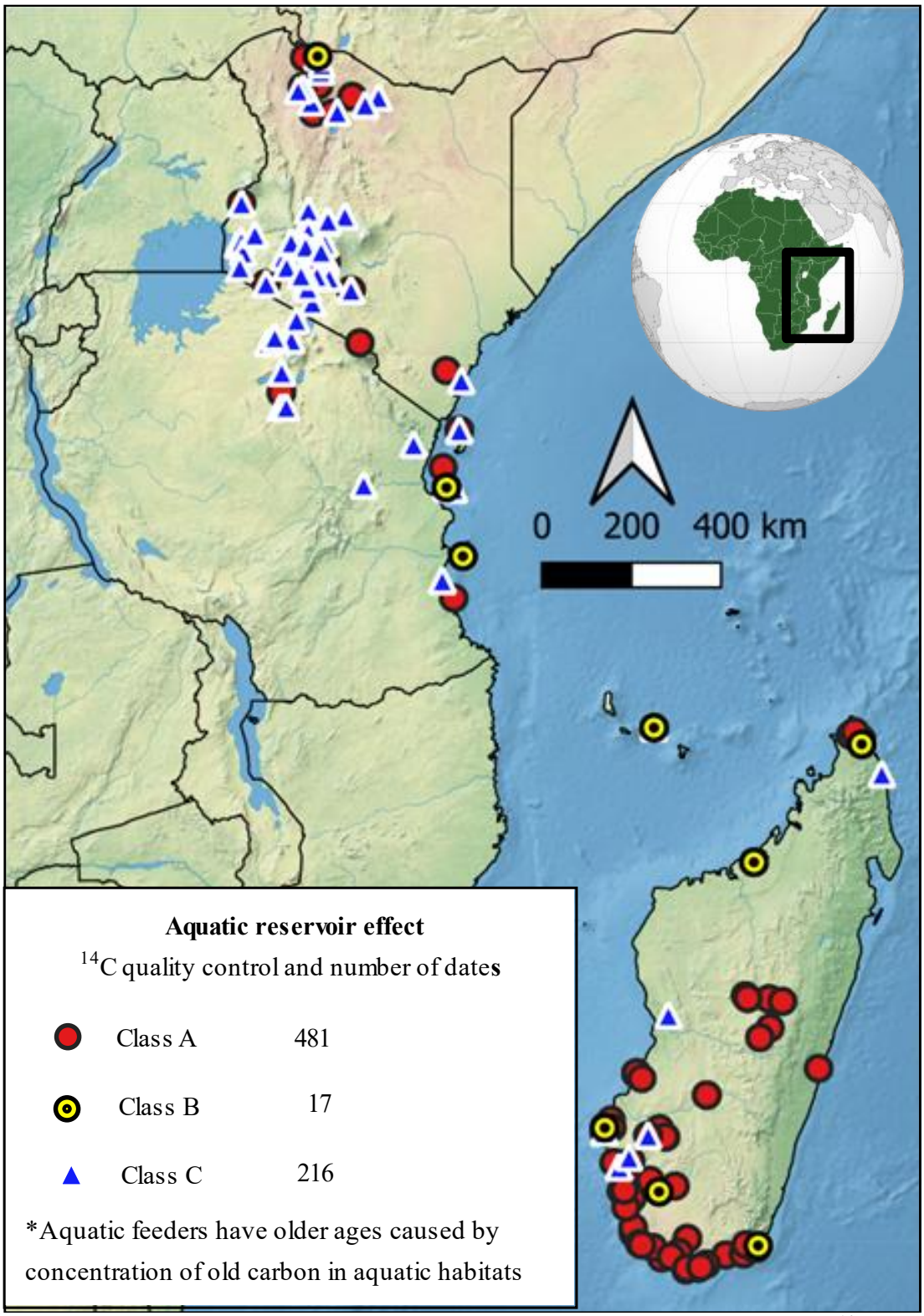


Figure 7.5. *Map of eastern Africa showing differences in the spatial distribution of ^{14}C dates from faunal material due to the aquatic reservoir effect. Note: Class A dates are considered to be the most reliable (Iminjili et al., 2025a; Iminjili et al., 2025b).*

The third criterion appraises the precision of a chronological determination. The basis for this is the pre-treatment method that is used. The pre-treatment method determines how effectively inorganic and organic contaminants are removed. These contaminants may skew an age determination (see Figure 7.6 and Table 7.4). The dataset did not include any information about pre-treatment methods, and these methods are rarely reported along with radiocarbon determinations in the study region. I used a coarse filter based on the publication date of the assay. This information is in column BL. I worked under the assumption that the accuracy of the ^{14}C dating technique for bone organics improved in 1971. This occurred when the Longin collagen extraction method was introduced (Brown et al., 1988). The accuracy of the technique was refined again in 1988. Ultrafiltration was introduced around that time as well (Brown et al., 1988). Around this time, researchers also started using AMS more regularly in radiocarbon dating of bone and charcoal samples (Schuur et al., 2016). Dates reported after 1988 were assigned to Class A. Those subjected to chromatographic methods were also assigned to Class A. Examples of these methods include XAD and amino acid isolation using HPLC. Dates reported between 1972 and 1988 were assigned to Class B. Those published before 1972 were assigned to Class C.

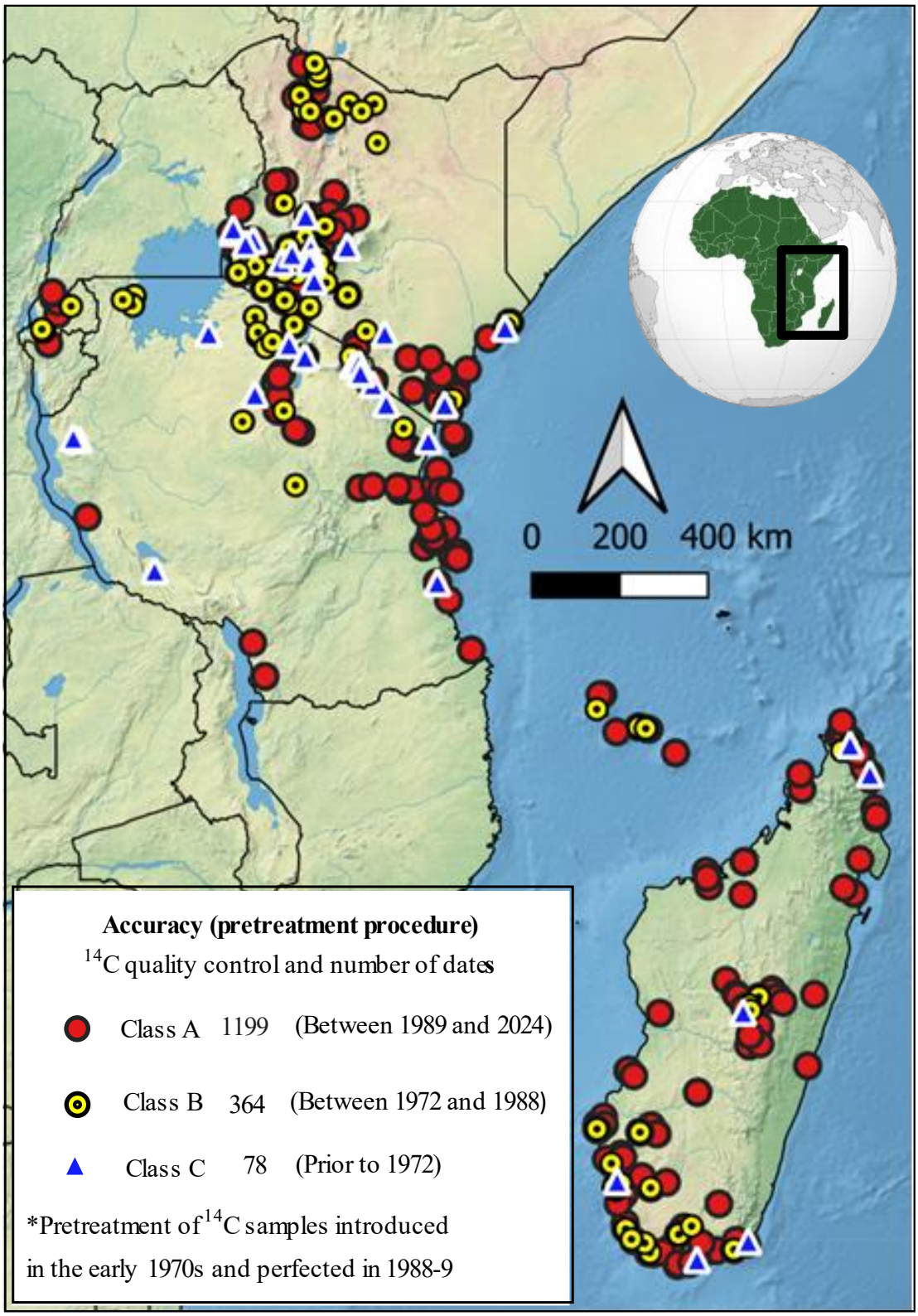


***Figure 7.6**: Map of eastern Africa showing differences in the spatial distribution of scientific dates, based on the accuracy of the pre-treatment procedure for ^{14}C dates. Note: Class A dates are the most reliable (Iminjili et al., 2025a; Iminjili et al., 2025b).*

7.7 – Data records

The *Wanyika* dataset (Iminjili et al., 2025a) comprises 75 fields, which are organized within eight major categories (see Table 7.5). Definitions of these 75 fields are provided below. The *Wanyika* dataset is spatiotemporal and flat-file, in which each row represents a scientific date associated with archaeological records. There are a total of 1,792 dataset records, each of which is associated with one of 422 sites. A "Yes" in the corresponding cell marks the presence of domesticated crop, faunal, iron, and/or ceramic finds, while a blank cell marks their absence. The dataset can be found in two formats: Excel and CSV. It is accessible via the repository *Wanyika* (https://pandoradata.earth/dataset/wanyika) within the AfriArch data community on the Pandora data platform https://pandoradata.earth/organization/afriarch (Pandora, 2024). This is the peer-reviewed version of the dataset and will not be updated. Updates will be included in a later version.

Table 7.5. *Data categories and field details. For definitions of column fields, see the section below.*

Column categories	**Data entry details**
Site details & metadata	Each row has the following unique identifiers: entry ID, site ID, name, country, region, vegetation cover, latitude and longitude coordinates, trench/site notes and context details.
Date	Date type, laboratory code number, mean BP date and standard deviation (uncalibrated in the case of radiocarbon measurements), minimum and maximum ranges and mean BCE/CE calendar dates, dated material, dated taxon, ceramic and regional cultural phase
Archaeobotanical	Presence of major African and exotic crops
Zooarchaeological	Presence of wild tetrapods, avian, aquatic, and indeterminate fauna, domesticates, human remains, introduced fauna, and extinct megafauna in Madagascar
Artefacts	Presence of iron artefacts and ceramics
Notes	Important qualitative site data
Quality control measures (Chronometric hygiene)	Applied to all dates: Based on stratigraphic integrity and reliability Applied to ^{14}C dates: Based on dated material and refined dating technique
Reference identification	Source references given in the *American Journal of Biological Anthropology* citation format and their Digital Object Identifier (DOI). Five fields are used to cite multiple references.

Definition of column fields

The column fields are labeled with letters of the alphabet, followed by the title of the column and an explanation of what the column represents.

A - Entry ID: This number indicates a specific date entry in a given row.

B - Site ID: This database number is assigned to a site by the system. Each site is assigned a unique number. All entries from the same site are given the same number.

C - Site Name: This refers to the name of the archaeological site.

D - Country: The name of the country in which the site is located. Possible options include Rwanda, Kenya, Tanzania, the Comoros Islands and Madagascar.

E - Country Region: The term 'region' refers to the specific area within a country where a site is located, as determined by administrative boundaries and latitude/longitude. Table 7.1 provides information on the demarcation of country regions.

F – Vegetation cover: This describes the site's dominant vegetation (White, 1983; Kingdon, 1984b; Burgess and Clarke, 2000; Kingdon, 2001; Iminjili et al., 2023). The subsequent six categories are encompassed: Forest/wood/grassland mosaic, montane forest, coastal forest mosaic, dry coastal wooded grassland, dry northern wooded grassland, and dry southern wooded grassland.

G - Latitude: The site's GIS coordinates are provided, expressed as decimal degrees of latitude relative to WGS84 (NIMA, January 2000).

H - Longitude: The site's GIS coordinates are provided, with the longitude expressed in decimal degrees relative to WGS84 (NIMA, January 2000).

I - Trench/Site Notes: The code numbers for excavation trenches, units, squares, quadrants, test pits, and features (e.g. burials, furnaces, and habitation sites) are captured, as well as any other

unique attributes that define a site (e.g. single-component or stratified sites, short- or long-term occupations).

J - Context: The context, number and/or measurement in centimeters, layer, level and stratum are all encompassed. Details that define time, space, matrix, and provenience are provided by it.

K - Date Type: This denotes the type of scientific dating method employed: ^{14}C, OSL, IRSL, TL or OH.

L - Labcode: This is a code number. It is designated by the host dating laboratory. The code number is given to the sample. The sample is used to generate a scientific date. It is usually a combination of letters and numbers. The letters represent the laboratory's designation and the number represents the sample's unique number. For example, OXA-14500.

M - Date BP: Uncalibrated date Before Present.

N - Date BP SD: Standard deviation for the uncalibrated date Before Present.

O - Min Chronology (Calibrated BCE/CE): Minimum calibrated date in calendar years (Before Common Era and Common Era).

P - Max Chronology (Calibrated BCE/CE): Maximum calibrated date in calendar years (Before Common Era and Common Era).

Q - Mean Chronology (Calibrated BCE/CE): Mean calibrated date in calendar years (Before Common Era and Common Era)**,** Minimum + Maximum / by 2 (calibrated date in calendar years).

R - Min Chronology (Calibrated BP - 1950): Minimum calibrated date Before Present (1950 minus Min Chronology calibrated BCE/CE).

S - Max Chronology (Calibrated BP - 1950): Maximum calibrated date Before Present (1950 minus Max Chronology calibrated BCE/CE).

T - Mean Chronology (Calibrated BP - 1950): Mean calibrated date Before Present (Minimum + Maximum / by 2 (Calibrated date Before Present).

U - Dated Material: The nature of the substance or specimen used to generate the date. Examples include charcoal, ceramics and bone collagen.

V - Dated Taxon: The lowest taxonomic order (i.e. species, genus, family, order or kingdom) of plant and animal remains (e.g. seeds, charred wood, bone/tooth collagen and apatite) used for dating is provided here.

W to AP - Archaeobotanical Information: Columns provide archaeobotanical information. A "Yes or blank cell" indicates the presence or absence of a specific crop. Represented African crops include finger millet (*Eleusine coracana*), pearl millet (*Pennisetum glaucum*), sorghum (*Sorghum bicolor*), cowpea (*Vigna unguiculata*), hyacinth bean (*Lablab purpureus*), Fig (*Ficus sp*.) and baobab (*Adansonia digitata*); exotic crops include rice (*Oryza sativa*), wheat (*Triticum aestivum*), coconut (*Cocos nucifera*), mung bean (*Vigna radiata*), pea (*Pisum*), red date (*Ziziphus jujuba*), and cotton (*Gossypium sp.*).

AQ to BB - Zooarchaeological Information: Columns provide zooarchaeological information for wild and pastoral species (but excluding introduced commensals like cat, dog, black rat). A "Yes or blank cell" indicates the presence or absence of a specific faunal taxon. Faunal taxa include wild tetrapods, avian, aquatic, and indeterminate fauna, as well as pastoral animals like bovids, cattle (*Bos taurus/indicus*), sheep (*Ovis aries*) and goat (*Capra hircus*), indeterminate Ovis/Capra, camel (*Camelus dromedary*), donkey (*Equus asinus*) and chicken (*Gallus gallus*). Directly dated remains of extinct megafauna in Madagascar (ratites, lemuroids, reptiles and non-primate mammals) and other translocated fauna (commensals cat, dog, black rat) are only recorded in the "Dated Taxon" column (column U).

BC to BD - Iron Smelting and Use: "Yes or blank cell" represents the presence or absence of evidence for iron smelting and use.

BE - Ceramics: "Yes or blank cell" represents the presence or absence of evidence for ceramics.

BF - Ceramic Phase (Pottery Ware): The names of the ceramic styles that are connected to the row data are listed here. These include the 25 major ceramic and pottery traditions and wares in eastern Africa. These are listed in Table 7.6.

BG - Regional Cultural Phase (Eastern Africa): This section provides an overview of the regional cultural phase represented by the recorded cultural assemblage (Table 7.6). These include the following: (a) the prehistoric period (applicable to Madagascar), the Late Stone Age (LSA), the Pastoral Neolithic (PN), the latter of which is divided into the Savanna Pastoral Neolithic (SPN) and the Elmenteitan Neolithic (EPN), and the Pastoral Iron Age (PIA); and (b) the Early Iron Age (EIA), the Middle Iron Age (MIA), and the Late Iron Age (LIA). For more information on the time period and ceramic tradition associated with each regional cultural phase, refer to Table 7.6.

Table 7.6. *Period and ceramic tradition associated with regional cultural phases.*

Regional Phase	**Estimated period**	**Ceramic tradition**
Prehistoric (Madagascar)	Pre-600 CE	-
Late Stone Age (LSA)	6000 BCE – 500 CE	Kansyore, Eburran, Lowasera
Savanna Pastoral Neolithic (SPN)	5000 BCE – 750 CE	Nderit and Ileret, Maringishu, Narosura, Akira
Elmenteitan Pastoral Neolithic (EPN)	1400 BCE – 750 CE	Elmenteitan
Pastoral Iron Age (PIA)	600 CE – 1800 CE	Turkwell, Lanet, Kisima, and Oldorotua
Early Iron Age (EIA)	500 BCE – 700 CE	Urewe, Lelesu, Kwale, Tana, Maore, Kilimanjaro, Swahili, Asian, Rezoky, Beropitika, Andaro, and Tranovato
Middle Iron Age (EIA)	701 CE – 1000 CE	
Later Iron Age (LIA)	1001CE – 1800 CE	

BH - General Notes: It provides important notes about the site and date. These include notes used for quality control assessments, such as notes on questionable dates and bioturbation-related anomalies.

BI - Mean Grade Chrono Hygiene 1 and 2: This is about the stratigraphic integrity grades. These are calculated using the stratigraphic integrity plus standard deviation (SD) mean scores. This is done to produce Class A-D dates. See the quality control section for more details.

BJ - Chrono Hygiene 3: The grade is predicated on the assumption that the ^{14}C date was affected by the long- or short-lived plant material. See Table 7.4.

BK - Chrono Hygiene 4: This grade is predicated on the probability that dated materials are impacted by the aquatic ^{14}C reservoir effect. See Table 7.4.

BL - Chrono Hygiene 5: This grade is predicated on the precision of the chronological determinations for the pre-treatment protocol of ^{14}C dates. See Table7.4.

BM - Date of Publication: The earliest year in which the date was disseminated is signified by this expression. The grades for "Chrono Hygiene 5" are calculated using this year. Accuracy (Pre-Treatment) ^{14}C Dates." I also use the publication year instead of the year of excavation for BP dates, because the primary publications used the year of excavation as "the present."

BN to BW - References and DOI 1-5: This provides bibliographic references and a Digital Object Identifier (DOI) or Uniform Resource Locator (URL) for each data source.

Technical Validation

The data in this dataset was primarily retrieved from peer-reviewed scientific journals, books, dissertations, monographs, and site reports written by researchers working in eastern Africa who have a strong reputation. In some instances, information from ongoing initiatives awaiting

dissemination has also been incorporated. Only data reported in uncalibrated years before the present with standard deviations and laboratory codes are included in the dataset. Throughout the dataset construction process, I carried out frequent checks and completed a final, comprehensive check towards the end to remove duplicate records and other errors. Roughly 20 records were omitted due to the absence of uncalibrated dates (reported in BCE/CE exclusively), standard deviation, or laboratory code. For instance, two dates from Engaruka and Kuumbi Cave in Tanzania were excluded due to the absence of standard deviations (Chami, 2009; Westerberg et al., 2010; Shipton et al., 2016). A distinctive instance in which four dates from the Serengeti (Tanzania) were erroneously published as Takwa dates (Kenya) was documented (Ambrose, 1984a; b; Wilson, 2019). These dates were also expunged from the dataset. The author of the Takwa report acknowledges the error on page 4, first sentence (Wilson, 2019). Geochron Laboratories also confirmed the accuracy of these dates through personal correspondence.

Usage Notes

As a member of the Afriarch community hosted on the Pandora platform, the *Wanyika* dataset (Iminjili et al., 2025a) adheres to the FAIR data principles. These principles encourage good data management practices by prompting scientists to make their datasets "findable," "accessible," "interoperable," and "reusable" (Wilkinson et al., 2016). The data is made findable and accessibility is enabled by the public availability afforded by Pandora's web presence. *Wanyika* (Iminjili et al., 2025a) champions the reutilisation of data by elucidating the findings of the quality control analysis and by being receptive to collaborations that can modernize the dataset as novel information emerges. The ongoing development of the Pandora platform includes Natural Language Model SQL (Standard Query Language) programming, which grants datasets such as *Wanyika*

interoperability. Furthermore, *Wanyika* has the potential to be integrated into semantically interoperable dataset systems, such as MAEASaM (Mapping Africa's Endangered Archaeological Sites and Monuments). The maps were generated using QGIS version 3.28.9 (QGIS Development Team, 2024), Natural Earth (Natural Earth, 2024), CSV data files (Microsoft, 2024), Adobe Photoshop (Adobe, 2024), and the Inkscape app (Inkscape, 2024).

Code availability

Four codes were utilized to calibrate the ^{14}C dates in OxCal for (1) terrestrial samples between -18° and 6° latitude, (2) terrestrial samples below -18° latitude, (3) marine samples, and (4) freshwater samples (only applicable to a sample above 0.5° latitude). The following is a list of the codes:

Terrestrial samples located between -18° and 6° latitude

```
Plot('terrestrial samples')
{
Curve('IntCal20,'IntCal20.14c');
Curve('SHCal','SHCal20.14c');
Mix_Curves('Mixed_terrestrial_curves','IntCal20', 'SHCal20' ,U(0,100));
R_Date('LAB_CODE',14C_MES,14C_UNC);
}
```

Terrestrial samples below -18° latitude

```
Plot('terrestrial samples') {
```

Curve('SHCal','SHCal20.14c');

R_Date('LAB_CODE',14C_MES,14C_UNC);

}

Marine samples

Plot(marine samples')

{

Curve('Marine20', 'Marine20.14c');

Delta_R('LocalMarine' , MARINE_DR, MARINE_DR_UNC);}

R_Date('LAB_CODE',14C_MES,14C_UNC);

}

Freshwater samples (only applicable to a sample above 0.5° latitude

Plot('freshwater samples')

{

Curve('IntCal20,'IntCal20.14c');

Delta_R('LocalFreshwater' , FRESHWATER_DR, FRESHWATER_DR_UNC);}

R_Date('LAB_CODE',14C_MES,14C_UNC);

}

Definition of terms for OxCal code for calibration of radiocarbon measurements

LAB_CODE stands for radiocarbon lab code

14C_MES stands for the uncalibrated radiocarbon measurement in years BP

14C_UNC stands for the 1-sigma error associated to 14C_MES

MARINE_DR stands for local marine ΔR value

MARINE_DR_UNC stands for the 1-sigma error associated to MARINE_DR

FRESHWATER_DR stands for local freshwater ΔR value

FRESHWATER_DR_UNC stands for the 1-sigma error associated to FRESHWATER_DR

Generating the *Wanyika* dataset is a significant achievement for late Holocene archaeology in eastern Africa. It is a foundational repository that provides a systematic structure upon which subsequent growth can be built. As an inventory of the region's archaeological record, the *Wanyika* dataset reveals which regions and time periods have been studied more than others, highlighting the strengths and weaknesses of the record. This archaeo-informatic dataset provides a new perspective on the region's archaeological record. Sophisticated, computer-aided programs can be used to explore the dataset for spatial-temporal modeling, addressing enigmatic questions and testing major hypotheses concerning ecology, complex subsistence strategies, the emergence of food production, and the dispersal of food-producing communities. The dataset and programs could also aid in refining and reformulating theories at regional and global scales. For example, they could help refine the pastoralist migration hypotheses and the western African agropastoralists' late-split riverine and late-split savannah migration hypotheses. The dataset also reveals research gaps in the archaeological record of eastern Africa during the late Holocene. It will be critical in shaping future research agendas and bridging the gap between archaeology and other disciplines.

Chapter 8 – Insights from isotopic and archaeo-informatic perspectives on the emergence and dispersal of food production and food-producing communities in coastal eastern Africa during the late Holocene

This chapter offers fresh, detailed insights into ecological fluctuations, intricate subsistence strategies, and the emergence and dispersal of food production and food-producing communities in eastern Africa's coastal strip, offshore islands, and interior during the late Holocene. These insights are revealed through multi-isotopic and archaeo-informatic analyses. The first section discusses the findings of case study one, which examined the ecological stability and persistence of foragers at Kuumbi Cave (KC) during the late Pleistocene and late Holocene epochs. The second section provides insights from case study two on patterns of carbon, nitrogen, oxygen and strontium isotopes, reflecting caprine management and complex economic adaptation strategies, at Unguja Ukuu (UU) and Fukuchani (FK) on Unguja Island, and at Panga ya Saidi (PYS) on the coastal strip of eastern Africa. The third section highlights insights from case study three concerning the *Wanyika* dataset, which addresses major research questions regarding the emergence of food production and the dispersal of food-producing communities in eastern Africa. The fourth section condenses the archaeological conundrum surrounding the emergence and dispersal of the 'Bantu agropastoral package' in the interior of eastern Africa, along the coast, and on the islands. Finally, section five summarizes insights from multi-isotopic and archaeo-informatic analyses, highlighting the complementarity of the two approaches applied in this thesis to test the postulates of the indigenous continuity and migration hypotheses in eastern African archaeology, as discussed in chapters one to four.

8.1 – Ecological stability and forager persistence at Kuumbi Cave during the late Pleistocene and late Holocene

As presented in chapter five, the stable carbon and oxygen isotope analysis of enamel samples from the faunal and human remains at the late Pleistocene to late Holocene KC site supports the hypothesis that:

1. *The stability of forests along the coastal strip and on offshore islands in eastern Africa may have played a significant role in the endurance of indigenous foraging communities at Kuumbi Cave when interacting with immigrating agropastoral groups during the Iron Age.*

Evidence from the KC site on Unguja Island, including isotopic and archaeological assemblage data, suggests that indigenous continuity was more prevalent than immigrant agropastoralism from mainland eastern Africa during the Iron Age. In theory, agropastoralists could have used KC for foraging activities either partially or exclusively. However, data from wild fauna and humans indicate that the indigenous foraging lifestyle—specializing in hunting small, forest-adapted mammals with bone points, traps, and crude stone tools—persisted from Phases IV to II and continued after a long Holocene hiatus, as evidenced in Phase I (the Iron Age) (Langley et al., 2016; Prendergast et al., 2016; Shipton et al., 2016; Faulkner et al., 2019). This occurred despite the evidence of the emergence of food production at KC during the Iron Age. The isotopic and archaeological records suggest that dense forests inhabited by small, forest-adapted fauna persisted at KC even during Phase I (the Iron Age), despite an increase in climatic variability and aridity across the region, as evidenced by changes in mangrove and tidal inundation dynamics at UU (Punwong et al., 2013; Englong et al., 2023). Previous zooarchaeological work at KC further supports the isotopic data (Prendergast et al., 2016). This work showed that the assemblage

comprised animals living in habitats ranging from closed forests and woodlands to open forests and grasslands, though forest and woodland habitats were overall dominant (Table A1:1 and Prendergast et al., 2016). The ubiquitous and abundant primate and hyrax species are arboreal and adapted to dense forest cover (White, 1983; Kingdon, 1984b; Fleagle, 1999; Burgess and Clarke, 2000; Kingdon, 2001; Olson et al., 2001; Fleagle and Kamilar, 2007). Most of the represented bovids are endemic to closed-forest habitats. However, some are found in more mixed mosaic habitats. These include klipspringer, bush duiker, and bushbuck (Gagnon and Chew, 2000; Cerling et al., 2003c). Bush pigs, giant pouched rats, and porcupines are found in a variety of habitats, ranging from forests to woodlands (Kingdon, 1984b; 2001). Grassland-adapted species are few and rare, and absent from the latter part of Phase I (reported as P1a in Prendergast et al., 2016). The isotope data also emphasize the importance of dense forests and woodlands as human-exploited environments at the site, with small patches of open forests and woodlands, thickets, bushlands, and grasslands present throughout the sequence. Notably, as with PYS, the $\delta^{13}C$ and $\delta^{18}O$ values of the KC faunal remains effectively distinguish among forest, woodland, and grassland conditions (Roberts et al., 2020), potentially achieving greater resolution within forest niches, as per Cerling et al. (2004).

Data from stable isotope analysis and zooarchaeology suggest that the past inhabitants of KC used animals well adapted to the local environment, which included diverse vegetation (Kingdon, 1984b; Burgess and Clarke, 2000; Kingdon, 2001; Prendergast et al., 2016). The preponderance of terrestrial fauna hail from closed and open forested niches ($\delta^{13}C$ values between −15 and −9‰, n=121). A minuscule proportion of the fauna appears to originate from dense forest ecosystems (ranging from −21 to −15‰, n = 7). These $\delta^{13}C$ readings are consistent with subcanopy and canopy habitats within the forest, ranging from −15 to −12 ‰, and with understory habitats, ranging from

−19 to −15 ‰. However, only a negligible proportion of the fauna exhibited values congruent with those observed in open woodland and grassland settings (−9 to 2 ‰, n = 19). A comparison of $\delta^{13}C$ readings over time suggests that, during Phases IV and III when grasslands expanded from the mainland to the island, hunters may have focused on the more open/peripheral parts of forests and woodlands (−15 to 1 ‰ for primates and hyraxes, −14 to −10 ‰ for browsing bovids, and −6 to −2 ‰ for grazers). During the islandization period (Phases II and I), however, hunters focused more on forest-dwelling prey: −19 to −10 ‰ for primates and hyraxes, −21 to −8 ‰ for browsing bovids, and −9 to −4 ‰ for zebras.

The scarcity and disappearance of grassland-adapted animals in KC from phases IV to I may be primarily caused by forest expansion and islandization (Prendergast et al., 2016). Human-induced changes during the Iron Age may have accelerated this process. This forest expansion is likely a consequence of the more humid Holocene weather conditions and the geographic setting of island formation, which resulted in more moist conditions (Punwong et al., 2012; 2013; Prendergast et al., 2016; Shipton et al., 2016; Punwong et al., 2018; Englong et al., 2023). Additionally, foragers do not appear to have had an imbalanced preference for grassland fauna in Phases IV and III. Despite the limited sample size, the grazer isotope values ($\delta^{13}C$ and $\delta^{18}O$) in Phases IV and III are notably higher and more narrowly distributed than the values observed in Phase II ($\delta^{13}C$: n = 2, mean = −6.3‰; $\delta^{18}O$: mean = −3.6‰). The low $\delta^{13}C$ and $\delta^{18}O$ values observed in Phase II could indicate a contraction of the grassland habitat, which may have led to a decline in grazing activity in the KC region. The precise times of extirpation are unclear, but the faunal data show that buffalo were only present in Phase III and waterbuck in Phases II, III, and IV. Reedbuck and zebra were present infrequently across all phases, and their absence became more pronounced in later Phase I. The indeterminate mammal size 3-4, which corresponds to the size of waterbuck, zebra, and

buffalo, was also scarce in Phases II and I. The arrival of Iron Age farmers may have worsened the problem of defaunation by contributing to the disappearance of the reedbuck and zebra in the KC sequence. The reedbuck is represented by $\delta^{13}C$ values in Phase III, while the zebra is represented by values in Phases IV and II. The values for these grazers are lower than −2‰ (between −8 and −2‰), whereas the values for these same grazers in the interior of eastern Africa are higher than −2‰. These low values suggest that these grazers struggled in environments with limited grazing and experimented with browse that did not favor them. The immigrating agropastoralists likely occupied these open habitats, accelerating the defaunation process.

A plethora of stable isotope studies have underscored the notion that the partitioning of food resources among arboreal primates may be reflected by $\delta^{18}O$ values, yet not by $\delta^{13}C$ values (Krigbaum et al., 2013; Roberts et al., 2017; Lowry et al., 2021). However, the KC primates' and hyraxes' $\delta^{13}C$ and $\delta^{18}O$ values appear to capture intraspecific vertical food resource partitioning (Figure 8.1). These values represent animals within a taxon that exploit resources along a gradient between the forest floor and the upper canopy. This could be considered intraspecific partitioning, which occurs when organisms of the same species are separated geographically or physiologically. Cercopithecines, including vervet and blue monkeys, are adaptable with a wide range of habitat preferences (Fleagle, 1999; Kingdon, 2001a; Campbell et al., 2006). They can be found in the canopy and subcanopy as well as the understory of forested habitats, open and closed woodlands, and thickets (Kingdon, 2001b). Tree hyraxes inhabit the understory, middle, and upper levels of forests, as well as evergreen thickets and forest mosaics (Kingdon, 2001a). The greater galago and the Zanzibar bush baby are omnivorous and can often be found in the understory and subcanopy of forests. These animals can adapt to different environments (ecological niches) based on competition levels (Kingdon, 2001b). The Zanzibar colobus's low range in $\delta^{13}C$ values and high

$\delta^{18}O$ values are explained by their exclusive canopy habitat. The eclectic behaviors of primates and hyraxes are reflected in their $\delta^{13}C$ and $\delta^{18}O$ values (see the summary statistics).

The hyrax is an extreme outlier, with high $\delta^{13}C$ (−2.5‰) and $\delta^{18}O$ (−0.2‰) values reflecting reliance on C_4 resources, which is unexpected. To my knowledge, no studies have reported a similar observation from hyraxes (Ambrose and DeNiro, 1986a; b; Kingdon, 2001; Cerling et al., 2004; la Grange, 2015).

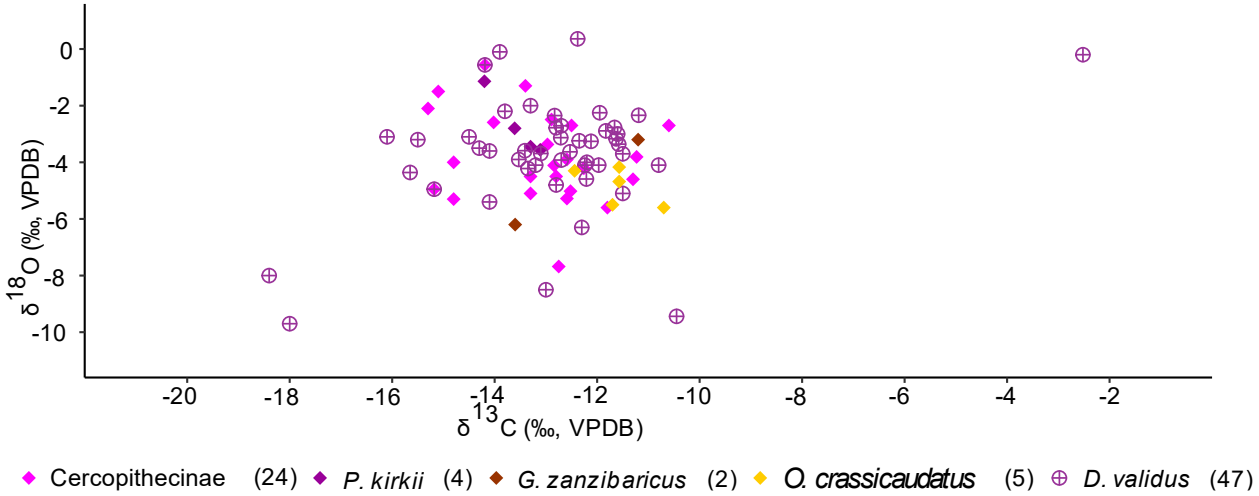


Figure 8.1. *Scatter plot showing the distribution of arboreal fauna (primates and hyraxes) at KC. The values mirror the exploitation of resources by animals within each given taxon along a gradient between the forest floor and upper canopy (Iminjili et al., 2023).*

Zooarchaeological analyses and faunal stable isotope values provide broad insights into the niches exploited by humans at KC. Additionally, the $\delta^{13}C$ and $\delta^{18}O$ values of the two humans (terminal Pleistocene: −12.1 and −5.4‰; Iron Age: −10.7 and −3.1‰) provide direct insights into the foragers' diets. Generally, human $\delta^{13}C$ values indicate a diet dominated by forest/woodland C_3 resources, which overlaps with the omnivorous fauna values at the site ($\delta^{13}C$: −13.6 to −9.8 ‰; $\delta^{18}O$: −6.8 to −1 ‰). The Iron Age sample has slightly higher $\delta^{13}C$ and $\delta^{18}O$ values than the

Pleistocene sample, but the small sample size prevents us from deriving any significant conclusions. These human and faunal values suggest that humans primarily subsisted on forest/woodland resources. However, there were varying contributions from denser canopied areas and more open settings. The abundance of arboreal and other forest-adapted taxa, particularly primates, hyraxes, and dwarf antelopes (Neotragini and Cephalophini), in the archaeological record supports the forest/woodland subsistence interpretation. The presence of unique stone tools and the absence of obsidian microliths, forager ceramics (as seen on the mainland), domestic animals, crops, and iron suggest that the indigenous foragers at KC endured for a long time without contact with the outside world, particularly mainland Africa (Prendergast et al., 2016; Shipton et al., 2016; Culley et al., 2021b).

Kuumbi Cave and the continuity of indigenous foragers in the broader eastern African context

Spatial variation in forager subsistence is revealed by comparing the zooarchaeological assemblage and isotopic datasets from KC with those from PYS and other interior eastern African sites (Robinson, 2017; 2019; Prendergast, 2020; Roberts et al., 2020; Jones and Brandt, 2022; Prendergast et al., 2023). Among known late Pleistocene and late Holocene sites, KC exhibits the highest proportion of forest-adapted species, including primates, hyraxes, bovids (Cephalophini and Neotragini), and rodents, in both NISP and MNI, compared to other eastern African zooarchaeological assemblages (Gifford-Gonzalez and Kimengich, 1984; Mehlman, 1989; Marean, 1992a; Prendergast et al., 2007; Prendergast et al., 2013; Robinson, 2017; Chritz et al., 2019; Robinson, 2019). A large number of forest-adapted species have been documented in the nearby Kenyan coastal sequence of PYS. These include suni, klipspringer, tree hyrax, vervet monkeys, blue monkeys, *Colobus* sp. (colobus monkeys), and giant pouched rats. Nevertheless,

the presence of a significant proportion of open woodland and grassland fauna indicates a greater persistence of forest mosaics at the PYS site. Examples include kongoni/topi *(Alcelaphus/Damaliscus)*, waterbuck, blue wildebeest, *(Connochaetes taurinus)*, buffalo, warthog *(Phacochoerus* sp.), and reedbuck (Shipton et al., 2018; Roberts et al., 2020; Culley et al., 2021a; Faulkner et al., 2021; Prendergast et al., 2023).

Pleistocene and Holocene sites in the eastern African interior have yielded fauna indicative of grassland environments. This suggests that these portions of eastern Africa were much more open in the past, except for the EYM rock shelter and Gamble's Cave in the central Rift Valley of Kenya. High numbers of hyper-grazers, including blue wildebeest, hartebeest, waterbuck, topi, reedbucks (*R. redunca, R. arundinum, R. fulvorufula)*, buffalo (*S. caffer, S.* cf. *antiquus)*, beisa oryx (*Oryx beisa)*, common and Grevy's zebra (*E. quagga* and *grevyi),* and warthog *(Phacochoerus africanus)*, have been recorded at sites in the Lake Eyasi basin, the Mbulu Plateau, and the Serengeti in Tanzania; the Lake Victoria and Lake Turkana regions in Kenya; and other related sites, such as Ele Bor, Lukenya Hill in Kenya, Porc Epic in Ethiopia, and Kalemba in Zambia (Figure 5.5 and Appendix 1) (Mehlman, 1989; Marean, 1992b; Gifford-Gonzalez, 2003; Dale, 2007; Prendergast et al., 2007; Prendergast, 2010a; Prendergast et al., 2013; Robinson, 2017; Grillo et al., 2018; Chritz et al., 2019; Robinson, 2019). Primates, hyraxes, and rodents are rare in interior eastern African sites. The stability of grasslands and open woodlands is confirmed by the relatively higher faunal $\delta^{13}C$ and $\delta^{18}O$ values from mainland eastern African sites compared to KC (Figures 5.5 and 5.6, Table 5.1, and Tables A1:1 and A1:2) (Robinson, 2017; Chritz et al., 2019; Robinson, 2019; Roberts et al., 2020). The ecological uniqueness of KC is highlighted by a comparative statistical analysis of equid and browser $\delta^{13}C$ values (Appendix 1). Additionally, statistical analyses suggest that foragers at KC hunted animals from the most complex ecological niches and the deepest, most

forested parts of the forest, more so than other eastern African sites (Figures 5.5–5.6 and Tables 5.1 and A1:1 and A1:2) (Robinson, 2017; Chritz et al., 2019; Robinson, 2019; Roberts et al., 2020).

A comparison of the $\delta^{13}C$ and $\delta^{18}O$ enamel values of humans from KC, PYS, and Kakapel reveals a similar spatial diversity (Roberts et al., 2020; Wang et al., 2020). The $\delta^{13}C$ and $\delta^{18}O$ values of the PYS humans are very similar to those of the KC humans and indicate a focus on tropical forest and woodland resources: −11.4 and −11.1 ‰ (MSA) and −11.1 and −11.0 ‰ (Iron Age) for $\delta^{13}C$; and −4.3 and −3.2 ‰ (MSA) and −3.2 and −3.1 ‰ (Iron Age) for $\delta^{18}O$. In contrast, Kakapel human isotope values from two individuals demonstrate a clear dietary shift over time, with Individual 1 (~4,000 BP) exhibiting lower $\delta^{13}C$ and $\delta^{18}O$ values of −10.6 and −1.4 ‰, respectively. Individual 2's (<2300 BP) higher $\delta^{13}C$ and $\delta^{18}O$ values (−4.4 and −1, respectively) have been associated with the high consumption of finger millet and sorghum. Long-term millet cultivation has been proposed for this site (Mueller et al., 2022). Dramatic changes associated with high consumption of domesticated C_4 crops are also suggested by some collagen values from Kakapel (below −8‰ when normalized to enamel level). The Kakapel situation demonstrates what might occur if cultivated C_4 crops had been adopted to a significant extent in the coastal areas. In a similar vein, humans who rely on cattle, sheep, and goats in eastern Africa have also been linked to higher "C_4" values (Ambrose, 1986; Bleasdale et al., 2020). The absence of this change at KC and PYS suggests a continued reliance on forest- and woodland-based dietary strategies in these areas. These consistently low $\delta^{13}C$ values suggest that KC and PYS humans didn't really adopt domestic crops like sorghum and finger millet as a major dietary source.

The choice of foragers to limit the uptake of agriculture, at least of C_4 crops such as millet and sorghum or grazing domesticates, during the Iron Age may have been influenced by the relative

stability of forest habitats at KC and PYS (Prendergast et al., 2016; Shipton et al., 2016; Shipton et al., 2018; Roberts et al., 2020; Prendergast et al., 2023). The continued focus of these populations on forest and woodland resources for their subsistence is suggested by human $\delta^{13}C$ and $\delta^{18}O$ values at Iron Age KC, as at PYS (Roberts et al., 2020). Therefore, the absence of domesticated animals at KC may indicate a community of foragers who were experimenting with food production rather than a community of incoming food producers. Further supporting this point are zooarchaeological and material culture evidence (Langley et al., 2016; Prendergast et al., 2016; Shipton et al., 2016). These include similar patterns of hunting and faunal diversity during the Iron Age; a lack of domesticated fauna; a stone tool assemblage; and an absence of iron, which is common in sites associated with established food production (Shipton et al., 2016). The site also yielded a version of the local Tana Tradition (TT) and Triangular Incised Ware (TIW) ceramics with a unique fabric composition, setting them apart from other Unguja Island sites, including UU and FK. KC ceramics exhibit a lower content of sand temper, a more intense firing process, and thicker body sherds (Shipton et al., 2016). Preliminary analyses of the site's archaeobotanical assemblages have found no unequivocal crop remains thus far, though this work is ongoing (Crowther et al., 2016b).

The material culture and genetics records of the KC and PYS sites also reflect patterns of diversity, complexity, and continuity (Prendergast et al., 2016; Shipton et al., 2016; Roberts et al., 2020; Wang et al., 2020; Lipson et al., 2022; Iminjili et al., 2025a; Iminjili et al., 2025b). After islandization, Unguja Island was likely submerged and abandoned, and then reoccupied by foraging immigrants from the coastal strip in reaction to the emergence of food-producing communities along the coast (Prendergast et al., 2016; Shipton et al., 2016). However, several lines of evidence suggest that the island was not completely submerged and that animals, and perhaps even humans, persisted until the Iron Age. The presence of diverse wild animals and plants of African origin on

the island during the Iron Age suggests that the island was not completely submerged (Prendergast et al., 2016). The persistence of hunting wild animals in Phase I with patterns similar to those of the late to terminal Pleistocene (Phases IV to II), the continuation of peculiar quartz and limestone stone tool technology differing from the microlith technology found at PYS and other sites in eastern Africa suggest that these foragers were indigenous to Unguja Island (Shipton et al., 2016; Goldstein et al., 2022b). The absence of obsidian microliths and other common types of stone tools found in mainland eastern Africa, as well as the absence of ceramics associated with foragers, such as Kansyore and Neolithic and Iron Age pastoralists, who are prevalent in the interior, suggests an absence of trade networks and producer-client relations, as well as fictitious blood alliances, between the KC foragers and the mainland (Shipton et al., 2016). The absence of an indigenous ceramic tradition among the coastal KC and PYS foragers suggests their isolation from interior populations (Shipton et al., 2016; Shipton et al., 2018; Faulkner et al., 2021). Strontium values from the KC Iron Age human also suggest that this individual was native to KC (reported in the Unguja Ukuu results chapter six).

The archaeological assemblage at KC, which includes Tana-TIW ceramics, suggests that, following the isolation of Unguja Island from the mainland during the early Holocene, the first contact with mainland human populations occurred during the Iron Age when western African agropastoralists arrived (Prendergast et al., 2016; Shipton et al., 2016). This is supported by aDNA evidence showing that although the KC (600 CE) and PYS (1540 CE) individuals are closely related to other foragers, they are distantly related within the forager pool (Skoglund et al., 2017; Prendergast et al., 2019b; Wang et al., 2020; Lipson et al., 2022). Specifically, the KC individual is more closely related to early to mid-Holocene Malawi foragers than the PYS individual is (Wang et al., 2020; Lipson et al., 2022). Conversely, the PYS individual is more closely related to

Neolithic Ethiopian foragers and modern Hadza and Sandawe foragers from Tanzania than the KC individual is (Wang et al., 2020; Lipson et al., 2022). The KC individual is more distantly related to all food producers in eastern Africa than the PYS individual (Wang et al., 2020; Lipson et al., 2022). The close relationship between the KC individual and Holocene Malawi foragers may have developed before islandization. The Makangale individual I (560 CE) identified as a forager is closely related to the KC Iron Age individual but not to the Makangale individual II (1350 CE), who is associated with agropastoralists of western African ancestry (Wang et al., 2020; Lipson et al., 2022). This Makangale individual II is closely related to late Iron Age central African, Ugandan (Munsa 1500 CE), and modern western African populations, as indicated by aDNA evidence (Wang et al., 2020; Lipson et al., 2022). These findings further support the existence of a long-term foraging population at KC that adapted to hunting small forest-dwelling mammals from Phases IV to II and beyond, even after interacting with agropastoralists who immigrated from mainland eastern Africa during Phase I (the Iron Age).

Together, the isotopes, the archaeological assemblage, and the aDNA evidence from KC and PYS suggest that, during the Iron Age in eastern Africa, indigenous continuity rather than migration primarily shaped human-environment interactions at certain sites on offshore islands, such as KC, and in the coastal strip, such as PYS (Roberts et al., 2020; Wang et al., 2020; Lipson et al., 2022; Iminjili et al., 2023). The moving frontier hypothesis describes this type of scenario with a static frontier (Lane, 2004). In this case, the boundary is created by the mutual coexistence of independent foragers and food producers, and is referred to as the static frontier. This phase typically involves limited and specific interactions between food producers and indigenous populations. These KC and PYS scenarios illustrate the absence of intense mosaic interactions (Kusimba and Kusimba, 2005; Crowther et al., 2018) involving multiple ceramic traditions, which represent island-

mainland intercultural coalescence. For instance, the Kansyore, Urewe, Narosura, and Elmenteita ceramic traditions intermingled in the Lake Victoria and central Rift Valley regions of eastern Africa (Kusimba and Kusimba, 2005). There is also a lack of mosaic interaction in stone technology at KC and PYS (Shipton et al., 2016; Goldstein et al., 2022b), as evidenced by the obsidian exchange between the Northern Island and the mainland around Lake Turkana (Ndiema, 2011; Ndiema et al., 2011).

Collectively, the $\delta^{13}C$ and $\delta^{18}O$ and the archaeological assemblage from KC and PYS suggest that the stable coastal forests influenced the adaptive trajectory of foragers at coastal sites differently than it did for foragers in the arid, wooded grasslands of eastern Africa's interior (Chritz et al., 2019; Robinson, 2019; 2022). According to the delayed return model, foragers who practice delayed return are more likely to adopt food production than those who practice immediate return (Woodburn, 1982; Dale et al., 2004; Layton and Rowley-Conwy, 2013). In African archaeological settings, delayed return foragers are characterized by their repeated use of sites, complex hunting skills (e.g., use of bone points and traps), and a rich, predictable resource base (Dale et al., 2004; Dale, 2007). By this definition, the KC foragers are considered delayed return foragers and thus expected to invent or take up food production easily. Examples from the interior of eastern Africa suggest that foragers practicing immediate return from the Eyasi Basin and foragers practicing delayed return from sites in the Lake Victoria region could have switched to food production (discussed in chapter two) (Dale et al., 2004; Prendergast et al., 2007; Prendergast, 2009; Prendergast and Mutundu, 2009; Dale and Ashley, 2010; Prendergast et al., 2013; Prendergast et al., 2014). However, the long-term records of the KC and PYS foragers do not conform to the postulates of the delayed return model because they did not evolve or adopt food production, even during their interactions with Iron Age agropastoralists (Prendergast et al., 2016; Shipton et al.,

2016; Shipton et al., 2018; Roberts et al., 2020; Faulkner et al., 2021). As with other examples worldwide, the KC and PYS records support the idea that delayed-return foraging is not a prerequisite for food production and that not all delayed-return foragers evolve food production (Layton and Rowley-Conwy, 2013). The fluctuating ecology and seasonally available resources of the interior of eastern Africa produced highly adaptive foragers who could easily switch subsistence strategies (Ambrose, 1997; Ambrose, 1998; Kusimba, 2005; Kusimba, 2013). In contrast, the stable coastal forests produced specialized foragers who hunted small, forest-adapted mammals that were easily accessible year-round (Prendergast et al., 2016; Shipton et al., 2016; Shipton et al., 2018; Roberts et al., 2020; Iminjili et al., 2023). This made it difficult for food production to circulate quickly among coastal foragers. Notably, coastal foragers persisted on the mainland of eastern Africa until the 20th century, particularly in southern Kenya and northern Tanzania (Stiles, 1981; 1982; Kassam, 1986; 1987; Walsh, 1990; 1993). They are still present in northern Kenya and southern Somalia.

8.2 – Caprine husbandry and complex subsistence strategies at Unguja Ukuu, Unguja Island, during the Iron Age

As presented in chapter six, the multi-isotope analysis of collagen carbon and nitrogen, as well as enamel carbon, oxygen, and strontium from caprine, wild fauna, and human remains from the Iron Age site of UU, supported by the associated archaeological assemblage, supports the hypothesis that:

2. *The Unguja Ukuu forest and marine ecosystem, along with its archaeological assemblage, portrays a complex caprine herding strategy intertwined with a mosaic economic livelihood that*

originates from the forested coastal region of eastern Africa. This coastal herding strategy differs greatly from those in the predominantly arid interior of eastern Africa.

Overall, analysis of stable isotope data from nine eastern African archaeological sites has demonstrated the valuable insights that multi-isotope studies can provide into herd animal diets and pastoral lifeways. While some samples did not yield sufficient collagen for analysis, 85% of the targeted samples did. Studying residual collagen extracts from the previous ZooMS analyses of material from UU, FK, and PYS highlights the value of these samples for further isotopic studies. Trends in the UU collagen dataset show that caprines generally have higher $\delta^{13}C$ and $\delta^{15}N$ values than wild animals. Similarly, the nine UU enamel $\delta^{13}C$ values suggest that the goats' values are higher than would be expected in an ecological setting dominated by C_3 resources, such as mangrove forests, which would have been utilized by caprines (Culley et al., 2021b). This is all the more surprising given that UU marine core records indicate a wetter climate characterized by the inland expansion of mangrove forests during the period of the UU site's occupation (Punwong et al., 2013; Englong et al., 2023). The caprine $\delta^{18}O$ values are below 1‰, with one value above 4‰. The UU human $\delta^{13}C$ and $\delta^{18}O$ values are within the range of the caprine values. The $^{87}Sr/^{86}Sr$ values suggest that the caprines and one human at UU have different origins, with some of the caprine values indicating a coastal mainland eastern African origin. Five goats have values above 0.710; two goats, one sheep, and one human have values between 0.709 and 0.710; and one goat has a value below 0.709. A comparison of collagen values between sites shows that the PYS sheep with the lowest $\delta^{13}C$ value and high $\delta^{15}N$ value are different from the UU and EYM sheep. Inter-site comparison of enamel values from the coastal sites shows that UU caprines have higher $\delta^{13}C$ and $\delta^{18}O$ values than KC wild browsers, but these values are almost similar to those of KC wild grazers. The UU human enamel values are within the range of the caprine values and different from the KC

and PYS human values, which are within the range of the KC wild browsers. Human $^{87}Sr/^{86}Sr$ values show that UU and KC are similar (between 0.709 and 0.710) and different from PYS humans (above 0.710). The cross-site comparison of enamel values demonstrates that, in general, caprines from UU possess lower $\delta^{13}C$ and $\delta^{18}O$ values compared to caprines from locations within the interior of eastern Africa (e.g. Dongodien, Gogo Falls, and Wadh Lang'o).

At UU, caprine isotope values suggest a diet dominated by ^{15}N-enriched C_4 resources (Figure 6.2-6.3). Two possible scenarios might explain these values. One is that caprines were consuming marine plants. The other is that they were eating manured farmland vegetation that, in some cases, grew in soils with marine nitrogen inputs. Direct feeding on marine plants would lead to a strong positive correlation in $\delta^{13}C_{coll}$ and $\delta^{15}N$ as demonstrated by sheep raised on islands and fed seaweed (Schulting et al., 2017; Blanz et al., 2020). Schulting et al (2017) demonstrated that juvenile sheep fed seaweed exhibited a correlated rise in $\delta^{13}C_{coll}$ values ranging from −18‰ to −12‰ and in $\delta^{15}N$ values ranging from 8‰ to 14‰ ($r^2 = 0.609$). In contrast, older sheep fed terrestrial C_3 vegetation exhibited randomly distributed values, with $\delta^{13}C_{coll}$ values ranging from −22‰ to −19‰ and $\delta^{15}N$ values ranging from 4‰ to 10‰. The UU caprines do not demonstrate the correlation in $\delta^{13}C_{coll}$ and $\delta^{15}N$ values observed for caprines that consume seaweed, and there are furthermore no known examples of caprines feeding on seaweed in Zanzibar. In a unique case, a caprine from the Takarkori site in Libya with $\delta^{13}C_{coll}$ and $\delta^{15}N$ values similar to those of the UU caprines is interpreted to have been consuming freshwater fish, and the presence of fish in the caprine's dung has been used to support this interpretation (di Lernia and Tafuri, 2013). The mixture of C_4 crop remains, including sorghum and pearl millet, recovered from the UU site, as well as the conspicuous marine waste middens (containing fish and marine shells) scattered across the 20-hectare site, likely represent a more realistic, indirect source of elevated $\delta^{13}C_{coll}$ and $\delta^{15}N$ in the UU

caprines (Juma, 2004; Crowther et al., 2016a; Fitton and Wynne-Jones, 2017; Horton, 2017; Prendergast et al., 2017b; Faulkner et al., 2018; Out, 2018; Wynne-Jones et al., 2021; Kotarba-Morley et al., 2022). The UU caprines may have been routinely herded onto farmland with spots rich in C_4 crops and grassy glades, which were supplemented by high concentrations of C_4 crop remains, grasses, livestock manure, and marine waste, such as fish and shells, in abandoned homes, kraals, and fish processing dumpsites. Alternatively, the caprines may have been penned and foddered on C_4 crops and grasses from these spots (Figure 6.2-6.3).

The UU and KC wild fauna isotopic value patterns suggest that inhabitants of the UU site used resources from the surrounding densely forested and open grassland areas (Figure 6.2-6.3). The scarcity of similarly low caprine values suggests that wildland caprine herding was uncommon in the surrounding forested areas, either because caprines did not venture there or because they were not permitted to do so. The UU human isotope values indicate an agropastoral diet dominated by C_4 resources in an open ecological setting, while the KC and PYS human isotope values, in contrast, indicate a forager diet dominated by C_3 resources in a forest mosaic ecological setting (Figure 6.3), in excellent agreement with archaeobotanical and zooarchaeological findings. The C_4 resources utilized by the UU human likely included the C_4 crops and caprine remains recovered from the site, while the C_3 resources utilized by the KC and PYS humans included the forest-adapted mammals recovered from the site, together with gathered plants and fruits. Overall, human values align with observations from caprines, which revealed a more diverse pastoral context in coastal settings. This context includes interplays of reliance on domestic herds within systems of diverse crop production and foraging in marine and forest environments (Figure 6.3). Together, this fits with other discussions that highlight how pastoral cultures and economies from the mainland and interior were

adapted within local contexts (Ambrose, 1998; 2003; Marshall et al., 2011; Janzen, 2015; Chritz et al., 2019; Janzen et al., 2020a; Robertshaw, 2021; Janzen, 2022).

The strontium and oxygen isotope values suggest that the UU caprines originated from varying geological substrates in either mainland eastern Africa or Unguja Island (Figure 6.3B). A comprehensive baseline study of the coastal strip and Zanzibar would best determine the origin of these caprines. Nevertheless, the caprine with the lowest $^{87}Sr/^{86}Sr$ value (0.7079) and the highest $\delta^{18}O$ value (4.4 ‰) in the dataset indicates translocation from the coastal hinterland or interior of eastern Africa. This value is similar to those of Carboniferous Karoo rocks in the Tanga/Duruma Basin in Kenya's interior (0.708) (Janzen et al., 2020b). The goat's $\delta^{18}O$ value (4.4‰) is also outside the range of Unguja fauna, and suggests that this individual was likely translocated from more open, arid areas in eastern Africa's interior hinterland coast. The $^{87}Sr/^{86}Sr$ values ranging from 0.7091 to 0.7099, meanwhile, suggest that these three caprines and three humans from UU and KC are native to Unguja Island, whereas values ranging from 0.710 to 0.713 imply that five of the UU caprines and the PYS human originated from a different geological formation of the same age (Figure 6.3B). These values also suggest that the vicinity of UU and PYS consists of older geological deposits, such as the Neoproterozoic Mozambique Belt (0.710 to 0.712), or that the UU caprines were translocated and the PYS humans migrated from the coastal strip-hinterland region of Tanzania, where the Neoproterozoic Mozambique Belt's geological strata are dominant. All caprines and humans with $^{87}Sr/^{86}Sr$ values greater than 0.709 have $\delta^{18}O$ values below 1‰, indicating that they originated from a forested ecological setting in the coastal strip and Unguja Island regions (Figure 6.3B). The four PYS human isotope values from different teeth indicate that this individual lived most of his or her life on the same geological substrate under forest mosaic ecological conditions (Figure 6.6B). These patterns in the overall caprine and human isotope values

reflect complex mosaic interaction patterns involving the coalescence of pastoralists, agropastoralists and native foragers in eastern Africa during the Iron Age (Lane, 2004; Kusimba and Kusimba, 2005; Russell et al., 2014; Lane, 2017; Crowther et al., 2018).

The differences in the isotope values for caprines on offshore islands and coastal mainland sites versus those of interior eastern African sites reflect clear environmental and socioeconomic differences between these regions (Figure 6.4-6.7 and 8.2). The offshore islands and coastal mainland sites are dominated by dense forest mosaic habitats, whereas the interior of eastern Africa consists of woody grassland mosaics (White, 1983; Kingdon, 1984b; 2001). Goat-dominated herds are common in woodland-forest habitats on the coast (e.g., UU and other archipelago sites) (Prendergast et al., 2017b; Culley et al., 2021b). While the data are not strong, it is possible that sheep-dominated herds, as seen at EYM, and mixed herds, as seen at Dongodien (identified by isotopes only) and at Luxmanda (identified by ZooMS and isotopes), were common in woody grassland habitats in eastern Africa (Ambrose and DeNiro, 1989; Chritz et al., 2019; Prendergast et al., 2019a). Sheep- and mixed-dominated herds, including goats, cattle, and camels, are prevalent among modern eastern African pastoralists (Fratkin, 2001; Bollig and Wotzka, 2013; FAO, 2018; Galaty, 2021; Stites et al., 2023; Ibeagha-Awemu et al., 2026). Examples include the Maasai, Samburu, Pokot, Turkana, Borana, and Somali peoples, who thrive in the region's semi-arid grasslands and Rift Valley settings. The coast has abundant marine resources, while the interior has seasonal C_3 and C_4 terrestrial resources that fluctuate over time due to climate change. There are also differences in the $\delta^{18}O$ values for these two regions due to differences in precipitation levels between the coast and the interior. The abundance of livestock remains and communal settlement patterns in archaeological sites in regions dominated by wild animals today suggests that Neolithic pastoralists in eastern Africa preferred wildland caprine herding (Bower et al., 1977;

Onyango-Abuje, 1977b; a; Ambrose, 1982; Gifford-Gonzalez and Kimengich, 1984; Marshall et al., 1984; Marshall, 1990; Bower, 1991; Ambrose, 1998; 2003; Lane, 2013a; Marshall et al., 2018), while the agropastoralists living at the coastal and island settings during the Iron Age supplemented wildland feeding with manured C_4 crops, and/or grass feeding and/or foddering (Juma, 2004; Crowther et al., 2016a; Fitton and Wynne-Jones, 2017; Prendergast et al., 2017b; Crowther et al., 2018; Faulkner et al., 2018; Wynne-Jones and LaViolette, 2018; Wynne-Jones et al., 2021; Kotarba-Morley et al., 2022).

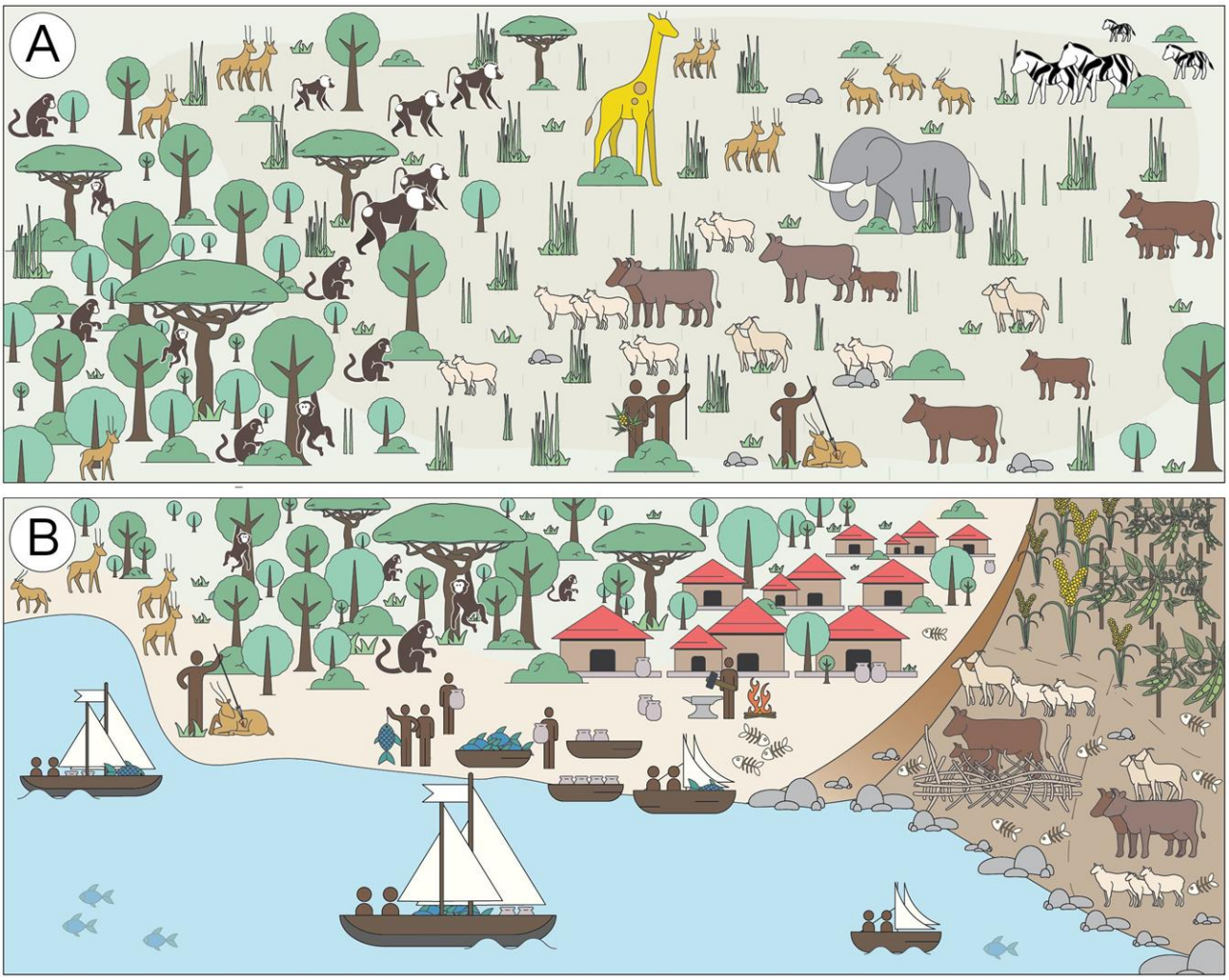


Figure 8.2. *Graphic representation of regional caprine husbandry strategies in eastern Africa, showing differences in herding practices. (A) Interior: Pastoralist wildland herding, where caprines are herded in proximity to wild animals and feed similarly. (B) Coast and Islands: Agropastoralist farmland herding, where caprines are herded in manured farmlands, including penning and paddocking, far from wild animals. They feed predominantly on cultivated crops, such as sorghum and millet. Note that the interior is dominated by large, grassland-adapted, wild animals, while the islands are dominated by small, forest-adapted animals. Agropastoralist communities on the islands are also involved in foraging, fishing, ironworking, and Indian Ocean trade. The figure was created for this study by Hans Sell (Graphic Designer for the Max Planck Institute of Geoanthropology, Jena, Germany).*

Unguja Ukuu and immigration from the interior of eastern Africa

Examining the isotope records and the entire archaeological assemblage from the UU site indicates that migration played a key role in establishing the UU settlements (Prendergast et al., 2016; Crowther et al., 2018). Unlike the KC isotopes and archaeological assemblage, which suggest continuity among indigenous foragers from the late Pleistocene to the Iron Age, the UU isotopes and assemblage indicate the sudden emergence of a new community. As discussed above, this UU community had complex subsistence strategies, including a caprine-focused agropastoral lifestyle among others (Prendergast et al., 2016; Crowther et al., 2018; Iminjili et al., 2025a; Iminjili et al., 2025b). The lack of forager deposits below the Iron Age deposits at UU and the sudden appearance of a densely populated twenty-acre settlement engaged in complex economic activities evident on the mainland suggests that migration from the eastern African coast was the predominant force in establishing these settlements rather than indigenous foragers inventing and adapting to this lifestyle (Iminjili et al., 2025a; Iminjili et al., 2025b). These immigrations and establishment of a trade port altered the UU ecological setting from forested to more open settlements, farmlands, and maritime-dominated zones. The caprine collagen and enamel values suggest herding on N-enriched C_4 resources that could have originated from manured farmlands and marine refuse composite zones. This herding strategy is different from the feeding patterns of wild animals in a forest mosaic ecological setting, as demonstrated by UU and KC wild animals. It is also different from the wildland livestock herding strategy practiced by pastoralists in the arid woody grasslands in the interior of eastern Africa. The presence of a low proportion of wild animals in the UU assemblage suggests an agropastoral tradition, but could also be footprints of assimilated foragers.

The patterns in the zooarchaeological, archaeobotanical, ceramic, and iron assemblages at UU are more similar to those found in the coastal mainland region and other offshore island sites, which are linked to agropastoral communities of western African ancestry that immigrated from the Great Lakes region of eastern Africa (Giblin and Fuller, 2011; Erendira Malinali Quintana and Prendergast, 2017; Lane, 2017; Crowther et al., 2018; Goldstein et al., 2024; Bostoen and Coutros, 2025; Goldstein et al., 2025; Iminjili et al., 2025a; Iminjili et al., 2025b). Assemblages from most coastal sites associated with agropastoralists are characterized by the presence of Kwale or Tana ceramics, alongside other components of the Bantu package, such as livestock remains (cattle, goats, and sheep), African domesticated crops, and iron artefacts (Crowther et al., 2018; Iminjili et al., 2025a; Iminjili et al., 2025b). Examples of such sites include Mgombani in Kenya, which has yielded four African domesticated crops and Tana ceramics, as well as Chombo, Kwale (700–900 CE), Mteza, Mtsengo, Shanga, Manda and Kizingitini, which have reported the presence of Kwale and/or Tana ceramics. Tanzanian sites such as Amboni Cave (400-500 CE), Mkukutu Kibiti (400-500 CE), Kivinja (500 CE), Kwale Island, Kilwa Kisiwani, Kimimba, Misasa, Mlongo, Tumbe and Pemba Village have also reported the presence of Kwale and/or Tana ceramics, alongside other artefacts. These coastal ceramics originated from the interior and are related to Kwale, Maore, Kilimanjaro, Lelesu and Urewe ceramics found in the Usambara, Kilimanjaro and Great Lakes regions of eastern Africa. Most of these date to before 200 CE, with Urewe extending back to 600 BCE (Iminjili et al., 2025a; Iminjili et al., 2025b).

Although limited, the aDNA record from the coastal region and the interior of eastern Africa suggests that the UU cultural phenomenon is associated with the migration of agropastoralists of western African ancestry (Skoglund et al., 2017; Prendergast et al., 2019b; Wang et al., 2020; Lipson et al., 2022). Individual II from the Makangale site, who is genetically similar to individuals

from the Great Lakes region and western Africa, as discussed above, and who was found in close association with Tana ceramics and black rat remains, which are also present in the UU assemblage, suggests that the UU settlement may be related to agropastoralist migrations from the interior of eastern Africa with genetic roots in western Africa (Prendergast et al., 2017a; Iminjili et al., 2025a; Iminjili et al., 2025b).

The KC and UU isotopic records and archaeological assemblages provide valuable insights into the moving frontier and subsistence mosaics hypotheses (Lane, 2004; Crowther et al., 2018). The KC archaeological record could represent the Pioneer Phase of the moving frontier hypothesis (Chapter Two), which marks the beginning of interaction between foragers and food producers. Conversely, this KC assemblage could represent a static frontier caused by the avoidance and self-preservation mechanisms of foragers and food producers, which limit intercultural and biological interactions. The UU site, on the other hand, represents the substitution and consolidation phases, which are characterized by the intensification of agropastoralism (Lane, 2004). This intensification is indicated by the subdivision of land into pasture and farmlands, the construction of permanent homes, the use of manure, and the existence of possibly stall grazing. Admixture and absorption likely led to the absorption of some foragers, while others withdrew to the margins. The mosaic interaction and subsistence mosaic hypotheses also predict these complexities in subsistence patterns at cosmopolitan sites like UU (Kusimba and Kusimba, 2005; Crowther et al., 2018). In the future, aDNA studies should confirm these patterns at UU. It would be interesting to determine whether the UU population had genetics similar to those of the Makangale (1350 CE) or if the population included individuals with mixed genetic backgrounds, similar to those of the Kakapel (1150 and 1800 CE), Elmeteitan (900 CE), and Kindoki (1800 CE) populations. It would also be

interesting to determine if the population included foragers with genetic similarities to those of the PYS, KC, and other interior eastern African foragers (archaeological and modern).

In conclusion, the isotopic data from the site and the archaeological assemblages have provided insights that highlight the persistence of indigenous foragers at KC and the emergence and establishment of immigrant agropastoralists at UU with complex subsistence strategies traceable to the coastal strip and interior of eastern Africa. The archaeological assemblages suggest that the Iron Age agropastoral interaction with UU, KC, and PYS was the first between these foragers and food producers, despite the fact that pastoralism had existed in the interior of eastern Africa since 3000 BCE. Overall, no evidence at Unguja Ukuu suggests the indigenous foragers independently invented these agropastoral cultural traits, as has been argued for the Kilimanjaro Chagga continuity (Chami and Silayo, 2023).

8.3 – *Wanyika* dataset and migrations in eastern Africa

The spatial-temporal patterns highlighted in the maps generated from the archaeo-informatics-oriented dataset of scientific dates and associated archaeological finds from sites in eastern Africa, as presented in chapter seven, support the hypothesis that:

3. *Taking an archaeoinformatics approach to the archaeological record of eastern Africa from 5000 BCE to 1800 CE provides broad and in-depth diachronic insights into human–environment interactions. These insights include connections between the ecology and the complex subsistence strategies employed by coastal and inland communities. This perspective should also reveal significant research gaps and biases that hinder rigorous hypothesis testing.*

Maps generated from the *Wanyika* dataset provide valuable insights that advance the testing of hypotheses and the development of theories at regional and global scales. I highlight these insights in three dimensions: (I) exposing spatial-temporal patterns in human-environment interactions, (II) identifying research gaps in archaeology, and (III) shaping future research agendas.

Exposing climate-driven ecological patterns, complex subsistence strategies and migrations

The diachronic configurations in the maps generated from the *Wanyika* dataset suggest aridity-driven migrations, with north-eastern African pastoralists originating from arid riverine ecological settings and western African agropastoralists originating from areas of dense forests and savanna woodlands (Iminjili et al., 2025a; Iminjili et al., 2025b). The maps indicate that pastoralists from northern Africa entered eastern Africa through northern Kenya, following well-watered savannah grasslands across the region while avoiding densely forested areas. Due to the arid ecological settings and prevalence of climate-related shocks, the pastoralists who entered eastern Africa evolved complex, adaptive subsistence strategies that included utilizing wild resources to a large extent in extremely arid ecological settings, particularly after catastrophic livestock loss (Ambrose, 1998; Gifford-Gonzalez, 2003; Ndiema, 2011; Ndiema et al., 2011). In certain circumstances, the data suggest that pastoralists shift to foraging after losing livestock and then shift back to pastoralism after replenishing their stock (Lane, 2013a). In optimal ecological settings, pastoralist sites record the utilization of livestock at over 90% and wild animals at under 10%. The archaeological record indicates that the central Rift Valley and the Serengeti region were optimal ecological settings where this high proportion of livestock utilization was common, as evidenced by the Hyrax Hill, Narosura, Maasai Gorge, Crescent Island, Serengeti, and Ngorongoro sites (Iminjili et al., 2025a; Iminjili et al., 2025b). These patterns are explained schematically in the

'trickle-and-splash' hypothesis. However, no follow-up studies have been conducted that use adequate scientific data to test this hypothesis by Bower (1991).

The maps also suggest that the agropastoralists of western African ancestry followed riparian, forested, and savannah woodland ecosystems from their point of origin to the Great Lakes region (Russell et al., 2014; Grollemund et al., 2015; Grollemund et al., 2023). The late-split riverine and late-split peeling-off hypotheses postulate that, during these migrations across the Congo forest region, the communities that migrated through the forest retained agropastoralism and a sedentary lifestyle, while the communities that migrated through the savannah woodlands switched to a foraging lifestyle that included gathering plants, hunting, and fishing (Russell et al., 2014; Grollemund et al., 2023). Once these communities reached the Great Lakes region, they consolidated most elements of the Bantu package, as evidenced by archaeological records from the Kakapel site in Kenya and multiple sites in Rwanda. These agropastoralists of western African ancestry then continued to track down forested areas through the Kilimanjaro-Usambara highlands, along the coast and onto the offshore islands, including Madagascar (Iminjili et al., 2025a; Iminjili et al., 2025b). Throughout this migration to the coast, the consumption of wild resources remained an important part of the agropastoralists' subsistence strategy, even as their crops and livestock husbandry became more complex.

Despite the limitations of the dataset, as discussed in Chapter 7, Section 7.1, "Sampling Strategy," the generated maps offer a broad overview of the spatial and temporal distribution of dates and archaeological assemblages (Figure 2.11 and 8.3). There is a systematic association between the spatial-temporal distribution of dates and the archaeobotanical, zooarchaeological, metallurgical, and ceramic remains associated with foragers, pastoralists, farmers, and Indian Ocean commerce

(Figure 2.11 and 8.3). Additionally, aDNA records reflect these assemblage patterns (Skoglund et al., 2017; Prendergast et al., 2019b; Wang et al., 2020; Lipson et al., 2022). When the contested dates are excluded (Figure 8.3a), yellow; (Mehlman, 1989; Prendergast et al., 2014; and Tryon et al., 2018; and Figure 8.3b), green; (Wright et al., 1984; and Chami, 1994), the dataset highlights the dispersal of pastoralism in the interior of eastern Africa from 3000 to 701 BCE (Figure 8.3a), followed by the dispersal of farming and agropastoralism, as well as metallurgy, from 600 BCE to 600 CE (Figure 8.3b). Finally, the dataset shows the dispersal of agropastoralism, involving both African and exotic crops, as well as metallurgy, to the coast, islands, and Madagascar from 601 to 1800 CE (Figure 8.3c). The earliest dates associated with the faunal (cattle and caprines) and ceramic remains of Pastoral Neolithic herders are found in northern Kenya (3000 BCE), followed by the central Rift Valley, the Serengeti, Lukenya, Tsavo, the Eyasi Basin, and the hinterland coast (2000 BCE) (Figure 8.3a and b).

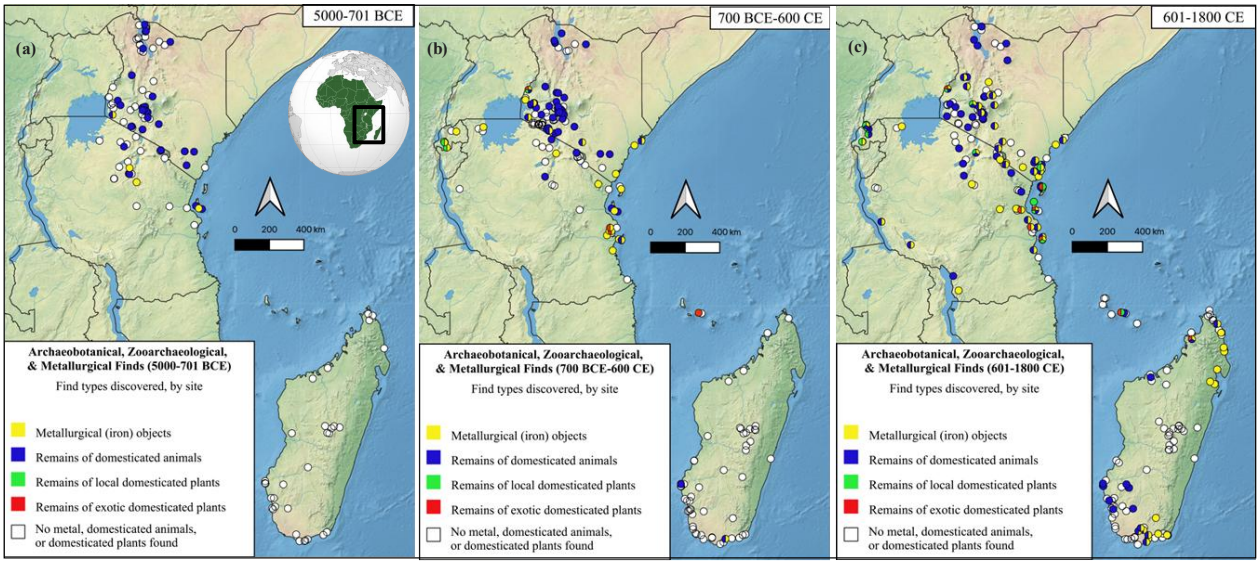


Figure 8.3. *Maps showing 3-time windows highlighting change in land use patterns in eastern Africa between 5000 BCE to 1800 CE: (a) the north-south dispersal of domesticated animals from the Lake Turkana region beginning 3000 BCE, (b) the west-east dispersal of African domesticated crops and iron technology from the Lake Victoria region, (c) convergence of domesticated animals and local crops, and exotic crops along the eastern Africa hinterland coast, islands and Madagascar (Iminjili et al., 2025a; Iminjili et al., 2025b). The figure was created for this study by Michael Fisher (Digital archaeologist, Max Planck Institute of Geoanthropology, Jena, Germany).*

The spatial-temporal distribution of dates, fauna, ceramics, and iron remains in the Pastoral Iron Age sites is complex and has not been well studied (Figure 2.11 and 8.3c). However, a pattern emerges indicating that some pastoralist communities migrated from the central Rift Valley floor to the western highlands, where they transitioned to agropastoralism. The conspicuous earthworks associated with these communities are only found in the central Rift Valley and in areas heading towards the western highlands and Mount Elgon. The manner in which these groups immigrated to the central Rift Valley remains unknown, as does the construction, plan, and use of these earthworks across the region, particularly the Lanet earthworks. Scattered concentrations of Pastoral Iron Age sites are also found in Laikipia, Mara-Serengeti, Lukenya, and the coastal hinterland. Further studies should reveal more complex spatial-temporal migration configurations and the origins of these communities.

Although there are few sites in the interior of eastern Africa (sites in Rwanda and Kakapel and Deloraine in Kenya), the dates and domesticated African crops (sorghum, pearl millet, finger millet, cow pea, and lablab bean) form a pattern indicating that farmers migrated from the Great Lakes region to the interior of eastern Africa, the hinterland and coastal strip, and later the offshore islands, including the Comoros and Madagascar (Figure 2.11 and 8.3b and c). These sites are also associated with cattle and goat remains, as well as iron and farming-related ceramics. The sites with domesticated crops in Rwanda and Kakapel have the earliest dates, followed by those in Deloraine and along the coast (Figure 2.11 and 8.3b and c). In addition to domesticated African crops, sites along the coastal strip reveal exotic crops, ceramics, and other material cultural artifacts, indicating transoceanic trade movements from the Arabian and Asian worlds (Figure 2.11 and 8.3b and c).

The spatial-temporal patterns of the distribution of 24 ceramic traditions in eastern Africa's interior, along the coast, and on offshore islands, including the Comoros and Madagascar, suggest that migration was the dominant force behind these dispersals (Figure 2.11 and 8.4-8.4). These ceramic traditions are also distributed in correlation with domesticated livestock and crops associated with migrations of pastoralists and farmers (Figure 2.11 and 8.3-8.4). The Nderit and Ileret traditions are the earliest dated traditions and are widely distributed from the northeastern region of Lake Turkana into the interior of eastern Africa (Figure 8.4A). The Elmenteitan tradition is primarily found on the western side of the Great Rift Valley, near the Lake Victoria region (Figure 8.4A). Other Pastoral Neolithic ceramics, such as the Maringishu, Narosura, and Akira traditions, as well as other Pastoral Iron Age ceramics, such as the Lanet, Kisima, and Oldorotua traditions, are mainly distributed from the Laikipia region in central Kenya to central Tanzania (Figures 8.4A and B). It is long overdue to revisit these ceramics based on a refined 'trickle and splash' hypothesis (Bower, 1991).

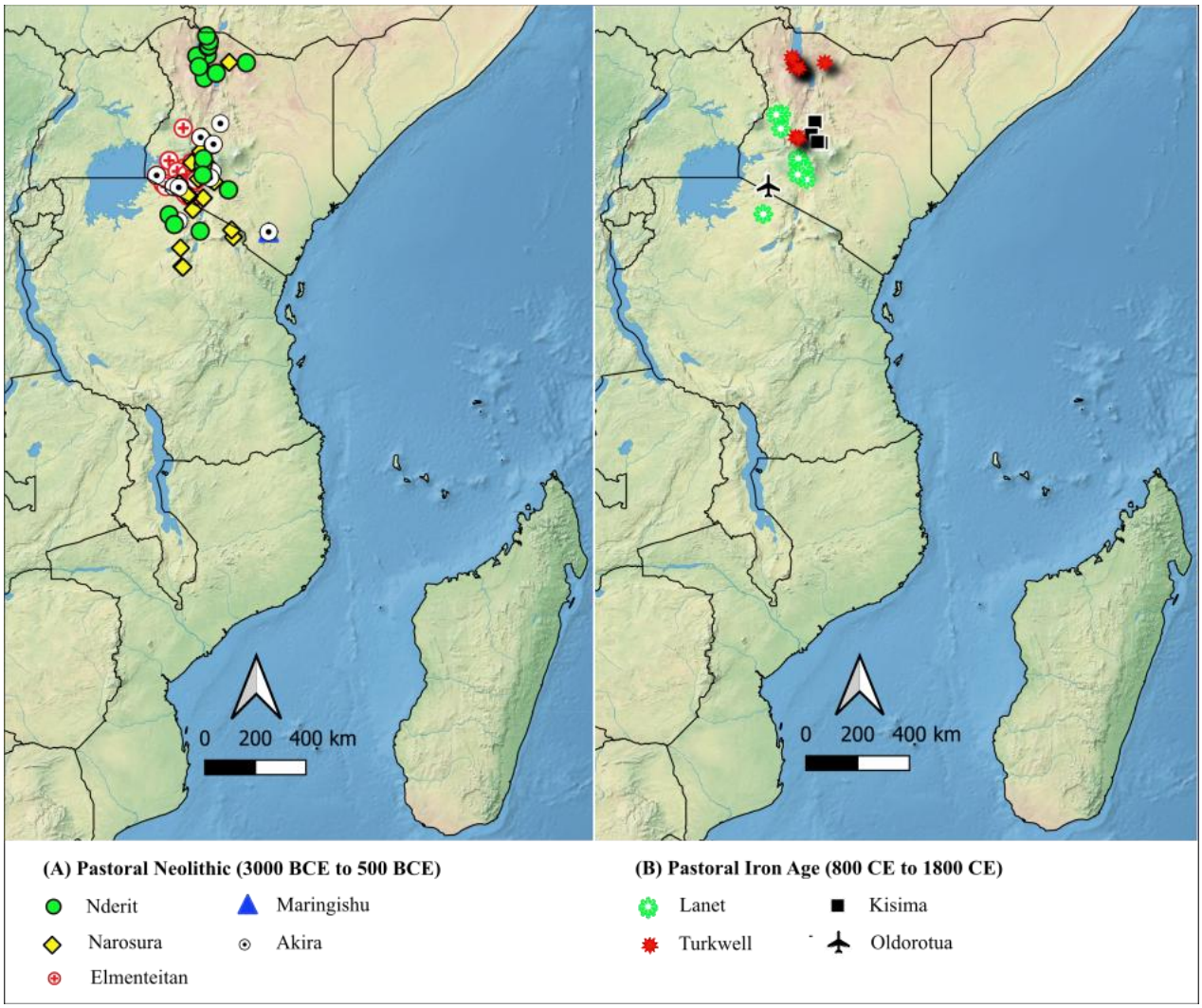


Figure 8.4. *Maps showing two time windows that highlight general patterns in the spatial and temporal distribution of ceramics related to pastoralists originating from the Lake Turkana region and circulating in the interior of eastern Africa: (A) the Pastoral Neolithic (3000–500 BCE) and (B) the Pastoral Iron Age (800 CE–1800 CE) (Iminjili et al., 2025a; Iminjili et al., 2025b).*

Ceramic traditions associated with farmers are also correlated with the distribution of domesticated crops and iron. The earliest farmer-associated ceramic traditions are found around the Great Lakes region (Urewe, Figure 8.5A-C), followed by the interior of eastern Africa (Lelesu, Kwale, Maore, and Kilimanjaro), then the coastal strip (Kwale and Tana), and finally the offshore islands, including the Comoros and Madagascar (Tana, Rezoky, Beropitika, Andaro, and Tranovato) (Figure 8.5C). The dates and co-distribution of ceramic traditions associated with Indian Ocean

commerce and agropastoralists along the eastern African coast also indicate migration patterns (Figure 8.5C). Lastly, the distribution of hunter-gatherer ceramics (Kansyore, Eburran, and Lowasera), which are associated with wild animals at some sites and with the ceramics of pastoralists and/or farmers, as well as wild and domesticated animals at others, indicates the existence of complex interaction patterns between indigenous foragers and immigrating food producers (Figure 2.11 and 8.4-8.5). The distribution of these ceramics provides a basis for considering hypotheses applied in central Africa, such as the spread-over-spread and peeling-off hypotheses. In general, it provides a basis for considering the late-split riverine and late-split savannah hypotheses in eastern Africa's archaeological record.

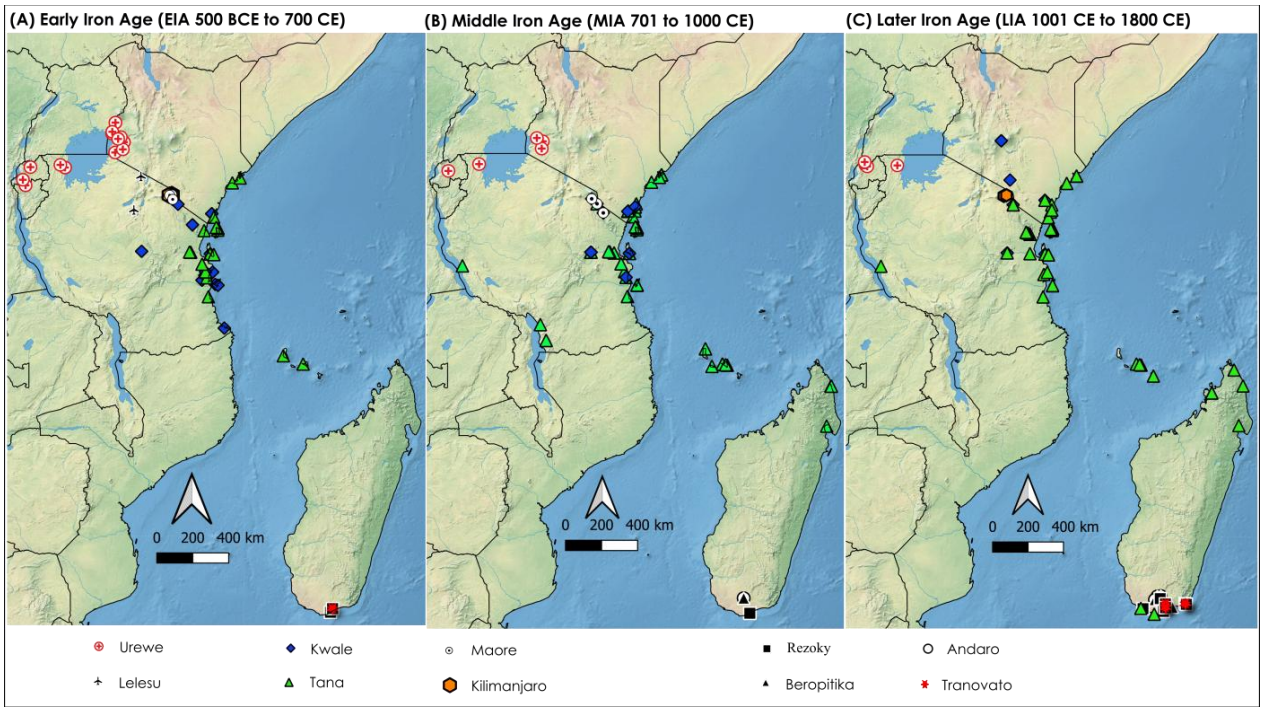


Figure 8.5. *Maps showing three time windows that highlight general patterns in the spatial and temporal distribution of farmer-related ceramics originating from the Lake Victoria region and circulating in eastern Africa's interior. (A) Urewe ceramic ware, found around Lake Victoria, has the earliest dates (earlier than 100 BCE). This is followed by Kwale, found in the coastal region, with the earliest dates around 1-200 CE. Next is Tana ware, with the earliest dates around 300-500 CE. (B) Kwale and Tana ware dominate the coast and become prevalent in the islands during the Middle Iron Age (700-1000 CE). (C) Tana ware spreads to Madagascar, where Rezoky, Andaro, Beropitika, and Tranovato become prevalent in southern Madagascar. (Iminjili et al., 2025a; Iminjili et al., 2025b).*

Patterns generated from aDNA also suggest that genes associated with pastoral communities circulated from Sudan, Ethiopia, and Somalia into eastern Africa's interior around 3000 BCE (Skoglund et al., 2017; Prendergast et al., 2019b; Wang et al., 2020; Lipson et al., 2022; Sirak et al., 2022). These aDNA records indicate that Neolithic pastoralists from Kenyan sites, such as Hyrax Hill (300 BCE), Lukenya (1600 BCE), and Molo Cave (600 CE), as well as Tanzanian sites, such as Luxmanda (1000 BCE), are in one cluster with modern Cushitic speakers inhabiting Ethiopia and Somalia. Iron Age pastoralists from Kenya cluster with modern Maasai speakers but are also close to Neolithic pastoralists. These findings suggest that the Neolithic and Iron Age pastoralists in Kenya and Tanzania originated in northeastern Africa. Similarly, as discussed in the

section above on UU, genes associated with farmers indicate an origin in western Africa via the Great Lakes region, circulating into the interior of eastern Africa, the coastal strip, and, later, offshore islands (Skoglund et al., 2017; Prendergast et al., 2019b; Wang et al., 2020; Lipson et al., 2022; Sirak et al., 2022). The carbon, oxygen, and nitrogen isotope data at UU suggest an anthropogenic effect on caprine diets, likely resulting from feeding on African domesticated crops by agropastoralists of western African ancestry. The UU human values also suggest an agropastoral lifestyle. The UU strontium values indicate a later generation of agropastoralists who migrated from the mainland. While genetic evidence is still needed to confirm this, similarities in ceramics and iron artefacts between UU and sites along the eastern African coastline and islands suggest this is indeed the case. Genetic evidence also suggests that foragers were dominant before 3000 BCE. This was followed by admixture, displacement, and the later dominance of pastoralists and farmers between 3000 BCE and 1800 CE (Skoglund et al., 2017; Raaum et al., 2018; Prendergast et al., 2019b; Wang et al., 2020; Lipson et al., 2022; Sirak et al., 2022). As discussed earlier, despite the predominance of immigrating food-producing communities, indigenous foragers persisted in certain regions, such as the coast, in sites such as KC and PYS. The carbon, oxygen, and strontium isotope data from the faunal and human assemblages at KC and PYS indicate this continuity, and again, the aDNA data from the KC and PYS individuals suggest the persistence of foragers even after interacting with food producers from the interior of eastern Africa. Evidence of genetic admixture between these African groups and Arabian and Asian groups has been found along the eastern coast of Africa (Raaum et al., 2018).

Megafauna extinction and migrations

The chronology and distribution of archaeological assemblages in Madagascar suggest that migration played a key role in the dispersal of humans, as well as of domesticated crops, animals, and other goods from Africa and Asia (Figure 8.6 and Table 8.1). Records show that from 5000 BCE to 600 CE, Madagascar was likely sparsely inhabited by foragers and dominated by more than 15 species of megafauna, including giant primates (lemuroids), elephant birds (ratites), giant tortoises, and pygmy hippopotamuses (Figure 8.6a and b and Table 8.1). The first recorded instances of domesticated crops, animals, and human remains date to the period between 601 and 1800 CE. This period is associated with the migration of agropastoralists to Madagascar (Figure 8.6c). Madagascar was also involved in Indian Ocean commerce during this time. The archaeological record documents an acceleration in the exploitation of ratite eggs and meat from megafauna by humans during this time. Ratite eggshells and burnt megafauna bones with cut marks from iron tools are common at sites dating to this period. The introduced animals in Madagascar include cattle, goats, sheep, dogs, cats, wild pigs, and black rats. This evidence suggests that human migration to Madagascar played a significant role in the megafauna's extinction. In general, the intensification of land use by agropastoralists of western African descent across the central and eastern African region could have played a significant role in the forest crisis of the period, bearing in mind the increasing evidence of charcoal produced by burning wood (Bayon et al., 2012b; Bayon et al., 2012a; Englong et al., 2023). However, aridity could have been the dominant force.

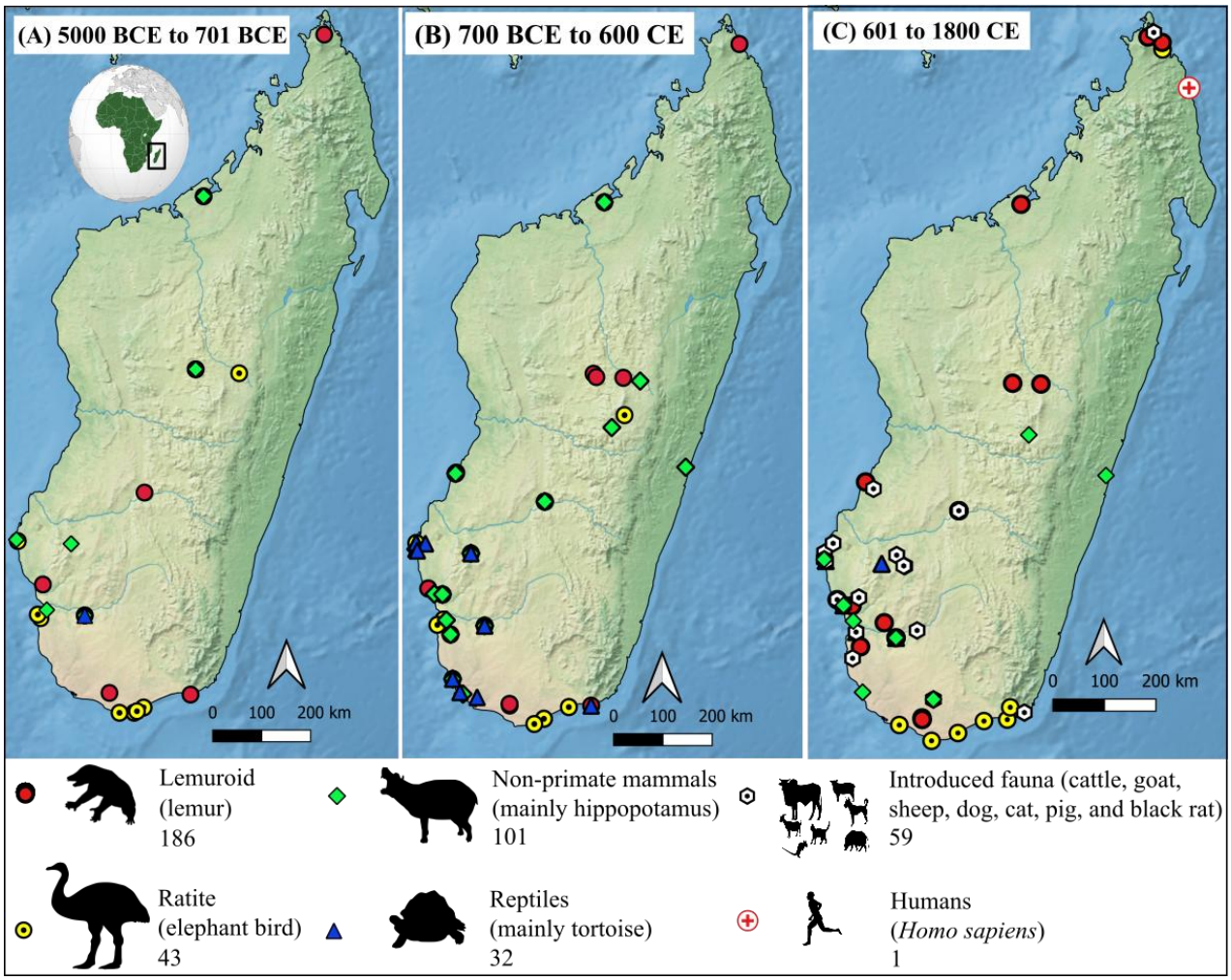


Figure 8.6. *Maps showing 3 time windows highlighting dates from extinct megafauna taxa tracking their late persistence and appearance of introduced species and humans in Madagascar (a-c). Map (c) shows that humans, introduced species, and extinct megafauna coexisted between 601 and 1800 CE (Iminjili et al., 2025a; Iminjili et al., 2025b).*

Table 8.1. *List of extinct faunal species including megafauna, introduced species and humans with direct dates from Madagascar tracking their coexistence. Note the disparity in direct human dates.*

Faunal Categories	**5000 – 701 BCE**	**700 BCE – 600 CE**	**601 – 1800 CE**
Lemuroids (lemurs)	*Archaeolemur edwardsi, Archaeolemur majori, Babakotia radofilai, Megaladapis edwardsi, Megaladapis grandidieri, Megaladapis madagascariensis, Megaladapis sp., Pachylemur jullyi, Pachylemur insignis, Palaeopropithecus ingens, Palaeopropithecus maximus* **27 dates**	*A. edwardsi, A. majori, Archaeolemur sp., M. edwardsi, M. madagascariensis, Megaladapis sp., P. jullyi, P. insignis, P. ingens, Paleopropithecus sp., Archaeoindris fontoynontii, Hadropithecus stenognathus, Mesopropithecus globiceps* **92 dates**	*Archaeolemur majori, Archaeolemur sp., M. edwardsi, M. grandidieri, M. madagascariensis, P. jullyi, P. insignis, P. ingens, Palaeopropithecus sp., H. stenognathus, Mesopropithecus pithecoides, Daubentonia robusta* **67 dates**
Ratites (elephant birds)	*Aepyornis maximus, Mullerornis modestus, Aepyornis sp.* **12 dates**	*A. maximus, M. modestus, Aepyornis sp., Mullerornis sp.* **20 dates**	*A. maximus, Aepyornis sp., Mullerornis sp.* **11 dates**
Reptiles (tortoise)	*Aldabrachelys sp.* **1 date**	*Aldabrachelys sp., Geochelone grandidieri, Geochelone abrupta, Geochelone sp.* **21 dates**	*Aldabrachelys sp., G. grandidieri , G. abrupta* **10 dates**
Non-primate mammals (mainly hippopotamus)	*Hippopotamus lemerlei, Hippopotamus sp., Cryptoprocta spelea* **29 dates**	*H. lemerlei, Hippopotamus laloumena, Hippopotamus sp., C. spelea Plesiorycteropus sp.* **42 dates**	*H. lemerlei, H. laloumena* **30 dates**
Introduced fauna (cattle, goat, sheep, dog, cat, pig, and black rat)			*Bos taurus indicus, Capra hircus, Ovis aries, Canis familiaris, Felis domesticus, Potamochoerus larvatus, Rattus rattus* **59 dates**
Hominin			*Homo sapiens* **1 date**

Exposing research gaps in archaeology

Wanyika (Iminjili et al., 2025a) is an inventory that summarizes the progress of archaeological research in eastern Africa. It systematically highlights available archaeological data and persistent data gaps. It can reveal geographical, temporal, and other biases in existing research and assess the robustness of available chronological information. *Wanyika* can be used to evaluate the precision

of dating methods based on standard deviation, as well as to identify uneven distributions of sites and chronological sequences (Figures 2.11 and 7.2 and Tables 7.1, 7.3, and 7.6). I summarize these highlights in four points.

i) Geographical disparities

The dataset shows that Kenya and Madagascar account for 75% of all recorded scientific dates in the study area, of which radiocarbon dates account for more than 90% (see Figures 2.11 and 7.2). However, there are no scientific dates from large areas of eastern Kenya and western Tanzania extending to the southeast. The four quality control measures indicate that over half of the dates in the study are of questionable quality. The stratigraphic integrity and reliability quality control measure shows that fewer than 15% of the dates are Class A (Figure 7.3). Nearly 50% of the ^{14}C dates are from plant material, of which only 7% are Class A (Figure 7.4). Forty percent of the radiocarbon dates are from faunal material with reservoir issues; of these, 30% are non-Class A (Figure 7.5). Almost 30% of the ^{14}C dates have issues related to pretreatment because they were produced before 1972, when pretreatment of ^{14}C samples was introduced (Figure 7.6). Figures 8.7a-b show that, apart from Cluster 2, the other groups generated by the mclust algorithm have major gaps in the spatiotemporal distribution of dates within the 5000 BCE to 1800 CE time period. Table 7.3 highlights more details on these disparities at the country and regional levels.

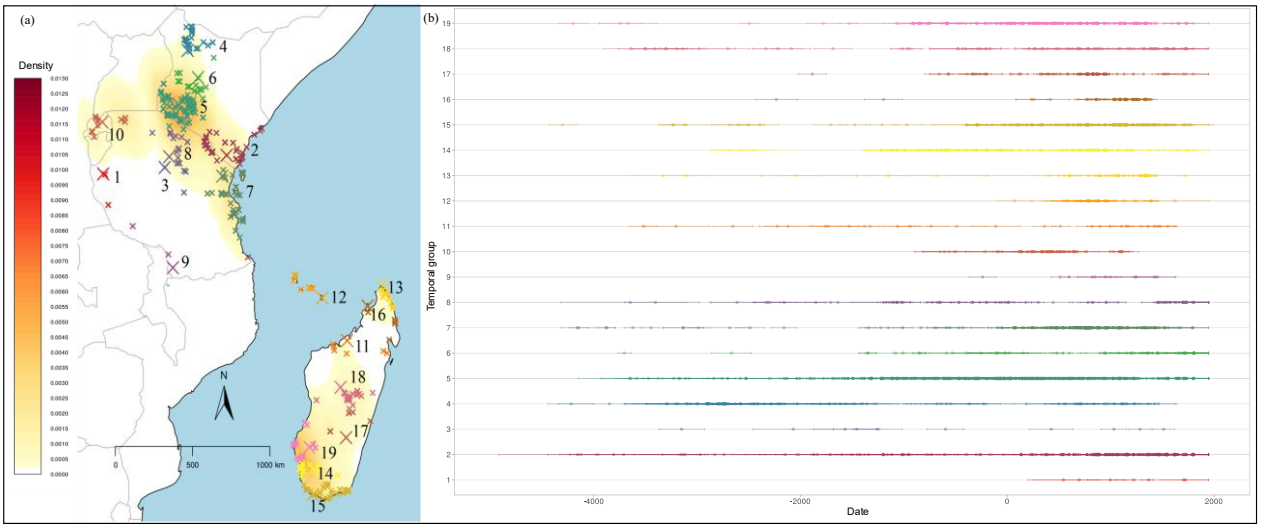


Figure 8.7. *a) Distribution of* Wanyika *archaeological sites located in Kenya, Tanzania, Comoros, and Madagascar, organized into k-means groups (Hartigan–Wong algorithm)(Hartigan and Wong, 1979). The groups are numbered 1-19. The larger symbols represent group centroids. b) Distribution of group dates (vertical tick marks with median value as a dot) within the 5000 BCE to 1800 CE time period* (Iminjili et al., 2025a; Iminjili et al., 2025b). *The figure was created for this study by Ricardo Fernandes (Archaeo-informatics expert, Max Planck Institute of Geoanthropology, Jena, Germany).*

Geographical disparities in the distribution of scientific dates, coupled with the fact that over 50% of data from covered regions is of poor quality, inadequately reflect complex spatiotemporal patterns of human-environment interactions. This is especially true for climate-induced ecological changes, the emergence of food production, the dispersal of food-producing communities, the exploitation of wild resources, and complex adaptive strategies, such as livestock herding and crop production, in subsistence strategies. This is particularly relevant when testing hypotheses about indigenous continuity and migration in eastern Africa. Currently, the dataset can only reflect broad patterns, offering limited insight and being full of paradoxes.

ii) Archaeobotany

The archaeobotanical record indicates that apart from Rwanda, the interior of eastern Africa has few records, comprising only two sites in Kenya and one in Tanzania (Figures 8.8 and Table 8.2).

Most archaeobotanical records come from the coastal hinterland, islands, and Madagascar. A synthesis of dates from four African crops (sorghum, pearl millet, finger millet, and cowpea) and three exotic crops (Asian rice, coconuts, and mung beans) reveals that there are only 51 direct dates from 19 sites (Figures 8.8 and Table 8.2). Rwanda has no direct dates from domesticated crops. Kenya, Tanzania, the Comoros Islands, and Madagascar have fewer than 25 direct dates from fewer than ten sites each. Kenya is the only country with direct finger millet dates. Madagascar has direct dates only for rice. Most crops have between one and five direct dates per site (Figures 8.8 and Table 8.2).

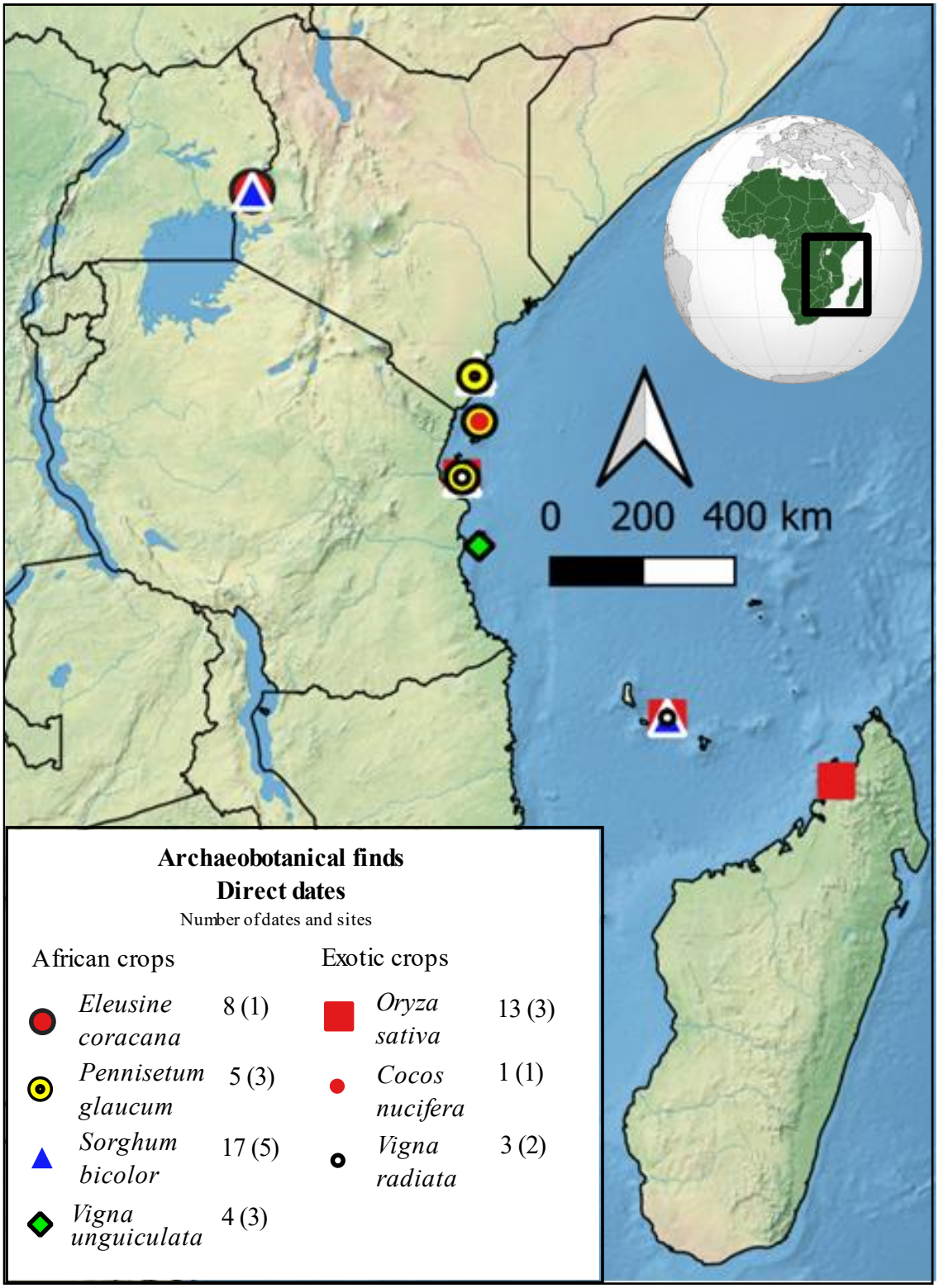


Figure 8.8. *Map of eastern Africa highlighting the disparities in the distribution of direct dates from domesticated crops: four African and three exotic breeds. n = total number of dates and number of sites in brackets (Iminjili et al., 2025a; Iminjili et al., 2025b).*

Table 8.2. *Highlighting the disparities in the distribution of the number of direct archaeobotanical dates from four African and three exotic crops, n = Total number of dates and number of sites in brackets.*

	Archaeobotanical finds							
		African crops				Exotic Crops		
Country	n	Finger millet *Eleusine coracana*	Pearl millet *Pennisetum glaucum*	Sorghum *Sorghum bicolor*	Cowpea *Vigna unguiculata*	Rice *Oryza sativa*	Coconut *Cocos nucifera*	Mung bean *Vigna radiata*
Rwanda	0	0	0	0	0	0	0	0
Kenya	16 (6)	8 (1)	2 (1)	5 (3)	1 (1)	0	0	0
Tanzania	23 (8)	0	3 (2)	11 (1)	3 (2)	3 (1)	1 (1)	2 (1)
Comoros	7 (4)	0	0	1 (1)	0	5 (1)	0	1 (1)
Madagascar	5 (1)	0	0	0	0	5 (1)	0	0
TOTAL	**51 (19)**	**8 (1)**	**5 (3)**	**17 (5)**	**4 (3)**	**13 (3)**	**1 (1)**	**3 (2)**

This dataset of archaeobotanical remains and associated dates is inadequate for providing in-depth insights into spatiotemporal trends in the emergence and intensification of crop production, particularly within the context of indigenous continuity and migration hypotheses. This is especially true of interior eastern Africa, where pastoralists from the northeast and agropastoralists from western Africa converged with indigenous foragers and formed complex patterns before dispersing to other regions of Africa. The dataset is insufficient to argue conclusively for or against Nilotic-, Cushitic-, or Bantu-speaking communities, or even indigenous foragers, as the pioneers who dispersed these crops in eastern Africa. The dataset is also inadequate for understanding the dispersal patterns of these crops across eastern Africa's interior to its coast and islands. For instance, it does not indicate which crops entered eastern Africa via the Congo Basin migration route and which entered through the Nile route. It also does not provide insight into whether these crops dispersed as a package from the interior to the coast, nor does it address whether these patterns changed across the region, as has been argued regarding central African migrations. Are the eastern African patterns, for example, similar to those projected by the late-split savanna-peeling-off hypothesis? In this hypothesis, migrating Bantu people became foragers while crossing the Congo Forest. They then returned to agropastoralism after entering the Great Lakes region, where they

relearned crop farming and adopted the five major African crops, including pearl millet and cowpea, from Nilotic and Cushitic pastoralists. This dataset from the interior is also inadequate for comparative analysis with coastal and island data to gain meaningful insights into patterns of emergence, complex adaptive strategies, and dispersal in these different ecological settings, particularly when contextualized within the indigenous continuity and migration hypothesis.

iii) Zooarchaeology

A synthesis of zooarchaeological dates from three types of livestock, three types of commensals, and human remains shows that only 134 direct dates exist from 63 sites in eastern Africa (see Figure 8.9 and Table 8.3). Goats and cats have the fewest dates. Kenya has few dates from livestock and black rats, but many dates from human remains. Tanzania has no direct dates from any livestock, dogs, or cats but has a high number of dates from black rats and humans. The Comoros Islands have no direct dates from zooarchaeological remains. Madagascar has the highest number of direct dates from livestock, commensals, and megafauna, but only one date from human remains.

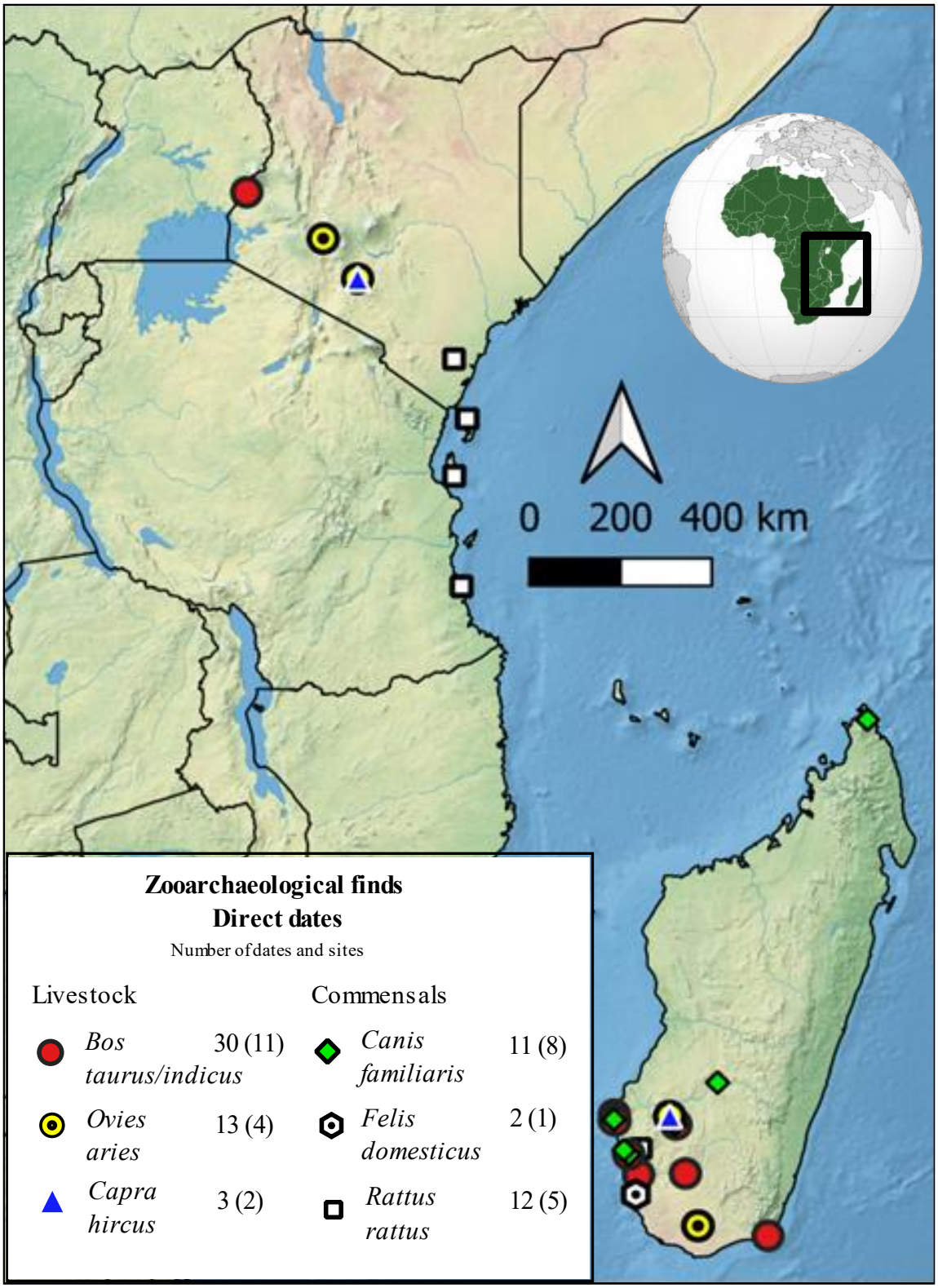


Figure 8.9. *Map of eastern Africa highlighting the disparities in the distribution of the number of direct zooarchaeological dates from three livestock and three commensals. n = total number of dates and number of sites in brackets (Iminjili et al., 2025a; Iminjili et al., 2025b).*

Table 8.3. *Highlighting the disparities in the distribution of the number of direct zooarchaeological dates from three livestock, three commensals, humans and megafauna per country, n = total number of dates and number of sites in brackets.*

	Zooarchaeological								
		Livestock			Commensals				
Country	n	Cattle *Bos taurus/ indicus*	Sheep *Ovis aries*	Goat *Capra hircus*	Dog *Canis familiaris*	Cat *Felis domesticus*	Black rat *Rattus rattus*	Humans *Homo sapiens*	Mega fauna
Kenya	52 (31)	2 (1)	2 (2)	2 (1)	0	0	1 (1)	45 (26)	0
Tanzania	27 (8)	0	0	0	0	0	10 (3)	17 (5)	0
Comoros	0	0	0	0	0	0	0	0	0
Madagascar	55 (24)	28 (10)	11 (2)	1 (1)	11 (8)	2 (1)	1 (1)	1 (1)	360 (46)
TOTAL	**134 (63)**	**30 (11)**	**13 (4)**	**3 (2)**	**11 (8)**	**2 (1)**	**12 (5)**	**63 (32)**	**360 (6)**

This zooarchaeological dataset is insufficient for providing definitive insights into the emergence and dispersal of pastoralism and the interactions between indigenous foragers and agropastoralists originating from western Africa (Figure 8.9 and Table 8.3). This is especially true when testing the indigenous continuity and migration hypotheses. The dataset is insufficient for determining patterns of livestock dispersal in relation to climate-driven ecological trends. For instance, did cattle, goats, and sheep disperse together from the interior to the coast and islands? Did patterns differ between the interior and the coast? How did these animals thrive in diverse eastern African ecological settings? Are there noticeable trends or shifts in the proportion of these livestock in line with vegetation patterns? Did caprines spread faster than cattle? Of the goats and sheep, which species spread faster across the interior of eastern Africa? Were the patterns in the interior similar to those on the coast and islands, despite their different ecological settings? Did cattle, goats, and sheep emerge on the coast and disperse together or separately? The human dataset and direct dates, particularly those from Madagascar, are inadequate for making claims about human-environment interactions. In general, the human dataset and direct dates from the represented regions in eastern Africa are insufficient to determine whether indigenous continuity or migration was the dominant force in dispersing food production and food-producing communities across the region.

iv) Metallurgy

Iron remains have been recovered from numerous sites in eastern Africa. However, only seven questionable direct dates from two sites are available (Figure 8.10) (Kusimba, 1993). Further dating and biogeochemical studies are needed to reveal iron's mobility and trade patterns on a regional scale. Due to technical complications, dating iron artifacts has proven to be significantly more complex than dating organic materials (Kusimba, 1993). The most accurate method is to use chronologically tightly associated radiocarbon dates from the iron and related organic remains in the context. Similar to the inadequacies in the archaeobotanical and zooarchaeological assemblages, the diachronic distribution of iron finds and dates is inadequate for providing in-depth insights into the emergence and dispersal of iron within the context of indigenous continuity and migration hypotheses.

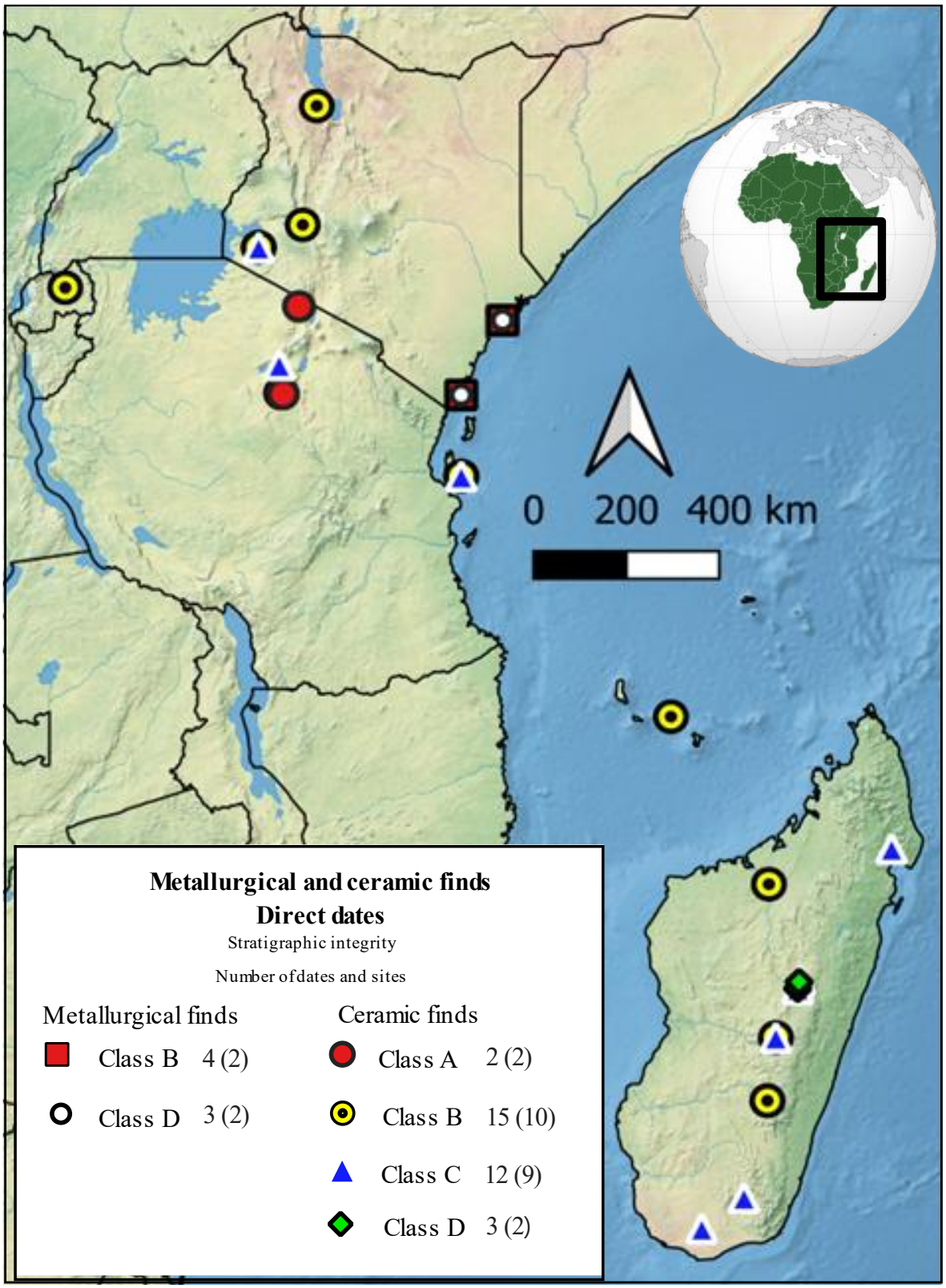


Figure 8.10. *Map of eastern Africa highlighting the disparities in the distribution of direct iron and ceramic dates according to the stratigraphic integrity and reliability of date quality control classes. n = total number of dates and number of sites in brackets (Iminjili et al., 2025a; Iminjili et al., 2025b).*

v) Ceramics

Many dated sites have ceramic remains associated with specific subsistence strategies or trade networks, such as pastoralism, hunting and gathering, farming, and Indian Ocean commerce. However, only 32 direct ceramic dates from 23 sites are available (Figure 8.10 and Table 8.4). Most ceramic traditions have been relatively dated using questionable archaeobotanical or zooarchaeological dates (Table 8.4). A review of dates for the appearance and persistence of the ceramic traditions after applying quality control shows that 16 of the 24 traditions in the table have a small sample size (column $n^1 \leq 3$) in Class A dates and only 18 have direct ceramic dates (column n^2). The lack of sample size in Class A dates and direct ceramic dates negatively impacts the ability to constrain the appearance and persistence of ceramic traditions (Table 8.4).

Table 8.4. *Chronology of 24 major ceramic traditions from interior eastern Africa, the coast, and islands limited to the period spanning 5000 BCE to 1800 CE, based on class A dates and all class dates in Figure 7.3. Some ceramic traditions do not have class A, B, and D dates.* ***n[1]*** *= total number of dates and* ***n[2]*** *= number of direct ceramic dates (from identified ceramic tradition).*

Ceramic Tradition	**Class**	**n[1]**	**n[2]**	**Chronology BP**	**Published Chronology** (range estimates based on multiple sources)
Kansyore	A	3	1	4190 – 1710	8200– 1500
	ABCD	33	1	4860 – 1710	
Lowasera	DC	4	0	4410 – 1530	Unreported
Eburran	B	8	0	3990 – 2560	5000 – 1200
	BCD	27	0	5960 – 895	
Nderit and Ileret	A	17	0	4385 – 2354	5000 – 1200
	ABCD	44	1	5420 – 1501	
Maringishu	BC	4	0	2987 – 1295	>1700
Narosura	A	13	1	4190 – 2145	2800 – 1400
	ABCD	81	2	4430 – 195	
Akira	A	2	0	2855 – 2675	1900 – 1200
	ABCD	44	0	2987 – 280	
Elmenteitan	A	7	0	2420 – 1500	3300 – 1200
	ABCD	100	0	4560 – 595	
Turkwell	B	3	0	1500 – 870	1800 – 950
	BCD	14	0	5420 – 748	
Lanet	A	8	0	386 – 164	1200 – 250
	ABC	26	0	4924 – 164	
Oldorotua	A	2	0	875 – 790	900 – 600
	ACD	7	0	1390 – 790	
Kisima	B	5	0	607 – 170	>800 – 200
Urewe	A	7	0	2280 – 951	2500 – 900
	ABCD	49	2	2560 – 940	
Lelesu	A	1	0	4190	1800 – 1600
	ABC	6	0	4190 – 1780	
Kwale	A	3	0	1646 – 1604	1800 – 950
	ABCD	62	0	5330 – 380	
Maore	B	7	0	1060 – 238	1700 – 950
	BCD	17	0	5330 – 238	
Kilimanjaro	CD	4	0	2260 – 525	800 – 500 CE
Tana	A	21	0	1276 – 522	1700 – 500
	ABCD	168	6	5332 – 490	
Asian	A	15	0	1276 – 470	1300 – 600
	ABCD	153	4	1960 – 238	
Swahili	A	3	0	582 – 470	750 – 500
	ABCD	33	1	1040 – 350	
Rezoky	A	3	0	560 – 355	900 – 400
	ABCD	17	0	1960 – 355	
Beropitika	A	1	0	1190	1000 – 600
	ABC	19	1	1320 – 220	
Andaro	A	1	0	1190	1100 – 800
	ABC	18	1	1320 – 220	
Tranovato	A	2	0	401 – 355	500 – 300
	ACD	6	0	1960 – 355	

Similar to the situation with iron, the ceramic records and direct dates in the *Wanyika* dataset are insufficient for providing definitive insights into the emergence of various ceramic traditions associated with food production and the dispersal of food-producing communities. This is particularly relevant when testing the indigenous continuity and migration hypotheses, especially the trickle-and-splash, spread-over-spread, and peeling-off hypotheses. The existing dataset lacks sufficient information on the initial appearance, development, dispersal, and final appearance of the nearly fifty different ceramic traditions scattered across eastern Africa. Although ceramic finds are indispensable for dating, few ceramic dates exist, and they pose specific scientific challenges. These challenges include contamination of food residues on the ceramics, destruction of organic samples during firing, and lack of correlation with dates from similar contexts, due to the old wood effect. These issues compromise the reliability of direct dates from ceramics. However, combining microCT scanning to identify short-lived plants, including African crops, embedded in ceramics could make ceramics one of the most reliable dating materials in eastern African archaeology. Using chronologically associated radiocarbon dates from ceramics and context-related assemblages could also be a workable option.

Shaping future research agendas

Projects focused on archaeological science, including new explorations and excavations, should be prioritized. These projects should include sampling for direct dating of as many archaeobotanical and zooarchaeological remains as possible from unexplored areas of the interior and offshore islands of Kenya and Tanzania, the Comoros, and Madagascar, as well as the entirety of eastern Africa. To make this *Wanyika* dataset more useful and accurate for computer and other high-tech analyses, we archaeologists must work hard over the next ten years to ensure that the number of

Class A radiocarbon dates, direct dates, and dated sites grows exponentially. Direct dates from archaeobotanical, zooarchaeological, and material culture remains, as well as other elements of the associated archaeological assemblage, are critical to resolving chronological and cultural discrepancies in the eastern African archaeological record (Sassoon, 1980; Horton, 1987; Wandibba, 1990; Robertshaw, 1991; Chami and Chami, 2001; Munene, 2002; Kusimba and Kusimba, 2005; Chami, 2009; Pearson et al., 2010; Nkirote, 2012; Mbogori, 2017; Douglass et al., 2019; Hixon et al., 2021a; Goldstein et al., 2024). More than 350 direct dates from Madagascar were used to highlight the persistence of megafauna (5000 BCE–1800 CE) and their coexistence with humans (600–1800 CE). This information has significantly informed the longstanding debate in the field of human-environment interaction studies (Burney et al., 2004; Pearson et al., 2010; Crowley et al., 2011; Crowley et al., 2017; Hansford et al., 2018; Douglass et al., 2019; Godfrey et al., 2019; Mitchell, 2020; Hixon et al., 2021a; Hixon et al., 2021b).

Goldstein et al. (2024) provided an example of chronological inconsistencies at the Kakapel Rock Shelter, which justifies the need for more direct dating methods in eastern Africa. The study reported different dates for charred finger millet seeds and indeterminate nuts found in the same context. The finger millet seeds yielded more recent dates (900–1,000 BP), while the indeterminate nuts yielded older dates (>5,000 BP), predating the onset of agriculture. There are other examples throughout the broader study region where artifacts from different periods appear to have been found in the same deposits due to bioturbation or other taphonomic factors. One example is the mixing of Iron Age artifacts (such as iron and Lelesu and Tana ceramics) with those from earlier cultures (such as Kansyore and Narosura ceramics). This has been seen in sites like Misasa (LaViolette et al., 1989; Chami, 1994), Kisese (Tryon et al., 2018), Mumba Rock Shelter (Mehlman, 1989; Prendergast et al., 2014), Mikindani (Pawlowicz, 2011; Pawlowicz, 2012; 2013;

Pawlowicz et al., 2014) in Tanzania, and Gogo Falls (Robertshaw, 1991; Munene, 2002; Lane, 2004; Kusimba and Kusimba, 2005), Wadh Lang'o (Lane et al., 2007a; Prendergast, 2009, 2010c), and Takwa (Wilson, 2019) (Kenya).

These discrepancies can be addressed through direct dating combined with archaeological and scientific approaches, such as microCT scanning and ZooMS. MicroCT scanning can identify charred, short-lived plant remains, e.g., seeds embedded in ceramics, which can be used for direct dating. This could be the best method to address bioturbation-affected ceramics used and the chronology of the different ceramic wares associated with foragers and agropastoralists (Table 8.4). ZooMS can distinguish between domesticated and wild animals, as well as detect discrepancies related to bioturbation between the pre-domestication and domestication periods at sites suspected of being affected by bioturbation. Excavations that include the recovery of archaeobotanical, zooarchaeological, and artifactual remains for direct dating and other scientific archaeological studies should be emphasized at sites across the eastern African region. These studies should extend from northern eastern Africa to the Great Lakes region, the coastal strip, and the offshore islands, including the Comoros and Madagascar.

The absence of direct human dates in Madagascar represents a significant scientific gap requiring urgent attention (Figure 8.11 and Table 8.1). The 62 direct human dates and associated genetic records (aDNA) from legacy sites in Kenya and Tanzania have been critical to reconstructing complex interactions among fishers, foragers, pastoralists, and farmers in eastern Africa and its littoral islands (Skoglund et al., 2017; Prendergast et al., 2019b; Wang et al., 2020; Bleasdale et al., 2021; Lipson et al., 2022; Sirak et al., 2022). A large number of direct human dates from all regions of Madagascar, together with associated aDNA studies, would help improve our ability to

address major questions about human-environment interactions. These questions include the timing of migrations and interactions of populations from Africa (hunter-gatherers, pastoralists, and farmers), Asia, and Arabia, as well as their ecological impacts, including megafaunal extinctions and climatic change. Expanding archaeological science research, including archaeobotanical studies, in all four regions of Madagascar will help answer these questions. The Comoros Islands should also be the focus of archaeological research, as they likely played a significant role in the dispersal of populations from Africa to Madagascar.

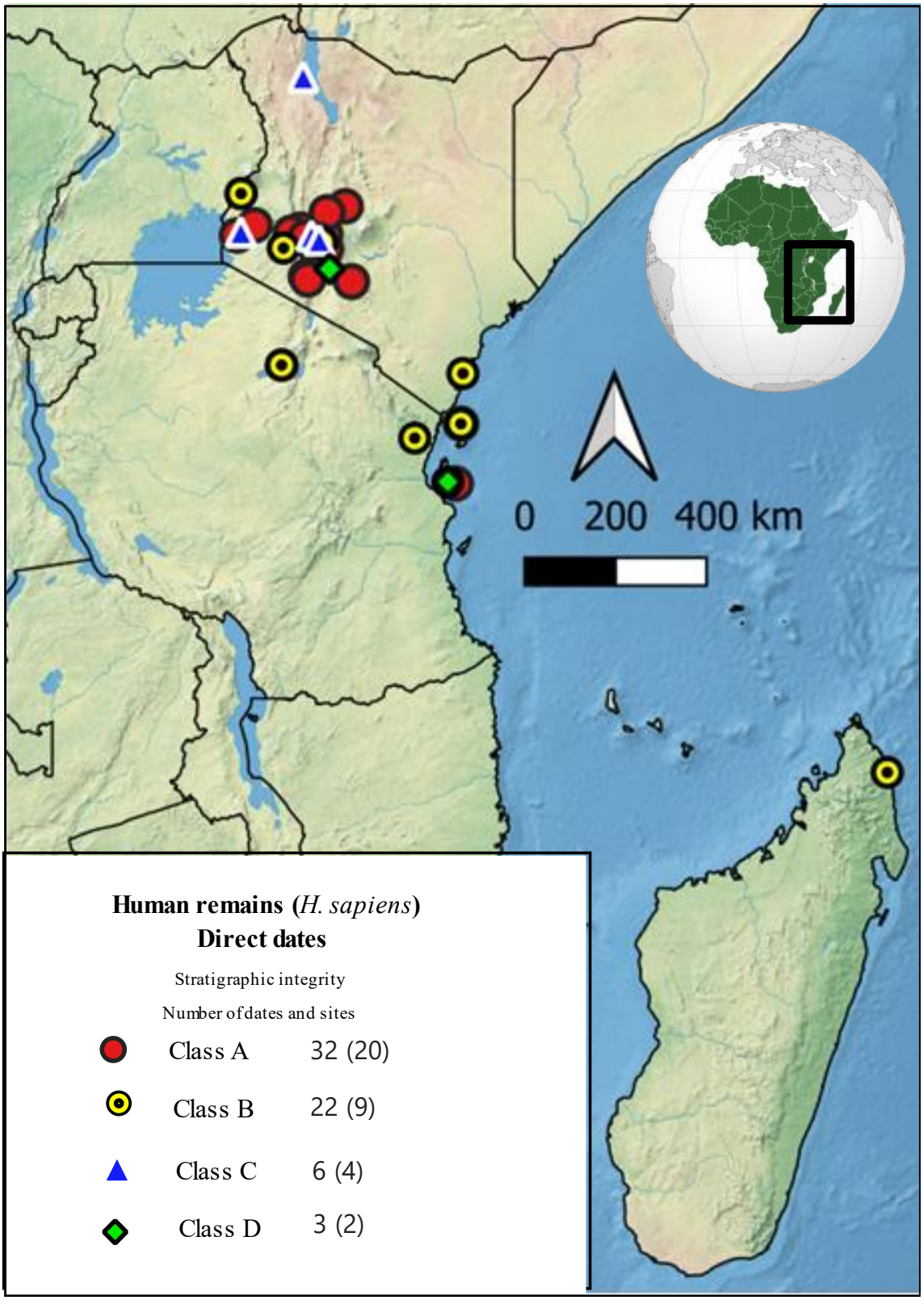


Figure 8.11. *Map of eastern Africa highlighting the disparities in the distribution of direct human dates. n = total number of dates and number of sites in brackets (Iminjili et al., 2025a; Iminjili et al., 2025b).*

The *Wanyika* dataset (Iminjili et al., 2025a) can be used for computational modeling with data-driven and hypothesis-testing approaches to study human-environment interactions and their impact on biodiversity. For example, it can be used to test the Subsistence Shift Hypothesis, the spread of food production in eastern Africa, and megafaunal extinctions in Madagascar (Godfrey et al., 2019; see Figure 8.5). Unlike global perspectives, which often rely on low-resolution modeling (Lemmen, 2009a; Lemmen, 2009b; Kaplan and Krumhardt, 2011; Kaplan et al., 2011; Klein Goldewijk et al., 2017; Prestele et al., 2017; Stephens et al., 2019), regional datasets like *Wanyika* offer finer-grained information that can be used to reconstruct clearer, more detailed patterns. This is illustrated by Kay et al.'s (2019) work exploring nonlinear trends in Western African land use over time and Russell et al's (Russell et al., 2014) work testing the migration hypotheses of Bantu farmers. Electronic Figure 1 in the *Wanyika* repository (https://pandoradata.earth/dataset/wanyika) illustrates modeling potential by showing a spatiotemporal kernel density estimate of site presence (Wand and Jones, 1994). This estimate was produced via the R-based IsoMemo app at https://github.com/Pandora-IsoMemo/iso-app. The figure reveals variability in site density over time and space within the *Wanyika* records.

8.4 – The 'Bantu package' dilemma

The origin and dispersal of the 'Bantu package' remains one of the most enigmatic questions in late Holocene archaeology in eastern Africa (Ambrose, 1982; Ehret, 1998; Sutton, 1998c; Ehret, 2001; Ambrose, 2003; Crowther et al., 2018). Here, the term 'Bantu package' refers to an assemblage comprising five domesticated African crops (sorghum, pearl millet, finger millet, cowpea and lablab bean), livestock (cattle, goats and sheep), Urewe-type ceramics and iron

artefacts. It is unclear whether the pioneers and participants in the long-term dispersal of livestock, African domesticated crops, and iron into the interior to the coast and islands of eastern Africa were predominantly pastoralists from the Sudan-Upper Nile region, the Ethiopia-Somali region, or agropastoralists from western Africa, or indigenous foragers. While it is now agreed that the Bantu did not originate in western Africa with this complete package, it is thought that it was assembled along the way and spread in multiple constellations. Evidence of the basic set of pearl millet, cowpeas, and iron has been found in the Congo forest (Kahlheber et al., 2009; Bostoen et al., 2015; Bostoen, 2018; Neumann et al., 2022). In the Great Lakes region, all the elements of the package have been found, although not necessarily in the same context, in sites dating from as early as 600 BCE to 200 CE (Phillipson, 1975; Van Noten, 1979; Schmidt and Childs, 1985; Raymaekers and Van Noten, 1986; Giblin and Fuller, 2011; Goldstein et al., 2024; Goldstein et al., 2025). The question of how, when, and by whom this package was assembled in the Great Lakes region remains a paradox that has divided scholars (Möhlig, 1977; Möhlig, 1981; Ehret and Posnansky, 1982; Ehret, 2001; 2002; Bostoen, 2018; Grollemund et al., 2023). Surprisingly, there is not enough adequate archaeological data to resolve this issue. The late-split savannah hypothesis suggests that some Bantu populations migrated through the Congo savannah woodlands, adopting a foraging lifestyle before relearning agropastoralism from Neolithic pastoralists in the Great Lakes region (Grollemund et al., 2023). It is said that these Bantu populations also acquired Urewe and iron technology from these pastoralists. In contrast, the Bantu populations migrating via the northern Congo forest route could have acquired this package along the Sahelian corridor and at the Nile River confluence before entering the Great Lakes region (Möhlig, 1977; Möhlig, 1981). After acquiring this package, the Bantu-speaking populations dispersed it in various forms, especially concerning crops and livestock breeds, based on ecological conditions, to the coastal strip and offshore islands, as far as Madagascar.

The inadequate archaeological record of all the elements of the Bantu package and their chronological appearance in the Great Lakes region, alongside the associated human populations, has highlighted the complexity of the process (Iminjili et al., 2025a; Iminjili et al., 2025b). In particular, the archaeobotanical evidence for the dispersal of sorghum, finger millet and lablab beans into eastern Africa via the Great Lakes region is contradictory. (Van Noten, 1979; Clist, 1987b; Van Grunderbeek and Roche, 2008b; Giblin and Fuller, 2011; Goldstein et al., 2024; Goldstein et al., 2025). Even though five types of African crops were being circulated in the Sahelian region and all the way to the Indian subcontinent by 1000 BCE, there is no evidence of these crops being used by Neolithic and Iron Age pastoralists in the Great Lakes region and eastern Africa in general. Sites in the Great Lakes region have produced evidence of Urewe ceramics and iron dating back to 600 BCE (Schmidt and Childs, 1985; Clist, 1987b; Van Grunderbeek, 1992). However, the earliest evidence for African crops dates to 300 BCE at Kakapel. Kakapel provides the best evidence for the earliest assemblage of the western African agropastoralist package found at a single site, albeit in a somewhat paradoxical pattern (Goldstein et al., 2024; Goldstein et al., 2025; Iminjili et al., 2025b). The site produced two of the five domesticated African crops, dating to 300 BCE: finger millet, which was domesticated in Ethiopia, and cowpea, which was domesticated in western Africa. It also produced Urewe ceramics and iron. Sorghum, which was domesticated in Ethiopia, has been found at Kakapel at later dates (1100–1300 CE) (Goldstein et al., 2024; Goldstein et al., 2025). Currently, there is no irrefutable evidence indicating the involvement of pastoralists from northeastern Africa in dispersing the Bantu package to the Great Lakes region (Bostoen, 2018). The human aDNA archives from KK exhibit a paradoxical pattern, suggesting admixture. Records from individuals KK 1150 CE and KK 1800 CE suggest genetic ancestry from both western African agropastoralists and northeastern African pastoralists (Wang

et al., 2020; Lipson et al., 2022). The Deloraine individual (900 CE), who is associated with finger millet, also has mixed ancestry from northeastern and western African communities.

By 400 CE, most of the African crops had been recorded at sites in Rwanda, with the exception of lablab beans, which first appear at Nguri in 1100 CE (Clist, 1987b; Van Grunderbeek and Roche, 2008a). By this time, most of these sites also had Urewe ceramics and iron. Sites along the coast had assemblages composed of Kwale and Tana ceramics by 200 CE. The Mgombani site, located on the Kenyan coast and dating to the mid-Iron Age, has one of the earliest recorded crop assemblages on the coast. It contains four African crops (sorghum, pearl millet, finger millet and possibly cowpea), as well as Kwale and Tana ceramics (Crowther et al., 2016b; Iminjili et al., 2025b). UU has the four African crops, but not lablab beans. It also has Tana ceramics and iron artefacts. The basic settlement pattern of the UU, which consists of rectangular structures made of wood and daub or coral stone with thatched roofs, is reminiscent of the agropastoral Bantu-speaker settlement patterns at coastal mainland sites in eastern Africa. These patterns can be traced back to sites in western Africa (Bostoen, 2018; Bostoen and Coutros, 2025).

Solving the 'Bantu package' dilemma is set to continue to be one of the most intensively studied topics in the study of late Holocene archaeology in eastern Africa moving forward. The archaeological record has yet to verify whether it was pastoralists from north-eastern Africa who circulated the agrarian package to the Great Lakes region before the Bantu agropastoralists adopted it and circulated it further into eastern Africa. Similarly, the reasons for the circulation of sorghum, pearl millet, finger millet, cowpeas and labab beans in the Sahelian region, the lower Nile, Egypt, Arabia and India via the Red Sea by 1000 BCE, yet their absence from the interior of eastern Africa until 600 BCE, remain to be verified. Similarly, the archaeological record should confirm whether

the Bantu package was circulated to the coast and islands by Bantu agropastoralists with a similar aDNA composition to the Makangale individual from 1400 CE or with a mosaic composition similar to the KK individuals (Wang et al., 2020; Lipson et al., 2022). The archaeological record should also verify whether some elements of the package were dropped along the way, or if they moved as a package from the Great Lakes region to the coast and islands. The reason why Urewe ceramics dominated the Great Lakes region for more than a millennium, while the design changed to Kwale, Maore and Tana ceramics towards the interior, coast and islands, also needs to be investigated.

8.5 – A synthesis of the multi-isotope and archaeo-informatic perspectives in the late-Holocene archaeology of coastal eastern Africa

The isotopic and archaeo-informatic perspectives complement each other by integrating context-site-specific and regional views to reveal specific details on the emergence of complex subsistence adaptive strategies and broader patterns in the dispersal of food-producing communities in the context of indigeneity and migration in the late Holocene archaeology of eastern Africa. The site-specific perspective offers a worm's-eye view, while the regional perspective offers a bird's-eye view. This complementarity provides a holistic view of late-Holocene archaeology of eastern Africa. I highlight this complementarity of perspectives, particularly in providing in-depth insights into spatial-temporal ecological trends and the emergence of complex subsistence strategies, including the specialized hunting of small, forest-adapted fauna; caprine herd management; and crop production. I also demonstrate this complementarity by providing in-depth insights into the

emergence and dispersal of food-producing communities to the coastal region and, more broadly, to eastern Africa.

Broadly speaking, the multifocal approach applied in this thesis reveals finer-grained insights into past ecological differences between the interior of eastern Africa and its coastal strip and offshore islands, which is significant in shaping diverse trajectories of complex subsistence adaptive strategies. The nearly identical $\delta^{13}C$ and $\delta^{18}O$ values from the KC and PYS foragers, which indicate the persistent use of forest resources even after interacting with agropastoralists, align well with the tenets of indigenous continuity and the stasis phase of the moving frontier hypothesis. The patterns of dietary similarity and difference between foragers (KC and PYS) and agropastoralists (KK and UU) are also reflected in the genetic composition of these groups. The carbon and oxygen isotope dataset, supported by zooarchaeological evidence from KC and PYS, suggests that although coastal foragers practiced a delayed return model similar to that of foragers in the Great Lakes region of eastern Africa, they did not rapidly transition to food production (see the discussion in Section 8.1). This finding contradicts the predictions of the delayed return model. Building upon and expanding these insights from the KC and PYS paleoecology and human foraging study to other sites in the interior and coastal regions of eastern Africa would represent milestone progress in understanding how different ecological settings contribute to indigenous continuity and migration in the archaeology of eastern Africa. This also includes knowledge of particular trends related to subsistence and technological complexity in island and mainland sites. It also includes knowledge of trends reflecting trade and symbolic alliance networks between island sites and the interior of eastern Africa before and after the introduction of food production to the coast (Section 8.1).

The multi-isotope study of caprines has also provided valuable insights into the emergence of complex subsistence strategies and the dispersal of food-producing communities at the UU, FK, and PYS sites (Section 8.2). The distinction of the UU caprine and human collagen $\delta^{13}C$ and $\delta^{15}N$, as well as the enamel $\delta^{13}C$ and $\delta^{18}O$ values, from the wild fauna values, echoes the tenets of the migration, moving frontier, mosaic interaction, and subsistence mosaic hypotheses on variability and complexity in subsistence patterns. The $\delta^{13}C$, $\delta^{15}N$, and $\delta^{18}O$ values suggest a distinct isotopic pool that defined the emergence and establishment of agropastoralism and complex livelihoods in the UU ecosystem. UU human enamel $\delta^{13}C$ and $\delta^{18}O$ values indicate a C_4 agropastoralist diet in open lands within a coastal forest ecosystem. Variations in $^{87}Sr/^{86}Sr$ and $\delta^{18}O$ values highlight mobility patterns among foragers, immigrants, and caprines. These results indicate that both KC and UU humans are native to the island, with some caprines possibly translocated from the mainland of eastern Africa. The PYS Iron Age individual (forager) showed consistent $^{87}Sr/^{86}Sr$, $\delta^{13}C$ and $\delta^{18}O$ values from four different teeth, backed by similar $\delta^{13}C$ and $\delta^{18}O$ values from the PYS MSA individual (also a forager) (Roberts et al., 2020). These values indicate consistency in the foragers' diet and sedentary lifestyle within the stable coastal forest ecological setting, which resonates with the tenets of the indigenous continuity hypothesis. Another significant point is the chronological shift noted between the Pastoral Neolithic caprine $\delta^{13}C$ and $\delta^{18}O$ values from Dongodien, which mimic the patterns of wild fauna with goats browsing and sheep grazing, and the Iron Age UU caprines, which include both goats and sheep as C_4 feeders. This could be built upon when testing ecological dynamics using data from other sites to examine the indigenous continuity, the late-split riverine and late-split savannah peeling-off migration hypotheses moving frontier and subsistence mosaics, and the foragers models, as discussed in Chapters 1 and 2.

Maps generated from the *Wanyika* archaeo-informatics dataset combined with genetic records reveal particularities and generalities in the diverse regional communities' shaping of complex subsistence adaptive strategies, as evidenced by the archaeological record of KC, UU, FK, PYS, and other sites in eastern Africa's interior (Section 8.3). For instance, the particularities of KC suggest that the population has been isolated from the mainland population since the islandization period (Terminal Pleistocene). Similarly, the particularities of PYS suggest isolation from KC and the interior, providing a unique case of a lack of trade networks and symbolic alliance relations between KC, PYS, and the interior of eastern Africa, as postulated by the mosaic interactions hypothesis. The generalities that bind these individuals as foragers, closely related to other foragers in eastern Africa, are also highlighted. The data also highlight the generalities that define subsistence dichotomies in the normative ecological approach and how these dichotomies become blurred in complex patterns, as postulated by the mosaic interaction hypothesis. Patterns of blurring among pastoral and forager lifestyles in the arid grasslands of northern Kenya and dichotomy patterns among these communities in well-watered grasslands close to the equator, in sites around the central Rift Valley, and in the Serengeti and Laikipia regions are also highlighted. The archaeology of agropastoralists from western Africa, how they interact with pastoralists of northern African descent, and their interaction with foragers is also highlighted. Genetic records from eastern Africa have provided in-depth insights into population shuffling and reshuffling patterns over time. In some regions, however, the data suggest limited cultural and biological interaction. When combined with isotopic and archaeoinformatics perspectives, these insights are important for tracking different hypotheses in the late Holocene archaeology of eastern Africa over time.

In general, the archaeo-informatics-oriented dataset combined with genetics provides a basic regional perspective that highlights the co-occurrence of indigenous continuity and migration in

the late Holocene archaeological record of eastern Africa, though migration is predominant. Maps generated from the dataset highlight the spatial and temporal patterns indicating that migration was the dominant force in the dispersal of different cultural groups, as well as the development of pastoralism and agropastoralism, in eastern Africa between 3000 BCE and 1800 CE. These maps and genetic records suggest that migrations were mostly systematic and unidirectional, with pastoralists originating from arid regions of Sudan, Ethiopia, and Somalia and heading towards well-watered grasslands close to the equator. Conversely, the agropastoralists originated from the forest and woodland regions of the Great Lakes and tracked forests and savannah woodlands close to and south of the equator. These agropastoralists continued to follow the forests, even to the islands and Madagascar. The maps and assemblage records also indicate interactions between agropastoralist communities and megafauna in Madagascar. For example, human-modified bones of the extinct dwarf hippopotamus (*Hippopotamus lemerlei*) and the giant bird (*Aepyornis maximus*) have been found in archaeological contexts at Lamborana, Itampolo, and Ambolisatra (MacPhee and Burney, 1991; Rakotozafy, 1996; Burney et al., 2004; Pearson et al., 2010; Hansford et al., 2018; Douglass et al., 2019; Godfrey et al., 2019), Additionally, giant bird eggshells from *A. maximus* and *Mullerornis modestus* have been found in archaeological contexts.

Similarly, maps generated from the dataset highlight major temporal and spatial research gaps that have hindered access to in-depth knowledge of complex subsistence strategies, such as specialized foraging and livestock and crop husbandry, as well as technological skills, such as ceramics and ironworking. These gaps have prevented an in-depth exploration of the emergence of food production and the dispersal of food-producing communities in eastern African archaeology. Filling these gaps could provide more details in the dataset, generated maps, and other modeling analyses, enabling them to offer valuable, in-depth insights. These insights could reveal the

particularities that shaped complex subsistence and adaptive strategies, as well as the generalities that reveal whether indigenous continuity or migration was dominant in the emergence of food production and the dispersal of food-producing communities in eastern Africa during the Iron Age.

In summary, isotopic and archaeo-informatic approaches generally have two major strengths that make them significant in contemporary archaeological studies in eastern Africa. They both reveal novel, previously inaccessible spatial and temporal insights into the archaeology of eastern Africa, and complement each other and other archaeological science approaches. Isotopic ecology provides finer-grained details on human-environment interactions in eastern Africa, shedding light on topics such as ecology, subsistence patterns, herding strategies and mobility patterns. This is achieved by analyzing zooarchaeological collections, which form part of a larger assemblage containing archaeobotanical, ceramic, iron and other finds. These finds have a defined chronological framework based on scientific dates. The archaeo-informatic approach to eastern African archaeological data reveals broad patterns generated from synthesized data from multiple sites, composed of contextual and site-specific details. Furthermore, although not yet applied in eastern Africa, machine learning and AI can process large amounts of data, enabling the automatic classification of artefacts and the identification of patterns invisible to human analysis. This archaeo-informatic perspective provides a novel way of studying late Holocene archaeological data from eastern Africa, highlighting patterns that provide in-depth insights into human-environment interactions during different time periods and climate conditions, as well as existing gaps in the research. Above all, data from other archaeological sciences, such as zooarchaeology, archaeobotany, aDNA and ZooMS, can easily complement isotope and archaeo-informatics perspectives, providing a comprehensive overview of late Holocene archaeology in eastern Africa.

On the other hand, isotopic and archaeo-informatic perspectives have two major weaknesses that limit their scientific potential. These include the intricate scientific procedures involved, from fieldwork to lab work and the final publication of data, and the involvement of complex technology with a 'black box' effect. Both approaches require scientifically rigorous archaeological excavations with well-defined stratigraphic units that have been accurately dated, as this is a prerequisite for accurate interpretation. Isotopic studies depend on excellent basic zooarchaeology, involving the identification of faunal remains to species level wherever possible. The archaeo-informatics dataset requires highly refined dates, high-resolution chronology at the site and regional scales, and accurate identification of the zooarchaeological and archaeobotanical assemblages at the species level. It also requires identification of ceramic and iron artefacts. As discussed earlier, more than half of the dated sites in eastern Africa have issues related to compromised scientific standards, including bioturbation, unreliable 20th-century laboratory procedures and a lack of taxonomic identification of the zooarchaeological and archaeobotanical assemblages. The "black box" nature of certain AI and analytical algorithms has the potential to obscure the rationale underpinning classifications, giving rise to the possibility of misinterpretation and category bias. Using complex technology defined by codes can result in a loss of understanding of what is happening to the data and of any anomalies that lead to errors which are difficult to detect. On a positive note, these are generally manageable and addressable challenges with consistent data refinement over time. Archaeological projects in eastern Africa are encouraged to embrace the complementarity of isotopic and archaeo-informatic perspectives inherent in comprehensive archaeological science studies. Additionally, the scope should be expanded to fill existing spatial and temporal gaps.

Chapter 9 – Conclusions, limitations and future work

9.1 – Conclusions

This thesis aimed to provide new, in-depth insights from multi-isotopic and archaeo-informatic perspectives on ecological trends, forager continuity, and complex subsistence strategies, including crop production, livestock herding, and wild resource use in the coastal strip, offshore islands, and the broader eastern African region during the late Holocene. Additionally, it sought to explore the emergence of food production and the dispersal of food-producing communities in this region. Previous archaeological studies relied heavily on indirect data from assemblages that underwent minimal basic zooarchaeological, archaeobotanical, ceramic, and metallurgical analyses. This data came from contexts with unreliable dates and was mainly from the arid interior of eastern Africa. This project employed a multi-isotopic study of zooarchaeological samples from coastal sites studied using archaeological science approaches. These approaches ensured stratigraphic integrity and the production of a large number of context-specific dates. They also allowed for the identification of zooarchaeological and archaeobotanical finds at the species level and the identification of material culture. The *Wanyika* dataset, which comprises scientific dates and associated archaeological assemblages from sites in eastern Africa spanning almost 7000 years, was synthesized from publications into an archaeo-informatic-oriented format and used to generate maps for diachronic analysis of the coastal sites and the broader eastern Africa.

The isotopic results suggest stability in dense, forested habitats at KC throughout periods of global aridity, as well as the islandisation of Unguja Island from the late Pleistocene to the late Holocene.

In particular, the results indicate an increase in forest cover during Phases I and II. This stability reinforced the continuity of the foraging population, even after interacting with food producers during the Iron Age. Strontium values suggest that the KC individual is indigenous, and artifactual and aDNA records indicate that there was no cultural or biological contact with other foragers or food producers from mainland eastern Africa after islandization to the early Iron Age. The isotopic results also reveal an abrupt appearance of an agropastoralist settlement at the UU site with complex subsistence strategies. These strategies involved herding goats away from wild animals onto farmland rich in livestock and marine manure, as well as domesticated C_4 crop residues and grasses. The isotopic results reveal that the UU individual is native and that a significant percentage of the caprines were translocated from the hinterland and coastal strip of mainland eastern Africa. Combined results from multi-isotope and multidisciplinary studies, an archaeo-informatics study and aDNA records revealed that indigenous continuity was prevalent at KC and PYS, whereas immigration by agropastoralists of western African ancestry was prevalent at UU.

In general, the archaeo-informatics study revealed that, although indigenous continuity and migration were prevalent in the dispersal of food production across the eastern African region, migration played a core role. The study also highlighted major research gaps in the late Holocene archaeological record of eastern Africa that impede hypothesis testing and scientific progress. This is the first time that a multidisciplinary study combining multi-isotope analysis and archaeo-informatics, with a broad perspective of archaeological sciences, has been used to discuss the emergence and dispersal of food production and food-producing communities in eastern Africa (Chapters 1–4). Taking this broad perspective could provide new insights into the particulars and generalities that shaped human–environment interactions in the late Holocene archaeological record of eastern Africa. These insights could inform or test hypotheses concerning indigenous

continuity, subsistence mosaics, pastoralist migrations and late-split riverine and savannah migrations, to name a few.

Stable carbon and oxygen isotope analyses were performed on enamel samples from wild animals and humans from various stratigraphic layers representing dry and wet periods globally from the late Pleistocene to the late Holocene at the KC site. These analyses evaluated the persistence of coastal forests from the late Pleistocene to the late Holocene and their role in the endurance of foragers interacting with food producers during the Iron Age. The results of the KC study are presented as case study one in chapter five. A multidisciplinary approach using multiple isotopes was applied to caprine, wild animal, and human collagen and enamel samples to determine if the feeding strategies of caprines at UU, FK, PYS, and KC differed from those of wild animals. This was also done to determine if some of the caprines at UU were translocated from mainland eastern Africa. The results of this multi-isotope study are presented in chapter six as case study two. Lastly, maps and tables generated from the *Wanyika* dataset, which is oriented toward archaeo-informatics, highlight basic diachronic insights into the emergence and dispersal of food production and food-producing communities. The maps and tables also reveal research gaps that have hindered testing of hypotheses regarding indigenous continuity, migration of pastoralists from northeastern Africa, and migration of agropastoralists from western Africa in eastern African archaeology. The results of this archaeo-informatics study are presented in chapter seven as case study three.

In case study one, I presented a multiproxy paleoecological study of finds from KC, a multi-stratified island site in coastal eastern Africa that has four major phases spanning from the late Pleistocene to the late Holocene (with a hiatus in between Phases II and I). Using published zooarchaeological data and new stable isotope data from the site, I demonstrated the continuity of

forest-dominated mosaic habitats near KC over the past 20,000 years, as well as the consistency of a specialized hunting strategy that targeted forest-adapted species from various ecological niches. I argued that the stable forest mosaic habitats of the eastern African coastal region and islands served as an optimal environment for foragers because they provided an abundant and consistent supply of resources year-round (Shipton et al., 2018). This remained true even during the glacial phase of orbital forcing when the interior of eastern Africa experienced aridity and was dominated by open woodlands and grasslands. This resulted in a shortage of water, food, and other resources. However, the expansion of forests following the formation of the island seems to have contributed to the extirpation of some fauna. The spread of food production may have exacerbated this turnover further. As Shipton et al. (2016) and Prendergast et al. (2016) have argued, the Iron Age inhabitants of KC were primarily foragers who experimented with food production. Their long-term multi-habitat foraging strategies dictated the adoption of new economic and social practices.

In case study two, I presented a multi-isotope study on caprine husbandry from two sites on Unguja Island and one coastal site in mainland eastern Africa, namely UU, FK, and PYS. My findings suggest that the caprines at the UU site predominantly consumed C_4 and $\delta^{15}N$-enriched resources, which might have originated from C_4 crops or grasses cultivated in manure-rich soils and areas with discarded marine resources. Though limited, caprine values from FK and PYS also suggest an anthropogenic effect on herding patterns, particularly with regard to $\delta^{15}N$-enriched resources. I also found evidence of spatial and temporal diversification in caprine husbandry strategies. These range from wildland herding by pastoralists during the Neolithic period to additional farmland herding, as well as likely penning and foddering with C_4 and $\delta^{15}N$-enriched resources by agropastoralists during the Iron Age. Furthermore, my results suggest that a significant proportion of the caprines at the UU site were translocated from the eastern African coastal strip and

hinterland. The diet of the agropastoralists at UU was dominated by C_4 crops, grasses, and the domesticated animals that fed on them. Meanwhile, at KC and PYS, foragers continued to rely on resources from the coastal forests for their diet, even though they interacted with food-producing communities. I argue that multi-isotope studies of caprines and wild animals, identified to the species level via ZooMS, from large sample sizes at eastern African archaeological sites can highlight the complex negotiation between incoming pastoral land uses, lifeways, and local environments and cultural practices in different parts of the region.

In case study three, I compile scientific dates and associated faunal, botanical, ceramic, and metallurgical findings from archaeological sites in eastern Africa, ranging from 5,000 BCE to 1,800 CE, into an archaeo-informatics-oriented dataset. Spatial-temporal maps created using the *Wanyika* dataset demonstrate that migration played a pivotal role in the dispersal of pastoralism across eastern Africa during the Neolithic and Iron Ages. The maps also show that migration was the dominant force in the dispersal of agropastoralism into the interior, as well as to the coastal strip, offshore islands, and Madagascar during the Iron Age. The maps also highlight the coexistence of megafauna with humans in Madagascar during the Iron Age, as well as the extinction of most of these megafauna taxa by 1200 CE. Similarly, maps generated from this dataset highlight major research gaps in the archaeological record of eastern Africa. Spatial-temporal maps show that large swaths of Kenya, Tanzania, the Comoros Islands, and Madagascar have not been explored for archaeological studies, and that dates are unevenly distributed in most regions. These gaps limit the dataset's accuracy when modeling and applying other modern analytical approaches that could aid in testing the indigenous continuity and migrations hypotheses in eastern African archaeology.

Chapter eight provided a detailed discussion of the main findings from the perspectives of isotopes and archaeo-informatics regarding ecological stability, the continuity of foragers, the development of complex subsistence strategies, and the emergence and dispersal of food production and food-producing communities in coastal and inland regions of eastern Africa. The chapter also emphasized the usefulness of these approaches when testing hypotheses of indigenous continuity and migration in eastern African archaeology. Further building upon these insights could greatly enrich hypothesis testing and theory building in archaeology at regional and global scales.

This final chapter summarizes the key findings from the three case studies and related milestones in late Holocene archaeology in eastern Africa. It also outlines the study's limitations and potential future research. The first section summarizes the insights from the case studies, indicating that despite the presence of food-producing communities near the cave, indigenous continuity was prevalent at the KC site during the Iron Age. It also suggests that the complex subsistence strategies at UU, including caprine herding, resulted from migrations by agropastoralists of western African ancestry. Overall, the case studies indicate that migration played a pivotal role in the dispersal of food production in eastern Africa, although indigenous continuity also played a part. The second section discusses milestone insights from the study beyond indigeneity and migration. It emphasizes the significant contributions of this thesis to archaeological study. These contributions include original, in-depth insights on human-environment interactions and primary isotopic datasets from KC, UU, FK, and PYS. Additionally, this project synthesized the *Wanyika* dataset of scientific dates from published archaeological sites in eastern Africa. These isotopic and scientific-date datasets will finally be included in regional and global databases for research purposes (Bird et al., 2022). Lastly, the third section discusses the limitations of this study and potential areas for

future research, particularly the use of isotopes and archaeo-informatics in late Holocene archaeology in eastern Africa.

9.2 – Milestones of this thesis in the late Holocene archaeology of eastern Africa

The isotopic record of carbon and oxygen values obtained from 229 faunal and human samples at the Kuumbi Cave site is unparalleled in the field of eastern African archaeology. PYS produced carbon and oxygen values from 134 samples, while other isotope paleoecology studies in mainland eastern Africa reported values from fewer than 100 samples. To bolster its potential for reuse, the primary isotopic dataset from this study has been published and will be included in the African Isotope Database and the Afriarch Isotopic Database hosted by the IsoMemo Network on the Pandora Platform (Goldstein et al., 2022a; Iminjili et al., 2023). Together, the Kuumbi Cave paleocology case study and the Panga ya Saidi study are notable for their in-depth insights into long-term, climate-driven ecological fluctuations and human-environment interactions from the late Pleistocene to the late Iron Age. These sites' deposits capture the dry and wet cycles of global climate change during a significant period of human history, a rare occurrence in eastern Africa. The two sites' archaeologically rich, multi-phased stratigraphic sequences, with their well-preserved zooarchaeological assemblages, are unmatched in the region. Isotopic insights from these sites will serve as a reference point for other isotope studies in the region. Isotopic value patterns from small, forest-adapted fauna provide valuable insights for spatial-temporal comparative studies with data from other offshore islands and interior eastern African sites. It will be a key area of research to see how glacial and interglacial, climate-driven ecological changes in eastern Africa's interior are represented in yet-to-be-discovered sites with multi-phased,

stratigraphic sequences from Lake Turkana, Lake Victoria, the central Rift Valley, the Eyasi region, and other offshore islands, such as Madagascar and the Comoros. Studies from several multi-phased archaeological sites in Madagascar could clarify whether foragers existed in Madagascar before the migration of agropastoralists of western African ancestry and their role in megafaunal extinctions.

Another milestone of this thesis is case study two's production of new multiple isotope values, including carbon, oxygen, nitrogen and strontium, from 62 bulk bone and enamel samples from caprines, wild animals and human remains from the three coastal sites of Unguja Ukuu, Fukuchani and Panga ya Saidi. These values will ultimately be published and included in regional and global isotopic databases to maximize the potential for reuse (Bird et al., 2021; Goldstein et al., 2022a). This case study of caprine husbandry has also provided significant insights on which future studies can build. Studying caprine husbandry using a multi-isotopic dataset from zooarchaeological samples identified to species via ZooMS is a significant step in advancing livestock husbandry studies in eastern Africa. Comparing wildland and farmland caprine husbandry strategies in the arid grasslands and forested coastal regions of eastern Africa has also provided valuable insights for future studies. Insights gained from integrating isotope and archaeological assemblage studies from UU, FK, PYS, and other sites in eastern Africa's interior are remarkable and worthy of application to other sites across the region. Another milestone achievement is using insights on agropastoralism—including crop and livestock production, exploitation of marine and wildlife resources, and involvement in the Indian Ocean trade—to untangle the isotopic record of four elements (C, O, N, and Sr). This approach could be applied to other sites. A regional, spatial, and temporal approach comparing the coastal strip and offshore islands to the interior of eastern Africa could inspire more archaeological studies on differences in caprine husbandry. Strontium values,

supported by carbon and oxygen data, have provided valuable insights into the translocation of goats from the hinterland to Unguja Ukuu. The strontium dataset from UU, PYS, and KC is a significant step in creating an isoscape of the coastal strip, Unguja Island, and other offshore islands, including Comoros and Madagascar. This isoscape will be valuable for studying human mobility patterns and the translocation of livestock and artifacts across the eastern African region and the Indian Ocean rim.

Lastly, another significant achievement of this thesis is the synthesis of 1,792 scientific dates and associated archaeological information from archaeological sites in eastern Africa spanning almost seven millennia into an archaeo-informatics-oriented dataset — the *Wanyika* Dataset — which has been published on the Pandora Data Platform (Iminjili et al., 2025a; Iminjili et al., 2025b). This dataset will significantly help to fill the gap in eastern African records within the global database of radiocarbon dates, while also increasing the reusability of scientific data from eastern Africa at global, continental, regional and local scales (Bird et al., 2022). Of the 180,070 radiocarbon dates published in the global database, only 11,120 come from Africa, primarily from northwestern and southern regions. The interior of eastern Africa is sparsely represented, and the Comoros and Madagascar islands are not represented at all. The 1,792 dates captured in the *Wanyika* dataset will strengthen the representation of eastern Africa in the global database. The dataset will facilitate modeling studies that include paleo-demographic research, Bayesian modeling, and summed probability distribution methodologies. Archaeological insights from the *Wanyika* dataset will encourage archaeological work and the production of scientific dates in areas that have not been covered. Once the archaeology of eastern Africa is well documented, this dataset could be used to study food security, biodiversity conservation, and other sustainable management practices that are only evident in the archaeological record. For instance, one could compare the nutrient value of

African crops found at archaeological sites with that of exotic modern crops found near the sites. I previously used the *Wanyika* dataset to write a published essay reviewing the contributions of pastoralism to ecological enrichment and conservation (ECHOES et al., 2024). The reuse potential of the dataset and the archaeological projects it will trigger will also benefit ongoing debates on megafauna extinctions in Madagascar.

9.3 – Limitations and future work

The three case studies presented in this thesis had several limitations that could be addressed in future research. The paleoecology and human foraging studies at KC and PYS did not have an adequate sample size of humans from the pre-Iron Age and Iron Age deposits. Additionally, most sites in the interior of eastern Africa with isotope data lack human values for the pre-Iron Age and Iron Age periods. Studies of paleoecology and human foraging based on carbon and oxygen isotopes from the coastal region are limited. To date, only two studies exist (PYS and KC). Isotope ecological studies in the interior of eastern Africa are also scarce. The caprine husbandry study faced a number of limitations that could similarly be addressed in future research. The samples used in this study are residues from a previous ZooMS study (Culley et al., 2021a; Culley et al., 2021b) that was focused on caprines rather than wild fauna. As a result, the study did not have adequate sample sizes from all taxonomic groups and contexts in the UU Early and Late Phases. Twenty samples (UU, FK, and PYS) were affected by the lack of collagen and failures to meet established standards of bone collagen preservation. Eight of these samples came from UU Trench 14 (seven from the Early Phase). There was also insufficient material for directly dating caprines. The lack of ZooMS identification to species level and direct dates on caprines from most of the

sites in the interior of eastern Africa, and the lack of a strontium baseline study for the coastal strip and Zanzibar also impose major limitations on the interpretation of these datasets.

Major research gaps in the archaeological record of eastern Africa, as highlighted by maps generated from the *Wanyika* dataset, limit the dataset's ability to test the finer details of indigenous continuity and migration hypotheses. The high number of unreliable dates and the disparities in the spatial-temporal distribution of dated sites across eastern Africa limit the use of this dataset in archaeo-informatics-oriented modeling experiments to test the indigenous continuity and migration hypotheses. The current archaeological data does not allow us to adequately assess the contribution of indigenous continuity hypotheses to the emergence and dispersal of food production and food-producing communities in eastern Africa's interior. The primary example from Mount Kilimanjaro supporting this hypothesis is based solely on ceramic and radiocarbon date datasets. No zooarchaeological, archaeobotanical, metallurgical, human osteological, or aDNA datasets were presented in support of the hypothesis. Most of the data used to support the hypothesis originates from sites with issues of stratigraphic integrity. Studies supporting migration hypotheses have also used these same datasets to bolster their arguments. The present archaeological data does not allow us to determine whether pastoralists from the north migrated with cattle, goats, and sheep as a package and if they had domesticated crops. Similarly, it is impossible to ascertain whether immigrating agropastoralists entered eastern Africa with livestock, African domesticated crops, ceramics, and metallurgy as a package. It is also impossible to conclusively determine which community—Cushitic-, Nilotic-, or Bantu-speaking—introduced and actively dispersed the five African domesticated crops in interior eastern Africa. The limited availability of dates and sites hinders our understanding of the contributions of the hypothesized late-split riverine and late-split savannah routes to agropastoralist migration and the spread-over-spread migration patterns across

eastern Africa. This is evident in the migration patterns observed among these agropastoralists in central Africa.

Future work in eastern Africa should consider applying both normative and idiographic approaches to late Holocene archaeology. Context-specific and broad regional to global hypotheses both contribute to a comprehensive understanding of past human-environment interactions. These hypotheses should be supported by insights from archaeological science, with an emphasis on isotopic and archaeo-informatic perspectives. Focusing on context, site-specific, and regional-scale perspectives based on a multidisciplinary approach, with isotopic and archaeo-informatics at the forefront, provides insights into both fine details and broad patterns across space and time. These fine details and broad patterns are important for discerning indigenous continuity and migration in the archaeological record, ultimately providing a comprehensive understanding of the emergence and dispersal of food production and food-producing communities in eastern Africa during the late Holocene. Biomolecular perspectives, attainable from ZooMS, aDNA, proteomics, and well-designed isotope research, should also be prioritized.

For the coastal region and the interior of eastern Africa, paleoecological studies on multi-stratified pre-Iron Age and Iron Age sites based on enamel carbon and oxygen isotopes, such as KC and PYS, with adequate numbers of human samples and more precise dates, should be prioritized. Multi-isotope studies incorporating both bulk and sequential analyses of three molar teeth are essential for paleoecological and mobility studies (Janzen, 2015; Janzen et al., 2020a; Janzen et al., 2020b; Culley et al., 2021b; Janzen et al., 2021; Janzen, 2022). Direct dates from caprines and other livestock in legacy and new collections from all archaeological sites are essential for precisely tracking their dispersal and addressing the large number of questionable stratigraphic dates. A

baseline study of strontium is also required for the coastal strip and islands. A multi-isotope perspective examining spatial and temporal changes in isotopes, such as $\delta^{13}C_{coll}$ and $\delta^{15}N$, in zooarchaeological collections, as well as ecological impacts over time, is also required. This includes periods before the introduction of food production, during the establishment of traditional African food production dominated by organic manure, and during the establishment of commercial farming dominated by synthetic/factory fertilizer. This approach would provide valuable insights into past and present interactions between humans and the environment. These insights could inform future decisions about the use of organic and synthetic fertilizers, among other things. (Novacek and Cleland, 2001; Causey and Lane, 2005; Erlandson and Braje, 2014; Marchant and Lane, 2014; Lane, 2015b; Marchant et al., 2017; Marchant et al., 2018; Boles et al., 2019; Courtney Mustaphi et al., 2019; Stephens et al., 2019; Boivin and Crowther, 2021; Marchant, 2021).

In order for the archaeo-informatic-oriented dataset to be most effective, archaeologists working in eastern Africa should be encouraged to adopt a broad-based archaeological science approach at all archaeological sites. This approach includes context-specific excavations, computer-aided recording and mapping, flotation, microscopy, and micro-CT scanning on ceramics; advanced zooarchaeology and archaeobotany, including identification to the species level of all faunal and plant remains; and the production of mass dates from a site, including context-specific direct dates from domesticated animals, crops, ceramics, metallurgy, and other artifacts. Studies on caprines, cattle, and humans using ZooMS, proteomics, and ancient genetics should be encouraged. These subdisciplines should produce their own archaeo-informatic-oriented datasets, which could be merged with the *Wanyika* dataset, the MAESaM database, and other datasets to develop an African archaeological database that would contribute to the global database. Archaeologists should also

explore regions that have not been worked on and establish archaeological projects there. An even spatial and temporal distribution of new sites and dates across eastern Africa could facilitate novel insights from archaeo-informatic modeling analyses and other technology-aided studies.

Adopting a broad archaeological sciences approach that incorporates isotopic and archaeo-informatic perspectives is likely to provide valuable insights that were previously inaccessible. These insights will enrich discussions about ecological trends, complex subsistence strategies, the emergence of food production, and the dispersal of food-producing communities in eastern Africa. Investigations guided by an integration of normative and idiographic hypotheses based on a multidisciplinary approach led by isotopic and archaeo-informatic-oriented perspectives are bound to piece together finer context-specific details and broader spatial-temporal patterns, thereby providing a comprehensive understanding of the contributions of indigenous foragers and immigrants in human-environment interactions in eastern Africa during the late Holocene. In this sense, the worm's-eye and bird's-eye views of the archaeological data complement each other to provide a holistic view. Going forward, to achieve a holistic understanding of the late Holocene archaeology of eastern Africa, it is vital to integrate these perspectives.

References

Åberg, G., Jacks, G., and Joseph Hamilton, P. (1989). Weathering rates and 87Sr/86Sr ratios: An isotopic approach. *Journal of Hydrology* 109(1)**,** 65–78. doi: https://doi.org/10.1016/0022-1694(89)90007-3.

Abungu, G.H.O. (1989). *Communities on the River Tana, Kenya: An archaeological study of relations between the Delta and the River Basin, 700-1890 A.D.* . PhD dissertation University of Cambridge

Abungu, G.H.O., and Mutoro, H. (1993). "Coast-interior settlements and social relations in the Kenya coastal hinterland," in *The Archaeology of Africa: Food, Metals and Towns,* eds. T. Shaw, P.J.J. Sinclair, B. Andah & A. Okpoko. (London: Routledge), 694–704.

Adams, W.Y., Van Gerven, D.P., and Levy, R.S. (1978). The Retreat from Migrationism. *Annual Review of Anthropology* 7(Volume 7, 1978)**,** 483–532. doi: https://doi.org/10.1146/annurev.an.07.100178.002411.

Adobe (2024). *Adobe Photoshop 2024* [Online]. Adobe Available: https://news.adobe.com/news/news-details/2024/New-Adobe-Photoshop-with-Advanced-Generative-Fill-and-Generate-Image-Brings-New-Superpowers-to-All/default.aspx [Accessed].

Alders, W. (2026). Townlands of the Swahili Coast: A Framework for Compact, High-Density Tropical Urbanism on Eastern Africa's Indian Ocean Rim. *Journal of Archaeological Research*. doi: 10.1007/s10814-025-09218-9.

Alonzi, E., Pacheco-Forés, S.I., Gordon, G.W., Kuijt, I., and Knudson, K.J. (2020). New understandings of the sea spray effect and its impact on bioavailable radiogenic strontium isotope ratios in coastal environments. *Journal of Archaeological Science: Reports* 33**,** 102462. doi: https://doi.org/10.1016/j.jasrep.2020.102462.

Ambrose, S. (1984a). *Holocene environments and human adaptations in the central Rift Valley, Kenya.* PhD, University of California.

Ambrose, S. (1984b). "The Introduction of Pastoral Adaptations to the Highlands of East Africa," in *From Hunters to Farmers: The Causes and Consequences of Food production in Africa,* eds. D. Clark & S.A. Brandt. (London: University of California Press), 212–421.

Ambrose, S. (1986). Stable carbon and nitrogen isotope analysis of human and animal diet in Africa. *Journal of Human Evolution* (15)**,** 707–731.

Ambrose, S. (1998). Chronology of the Later Stone Age and food production in East Africa. *Journal of Archaeological Science* 25(4)**,** 377–392. doi: https://doi.org/10.1006/jasc.1997.0277.

Ambrose, S. (2003). "East African Neolithic", in: *Encyclopaedia of Prehistory.* (eds.) P.N. Peregrine & M. Ember. (New York: Kluwer Academic).

Ambrose, S.H. (1982). "Archaeology and Linguistic Reconstructions of History in East Africa," in *The Archaeological and Linguistic Reconstruction of African History,* eds. E. Christopher & P. Merrick. (Berkeley: University of California Press), 104–157.

Ambrose, S.H. (1990). Preparation and characterization of bone and tooth collagen for isotopic analysis. *Journal of Archaeological Science* 17(4)**,** 431–451. doi: https://doi.org/10.1016/0305-4403(90)90007-R.

Ambrose, S.H. (1993). "Isotopic analysis of paleodiets: methodological and interpretive considerations," in *Investigations of Ancient Human Tissue: Chemical Analysis in Anthropology,* ed. M.K. Sanford. (Langhorne, P.A.: Gordon and Breach Science Publishers), 59–129.

Ambrose, S.H. (1997). "Hunter-gatherer adaptations to climate change in the Kenya Rift Valley," in *Preliminary Report on Research on Permit OP.13/001/16C 26/19*. (Nairobi: Kenya).

Ambrose, S.H., Ambrose, S.H., and Katzenburg, M.A. (2000). *Biogeochemical Approaches to Palaeodietary Analysis.*

Ambrose, S.H., Collett, D., Collett, D., and Marshall, F. (1984). Excavations at Deloraine, Rongai, 1978. *Azania: Archaeological Research in Africa* 19(1)**,** 79–104. doi: 10.1080/00672708409511329.

Ambrose, S.H., and DeNiro, M.J. (1986a). The isotopic ecology of East African mammals. *Oecologia* 69(3)**,** 395–406. doi: 10.1007/bf00377062.

Ambrose, S.H., and DeNiro, M.J. (1986b). Reconstruction of African human diet using bone collagen carbon and nitrogen isotope ratios. *Nature* 319(6051)**,** 321–324.

Ambrose, S.H., and DeNiro, M.J. (1989). Climate and habitat reconstruction using stable carbon and nitrogen isotope ratios of collagen in prehistoric herbivore teeth from Kenya. *Quaternary Research* 31(3)**,** 407–422. doi: https://doi.org/10.1016/0033-5894(89)90048-3.

Ambrose, S.H., and Norr, L. (1993). "Experimental Evidence for the Relationship of the Carbon Isotope Ratios of Whole Diet and Dietary Protein to Those of Bone Collagen and Carbonate," in *Prehistoric Human Bone: Archaeology at the Molecular Level,* eds. J.B. Lambert & G. Grupe. (Berlin, Heidelberg: Springer Berlin Heidelberg), 1–37.

Ambrose, S.H., Norr, L., Lambert, J., and Grupe, G. (1993). *Prehistoric Human Bone.*

Amy, S.J. (2020). *Inside perspectives on ceramic manufacturing: Visualizing ancient potting practices through Micro-CT scanning.* Doctor of Philosophy, The University of Western Ontario.

Anderson, A., Clark, G., Haberle, S., Higham, T., Nowak-Kemp, M., Prendergast, A., et al. (2018). New evidence of megafaunal bone damage indicates late colonization of Madagascar. *PLOS ONE* 13(10)**,** e0204368. doi: 10.1371/journal.pone.0204368.

Anderson, C., and Cabana, G. (2006). Does δ15N in river food webs reflect the intensity and origin of N loads from the watershed? *The Science of the total environment* 367**,** 968–978. doi: 10.1016/j.scitotenv.2006.01.029.

Anderson, D.G. (2024). Modern archaeological research and the importance of information management. *Proceedings of the National Academy of Sciences* 121(16)**,** e2403792121. doi: doi:10.1073/pnas.2403792121.

Ansari Pour, N., Plaster, C.A., and Bradman, N. (2013). Evidence from Y-chromosome analysis for a late exclusively eastern expansion of the Bantu-speaking people. *European Journal of Human Genetics* 21(4)**,** 423–429. doi: 10.1038/ejhg.2012.176.

Anthony, D.W. (2023). Ancient DNA and migrations: New understandings and misunderstandings. *Journal of Anthropological Archaeology* 70**,** 101508. doi: https://doi.org/10.1016/j.jaa.2023.101508.

Arthur, J.W., Curtis, M.C., Arthur, K.J.W., Coltorti, M., Pieruccini, P., Lesur, J., et al. (2019). The Transition from Hunting–Gathering to Food Production in the Gamo Highlands of Southern Ethiopia. *African Archaeological Review* 36(1)**,** 5–65. doi: 10.1007/s10437-018-09322-w.

Åse, L.-E. (1981). Studies of Shores and Shore Displacement on the Southern Coast of Kenya—Especially in Kilifi District. *Geografiska Annaler: Series A, Physical Geography* 63(3-4)**,** 303–310. doi: 10.1080/04353676.1981.11880045.

Ashley, C.Z. (2010). Towards a Socialised Archaeology of Ceramics in Great Lakes Africa. *The African Archaeological Review* 27(2)**,** 135–163.

Ashley, C.Z., and Grillo, K.M. (2015). Archaeological ceramics from eastern Africa: past approaches and future directions. *Azania: Archaeological Research in Africa* 50(4)**,** 460–480. doi: 10.1080/0067270X.2015.1102939.

Aston, F.W. (1922). *Isotopes.* London: Edward Arnold & Co.

Bajaj, N.S., and Palan, C.B. (2022). "Understanding OSL radiation dosimetry and its application," in *Radiation Dosimetry Phosphors*, eds. S. Dhoble, V. Chopra, V. Nayar, G. Kitis, D. Poelman & H. Swart. Woodhead Publishing), 99–128.

Balasse, M. (2014). "Isotopic Studies of Husbandry Practices," in *Encyclopedia of Global Archaeology*, ed. C. Smith. (New York, NY: Springer New York), 4120–4128.

Balasse, M., and Ambrose, S.H. (2005). Distinguishing sheep and goats using dental morphology and stable carbon isotopes in C4 grassland environments. *Journal of Archaeological Science* 32**,** 691–702.

Balasse, M., Bocherens, H., Mariotti, A., and Ambrose, S.H. (2001). Detection of Dietary Changes by Intra-tooth Carbon and Nitrogen Isotopic Analysis: An Experimental Study of Dentine Collagen of Cattle (Bos taurus). *Journal of Archaeological Science* 28(3)**,** 235–245. doi: https://doi.org/10.1006/jasc.1999.0535.

Barron, A., Datan, I., Bellwood, P., Wood, R., Fuller, D.Q., and Denham, T. (2020a). Sherds as archaeobotanical assemblages: Gua Sireh reconsidered. *Antiquity* 94(377)**,** 1325–1336. doi: 10.15184/aqy.2020.166.

Barron, A., Fuller, D.Q., Stevens, C., Champion, L., Winchell, F., and Denham, T. (2020b). Snapshots in time: MicroCT scanning of pottery sherds determines early domestication of sorghum (Sorghum bicolor) in East Africa. *Journal of Archaeological Science* 123**,** 105259. doi: https://doi.org/10.1016/j.jas.2020.105259.

Barthelme, J. (1977). Holocene sites North-East of Lake Turkana: A preliminary report. *Azania: Archaeological Research in Africa* 12(1)**,** 33–41. doi: 10.1080/00672707709511246.

Barthelme, J. (1985). *Fisher-Hunters and Neolithic Pastoralists in East Turkana, Kenya.* Oxford: Cambridge Monographs in African Archaeology 13 (B.A.R. International Series 254).

Bateman, A.S., and Kelly, S.D. (2007). Fertilizer nitrogen isotope signatures. *Isotopes in Environmental and Health Studies* 43(3)**,** 237–247. doi: 10.1080/10256010701550732.

Bayon, G., Dennielou, B., Etoubleau, J., Ponzevera, E., Toucanne, S., and Bermell, S. (2012a). Intensifying Weathering and Land Use in Iron Age Central Africa. *Science* 335(6073)**,** 1219–1222. doi: doi:10.1126/science.1215400.

Bayon, G., Dennielou, B., Etoubleau, J., Ponzevera, E., Toucanne, S., and Bermell, S. (2012b). Response to Comments on "Intensifying Weathering and Land Use in Iron Age Central Africa". *Science* 337**,** 1040–1040. doi: 10.1126/science.1222458.

Beaujard, P. (2007). East Africa, the Comoros Islands and Madagascar before the sixteenth century: On a neglected part of the world system. *AZANIA: Journal of the British Institute in Eastern Africa* 42**,** 15–35. doi: 10.1080/00672700709480448.

Beck, C.C., Feibel, C.S., Wright, J.D., and Mortlock, R.A. (2019). Onset of the African Humid Period by 13.9 kyr BP at Kabua Gorge, Turkana Basin, Kenya. *The Holocene* 29(6)**,** 1011–1019. doi: 10.1177/0959683619831415.

Bentley, R.A. (2006a). Strontium Isotopes from the Earth to the Archaeological Skeleton: A Review. *Journal of Archaeological Method and Theory* 13**,** 135–187. doi: 10.1007/s10816-006-9009-x.

Bentley, R.A. (2006b). Strontium isotopes from the earth to the archaeological skeleton: a review. *Journal of Archaeological Method and Theory* 13(3).

Bentley, R.A., and Maschner, H. (2007). "Introduction to Archaeological Theory."), 1–8.

Bergner, A., Trauth, M., and Bookhagen, B. (2003). Paleoprecipitation estimates for the Lake Naivasha basin (Kenya) during the last 175 k.y. using a lake-balance model. *Global and Planetary Change* 36**,** 117–136. doi: 10.1016/S0921-8181(02)00178-9.

Billings, T.N., Scott, E., Cocozza, C., Hixon, S., Boivin, N., Roberts, P., et al. (2025). The North American Repository for Archaeological Isotopes. *Scientific Data* 12(1)**,** 50. doi: 10.1038/s41597-024-04175-2.

Binford, L.R. (1962). Archaeology as Anthropology. *American Antiquity* 28(2)**,** 217–225. doi: 10.2307/278380.

Binford, L.R. (1968). Some Comments on Historical versus Processual Archaeology. *Southwestern Journal of Anthropology* 24(3)**,** 267–275.

Bird, D., Freeman, J., Robinson, E., Maughan, G., Finley, J.B., Lambert, P.M., et al. (2020). A first empirical analysis of population stability in North America using radiocarbon records. *The Holocene* 30(9)**,** 1345–1359. doi: 10.1177/0959683620919975.

Bird, D., Miranda, L., Vander Linden, M., Robinson, E., Bocinsky, R.K., Nicholson, C., et al. (2022). p3k14c, a synthetic global database of archaeological radiocarbon dates. *Scientific Data* 9(1)**,** 27. doi: 10.1038/s41597-022-01118-7.

Bird, M.I., Crabtree, S.A., Haig, J., Ulm, S., and Wurster, C.M. (2021). A global carbon and nitrogen isotope perspective on modern and ancient human diet. *Proceedings of the National Academy of Sciences* 118(19)**,** e2024642118. doi: doi:10.1073/pnas.2024642118.

Black, E. (2005). The relationship between Indian Ocean sea-surface temperature and East African rainfall: One contribution of 24 to a Discussion Meeting 'Atmosphere-ocean-ecology dynamics in the Western Indian Ocean'. *Philosophical Transactions of The Royal Society A: Mathematical, Physical and Engineering Sciences* 363**,** 43–47. doi: 10.1098/rsta.2004.1474.

Blanz, M., Ascough, P., Mainland, I., Martin, P., Taggart, M.A., Dieterich, B., et al. (2019). Seaweed fertilisation impacts the chemical and isotopic composition of barley: Implications for analyses of archaeological skeletal remains. *Journal of Archaeological Science* 104**,** 34–44. doi: https://doi.org/10.1016/j.jas.2019.02.003.

Blanz, M., Mainland, I., Richards, M., Balasse, M., Ascough, P., Wolfhagen, J., et al. (2020). Identifying seaweed consumption by sheep using isotope analysis of their bones and teeth: Modern reference δ13C and δ15N values and their archaeological implications.

Journal of Archaeological Science 118**,** 105140. doi: https://doi.org/10.1016/j.jas.2020.105140.

Bleasdale, M., Derbyshire, S., Lucas, M., Lowasa, L., Lehn, C., Nami, J.E., et al. (2026). Exploring Contemporary Pastoral Variability through Stable Isotope Analysis in the Turkana Basin, Kenya. *Current Anthropology* 67(1)**,** 28–55. doi: 10.1086/739930.

Bleasdale, M., Richter, K.K., Janzen, A., Brown, S., Scott, A., Zech, J., et al. (2021). Ancient proteins provide evidence of dairy consumption in eastern Africa. *Nature Communications* 12(1)**,** 632. doi: 10.1038/s41467-020-20682-3.

Bleasdale, M., Wotzka, H.-P., Eichhorn, B., Mercader, J., Styring, A., Zech, J., et al. (2020). Isotopic and microbotanical insights into Iron Age agricultural reliance in the Central African rainforest. *Communications Biology* 3(1)**,** 619. doi: 10.1038/s42003-020-01324-2.

Blum, J.D., Erel, Y., and Brown, K. (1993). 87Sr/86Sr ratios of sierra nevada stream waters: Implications for relative mineral weathering rates. *Geochimica et Cosmochimica Acta* 57(21)**,** 5019–5025. doi: https://doi.org/10.1016/S0016-7037(05)80014-6.

Blum, J.D., Taliaferro, E.H., Weisse, M.T., and Holmes, R.T. (2000). Changes in Sr/Ca, Ba/Ca and 87Sr/86Sr ratios between trophic levels in two forest ecosystems in the northeastern U.S.A. *Biogeochemistry* 49(1)**,** 87–101. doi: 10.1023/a:1006390707989.

Blumenthal, S.A., Rothman, J.M., Chritz, K.L., and Cerling, T.E. (2016). Stable isotopic variation in tropical forest plants for applications in primatology. *American journal of primatology* 78(10)**,** 1041–1054. doi: 10.1002/ajp.22488.

Bluszcz, A. (Year). "OSL Dating in Archaeology": Springer Netherlands), 137–149.

Bobe, R. (2006). The evolution of arid ecosystems in eastern Africa. *Journal of Arid Environments* 66**,** 564–584.

Bobe, R. (2011). Fossil mammals and paleoenvironments in the Omo-Turkana Basin. *Evolutionary Anthropology: Issues, News, and Reviews* 20(6)**,** 254–263. doi: 10.1002/evan.20330.

Bobe, R., and Behrensmeyer, A.K. (2004). The expansion of grassland ecosystems in Africa in relation to mammalian evolution and the origin of the genus *Homo*. *Palaeogeography, Palaeoclimatology, Palaeoecology* 207**,** 399–420.

Bobe, R., Behrensmeyer, A.K., and Chapman, R.E. (2002). Faunal change, environmental variability and late Pliocene hominin evolution. *Journal of Human Evolution* 42(4)**,** 475–497.

Bobe, R., and Carvalho, S. (2019). Hominin diversity and high environmental variability in the Okote Member, Koobi Fora Formation, Kenya. *Journal of Human Evolution* 126**,** 91–105. doi: https://doi.org/10.1016/j.jhevol.2018.10.012.

Bobe, R., and Eck, G.G. (2001). Responses of African bovids to Pliocene climatic change. *Paleobiology* 27(2)**,** 1 – 47.

Bocquet-Appel, J.-P., Naji, S., Vander Linden, M., and Kozlowski, J. (2012). Understanding the rates of expansion of the farming system in Europe. *Journal of Archaeological Science - J ARCHAEOL SCI* 39. doi: 10.1016/j.jas.2011.10.010.

Boivin, N., and Crowther, A. (2021). Mobilizing the past to shape a better Anthropocene. *Nature Ecology & Evolution* 5(3)**,** 273–284. doi: 10.1038/s41559-020-01361-4.

Boivin, N., Crowther, A., Helm, R., and Fuller, D.Q. (2013). East Africa and Madagascar in the Indian Ocean world. *Journal of World Prehistory* 26(3)**,** 213–281. doi: 10.1007/s10963-013-9067-4.

Boivin, N., Crowther, A., Prendergast, M., and Fuller, D.Q. (2014). Indian Ocean food globalisation and Africa. *The African Archaeological Review* 31(4)**,** 547–581.

Boivin, N., Fuller, D.Q., and Crowther, A. (2012). Old World globalization and the Columbian exchange: comparison and contrast. *World Archaeology* 44(3)**,** 452–469. doi: 10.1080/00438243.2012.729404.

Boles, O.J.C., Shoemaker, A., Courtney Mustaphi, C.J., Petek, N., Ekblom, A., and Lane, P.J. (2019). Historical ecologies of pastoralist overgrazing in Kenya: Long-term perspectives on cause and effect. *Human Ecology* 47(3)**,** 419–434. doi: 10.1007/s10745-019-0072-9.

Bollig, M., and Wotzka, H.-P. (2013). *Pastoralism in Africa: Past, Present and Future.* Oxford: Berghahn Books.

Bonnefille, R. (1995). "A Reassesment of the Plio-Pleistocene Pollen Record of East Africa," in *Paleoclimate and Evolution with Emphasis on Human Origins,* eds. E.S. Vrba, G.H. Denton, T.C. Patridge & L.H. Burckle. (New Haven: Yale University Press), 299–310.

Bonnefille, R. (2010). Cenozoic vegetation, climate changes and hominid evolution in tropical Africa. *Global and Planetary Change* 72(4)**,** 390–411. doi: https://doi.org/10.1016/j.gloplacha.2010.01.015.

Bonnefille, R., Roeland, J.C., and Guiot, J. (1990). Temperature and rainfall estimates for the past 40,000 years in equatorial Africa. *Nature* 346(6282)**,** 347–349. doi: https://doi.org/10.1038/346347a0.

Bostoen, K. (2018). "The Bantu Expansion". Oxford University Press).

Bostoen, K., Clist, B., Doumenge, C., Grollemund, R., Hombert, J.-M., Muluwa, J.K., et al. (2015). Middle to Late Holocene Paleoclimatic Change and the Early Bantu Expansion in the Rain Forests of Western Central Africa. *Current Anthropology* 56(3)**,** 354–384. doi: 10.1086/681436.

Bostoen, K., and Coutros, P. (2025). "Introduction to a New Archaeology of the Bantu Expansion."), 1–24.

Bouimetarhan, I., Dupont, L., Kuhlmann, H., Pätzold, J., Prange, M., Schefuß, E., et al. (2015). Northern Hemisphere control of deglacial vegetation changes in the Rufiji uplands (Tanzania). *Clim. Past* 11(5)**,** 751–764. doi: 10.5194/cp-11-751-2015.

Bower, J. (1991). The Pastoral Neolithic of East Africa. *Journal of World Prehistory* 5(1)**,** 49–82. doi: 10.1007/BF00974732.

Bower, J.R.F., and Nelson, C.M. (1978). Early pottery and pastoral cultures of the central Rift Valley, Kenya. *Man* 13(4)**,** 554–566. doi: 10.2307/2801248.

Bower, J.R.F., Nelson, C.M., Waibel, A.F., and Wandibba, S. (1977). The University of Massachusetts' Later Stone Age/Pastoral 'Neolithic' comparative study in central Kenya: an overview. *Azania: Archaeological Research in Africa* 12(1)**,** 119–146. doi: 10.1080/00672707709511251.

Braje, T.J., Leppard, T.P., Fitzpatrick, S.M., and Erlandson, J.M. (2017). Archaeology, historical ecology and anthropogenic island ecosystems. *Environmental Conservation* 44(3)**,** 286–297. doi: 10.1017/S0376892917000261.

Britton, K., Crowley, B., Bataille, C., Miller, J., and Wooller, M. (2022). Editorial: A Golden Age for Strontium Isotope Research? Current Advances in Paleoecological and Archaeological Research. *Frontiers in Ecology and Evolution* 9. doi: 10.3389/fevo.2021.820295.

Brock, F., Higham, T., and Ramsey, C.B. (2013). Comments on the Use of Ezee-Filters™ and Ultrafilters at Orau. *Radiocarbon* 55(1)**,** 211–212. doi: 10.2458/azu_js_rc.v55i1.16480.

Bronk Ramsey, C. (2009). Bayesian analysis of radiocarbon dates. *Radiocarbon* 51(1)**,** 337–360. doi: 10.1017/S0033822200033865.

Brown, T.A., Nelson, D.E., Vogel, J.S., and Southon, J.R. (1988). Improved collagen extraction by modified longin method. *Radiocarbon* 30(2)**,** 171–177. doi: 10.1017/S0033822200044118.

Buchanan, B., Hamilton, M., Edinborough, K., O'Brien, M.J., and Collard, M. (2011). A comment on Steele's (2010) "radiocarbon dates as data: quantitative strategies for estimating colonization front speeds and event densities". *Journal of Archaeological Science* 38(9)**,** 2116–2122. doi: https://doi.org/10.1016/j.jas.2011.02.026.

Buchmann, N., and Ehleringer, J.R. (1998). CO2 concentration profiles, and carbon and oxygen isotopes in C3 and C4 crop canopies. *Agricultural and Forest Meteorology* 89(1)**,** 45–58. doi: https://doi.org/10.1016/S0168-1923(97)00059-2.

Buchmann, N., Guehl, J.M., Barigah, T.S., and Ehleringer, J.R. (1997). Interseasonal comparison of CO2 concentrations, isotopic composition, and carbon dynamics in an Amazonian rainforest (French Guiana). *Oecologia* 110(1)**,** 120–131. doi: 10.1007/s004420050140.

Burgess, N.D., and Clarke, G.P. (2000). *Coastal Forests of Eastern Africa.* Cambridge: IUCN - The World Conservation Union.

Burmeister, S. (2000). Archaeology and Migration: Approaches to an Archaeological Proof of Migration. *Current Anthropology* 41(4)**,** 539–567. doi: 10.1086/317383.

Burmeister, S. (2019). "Archaeological Migration Research is Interdisciplinary, or it is Nothing. Ten Essentials How to Think About the Archaeological Study of Migration", in: *Mobility and Migration: Concepts, Methods, Results (Denisova Cave (Altai, Russia)* (eds.) V.I. Molodin & L.N. Mylnikova. (Novosibirsk).

Burney, D.A. (1997). "Theories and facts regarding Holocene environmental change before and after human colonization," in *Natural Change and Human Impacts in Madagascar,* eds. S.M. Goodman & B.D. Patterson. (Washington, DC: Smithsonian Press), 142–168.

Burney, D.A. (1999). "Rates, patterns, and processes of landscape transformation and extinction in Madagascar," in *Extinction in Near Time,* ed. R.D.E. MacPhee. (New York: Kluwer/Plenum), 145–164.

Burney, D.A., Burney, L.P., Godfrey, L.R., Jungers, W.L., Goodman, S.M., Wright, H.T., et al. (2004). A chronology for late prehistoric Madagascar. *Journal of Human Evolution* 47(1)**,** 25–63. doi: https://doi.org/10.1016/j.jhevol.2004.05.005.

Butzer, K.W., Isaac, G.L., Richardson, J.L., and Washbourn-Kamau, C. (1972). Radiocarbon Dating of East African Lake Levels. *Science* 175(4026)**,** 1069–1076. doi: doi:10.1126/science.175.4026.1069.

Buzon, M.R., Simonetti, A., and Creaser, R.A. (2007). Migration in the Nile Valley during the New Kingdom period: a preliminary strontium isotope study. *Journal of Archaeological Science* 34**,** 1391–1401.

Camberlin, P. (2018). "Climate of Eastern Africa". Oxford University Press).

Campbell, C., Fuentes, C., Mackonnon, K.M., Panger, M., and Bearder, S.K. (2006). *Primates in Perspective.* New York: Oxford University Press.

Capo, R.C., Stewart, B.W., and Chadwick, O.A. (1998). Strontium isotopes as tracers of ecosystem processes: theory and methods. *Geoderma* 82(1)**,** 197–225. doi: https://doi.org/10.1016/S0016-7061(97)00102-X.

Carter, M., and Bradbury, M. (2015). Oxygen isotope ratios in Primate bone carbonate reflect amount of leaves and vertical stratification in the diet. *American journal of primatology* 78. doi: 10.1002/ajp.22432.

Carter, M.L. (2001). *Sensitivity of stable isotopes (carbon-13, nitrogen-15, and oxygen-18) in bone to dietary specialization and niche separation among sympatric primates in Kibale National Park, Uganda.* PhD Dissertation The University of Chicago, The University of Chicago.

Cartigny, P., and Busigny, V. (2018). "Nitrogen isotopes."), 991–1003.

Causey, M. (2009). Delineating pastoralist behaviour and long-term environmental change: a GIS landscape approach on the Laikipia Plateau, Kenya, University of Oxford, 2008. *Azania: Archaeological Research in Africa* 44(1)**,** 155–155. doi: 10.1080/00671990902796200.

Causey, M., and Lane, P. (2005). GIS and landscape archaeology: delineating the possible long-term environmental effects of pastoralism on the Laikipia Plateau, Kenya. *Nyame Akuma* (64)**,** 24–32.

Cerling, T., Andanje, S.A., Blumenthal, S.A., Brown, F.H., Chritz, K.L., Harris, J.M., et al. (2015). Dietary changes of large herbivores in the Turkana Basin, Kenya from 4 to 1 Ma. *Proceedings of the National Academy of Sciences* 112(37)**,** 11467–11472. doi: 10.1073/pnas.1513075112.

Cerling, T., Harris, J.M., Leakey, M.G., Passey, B.H., and Levin, N. (2010). "Stable Carbon and Oxygen Isotopes in East African Mammals: Modern and Fossil," in *Cenozoic Mammals of Africa,* eds. L. Werdelin & W.J. Sanders. (Los Angeles: University of California Press), 949–960.

Cerling, T.E., and Harris, J.M. (1999). Carbon isotope fractionation between diet and bioapatite in ungulate mammals and implications for ecological and paleoecological studies. *Oecologia* 120**,** 347–363.

Cerling, T.E., Harris, J.M., Ambrose, S., Leakey, M.G., and Solounias, N. (1997). Dietary and Environmental Reconstruction with Stable Isotope Analyses of Herbivore Tooth Enamel from the Miocene Locality of Fort Ternan, Kenya. *Journal of Human Evolution* 33**,** 635–650.

Cerling, T.E., Harris, J.M., and Leakey, M.G. (1999). Browsing and grazing in elephants: the isotope record of modern and fossil proboscideans. *Oecologia* 120**,** 364–374.

Cerling, T.E., Harris, J.M., and Leakey, M.G. (2003a). "Isotope Paleoecology of the Nawata and Nachukui Formations at Lothagam, Turkana Basin, Kenya," in *Lothagam: the Dawn of Humanity in Eastern Africa,* eds. M.G. Leakey & J.M. Harris. (New York: Columbia University Press), 605–624.

Cerling, T.E., Harris, J.M., and Leakey, M.G. (2005). "Environmentally Driven Dietary Adaptations in African Mammals," in *A History of Atmospheric CO_2 and its Effects on Plants, Animals, and Ecosystems,* eds. J.R. Ehleringer, T.E. Cerling & M.D. Dearing. (New York: Springer-Verlag), 258–272.

Cerling, T.E., Harris, J.M., Leakey, M.G., and Mudida, N. (2003b). "Stable Isotope Ecology of Northern Kenya, with Emphasis on the Turkana Basin," in *Lothagam: The Dawn of Humanity in Eastern Africa*, eds. M.G. Leakey & J.M. Harris. (New York: Columbia University Press), 583–603.

Cerling, T.E., Harris, J.M., and Passey, B.H. (2003c). Diets of East African Bovidae based on stable isotope analysis. *Journal of Mammology* 84(2)**,** 456–470. doi: https://doi.org/10.1644/1545-1542(2003)084<0456:DOEABB>2.0.CO;2.

Cerling, T.E., Hart, J.A., and Hart, T.B. (2004). Stable isotope ecology in the Ituri forest. *Oecologia* 138(1)**,** 5–12. doi: 10.1007/s00442-003-1375-4.

Cerling, T.E., Hay, R.L., and O'Neil, J.R. (1977). Isotopic Evidence for Dramatic Climatic Changes in East Africa During the Pleistocene. *Nature* 267(5607)**,** 137–138.

Cerling, T.E., Manthi, F.K., Mbua, E.N., Leakey, L.N., Leakey, M.G., Leakey, R.E., et al. (2013). Stable isotope-based diet reconstructions of Turkana Basin hominins. *Proceedings of the National Academy of Sciences* 110(26)**,** 10501–10506. doi: 10.1073/pnas.1222568110.

Cerling, T.E., Mbua, E., Kirera, F.M., Manthi, F.K., Grine, F.E., Leakey, M.G., et al. (2011a). Diet of *Paranthropus boisei* in the early Pleistocene of East Africa. *Proceedings of the National Academy of Sciences* 1073(10)**,** 1–5.

Cerling, T.E., and Sharp, Z.D. (1996). Stable Carbon and Oxygen Isotope Analysis of Fossil Tooth Enamel Using Laser Ablation. *Palaeogeography, Palaeoclimatology, Palaeoecology* 126(1-2)**,** 173–186.

Cerling, T.E., Wynn, J.G., Andanje, S.A., Bird, M.I., Korir, D.K., Levin, N.E., et al. (2011b). Woody cover and hominin environments in the past 6 million years. *Nature* 476(7358)**,** 51–56.

Chami, F. (1994). *The Tanzanian coast in the early first millenium AD: An archaeology of the iron-working, farming communities.* PhD dissertation, Uppsala University.

Chami, F. (2001a). "Chicken bones from a Neolithic limestone cave site, Zanzibar: Contact between East Africa and Asia," in *People, Contacts and the Environments in the African Past*, eds. F. Chami, G. Pwiti & C. Radimilahy. (Dar es Salaam University of Dar es Salaam), 84–97.

Chami, F. (2003a). "Climate change on the coast of East Africa since 3000 BC: Archaeological indicators," in *Climate, trade, and modes of production in the Sub-Saharan Africa*, eds. F. Chami, G. Pwiti & C. Radimilahy. (Dar es Salaam: Dar es Salaam University Press), 1–20.

Chami, F. (2003b). "Early ironworking communities on the East African coast: Excavations at Kivinja, Tanzania," in *East African Archaeology: Foragers, Potters, Smiths, and Traders,*

eds. C. Kusimba & S. Kusimba. (Philadelphia: University of Pennsylvania Museum), 87–98.

Chami, F. (2004). "The archaeology of the Mafia Archipelago, Tanzania," in *African Archaeology Network: reports and Views,* eds. F. Chami, G. Pwiti & C. Radimilahy. (Dar es Salaam: Dar es Salaam University Press), 73–101.

Chami, F. (2006). *The Unity of African Ancient History: 3000 BC - AD 500.* Mauritius: E&D Publishers.

Chami, F., and Msemwa, P.J. (1997a). The excavation at Kwale Island, South of Dar es Salaam, Tanzania. *Nyame akuma***,** 45–56.

Chami, F., Pwiti, G., and Radimilahy, C. (2001). *People, Contacts and the Environments in the African Past.* Dar es Salaam University of Dar es Salaam

Chami, F.A. (1992). Limbo: Early iron-working in south-eastern Tanzania. *Azania: Archaeological Research in Africa* 27(1)**,** 45–52. doi: 10.1080/00672709209511430.

Chami, F.A. (1998). A review of Swahili archaeology. *The African Archaeological Review* 15(3)**,** 199–218.

Chami, F.A. (1999). The Early Iron Age on Mafia Island and its relationship with the mainland. 1–10. doi: 10.2307/al.ch.document.sip200023.

Chami, F.A. (2001b). A Response to Christopher Ehret's "Bantu Expansions". *The International Journal of African Historical Studies* 34(3)**,** 647–651. doi: 10.2307/3097559.

Chami, F.A. (2007). Diffusion in the studies of the African past: reflections from new archaeological findings. *The African Archaeological Review* 24(1/2)**,** 1–14. doi: 10.2307/40645410.

Chami, F.A. (2009). *Zanzibar and the Swahili Coast from c.30,000 Years Ago.* Dar es Salaam: E&D Vision Publishing.

Chami, F.A., and Chami, R. (2001). Narosura pottery from the southern coast of Tanzania: First incontro- vertible coastal Later Stone Age pottery. *Nyame akuma***,** 29–35.

Chami, F.A., and Kwekason, A. (2003). Neolithic pottery traditions from the Islands, the Coast and the Interior of East Africa. *The African Archaeological Review* 20(2)**,** 65–80.

Chami, F.A., and Msemwa, P.J. (1997b). A new look at culture and trade on the Azanian coast. *Current Anthropology* 38(4)**,** 673–677.

Chami, F.A., and Silayo, V.V. (2023). Neolithic and Early Iron Age settlements of Mount Kilimanjaro's southern slopes: Re-examining a controversial cultural heritage. *Utafiti* 18(2)**,** 135–159. doi: https://doi.org/10.1163/26836408-15020080.

Chapman, S. (1966). A Sirikwa hole on Mount Elgon. *Azania: Archaeological Research in Africa* 1(1)**,** 139–148. doi: 10.1080/00672706609511346.

Chaput, M.A., Kriesche, B., Betts, M., Martindale, A., Kulik, R., Schmidt, V., et al. (2015). Spatiotemporal distribution of Holocene populations in North America. *Proceedings of the National Academy of Sciences* 112(39)**,** 12127–12132. doi: doi:10.1073/pnas.1505657112.

Chritz, K.L., Cerling, T.E., Freeman, K.H., Hildebrand, E.A., Janzen, A., and Prendergast, M.E. (2019). Climate, ecology, and the spread of herding in eastern Africa. *Quaternary Science Reviews* 204**,** 119–132. doi: https://doi.org/10.1016/j.quascirev.2018.11.029.

Chritz, K.L., and Kinyanjui, R.N. (2025). Human-environment interactions during the emergence of food production in the Turkana Basin, Kenya. *Past Global Changes Magazine* 33(1)**,** 10–11. doi: https://doi.org/10.22498/pages.33.1.10.

Clark, D., and Brandt, S.A. (1984). *From Hunters to Farmers: The Causes and Consequences of Food Production in Africa.* London: University of California Press.

Clist, B. (1987a). A critical reappraisal of the chronological framework of the early Urewe Iron Age industry. *Muntu: revue scientifique et culturelle du CICIBA* (6)**,** 35–62.

Clist, B. (1987b). A critical reappraisal of the chronological framework of the early Urewe Iron Age industry. *Muntu* 6**,** 35–62.

Clist, B., Denbow, J., Jesus, M., Lanfranchi, R., and Mbida Mindzie, C. (2021). Saving 1,000 years of African history: there is no evidence of a population collapse in Congo rainforest from 400 to 600 CE -2. The pottery styles. *Science Advances* 7.

Clist, B., Denbow, J., and Lanfranchi, R. (2023). Using the radiocarbon dates of Central Africa for studying long-term demographic trends of the last 50,000 years: potential and pitfalls. *Azania: Archaeological Research in Africa* 58**,** 1–59. doi: 10.1080/0067270X.2023.2215649.

Codron, D., Sponheimer, M., Codron, J., Newton, I., Lanham, J., and Clauss, M. (2012). The confounding effects of source isotopic heterogeneity on consumer-diet and tissue-tissue stable isotope relationships. *Oecologia* 169**,** 939–953. doi: 10.1007/s00442-012-2274-3.

Collett, D., and Robertshaw, P. (1983). Pottery traditions of early pastoral communities in Kenya. *Azania: Archaeological Research in Africa* 18(1)**,** 107–125. doi: 10.1080/00672708309511317.

Collett, D.P. (1985). *The spread of early iron producing communities in eastern Africa.* PhD Dissertation University of Cambridge.

Collett, D.P., and Robertshaw, P.T. (1980). Early Iron Age and Kansyore Pottery: Finds from Gogo Falls, South Nyanza. *Azania: Archaeological Research in Africa* 15(1)**,** 133–145. doi: 10.1080/00672708009511280.

Courtney Mustaphi, C., Capitani, C., Boles, O., Kariuki, R., Newman, R., Munishi, L., et al. (2019). Integrating evidence of land use and land cover change for land management policy formulation along the Kenya-Tanzania borderlands. *Anthropocene* 28. doi: 10.1016/j.ancene.2019.100228.

Courtney Mustaphi, C., and Marchant, R. (2016). A database of radiocarbon dates for palaeoenvironmental research in eastern Africa. *Open Quaternary* 2**,** 1–7. doi: 10.5334/oq.22.

Courtney Mustaphi, C.J., Kinyanjui, R., Shoemaker, A., Mumbi, C., Muiruri, V., Marchant, L., et al. (2021). A 3000-year record of vegetation changes and fire at a high-elevation wetland on Kilimanjaro, Tanzania. *Quaternary Research* 99**,** 34–62. doi: 10.1017/qua.2020.76.

Coutros, P.R., Matonda, I., Doman, J.H., Pacchiarotti, S., Mesfin, I., and Bostoen, K. (2024). The beginning of the Iron Age south of the Congo rainforest: the first archaeological investigations around Idiofa (Congo), c. 146 BC – AD 1648. *Azania: Archaeological Research in Africa* 59(2)**,** 213–248. doi: 10.1080/0067270X.2024.2296802.

Craig, H. (1953). The geochemistry of the stable carbon isotopes. *Geochimica et Cosmochimica Acta* 3(2)**,** 53–92. doi: https://doi.org/10.1016/0016-7037(53)90001-5.

Craine, J.M., Brookshire, E.N.J., Cramer, M.D., Hasselquist, N.J., Koba, K., Marin-Spiotta, E., et al. (2015a). Ecological interpretations of nitrogen isotope ratios of terrestrial plants and soils. *Plant and Soil* 396(1)**,** 1–26. doi: 10.1007/s11104-015-2542-1.

Craine, J.M., Elmore, A.J., Wang, L., Augusto, L., Baisden, W.T., Brookshire, E.N.J., et al. (2015b). Convergence of soil nitrogen isotopes across global climate gradients. *Scientific Reports* 5(1)**,** 8280. doi: 10.1038/srep08280.

Crombé, P., and Robinson, E. (2014). 14C Dates as demographic proxies in Neolithisation models of northwestern Europe: a critical assessment using Belgium and northeast France as a case-study. *Journal of Archaeological Science* 52. doi: 10.1016/j.jas.2014.02.001.

Crowley, B. (2012). Stable isotope techniques and applications for primatologists. *International Journal of Primatology* 33. doi: 10.1007/s10764-012-9582-7.

Crowley, B.E. (2010). A refined chronology of prehistoric Madagascar and the demise of the megafauna. *Quaternary Science Reviews* 29(19)**,** 2591–2603. doi: https://doi.org/10.1016/j.quascirev.2010.06.030.

Crowley, B.E., Godfrey, L.R., Bankoff, R.J., Perry, G.H., Culleton, B.J., Kennett, D.J., et al. (2017). Island-wide aridity did not trigger recent megafaunal extinctions in Madagascar. *Ecography* 40(8)**,** 901–912. doi: https://doi.org/10.1111/ecog.02376.

Crowther, A., Faulkner, P., Prendergast, M.E., Quintana Morales, E.M., Horton, M., Wilmsen, E., et al. (2016a). Coastal subsistence, maritime trade, and the colonization of small offshore islands in eastern African prehistory. *The Journal of Island and Coastal Archaeology* 11(2)**,** 211–237. doi: 10.1080/15564894.2016.1188334.

Crowther, A., Horton, M., Kotarba-Morley, A., Prendergast, M., Quintana Morales, E., Wood, M., et al. (2014). Iron Age agriculture, fishing and trade in the Mafia Archipelago, Tanzania: new evidence from Ukunju Cave. *Azania: Archaeological Research in Africa* 49(1)**,** 21–44. doi: 10.1080/0067270X.2013.878104.

Crowther, A., Lucas, L., Helm, R., Horton, M., Shipton, C., Wright, H.T., et al. (2016b). Ancient crops provide first archaeological signature of the westward Austronesian expansion. *Proceedings of the National Academy of Sciences of the United States of America* 113(24)**,** 6635–6640. doi: 10.1073/pnas.1522714113.

Crowther, A., Prendergast, M.E., Fuller, D.Q., and Boivin, N. (2018). Subsistence mosaics, forager-farmer interactions, and the transition to food production in eastern Africa. *Quaternary International* 30**,** 1–20. doi: https://doi.org/10.1016/j.quaint.2017.01.014.

Cubas, M., Lucquin, A., Robson, H.K., Colonese, A.C., Arias, P., Aubry, B., et al. (2020). Latitudinal gradient in dairy production with the introduction of farming in Atlantic Europe. *Nature Communications* 11(1)**,** 2036. doi: 10.1038/s41467-020-15907-4.

Culley, C., Janzen, A., Brown, S., Prendergast, M.E., Shipton, C., Ndiema, E., et al. (2021a). Iron Age hunting and herding in coastal eastern Africa: ZooMS identification of domesticates and wild bovids at Panga ya Saidi, Kenya. *Journal of Archaeological Science* 130**,** 105368. doi: https://doi.org/10.1016/j.jas.2021.105368.

Culley, C., Janzen, A., Brown, S., Prendergast, M.E., Wolfhagen, J., Abderemane, B., et al. (2021b). Collagen fingerprinting traces the introduction of caprines to island eastern Africa. *Royal Society Open Science* 8(7)**,** 202341. doi: doi:10.1098/rsos.202341.

Currie, T.E., Meade, A., Guillon, M., and Mace, R. (2013). Cultural phylogeography of the Bantu Languages of sub-Saharan Africa. *Proceedings. Biological sciences* 280(1762)**,** 20130695–20130695. doi: 10.1098/rspb.2013.0695.

D'Andrea, A.C., Richards, M.P., Pavlish, L.A., Wood, S., Manzo, A., and Wolde-Kiros, H.S. (2011). Stable isotopic analysis of human and animal diets from two pre-Aksumite/Proto-Aksumite archaeological sites in northern Ethiopia. *Journal of Archaeological Science* 38(2)**,** 367–374. doi: https://doi.org/10.1016/j.jas.2010.09.015.

da Silveira, L.S.L. (Year). "Oxygen and Hydrogen Isotope Ratios in Plant Cellulose: Mechanisms and Applications", in: *Stable Isotopes in Ecological Research Conference*, eds. P.W. Rundel, J.R. Ehleringer & K.A. Nagy: Springer New York), 124–141.

Dale, D. (2000). Recent archaeological investigation of Kansyore sites in western Kenya. *Azania: Archaeological Research in Africa* 35(1)**,** 204–207. doi: 10.1080/00672700009511604.

Dale, D., and Ashley, C.Z. (2010). Holocene hunter-fisher-gatherer communities: new perspectives on Kansyore Using communities of Western Kenya. *Azania: Archaeological Research in Africa* 45(1)**,** 24–48. doi: 10.1080/00672700903291716.

Dale, D., Marshall, F., and Pilgram, T. (2004). "Delayed-Return Hunter-Gatherer in Africa? Historic Perspectives from the Okiek and Archaeological Perspectives from the Kansyore," in *Hunters and Gatherers in Theory and Archaeology,* ed. G. Crothers. (Carbondale: Southern Illinois University), 340–375.

Dale, D.D. (2007). *An archaeological investigation of the Kansyore, Later Stone Age hunter-gatherers in East Africa.* PhD Washington University in Saint Louis.

Davidson, B., Mhina, J.E.F., and Ogot, B.A. (1967). *The Growth of African Civilization: East and Central Africa to the Late Nineteenth Century.* Nairobi: Longmans of Kenya Limited.

Davies, M. (2008). The irrigation system of the Pokot, northwest Kenya. *Azania: Archaeological Research in Africa* 43(1)**,** 50–76. doi: 10.1080/00672700809480459.

Davies, M.I.J., Kipruto, T.K., and Moore, H.L. (2014). Revisiting the irrigated agricultural landscape of the Marakwet, Kenya: tracing local technology and knowledge over the recent past. *Azania: Archaeological Research in Africa* 49(4)**,** 486–523. doi: 10.1080/0067270X.2014.979527.

Davison, K., Dolukhanov, P.M., Sarson, G., Shukurov, A., and Zaytseva, G. (2006). Multiple Sources of the European Neolithic: Mathematical Modelling Constrained by Radiocarbon Dates. *Quaternary International* 203. doi: 10.1016/j.quaint.2008.04.013.

Davison, S. (1993). Early pottery on the Tiwi coast, south of Mombasa. *Azania: Archaeological Research in Africa* 28(1)**,** 127–130. doi: 10.1080/00672709309511651.

Dawson, T.E., Brooks, P.D., and (2001). "Fundamentals of Stable Isotope Chemistry and Measurement.," in *Stable Isotope Techniques in the Study of Biological Processes and Functioning of Ecosystems,* ed. M. Unkovich. Kluwer Academic Publishers).

Dawson, T.E., Mambelli, S., Plamboeck, A.H., Templer, P.H., and Tu, K.P. (2002). Stable isotopes in plant ecology. *Annual Review of Ecology and Systematics* 33(1)**,** 507–559. doi: doi:10.1146/annurev.ecolsys.33.020602.095451.

De Cort, G., Bessems, I., Keppens, E., Mees, F., Cumming, B., and Verschuren, D. (2013). Late-Holocene and recent hydroclimatic variability in the central Kenya Rift Valley: The sediment record of hypersaline lakes Bogoria, Nakuru and Elementeita. *Palaeogeography, Palaeoclimatology, Palaeoecology* 388**,** 69–80. doi: https://doi.org/10.1016/j.palaeo.2013.07.029.

de Filippo, C., Bostoen, K., Stoneking, M., and Pakendorf, B. (2012). Bringing together linguistic and genetic evidence to test the Bantu expansion. *Proceedings of the Royal Society B: Biological Sciences* 279(1741)**,** 3256–3263. doi: 10.1098/rspb.2012.0318.

de Freitas, A.D.S., de Sá Barretto Sampaio, E.V., de Souza Ramos, A.P., de Vasconcellos Barbosa, M.R., Lyra, R.P., and Araújo, E.L. (2015). Nitrogen isotopic patterns in tropical forests along a rainfall gradient in Northeast Brazil. *Plant and Soil* 391(1)**,** 109–122. doi: 10.1007/s11104-015-2417-5.

De Glanville, W., Davis, A., Allan, K., Buza, J., Claxton, J., Crump, J., et al. (2020). *Classification and characterisation of livestock production systems in northern Tanzania.*

de Maret, P. (2013). "Archaeologies of the Bantu Expansion," in *The Oxford Handbook of African Archaeology,* eds. P. Mitchell & P.J. Lane. Oxford University Press), 0.

de Maret, P. (2025). "A New Bantu Story with More than a Few Thorny Issues."), 83–102.

DeNiro, M.J. (1985). Postmortem preservation and alteration of in vivo bone collagen isotope ratios in relation to palaeodietary reconstruction. *Nature* 317(6040)**,** 806–809. doi: 10.1038/317806a0.

DeNiro, M.J., and Epstein, S. (1978). Influence of diet on the distribution of carbon isotopes in animals. *Geochimica et Cosmochimica Acta* 42(5)**,** 495–506.

Deniro, M.J., and Epstein, S. (1981). Influence of diet on the distribution of nitrogen isotopes in animals. *Geochimica et Cosmochimica Acta* 45(3)**,** 341–351. doi: https://doi.org/10.1016/0016-7037(81)90244-1.

Dewar, R.E., Radimilahy, C., Wright, H.T., Jacobs, Z., Kelly, G.O., and Berna, F. (2013). Stone tools and foraging in northern Madagascar challenge Holocene extinction models. *Proceedings of the National Academy of Sciences* 110(31)**,** 12583–12588. doi: 10.1073/pnas.1306100110.

di Lernia, S., and Tafuri, M.A. (2013). Persistent deathplaces and mobile landmarks: The Holocene mortuary and isotopic record from Wadi Takarkori (SW Libya). *Journal of Anthropological Archaeology* 32(1)**,** 1–15. doi: https://doi.org/10.1016/j.jaa.2012.07.002.

Dickin, A.P. (2018a). *Radiogenic Isotope Geology.* Cambridge: Cambridge University Press.

Dickin, A.P. (2018b). "The Rb–Sr Method," in *Radiogenic Isotope Geology,* ed. A.P. Dickin. 3 ed (Cambridge: Cambridge University Press), 40–66.

Djindjian, F. Big data and archaeology *Humanities Arts and Society*

Douglass, K., Hixon, S., Wright, H.T., Godfrey, L.R., Crowley, B.E., Manjakahery, B., et al. (2019). A critical review of radiocarbon dates clarifies the human settlement of Madagascar. *Quaternary Science Reviews* 221**,** 105878. doi: https://doi.org/10.1016/j.quascirev.2019.105878.

Dühnforth, M., Bergner, A.G.N., and Trauth, M.H. (2006). Early Holocene water budget of the Nakuru-Elmenteita basin, Central Kenya Rift. *Journal of Paleolimnology* 36(3)**,** 281–294. doi: 10.1007/s10933-006-9003-z.

Duller, G. (2008). *Luminescence Dating : Guidelines on using luminescence dating in archaeology.*

Dyvart, K.F., Sealy, J., and Fredriksen, P.D. (2018). Osteological and stable isotope (δ13C and δ15N) analysis of faunal remains from Khami, Zimbabwe. *Azania: Archaeological Research in Africa* 53(4)**,** 507–527. doi: 10.1080/0067270X.2018.1540215.

ECHOES, Zuccarelli Freire, V., Ziegler, M.J., Caetano-Andrade, V., Iminjili, V., Lellau, R., et al. (2024). Addressing the Anthropocene from the Global South: integrating paleoecology, archaeology and traditional knowledge for COP engagement. *Frontiers in Earth Science* 12. doi: 10.3389/feart.2024.1470577.

Eerkens, J.W., Vaughn, K.J., Linares-Grados, M., and Beckham, C. (2024). Long-Term Camelid Husbandry and Agricultural Intensification in the Southern Nasca Region, Peru: Insight from Faunal Isotopes. *Latin American Antiquity* 35(3)**,** 694–711. doi: 10.1017/laq.2023.44.

Ehret, C. (1974). *Ethiopians and East Africans* Nairobi.

Ehret, C. (1997). "Historical Linguistics", in: *Encyclopedia of Africa South Of the Sahara.* (ed.) J. Middleton. (New York: Charles Scribner's Sons).

Ehret, C. (1998). *An African Classical Age: Eastern and Southern Africa in World History, 1000 BC to AD 400.* Charlottesville: University of Virginia Press.

Ehret, C. (2000). "Language and history," in *African Languages: an introduction,* eds. B. Heine & D. Nurse. (Cambridge: Cambridge University Press), 272–297.

Ehret, C. (2001). Bantu expansions: re-envisioning a central problem of early African history. *International Journal of African Historical Studies* (34)**,** 5–43.

Ehret, C. (2002). *The Civilizations of Africa: A History to 1800.* Charlottesville: University Press of Virginia.

Ehret, C., and Posnansky, M. (1968). *The Archaeological and Linguistic Reconstruction of African History.* Berkeley University of California Press

Ehret, C., and Posnansky, M. (1982). *The Archaeological and Linguistic Reconstruction of African History.* Berkeley: University of California Press.

Ekblom, A., Lane, P., Radimilahy, C., Rakotoarisoa, J.-A., Sinclair, P., and Virah-Sawmy, M. (2016). "Migration and Interaction between Madagascar and Eastern Africa, 500 BCE–1000 CE: An Archaeological Perspective."), 195–230.

Englong, A., Punwong, P., Marchant, R., Seelanan, T., Wynne-Jones, S., and Chirawatkul, P. (2023). High-Resolution Multiproxy Record of Environmental Changes and Anthropogenic Activities at Unguja Ukuu, Zanzibar, Tanzania during the Last 5000 Years. *Quaternary* 6**,** 21. doi: 10.3390/quat6010021.

Erendira Malinali Quintana, M., and Prendergast, M. (2017). "Animals and their uses in the Swahili world," in *The Swahli World,* eds. S.W. Jones & A. LaViolette. (London: Routledge), 702.

Erickson, P.A., and Murphy, L.D. (2003). *A History of Anthropological theory.* Ontario: Broadview Press.

Erlandson, J., and Braje, T. (2014). Archaeology and the Anthropocene. *Anthropocene*.

Evans, J., Stoodley, N., and Chenery, C. (2006). A strontium and oxygen isotope assessment of a possible fourth century immigrant population in a Hampshire cemetery, southern England. *Journal of Archaeological Science* 33(2)**,** 265–272. doi: https://doi.org/10.1016/j.jas.2005.07.011.

Evans, J.A., and Chenery, C.A. (2006). Bronze age childhood migration of individuals near Stonehenge, revealed by strontium and oxygen isotope tooth enamel analysis. *Archaeometry* 48**,** 309–321.

Evans, R.D. (2001). Physiological Mechanisms Influencing Plant Nitrogen Isotope Composition. *Trends in Plant Science* 6(3)**,** 121–126.

Fagan, B.M. (1966). Radiocarbon Dates for Sub-Saharan Africa-IV. *The Journal of African History* 7(3)**,** 495–506.

FAO (2018). "Pastoralism in Africa's drylands. Rome. 52 pp. Licence: CC BY-NC-SA 3.0 IGO.".).

Farquhar, G.D., Ehleringer, J.R., and Hubick, K.T. (1989). Carbon isotope discrimination and photosynthesis. *Annual Review of Plant Physiology and Plant Molecular Biology* 40(1)**,** 503–537. doi: doi:10.1146/annurev.pp.40.060189.002443.

Faulkner, P., Harris, M., Ali, A.K., Haji, O., Crowther, A., Horton, M.C., et al. (2018). Characterising marine mollusc exploitation in the eastern African Iron Age: Archaeomalacological evidence from Unguja Ukuu and Fukuchani, Zanzibar. *Quaternary International* 471**,** 66–80. doi: https://doi.org/10.1016/j.quaint.2017.08.051.

Faulkner, P., Harris, M., Haji, O., Ali, A.K., Crowther, A., Shipton, C., et al. (2019). Long-term trends in terrestrial and marine invertebrate exploitation on the eastern African coast: Insights from Kuumbi Cave, Zanzibar. *The Journal of Island and Coastal Archaeology* 14(4)**,** 479–514. doi: 10.1080/15564894.2018.1501442.

Faulkner, P., Miller, J.M., Quintana Morales, E.M., Crowther, A., Shipton, C., Ndiema, E., et al. (2021). 67,000 years of coastal engagement at Panga ya Saidi, eastern Africa. *PLOS ONE* 16(8)**,** e0256761. doi: 10.1371/journal.pone.0256761.

Faulkner, P., Sarathi, A., Crowther, A., Smith, T., Harris, M., Ali, A.K., et al. (2022). Human-ecodynamics and the intertidal zones of the Zanzibar Archipelago. *Frontiers in Earth Science* 10. doi: 10.3389/feart.2022.982694.

Faure, G., and Mensing, T.M. (2005). *Isotopes: Principles and Applications.* New Jersey Wiley.

Faure, G., and Powel, J.L. (1972). *Strontium Isotope Geology.*

Feathers, J. (2003). Use of luminescence dating in archaeology. *Meas. Sci. Technol* 14**,** 1493–1509. doi: 10.1088/0957-0233/14/9/302.

Fenner, J.N., Gagan, M.K., Cowley, J., Armstrong, R., and Prasetyo, B. (2016). Investigating the presence of foreigners and pig husbandry in ancient Bali: Stable isotopes in human and domestic animal tooth enamel. *Journal of Archaeological Science: Reports* 10**,** 272–281. doi: https://doi.org/10.1016/j.jasrep.2016.09.014.

Fernandes, R. (2013). A freshwater lake saga: Carbon routing within the aquatic food web of Lake Schwerin. *Radiocarbon* 55. doi: 10.2458/azu_js_rc.55.16357.

Fernandes, R. (2016). A Simple(R) model to predict the source of dietary carbon in individual consumers. *Archaeometry* 58(3)**,** 500–512. doi: https://doi.org/10.1111/arcm.12193.

Fernandes, R., Grootes, P., Nadeau, M.-J., and Nehlich, O. (2015). Quantitative diet reconstruction of a Neolithic population using a Bayesian mixing model (FRUITS): The case study of Ostorf (Germany). *American Journal of Physical Anthropology* 158(2)**,** 325–340. doi: https://doi.org/10.1002/ajpa.22788.

Fernandes, R., Rinne, C., Nadeau, M.-J., and Grootes, P. (2016). Towards the use of radiocarbon as a dietary proxy: Establishing a first wide-ranging radiocarbon reservoir effects baseline for Germany. *Environmental Archaeology* 21(3)**,** 285–294. doi: 10.1179/1749631414Y.0000000034.

Finucane, B., Agurto, P.M., and Isbell, W.H. (2006). Human and animal diet at Conchopata, Peru: stable isotope evidence for maize agriculture and animal management practices during the Middle Horizon. *Journal of Archaeological Science* 33(12)**,** 1766–1776. doi: https://doi.org/10.1016/j.jas.2006.03.012.

Fischer-Ausserer, K., Börner, W., and Goriany, M. (2003). "Archaeological Information. An Information Scientist Looks on Archaeology," in *Enter the Past. The E-way into the four Dimensions of Cultural Heritage. CAA 2003. Computer Applications and Quantitative Methods in Archaeology (BAR International Series 1227)*.).

Fischer, M.L., Markowska, M., Bachofer, F., Foerster, V.E., Asrat, A., Zielhofer, C., et al. (2020). Determining the Pace and Magnitude of Lake Level Changes in Southern Ethiopia Over the Last 20,000 Years Using Lake Balance Modeling and SEBAL. *Frontiers in Earth Science* Volume 8 - 2020. doi: 10.3389/feart.2020.00197.

Fisher, E. (2020). "Archaeoinformatics". Oxford University Press).

Fitton, T., and Wynne-Jones, S. (2017). Understanding the layout of early coastal settlement at Unguja Ukuu, Zanzibar. *Antiquity* 91**,** 1268–1284. doi: 10.15184/aqy.2017.141.

Fitzpatrick, S.M., Rick, T.C., and Erlandson, J.M. (2015). Recent progress, trends, and developments in island and coastal archaeology. *The Journal of Island and Coastal Archaeology* 10(1)**,** 3–27. doi: 10.1080/15564894.2015.1013647.

Fleagle, J. (1999). *Primate Adaptation and Evolution.* San Diego: Academic Press.

Fleagle, J., and Kamilar, J. (2007). Primate diversity: Past, present, and future. *Evolutionary Anthropology: Issues, News, and Reviews* 16(3)**,** 83–85.

Foerster, V., Vogelsang, R., Junginger, A., Asrat, A., Lamb, H.F., Schaebitz, F., et al. (2015). Environmental change and human occupation of southern Ethiopia and northern Kenya during the last 20,000 years. *Quaternary Science Reviews* 129**,** 333–340. doi: https://doi.org/10.1016/j.quascirev.2015.10.026.

Fortes-Lima, C.A., Burgarella, C., Hammarén, R., Eriksson, A., Vicente, M., Jolly, C., et al. (2024). The genetic legacy of the expansion of Bantu-speaking peoples in Africa. *Nature* 625(7995)**,** 540–547. doi: 10.1038/s41586-023-06770-6.

Fraedrich, K., Jiang, J., Gerstengarbe, F.-W., and Werner, P.C. (1997). Multiscale detection of abrupt climate changes: application to River Nile flood levels. *International Journal of Climatology* 17(12)**,** 1301–1315. doi: https://doi.org/10.1002/(SICI)1097-0088(199710)17:12<1301::AID-JOC196>3.0.CO;2-W.

Francey, R.J., Allison, C.E., Etheridge, D.M., Trudinger, C.M., Enting, I.G., Leuenberger, M., et al. (1999). A 1000-year high precision record of $\delta^{13}C$ in atmospheric CO_2. *Tellus B* 51(2)**,** 170–193. doi: 10.1034/j.1600-0889.1999.t01-1-00005.x.

Fraser, R.A., Bogaard, A., Heaton, T.H.E., Charles, M.P., Jones, G., Christensen, B.T., et al. (2011). Manuring and stable nitrogen isotope ratios in cereals and pulses : towards a new archaeobotanical approach to the inference of land use and dietary practices. *Journal of Archaeological Science* 38**,** 2790–2804.

Fratkin, E. (2001). East African Pastoralism in Transition: Maasai, Boran, and Rendille Cases. *African Studies Review* 44(3)**,** 1–25. doi: 10.2307/525591.

Fuller, D.Q. (2003). "African crops in prehistoric South Asia: a critical review," in *Food, Fuel and Fields: Progress in African Archaeobotany,* eds. K. Neumann, A. Butler & S. Kahlheber. (Cologne: Heinrich-Barth-Institut), 239–271.

Fuller, D.Q., Barron, A., Champion, L., Dupuy, C., Commelin, D., Raimbault, M., et al. (2021). Transition From Wild to Domesticated Pearl Millet (Pennisetum glaucum) Revealed in Ceramic Temper at Three Middle Holocene Sites in Northern Mali. *Afr Archaeol Rev* 38(2)**,** 211–230. doi: 10.1007/s10437-021-09428-8.

Fuller, D.Q., Champion, L., and Stevens, C. (2019). "Comparing the tempo of cereal dispersal and the agricultural transition: two African and one West Asian trajectory," in *Trees, Grasses and Crops: People and Plants in Sub-Saharan Africa and Beyond,* eds. B. Eichhorn & A. Hohn. (Bonn: Verlag Dr. Rudolf Habelt GmbH).

Fuller, D.Q., and Stevens, C.J. (2018). "Sorghum Domestication and Diversification: A Current Archaeobotanical Perspective," in *Plants and People in the African Past: Progress in African Archaeobotany,* eds. A.M. Mercuri, A.C. D'Andrea, R. Fornaciari & A. Höhn. (Cham: Springer International Publishing), 427–452.

Gagnon, M., and Chew, A.E. (2000). Dietary preferences in extant African Bovidae. *Journal of Mammalogy* 81(2)**,** 490–511. doi: https://doi.org/10.1644/1545-1542(2000)081<0490:DPIEAB>2.0.CO;2.

Galaty, J. (2021). "Pastoralism in Eastern Africa," in *Oxford Research Encyclopedia of African History.* (Oxford: Oxford University Press).

Galaty, J.G. (1982). Being 'Maasai'; being 'people of cattle'; ethnic shiftes in East Africa. *American Ethnologist* 9**,** 1–20.

Galaty, J.G. (1993). "Maasai Expansion and the New East African Pastoralism," in *Being Maasai: Ethnicity and identity in East Africa,* eds. T. Spear & R. Waller. (London: James Currey), 61–86.

Galaty, J.G. (2016). Reasserting the commons: Pastoral contestations of private and state lands in East Africa. *International Journal of the Commons*. doi: 10.18352/ijc.720.

Garcin, Y., Melnick, D., Strecker, M.R., Olago, D., and Tiercelin, J.-J. (2012). East African mid-Holocene wet–dry transition recorded in palaeo-shorelines of Lake Turkana, northern Kenya Rift. *Earth and Planetary Science Letters* 331-332**,** 322–334. doi: https://doi.org/10.1016/j.epsl.2012.03.016.

Garten, C., Hanson, P., Todd, D., Lu, B., and Brice, D. (2008). "Natural 15N- and 13C-Abundance as Indicators of Forest Nitrogen Status and Soil Carbon Dynamics."), 61–82.

Gasse, F. (2000). Hydrological changes in the African tropics since the Last Glacial Maximum. *Quaternary Science Reviews* 19(1)**,** 189–211. doi: https://doi.org/10.1016/S0277-3791(99)00061-X.

Gattiglia, G. (2015). Think big about data: Archaeology and the Big Data challenge. *Archäologische Informationen* 38. doi: 10.11588/ai.2015.1.26155.

Gelorini, V., and Verschuren, D. (2013). Historical climate-human-ecosystem interaction in East Africa: a review. *African Journal of Ecology* 51(3)**,** 409–421. doi: 10.1111/aje.12045.

Gerschlauer, F., Saiz, G., Schellenberger Costa, D., Kleyer, M., Dannenmann, M., and Kiese, R. (2019). Stable carbon and nitrogen isotopic composition of leaves, litter, and soils of various ecosystems along an elevational and land-use gradient at Mount Kilimanjaro, Tanzania. *Biogeosciences* 16(2)**,** 409–424. doi: 10.5194/bg-16-409-2019.

Giblin, J., and Fuller, D. (2011). First and second millennium AD agriculture in Rwanda: archaeobotanical finds and radiocarbon dates from seven sites. *Vegetation History and Archaeobotany* 20**,** 253–265. doi: 10.1007/s00334-011-0288-0.

Giblin, J., and Humphris, J. (2010). An Urewe burial in Rwanda: Exchange, health, wealth and violence c. AD 400. *Azania: Archaeological Research in Africa* 45**,** 276–297. doi: 10.1080/0067270X.2010.521677.

Giblin, J.D. (2008). New work on the later archaeology of Rwanda 2006 to 2007 : A preliminary fieldwork report. *Nyame akuma***,** 45–55.

Gifford-Gonzalez, D. (1998). Early Pastoralists in East Africa: Ecological and Social Dimensions. *Journal of Anthropological Archaeology* 17(2)**,** 166–200. doi: https://doi.org/10.1006/jaar.1998.0322.

Gifford-Gonzalez, D. (2003). The fauna from Ele Bor: evidence for the persistence of foragers into the later Holocene of arid North Kenya. *African Archaeological Review* 20(2)**,** 81–119. doi: 10.1023/A:1024410814287.

Gifford-Gonzalez, D. (2017). "Animal disease challenges" fifteen years later: The hypothesis in light of new data. *Quaternary International* 436**,** 283–293. doi: https://doi.org/10.1016/j.quaint.2015.10.054.

Gifford-Gonzalez, D.P., and Kimengich, J. (1984). "Faunal Evidence for Early Stock-keeping in the Central Rift of Kenya: Preliminary Finds," in *Origin and Early Development of Food-Producing Cultures in North-Eastern Africa,* eds. L. Krzyzaniak & M. Kobusiewicz. (Poznan: Polish Academy of Sciences and Poznan Archaeological Museum), 457–471.

Gifford, D.P., Isaac, G.L., and Nelson, C.M. (1980). Evidence for predation and pastoralism at Prolonged Drift: a Pastoral Neolithic site in Kenya. *Azania: Archaeological Research in Africa* 15(1)**,** 57–108. doi: 10.1080/00672708009511277.

Gillis, R.E., Eckelmann, R., Filipović, D., Müller-Scheeßel, N., Cheben, I., Furholt, M., et al. (2020). Stable isotopic insights into crop cultivation, animal husbandry, and land use at the Linearbandkeramik site of Vráble-Veľké Lehemby (Slovakia). *Archaeological and Anthropological Sciences* 12(11)**,** 256. doi: 10.1007/s12520-020-01210-2.

Giraldo, J., del Valle, J., González-Caro, S., and Sierra, C. (2022). Intra-annual isotope variations in tree rings reveal growth rhythms within the least rainy season of an ever-wet tropical forest. *Trees*. doi: 10.1007/s00468-022-02271-7.

Githumbi, E.N., Courtney Mustaphi, C.J., Yun, K.J., Muiruri, V., Rucina, S.M., and Marchant, R. (2018). Late Holocene wetland transgression and 500 years of vegetation and fire variability in the semi-arid Amboseli landscape, southern Kenya. *Ambio* 47(6)**,** 682–696. doi: 10.1007/s13280-018-1014-2.

Gkiasta, M., Russell, T., Shennan, S., and Steele, J. (2004). Neolithic transition in Europe: The radiocarbon record revisited. *Gkiasta, M. and Russell, T. and Shennan, S. and Steele, J. (2003) Neolithic transition in Europe: the radiocarbon record revisited. Antiquity, 77 (295). pp. 45-62. ISSN 0003598X* 77. doi: 10.1017/S0003598X00061330.

Godfrey, L.R., Scroxton, N., Crowley, B.E., Burns, S.J., Sutherland, M.R., Pérez, V.R., et al. (2019). A new interpretation of Madagascar's megafaunal decline: The "Subsistence Shift Hypothesis". *Journal of Human Evolution* 130**,** 126–140. doi: https://doi.org/10.1016/j.jhevol.2019.03.002.

Goldstein, S., Hixon, S., Scott, E., Wolfhagen, J., Iminjili, V., Janzen, A., et al. (2022a). Presenting the AfriArch Isotopic Database. *Journal of Open Archaeology Data* 10. doi: 10.5334/joad.94.

Goldstein, S., O'Brien, K., Adum, A., and Mwangi, J. (2023). A multi-component forager-to-herder sequence at Kapsoo Rockshelter (Chebinyiny) on the Uasin Gishu Plateau, Kenya. *Azania: Archaeological Research in Africa***,** 1–27. doi: 10.1080/0067270X.2023.2259751.

Goldstein, S.T., Mueller, N.G., Finestone, E., Sawchuk, E.A., Juengst, S., Otwani, A.O., et al. (2025). Cultural, economic, and settlement shifts over the last 9,000 years at Kakapel Rockshelter, Western Kenya. *PLOS ONE* 20(8)**,** e0328805. doi: 10.1371/journal.pone.0328805.

Goldstein, S.T., Mueller, N.G., Janzen, A., Finestone, E., Sawchuk, E.A., Juengst, S., et al. (forthcoming). A 9,000 year record of subsistence transitons and population change at Kakapel Rockshelter, western Kenya. *PLOS*

Goldstein, S.T., Mueller, N.G., Janzen, A., Ogola, C., Dal Martello, R., Fernandes, R., et al. (2024). Early agriculture and crop transitions at Kakapel Rockshelter in the Lake Victoria region of eastern Africa. *Proceedings of the Royal Society B: Biological Sciences* 291(2026)**,** 20232747. doi: doi:10.1098/rspb.2023.2747.

Goldstein, S.T., Shipton, C., Miller, J.M., Ndiema, E., Boivin, N., and Petraglia, M. (2022b). Hunter-gatherer technological organization and responses to Holocene climate change in coastal, lakeshore, and grassland ecologies of eastern Africa. *Quaternary Science Reviews* 280**,** 107390. doi: https://doi.org/10.1016/j.quascirev.2022.107390.

Goodman, S., Raherilalao, M.J., and Muldoon, K. (2013). Bird fossils from Ankilitelo Cave: Inference about Holocene environmental changes in Southwestern Madagasca. *Zootaxa* 3750**,** 534–548. doi: 10.11646/zootaxa.3750.5.6.

Goodman, S.M. (Year). "Holocene bird subfossils from the sites of Ampasambazimba, Antsirabe and Ampoza, Madagascar: changes in the avifauna of south central Madagascar over the past few millennia", in: *Proceedings of the 22nd International Ornithological Congress*, eds. N.J. Adams & R.H. Slotow: BirdLife South Africa), 3071–3083.

Goodman, S.M., and Rakotozafy, L.M.A. (1997). "Subfossil birds from coastal sites in western and southwestern Madagascar: a paleoenvironmental reconstruction," in *Natural Change and Human Impacts in Madagascar,* eds. S.M. Goodman & B. Patterson. (Washington DC: Smithsonian Institution Press), 142–168.

Gramly, R.M. (1975). *Pastoralists and hunters: recent prehistory in southern Kenya and northern Tanzania.* PhD Harvard University.

Gramly, R.M., and Rightmire, G.P. (1973). A fragmentary cranium and dated later Stone Age assemblage from Lukenya Hill, Kenya. *Man.* 8**,** 571–579.

Greenberg, J.H. (1963). *The Languages of Africa.* The Hague: Mouton.

Greiner, C., Vehrs, H.-P., and Bollig, M. (2021). Land-use and Land-cover Changes in Pastoral Drylands: Long-term Dynamics, Economic Change, and Shifting Socioecological Frontiers in Baringo, Kenya. *Human Ecology* 49(5)**,** 565–577. doi: 10.1007/s10745-021-00263-8.

Grillo, K., McKeeby, Z., and Hildebrand, E. (2020a). "Nderit Ware" and the origins of pastoralist pottery in eastern Africa. *Quaternary International*. doi: 10.1016/j.quaint.2020.06.032.

Grillo, K., Prendergast, M., Contreras, D., Fitton, T., Gidna, A., Goldstein, S., et al. (2018). Pastoral Neolithic settlement at Luxmanda, Tanzania. *Journal of Field Archaeology* 43**,** 102–120. doi: 10.1080/00934690.2018.1431476.

Grillo, K.M., Dunne, J., Marshall, F., Prendergast, M.E., Casanova, E., Gidna, A.O., et al. (2020b). Molecular and isotopic evidence for milk, meat, and plants in prehistoric eastern African herder food systems. *Proceedings of the National Academy of Sciences* 117(18)**,** 9793–9799. doi: 10.1073/pnas.1920309117.

Grillo, K.M., and Hildebrand, E.A. (2013). The context of early megalithic architecture in eastern Africa: the Turkana Basin c. 5000-4000 BP. *Azania: Archaeological Research in Africa* 48(2)**,** 193–217. doi: 10.1080/0067270X.2013.789188.

Grillo, K.M., McKeeby, Z., and Hildebrand, E.A. (2022). “Nderit Ware” and the origins of pastoralist pottery in eastern Africa. *Quaternary International* 608-609**,** 226–242. doi: https://doi.org/10.1016/j.quaint.2020.06.032.

Grollemund, R., Branford, S., Bostoen, K., Meade, A., Venditti, C., and Pagel, M. (2015). Bantu expansion shows that habitat alters the route and pace of human dispersals. *Proceedings of the National Academy of Sciences* 112(43)**,** 13296–13301. doi: doi:10.1073/pnas.1503793112.

Grollemund, R., Schoenbrun, D., and Vansina, J. (2023). Moving Histories: Bantu Language Expansions, Eclectic Economies, and Mobilities. *The Journal of African History* 64(1)**,** 13–37. doi: 10.1017/S0021853722000780.

Guiserix, D., Albalat, E., Ueckermann, H., Davechand, P., Iaccheri, L., Bybee, G., et al. (2022). Simultaneous analysis of stable and radiogenic strontium isotopes in reference materials, plants and modern tooth enamel. *Chemical Geology* 606**,** 121000. doi: 10.1016/j.chemgeo.2022.121000.

Hajdas, I. (2008). Radiocarbon dating and its applications in Quaternary studies. *Quaternary Science Journal* 57. doi: 10.3285/eg.57.1-2.1.

Hajdas, I., Kull, C., and Kiefer, T. (2006). ^{14}C- Chronology. *PAGES magazine*.

Hakenbeck, S. (2013). Potential and limitations of isotope analysis in early medieval archaeology. *Postclassical Archaeologies* 3**,** 109–125.

Håland, R., and Msuya, C.S. (2000). Pottery production, iron working, and trade in the Early Iron Age: the case of Dakawa, east-central Tanzania. *Azania: Archaeological Research in Africa* 35(1)**,** 75–106. doi: 10.1080/00672700009511597.

Hamilton, M.J., and Buchanan, B. (2007). Spatial gradients in Clovis-age radiocarbon dates across North America suggest rapid colonization from the north. *Proceedings of the National Academy of Sciences* 104(40)**,** 15625–15630. doi: doi:10.1073/pnas.0704215104.

Hamilton, R.W. (1920). Land Tenure among the Bantu Wanyika of East Africa. *Journal of the Royal African Society* 20(77)**,** 13–18.

Hannaford, M.J. (2023). Deep histories of food systems in eastern Africa and current patterns of food insecurity. *Nature Food* 4(11)**,** 949–960. doi: 10.1038/s43016-023-00879-7.

Hansford, J., Wright, P.C., Rasoamiaramanana, A., Pérez, V.R., Godfrey, L.R., Errickson, D., et al. (2018). Early Holocene human presence in Madagascar evidenced by exploitation of avian megafauna. *Science Advances* 4(9)**,** eaat6925. doi: 10.1126/sciadv.aat6925.

Hare, V.J., and Loftus, E. (2018). "Scientific Dating Methods in African Archaeology". Oxford University Press).

Harris, M. (2001). *The Rise of Anthropological Theory : A History of Theories of Culture.* Walnut Creek, CA: AltaMira Press.

Hartigan, J.A., and Wong, M.A. (1979). Algorithm AS 136: A k-means clustering algorithm. *Journal of the Royal Statistical Society. Series C (Applied Statistics)* 28(1)**,** 100–108. . doi: https://doi.org/10.2307/2346830.

Hartman, G. (2011). Are elevated δ15N values in herbivores in hot and arid environments caused by diet or animal physiology? *Functional Ecology* 25(1)**,** 122–131. doi: https://doi.org/10.1111/j.1365-2435.2010.01782.x.

Hassan, F.A. (1981). Historical Nile floods and their implications for climatic change. *Science* 212(4499)**,** 1142–1145. doi: 10.1126/science.212.4499.1142.

Hastenrath, S., and Kutzbach, J.E. (1983). Paleoclimatic estimates from water and energy budgets of East African Lakes. *Quaternary Research* 19(2)**,** 141–153. doi: https://doi.org/10.1016/0033-5894(83)90001-7.

Heaton, T.J., Köhler, P., Butzin, M., Bard, E., Reimer, R.W., Austin, W.E.N., et al. (2020). Marine20—The Marine Radiocarbon Age Calibration Curve (0–55,000 cal BP). *Radiocarbon* 62(4)**,** 779–820. doi: 10.1017/RDC.2020.68.

Helm, R., Crowther, A., Shipton, C., Tengeza, A., Fuller, D., and Boivin, N. (2012). Exploring agriculture, interaction and trade on the eastern African littoral: preliminary results from Kenya. *Azania Archaeological Research in Africa* 47. doi: 10.1080/0067270X.2011.647947.

Helm, R.M. (2000). Recent archaeological research on the iron-working, farming communities of coastal Kenya. *Azania: Archaeological Research in Africa* 35(1)**,** 183–189. doi: 10.1080/00672700009511601.

Henton, E., Martin, L., Garrard, A., Jourdan, A.-L., Thirlwall, M., and Boles, O. (2017). Gazelle seasonal mobility in the Jordanian steppe: The use of dental isotopes and microwear as environmental markers, applied to Epipalaeolithic Kharaneh IV. *Journal of Archaeological Science: Reports* 11**,** 147–158. doi: https://doi.org/10.1016/j.jasrep.2016.11.031.

Hildebrand, E.A., and Grillo, K.M. (2012). Early herders and monumental sites in eastern Africa: dating and interpretation. *Antiquity* 86(332)**,** 338–352. doi: 10.1017/S0003598X00062803.

Hildebrand, E.A., Grillo, K.M., Sawchuk, E.A., Pfeiffer, S.K., Conyers, L.B., Goldstein, S.T., et al. (2018). A monumental cemetery built by eastern Africa's first herders near Lake Turkana, Kenya. *Proceedings of the National Academy of Sciences* 115(36)**,** 8942–8947. doi: 10.1073/pnas.1721975115.

Hildebrand, E.A., Shea, J.J., and Grillo, K.M. (2011). Four middle Holocene pillar sites in West Turkana, Kenya. *Journal of Field Archaeology* 36(3)**,** 181–200. doi: 10.1179/009346911X12991472411088.

Hixon, S., Douglass, K., Crowley, B., Rakotozafy, L., Clark, G., Anderson, A., et al. (2021a). Late Holocene spread of pastoralism coincides with endemic megafaunal extinction on Madagascar. *Proceedings. Biological sciences* 288**,** 20211204. doi: 10.1098/rspb.2021.1204.

Hixon, S.W., Curtis, J.H., Brenner, M., Douglass, K.G., Domic, A.I., Culleton, B.J., et al. (2021b). Drought coincided with, but does not explain, Late Holocene megafauna extinctions in SW Madagascar. *Climate* 9(9)**,** 138.

Hixon, S.W., Douglass, K.G., Godfrey, L.R., Eccles, L., Crowley, B.E., Rakotozafy, L.M.A., et al. (2021c). Ecological consequences of a Millennium of introduced dogs on Madagascar. *Frontiers in Ecology and Evolution* 9. doi: 10.3389/fevo.2021.689559.

Hoefs, J. (2009). *Stable Isotope Geochemistry.* Gottingen Springer-Verlag Berlin Heidelberg

Hofmanová, Z., Kreutzer, S., Hellenthal, G., Sell, C., Diekmann, Y., Díez-del-Molino, D., et al. (2016). Early farmers from across Europe directly descended from Neolithic Aegeans. *Proceedings of the National Academy of Sciences* 113(25)**,** 6886–6891. doi: doi:10.1073/pnas.1523951113.

Högberg, A., Brink, K., Brorsson, T., and Malmström, H. (2025). Transdisciplinary Theoretical Approaches to Migration Studies in Archaeology. *Cambridge Archaeological Journal* 35(3)**,** 418–434. doi: 10.1017/S0959774325000046.

Hogberg, P. (1997). Tansley Review No. 95 ^{15}N Natural Abundance in Soil-Plant Systems. *New Phytol* 137**,** 179–203.

Hogg, A.G., Heaton, T.J., Hua, Q., Palmer, J.G., Turney, C.S.M., Southon, J., et al. (2020). SHCal20 Southern Hemisphere Calibration, 0–55,000 Years cal BP. *Radiocarbon* 62(4)**,** 759–778. doi: 10.1017/RDC.2020.59.

Holt, E., Evans, J.A., and Madgwick, R. (2021). Strontium (87Sr/86Sr) mapping: A critical review of methods and approaches. *Earth-Science Reviews* 216**,** 103593. doi: https://doi.org/10.1016/j.earscirev.2021.103593.

Hopkins, D.W., Wheatley, R.E., and Robinson, D. (2020). "Stable isotope studies of soil nitrogen."), 75–88.

Horton, M. (1996). *Shanga: The archaeology of a Muslim trading community on the coast of East Africa.* London: The British Institute in Eastern Africa.

Horton, M. (2017). "Zanzibar and Pemba: the archaeology of an Indian Ocean Archipelago". British Institute in Eastern Africa.).

Horton, M., and Middleton, J. (2000). *The Swahili: The Social Landscape of a Mercantile Society.* Oxford: Blackwell Publishers.

Horton, M., Olsen, J., Fleisher, J., and Wynne-Jones, S. (2022). The chronology of Kilwa Kisiwani, AD 800–1500. *African Archaeological Review* 39. doi: 10.1007/s10437-022-09476-8.

Huffman, T., and Vogel, J. (1991). The chronology of Great Zimbabwe. *The South African Archaeological Bulletin* 46**,** 61. doi: 10.2307/3889086.

Huffman, T.N. (1970). The Early Iron Age and the spread of the Bantu. *The South African Archaeological Bulletin* 25(97)**,** 3–21. doi: 10.2307/3888762.

Huffman, T.N., and Herbert, R.K. (1994). New perspectives on eastern Bantu. *Azania: Archaeological Research in Africa* 29-30(1)**,** 27–36. doi: 10.1080/00672709409511659.

Huggett, J. (2020). Is Big Digital Data different? Towards a new archaeological paradigm. *Journal of Field Archaeology* 45(sup1)**,** S8–S17. doi: 10.1080/00934690.2020.1713281.

Iacumin, P., Bocherens, H., Chaix, L., and Marioth, A. (1998). Stable Carbon and Nitrogen Isotopes as Dietary Indicators of Ancient Nubian Populations (Northern Sudan). *Journal of Archaeological Science* 25(4)**,** 293–301. doi: https://doi.org/10.1006/jasc.1997.0206.

Ibeagha-Awemu, E.M., Osei-Amponsah, R., and Bemji, M.N. (2026). "African Livestock Production Systems: The Past, Present and the Projected Future," in *African Livestock Genetic Resources and Sustainable Breeding Strategies: Unlocking a Treasure Trove and Guide for Improved Productivity,* eds. E.M. Ibeagha-Awemu, S.O. Peters, A. Djikeng & J.E.O. Rege. (Cham: Springer Nature Switzerland), 13–64.

Iminjili, V. (2012). *The utility of refined δ13C values in hominin paleoecology.* Master of Arts, University of Georgia.

Iminjili, V., Crowther, A., Fisher, M., Kay, A., Roberts, P., Goldstein, S., et al. (2025a). Wanyika: A dataset of scientific dates from archaeological sites in eastern Africa spanning 5000 BCE to 1800 CE. doi: https://www.doi.org/10.48493/mwsp-e133

Iminjili, V., Crowther, A., Fisher, M.T., Kay, A., Roberts, P., Goldstein, S., et al. (2025b). A dataset of scientific dates from archaeological sites in eastern Africa spanning 5000 BCE to 1800 CE. *Scientific Data* 12(1)**,** 801. doi: 10.1038/s41597-025-05138-x.

Iminjili, V., and Fernandes, R. (2023). Zanadamu: An African hominin isotopic dataset. *Data in Brief* 50**,** 109522. doi: https://doi.org/10.1016/j.dib.2023.109522.

Iminjili, V., Stewart, M., Culley, C., Hixon, S., Goldstein, S., Bleasdale, M., et al. (2023). Late Pleistocene to late Holocene palaeoecology and human foraging at Kuumbi Cave, Zanzibar Island. *Frontiers in Environmental Archaeology* 2. doi: 10.3389/fearc.2023.1080785.

Inkscape. 2024. Vector graphics editor. Available: https://inkscape.org/release/inkscape-1.3.2/windows/64-bit/msi/?redirected=1.

Ito, P.K. (1980). 7 Robustness of ANOVA and MANOVA test procedures. *Handbook of Statistics* 1**,** 199–236.

Janzen, A. (2015). *Mobility and herd management strategies of early pastoralists in South Central Kenya.* PhD, University of California.

Janzen, A. (2022). Insights into herd management among East Africa's earliest pastoralists: Combining zooarchaeological data and stable isotope analysis. *Quaternary international***,** pp. —2022. doi: 10.1016/j.quaint.2022.05.018.

Janzen, A., Balasse, M., and Ambrose, S.H. (2020a). Early pastoral mobility and seasonality in Kenya assessed through stable isotope analysis. *Journal of Archaeological Science* 117**,** 105099. doi: https://doi.org/10.1016/j.jas.2020.105099.

Janzen, A., Bataille, C., Copeland, S.R., Quinn, R.L., Ambrose, S.H., Reed, D., et al. (2020b). Spatial variation in bioavailable strontium isotope ratios (87Sr/86Sr) in Kenya and northern Tanzania: Implications for ecology, paleoanthropology, and archaeology. *Palaeogeography, Palaeoclimatology, Palaeoecology* 560**,** 109957. doi: https://doi.org/10.1016/j.palaeo.2020.109957.

Janzen, A., Richter, K.K., Mwebi, O., Brown, S., Onduso, V., Gatwiri, F., et al. (2021). Distinguishing African bovids using Zooarchaeology by Mass Spectrometry (ZooMS): New peptide markers and insights into Iron Age economies in Zambia. *PLOS ONE* 16(5)**,** e0251061. doi: 10.1371/journal.pone.0251061.

Jiang, J., Mendelssohn, R., Schwing, F., and Fraedrich, K. (2002). Coherency detection of multiscale abrupt changes in historic Nile flood levels. *Geophysical Research Letters* 29(8)**,** 112–111–112–114. doi: https://doi.org/10.1029/2002GL014826.

Jim, S., Ambrose, S., and Evershed, R. (2004). Stable carbon isotopic evidence for differences in the dietary origin of bone cholesterol, collagen and apatite: Implications for their use in palaeodietary reconstruction. *Geochimica et Cosmochimica Acta* 68**,** 61–72. doi: 10.1016/S0016-7037(03)00216-3.

Jones, M.B., and Brandt, S.A. (2022). 20,000 years of small game hunting in southern Somalia. *Quaternary International*. doi: https://doi.org/10.1016/j.quaint.2022.06.004.

Julien, M.-A., Bocherens, H., Burke, A., Drucker, D.G., Patou-Mathis, M., Krotova, O., et al. (2012). Were European steppe bison migratory? 18O, 13C and Sr intra-tooth isotopic variations applied to a palaeoethological reconstruction. *Quaternary International* 271**,** 106–119. doi: https://doi.org/10.1016/j.quaint.2012.06.011.

Juma, A. (2004). *Unguja Ukuu on Zanzibar : An archaeological study of early urbanism.* Doctoral thesis, monograph, Afrikansk och jämförande arkeologi.

Kabiru, A. (2017). *An exploratory study of Middle Stone Age and Later Stone Age site locations in Kenya's central Rift Valley using landscape analysis: A GIS approach.* MSC, Lund University.

Kahlheber, S., Bostoen, K., and Neumann, K. (2009). Early Plant Cultivation in the Central African Rain Forest: First Millennium BC Pearl Millet from South Cameroon. *Journal of African Archaeology* 7**,** 253–272. doi: 10.3213/1612-1651-10142.

[Dataset] Kaplan, J.O., and Krumhardt, K.M. (2011). *The KK10 Anthropogenic Land Cover Change scenario for the preindustrial Holocene, link to data in NetCDF format.* PANGAEA. doi: 10.1594/PANGAEA.871369. Available: https://doi.org/10.1594/PANGAEA.871369.

Kaplan, J.O., Krumhardt, K.M., Ellis, E.C., Ruddiman, W.F., Lemmen, C., and Goldewijk, K.K. (2011). Holocene carbon emissions as a result of anthropogenic land cover change. *The Holocene* 21(5)**,** 775–791. doi: 10.1177/0959683610386983.

Karanth, K.P., Delefosse, T., Rakotosamimanana, B., Parsons, T.J., and Yoder, A.D. (2005). Ancient DNA from giant extinct lemurs confirms single origin of Malagasy primates. *Proceedings of the National Academy of Sciences* 102(14)**,** 5090–5095. doi: doi:10.1073/pnas.0408354102.

Karega, M. (1996). The east African Neolithic: An alternative view. *African Archaeological Review* 13(4)**,** 247–254. doi: 10.1007/BF02126098.

Kassam, A. (1986). The Gabbra Pastoralist/Waata Hunter-Gatherer Symbiosis: A Symbolic Interpretation. *Sprache und Geschichte in Afrika* 7(1)**,** 189–204.

Kassam, A. (1987). The Process of Becoming: Gabra Oromo Transition Rites (Jilla). *Azania: Archaeological Research in Africa* 22(1)**,** 55–75. doi: 10.1080/00672708709511381.

Kay, A.U., Fuller, D.Q., Neumann, K., Eichhorn, B., Höhn, A., Morin-Rivat, J., et al. (2019). Diversification, intensification and specialization: changing land use in western Africa from 1800 BC to AD 1500. *Journal of World Prehistory* 32(2)**,** 179–228. doi: 10.1007/s10963-019-09131-2.

Kay, A.U., and Kaplan, J.O. (2015). Human subsistence and land use in sub-Saharan Africa, 1000BC to AD1500: A review, quantification, and classification. *Anthropocene* 9**,** 14–32. doi: https://doi.org/10.1016/j.ancene.2015.05.001.

Keeling, R.F., Piper, S.C., Bollenbacher, A.F., and Walker, S.J. (2010). "Monthly Atmospheric 13C/12C Isotopic Ratios for 11 SIO Stations," in *Trends: A Compendium of Data on Global Change*. (Oak Ridge, Tenn: Carbon Dioxide Information Analysis Center, Oak Ridge National Laboratory, U.S. Department of Energy).

Kenyatta, J. (1968). *Facing Mount Kenya.* London: Secker and Warburg Originally published in 1938.

Kiage, L.M., and Liu, K.-b. (2009). Palynological evidence of climate change and land degradation in the Lake Baringo area, Kenya, East Africa, since AD 1650. *Palaeogeography, Palaeoclimatology, Palaeoecology* 279(1)**,** 60–72. doi: https://doi.org/10.1016/j.palaeo.2009.05.001.

Kiage, L.M., and Liu, K. (2006). Late Quaternary paleoenvironmental changes in East Africa: a review of multiproxy evidence from palynology, lake sediments, and associated records. *Progress in Physical Geography* 30(5)**,** 633 – 658. doi: https://doi.org/10.1177/0309133306071146.

Killick, D. (2006). Archaeological science and African archaeology. 4**,** 1–2.

Kinaston, R.L. (2023). "Isotopes, Domestication, and Past Animal Husbandry Practices: A Review of the Formative Studies," in *Exploring Human Behavior Through Isotope Analysis: Applications in Archaeological Research*, eds. M.M. Beasley & A.D. Somerville. (Cham: Springer International Publishing), 155–180.

Kingdon, J. (1984a). "East African Environment," in *East African Mammals: an Atlas of Evolution in Africa*, ed. J. Kingdon. (Chicago: The University of Chicago Press), 8–21.

Kingdon, J. (1984b). *East African Mammals: An Atlas of Evolution in Africa.* Chicago: The University of Chicago Press.

Kingdon, J. (1984c). "Vegetation," in *East African Mammals: an Atlas of Evolution in Africa*, ed. J. Kingdon. (Chicago: The University of Chicago Press), 22–44.

Kingdon, J. (1997). "The African Environment," in *The Kingdon Field Guide to African Mammals*, ed. J. Kingdon. (London: Academic Press), 447–458.

Kingdon, J. (2001). *The Kingdon Field Guide to African Mammals.* San Diego: Academic Press.

Kintigh, K. (2006). The promise and challenge of archaeological data integration. *American Antiquity* 71**,** 567–578. doi: 10.1017/S0002731600039810.

Kinyanjui, R.N., Mashaka, H.K., Chritz, K.L., Wemanya, S.N., Ndiema, E.K., Braun, D.R., et al. (2026). Holocene vegetation dynamics of the Koobi Fora Basin, East Turkana, Kenya: Insights from phytolith analysis. *Quaternary International* 759**,** 110131. doi: https://doi.org/10.1016/j.quaint.2026.110131.

Kirkels, F.M.S.A., de Boer, H.J., Concha Hernández, P., Martes, C.R.T., van der Meer, M.T.J., Basu, S., et al. (2022). Carbon isotopic ratios of modern C3 and C4 vegetation on the Indian peninsula and changes along the plant–soil–river continuum – implications for vegetation reconstructions. *Biogeosciences* 19(17)**,** 4107–4127. doi: 10.5194/bg-19-4107-2022.

Kiura, P. (2008a). *Ethnoarchaeological and Stable Isotopes in the Study of People's Diets: The Diets of the Dassanech, Gabra, and Elmolo People of Northern Kenya* Amazon: VDM Verlag Dr. Mueller e.K.

Kiura, P.W. (2005). *An Actualistic and Stable Isotope Study on the Diet of Three Modern groups of People in Northern Kenya.* Anthropology, Rutgers

Kiura, P.W. (2008b). *Ethnoarchaeological and Stable Isotope in the Study of People's Diets: The Diets of the Dassanech, Gabra and Elmolo People of Northern Kenya.* Germany: VDM Verlag Dr. Müller.

Klein Goldewijk, K., Beusen, A., Doelman, J., and Stehfest, E. (2017). Anthropogenic land use estimates for the Holocene – HYDE 3.2. *Earth Syst. Sci. Data* 9(2)**,** 927–953. doi: 10.5194/essd-9-927-2017.

Koch, P.L., Heisinger, J., Moss, C., Carlson, R.W., Fogel, M.L., and Behrensmeyer, A.K. (1995). Isotopic Tracking of Change in Diet and Habitat Use in African Elephants. *Science* 267(5202)**,** 1340–1343. doi: 10.1126/science.267.5202.1340.

Kochi, S., Pérez, S.A., Tessone, A., Ugan, A., Tafuri, M.A., Nye, J., et al. (2018). δ13C and δ15N variations in terrestrial and marine foodwebs of Beagle Channel in the Holocene. Implications for human paleodietary reconstructions. *Journal of Archaeological Science: Reports* 18**,** 696–707. doi: https://doi.org/10.1016/j.jasrep.2017.11.036.

Kohn, M.J., Schoeninger, M.J., and Valley, J.W. (1996). Herbivore tooth oxygen isotope compositions: effects of diet and physiology. *Geochimica et Cosmochimica Acta* 60(20)**,** 3889–3896. doi: https://doi.org/10.1016/0016-7037(96)00248-7.

Kohn, M.J., Schoeninger, M.J., and Valley, J.W. (1998). Variability in oxygen isotope compositions of herbivore teeth: reflections of seasonality or developmental physiology? *Chemical Geology* 152(1-2)**,** 97–112.

Koile, E., Greenhill, S.J., Blasi, D.E., Bouckaert, R., and Gray, R.D. (2022). Phylogeographic analysis of the Bantu language expansion supports a rainforest route. *Proceedings of the National Academy of Sciences* 119(32)**,** e2112853119. doi: doi:10.1073/pnas.2112853119.

Kotarba-Morley, A., Kourampas, N., Morley, M., McAdams, C., Crowther, A., Faulkner, P., et al. (2022). Coastal landscape changes at Unguja Ukuu, Zanzibar: Contextualizing the archaeology of an early Islamic port of trade. *The Journal of Island and Coastal Archaeology* 19**,** 1–35. doi: 10.1080/15564894.2022.2030441.

Krigbaum, J., Berger, M.H., Daegling, D.J., and McGraw, W.S. (2013). Stable isotope canopy effects for sympatric monkeys at Tai Forest Cote d'Ivoire. *Biology Letters* 9(4)**,** 20130466. doi: doi:10.1098/rsbl.2013.0466.

Krzyzaniak, L., and Kobusiewicz, M. (1984). *Origin and Early Development of Food-Producing Cultures in North-Eastern Africa.* Poznan: Polish Academy of Sciences and Poznan Archaeological Museum.

Kusimba, C., Kusimba, S., and Wright, D. (2005). The development and collapse of precolonial ethnic mosaics in Tsavo, Kenya. *Journal of African Archaeology* 3**,** 243–265. doi: 10.3213/1612-1651-10053.

Kusimba, C., and Walz, J.R. (2021). Debating the Swahili: Archaeology since 1990 and into the future. *Archaeologies*. doi: 10.1007/s11759-021-09434-x.

Kusimba, C.M. (1993). *The archaeology and ethnography of iron metallurgy of the Kenya coast.* PhD unpublished dissertation, Bryn Mawr College

Kusimba, C.M., and Kusimba, S.B. (2005). "Mosaics and interactions: East Africa, 2000 b.p. to the present," in *African Archaeology: A Critical Introduction,* ed. A. Stahl. (Oxford: Blackwell), 392 – 419.

Kusimba, C.M., Kusimba, S.B., and Dussubieux, L. (2013). Beyond the coastalscapes: preindustrial social and political networks in East Africa. *African Archaeological Review* 30(4)**,** 399–426. doi: 10.1007/s10437-013-9133-4.

Kusimba, C.M., and Sibel, B.K. (2004). *East African Archaeology.* Philadelphia: University of Pennsylvania Press.

Kusimba, C.M., and Walz, J.R. (2018). When Did the Swahili become maritime?: A reply to Fleisher et al. (2015), and to the resurgence of maritime myopia in the archaeology of the East African Coast. *American Anthropologist* 120(3)**,** 429–443. doi: https://doi.org/10.1111/aman.13059.

Kusimba, S.B. (1999). Hunter–gatherer land use patterns in Later Stone Age East Africa. *Journal of Anthropological Archaeology* 18(2)**,** 165–200. doi: https://doi.org/10.1006/jaar.1998.0335.

Kusimba, S.B. (2005). What Is a hunter-gatherer? Variation in the archaeological record of eastern and southern Africa. *Journal of Archaeological Research* 13(4)**,** 337–366. doi: 10.1007/s10814-005-5111-y.

Kusimba, S.B. (2013). "Hunter-Gatherer-Fishers of Eastern and South-Central Africa Since 20,000 Years Ago", in: *The Oxford Handbook of African Archaeology.* (eds.) P. Mitchell & P.J. Lane. (Oxford: Oxford University Press).

Kwekason, A.P. (2007). "Pre-early ironworking sedentary communities on the southern coast of Tanzania," in *Studies in the African Past* eds. G. Pwiti, C. Radimilaly & F. Chami. (Dar es Salaam: Dar es Salaam University Press).

la Grange, L. (2015). *Rock Hyraxes (Procavia capensis) and their Environments: $\delta^{13}C_{collagen}$ and $\delta^{15}N_{collagen}$ as Environmetal Indicators.* Master of Philosophy, University of Cape Town.

Laffranchi, Z., Huertas, A.D., Jiménez Brobeil, S.A., Torres, A.G., and Riquelme Cantal, J.A. (2016). Stable C & N isotopes in 2100 Year-B.P. human bone collagen indicate rare dietary dominance of C4 plants in NE-Italy. *Scientific Reports* 6(1)**,** 38817. doi: 10.1038/srep38817.

Lamb, H., Darbyshire, I., and Verschuren, D. (2003). Vegetation response to rainfall variation and human impact in central Kenya during the past 1100 years. *The Holocene* 13(2)**,** 285–292. doi: 10.1191/0959683603hl618rr.

Lane, P. (2004). The moving frontier and the transition to food production in Kenya. *Azania: Archaeological Research in Africa* 39(1)**,** 243 – 264.

Lane, P. (2011). An Outline of the Later Holocene archaeology and precolonial history of the Ewaso Basin, Kenya. *Smithsonian Contributions to Zoology* 632. doi: 10.5479/si.00810282.632.11.

Lane, P. (2013a). "The Archaeology of Pastoralism and Stock-Keeping in East Africa", in: *The Oxford Handbook of African Archaeology.* (eds.) P. Mitchell & P. Lane. (Oxford: Oxford University Press).

Lane, P. (2013b). "Trajectories of Pastoralism in Northern and Central Kenya: An Overview of the Archaeological and Environmental Evidence," in *Pastoralism in Africa: Past, Present and Future,* eds. M. Bollig & H.-P. Wotzka. (Oxford: Berghahn Books), 104–144.

Lane, P. (2015a). "Ethnicity, archaeological ceramics and changing paradigms in East African archaeology," in *Ethnic Ambiguity and the African Past,* eds. C.M. Kevin & R. Francois. (Walnut Creek, CA: Left Coast Press Inc.), 245–271.

Lane, P., Ashley, C., and Oteyo, G. (2006). New dates for Kansyore and Urewe Wares from northern Nyanza, Kenya. *Azania: Archaeological Research in Africa* 41(1)**,** 123–138. doi: 10.1080/00672700609480438.

Lane, P., Ashley, C., Seitsonen, O., Harvey, P., Mire, S., and Odede, F. (2007). The transition to farming in eastern Africa: new faunal and dating evidence from Wadh Lang'o and Usenge, Kenya. *Antiquity* 81(311)**,** 62–81. doi: 10.1017/S0003598X00094849.

Lane, P.J. (2015b). Archaeology in the age of the Anthropocene: A critical assessment of its scope and societal contributions. *Journal of Field Archaeology* 40(5)**,** 485–498. doi: 10.1179/2042458215Y.0000000022.

Lane, P.J. (Year). "People, Pots, Words and Genes: Multiple sources and recon-structions of the transition to food production in eastern Africa", in: *Cultural and Linguistic Transition explored. Proceedings of the ATrA closing workshop Trieste, May 25-26, 2016*, ed. I. Micheli: Trieste, EUT Edizioni Università di), 60–77.

Langley, M.C., Prendergast, M.E., Shipton, C., Quintana Morales, E.M., Crowther, A., and Boivin, N. (2016). Poison arrows and bone utensils in late Pleistocene eastern Africa: evidence from Kuumbi Cave, Zanzibar. *Azania: Archaeological Research in Africa* 51(2)**,** 155–177. doi: 10.1080/0067270X.2016.1173302.

Lawler, A. (2018). Scarred bird bones reveal early settlement on Madagascar. *Science* 361(6407)**,** 1059–1059. doi: doi:10.1126/science.361.6407.1059.

Layton, R., and Rowley-Conwy, P. (2013). Wild things in the north? Hunter-gatherers and the tyranny of the colonial perspective. *Anthropologie (Brno. Print)* 51(2)**,** 213–230. doi: http://puvodni.mzm.cz/Anthropologie/article.php?ID=1515.

Lazzerini, N., Balter, V., Coulon, A., Tacail, T., Marchina, C., Lemoine, M., et al. (2021). Monthly mobility inferred from isoscapes and laser ablation strontium isotope ratios in caprine tooth enamel. *Scientific Reports* 11(1)**,** 2277. doi: 10.1038/s41598-021-81923-z.

Le Meillour, L., Zazzo, A., Zirah, S., Tombret, O., Barriel, V., Arthur, K.W., et al. (2023). The name of the game: palaeoproteomics and radiocarbon dates further refine the presence and dispersal of caprines in eastern and southern Africa. *Royal Society Open Science* 10(11)**,** 231002. doi: doi:10.1098/rsos.231002.

Leakey, M. (1943). Report on the excavations at Hyrax Hill, Nakuru, Kenya Colony, 1937-1938. *Transactions of the Royal Society of South Africa* 30(4)**,** 271–409.

Lee-Thorp, J., Likius, A., Mackaye, H.T., Vignaud, P., Sponheimer, M., and Brunet, M. (2012). Isotopic evidence for an early shift to C4 resources by Pliocene hominins in Chad. *Proceedings of the National Academy of Sciences* 109(50)**,** 20369–20372. doi: 10.1073/pnas.1204209109.

Lee-Thorp, J., Sponheimer, M., and van der Merwe, N.J. (2003). What do stable isotopes tell us about hominid dietary and ecological niches in the Pliocene? *International Journal of Osteoarchaeology* 13(1-2)**,** 104–113.

Lee-Thorp, J.A. (2008). On isotopes and old bones. *Archaeometry* 50(6)**,** 925–950. doi: 10.1111/j.1475-4754.2008.00441.x.

Lee-Thorp, J.A., Sealy, J.C., and van der Merwe, N.J. (1989). Stable carbon isotope ratio differences between bone collagen and bone apatite, and their relationship to diet. *Journal of Archaeological Science* 16(6)**,** 585–599. doi: https://doi.org/10.1016/0305-4403(89)90024-1.

Lee-Thorp, J.A., and Sponheimer, M. (2013). "Contribution of Stable Light Isotopes to Paleoenvironmental Reconstruction," in *HandBook of Paleoanthropology*, eds. W. Henke, I. Tattersall & T. Hardt. (Berlin: Springer-Verlag), 289–310.

Lee-Thorp, J.A., Sponheimer, M., Passey, B.H., de Ruiter, D.J., and Cerling, T.E. (2010). Stable isotopes in fossil hominin tooth enamel suggest a fundamental dietary shift in the

Pliocene. *Philos Trans R Soc Lond B Biol Sci* 365(1556)**,** 3389–3396. doi: 10.1098/rstb.2010.0059.

LeFebvre, M.J., Brenskelle, L., Wieczorek, J., Kansa, S.W., Kansa, E.C., Wallis, N.J., et al. (2019). ZooArchNet: Connecting zooarchaeological specimens to the biodiversity and archaeology data networks. *PLOS ONE* 14(4)**,** e0215369. doi: 10.1371/journal.pone.0215369.

Leggett, S., Rose, A., Praet, E., and Le Roux, P. (2021). Multi-tissue and multi-isotope (δ13C, δ15N, δ18O and 87/86Sr) data for early medieval human and animal palaeoecology. *Ecology* 102(6)**,** e03349. doi: https://doi.org/10.1002/ecy.3349.

Leichliter, J., Lüdecke, T., Foreman, A., Bourgon, N., Duprey, N., Vonhof, H., et al. (2022). Nitrogen isotopic composition of tooth enamel organic matter records trophic position in modern and fossil ecosystems. *Research Square*. doi: 10.21203/rs.3.rs-1942250/v1.

Leichliter, J.N., Lüdecke, T., Foreman, A.D., Bourgon, N., Duprey, N.N., Vonhof, H., et al. (2023). Tooth enamel nitrogen isotope composition records trophic position: a tool for reconstructing food webs. *Commun Biol* 6(1)**,** 373. doi: 10.1038/s42003-023-04744-y.

Lemmen, C. (2009a). World distribution of land cover changes during pre- and protohistoric times and estimation of induced carbon releases *Géomorphologie : Relief, Processus, Environnement* 4.

[Dataset] Lemmen, C. (2009b). *World distribution of land cover changes, model in NetCDF format.* PANGAEA. doi: 10.1594/PANGAEA.737958. Available: https://doi.org/10.1594/PANGAEA.737958.

Lemmen, C. (2011). Mechanisms Shaping the Transition to Farming in Europe and the North American Woodland. *Archaeology, Ethnology and Anthropology of Eurasia* 41. doi: 10.1016/j.aeae.2014.03.007.

Lemmen, C., Gronenborn, D., and Wirtz, K.W. (2011). A simulation of the Neolithic transition in Western Eurasia. *Journal of Archaeological Science* 38(12)**,** 3459–3470. doi: https://doi.org/10.1016/j.jas.2011.08.008.

Levin, N., Simpson, S.W., Quade, J., Cerling, T.E., and Frost, S. (2008). Herbivore enamel carbon isotopic composition and the environmental context of *Ardipithecus* at Gona, Ethiopia. *Geological Society of America* (Special paper 446)**,** 251–234. doi: https://doi.org/10.1130/2008.2446(10).

Levin, N.E., Cerling, T.E., Passey, B.H., Harris, J.M., and Ehleringer, J.R. (2006). A Stable isotope aridity index for terrestrial environments. *Proceedings of the National Academy of Sciences* 103(30)**,** 11201–11205. doi: 10.1073/pnas.0604719103.

Li, S., Schlebusch, C., and Jakobsson, M. (2014). Genetic variation reveals large-scale population expansion and migration during the expansion of Bantu-speaking peoples. *Proceedings of the Royal Society B: Biological Sciences* 281(1793). doi: 10.1098/rspb.2014.1448.

Liao, J.D., Boutton, T., and Jastrow, J. (2006). Organic Matter Turnover in Soil Physical Fractions Following Woody Plant Invasion of Grassland: Evidence From Natural 13C and 15N. *Soil Biology and Biochemistry* 38**,** 3197–3210. doi: 10.1016/j.soilbio.2006.04.004.

Limburg, K. (2004). The Biogeochemistry of Strontium: A review of H.T. Odum's contributions. *Ecological Modelling - ECOL MODEL* 178**,** 31–33. doi: 10.1016/j.ecolmodel.2003.12.022.

Lipson, M., Sawchuk, E.A., Thompson, J.C., Oppenheimer, J., Tryon, C.A., Ranhorn, K.L., et al. (2022). Ancient DNA and deep population structure in sub-Saharan African foragers. *Nature*. doi: 10.1038/s41586-022-04430-9.

Liritzis, I., Singhvi, A.K., Feathers, J.K., Wagner, G.A., Kadereit, A., Zacharias, N., et al. (2013). *Luminescence Dating in Archaeology, Anthropology, and Geoarchaeology An Overview.* London: Springer

Liu, J. (2019). The Impact of Bantu Migration on Agriculture in Sub-Saharan Africa. *International Journal of New Developments in Engineering and Society* Vol.3(Issue 2)**,** 28–34. doi: https://doi.org/10.25236/IJNDES.19204.

Liu, X., Rendle-Buehring, R., and Henrich, R. (2017). Geochemical composition of Tanzanian shelf sediments indicates Holocene climatic and sea-level changes. *Quaternary Research* 87**,** 442–454. doi: 10.1017/qua.2017.12.

Lofgren, L. (1967). Stone structures of South Nyanza, Kenya *Azania* 2**,** 75–88.

Loftus, E. (2021). "Isotopes and Diet in African Hominins and Hunter-Gatherers". Oxford University Press).

Loftus, E., Mitchell, P.J., and Ramsey, C.B. (2019). An archaeological radiocarbon database for southern Africa. *Antiquity* 93(370)**,** 870–885. doi: 10.15184/aqy.2019.75.

Loftus, E., Roberts, P., and Lee-Thorp, J.A. (2016). An isotopic generation: four decades of stable isotope analysis in African archaeology. *Azania: Archaeological Research in Africa* 51(1)**,** 88–114. doi: 10.1080/0067270X.2016.1150083.

Long, T., Chen, H., Leipe, C., Wagner, M., and Tarasov, P.E. (2022). Modelling the chronology and dynamics of the spread of Asian rice from ca. 8000 BCE to 1000 CE. *Quaternary International* 623**,** 101–109. doi: https://doi.org/10.1016/j.quaint.2021.11.016.

Longin, R. (1971). New method of collagen extraction for radiocarbon dating. *Nature* 230(5291)**,** 241–242. doi: 10.1038/230241a0.

Longo, L., Brcic, M., Cabitza, F., Choi, J., Confalonieri, R., Ser, J.D., et al. (2024). Explainable Artificial Intelligence (XAI) 2.0: A manifesto of open challenges and interdisciplinary research directions. *Information Fusion* 106**,** 102301. doi: https://doi.org/10.1016/j.inffus.2024.102301.

Lyaya, E.C. (2020). Change and continuity in metal technology: iron production in the first and second millennium CE in Mbinga, southwestern Tanzania. *Archaeological and Anthropological Sciences* 12(6)**,** 125. doi: 10.1007/s12520-020-01064-8.

Lynch, B.M., and Robbins, L.H. (1979). Cushitic and nilotic prehistory: New Archaeological evidence from North-West Kenya. *The Journal of African History* 20(3)**,** 319–328. doi: 10.1017/S0021853700017333.

M'Mbogori, F.N. (2017). "Farming and Herding in Eastern Africa: Archaeological and Historical Perspectives." Oxford University Press).

Macharia, A.N., Uno, K.T., Cerling, T.E., and Brown, F.H. (2012). Isotopically distinct modern carbonates in abandoned livestock corrals in northern Kenya. *Journal of Archaeological Science* 39(7)**,** 2198–2205. doi: https://doi.org/10.1016/j.jas.2012.02.005.

MacPhee, R.D.E. (1986). Environment, extinction, and Holocene vertebrate localities in southern Madagascar. *National Geographic Research* (2)**,** 441–455.

MacPhee, R.D.E., and Burney, D.A. (1991). Dating of modified femora of extinct dwarf hippopotamus from southern Madagascar: Implications for constraining human colonization and vertebrate extinction events. *Journal of Archaeological Science* 18(6)**,** 695–706. doi: https://doi.org/10.1016/0305-4403(91)90030-S.

MacPhee, R.D.E., Burney, D.A., and Wells, N.A. (1985). Early Holocene chronology and environment of Ampasambazimba, A Malagasy subfossil lemur site. *International Journal of Primatology* 6**,** 463–489.

Madgwick, R., Lamb, A., Sloane, H., Nederbragt, A., Albarella, U., Parker Pearson, M., et al. (2021). A veritable confusion: use and abuse of isotope analysis in archaeology. *Archaeological Journal* 178(2)**,** 361–385. doi: 10.1080/00665983.2021.1911099.

Maggs, T. (1977). Some recent radiocarbon dates from eastern and southern Africa. *The Journal of African History* 18(2)**,** 161–191.

Mahan, S., Rittenour, T., Nelson, M., Ataee, N., Brown, N., DeWitt, R., et al. (2022). Guide for interpreting and reporting luminescence dating results. *GSA Bulletin*. doi: 10.1130/B36404.1.

Mahaney, W.C. (1988). Holocene glaciations and paleoclimate of mount Kenya and other East African mountains. *Quaternary Science Reviews* 7(2)**,** 211–225. doi: https://doi.org/10.1016/0277-3791(88)90007-8.

Makarewicz, C., and Tuross, N. (2006). Foddering by Mongolian pastoralists is recorded in the stable carbon (δ13C) and nitrogen (δ15N) isotopes of caprine dentinal collagen. *Journal of Archaeological Science* 33(6)**,** 862–870. doi: https://doi.org/10.1016/j.jas.2005.10.016.

Makarewicz, C., and Tuross, N. (2012). Finding Fodder and Tracking Transhumance: Isotopic Detection of Goat Domestication Processes in the Near East. *Current Anthropology* 53(4)**,** 495–505. doi: 10.1086/665829.

Makarewicz, C.A. (2014). Winter pasturing practices and variable fodder provisioning detected in nitrogen (δ15N) and carbon (δ13C) isotopes in sheep dentinal collagen. *Journal of Archaeological Science* 41**,** 502–510. doi: https://doi.org/10.1016/j.jas.2013.09.016.

Makarewicz, C.A., and Pederzani, S. (2017). Oxygen (δ18O) and carbon (δ13C) isotopic distinction in sequentially sampled tooth enamel of co-localized wild and domesticated caprines: Complications to establishing seasonality and mobility in herbivores. *Palaeogeography, Palaeoclimatology, Palaeoecology* 485**,** 1–15. doi: https://doi.org/10.1016/j.palaeo.2017.01.010.

Maley, J., Doumenge, C., Giresse, P., Mahe, G., Philippon, N., Hubau, W., et al. (2018). Late Holocene forest contraction and fragmentation in central Africa *Quaternary Research***,** 1–17. doi: doi:10.1017/qua.2017.97.

Maley J. et al. (2012). *Science* 337(1040). doi: www.sciencemag.org/cgi/content/full/337/6098/1040-d.

Malone, M.A., MacLatchy, L.M., Mitani, J.C., Kityo, R., and Kingston, J.D. (2021). A chimpanzee enamel-diet δ13C enrichment factor and a refined enamel sampling strategy: Implications for dietary reconstructions. *Journal of Human Evolution* 159**,** 103062. doi: https://doi.org/10.1016/j.jhevol.2021.103062.

Mapunda, B.B. (1995). *An archaeological view of the history and variation of ironworking in southwestern Tanzania* PhD dissertation, University of Florida.

Marchant, R. (2021). "Climate Change in Eastern Africa". Oxford University Press).

Marchant, R., Courtney-Mustaphi, C., and Githumbi, E. (2017). Entangled ecosystem-people-animal interactions: perspectives from the East African savannas. *PAGES magazine***,** 80–81. doi: https://doi.org/10.22498/pages.25.2.80.

Marchant, R., and Lane, P. (2014). Past perspectives for the future: foundations for sustainable development in East Africa. *Journal of Archaeological Science* 51**,** 12–21. doi: https://doi.org/10.1016/j.jas.2013.07.005.

Marchant, R., Richer, S., Boles, O., Capitani, C., Courtney-Mustaphi, C.J., Lane, P., et al. (2018). Drivers and trajectories of land cover change in East Africa: Human and environmental interactions from 6000 years ago to present. *Earth-Science Reviews* 178**,** 322–378. doi: https://doi.org/10.1016/j.earscirev.2017.12.010.

Marchenko, Z.V., Svyatko, S.V., and Grishin, A.E. (2021). δ13C and δ15N isotope analysis of modern freshwater fish in the south of Western Siberia and its potential for palaeoreconstructions. *Quaternary International* 598**,** 97–109. doi: https://doi.org/10.1016/j.quaint.2021.06.006.

Marciniak, A., Evans, J., Henton, E., Perason, J., Lisowski, M., Bartkowiak, M., et al. (2017). Animal husbandry in the Early and Middle Neolithic settlement at Kopydłowo in the Polish lowlands. A multi-isotope perspective. *Archaeol Anthropol Sci* 9. doi: 10.1007/s12520-017-0485-6.

Marean, C.W. (1992a). Hunter to herder: large mammal remains from the hunter-gatherer occupation at Enkapune Ya Muto Rock-shelter, central Rift, Kenya. *African Archaeological Review* 10(1)**,** 65–127. doi: 10.1007/BF01117697.

Marean, C.W. (1992b). Implications of late Quaternary mammalian fauna from Lukenya Hill (South-central Kenya) for paleoenvironmental change and faunal extinctions. *Quaternary Research* 37(2)**,** 239–255. doi: 10.1016/0033-5894(92)90085-W.

Marean, C.W., Mudida, N., and Reed, K.E. (1994). Holocene paleoenvironmental change in the Kenyan central Rift as indicated by micromammals from Enkapune Ya Muto Rockshelter. *Quaternary Research* 41(3)**,** 376–389. doi: 10.1006/qres.1994.1042.

Marlowe, F.W. (2010). The Hadza: Hunter–Gatherers of Tanzania. *The Hadza: Hunter-Gatherers of Tanzania*.

Marsh, E.J., Bruno, M.C., Fritz, S.C., Baker, P., Capriles, J.M., and Hastorf, C.A. (2018). IntCal, SHCal, or a Mixed Curve? Choosing a 14C Calibration Curve for Archaeological and Paleoenvironmental Records from Tropical South America. *Radiocarbon* 60(3)**,** 925–940. doi: 10.1017/RDC.2018.16.

Marshall, F. (1990). Origins of specialized pastoral production in East Africa. *American Anthropologist* 92(4)**,** 873–894. doi: 10.1525/aa.1990.92.4.02a00020.

Marshall, F., Grillo, K., and Arco, L. (2011). "Prehistoric pastoralists and social responses to climatic risk in East Africa," in *Sustainable lifeways: cultural persistence in an ever-changing environment*, eds. N. Miller, K. Moore & K. Ryan. (Philadelphia: University of Pennsylvania Press).

Marshall, F., and Hildebrand, E. (2002). Cattle before crops: the beginnings of food production in Africa. *Journal of World Prehistory* 16(2)**,** 99–143. doi: DOI:10.1023/A:1019954903395

Marshall, F., Reid, R.E.B., Goldstein, S., Storozum, M., Wreschnig, A., Hu, L., et al. (2018). Ancient herders enriched and restructured African grasslands. *Nature* 561(7723)**,** 387–390. doi: 10.1038/s41586-018-0456-9.

Marshall, F., Stewart, K., and Barthelme, J. (1984). Early domestic stock at Dongodien in northern Kenya. *Azania: Archaeological Research in Africa* 19(1)**,** 120–127. doi: 10.1080/00672708409511332.

Marshall, F.B. (1986). *Aspects of the advent of pastoral economics in East Africa.* PhD University of California

Martinón-Torres, M., and Killick, D. (2015). "Archaeological Theories and Archaeological Sciences," in *The Oxford Handbook of Archaeological Theory,* eds. A. Gardner, M. Lake & U. Sommer. (Oxford Oxford University Press).

Marwick, B. (2017). Computational Reproducibility in Archaeological Research: Basic Principles and a Case Study of Their Implementation. *Journal of Archaeological Method and Theory* 24(2)**,** 424–450. doi: 10.1007/s10816-015-9272-9.

Maxon, R.M. (2009). *East Africa: An Introductory History.* Morgantown: West Virginia University Press.

McGee, R.J., and Warms, R.L. (2008). *Anthropological Theory: An Introductory History.* New York: Mc Graw Hill.

McIntosh, R.J., Maley, J., and Vernet, R. (2015). African Palaeoclimate and Human Response: A Special Issue of the African Archaeological Review. *African Archaeological Review* 32(2)**,** 167–177. doi: 10.1007/s10437-015-9187-6.

McSparron, C., Donnelly, C., Murphy, E., and Geber, J. (2020). Migration, Group Agency, and Archaeology: A New Theoretical Model. *International Journal of Historical Archaeology* 24(2)**,** 219–232. doi: 10.1007/s10761-019-00519-6.

Mehlman, M.J. (1989). *Later Quaternary Archaeological Sequences in Northern Tanzania.* PhD, University of Illinois at Urbana-Champaign.

Michels, J.W., Tsong, I.S.T., and Nelson, C.M. (1983). Obsidian Dating and East African Archeology. *Science* 219(4583)**,** 361–366. doi: doi:10.1126/science.219.4583.361.

Microsoft (2024). *Import or export text (.txt or .csv) files* [Online]. Microsoft. Available: https://support.microsoft.com/en-us/office/import-or-export-text-txt-or-csv-files-5250ac4c-663c-47ce-937b-339e391393ba [Accessed 2024].

Mitchell, P. (2020). Settling Madagascar: When Did People First Colonize the World's Largest Island? *The Journal of Island and Coastal Archaeology* 15(4)**,** 576–595. doi: 10.1080/15564894.2019.1582567.

Mitchell, P., and Lane, P. (2013). *The Oxford Handbook of African Archaeology.* Oxford: Oxford University Press.

Möhlig, W.J.G. (1977). "Zur frühen Siedlungsgeschichte der Savannen-Bantu aus lauthistorischer Sicht," in *Zur Sprachgeschichte und Ethnohistorie in Afrika,* ed. W.J.G. Möhlig.).

Möhlig, W.J.G.I. (1981). *Stratification in the History of the Bantu Languages.*

Moore, J., Rose, A., Anderson, S., Evans, J., Nowell, G., Gröcke, D.R., et al. (2020). A multi-isotope (C, N, O, Sr, Pb) study of Iron Age and Roman period skeletons from east Edinburgh, Scotland exploring the relationship between decapitation burials and geographical origins. *Journal of Archaeological Science: Reports* 29**,** 102075. doi: https://doi.org/10.1016/j.jasrep.2019.102075.

Morales, E.M.Q. (2013). *Reconstructing Swahili Foodways: the archaeology of fishing and fish consumption in coastal East Africa, AD 500-1500.* PhD Unpublished Dissertation, University of Bristol.

Moreau, R.E., and Pakenham, R.H.W. (1940). Faunistics and Ages of the East African Islands. *Nature* 146(3701)**,** 462–462. doi: 10.1038/146462a0.

Moreau, R.E., and Pakenham, R.H.W. (1941). The land vertebrates of Pemba, Zanzibar, and Mafia: zoogeographical study. *Proceedings of the Zoological Society of London* 110 (Series A)**,** 97–128.

Morel, M. (2023). *Iron metallurgy in Northeastern Madagascar: Study of Rasikajy metallurgical production between the 11th abd 15th Centuries.* PhD Thesis.

Morton, R.F. (1972). The Shungwaya myth of Miji Kenda origins: a problem of late nineteenth-century Kenya coastal history. *International Journal of African Historical Studies* 5**,** 397–423.

Mosley, P.N., and Davison, S. (1992). Ugunja: a new Kansyore (Oltome) site. *Azania: Archaeological Research in Africa* 27(1)**,** 129–134. doi: 10.1080/00672709209511433.

Moullou, D., Vital, R., Sylaiou, S., and Ragia, L. (2024). Digital Tools for Data Acquisition and Heritage Management in Archaeology and Their Impact on Archaeological Practices. *Heritage* 7(1)**,** 107–121.

Mturi, A.A. (1986). The Pastoral Neolithic of West Kilimanjaro. *Azania: Archaeological Research in Africa* 21(1)**,** 53–63. doi: 10.1080/00672708609511367.

Mudge, P.L., Schipper, L.A., Baisden, W.T., Ghani, A., and Lewis, R.W. (2014). Changes in soil C, N and δ15N along three forest–pasture chronosequences in New Zealand. *Soil Research* 52(1)**,** 27–37. doi: https://doi.org/10.1071/SR13183.

Mueller, N., Goldstein, S., Odeny, D., and Boivin, N. (2022). Variability and preservation biases in the archaeobotanical record of Eleusine coracana (finger millet): evidence from Iron Age Kenya. *Vegetation History and Archaeobotany* 31. doi: 10.1007/s00334-021-00853-y.

Mulrooney, M., Bickler, S., Allen, M., and Ladefoged, T. (2011). High-precision dating of colonization and settlement in East Polynesia. *Proceedings of the National Academy of Sciences of the United States of America* 108**,** E192–194; author reply E195. doi: 10.1073/pnas.1100447108.

Munene, K. (2002). *Holocene Foragers, Fishers, and Herders of Western Kenya.* Oxford: Archaopress.

Murphy, B.P., and Bowman, D.M.J.S. (2009). The carbon and nitrogen isotope composition of Australian grasses in relation to climate. *Functional Ecology* 23(6)**,** 1040–1049. doi: https://doi.org/10.1111/j.1365-2435.2009.01576.x.

Mutundu, K.K. (2010). An ethnoarchaeological framework for the identification and distinction of late Holocene archaeological sites in East Africa. *Azania: Archaeological Research in Africa* 45(1)**,** 6–23.

Natural Earth. 2024. Free vector and raster map data at 1:10m, 1:50m, and 1:110m scales. Available: https://www.naturalearthdata.com/downloads/.

Ndiema, E.K. (2011). *Mobility and subsistence patterns among mid-Holocene pastoralists at Koobi Fora, northern Kenya: new archaeological sites and evidence from obsidian sourcing and geochemical characterization* PhD Rutgers, The State University of New Jersey.

Ndiema, K., Dillian, C., Braun, D., Harris, J., and Kiura, P. (2011). Transport and subsistence patterns at the transition to pastoralism, Koobi Fora, Kenya. *Archaeometry* 53. doi: 10.1111/j.1475-4754.2011.00595.x.

Nelson, C.M., and Kimengich, J. (1984). "Early Phases of Pastoral Adaptation in the Central Highlands of Kenya," in *Origin and Early Development of Food-Producing Cultures in North-Eastern Africa*, eds. L. Krzyzaniak & M. Kobusiewicz. (Poznan: Polish Academy of Sciences).

Neumann, K., Eichhorn, B., and Wotzka, H.-P. (2022). Iron Age plant subsistence in the Inner Congo Basin (DR Congo). *Vegetation History and Archaeobotany*. doi: 10.1007/s00334-021-00865-8.

NIMA (January 2000). "World Geodetic System 1984: Its Definiton and Relations with Local Geodetic Systems ", in: *Technical Report.* National Imagery and Mapping Agency).

Nitsche, C., Schreurs, G., and Serneels, V. (2023). The enigmatic softstone vessels of northern Madagascar: Petrological investigations of a Medieval Quarry. *Journal of Field Archaeology* 48(1)**,** 55–72. doi: 10.1080/00934690.2022.2092689.

Nkirote, M.M.F. (2012). Population and ceramic traditions: revisiting the Tana ware of coastal Kenya (7th–14th century AD). *Azania: Archaeological Research in Africa* 47(2)**,** 245–246. doi: 10.1080/0067270X.2012.674423.

Novacek, M.J., and Cleland, E.E. (2001). The current biodiversity extinction event: Scenarios for mitigation and recovery. *Proceedings of the National Academy of Sciences of the United States of America* 98(10)**,** 5466–5470. doi: 10.1073/pnas.091093698.

Nurse, D. (1994). 'Historical' classifications of the Bantu languages. *Azania: Archaeological Research in Africa* 29-30(1)**,** 65–81. doi: 10.1080/00672709409511662.

O'Connell, T.C. (2025). The signal and the noise: inherent challenges for isotopic studies in bioarchaeology. *Journal of Archaeological Science* 183**,** 106379. doi: https://doi.org/10.1016/j.jas.2025.106379.

O'Malley, C.P.B., White, N.J., Stephenson, S.N., and Roberts, G.G. (2021). Large-Scale Tectonic Forcing of the African Landscape. *Journal of Geophysical Research: Earth Surface* 126(12)**,** e2021JF006345. doi: https://doi.org/10.1029/2021JF006345.

Odede, F. (2008). Gunda-buche: the bank-and-dicth fortified settlement enclosures of western Kenya, Lake Victoria Basin. *Azania: Archaeological Research in Africa* 43(1)**,** 36–49.

Odner, K. (1971a). An archaeological survey of Iramba, Tanzania. *Azania: Archaeological Research in Africa* 6(1)**,** 151–198. doi: 10.1080/00672707109511550.

Odner, K. (1971b). A preliminary report on an archaeological survey on the slopes of Kilimanjaro. *Azania: Archaeological Research in Africa* 6(1)**,** 131–149. doi: 10.1080/00672707109511549.

Odner, K. (1971c). Usangi Hospital and other archaeological sites in the North Pare Mountains, North-eastern Tanzania. *Azania: Archaeological Research in Africa* 6(1)**,** 89–130. doi: 10.1080/00672707109511548.

Odner, K. (1972). Excavations at Narosura, a stone bowl site in the southern Kenya Highlands. *Azania: Archaeological Research in Africa* 7(1)**,** 25–92. doi: 10.1080/00672707209511557.

Oelze, V.M., Head, J.S., Robbins, M.M., Richards, M., and Boesch, C. (2014). Niche differentiation and dietary seasonality among sympatric gorillas and chimpanzees in Loango National Park (Gabon) revealed by stable isotope analysis. *Journal of Human Evolution* 66**,** 95–106. doi: https://doi.org/10.1016/j.jhevol.2013.10.003.

Ogot, B.A. (1976). *Kenya Before 1900* Nairobi: East African Publishing House.

Ojiambo, S., Lyons, W., Welch, K., Poreda, R., and Johannesson, K. (2003). Strontium isotopes and rare earth elements as tracers of groundwater-lake water interactions, Lake Naivasha, Kenya. *Applied Geochemistry* 18**,** 1789–1805. doi: 10.1016/S0883-2927(03)00104-5.

Olaka, L., and Ebinger, C.J. (2023). Tectonic and Paleoclimatic Setting for Hominin Evolution in Eastern Africa. *Elements* 19(2)**,** 82–87. doi: 10.2138/gselements.19.2.82.

Oliver, R. (1966). The Problem of the Bantu Expansion. *The Journal of African History* 7(3)**,** 361–376. doi: 10.1017/S0021853700006472.

Olson, D.M., Dinerstein, E., Wikramanayake, E.D., Burgess, N.D., Powell, G.V.N., Underwood, E.C., et al. (2001). Terrestrial Ecoregions of the World: A New Map of Life on Earth: A new global map of terrestrial ecoregions provides an innovative tool for conserving biodiversity. *BioScience* 51(11)**,** 933–938. doi: 10.1641/0006-3568(2001)051[0933:Teotwa]2.0.Co;2.

Onjala, I.O. (2003). Spatial distribution and settlement system of the stone structures of south-western Kenya *Azania: Archaeological Research in Africa* 38(1)**,** 99–120.

Onyango-Abuje, J.C. (1977a). *A contribution to the study of the Neolithic in East Africa with particular reference to the Naivasha-Nakuru Basin.* PhD, University of California.

Onyango-Abuje, J.C. (1977b). Crescent Island: A preliminary report on excavations at an East African Neolithic site. *Azania: Archaeological Research in Africa* 12(1)**,** 147–159. doi: 10.1080/00672707709511252.

Oslisly, R., White, L., Bentaleb, I., Favier, C., Fontugne, M., Gillet, J.-F., et al. (2013). Climatic and cultural changes in the west Congo Basin forests over the past 5000 years. *Philosophical Transactions of the Royal Society B: Biological Sciences* 368(1625). doi: 10.1098/rstb.2012.0304.

Ostrom, N.E., and Ostrom, P.H. (1998). "Nitrogen isotopes," in *Geochemistry*. (Dordrecht: Springer Netherlands), 431–434.

Out, W.A. (2018). *Unguja Ukuu, Zanzibar (FHM 4296/2540). Preliminary analysis of charcoal samples from artefact concentrations and domestic structures.*

Owen, R.B., Barthelme, J.W., Renaut, R.W., and Vincens, A. (1982). Palaeolimnology and archaeology of Holocene deposits north-east of Lake Turkana, Kenya. *Nature* 298(5874)**,** 523–529. doi: 10.1038/298523a0.

Pakendorf, B., Bostoen, K., and Filippo, C. (2011). Molecular Perspectives on the Bantu Expansion: A Synthesis. *Language Dynamics and Change* 1**,** 50–88. doi: 10.1163/221058211X570349.

Pandora (2024). Pandora data platform. doi: https://pandoradata.earth/organization/afriarch.

Passey, B.H., and Cerling, T.E. (2002). Tooth Enamel Mineralization in Ungulates: Implications for Recovering a Primary Isotopic Time-Series. *Geochimica et Cosmochimica Acta* 66(18)**,** 3225–3234.

Patin, E., Lopez, M., Grollemund, R., Verdu, P., Harmant, C., Quach, H., et al. (2017). Dispersals and genetic adaptation of Bantu-speaking populations in Africa and North America. *Science* 356(6337)**,** 543–546. doi: doi:10.1126/science.aal1988.

Patridge, T.C. (2010). "Tectonics and geomorphology of Africa during the Phanerozoic," in *Cenozoic Mammals of Africa,* eds. L. Werdelin & W.J. Sanders. (Berkeley: University of California Press), 3–17.

Pawlowicz, M.C. (2011). *Finding their place in the Swahili world: an archaeological exploration of southern Tanzania.* PhD University of Virginia

Pearson, C., Leavitt, S., Kromer, B., Solanki, S., and Usoskin, I. (2021). Dendrochronology and radiocarbon dating *Radiocarbon* 64**,** 1–20. doi: 10.1017/RDC.2021.97.

Pearson, M.P., Godden, K., Ramilisonina, Retsihisatse, Schwenninger, J.-L., Heurtebize, G., et al. (2010). *Pastoralists, Warriors and Colonists: The Archaeology of Southern Madagascar.* Oxford: Archaeopress.

Peregrine, P.N., and Ember, M. (2003). *Encyclopaedia of Prehistory* New York: Kluwer Academic.

Petchey, F., Ulm, S., David, B., McNiven, I.J., Asmussen, B., Tomkins, H., et al. (2012). 14C Marine reservoir variability in herbivores and deposit-feeding gastropods from an open coastline, Papua New Guinea. *Radiocarbon* 54(3-4)**,** 967–978. doi: 10.1017/S0033822200047603.

Petek-Sargeant, N. (2025). The Turkwel settlement at Oltioki in Baringo: exploring cultural variation in the terminal Pastoral Neolithic of Kenya. *Azania: Archaeological Research in Africa* 60(4)**,** 632–672. doi: 10.1080/0067270X.2025.2520652.

Petek, N., and Lane, P. (2017). Ethnogenesis and surplus food production: communitas and identity building among nineteenth- and early twentieth-century Ilchamus, Lake Baringo, Kenya. *World Archaeology* 49(1)**,** 40–60. doi: 10.1080/00438243.2016.1259583.

Phillipson, D.W. (1975). The chronology of the Iron Age in Bantu Africa. *The Journal of African History* 16(3)**,** 321–342. doi: 10.1017/S0021853700014298.

Phillipson, D.W. (1977). *The Later Prehistory of Eastern and Southern Africa.*

Phillipson, D.W. (1979). Some Iron Age sites in the Lower Tana Valley *Azania: Archaeological Research in Africa* 14(1)**,** 155–160. doi: 10.1080/00672707909511270.

Phillipson, D.W. (1984). "Aspects of early food production in northern Kenya," in *Origins and Early Development Food-Producing Cultures in Northeastern Africa,* ed. L. Kryzyzaniak. (Poznan: Polish Academy of Science), 489–495.

Pickard, C., Schoop, U.-D., Bartosiewicz, L., Gillis, R., and Sayle, K.L. (2017). Animal keeping in Chalcolithic north-central Anatolia: what can stable isotope analysis add? *Archaeological and Anthropological Sciences* 9(7)**,** 1349–1362. doi: 10.1007/s12520-016-0386-0.

Pin, C., Briot, D., Bassin, C., and Poitrasson, F. (1994). Concomitant separation of strontium and samarium-neodymium for isotopic analysis in silicate samples, based on specific extraction chromatography. *Analytica Chimica Acta* 298(2)**,** 209–217. doi: https://doi.org/10.1016/0003-2670(94)00274-6.

Plomp, E., Holstein, I., Kootker, L., Verdegaal-Warmerdam, S., Forouzanfar, T., and Davies, G. (2020). Strontium, oxygen, and carbon isotope variation in modern human dental enamel. *American Journal of Physical Anthropology* 172. doi: 10.1002/ajpa.24059.

Pluckhahn, T., Wallis, N., and Thompson, V. (2020). The History and Future of Migrationist Explanations in the Archaeology of the Eastern Woodlands with a Synthetic Model of Woodland Period Migrations on the Gulf Coast. *Journal of Archaeological Research* 28. doi: 10.1007/s10814-019-09140-x.

Pouwels, R.L. (2002). Eastern Africa and the Indian Ocean to 1800: Reviewing relations in historical perspective. *The International Journal of African Historical Studies* 35(2/3)**,** 385–425. doi: 10.2307/3097619.

Prendergast, M. (2010a). Kansyore fisher-foragers and transitions to food production in East Africa: The view from Wadh Lang'o, Nyanza Province, Western Kenya. *Azania: Archaeological Research in Africa* 45**,** 83–111. doi: 10.1080/00672700903291765.

Prendergast, M. (2011). "Hunters and Herders at the Periphery: The Spread of Herding in Eastern Africa," in *People and Animals in Holocene Africa: Recent Advances in Archaeozoology,* eds. H. Jousse & J. Lesur. (Frankfurt: Africa Magna Verlag).

Prendergast, M., Luque, L., Dominguez-Rodrigo, M., Diez-Martín, F., Mabulla, A.Z.P., and Barba, R. (2007). New excavations at Mumba Rockshelter, Tanzania. *Journal of African Archaeology* 5**,** 217–243. doi: 10.3213/1612-1651-10093.

Prendergast, M., Rouby, H., Punnwong, P., Marchant, R., Crowther, A., Kourampas, N., et al. (2016). Continental island formation and the archaeology of defaunation on Zanzibar, eastern Africa. *PLOS ONE* 11(2)**,** e0149565. doi: 10.1371/journal.pone.0149565.

Prendergast, M.E. (2009). Forager variability and transitions to food production in secondary settings: Kansyore and Pastoral Neolithic economies in East Africa. *Azania: Archaeological Research in Africa* 44(2)**,** 276–277. doi: 10.1080/00671990903052330.

Prendergast, M.E. (2010b). Diversity in East African foraging and food producing communities. *Azania: Archaeological Research in Africa* 45(1)**,** 1–5. doi: 10.1080/00672700903291674.

Prendergast, M.E. (2010c). Kansyore fisher-foragers and transitions to food production in East Africa: the view from Wadh Lang'o, Nyanza Province, Western Kenya. *Azania: Archaeological Research in Africa* 45(1)**,** 83–111. doi: 10.1080/00672700903291765.

Prendergast, M.E. (2020). "The History of Eastern African Foragers". (Oxford: Oxford University Press).

Prendergast, M.E., and Beyin, A. (2018). Fishing in a fluctuating landscape: terminal Pleistocene and early Holocene subsistence strategies in the Lake Turkana Basin, Kenya. *Quaternary International* 471**,** 203–218. doi: https://doi.org/10.1016/j.quaint.2017.04.022.

Prendergast, M.E., Buckley, M., Crowther, A., Frantz, L., Eager, H., Lebrasseur, O., et al. (2017a). Reconstructing Asian faunal introductions to eastern Africa from multi-proxy biomolecular and archaeological datasets. *PLOS ONE* 12(8)**,** e0182565. doi: 10.1371/journal.pone.0182565.

Prendergast, M.E., Grillo, K.M., Mabulla, A.Z.P., and Wang, H. (2014). New dates for Kansyore and Pastoral Neolithic ceramics in the Eyasi Basin, Tanzania. *Journal of African Archaeology* 12(1)**,** 89–98.

Prendergast, M.E., Janzen, A., Buckley, M., and Grillo, K.M. (2019a). Sorting the sheep from the goats in the Pastoral Neolithic: morphological and biomolecular approaches at Luxmanda, Tanzania. *Archaeological and Anthropological Sciences* 11(6)**,** 3047–3062. doi: 10.1007/s12520-018-0737-0.

Prendergast, M.E., Lipson, M., Sawchuk, E.A., Olalde, I., Ogola, C.A., Rohland, N., et al. (2019b). Ancient DNA reveals a multistep spread of the first herders into sub-Saharan Africa. *Science* 365(6448)**,** eaaw6275. doi: 10.1126/science.aaw6275.

Prendergast, M.E., Mabulla, A.Z.P., Grillo, K.M., Broderick, L.G., Seitsonen, O., Gidna, A.O., et al. (2013). Pastoral Neolithic sites on the southern Mbulu Plateau, Tanzania. *Azania: Archaeological Research in Africa* 48(4)**,** 498–520. doi: 10.1080/0067270X.2013.841927.

Prendergast, M.E., Miller, J., Mwebi, O., Ndiema, E., Shipton, C., Boivin, N., et al. (2023). Small game forgotten: Late Pleistocene foraging strategies in eastern Africa, and remote capture at Panga ya Saidi, Kenya. *Quaternary Science Reviews* 305(108032). doi: https://doi.org/10.1016/j.quascirev.2023.108032.

Prendergast, M.E., and Mutundu, K.K. (2009). "Late Holocene zooarchaeology in East Africa: Ethnographic analogues and interpretive challenges," in *Tracking Down the Past: Ethnohistory Meets Archaeology,* eds. G. Grupe, G. McGlynn & J. Peters. Documenta Archaeologiae), 203–232.

Prendergast, M.E., Quintana Morales, E.M., Crowther, A., Horton, M.C., and Boivin, N.L. (2017b). Dietary diversity on the Swahili coast: the fauna from two Zanzibar trading locales. *International journal of osteoarchaeology* 27(4)**,** 621–637. doi: 10.1002/oa.2585.

Prestele, R., Arneth, A., Bondeau, A., de Noblet-Ducoudré, N., Pugh, T.A.M., Sitch, S., et al. (2017). Current challenges of implementing anthropogenic land-use and land-cover change in models contributing to climate change assessments. *Earth Syst. Dynam.* 8(2)**,** 369–386. doi: 10.5194/esd-8-369-2017.

Preusser, F., Degering, D., Fuchs, M., Hilgers, A., Kadereit, A., Klasen, N., et al. (2008). Luminescence dating: basics, methods and application. *Eiszeitalter & Gegenwart / Quaternary Science Journal* 57**,** 95–149.

Price, T.D., Manzanilla, L., and Middleton, W.D. (2000). Immigration and the ancient city of Teotihuacan in Mexico: a study using strontium isotope ratios in human bone and teeth. *Journal of Archaeological Science* (27)**,** 903–913.

Punwong, P., Marchant, R., and Selby, K. (2012). Holocene mangrove dynamics and environmental change in the Rufiji Delta, Tanzania. *Vegetation History and Archaeobotany* 22. doi: 10.1007/s00334-012-0383-x.

Punwong, P., Marchant, R., and Selby, K. (2013). Holocene mangrove dynamics from Unguja Ukuu, Zanzibar. *Quaternary International* 298**,** 4–19. doi: https://doi.org/10.1016/j.quaint.2013.02.007.

Punwong, P., Selby, K., and Marchant, R. (2018). Holocene mangrove dynamics and relative sea-level changes along the Tanzanian coast, East Africa. *Estuarine, Coastal and Shelf Science* 212**,** 105–117. doi: https://doi.org/10.1016/j.ecss.2018.07.004.

QGIS Development Team. 2024. QGIS Geographic Information System, version 3.28. Open Source Geospatial Foundation Project Available: https://docs.qgis.org/3.28/pdf/en/QGIS-3.28-DesktopUserGuide-en.pdf.

R Core Team. 2013. R: A language and environment for statistical computing. *R Foundation for Statistical Computing* [Online]. Available: http://www.R-project.org/.

Radimilahy, C. (1998). *Mahilaka : An archaeological investigation of an early town in northwestern Madagascar.* Doctoral thesis, comprehensive summary, Acta Universitatis Upsaliensis.

Rakotozafy, L.M.A. (1996). *Etude de la constitution du regime alimentaire des habitants du site de Mahilaka du XI au XIV siecle a partir des products de fouilles archeologiques.* Doctorate, Universite DAntananarivo

Rakotozafy, L.M.A., and Goodman, S.M. (2005). Contribution à l'étude zooarchéologique de la région du Sud-ouest et extrême Sud de Madagascar sur la base des collections de l'ICMAA de l'Université d'Antananarivo. *TALOHA revue scientifique internationale des civilisations* (14-15)**,** 1–15.

Ramachandran, P., Ramachandran, R., Ray, A., and Rixen, T. (2008). Nitrogen cycling: A review of the processes, transformations and fluxes in coastal ecosystems. *Current Science* 94.

Raymaekers, J., and Van Noten, F. (1986). Early iron furnaces with 'bricks' in Rwanda: Complementary evidence from Mutwarubona. *Azania: Archaeological Research in Africa* 21(1)**,** 65–84. doi: 10.1080/00672708609511368.

Reimer, P.J., Austin, W.E.N., Bard, E., Bayliss, A., Blackwell, P.G., Bronk Ramsey, C., et al. (2020). The IntCal20 Northern Hemisphere Radiocarbon Age Calibration Curve (0–55 cal kBP). *Radiocarbon* 62(4)**,** 725–757. doi: 10.1017/RDC.2020.41.

Reimer, P.J., and Reimer, R.W. (2001). A Marine Reservoir Correction Database and On-Line Interface. *Radiocarbon* 43(2A)**,** 461–463. doi: 10.1017/S0033822200038339.

Revel, M., Ducassou, E., Skonieczny, C., Colin, C., Bastian, L., Bosch, D., et al. (2015). 20,000 years of Nile River dynamics and environmental changes in the Nile catchment area as inferred from Nile upper continental slope sediments. *Quaternary Science Reviews* 130**,** 200–221. doi: https://doi.org/10.1016/j.quascirev.2015.10.030.

Rey-Iglesia, A., Wilson, T., Routledge, J., Skovrind, M., Garde, E., Heide-Jørgensen, M.P., et al. (2022). Combining δ13C and δ15N from bone and dentine in marine mammal palaeoecological research: insights from toothed whales. *bioRxiv***,** 2021.2012.2013.472362. doi: 10.1101/2021.12.13.472362.

Richardson, J.L., and Richardson, A.E. (1972). History of an African Rift Lake and Its Climatic Implications. *Ecological Monographs* 42(4)**,** 499–534. doi: https://doi.org/10.2307/1942169.

Rick, T.C., Kirch, P.V., Erlandson, J.M., and Fitzpatrick, S.M. (2013). Archeology, deep history, and the human transformation of island ecosystems. *Anthropocene* 4**,** 33–45. doi: https://doi.org/10.1016/j.ancene.2013.08.002.

Ring, U. (2018). "Tectonic Dynamics in the African Rift Valley and Climate Change". Oxford University Press).

Robakiewicz, E., Bergner, A., Mingram, J., Trauth, M., and Junginger, A. (2019). *25,000 years of moisture variability at Lake Nakuru, Central Kenya Rift.*

Robakiewicz, E., Bergner, A.G.N., Rosca, C., Kübler, S., Ketzer, V., Trauth, M.H., et al. (2025). Moisture availability and productivity at Lake Nakuru, Kenya leading into the African Humid Period. *Quaternary Science Reviews* 369**,** 109579. doi: https://doi.org/10.1016/j.quascirev.2025.109579.

Roberts, P., Perera, N., Wedage, O., Deraniyagala, S., Perera, J., Eregama, S., et al. (2017). Fruits of the forest: Human stable isotope ecology and rainforest adaptations in Late Pleistocene and Holocene (~36 to 3 ka) Sri Lanka. *Journal of Human Evolution* 106**,** 102–118. doi: https://doi.org/10.1016/j.jhevol.2017.01.015.

Roberts, P., Prendergast, M.E., Janzen, A., Shipton, C., Blinkhorn, J., Zech, J., et al. (2020). Late Pleistocene to Holocene human palaeoecology in the tropical environments of coastal eastern Africa. *Palaeogeography, Palaeoclimatology, Palaeoecology* 537**,** 109438. doi: https://doi.org/10.1016/j.palaeo.2019.109438.

Robertshaw, P. (1984). Archaeology in eastern Africa: recent developments and more dates. *The Journal of African History* 25**,** 369–393. doi: 10.1017/S0021853700028449.

Robertshaw, P. (1991). Gogo Falls. *Azania: Archaeological Research in Africa* 26**,** 63–195. doi: 10.1080/00672709109511425.

Robertshaw, P. (1994). Lake Victoria and Eastwards: Urewe, its antecedents and its neighbours. *Azania: Archaeological Research in Africa* 29-30(1)**,** 312–312. doi: 10.1080/00672709409511687.

Robertshaw, P. (2021). "Archaeology of Early Pastoralism in East Africa". (Oxford: Oxford University Press).

Robertshaw, P., Collett, D., Gifford, D., and Mbae, N.B. (1983). Shell middens on the shores of Lake Victoria. *Azania: Archaeological Research in Africa* 18(1)**,** 1–43. doi: 10.1080/00672708309511313.

Robertshaw, P., and Taylor, D. (2000). Climate change and the rise of political complexity in western Uganda *The Journal of African History* 41(1)**,** 1–28. doi: 10.1017/S0021853799007653.

Robertshaw, P.T. (1990a). *Early Pastoralists of South-western Kenya.* Nairobi: British Institute in Eastern Africa.

Robertshaw, P.T. (1990b). "Pottery Assemblages from the Lemek-Mara Region," in *Early Pastoralists of South-western Kenya,* ed. P.T. Robertshaw. (Nairobi: British Institute in Eastern Africa), 183–204.

Robertson, J.H., and Bradley, R. (2000). A New Paradigm: The African Early Iron Age without Bantu Migrations. *History in Africa* 27**,** 287–323. doi: 10.2307/3172118.

Robinson, J.R. (2017). Thinking locally: environmental reconstruction of Middle and Later Stone Age archaeological sites in Ethiopia, Kenya, and Zambia based on ungulate stable isotopes. *J Hum Evol* 106**,** 19–37. doi: 10.1016/j.jhevol.2017.01.013.

Robinson, J.R. (2019). A Holocene paleoenvironmental record based on ungulate stable isotopes from Lukenya Hill, Kenya. *Journal of Archaeological Science: Reports* 28**,** 102016. doi: https://doi.org/10.1016/j.jasrep.2019.102016.

Robinson, J.R. (2022). Investigating habitat heterogeneity of Late Pleistocene archaeological sites in eastern Africa from stable isotopes. *Historical Biology* 34(4)**,** 674–693. doi: 10.1080/08912963.2021.1942465.

Russell, J., Verschuren, D., and Eggermont, H. (2007). Spatial complexity of 'Little Ice Age' climate in East Africa: Sedimentary records from two crater lake basins in western Uganda. *Holocene* 17**,** 183–193. doi: 10.1177/0959683607075832.

Russell, T., Silva, F., and Steele, J. (2014). Modelling the spread of farming in the Bantu-speaking regions of Africa: an archaeology-based phylogeography. *PloS one* 9(1)**,** e87854–e87854. doi: 10.1371/journal.pone.0087854.

Samec, C.T., Yacobaccio, H.D., and Panarello, H.O. (2018). Stable isotope compositions of South American camelids in the Dry Puna of Argentina: A frame of reference for the study of prehistoric herding and hunting strategies. *Journal of Archaeological Science: Reports* 18**,** 628–636. doi: https://doi.org/10.1016/j.jasrep.2017.10.042.

Sawchuk, E.A. (2019). *Social change and human population movements — dental morphology in Holocene Eastern Africa.* PhD Dissertation, University of Toronto.

Sawchuk, E.A., Goldstein, S.T., Grillo, K.M., and Hildebrand, E.A. (2018). Cemeteries on a moving frontier: Mortuary practices and the spread of pastoralism from the Sahara into eastern Africa. *Journal of Anthropological Archaeology* 51**,** 187–205. doi: https://doi.org/10.1016/j.jaa.2018.08.001.

Sawchuk, E.A., Hildebrand, E.A., Hill, A.C., Contreras, D.A., Edung, J.E., Janzen, A., et al. (2022). The Jarigole mortuary tradition reconsidered. *Antiquity* 96(390)**,** 1460–1477. doi: 10.15184/aqy.2022.141.

Schaebitz, F., Asrat, A., Lamb, H.F., Cohen, A.S., Foerster, V., Duesing, W., et al. (2021). Hydroclimate changes in eastern Africa over the past 200,000 years may have influenced early human dispersal. *Communications Earth & Environment* 2(1)**,** 123. doi: 10.1038/s43247-021-00195-7.

Schiffer, M.B. (1986). Radiocarbon dating and the "old wood" problem: The case of the Hohokam chronology. *Journal of Archaeological Science* 13(1)**,** 13–30. doi: https://doi.org/10.1016/0305-4403(86)90024-5.

Schmidt, P.R. (1975). A New look at interpretations of the Early Iron Age in East Africa. *History in Africa* 2**,** 127–136. doi: 10.2307/3171469.

Schmidt, P.R., and Childs, S.T. (1985). Innovation and industry during the Early Iron Age in East Africa: the KM2 and KM3 sites of northwest Tanzania. *African Archaeological Review* 3(1)**,** 53–94. doi: 10.1007/BF01117455.

Schmidt, S.C., and Hageneuer, S. (2024). Digital and computational archaeology in Germany. *it - Information Technology* 66(6)**,** 269–277. doi: doi:10.1515/itit-2024-0091.

Schoeninger, M.J. (1995). Stable isotope studies in human evolution. *Evolutionary Anthropology: Issues, News, and Reviews* 4(3)**,** 83–98. doi: 10.1002/evan.1360040305.

Schoeninger, M.J. (2014). Stable Isotope Analyses and the Evolution of Human Diets. *Annual Review of Anthropology* 43(1)**,** 413–430. doi: 10.1146/annurev-anthro-102313-025935.

Schoeninger, M.J., and DeNiro, M.J. (1984). Nitrogen and carbon isotopic composition of bone collagen from marine and terrestrial animals. *Geochimica et Cosmochimica Acta* 48(4)**,** 625–639. doi: https://doi.org/10.1016/0016-7037(84)90091-7.

Schulting, R.J., Vaiglova, P., Crozier, R., and Reimer, P.J. (2017). Further isotopic evidence for seaweed-eating sheep from Neolithic Orkney. *Journal of Archaeological Science: Reports* 11**,** 463–470. doi: https://doi.org/10.1016/j.jasrep.2016.12.017.

Schuur, E.A.G., Druffel, E.R.M., and Trumbore, S.E. (2016). *Radiocarbon and Climate Change Mechanisms, Applications and Laboratory Techniques.* Switzerland: Springer Cham.

Schwarcz, H.P. (2000). "Radicarbon Dating," in *Encyclopedia of Human Evolution,* eds. E. Delson, I. Tattersal, J.A.V. Couvering & A.S. Brooks.), 610–611.

Schwarcz, H.P., and Schoeninger, M.J. (2012). "Stable Isotopes of Carbon and Nitrogen as Tracers for Paleo-Diet Reconstruction," in *Handbook of Environmental Isotope Geochemistry: Vol I*, ed. M. Baskaran. (Berlin, Heidelberg: Springer Berlin Heidelberg), 725–742.

Sealy, J., Johnson, M., Richards, M., and Nehlich, O. (2014). Comparison of two methods of extracting bone collagen for stable carbon and nitrogen isotope analysis: comparing whole bone demineralization with gelatinization and ultrafiltration. *Journal of Archaeological Science* 47**,** 64–69. doi: https://doi.org/10.1016/j.jas.2014.04.011.

Sealy, J.C., Merwe, N.v.d., Thorp, J.A.L., and Lanham, J.L. (1987). Nitrogen isotopic ecology in southern Africa: Implications for environmental and dietary tracing. *Geochimica et Cosmochimica Acta* 51**,** 2707–2717.

Sealy, J.C., van der Merwe, N.J., Sillen, A., Kruger, F.J., and Krueger, H.W. (1991). 87Sr86Sr as a dietary indicator in modern and archaeological bone. *Journal of Archaeological Science* 18(3)**,** 399–416. doi: https://doi.org/10.1016/0305-4403(91)90074-Y.

Sefton, J., Woodroffe, S., and Ascough, P. (2021). "Radiocarbon dating of mangrove sediments."), 199–215.

Seidensticker, D., Hubau, W., Verschuren, D., Fortes-Lima, C., de Maret, P., Schlebusch, C.M., et al. (2021). Population collapse in Congo rainforest from 400 CE urges reassessment of the Bantu Expansion. *Sci Adv* 7(7). doi: 10.1126/sciadv.abd8352.

Seitsonen, O. (2012). Pastoral Neolithic studies in northern Tanzania: an interim report on XRF and stable isotope analyses in the Engaruka area. *Nyame Akuma* (77)**,** 11–23.

Serneels, V., Morel, M., Nitsche, C., Radimilah, C., Rakotoarisoa, J.-A., Rasoarifetra, B., et al. (2020). Pierre et fer à Madagascar (3) – La carrière de Bobalila. *SLSA Jahresbericht – Rapport annuel – 2019* 291–352. doi: https://www.unifr.ch/geo/archaeometry/en/assets/public/assets/public/uploads/slsa_jb2019_(p291-352)_madagascar-bobalila_low.pdf.

Serneels, V., Morel, M., Nitsche, C., Radimilahy, C., Rakotoarisoa, J.-A., B, B., et al. (2018). Pierre et Fer à Madagascar (1) - Vestiges sidérurgiques de Benavony et de la rivière Matavy. *SLSA Jahresbericht – Rapport annuel – Annual report 2017*. doi: 10.13140/RG.2.2.28729.52326.

Serneels, V., Morel, M., Nitsche, C., Radimilahy, C., Rakotoarsisoa, J.-A., Rasoarifetra, B., et al. (2019). Pierre et fer à Madagascar (2) – Les scories d'Amboronala et lescarrières de Milanoa. *SLSA Jahresbericht – Rapport annuel 2018***,** 313–366. doi: https://www.unifr.ch/geo/archaeometry/en/assets/public/files/Serneels%20et%20al%202018%20(SLSA).pdf.

Shahack-Gross, R., Simons, A., and Ambrose, S.H. (2008). Identification of pastoral sites using stable nitrogen and carbon isotopes from bulk sediment samples: a case study in modern and archaeological pastoral settlements in Kenya. *Journal of Archaeological Science* 35(4)**,** 983–990. doi: https://doi.org/10.1016/j.jas.2007.07.002.

Shennan, S. (2018). "The Spread of Farming into Central Europe," in *The First Farmers of Europe: An Evolutionary Perspective,* ed. S. Shennan. (Cambridge: Cambridge University Press), 79–105.

Shennan, S., Downey, S.S., Timpson, A., Edinborough, K., Colledge, S., Kerig, T., et al. (2013). Regional population collapse followed initial agriculture booms in mid-Holocene Europe. *Nature Communications* 4(1)**,** 2486. doi: 10.1038/ncomms3486.

Shipton, C., Crowther, A., Kourampas, N., Prendergast, M.E., Horton, M., Douka, K., et al. (2016). Reinvestigation of Kuumbi Cave, Zanzibar, reveals Later Stone Age coastal habitation, early Holocene abandonment and Iron Age reoccupation. *Azania: Archaeological Research in Africa* 51(2)**,** 197–233. doi: 10.1080/0067270X.2016.1173308.

Shipton, C., Helm, R., Boivin, N., Crowther, A., Austin, P., and Fuller, D. (2013). Intersections, Networks and the Genesis of Social Complexity on the Nyali Coast of East Africa. *African Archaeological Review* 30. doi: 10.1007/s10437-013-9140-5.

Shipton, C., Roberts, P., Archer, W., Armitage, S.J., Bita, C., Blinkhorn, J., et al. (2018). 78,000-year-old record of Middle and Later Stone Age innovation in an East African tropical forest. *Nature Communications* 9(1)**,** 1832. doi: 10.1038/s41467-018-04057-3.

Shoemaker, A. (2018). *Pastoral pasts in the Amboseli landscape: An archaeological exploration of the Amboseli ecosystem from the later Holocene to the colonial Period.* PhD, Uppsala University.

Simonetti, A., and Buzon, M.R. (2025). Isotopes in Archeology: Perspectives on Post-Mortem Alteration and Climate Change. *Geosciences* 15(8)**,** 307.

Simons, E.L. (1997). "Lemurs: old and new," in *Natural Change and Human Impacts in Madagascar*, eds. S.M. Goodman & B.D. Patterson. (Washington DC: Smithsonian Press), 142–168.

Sinclair, P., Juma, A., and Chami, F. (2006). *Excavations at Kuumbi Cave on Zanzibar 2005*. Dar es Salaam: Dar es Salaam University Press.

Sinclair, P.J.J. (1991). Archaeology in eastern Africa: an overview of current chronological issues. *The Journal of African History* 32(2)**,** 179–219. doi: 10.1017/S0021853700025706.

Sinninghe Damsté, J.S., Verschuren, D., Ossebaar, J., Blokker, J., van Houten, R., van der Meer, M.T.J., et al. (2011). A 25,000-year record of climate-induced changes in lowland vegetation of eastern equatorial Africa revealed by the stable carbon-isotopic composition of fossil plant leaf waxes. *Earth and Planetary Science Letters* 302(1)**,** 236–246. doi: https://doi.org/10.1016/j.epsl.2010.12.025.

Sirak, K.A., Sawchuk, E.A., and Prendergast, M.E. (2022). "Ancient Human DNA and African Population History". Oxford University Press).

Skoglund, P., Thompson, J.C., Prendergast, M.E., Mittnik, A., Sirak, K., Hajdinjak, M., et al. (2017). Reconstructing prehistoric African population structure. *Cell* 171(1)**,** 59–71.e21. doi: 10.1016/j.cell.2017.08.049.

Slovak, N.M., and Paytan, A. (2011). "Applications of Sr isotopes in archaeology," in *Handbook of Environmental Isotope Geochemistry: Advances in Isotope Geochemistry*, ed. M. Baskaran. (Berlin: Springer-Verlag), 743–768.

Smith, B.N., and Epstein, S. (1971). Two categories of 13C/12C ratios for higher plants *Plant Physiology* 47(3)**,** 380–384. doi: 10.1104/pp.47.3.380.

Smith, C.C., Morgan, M.E., and Pilbeam, D. (2010). Isotopic ecology and dietary profiles of Liberian chimpanzees. *Journal of Human Evolution* 58(1)**,** 43–55.

Snoeck, C., Ryan, S., Pouncett, J., Pellegrini, M., Claeys, P., Wainwright, A., et al. (2019). Towards a biologically available strontium isotope baseline for Ireland. *Science of The Total Environment* in press. doi: 10.1016/j.scitotenv.2019.136248.

Soper, R. (1967a). Iron Age sites in North-Eastern Tanzania. *Azania: Archaeological Research in Africa* 2(1)**,** 19–36. doi: 10.1080/00672706709511438.

Soper, R. (1967b). Kwale: An Early Iron Age site in South-eastern Kenya. *Azania: Archaeological Research in Africa* 2(1)**,** 1–17. doi: 10.1080/00672706709511437.

Soper, R. (1971). Early Iron Age Pottery Types from East Africa: Comparative Analysis. *Azania: Archaeological Research in Africa* 6(1)**,** 39–52. doi: 10.1080/00672707109511546.

Soper, R. (1975). Notes on some caves in Kilifi District. *Caves Exploration Group of the East African Society*.

Soper, R. (1976). Archaeological sites in the Chyulu Hills, Kenya. *Azania: Archaeological Research in Africa* 11(1)**,** 83–116. doi: 10.1080/00672707609511232.

Soper, R. (1979). Iron Age Archaeology and Traditional History in Embu, Mbeere and Chuka Areas of Central Kenya. *Azania: Archaeological Research in Africa* 14(1)**,** 31–59. doi: 10.1080/00672707909511262.

Soper, R.C. (1969). Radiocarbon dating of "dimple-based ware" in western Kenya *Azania: Archaeological Research in Africa* 4(1)**,** 148–153. doi: 10.1080/00672706909511514.

Sponheimer, M. (2013). "Hominin Paleodiets: The Contribution of Stable Isotopes," in *Handbook of Paleoanthropology,* eds. W. Henke, I. Tattersal & T. Hardt. (Berlin: Springer-Verlag), 555–586.

Sponheimer, M., Alemseged, Z., Cerling, T.E., Grine, F.E., Kimbel, W.H., Leakey, M.G., et al. (2013). Isotopic evidence of early hominin diets. *Proceedings of the National Academy of Sciences* 110(26)**,** 10513–10518. doi: 10.1073/pnas.1222579110.

Sponheimer, M., Codron, D., Passey, B.H., Ruiter, D.d., Cerling, T.E., and Lee-Thorp, J.A. (2009). Using carbon isotopes to track dietary change in modern, historical, and ancient primates. *American Journal of Physical Anthropology* 140**,** 661–670.

Sponheimer, M., Lee-Thorp, J., Ruiter, D.d., Codron, D., Codron, J., Baugh, A.T., et al. (2005a). Hominins, sedges, and termites: new carbon isotope data from the Sterkfontein Valley and Kruger National Park. *Journal of Human Evolution* 48**,** 301–312. doi: https://doi.org/10.1016/j.jhevol.2004.11.008.

Sponheimer, M., and Lee-Thorp, J.A. (2003). Using carbon isotope data of fossil bovid communities for palaeoenvironmental reconstruction. *South African Journal of Science* 99**,** 273–275.

Sponheimer, M., and Lee-Thorp, J.A. (2007). "Hominin Paleodiets: The Contribution of Stable Isotopes," in *Handbook of Paleoanthropology,* eds. W. Henke, I. Tattersal & T. Hardt. (Berlin: Springer-Verlag), 555–585.

Sponheimer, M., Passey, B.H., de Ruiter, D.J., Guatelli-Steinberg, D., Cerling, T.E., and Lee-Thorp, J.A. (2006b). Isotopic evidence for dietary variability in the early hominin *Paranthropus robustus*. *Science* 314**,** 980–982.

Sponheimer, M., Ruiter, D., Lee-Thorp, J., and Späth, A. (2005b). Sr/Ca and early hominin diets revisited: new data from modern and fossil tooth enamel. *Journal of human evolution* 48**,** 147–156. doi: 10.1016/j.jhevol.2004.09.003.

Stager, J.C., Cumming, B., and Meeker, L. (1997). A High-Resolution 11,400-Yr Diatom Record from Lake Victoria, East Africa. *Quaternary Research* 47(1)**,** 81–89. doi: 10.1006/qres.1996.1863.

Stager, J.C., Cumming, B.F., and Meeker, L.D. (2003). A 10,000-year high-resolution diatom record from Pilkington Bay, Lake Victoria, East Africa. *Quaternary Research* 59(2)**,** 172–181. doi: 10.1016/S0033-5894(03)00008-5.

Stager, J.C., Cumming, B.F., and Meeker, L.D. (2017). A 10,000-year high-resolution diatom record from Pilkington Bay, Lake Victoria, East Africa. *Quaternary Research* 59(2)**,** 172–181. doi: 10.1016/s0033-5894(03)00008-5.

Stager, J.C., and Johnson, T.C. (2000). A 12,400 14c yr offshore diatom record from East central Lake Victoria, East Africa. *Journal of Paleolimnology* 23**,** 373–383.

Stager, J.C., and Johnson, T.C. (2008). The Late Pleistocene desiccation of Lake Victoria and the origin of its endemic biota. *Hydrobiologia* 596**,** 5–16. doi: 10.1007/s10750-007-9158-2.

Stager, J.C., Ryves, D., Cumming, B.F., Meeker, L.D., and Beer, J. (2005a). Solar variability and the levels of Lake Victoria, East Africa, during the last millenium. *Journal of Paleolimnology* 33(2)**,** 243–251. doi: 10.1007/s10933-004-4227-2.

Stager, J.C., Westwood, J., Grzesik, D., and Cumming, B.F. (2005b). A 5500-year environmental history of Lake Nabugabo, Uganda. *Palaeogeography, Palaeoclimatology, Palaeoecology* 218(3)**,** 347–354. doi: https://doi.org/10.1016/j.palaeo.2004.12.025.

Stahl, A. (2005). *African Archaeology: A Critical Introduction.* Oxford: Blackwell.

Steele, J. (2010). Radiocarbon dates as data: quantitative strategies for estimating colonization front speeds and event densities. *Journal of Archaeological Science* 37(8)**,** 2017–2030. doi: https://doi.org/10.1016/j.jas.2010.03.007.

Stephens, L., Fuller, D., Boivin, N., Rick, T., Gauthier, N., Kay, A., et al. (2019). Archaeological assessment reveals Earth's early transformation through land use. *Science* 365(6456)**,** 897–902. doi: 10.1126/science.aax1192.

Stewart, B., Zhao, Y., Mitchell, P., Dewar, G., Gleason, J., and Blum, J. (2020). Ostrich eggshell bead strontium isotopes reveal persistent macroscale social networking across late Quaternary southern Africa. *Proceedings of the National Academy of Sciences*. doi: 10.1073/pnas.1921037117.

Stewart, K.A. (1993). Iron Age ceramic studies in Great Lakes eastern Africa: a critical and historiographical review. *African Archaeological Review* 11(1)**,** 21–37. doi: 10.1007/BF01118141.

Stiles, D. (1981). Hunters of the Northern East African Coast: Origins and Historical Processes. *Africa* 51. doi: 10.2307/1159358.

Stiles, D. (1982). A history of the hunting peoples of the northern East Africa coast: Ecological and socio-economic consideractions *Paideuma* 28**,** 165–174.

Stites, E., Gargule, A., Lyer, P., and Young, H. (2023). "Mobility Matters: The Benefits of Pastoralists Mobility for Nutrition in Marsabit and Isiolo Counties, Kenya", in: *Briefing Paper*).

Sutton, J. (1998a). Engaruka: an irrigation agricultural community in northern Tanzanian before the Maasai era. *Azania: Archaeological Research in Africa* 33(1)**,** 1–37. doi: 10.1080/00672709809511463.

Sutton, J.E.G. (1965). Sirikwa holes, stone houses and their makers in the western highlands of Kenya. *Man* 65**,** 113–115.

Sutton, J.E.G. (1966). The archaeology and early peoples of the highlands of Kenya and northern Tanzania. *Azania: Archaeological Research in Africa* 1(1)**,** 37–57. doi: 10.1080/00672706609511340.

Sutton, J.E.G. (1973). *The Archaeology of the Western Highlands of Kenya.* Nairobi: British Institute in Eastern Africa.

Sutton, J.E.G. (1987). Hyrax Hill and the Sirikwa. *Azania: Archaeological Research in Africa* 22(1)**,** 1–36. doi: 10.1080/00672708709511378.

Sutton, J.E.G. (1993a). "Becoming Maasailand," in *Being Maasai: Ethnicity and Identity in East Africa,* eds. T. Spear & W. Waller. (London: James Currey), 38–60.

Sutton, J.E.G. (1993b). Further excavations, and the Iron Age sequence of the Central Rift. *Azania: Archaeological Research in Africa* 28(1)**,** 103–125. doi: 10.1080/00672709309511650.

Sutton, J.E.G. (1994–95). *The Growth of Farming Communities in Africa South of the Equator.* London: Bristish Institute in Eastern Africa.

Sutton, J.E.G. (1998b). Farmers, cattle-herders and rulers in western Uganda, AD 1000–1500. *Azania: Archaeological Research in Africa* 33(1)**,** 39–72. doi: 10.1080/00672709809511464.

Sutton, J.E.G. (1998c). Hyrax Hill and the later archaeology of the central Rift Valley of Kenya. *Azania* XXXIII.

Sutton, J.E.G. (1998d). Irrigation agriculture in the northern Tanzanian Rift Valley before the Maasai era. *Azania: Archaeological Research in Africa* 33(1)**,** 1–37. doi: 10.1080/00672709809511463.

Szostek, K., Madrzyk, K., and Cienkosz-Stepanczak, B. (2015). Strontium isotopes as an indicator of human migration - easy questions, difficult answers. *Anthropological Review* 78(2)**,** 133–156.

Szpak, P. (2014). Complexities of nitrogen isotope biogeochemistry in plant-soil systems: implications for the study of ancient agricultural and animal management practices. *Frontiers in Plant Science* 5. doi: 10.3389/fpls.2014.00288.

Tafuri, M.A., Bentley, R.A., Manzi, G., and di Lernia, S. (2006). Mobility and kinship in the prehistoric Sahara: Strontium isotope analysis of Holocene human skeletons from the Acacus Mts. (southwestern Libya). *Journal of Anthropological Archaeology* 25(3)**,** 390–402. doi: https://doi.org/10.1016/j.jaa.2006.01.002.

Talbot, M.R., and Lærdal, T. (2000). The Late Pleistocene - Holocene palaeolimnology of Lake Victoria, East Africa, based upon elemental and isotopic analyses of sedimentary organic matter. *Journal of Paleolimnology* 23**,** 141–164. doi: DOI:10.1023/A:1008029400463.

Tarrant, D., Hepburn, J., Renson, V., and Richards, M. (2024). A pilot bioavailable strontium isotope baseline map of Southern British Columbia, Canada. *FACETS* 9**,** 1–11. doi: 10.1139/facets-2023-0173.

Taylor, R.D.F. (1966). The Gumba and 'Gumba Pits' of the Fort Hall District, Kenya. *Azania: Archaeological Research in Africa* 1(1)**,** 111–117. doi: 10.1080/00672706609511344.

Taylor, R.E., and Aitken, M.J. (1997). *Chronometric Dating in Archaeology*. New York: Plenum Press.

Tejada, J.V., Flynn, J.J., Antoine, P.-O., Pacheco, V., Salas-Gismondi, R., and Cerling, T.E. (2020). Comparative isotope ecology of western Amazonian rainforest mammals. *Proceedings of the National Academy of Sciences* 117(42)**,** 26263–26272. doi: 10.1073/pnas.2007440117.

Thoennessen, M. (2016). "Isotopes of Stable Elements," in *The Discovery of Isotopes: A Complete Compilation*. (Cham: Springer International Publishing), 23–37.

Thompson, L.G., Mosley-Thompson, E., Davis, M.E., Henderson, K.A., Brecher, H.H., Zagorodnov, V.S., et al. (2002). Kilimanjaro Ice Core Records: Evidence of Holocene Climate Change in Tropical Africa. *Science* 298(5593)**,** 589–593. doi: 10.1126/science.1073198.

Tierney, J., Russell, J., Sinninghe-Damste, J., Huang, Y., and Verschuren, D. (2011). Late Quaternary behavior of the East African monsoon and the importance of the Congo Air Boundary. *Quaternary Science Reviews - QUATERNARY SCI REV* 30**,** 798–807. doi: 10.1016/j.quascirev.2011.01.017.

Tishkoff, S.A., Gonder, M.K., Henn, B.M., Mortensen, H., Knight, A., Gignoux, C., et al. (2007). History of Click-Speaking Populations of Africa Inferred from mtDNA and Y

Chromosome Genetic Variation. *Molecular Biology and Evolution* 24(10)**,** 2180–2195. doi: 10.1093/molbev/msm155.

Tite, M.S., and Waine, J. (1962). Thermoluminescent dating: A re-appraisal. *Archaeometry* 5(1)**,** 53–79. doi: https://doi.org/10.1111/j.1475-4754.1962.tb00554.x.

Trigger, B. (2006). "Culture-Historical Archaeology," in *A History of Archaeological Thought*, ed. B.G. Trigger. 2 ed (Cambridge: Cambridge University Press), 211–313.

Trigger, B.G. (1989). *A History of Archaeological Thought.* Cambridge: Cambridge University Press.

Trigger, B.G. (2007). *A History of Archaeological Thought* New York: Cambridge University Press.

Tryon, C.A., and Faith, J.T. (2016). A demographic perspective on the Middle to Later Stone Age transition from Nasera rockshelter, Tanzania. *Philosophical Transactions of the Royal Society B: Biological Sciences* 371(1698)**,** 20150238. doi: doi:10.1098/rstb.2015.0238.

Turakhujaev, K. (2025). *Responsible Data Science: Fairness Audit of Black Box Models.*

Tykot, R.H. (Year). "Stable isotopes and diet : You are what you eat").

Tykot, R.H., van der Merwe, N.J., and Hammond, N. (1996). "Stable Isotope Analysis of Bone Collagen, Bone Apatite, and Tooth Enamel in the Reconstruction of Human Diet," in *Archaeological Chemistry*. American Chemical Society), 355–365.

United Nations Statistics Division (2011). *Standard Country and Area Codes Classifications (M49)* [Online]. United Nations Available: https://web.archive.org/web/20110713041240/http://millenniumindicators.un.org/unsd/methods/m49/m49regin.htm [Accessed].

Uno, K.T., Cerling, T.E., Harris, J.M., Kunimatsu, Y., Leakey, M.G., Nakatsukasa, M., et al. (2011). Late Miocene to Pliocene carbon isotope record of differential diet change among East African herbivores. *Proceedings of the National Academy of Sciences*. doi: 10.1073/pnas.1018435108.

Valenzuela-Suau, L., Valenzuela-Lamas, S., Ramis, D., and Bosch, D. (2022). Caprine Mobility on the Balearic Islands During the Middle and Late Bronze Age (ca. 1600–850 BC): First Results Based on Strontium Isotopes (87Sr/86Sr). *Environmental Archaeology* 27(5)**,** 484–495. doi: 10.1080/14614103.2021.1921675.

van der Merwe, N.J. (1982). Carbon isotopes, photosynthesis, and archaeology: different pathways of photosynthesis cause characteristic changes in carbon isotope ratios that make possible the study of prehistoric human diets. *American Scientist* 70(6)**,** 596–606.

van der Merwe, N.J. (1992). "Light stable isotopes and the reconstruction of prehistoric diets," in *New Developments in Archaeological Science,* ed. J. van der Merwe Nicholas.), 247–264.

van der Merwe, N.J., and Medina, E. (1989). Photosynthesis and $^{13}C/^{12}C$ ratios in Amazonian rain forests. *Geochimica et Cosmochimica Acta* 53(5)**,** 1091–1094.

van der Merwe, N.J., and Medina, E. (1991). The canopy effect, carbon isotope ratios and foodwebs in Amazonia. *Journal of Archaeological Science* 18(3)**,** 249–259.

van der Plas, G., Rucina, S., Andreas, H., Marchant, R., Hooghiemstra, H., Schüler, L., et al. (2020). Climate-human-landscape interaction in the eastern foothills of Mt. Kilimanjaro (equatorial East Africa) during the last two millennia. *The Holocene***,** 095968362098169. doi: 10.1177/0959683620981694.

van Dommelen, P. (2014). Moving On: Archaeological Perspectives on Mobility and Migration. *World Archaeology* 46(4)**,** 477–483. doi: 10.1080/00438243.2014.933359.

Van Grunderbeek, M.-C. (1988). Essai d'étude typologique de céramique urewe de la région des collines au Burundi et Rwanda. *Azania: Archaeological Research in Africa* 23(1)**,** 11–55. doi: 10.1080/00672708809511386.

Van Grunderbeek, M.-C. (1992). Essai de délimitation chronologique de l'Age du Fer Ancien au Burundi, au Rwanda et dans la région des Grands Lacs. *Azania: Archaeological Research in Africa* 27(1)**,** 53–80. doi: 10.1080/00672709209511431.

Van Grunderbeek, M.-C., and Roche, E. (2008a). *Environment degradation resulting from human activities. Essay to further recognition through pollen and charcoal analysis. SAfA-website http://safa.rice.edu/About_SAfA/SAfA_2008_Conference-Proceedings_by_Program_Session.*

Van Grunderbeek, M.-C., and Roche, E. (2008b). *Multi-Disciplinary Evidence of Mixed Farming during the Early Iron Age in Rwanda and Burundi. (presented at the World Archaeological Congress, Washington 2003) in. T.P. Denham, J. Iriarte, L. Vrydaghs (eds) Rethinking Agriculture. Archaeological en Ethnoarchaeological Perspectives, One World Archaeology 51, Left Coast Press, inc. California, pp.299-319.*

van Klinken, G.J. (1999). Bone Collagen Quality Indicators for Palaeodietary and Radiocarbon Measurements. *Journal of Archaeological Science* 26(6)**,** 687–695. doi: https://doi.org/10.1006/jasc.1998.0385.

Van Noten, F. (1979). The Early Iron Age in the Interlacustrine region: The diffusion of iron technology. *Azania: Archaeological Research in Africa* 14(1)**,** 61–80. doi: 10.1080/00672707909511263.

Vansina, J. (1995). New Linguistic Evidence and 'The Bantu Expansion'. *The Journal of African History* 36(2)**,** 173–195. doi: 10.1017/S0021853700034101.

VanValkenburgh, P., and Dufton, J.A. (2020). Big Archaeology: Horizons and blindspots. *Journal of Field Archaeology* 45(sup1)**,** S1–S7. doi: 10.1080/00934690.2020.1714307.

Ventresca Miller, A., and Makarewicz, C. (2017). "Isotopic Investigations of Pastoralism in Prehistory (1st ed.)". Routledge).

Verschuren, D. (2004a). "Decadal and Century-Scale Climate Variability in Tropical Africa during the Past 2000 years," in *Past Climate Variability through Europe and Africa*, eds. R.W. Battarbee, F. Gasse & C.E. Stickley. (Dordrecht: Springer Netherlands), 139–158.

Verschuren, D. (2004b). "The Last 2000 Years in Tropical Africa," in *Past Climate Variability Through Europe and Africa*, eds. R.W. Battarbee, F. Gasse & C.E. Stickley. (Dordrecht: Springer), 139–158.

Verschuren, D., Laird, K.R., and Cumming, B.F. (2000). Rainfall and drought in equatorial East Africa during the past 1,100 years. *Nature* 403**,** 410–414.

Verschuren, D., Sinninghe Damsté, J.S., Moernaut, J., Kristen, I., Blaauw, M., Fagot, M., et al. (2009). Half-precessional dynamics of monsoon rainfall near the East African Equator. *Nature* 462(7273)**,** 637–641. doi: 10.1038/nature08520.

Walsh, M. (1993). The Vuna and the Degere: remnants and outcasts among the Duruma and Digo of Kenya and Tanzania. *Bulletin of the International Committee on Urgent Anthropological and Ethnological Research. International Committee on Urgent Anthropological and Ethnological Research* 34-35**,** 133–147.

Walshaw, S.C. (2005). *Swahili urbanization, trade, and food production: botanical perspectives from Pemba Island, Tanzania, A.D. 600-1500.* PhD Unpublished Dissertation, Washington University.

Wandibba, S. (1985). "A survey of the archaeology of Bungoma District," in *History and Culture in Westem Kenya: The People of Bungoma District through Time*, ed. S. Wandibba. (Nairobi: Gideon S. Were Press), 11–17.

Wandibba, S. (1990). Ancient and modern ceramic traditions in the Lake Victoria Basin of Kenya. *Azania: Archaeological Research in Africa* 25(1)**,** 69–78. doi: 10.1080/00672709009511409.

Wang, K., Goldstein, S., Bleasdale, M., Clist, B., Bostoen, K., Bakwa-Lufu, P., et al. (2020). Ancient genomes reveal complex patterns of population movement, interaction, and replacement in sub-Saharan Africa. *Science Advances* 6(24)**,** eaaz0183. doi: 10.1126/sciadv.aaz0183.

Werdelin, L., and Sanders, W.J. (2010). *Cenozoic Mammals of Africa.* Berkeley: University of California Press.

Were, G.S., and Wilson, D.A. (1970). *East Africa Through a Thousand Years: AD 1000 to the Present Day.* Ibadan: Evans Brothers Limited.

Werner, A. (1915). The Bantu coast tribes of the East African Protectorate. *The Journal Of The Royal Anthropological Institute Of Great Britain And Ireland* 45**,** 326–354.

Westerberg, L.-O., Holmgren, K., BÖRjeson, L., HÅKansson, N.T., Laulumaa, V., Ryner, M., et al. (2010). The development of the ancient irrigation system at Engaruka, northern Tanzania: physical and societal factors. *The Geographical Journal* 176(4)**,** 304–318.

White, F. (1983). *The Vegetation of Africa: A Descriptive Memoir to Accompany the UNESCO/AETFAT/UNSO Vegetation Maps of Africa (3 plates), 1:5,000,000.* Paris: UNESCO.

White, T.D., Ambrose, S.H., Suwa, G., Su, D.F., DeGusta, D., Bernor, R.L., et al. (2009). Macrovertebrate paleontology and the Pliocene habitat of *Ardipithecus ramidus*. *Science* 326(5949)**,** 67, 87–93. doi: 10.1126/science.1175822.

White, T.D., Ambrose, S.H., Suwa, G., and WoldeGabriel, G. (2010). Response to comment on the paleoenvironment of Ardipithecus ramidus. *Science* 328(5982)**,** 1105. doi: 10.1126/science.1185466.

Whitehouse, W., and Putman, J. (1953). *Radioactive Isotopes.* Oxford: Oxford University Press; Clarendon Press.

Whiteley, P.M., Xue, M., and Wheeler, W.C. (2019). Revising the Bantu tree. *Cladistics* 35(3)**,** 329–348. doi: https://doi.org/10.1111/cla.12353.

Wilkin, S., Ventresca Miller, A., Miller, B.K., Spengler, R.N., Taylor, W.T.T., Fernandes, R., et al. (2020). Economic diversification supported the growth of Mongolia's nomadic empires. *Scientific Reports* 10(1)**,** 3916. doi: 10.1038/s41598-020-60194-0.

Wilkinson, M.D., Dumontier, M., Aalbersberg, I.J., Appleton, G., Axton, M., Baak, A., et al. (2016). The FAIR Guiding Principles for scientific data management and stewardship. *Scientific Data* 3(1)**,** 160018. doi: 10.1038/sdata.2016.18.

Williams, A.N. (2012). The use of summed radiocarbon probability distributions in archaeology: a review of methods. *Journal of Archaeological Science* 39(3)**,** 578–589. doi: https://doi.org/10.1016/j.jas.2011.07.014.

Williams, A.N., Veth, P., Steffen, W., Ulm, S., Turney, C.S.M., Reeves, J.M., et al. (2015). A continental narrative: Human settlement patterns and Australian climate change over the last 35,000 years. *Quaternary Science Reviews* 123**,** 91–112. doi: https://doi.org/10.1016/j.quascirev.2015.06.018.

Willis, J. (1996). The Northern Kayas of the Mijikenda. *Azania: Archaeological Research in Africa* 31(1)**,** 75–98. doi: 10.1080/00672709609511457.

Wilson, T.H. (2019). "Settlement archaeology at Takwa", (ed.) N.M.o. Kenya. (Nairobi).

Wilson, T.H., and Omar, A.L. (1997). Archaeological investigations at Pate. *Azania: Archaeological Research in Africa* 32(1)**,** 31–76. doi: 10.1080/00672709709511587.

Winchell, F., Brass, M., Manzo, A., Beldados, A., Perna, V., Murphy, C., et al. (2018). On the Origins and Dissemination of Domesticated Sorghum and Pearl Millet across Africa and into India: a View from the Butana Group of the Far Eastern Sahel. *African Archaeological Review* 35(4)**,** 483–505. doi: 10.1007/s10437-018-9314-2.

Wood, M., Panighello, S., Orsega, E.F., Robertshaw, P., van Elteren, J.T., Crowther, A., et al. (2017). Zanzibar and Indian Ocean trade in the first millennium CE: the glass bead evidence. *Archaeological and Anthropological Sciences* 9(5)**,** 879–901. doi: 10.1007/s12520-015-0310-z.

Woodburn, J. (1982). Egalitarian Societies. *Man* 17(3)**,** 431–451. doi: 10.2307/2801707.

Woodroffe, S.A., Long, A.J., Punwong, P., Selby, K., Bryant, C.L., and Marchant, R. (2015). Radiocarbon dating of mangrove sediments to constrain Holocene relative sea-level change on Zanzibar in the southwest Indian Ocean. *The Holocene* 25(5)**,** 820–831. doi: 10.1177/0959683615571422.

Wotzka, H.P. (1995). Studien zur Archäologie des zentralafrikanischen Regenwaldes: Die Keramik des inneren Zaïre-Beckens und ihre Stellung im Kontext der Bantu-Expansion. *Africa Praehistorica 6*.

Wright, D. (2003). Archaeological investigations of three Pastoral Neolithic sites in Tsavo National Park, Kenya. *Azania: Archaeological Research in Africa* 38(1)**,** 183–188. doi: 10.1080/00672700309480370.

Wright, D.K. (2005a). *Environment, chronology and resource exploitation of the Pastoral Neolithic in Tsavo, Kenya.* PhD, University of Illinois.

Wright, D.K. (2017). Accuracy vs. Precision: Understanding potential errors from radiocarbon dating on African landscapes. *African Archaeological Review* 34(3)**,** 303–319. doi: 10.1007/s10437-017-9257-z.

Wright, H.T. (1992). Early Islam, oceanic trade and town development on Nzwani: The Comorian Archipelago in the 11th-15th Centuries AD. *Azania* 27**,** 81–128.

Wright, H.T., Andrianalvoarivony, R., Bailiff, I., Burney, D., Haas, H., Raharijaona, V., et al. (1992). Datation absolue de sites archeologiques du centre de Madagascar: presentation des determinations. *Taloha* 11**,** 121–146.

Wright, H.T., and Fanony, F. (1992). The evolution of settlement systems in the Mananara River Valley: archaeological reconnaissance of 1983-1990. *TALOHA* (11)**,** 16–64.

Wright, H.T., Griffin, W., and Ramilisonina (2015). Early settlements near Belo-Sur-Mer. *Unpublished*.

Wright, L.E. (2005b). Identifying immigrants to Tikal, Guatemala: defining local variability in strontium isotope ratios of human tooth enamel. *Journal of Archaeological Science* (32)**,** 555–566.

Wynn, J.G. (2004). Influence of Plio-Pleistocene aridification on human evolution: Evidence from paleosols of the Turkana Basin, Kenya. *American Journal of Physical Anthropology* 123(2)**,** 106–118. doi: 10.1002/ajpa.10317.

Wynn, J.G., Alemseged, Z., Bobe, R., Grine, F.E., Negash, E.W., and Sponheimer, M. (2020). Isotopic evidence for the timing of the dietary shift toward C4 foods in eastern African Paranthropus. *Proceedings of the National Academy of Sciences* 117(36)**,** 21978–21984. doi: doi:10.1073/pnas.2006221117.

Wynn, J.G., Sponheimer, M., Kimbel, W.H., Alemseged, Z., Reed, K., Bedaso, Z.K., et al. (2013). Diet of Australopithecus afarensis from the Pliocene Hadar Formation, Ethiopia. *Proceedings of the National Academy of Sciences* 110(26)**,** 10495–10500. doi: 10.1073/pnas.1222559110.

Wynne-Jones, S., and Fleisher, J. (2015). Fifty years in the archaeology of the eastern African coast: A methodological history. *Azania Archaeological Research in Africa* 50**,** 519–541. doi: 10.1080/0067270X.2015.1102943.

Wynne-Jones, S., and LaViolette, A. (2018). *The Swahili World* London: Routledge Taylor and Francis Group.

Wynne-Jones, S., Sulas, F., Out, W.A., Kristiansen, S.M., Fitton, T., Ali, A.K., et al. (2021). Urban chronology at a human scale on the coast of East Africa in the 1st Millennium a.d. *Journal of Field Archaeology* 46(1)**,** 21–35. doi: 10.1080/00934690.2020.1854549.

Yang, L., Pei, X., Yuan, H., Xue, Y., Shao, J., Hou, K., et al. (2025). Millet-based agricultural intensification in Guanzhong Basin China during late Yangshao Culture period by isotopic analysis. *npj Heritage Science* 13. doi: 10.1038/s40494-025-01814-8.

Young, R., and Thompson, G. (1999). "Missing Plant Foods? Where is the Archaeobotanical Evidence for Sorghum and Finger Millet in East Africa?," in *The Exploitation of Plant Resources in Ancient Africa*, ed. M. van der Veen. (Boston, MA: Springer US), 63–72.

Ziegler, M., Simon, M.H., Hall, I.R., Barker, S., Stringer, C., and Zahn, R. (2013). Development of Middle Stone Age innovation linked to rapid climate change. *Nature Communications* 4(1)**,** 1905. doi: 10.1038/ncomms2897.

Ziemann, M., Poulain, P., and Bora, A. (2023). The five pillars of computational reproducibility: bioinformatics and beyond. *Brief Bioinform* 24(6). doi: 10.1093/bib/bbad375.

Appendix 1 – Tables and statistical analysis associated with "Chapter 5: The Kuumbi Cave isotopic case study"

Tables on isotopic data

Table A1:1 An isotopic dataset of faunal enamel ^{13}C and ^{18}O values, inclusive of sample taxon and age from Kuumbi Cave, Unguja Island (Iminjili et al., 2023).

	Phase	Context	Age	Taxon	$\delta^{13}C$	$\delta^{18}O$	Diet
1	Phase 1	1007	Iron Age (2,000-500 BP)	Bovid Size 1	-13.5	-5.3	Browser
2	Phase 3	1018	Late Pleistocene LSA (18,830-17,080 BP)	Bovid Size 1	-11.6	-2.3	NA
3	Phase 2	1015	Terminal Pleistocene LSA (13,040-11,340 BP)	Bovid Size 2	-8.6	-4.3	NA
4	Phase 3	1024	Late Pleistocene LSA (18,830-17,080 BP)	Bovid Size 2	-12.6	-2.4	NA
5	Phase 3	1019	Late Pleistocene LSA (18,830-17,080 BP)	Bovid Size 2	-10.8	-2.8	Browser
6	Phase 1	1007	Iron Age (2,000-500 BP)	Cephalophinae	-13.6	-5.3	Browser
7	Phase 1	1007	Iron Age (2,000-500 BP)	Cephalophinae	-14.4	-5.7	Browser
8	Phase 1	1011	Iron Age (2,000-500 BP)	Cephalophinae	-15.2	-6.4	Browser
9	Phase 1	1011	Iron Age (2,000-500 BP)	Cephalophinae	-13.4	-4.9	Browser
10	Phase 1	1011	Iron Age (2,000-500 BP)	Cephalophinae	-12.9	-5.8	Browser
11	Phase 2	1015	Terminal Pleistocene LSA (13,040-11,340 BP)	Cephalophinae	-13.2	-4.3	Browser
12	Phase 2	1015	Terminal Pleistocene LSA (13,040-11,340 BP)	Cephalophinae	-12.7	-3.7	Browser
13	Phase 2	1015	Terminal Pleistocene LSA (13,040-11,340 BP)	Cephalophinae	-14.1	-5.0	Browser
14	Phase 2	1015	Terminal Pleistocene LSA (13,040-11,340 BP)	Cephalophinae	-19.0	-10.3	Browser
15	Phase 2	1015	Terminal Pleistocene LSA (13,040-11,340 BP)	Cephalophinae	-14.2	-6.3	Browser
16	Phase 2	1015	Terminal Pleistocene LSA (13,040-11,340 BP)	Cephalophinae	-14.5	-2.6	Browser
17	Phase 2	1017	Terminal Pleistocene LSA (13,040-11,340 BP)	Cephalophinae	-12.1	-4.2	Browser
18	Phase 2	1017	Terminal Pleistocene LSA (13,040-11,340 BP)	Cephalophinae	-12.6	-4.4	Browser
19	Phase 2	1017	Terminal Pleistocene LSA (13,040-11,340 BP)	Cephalophinae	-10.7	-4.9	Browser
20	Phase 2	1017	Terminal Pleistocene LSA (13,040-11,340 BP)	Cephalophinae	-12.8	-3.8	Browser

	Phase	Context	Age	Taxon	$\delta^{13}C$	$\delta^{18}O$	Diet
21	Phase 2	1017	Terminal Pleistocene LSA (13,040-11,340 BP)	Cephalophinae	-12.4	-3.8	Browser
22	Phase 3	1018	Late Pleistocene LSA (18,830-17,080 BP)	Cephalophinae	-12.8	-4.1	Browser
23	Phase 3	1018	Late Pleistocene LSA (18,830-17,080 BP)	Cephalophinae	-12.5	-4.2	Browser
24	Phase 3	1018	Late Pleistocene LSA (18,830-17,080 BP)	Cephalophinae	-12.1	-3.7	Browser
25	Phase 3	1018	Late Pleistocene LSA (18,830-17,080 BP)	Cephalophinae	-12.8	-3.3	Browser
26	Phase 3	1018	Late Pleistocene LSA (18,830-17,080 BP)	Cephalophinae	-11.4	-2.3	Browser
27	Phase 3	1018	Late Pleistocene LSA (18,830-17,080 BP)	Cephalophinae	-11.9	-4.8	Browser
28	Phase 3	1018	Late Pleistocene LSA (18,830-17,080 BP)	Cephalophinae	-12.7	-2.8	Browser
29	Phase 3	1018	Late Pleistocene LSA (18,830-17,080 BP)	Cephalophinae	-12.6	-3.2	Browser
30	Phase 3	1018	Late Pleistocene LSA (18,830-17,080 BP)	Cephalophinae	-10.1	-3.8	Browser
31	Phase 3	1019	Late Pleistocene LSA (18,830-17,080 BP)	Cephalophinae	-10.8	-3.8	Browser
32	Phase 3	1019	Late Pleistocene LSA (18,830-17,080 BP)	Cephalophinae	-11.9	-4.3	Browser
33	Phase 3	1019	Late Pleistocene LSA (18,830-17,080 BP)	Cephalophinae	-11.7	-3.8	Browser
34	Phase 3	1019	Late Pleistocene LSA (18,830-17,080 BP)	Cephalophinae	-11.4	-2.8	Browser
35	Phase 3	1019	Late Pleistocene LSA (18,830-17,080 BP)	Cephalophinae	-11.8	-2.9	Browser
36	Phase 3	1022	Late Pleistocene LSA (18,830-17,080 BP)	Cephalophinae	-13.2	-4.5	Browser
37	Phase 3	1022	Late Pleistocene LSA (18,830-17,080 BP)	Cephalophinae	-12.8	-3.1	Browser
38	Phase 3	1023	Late Pleistocene LSA (18,830-17,080 BP)	Cephalophinae	-11.3	-2.1	Browser
39	Phase 3	1024	Late Pleistocene LSA (18,830-17,080 BP)	Cephalophinae	-11.9	-3.4	Browser
40	Phase 3	1024	Late Pleistocene LSA (18,830-17,080 BP)	Cephalophinae	-10.7	-3.0	Browser
41	Phase 3	1024	Late Pleistocene LSA (18,830-17,080 BP)	Cephalophinae	-11.7	-2.8	Browser
42	Phase 3	1024	Late Pleistocene LSA (18,830-17,080 BP)	Cephalophinae	-12.9	-3.6	Browser
43	Phase 3	1024	Late Pleistocene LSA (18,830-17,080 BP)	Cephalophinae	-11.6	-3.3	Browser
44	Phase 3	1024	Late Pleistocene LSA (18,830-17,080 BP)	Cephalophinae	-12.3	-2.6	Browser
45	Phase 3	1024	Late Pleistocene LSA (18,830-17,080 BP)	*Cephalophus adersi*	-12.6	-3.0	Browser
46	Phase 1	1002	Iron Age (2,000-500 BP)	*Philantomba monticola*	-11.4	-3.4	Browser
47	Phase 1	1002	Iron Age (2,000-500 BP)	*Philantomba monticola*	-11.1	-3.7	Browser
48	Phase 1	1002	Iron Age (2,000-500 BP)	*Philantomba monticola*	-11.2	-3.0	Browser

	Phase	Context	Age	Taxon	$\delta^{13}C$	$\delta^{18}O$	Diet
49	Phase 1	1002	Iron Age (2,000-500 BP)	*Philantomba monticola*	-11.3	-2.5	Browser
50	Phase 1	1003	Iron Age (2,000-500 BP)	*Philantomba monticola*	-10.6	-3.9	Browser
51	Phase 1	1003	Iron Age (2,000-500 BP)	*Philantomba monticola*	-11.3	-7.8	Browser
52	Phase 1	1003	Iron Age (2,000-500 BP)	*Philantomba monticola*	-11.7	-4.2	Browser
53	Phase 1	1003	Iron Age (2,000-500 BP)	*Philantomba monticola*	-12.4	-3.4	Browser
54	Phase 1	1003	Iron Age (2,000-500 BP)	*Philantomba monticola*	-15.5	-8.1	Browser
55	Phase 1	1004	Iron Age (2,000-500 BP)	*Philantomba monticola*	-12.7	-3.7	Browser
56	Phase 1	1004	Iron Age (2,000-500 BP)	*Philantomba monticola*	-11.7	-3.9	Browser
57	Phase 1	1004	Iron Age (2,000-500 BP)	*Philantomba monticola*	-11.8	-3.7	Browser
58	Phase 1	1004	Iron Age (2,000-500 BP)	*Philantomba monticola*	-11.9	-3.8	Browser
59	Phase 4	1025	Sterile (>20,000 BP)	*Philantomba monticola*	-11.0	-3.5	Browser
60	Phase 4	1025	Sterile (>20,000 BP)	*Philantomba monticola*	-11.2	-4.0	Browser
61	Phase 1	1002	Iron Age (2,000-500 BP)	*Cephalophus sp.*	-13.1	-6.4	Browser
62	Phase 1	1003	Iron Age (2,000-500 BP)	*Cephalophus sp.*	-12.9	-4.8	Browser
63	Phase 1	1005	Iron Age (2,000-500 BP)	*Cephalophus sp.*	-12.4	-4.4	Browser
64	Phase 1	1005	Iron Age (2,000-500 BP)	*Cephalophus sp.*	-12.6	-3.9	Browser
65	Phase 1	1013	Holocene (2,000-500 BP)	Cercopithecinae	-14.0	-2.6	Browser
66	Phase 1	1002	Iron Age (2,000-500 BP)	Cercopithecinae	-10.6	-2.7	Browser
67	Phase 1	1002	Iron Age (2,000-500 BP)	Cercopithecinae	-12.8	-4.5	Browser
68	Phase 1	1002	Iron Age (2,000-500 BP)	Cercopithecinae	-11.2	-3.8	Browser
69	Phase 1	1004	Iron Age (2,000-500 BP)	Cercopithecinae	-12.3	-4.2	Browser
70	Phase 1	1005	Iron Age (2,000-500 BP)	Cercopithecinae	-12.6	-3.9	Browser
71	Phase 1	1007	Iron Age (2,000-500 BP)	Cercopithecinae	-13.4	-1.3	Browser
72	Phase 1	1007	Iron Age (2,000-500 BP)	Cercopithecinae	-13.3	-5.1	Browser
73	Phase 1	1007	Iron Age (2,000-500 BP)	Cercopithecinae	-14.8	-5.3	Browser
74	Phase 1	1007	Iron Age (2,000-500 BP)	Cercopithecinae	-13.3	-4.5	Browser
75	Phase 1	1010	Iron Age (2,000-500 BP)	Cercopithecinae	-12.6	-5.3	Browser
76	Phase 1	1011	Iron Age (2,000-500 BP)	Cercopithecinae	-15.2	-5.0	Browser

	Phase	Context	Age	Taxon	$\delta^{13}C$	$\delta^{18}O$	Diet
77	Phase 1	1011	Iron Age (2,000-500 BP)	Cercopithecinae	-14.2	-0.6	Browser
78	Phase 1	1011	Iron Age (2,000-500 BP)	Cercopithecinae	-12.5	-5.0	Browser
79	Phase 1	1011	Iron Age (2,000-500 BP)	Cercopithecinae	-11.3	-4.6	Browser
80	Phase 1	1011	Iron Age (2,000-500 BP)	Cercopithecinae	-11.8	-5.6	Browser
81	Phase 2	1015	Terminal Pleistocene LSA (13,040-11,340 BP)	Cercopithecinae	-14.8	-4.0	Browser
82	Phase 2	1015	Terminal Pleistocene LSA (13,040-11,340 BP)	Cercopithecinae	-15.1	-1.5	Browser
83	Phase 2	1015	Terminal Pleistocene LSA (13,040-11,340 BP)	Cercopithecinae	-15.3	-2.1	Browser
84	Phase 2	1015	Terminal Pleistocene LSA (13,040-11,340 BP)	Cercopithecinae	-12.5	-2.7	Browser
85	Phase 2	1016	Terminal Pleistocene LSA (13,040-11,340 BP)	Cercopithecinae	-12.9	-2.5	Browser
86	Phase 2	1016	Terminal Pleistocene LSA (13,040-11,340 BP)	Cercopithecinae	-12.8	-4.1	Browser
87	Phase 3	1020	Late Pleistocene LSA (18,830-17,080 BP)	Cercopithecinae	-13.0	-3.4	Browser
88	Phase 4	1026	Sterile (>20,000 BP)	Cercopithecinae	-12.8	-7.7	Browser
89	Phase 1	1004	Iron Age (2,000-500 BP)	*Colobus kirki*	-13.1	-3.6	Browser
90	Phase 1	1004	Iron Age (2,000-500 BP)	*Colobus kirki*	-13.6	-2.8	Browser
91	Phase 1	1011	Iron Age (2,000-500 BP)	*Colobus kirki*	-13.3	-3.5	Browser
92	Phase 3	1019	Late Pleistocene LSA (18,830-17,080 BP)	*Colobus kirki*	-14.2	-1.1	Browser
93	Phase 1	1013	Holocene (2,000-500 BP)	*Cricetomys gambianus*	-11.7	-3.7	Omnivore
94	Phase 1	1002	Iron Age (2,000-500 BP)	*Cricetomys gambianus*	-10.3	-4.9	Omnivore
95	Phase 1	1004	Iron Age (2,000-500 BP)	*Cricetomys gambianus*	-10.9	-4.1	Omnivore
96	Phase 1	1004	Iron Age (2,000-500 BP)	*Cricetomys gambianus*	-12.7	-6.8	Omnivore
97	Phase 1	1004	Iron Age (2,000-500 BP)	*Cricetomys gambianus*	-9.8	-4.5	Omnivore
98	Phase 1	1004	Iron Age (2,000-500 BP)	*Cricetomys gambianus*	-11.8	-5.2	Omnivore
99	Phase 1	1007	Iron Age (2,000-500 BP)	*Cricetomys gambianus*	-12.6	-5.2	Omnivore
100	Phase 1	1008	Iron Age (2,000-500 BP)	*Cricetomys gambianus*	-12.4	-5.2	Omnivore
101	Phase 1	1008	Iron Age (2,000-500 BP)	*Cricetomys gambianus*	-11.8	-4.9	Omnivore
102	Phase 1	1008	Iron Age (2,000-500 BP)	*Cricetomys gambianus*	-11.0	-4.7	Omnivore
103	Phase 2	1015	Terminal Pleistocene LSA (13,040-11,340 BP)	*Cricetomys gambianus*	-12.1	-1.0	Omnivore
104	Phase 2	1016	Terminal Pleistocene LSA (13,040-11,340 BP)	*Cricetomys gambianus*	-12.0	-3.7	Omnivore

	Phase	Context	Age	Taxon	$\delta^{13}C$	$\delta^{18}O$	Diet
105	Phase 3	1020	Late Pleistocene LSA (18,830-17,080 BP)	*Cricetomys gambianus*	-11.2	-4.0	Omnivore
106	Phase 3	1020	Late Pleistocene LSA (18,830-17,080 BP)	*Cricetomys gambianus*	-12.1	-3.6	Omnivore
107	Phase 1	1003	Iron Age (2,000-500 BP)	*Dendrohyrax validus*	-12.1	-3.3	Browser
108	Phase 1	1003	Iron Age (2,000-500 BP)	*Dendrohyrax validus*	-12.2	-4.6	Browser
109	Phase 1	1003	Iron Age (2,000-500 BP)	*Dendrohyrax validus*	-11.6	-3.2	Browser
110	Phase 1	1003	Iron Age (2,000-500 BP)	*Dendrohyrax validus*	-10.8	-4.1	Browser
111	Phase 1	1003	Iron Age (2,000-500 BP)	*Dendrohyrax validus*	-12.2	-4.0	Browser
112	Phase 1	1004	Iron Age (2,000-500 BP)	*Dendrohyrax validus*	-18.0	-9.7	Browser
113	Phase 1	1004	Iron Age (2,000-500 BP)	*Dendrohyrax validus*	-12.4	-3.2	Browser
114	Phase 1	1004	Iron Age (2,000-500 BP)	*Dendrohyrax validus*	-11.5	-5.1	Browser
115	Phase 1	1005	Iron Age (2,000-500 BP)	*Dendrohyrax validus*	-12.2	-4.1	Browser
116	Phase 1	1007	Iron Age (2,000-500 BP)	*Dendrohyrax validus*	-11.5	-3.7	Browser
117	Phase 1	1007	Iron Age (2,000-500 BP)	*Dendrohyrax validus*	-13.5	-3.9	Browser
118	Phase 1	1007	Iron Age (2,000-500 BP)	*Dendrohyrax validus*	-15.7	-4.4	Browser
119	Phase 1	1007	Iron Age (2,000-500 BP)	*Dendrohyrax validus*	-11.2	-2.3	Browser
120	Phase 1	1007	Iron Age (2,000-500 BP)	*Dendrohyrax validus*	-13.0	-8.5	Browser
121	Phase 1	1011	Iron Age (2,000-500 BP)	*Dendrohyrax validus*	-14.1	-5.4	Browser
122	Phase 1	1011	Iron Age (2,000-500 BP)	*Dendrohyrax validus*	-12.8	-4.8	Browser
123	Phase 1	1011	Iron Age (2,000-500 BP)	*Dendrohyrax validus*	-15.2	-5.0	Browser
124	Phase 1	1011	Iron Age (2,000-500 BP)	*Dendrohyrax validus*	-14.2	-0.6	Browser
125	Phase 1	1011	Iron Age (2,000-500 BP)	*Dendrohyrax validus*	-12.3	-6.3	Browser
126	Phase 2	1015	Terminal Pleistocene LSA (13,040-11,340 BP)	*Dendrohyrax validus*	-16.1	-3.1	Browser
127	Phase 2	1015	Terminal Pleistocene LSA (13,040-11,340 BP)	*Dendrohyrax validus*	-14.5	-3.1	Browser
128	Phase 2	1015	Terminal Pleistocene LSA (13,040-11,340 BP)	*Dendrohyrax validus*	-15.5	-3.2	Browser
129	Phase 2	1015	Terminal Pleistocene LSA (13,040-11,340 BP)	*Dendrohyrax validus*	-13.9	-0.1	Browser
130	Phase 2	1015	Terminal Pleistocene LSA (13,040-11,340 BP)	*Dendrohyrax validus*	-18.4	-8.0	Browser
131	Phase 2	1015	Terminal Pleistocene LSA (13,040-11,340 BP)	*Dendrohyrax validus*	-13.2	-4.1	Browser
132	Phase 2	1015	Terminal Pleistocene LSA (13,040-11,340 BP)	*Dendrohyrax validus*	-13.8	-2.2	Browser

	Phase	Context	Age	Taxon	$\delta^{13}C$	$\delta^{18}O$	Diet
133	Phase 2	1016	Terminal Pleistocene LSA (13,040-11,340 BP)	*Dendrohyrax validus*	-13.1	-3.7	Browser
134	Phase 3	1018	Late Pleistocene LSA (18,830-17,080 BP)	*Dendrohyrax validus*	-2.5	-0.2	Browser
135	Phase 3	1018	Late Pleistocene LSA (18,830-17,080 BP)	*Dendrohyrax validus*	-11.6	-3.0	Browser
136	Phase 3	1018	Late Pleistocene LSA (18,830-17,080 BP)	*Dendrohyrax validus*	-12.4	0.4	Browser
137	Phase 3	1018	Late Pleistocene LSA (18,830-17,080 BP)	*Dendrohyrax validus*	-14.1	-3.6	Browser
138	Phase 3	1018	Late Pleistocene LSA (18,830-17,080 BP)	*Dendrohyrax validus*	-13.3	-2.0	Browser
139	Phase 3	1019	Late Pleistocene LSA (18,830-17,080 BP)	*Dendrohyrax validus*	-12.8	-2.8	Browser
140	Phase 3	1019	Late Pleistocene LSA (18,830-17,080 BP)	*Dendrohyrax validus*	-12.7	-3.1	Browser
141	Phase 3	1019	Late Pleistocene LSA (18,830-17,080 BP)	*Dendrohyrax validus*	-13.4	-3.6	Browser
142	Phase 3	1019	Late Pleistocene LSA (18,830-17,080 BP)	*Dendrohyrax validus*	-12.7	-3.9	Browser
143	Phase 3	1019	Late Pleistocene LSA (18,830-17,080 BP)	*Dendrohyrax validus*	-12.5	-3.6	Browser
144	Phase 3	1024	Late Pleistocene LSA (18,830-17,080 BP)	*Dendrohyrax validus*	-12.8	-2.4	Browser
145	Phase 3	1024	Late Pleistocene LSA (18,830-17,080 BP)	*Dendrohyrax validus*	-12.7	-2.7	Browser
146	Phase 3	1024	Late Pleistocene LSA (18,830-17,080 BP)	*Dendrohyrax validus*	-13.4	-4.2	Browser
147	Phase 3	1024	Late Pleistocene LSA (18,830-17,080 BP)	*Dendrohyrax validus*	-12.0	-4.1	Browser
148	Phase 3	1024	Late Pleistocene LSA (18,830-17,080 BP)	*Dendrohyrax validus*	-14.3	-3.5	Browser
149	Phase 4	1025	Sterile (>20,000 BP)	*Dendrohyrax validus*	-11.6	-3.4	Browser
150	Phase 4	1025	Sterile (>20,000 BP)	*Dendrohyrax validus*	-11.8	-2.9	Browser
151	Phase 4	1025	Sterile (>20,000 BP)	*Dendrohyrax validus*	-12.0	-2.3	Browser
152	Phase 4	1025	Sterile (>20,000 BP)	*Dendrohyrax validus*	-11.7	-2.8	Browser
153	Phase 4	1025	Sterile (>20,000 BP)	*Dendrohyrax validus*	-10.5	-9.4	Browser
154	Phase 2	1017	Terminal Pleistocene LSA (13,040-11,340 BP)	*Equus quaaga*	-4.3	-3.1	Grazer
155	Phase 2	1017	Terminal Pleistocene LSA (13,040-11,340 BP)	*Equus quaaga*	-8.2	-4.2	Grazer
156	Phase 3	1018	Late Pleistocene LSA (18,830-17,080 BP)	*Equus quaaga*	-2.0	-1.8	Grazer
157	Phase 3	1018	Late Pleistocene LSA (18,830-17,080 BP)	*Equus quaaga*	-2.6	-1.2	Grazer
158	Phase 3	1018	Late Pleistocene LSA (18,830-17,080 BP)	*Equus quaaga*	-3.5	-1.4	Grazer
159	Phase 3	1019	Late Pleistocene LSA (18,830-17,080 BP)	*Equus quaaga*	-4.1	-2.0	Grazer
160	Phase 3	1019	Late Pleistocene LSA (18,830-17,080 BP)	*Equus quaaga*	-3.8	-1.9	Grazer

	Phase	Context	Age	Taxon	$\delta^{13}C$	$\delta^{18}O$	Diet
161	Phase 4	1025	Sterile (>20,000 BP)	*Equus quaaga*	-4.0	-3.7	Grazer
162	Phase 4	1025	Sterile (>20,000 BP)	*Equus quaaga*	-2.0	-2.9	Grazer
163	Phase 1	1005	Iron Age (2,000-500 BP)	*Galago zanzibaricus*	-13.6	-6.2	Omnivore
164	Phase 1	1007	Iron Age (2,000-500 BP)	*Galago zanzibaricus*	-11.2	-3.2	Omnivore
165	Phase 2	1017	Terminal Pleistocene LSA (13,040-11,340 BP)	*Hystrix cristata*	-12.8	-4.1	Omnivore
166	Phase 1	1012	Holocene (2,000-500 BP)	*Lepus sp.*	-9.2	-6.0	Mixed
167	Phase 2	1017	Terminal Pleistocene LSA (13,040-11,340 BP)	*Lepus sp.*	-10.2	-3.3	Mixed
168	Phase 3	1019	Late Pleistocene LSA (18,830-17,080 BP)	Neotragini	-13.4	-4.0	Browser
169	Phase 3	1019	Late Pleistocene LSA (18,830-17,080 BP)	Neotragini	-11.7	-2.4	Browser
170	Phase 3	1019	Late Pleistocene LSA (18,830-17,080 BP)	Neotragini	-12.2	-3.1	Browser
171	Phase 3	1019	Late Pleistocene LSA (18,830-17,080 BP)	Neotragini	-13.7	-2.9	Browser
172	Phase 3	1019	Late Pleistocene LSA (18,830-17,080 BP)	Neotragini	-12.8	-3.6	Browser
173	Phase 3	1019	Late Pleistocene LSA (18,830-17,080 BP)	Neotragini	-11.4	-3.4	Browser
174	Phase 3	1019	Late Pleistocene LSA (18,830-17,080 BP)	Neotragini	-12.2	-3.9	Browser
175	Phase 1	1002	Iron Age (2,000-500 BP)	*Neotragus moschatus*	-17.4	-10.0	Browser
176	Phase 1	1002	Iron Age (2,000-500 BP)	*Neotragus moschatus*	-11.0	-2.9	Browser
177	Phase 1	1003	Iron Age (2,000-500 BP)	*Neotragus moschatus*	-13.0	-5.1	Browser
178	Phase 1	1003	Iron Age (2,000-500 BP)	*Neotragus moschatus*	-15.3	-6.2	Browser
179	Phase 1	1007	Iron Age (2,000-500 BP)	*Neotragus moschatus*	-12.7	-4.2	Browser
180	Phase 1	1007	Iron Age (2,000-500 BP)	*Neotragus moschatus*	-12.4	-5.0	Browser
181	Phase 1	1011	Iron Age (2,000-500 BP)	*Neotragus moschatus*	-13.0	-3.5	Browser
182	Phase 1	1011	Iron Age (2,000-500 BP)	*Neotragus moschatus*	-13.1	-3.5	Browser
183	Phase 1	1011	Iron Age (2,000-500 BP)	*Neotragus moschatus*	-11.3	-4.6	Browser
184	Phase 1	1011	Iron Age (2,000-500 BP)	*Neotragus moschatus*	-14.1	-5.9	Browser
185	Phase 1	1011	Iron Age (2,000-500 BP)	*Neotragus moschatus*	-12.3	-3.7	Browser
186	Phase 2	1015	Terminal Pleistocene LSA (13,040-11,340 BP)	*Neotragus moschatus*	-14.8	-3.3	Browser
187	Phase 2	1016	Terminal Pleistocene LSA (13,040-11,340 BP)	*Neotragus moschatus*	-13.0	-4.0	Browser
188	Phase 2	1017	Terminal Pleistocene LSA (13,040-11,340 BP)	*Neotragus moschatus*	-11.5	-3.0	Browser

	Phase	Context	Age	Taxon	$\delta^{13}C$	$\delta^{18}O$	Diet
189	Phase 3	1018	Late Pleistocene LSA (18,830-17,080 BP)	*Neotragus moschatus*	-12.1	-0.9	Browser
190	Phase 3	1018	Late Pleistocene LSA (18,830-17,080 BP)	*Neotragus moschatus*	-10.9	-3.7	Browser
191	Phase 3	1018	Late Pleistocene LSA (18,830-17,080 BP)	*Neotragus moschatus*	-12.7	-5.8	Browser
192	Phase 3	1018	Late Pleistocene LSA (18,830-17,080 BP)	*Neotragus moschatus*	-13.3	-6.0	Browser
193	Phase 3	1024	Late Pleistocene LSA (18,830-17,080 BP)	*Neotragus moschatus*	-12.3	-3.7	Browser
194	Phase 3	1024	Late Pleistocene LSA (18,830-17,080 BP)	*Neotragus moschatus*	-12.1	-3.8	Browser
195	Phase 3	1024	Late Pleistocene LSA (18,830-17,080 BP)	*Neotragus moschatus*	-11.8	-4.6	Browser
196	Phase 3	1024	Late Pleistocene LSA (18,830-17,080 BP)	*Neotragus moschatus*	-11.9	-3.8	Browser
197	Phase 3	1024	Late Pleistocene LSA (18,830-17,080 BP)	*Neotragus moschatus*	-12.4	-3.1	Browser
198	Phase 3	1024	Late Pleistocene LSA (18,830-17,080 BP)	*Neotragus moschatus*	-12.4	-3.5	Browser
199	Phase 4	1025	Sterile (>20,000 BP)	*Neotragus moschatus*	-12.3	-2.8	Browser
200	Phase 4	1025	Sterile (>20,000 BP)	*Neotragus moschatus*	-12.0	-3.7	Browser
201	Phase 1	1003	Iron Age (2,000-500 BP)	*Otolemur crassicaudatus*	-11.6	-4.7	Omnivore
202	Phase 1	1004	Iron Age (2,000-500 BP)	*Otolemur crassicaudatus*	-11.6	-4.2	Omnivore
203	Phase 1	1004	Iron Age (2,000-500 BP)	*Otolemur crassicaudatus*	-10.7	-5.6	Omnivore
204	Phase 1	1005	Iron Age (2,000-500 BP)	*Otolemur crassicaudatus*	-11.7	-5.5	Omnivore
205	Phase 1	1007	Iron Age (2,000-500 BP)	*Otolemur crassicaudatus*	-12.4	-4.3	Omnivore
206	Phase 3	1019	Late Pleistocene LSA (18,830-17,080 BP)	*Ourebia ourebi*	-5.0	-2.7	Mixed
207	Phase 1	1004	Iron Age (2,000-500 BP)	*Potamochoerus larvatus*	-11.3	-4.2	Browser
208	Phase 1	1007	Iron Age (2,000-500 BP)	*Potamochoerus larvatus*	-12.6	-2.8	Browser
209	Phase 2	1015	Terminal Pleistocene LSA (13,040-11,340 BP)	*Potamochoerus larvatus*	-11.7	-4.3	Browser
210	Phase 3	1018	Late Pleistocene LSA (18,830-17,080 BP)	*Potamochoerus larvatus*	-13.2	-4.9	Browser
211	Phase 3	1019	Late Pleistocene LSA (18,830-17,080 BP)	*Potamochoerus larvatus*	-11.7	-3.4	Browser
212	Phase 3	1019	Late Pleistocene LSA (18,830-17,080 BP)	*Potamochoerus larvatus*	-12.1	-3.1	Browser
213	Phase 2	1015	Terminal Pleistocene LSA (13,040-11,340 BP)	*Oreotragus oreotragus*	-20.4	-10.8	Browser
214	Phase 3	1019	Late Pleistocene LSA (18,830-17,080 BP)	*Redunca redunca*	-4.6	-2.1	Grazer
215	Phase 3	1019	Late Pleistocene LSA (18,830-17,080 BP)	*Redunca redunca*	-5.5	-3.6	Grazer
216	Phase 3	1019	Late Pleistocene LSA (18,830-17,080 BP)	*Redunca redunca*	-1.9	-1.9	Grazer

	Phase	Context	Age	Taxon	$\delta^{13}C$	$\delta^{18}O$	Diet
217	Phase 3	1019	Late Pleistocene LSA (18,830-17,080 BP)	*Redunca redunca*	-3.5	-0.7	Grazer
218	Phase 3	1019	Late Pleistocene LSA (18,830-17,080 BP)	*Redunca redunca*	-2.9	-2.4	Grazer
219	Phase 3	1022	Late Pleistocene LSA (18,830-17,080 BP)	*Redunca redunca*	-4.8	-2.3	Grazer
220	Phase 1	1003	Iron Age (2,000-500 BP)	Macroscelidea	-10.5	-4.0	Omnivore
221	Phase 1	1004	Iron Age (2,000-500 BP)	Macroscelidea	-12.4	-4.2	Omnivore
222	Phase 1	1007	Iron Age (2,000-500 BP)	Macroscelidea	-11.1	-5.8	Omnivore
223	Phase 2	1015	Terminal Pleistocene LSA (13,040-11,340 BP)	Macroscelidea	-12.8	-2.7	Omnivore
224	Phase 3	1018	Late Pleistocene LSA (18,830-17,080 BP)	Suid indet.	-4.9	-2.8	NA
225	Phase 4	1025	Sterile (>20,000 BP)	Suid indet.	-7.9	-3.6	NA
226	Phase 1	1004	Iron Age (2,000-500 BP)	*Sylvicapra grimmia*	-13.5	-4.5	Browser
227	Phase 2	1015	Terminal Pleistocene LSA (13,040-11,340 BP)	*Sylvicapra grimmia*	-16.4	-5.3	Browser
228	Phase 3	1019	Late Pleistocene LSA (18,830-17,080 BP)	*Tragelaphus scriptus*	-12.3	-2.7	Browser
229	Phase 1	1002	Iron Age (2,000-500 BP)	*Tragelaphus scriptus*	-11.4	-4.4	Browser

Table A1:2 An isotopic dataset of published faunal enamel $\delta^{13}C$ and $\delta^{18}O$ values, including sample taxon and age, from archaeological sites in eastern Africa's interior (Robinson, 2017; Chritz et al., 2019; Robinson, 2022).

	Region	**Site**	**Age**	**Taxon**	δ^{13}**C**	δ^{18}**O**	**Diet**
1	L. Turkana	514.00	7300 BP	Alcelaphine	2.0	-0.2	Grazer
2	L. Turkana	514.00	7300 BP	*Equus* sp.	-0.2	2.5	Grazer
3	L. Turkana	514.00	7300 BP	*Equus* sp.	0.2	3.8	Grazer
4	L. Turkana	514.00	7300 BP	*Equus* sp.	1.3	3.6	Grazer
5	L. Turkana	514.00	7300 BP	*Hippopotamus amphibius*	-0.6	-2.1	Grazer
6	L. Turkana	514.00	7300 BP	*Phacochoerus* sp.	0.4	-0.9	Grazer
7	L. Turkana	514.00	7300 BP	*Phacochoerus* sp.	2.3	3.7	Grazer
8	L. Turkana	AW	7900 BP	Mammal	-1.2	2.2	Grazer
9	L. Turkana	AW	7900 BP	*Hippopotamus amphibius*	-1.2	-2.2	Grazer
10	L. Turkana	AW	7900 BP	*Hippopotamus amphibius*	-0.7	-2.2	Grazer
11	L. Turkana	AW	7900 BP	*Hippopotamus amphibius*	0.0	-2.2	Grazer
12	L. Turkana	AW	7900 BP	*Hippopotamus amphibius*	0.6	0.9	Grazer
13	L. Turkana	AW	7900 BP	*Hippopotamus amphibius*	1.8	-0.3	Grazer
14	L. Turkana	AW	7900 BP	*Hippopotamus amphibius*	2.9	0.3	Grazer
15	L. Turkana	AW	7900 BP	*Phacochoerus* sp.	-0.2	-2.2	Grazer
16	L. Turkana	AW	7900 BP	*Phacochoerus* sp.	2.5	5.1	Grazer
17	L. Turkana	AW	7900 BP	Reduncini	0.2	-2.4	Grazer
18	L. Turkana	Equid Site	10000 BP	Alcelaphine	0.5	3.0	Grazer
19	L. Turkana	Equid Site	10000 BP	Alcelaphine	1.4	6.2	Grazer
20	L. Turkana	Equid Site	10000 BP	Alcelaphine	2.3	4.1	Grazer
21	L. Turkana	Equid Site	10000 BP	Bovid	-0.9	2.1	Grazer
22	L. Turkana	Equid Site	10000 BP	*Equus* sp.	-2.0	1.1	Grazer
23	L. Turkana	Equid Site	10000 BP	*Equus* sp.	-1.9	-2.5	Grazer
24	L. Turkana	Equid Site	10000 BP	*Equus* sp.	-1.1	1.7	Grazer
25	L. Turkana	Equid Site	10000 BP	*Equus* sp.	-0.4	3.6	Grazer
26	L. Turkana	Equid Site	10000 BP	*Equus* sp.	-0.4	3.6	Grazer

	Region	Site	Age	Taxon	$\delta^{13}C$	$\delta^{18}O$	Diet
27	L. Turkana	Equid Site	10000 BP	*Equus* sp.	-0.3	2.3	Grazer
28	L. Turkana	Equid Site	10000 BP	*Equus* sp.	-0.2	3.5	Grazer
29	L. Turkana	Equid Site	10000 BP	*Equus* sp.	-0.1	2.5	Grazer
30	L. Turkana	Equid Site	10000 BP	*Equus* sp.	-0.1	2.5	Grazer
31	L. Turkana	Equid Site	10000 BP	*Equus* sp.	0.0	2.4	Grazer
32	L. Turkana	Equid Site	10000 BP	*Equus* sp.	0.1	4.1	Grazer
33	L. Turkana	Equid Site	10000 BP	*Equus* sp.	0.1	2.4	Grazer
34	L. Turkana	Equid Site	10000 BP	*Equus* sp.	0.4	3.3	Grazer
35	L. Turkana	Equid Site	10000 BP	*Equus* sp.	0.6	1.2	Grazer
36	L. Turkana	Equid Site	10000 BP	*Equus* sp.	0.6	3.4	Grazer
37	L. Turkana	Equid Site	10000 BP	*Equus* sp.	0.6	5.8	Grazer
38	L. Turkana	Equid Site	10000 BP	*Equus* sp.	1.1	0.8	Grazer
39	L. Turkana	Equid Site	10000 BP	*Phacochoerus* sp.	0.3	3.1	Grazer
40	L. Turkana	Equid Site	10000 BP	Reduncini	2.0	2.8	Grazer
41	L. Turkana	Equid Site	10000 BP	*Phacochoerus* sp.	0.0	3.0	Grazer
42	L. Turkana	Dongodien	3950 BP	Alcelaphine	-1.6	3.4	Grazer
43	L. Turkana	Dongodien	3950 BP	Alcelaphine	-1.3	4.5	Grazer
44	L. Turkana	Dongodien	3950 BP	Alcelaphine	0.3	2.8	Grazer
45	L. Turkana	Dongodien	3950 BP	Antilopini	-4.5	0.6	Mixed
46	L. Turkana	Dongodien	3950 BP	Antilopini	-3.0	4.1	Mixed
47	L. Turkana	Dongodien	3950 BP	Antilopini	-2.2	4.0	Mixed
48	L. Turkana	Dongodien	3950 BP	Bovid	1.6	3.6	Grazer
49	L. Turkana	Dongodien	3950 BP	Caprini	-4.5	6.0	Mixed
50	L. Turkana	Dongodien	3950 BP	Mammal	-6.0	5.3	Mixed
51	L. Turkana	Dongodien	3950 BP	Mammal	-4.2	3.5	Mixed
52	L. Turkana	Dongodien	3950 BP	Mammal	-0.5	1.9	Grazer
53	L. Turkana	Dongodien	3950 BP	Caprini	-1.4	1.8	Grazer
54	L. Turkana	Dongodien	3950 BP	Caprini	-7.9	3.2	Mixed

	Region	Site	Age	Taxon	$\delta^{13}C$	$\delta^{18}O$	Diet
55	L. Turkana	Dongodien	3950 BP	Caprini	-7.5	1.5	Mixed
56	L. Turkana	Dongodien	3950 BP	Caprini	-6.8	5.2	Mixed
57	L. Turkana	Dongodien	3950 BP	Caprini	-5.5	4.7	Mixed
58	L. Turkana	Dongodien	3950 BP	Caprini	-5.3	4.8	Mixed
59	L. Turkana	Dongodien	3950 BP	Caprini	-4.8	5.1	Mixed
60	L. Turkana	Dongodien	3950 BP	Caprini	-4.5	6.0	Mixed
61	L. Turkana	Dongodien	3950 BP	Caprini	-3.7	2.1	Mixed
62	L. Turkana	Dongodien	3950 BP	Caprini	-3.4	4.9	Mixed
63	L. Turkana	Dongodien	3950 BP	Caprini	-3.1	4.4	Mixed
64	L. Turkana	Dongodien	3950 BP	Caprini	-2.9	6.7	Mixed
65	L. Turkana	Dongodien	3950 BP	Caprini	-2.3	4.6	Grazer
66	L. Turkana	Dongodien	3950 BP	Caprini	-2.1	5.1	Grazer
67	L. Turkana	Dongodien	3950 BP	Caprini	-1.6	4.6	Grazer
68	L. Turkana	Dongodien	3950 BP	Caprini	-1.5	5.8	Grazer
69	L. Turkana	Dongodien	3950 BP	Caprini	0.0	4.1	Grazer
70	L. Turkana	Dongodien	3950 BP	Caprini	0.1	3.6	Grazer
71	L. Turkana	Dongodien	3950 BP	*Equus* sp.	-0.2	0.6	Grazer
72	L. Turkana	Dongodien	3950 BP	*Hippopotamus amphibius*	0.0	0.4	Grazer
73	L. Turkana	Dongodien	3950 BP	Caprini	-5.9	4.4	Mixed
74	L. Turkana	Dongodien	3950 BP	Caprini	-5.4	2.4	Mixed
75	L. Turkana	Dongodien	3950 BP	*Eudorcas thomsonii*	-3.3	3.8	Mixed
76	Ele Bor A	EBA	1300 BP	Antilopini	-8.7	1.8	Mixed
77	Ele Bor A	EBA	1300 BP	Antilopini	-5.5	3.5	Mixed
78	Ele Bor A	EBA	1300 BP	Antilopini	-1.2	1.0	Grazer
79	Ele Bor A	EBA	1300 BP	*Nanger granti*	-3.8	-4.3	Mixed
80	Ele Bor A	EBA	1300 BP	*Nanger granti*	-2.5	-0.3	Mixed
81	Ele Bor A	EBA	1300 BP	*Nanger granti*	-1.5	3.3	Mixed
82	Ele Bor A	EBA	1300 BP	*Nanger granti*	3.3	2.7	Mixed

	Region	Site	Age	Taxon	$\delta^{13}C$	$\delta^{18}O$	Diet
83	Ele Bor A	EBA	1300 BP	*Madoqua* sp.	-12.6	0.1	Browser
84	Ele Bor A	EBA	1300 BP	*Madoqua* sp.	-11.5	3.6	Browser
85	Ele Bor A	EBA	1300 BP	*Madoqua* sp.	-7.9	1.4	Browser
86	Ele Bor A	EBA	1300 BP	*Oryx beisa*	1.3	-0.1	Grazer
87	Ele Bor A	EBA	4600 BP	*Equus* sp.	0.1	1.3	Grazer
88	Ele Bor A	EBA	4600 BP	*Equus* sp.	0.9	1.1	Grazer
89	Ele Bor A	EBA	4600 BP	Antilopini	-9.3	5.5	Mixed
90	Ele Bor A	EBA	4600 BP	Antilopini	-9.1	0.7	Mixed
91	Ele Bor A	EBA	4600 BP	Antilopini	-7.6	1.5	Mixed
92	Ele Bor A	EBA	4600 BP	Antilopini	-7.3	5.0	Mixed
93	Ele Bor A	EBA	4600 BP	Antilopini	-6.5	2.5	Mixed
94	Ele Bor A	EBA	4600 BP	Antilopini	-5.8	-2.8	Mixed
95	Ele Bor A	EBA	4600 BP	Antilopini	-3.7	1.8	Mixed
96	Ele Bor A	EBA	4600 BP	Antilopini	-1.7	2.8	Grazer
97	Ele Bor A	EBA	4600 BP	Antilopini	-1.4	4.2	Grazer
98	Ele Bor A	EBA	4600 BP	Antilopini	-0.8	5.3	Grazer
99	Ele Bor A	EBA	4600 BP	Antilopini	-0.8	3.6	Grazer
100	Ele Bor A	EBA	4600 BP	Antilopini	-0.2	2.3	Grazer
101	Ele Bor A	EBA	4600 BP	Antilopini	0.2	1.6	Grazer
102	Ele Bor A	EBA	4600 BP	*Giraffa camelopardalis*	-12.4	5.4	Browser
103	Ele Bor A	EBA	4600 BP	*Madoqua* sp.	-11.8	1.6	Browser
104	Ele Bor A	EBA	4600 BP	*Oryx beisa*	-4.7	2.8	Grazer
105	Ele Bor A	EBA	4600 BP	*Oryx beisa*	-0.7	3.2	Grazer
106	Ele Bor A	EBA	4600 BP	*Oryx beisa*	2.1	1.6	Grazer
107	Ele Bor A	EBA	4600 BP	*Oryx beisa*	2.2	2.2	Grazer
108	Ele Bor A	EBA	4600 BP	*Oryx beisa*	2.6	0.2	Grazer
109	Ele Bor A	EBA	4600 BP	*Oryx beisa*	2.7	0.6	Grazer
110	Ele Bor A	EBA	4600 BP	*Oryx beisa*	3.4	-0.8	Grazer

	Region	Site	Age	Taxon	$\delta^{13}C$	$\delta^{18}O$	Diet
111	Ele Bor A	EBA	4600 BP	*Oryx beisa*	4.0	2.9	Grazer
112	Ele Bor A	EBA	4600 BP	*Phacochoerus* sp.	-11.1	0.7	Grazer
113	Ele Bor A	EBA	4600 BP	*Sylvicapra grimmia*	-2.1	1.8	Browser
114	Ele Bor A	EBA	4600 BP	*Taurotragus oryx*	-12.2	7.0	Browser
115	Ele Bor A	EBA	4600 BP	*Taurotragus oryx*	-11.5	3.2	Browser
116	Ele Bor A	EBA	4600 BP	*Taurotragus oryx*	-10.1	6.3	Browser
117	Ele Bor A	EBA	4600 BP	*Taurotragus oryx*	-9.0	5.1	Browser
118	Ele Bor A	EBA	7500 BP	Antilopini	-7.8	1.4	Mixed
119	Ele Bor A	EBA	7500 BP	Antilopini	-3.8	2.7	Mixed
120	Ele Bor A	EBA	7500 BP	Antilopini	-3.3	3.7	Mixed
121	Ele Bor A	EBA	7500 BP	*Oryx beisa*	2.4	4.1	Grazer
122	Ele Bor A	EBA	7500 BP	*Taurotragus oryx*	-8.9	5.6	Browser
123	Ele Bor A	EBA	7500 BP	*Taurotragus oryx*	-3.7	1.5	Browser
124	Ele Bor A	EBA	7500 BP	*Taurotragus oryx*	1.5	1.1	Browser
125	L. Turkana	FxJj12	8900 BP	Alcelaphine	2.0	3.2	Grazer
126	L. Turkana	FxJj12	8900 BP	Alcelaphine	1.4	-1.8	Grazer
127	L. Turkana	GaJj11	10050 BP	Mammal	2.7	2.5	Grazer
128	L. Turkana	GaJj11	10050 BP	*Hippopotamus amphibius*	-2.1	-2.0	Grazer
129	L. Turkana	GaJj11	10050 BP	*Hippopotamus amphibius*	0.1	-2.3	Grazer
130	L. Turkana	GaJj2	4650 BP	*Aepyceros melampus*	-7.2	2.3	Mixed
131	L. Turkana	GaJj2	4650 BP	Alcelaphine	-5.4	3.9	Grazer
132	L. Turkana	GaJj2	4650 BP	Alcelaphine	-1.4	2.4	Grazer
133	L. Turkana	GaJj2	4650 BP	Alcelaphine	-1.2	1.2	Grazer
134	L. Turkana	GaJj2	4650 BP	Alcelaphine	-1.2	2.5	Grazer
135	L. Turkana	GaJj2	4650 BP	Alcelaphine	3.2	0.5	Grazer
136	L. Turkana	GaJj2	4650 BP	Mammal	-4.4	2.2	Grazer
137	L. Turkana	GaJj2	4650 BP	Mammal	-1.9	1.4	Grazer
138	L. Turkana	GaJj2	4650 BP	Mammal	1.9	3.8	Grazer

	Region	Site	Age	Taxon	$\delta^{13}C$	$\delta^{18}O$	Diet
139	L. Turkana	GaJj2	4650 BP	Caprini	-6.0	1.7	Mixed
140	L. Turkana	GaJj2	4650 BP	Mammal	1.3	4.1	Grazer
141	L. Turkana	GaJj2	4650 BP	*Madoqua* sp.	-6.5	2.6	Browser
142	L. Turkana	GaJj2	4650 BP	*Hippopotamus amphibius*	-4.1	-0.6	Grazer
143	L. Turkana	GaJj2	4650 BP	*Hippopotamus amphibius*	-1.2	0.5	Grazer
144	L. Turkana	GaJj2	4650 BP	*Hippopotamus amphibius*	-0.9	-1.4	Grazer
145	L. Turkana	GaJj2	4650 BP	Neotragini	-1.9	-0.3	Grazer
146	L. Turkana	GaJj2	4650 BP	Neotragini	1.7	2.0	Grazer
147	L. Turkana	GaJj2	4650 BP	*Phacochoerus* sp.	-2.4	-1.4	Grazer
148	L. Turkana	GaJj2	4650 BP	*Phacochoerus* sp.	-1.2	0.6	Grazer
149	L. Turkana	GaJj2	4650 BP	*Phacochoerus* sp.	-0.2	1.7	Grazer
150	L. Turkana	GaJj2	4650 BP	*Phacochoerus* sp.	2.0	1.2	Grazer
151	L. Victoria	Gogo Falls	1700 BP	*Damaliscus* sp.	2.2	1.3	Grazer
152	L. Victoria	Gogo Falls	1700 BP	*Damaliscus* sp.	0.6	-0.3	Grazer
153	L. Victoria	Gogo Falls	1700 BP	*Damaliscus* sp.	0.6	0.1	Grazer
154	L. Victoria	Gogo Falls	1700 BP	*Damaliscus* sp.	2.2	1.3	Grazer
155	L. Victoria	Gogo Falls	1700 BP	*Damaliscus* sp.	2.8	1.5	Grazer
156	L. Victoria	Gogo Falls	1700 BP	Alcelaphine	-0.4	-0.4	Grazer
157	L. Victoria	Gogo Falls	1700 BP	Alcelaphine	0.0	-0.3	Grazer
158	L. Victoria	Gogo Falls	1700 BP	Alcelaphine	0.1	1.5	Grazer
159	L. Victoria	Gogo Falls	1700 BP	Alcelaphine	0.2	1.5	Grazer
160	L. Victoria	Gogo Falls	1700 BP	Alcelaphine	1.3	0.3	Grazer
161	L. Victoria	Gogo Falls	1700 BP	Alcelaphine	1.8	0.7	Grazer
162	L. Victoria	Gogo Falls	1700 BP	Alcelaphine	2.1	-2.1	Grazer
163	L. Victoria	Gogo Falls	1700 BP	Alcelaphine	3.0	1.9	Grazer
164	L. Victoria	Gogo Falls	1700 BP	Alcelaphine	3.2	2.4	Grazer
165	L. Victoria	Gogo Falls	1700 BP	Alcelaphine	1.4	0.8	Grazer
166	L. Victoria	Gogo Falls	1700 BP	Alcelaphine	3.0	1.9	Grazer

	Region	Site	Age	Taxon	$\delta^{13}C$	$\delta^{18}O$	Diet
167	L. Victoria	Gogo Falls	1700 BP	*Bos taurus*	-1.0	1.0	Grazer
168	L. Victoria	Gogo Falls	1700 BP	*Bos taurus*	-0.8	-2.7	Grazer
169	L. Victoria	Gogo Falls	1700 BP	*Bos taurus*	0.7	0.5	Grazer
170	L. Victoria	Gogo Falls	1700 BP	*Bos taurus*	1.3	2.5	Grazer
171	L. Victoria	Gogo Falls	1700 BP	*Bos taurus*	1.5	1.2	Grazer
172	L. Victoria	Gogo Falls	1700 BP	*Bos taurus*	1.8	0.3	Grazer
173	L. Victoria	Gogo Falls	1700 BP	*Bos taurus*	2.0	1.8	Grazer
174	L. Victoria	Gogo Falls	1700 BP	*Bos taurus*	2.5	2.3	Grazer
175	L. Victoria	Gogo Falls	1700 BP	*Bos taurus*	2.7	2.8	Grazer
176	L. Victoria	Gogo Falls	1700 BP	*Bos taurus*	2.8	0.8	Grazer
177	L. Victoria	Gogo Falls	1700 BP	*Bos taurus*	2.9	1.7	Grazer
178	L. Victoria	Gogo Falls	1700 BP	*Bos taurus*	3.2	2.1	Grazer
179	L. Victoria	Gogo Falls	1700 BP	*Bos taurus*	3.4	2.3	Grazer
180	L. Victoria	Gogo Falls	1700 BP	Caprini	-2.1	-0.6	Grazer
181	L. Victoria	Gogo Falls	1700 BP	Caprini	-2.0	1.6	Grazer
182	L. Victoria	Gogo Falls	1700 BP	Caprini	-0.9	3.2	Grazer
183	L. Victoria	Gogo Falls	1700 BP	Caprini	-0.7	-2.8	Grazer
184	L. Victoria	Gogo Falls	1700 BP	Caprini	-0.4	2.0	Grazer
185	L. Victoria	Gogo Falls	1700 BP	Caprini	0.2	1.9	Grazer
186	L. Victoria	Gogo Falls	1700 BP	Caprini	0.4	3.3	Grazer
187	L. Victoria	Gogo Falls	1700 BP	Caprini	0.5	4.3	Grazer
188	L. Victoria	Gogo Falls	1700 BP	Caprini	0.5	3.8	Grazer
189	L. Victoria	Gogo Falls	1700 BP	Caprini	0.7	1.6	Grazer
190	L. Victoria	Gogo Falls	1700 BP	Caprini	0.9	0.7	Grazer
191	L. Victoria	Gogo Falls	1700 BP	Caprini	1.7	1.3	Grazer
192	L. Victoria	Gogo Falls	1700 BP	Caprini	2.2	3.0	Grazer
193	L. Victoria	Gogo Falls	1700 BP	Caprini	2.6	2.9	Grazer
194	L. Victoria	Gogo Falls	1700 BP	*Sylvicapra grimmia*	-8.8	-1.1	Browser

	Region	Site	Age	Taxon	$\delta^{13}C$	$\delta^{18}O$	Diet
195	L. Victoria	Gogo Falls	1700 BP	*Equus* sp.	0.8	1.3	Grazer
196	L. Victoria	Gogo Falls	1700 BP	*Equus* sp.	0.9	2.4	Grazer
197	L. Victoria	Gogo Falls	1700 BP	*Equus* sp.	1.3	0.0	Grazer
198	L. Victoria	Gogo Falls	1700 BP	*Equus* sp.	1.5	1.9	Grazer
199	L. Victoria	Gogo Falls	1700 BP	*Equus* sp.	2.0	1.4	Grazer
200	L. Victoria	Gogo Falls	1700 BP	*Equus* sp.	0.3	1.7	Grazer
201	L. Victoria	Gogo Falls	1700 BP	*Equus* sp.	0.6	1.3	Grazer
202	L. Victoria	Gogo Falls	1700 BP	*Equus* sp.	0.0	-0.3	Grazer
203	L. Victoria	Gogo Falls	1700 BP	*Equus* sp.	0.1	1.0	Grazer
204	L. Victoria	Gogo Falls	1700 BP	*Equus* sp.	0.1	1.4	Grazer
205	L. Victoria	Gogo Falls	1700 BP	*Equus* sp.	0.5	-0.5	Grazer
206	L. Victoria	Gogo Falls	1700 BP	*Equus* sp.	0.6	1.2	Grazer
207	L. Victoria	Gogo Falls	1700 BP	*Equus* sp.	1.6	2.4	Grazer
208	L. Victoria	Gogo Falls	1700 BP	Hippotragini	1.4	-2.1	Grazer
209	L. Victoria	Gogo Falls	1700 BP	Hippotragini	2.7	0.3	Grazer
210	L. Victoria	Gogo Falls	1700 BP	Hippotragini	0.4	1.1	Grazer
211	L. Victoria	Gogo Falls	1700 BP	Hippotragini	2.3	0.4	Grazer
212	L. Victoria	Gogo Falls	1700 BP	*Ourebia ourebi*	-1.0	2.1	Mixed
213	L. Victoria	Gogo Falls	1700 BP	*Ourebia ourebi*	-0.6	0.9	Mixed
214	L. Victoria	Gogo Falls	1700 BP	*Ourebia ourebi*	-0.3	1.9	Mixed
215	L. Victoria	Gogo Falls	1700 BP	*Ourebia ourebi*	0.0	-1.1	Mixed
216	L. Victoria	Gogo Falls	1700 BP	*Ourebia ourebi*	0.9	0.8	Mixed
217	L. Victoria	Gogo Falls	1700 BP	*Ourebia ourebi*	0.9	-3.0	Mixed
218	L. Victoria	Gogo Falls	1700 BP	*Ourebia ourebi*	1.0	0.7	Mixed
219	L. Victoria	Gogo Falls	1700 BP	*Ourebia ourebi*	1.2	0.5	Mixed
220	L. Victoria	Gogo Falls	1700 BP	*Phacochoerus* sp.	-1.2	-1.9	Grazer
221	L. Victoria	Gogo Falls	1700 BP	*Phacochoerus* sp.	-0.3	-0.2	Grazer
222	L. Victoria	Gogo Falls	1700 BP	*Phacochoerus* sp.	0.4	1.7	Grazer

	Region	Site	Age	Taxon	$\delta^{13}C$	$\delta^{18}O$	Diet
223	L. Victoria	Gogo Falls	1700 BP	*Phacochoerus* sp.	0.7	1.4	Grazer
224	L. Victoria	Gogo Falls	1700 BP	*Potamochoerus larvatus*	-3.9	-2.8	Browser
225	L. Victoria	Gogo Falls	1700 BP	Reduncini	-1.0	-0.2	Grazer
226	L. Victoria	Gogo Falls	1700 BP	Reduncini	-0.4	-0.3	Grazer
227	L. Victoria	Gogo Falls	1700 BP	Reduncini	0.0	0.6	Grazer
228	L. Victoria	Gogo Falls	1700 BP	Reduncini	2.3	1.3	Grazer
229	L. Victoria	Gogo Falls	1700 BP	Reduncini	2.8	0.9	Grazer
230	L. Victoria	Gogo Falls	1700 BP	*Taurotragus oryx*	-9.6	-0.2	Browser
231	L. Victoria	Gogo Falls	1700 BP	*Taurotragus oryx*	-5.8	2.3	Browser
232	L. Victoria	Gogo Falls	1700 BP	*Taurotragus oryx*	-3.9	0.0	Browser
233	L. Victoria	Gogo Falls	1700 BP	*Taurotragus oryx*	-6.9	-0.6	Browser
234	L. Victoria	Gogo Falls	1700 BP	*Taurotragus oryx*	-4.1	1.2	Browser
235	L. Victoria	Gogo Falls	1700 BP	*Hippopotamus amphibius*	0.2	-2.6	Grazer
236	L. Victoria	Gogo Falls	1700 BP	*Hippopotamus amphibius*	1.0	-2.6	Grazer
237	L. Victoria	Kanam E	8200 BP	*Alcelaphus buselaphus*	-0.1	-1.4	Grazer
238	L. Victoria	Kanam E	8200 BP	*Hippopotamus amphibius*	-6.5	-3.7	Grazer
239	L. Victoria	Kanam E	8200 BP	*Hippopotamus amphibius*	-2.9	-0.9	Grazer
240	L. Victoria	Kanam E	8200 BP	*Hippopotamus amphibius*	-1.9	-3.5	Grazer
241	L. Victoria	Kanam E	8200 BP	*Phacochoerus* sp.	0.3	-0.2	Grazer
242	L. Victoria	Kanam E	8200 BP	*Syncerus caffer*	0.7	-1.9	Grazer
243	L. Victoria	Kanam E	8200 BP	*Syncerus caffer*	3.3	-0.6	Grazer
244	L. Victoria	Kanam E	8200 BP	Alcelaphine	2.2	-1.1	Grazer
245	L. Victoria	Kanam E	8200 BP	Bovid	2.9	-0.7	Grazer
246	L. Victoria	Kanam E	8200 BP	*Hippopotamus amphibius*	-3.9	-3.5	Grazer
247	L. Victoria	Kanam E	8200 BP	*Loxodonta africana*	-7.0	-1.4	Browser
248	L. Victoria	Kanam E	8200 BP	*Phacochoerus* sp.	-8.7	-2.4	Grazer
249	L. Victoria	Kanam E	8200 BP	*Redunca redunca*	2.1	-1.5	Grazer
250	L. Victoria	Kanam E	8200 BP	*Syncerus caffer*	-0.8	0.4	Grazer

	Region	Site	Age	Taxon	$\delta^{13}C$	$\delta^{18}O$	Diet
251	L. Turkana	Lothagam L	8300 BP	Alcelaphine	-2.0	-0.2	Grazer
252	L. Turkana	Lothagam L	8300 BP	*Papio* sp.	-6.9	-0.5	Omnivore
253	L. Turkana	Lothagam L	8300 BP	Mammal	-1.5	0.0	Grazer
254	L. Turkana	Lothagam L	8300 BP	Mammal	0.1	3.3	Grazer
255	L. Turkana	Lothagam L	8300 BP	Mammal	0.2	0.9	Grazer
256	L. Turkana	Lothagam L	8300 BP	Mammal	1.6	2.3	Grazer
257	L. Turkana	Lothagam L	8300 BP	Mammal	2.1	-0.4	Grazer
258	L. Turkana	Lothagam L	8300 BP	*Equus* sp.	-0.1	3.5	Grazer
259	L. Turkana	Lothagam L	8300 BP	*Equus* sp.	0.5	4.8	Grazer
260	L. Turkana	Lothagam L	8300 BP	*Equus* sp.	0.7	3.0	Grazer
261	L. Turkana	Lothagam L	8300 BP	*Equus* sp.	1.3	4.1	Grazer
262	L. Turkana	Lothagam L	8300 BP	*Hippopotamus amphibius*	-2.2	-1.8	Grazer
263	L. Turkana	Lothagam L	8300 BP	*Hippopotamus amphibius*	-0.9	-2.2	Grazer
264	L. Turkana	Lothagam L	8300 BP	*Hippopotamus amphibius*	0.0	-2.4	Grazer
265	L. Turkana	Lothagam L	8300 BP	*Hippopotamus amphibius*	0.0	-2.1	Grazer
266	L. Turkana	Lothagam L	8300 BP	*Hippopotamus amphibius*	0.1	-1.8	Grazer
267	L. Turkana	Lothagam L	8300 BP	*Phacochoerus* sp.	-1.0	-0.8	Grazer
268	L. Turkana	Lothagam L	8300 BP	*Phacochoerus* sp.	-0.2	0.6	Grazer
269	L. Turkana	Lothagam L	8300 BP	*Phacochoerus* sp.	1.2	-1.2	Grazer
270	L. Turkana	Lothagam L	8300 BP	*Phacochoerus* sp.	1.5	-1.1	Grazer
271	L. Turkana	Lothagam L	8300 BP	*Phacochoerus* sp.	3.1	-0.5	Grazer
272	L. Turkana	Lothagam L	8300 BP	*Syncerus caffer*	-0.2	1.8	Grazer
273	L. Turkana	Lothagam L	8300 BP	*Syncerus caffer*	2.8	-0.8	Grazer
274	L. Turkana	Lothagam L	8300 BP	*Oryx beisa*	1.4	4.9	Grazer
275	L. Victoria	Luanda	8400 BP	Alcelaphine	3.1	0.3	Grazer
276	L. Victoria	Luanda	8400 BP	Alcelaphine	2.4	-2.8	Grazer
277	L. Victoria	Luanda	8400 BP	Bovid	3.2	-1.2	Grazer
278	L. Victoria	Luanda	8400 BP	Bovid	1.4	-0.2	Grazer

	Region	Site	Age	Taxon	$\delta^{13}C$	$\delta^{18}O$	Diet
279	L. Victoria	Luanda	8400 BP	Bovid	3.6	-0.8	Grazer
280	L. Victoria	Luanda	8400 BP	Bovid	0.5	2.3	Grazer
281	L. Victoria	Luanda	8400 BP	Bovid	1.2	-3.4	Grazer
282	L. Victoria	Luanda	8400 BP	Bovid	1.3	-1.5	Grazer
283	L. Victoria	Luanda	8400 BP	Bovid	1.7	-1.0	Grazer
284	L. Victoria	Luanda	8400 BP	Bovid	1.7	-2.0	Grazer
285	L. Victoria	Luanda	8400 BP	*Connochaetes taurinus*	1.6	-0.7	Grazer
286	L. Victoria	Luanda	8400 BP	*Connochaetes taurinus*	2.6	-0.3	Grazer
287	L. Victoria	Luanda	8400 BP	*Connochaetes taurinus*	-0.1	0.4	Grazer
288	L. Victoria	Luanda	8400 BP	*Connochaetes taurinus*	1.6	0.0	Grazer
289	L. Victoria	Luanda	8400 BP	*Connochaetes taurinus*	2.6	0.6	Grazer
290	L. Victoria	Luanda	8400 BP	*Connochaetes taurinus*	3.4	0.2	Grazer
291	L. Victoria	Luanda	8400 BP	*Connochaetes taurinus*	3.6	-0.5	Grazer
292	L. Victoria	Luanda	8400 BP	*Equus* sp.	0.6	-0.6	Grazer
293	L. Victoria	Luanda	8400 BP	*Hippopotamus amphibius*	-5.7	-4.1	Grazer
294	L. Victoria	Luanda	8400 BP	*Hippopotamus amphibius*	-5.5	-2.3	Grazer
295	L. Victoria	Luanda	8400 BP	*Hippopotamus amphibius*	-5.5	-4.6	Grazer
296	L. Victoria	Luanda	8400 BP	*Hippopotamus amphibius*	-3.4	-3.0	Grazer
297	L. Victoria	Luanda	8400 BP	*Hippopotamus amphibius*	-3.2	-2.8	Grazer
298	L. Victoria	Luanda	8400 BP	*Hippopotamus amphibius*	-1.9	-3.1	Grazer
299	L. Victoria	Luanda	8400 BP	*Kobus ellipsiprymnus*	1.5	-1.2	Grazer
300	L. Victoria	Luanda	8400 BP	*Kobus ellipsiprymnus*	2.4	-4.7	Grazer
301	L. Victoria	Luanda	8400 BP	*Kobus ellipsiprymnus*	3.0	-0.1	Grazer
302	L. Victoria	Luanda	8400 BP	*Kobus kob*	1.3	-1.4	Grazer
303	L. Victoria	Luanda	8400 BP	*Kobus kob*	1.8	-1.0	Grazer
304	L. Victoria	Luanda	8400 BP	*Kobus kob*	3.0	0.0	Grazer
305	L. Victoria	Luanda	8400 BP	*Phacochoerus* sp.	0.2	-0.6	Grazer
306	L. Victoria	Luanda	8400 BP	*Phacochoerus* sp.	1.1	1.4	Grazer

	Region	Site	Age	Taxon	$\delta^{13}C$	$\delta^{18}O$	Diet
307	L. Victoria	Luanda	8400 BP	*Potamochoerus larvatus*	-11.8	-5.5	Omnivore
308	L. Victoria	Luanda	8400 BP	*Potamochoerus larvatus*	-7.8	-4.2	Omnivore
309	L. Victoria	Luanda	8400 BP	*Redunca* sp.	0.3	0.0	Grazer
310	L. Victoria	Luanda	8400 BP	*Redunca* sp.	3.0	-1.5	Grazer
311	L. Victoria	Luanda	8400 BP	*Syncerus caffer*	3.4	-1.8	Grazer
312	L. Victoria	Luanda	8400 BP	*Syncerus caffer*	-1.4	0.3	Grazer
313	L. Victoria	Luanda	8400 BP	*Syncerus caffer*	0.1	-0.6	Grazer
314	L. Victoria	Luanda	8400 BP	*Syncerus caffer*	0.5	-0.7	Grazer
315	L. Victoria	Luanda	8400 BP	*Syncerus caffer*	0.7	0.5	Grazer
316	L. Victoria	Luanda	8400 BP	*Syncerus caffer*	1.5	-3.3	Grazer
317	L. Victoria	Luanda	8400 BP	*Syncerus caffer*	1.9	-1.7	Grazer
318	L. Victoria	Luanda	8400 BP	*Syncerus caffer*	1.9	-0.1	Grazer
319	L. Victoria	Luanda	8400 BP	*Syncerus caffer*	2.1	-0.9	Grazer
320	L. Victoria	Luanda	8400 BP	*Syncerus caffer*	2.3	-2.1	Grazer
321	L. Victoria	Luanda	8400 BP	*Syncerus caffer*	2.9	-1.3	Grazer
322	L. Victoria	Luanda	8400 BP	*Syncerus caffer*	3.0	-2.5	Grazer
323	L. Victoria	Luanda	8400 BP	*Syncerus caffer*	3.1	-2.3	Grazer
324	L. Victoria	Luanda	8400 BP	*Syncerus caffer*	3.2	-2.8	Grazer
325	L. Victoria	Luanda	8400 BP	*Syncerus caffer*	3.7	-1.6	Grazer
326	L. Victoria	Luanda	8400 BP	*Syncerus caffer*	3.7	-3.2	Grazer
327	L. Victoria	Luanda	8400 BP	*Syncerus caffer*	3.8	-1.9	Grazer
328	L. Victoria	Wadh Lang'o	1300 BP	Alcelaphine	3.0	5.2	Grazer
329	L. Victoria	Wadh Lang'o	1300 BP	Alcelaphine	0.0	4.0	Grazer
330	L. Victoria	Wadh Lang'o	1300 BP	Alcelaphine	1.8	1.3	Grazer
331	L. Victoria	Wadh Lang'o	1300 BP	Alcelaphine	2.2	2.8	Grazer
332	L. Victoria	Wadh Lang'o	1300 BP	Alcelaphine	2.7	4.1	Grazer
333	L. Victoria	Wadh Lang'o	1300 BP	Alcelaphine	3.0	3.6	Grazer
334	L. Victoria	Wadh Lang'o	1300 BP	Bovid	-2.3	2.1	Grazer

	Region	Site	Age	Taxon	$\delta^{13}C$	$\delta^{18}O$	Diet
335	L. Victoria	Wadh Lang'o	1300 BP	Bovid	1.7	-0.5	Grazer
336	L. Victoria	Wadh Lang'o	1300 BP	Bovid	0.3	3.1	Grazer
337	L. Victoria	Wadh Lang'o	1300 BP	Bovid	2.0	2.5	Grazer
338	L. Victoria	Wadh Lang'o	1300 BP	Bovid	2.2	5.7	Grazer
339	L. Victoria	Wadh Lang'o	1300 BP	Bovid	-0.7	2.2	Grazer
340	L. Victoria	Wadh Lang'o	1300 BP	Caprini	1.6	4.1	Grazer
341	L. Victoria	Wadh Lang'o	1300 BP	Caprini	3.1	4.7	Grazer
342	L. Victoria	Wadh Lang'o	1300 BP	Caprini	-1.4	0.1	Grazer
343	L. Victoria	Wadh Lang'o	1300 BP	Caprini	-0.5	4.3	Grazer
344	L. Victoria	Wadh Lang'o	1300 BP	Caprini	-0.3	1.7	Grazer
345	L. Victoria	Wadh Lang'o	1300 BP	Caprini	-0.2	2.0	Grazer
346	L. Victoria	Wadh Lang'o	1300 BP	Caprini	1.1	2.6	Grazer
347	L. Victoria	Wadh Lang'o	1300 BP	Caprini	1.7	3.9	Grazer
348	L. Victoria	Wadh Lang'o	1300 BP	Caprini	2.1	4.1	Grazer
349	L. Victoria	Wadh Lang'o	1300 BP	Caprini	2.2	-2.4	Grazer
350	L. Victoria	Wadh Lang'o	1300 BP	Caprini	2.2	-0.3	Grazer
351	L. Victoria	Wadh Lang'o	1300 BP	Caprini	2.8	5.4	Grazer
352	L. Victoria	Wadh Lang'o	1300 BP	Caprini	4.0	5.0	Grazer
353	L. Victoria	Wadh Lang'o	1300 BP	*Redunca redunca*	-3.3	-1.6	Grazer
354	L. Victoria	Wadh Lang'o	1300 BP	*Redunca redunca*	-0.7	1.7	Grazer
355	L. Victoria	Wadh Lang'o	1300 BP	*Redunca redunca*	2.6	0.7	Grazer
356	L. Victoria	Wadh Lang'o	1300 BP	*Redunca redunca*	2.5	0.4	Grazer
357	L. Victoria	Wadh Lang'o	1800 BP	*Bos taurus*	1.8	3.6	Grazer
358	L. Victoria	Wadh Lang'o	1800 BP	Bovid	-0.6	4.7	Grazer
359	L. Victoria	Wadh Lang'o	1800 BP	Caprini	0.1	1.6	Grazer
360	L. Victoria	Wadh Lang'o	1800 BP	Caprini	2.7	1.1	Grazer
361	L. Victoria	Wadh Lang'o	1800 BP	Caprini	-0.7	2.1	Grazer
362	L. Victoria	Wadh Lang'o	1800 BP	Caprini	-0.1	0.1	Grazer

	Region	Site	Age	Taxon	$\delta^{13}C$	$\delta^{18}O$	Diet
363	L. Victoria	Wadh Lang'o	1800 BP	Caprini	2.0	3.7	Grazer
364	L. Victoria	Wadh Lang'o	1800 BP	Caprini	-2.2	4.2	Grazer
365	L. Victoria	Wadh Lang'o	1800 BP	Bovid	2.2	-2.4	Grazer
366	L. Victoria	Wadh Lang'o	1800 BP	*Connochaetus taurinus*	2.8	1.9	Grazer
367	L. Victoria	Wadh Lang'o	1800 BP	*Phacochoerus* sp.	0.4	-0.1	Grazer
368	L. Victoria	Wadh Lang'o	1800 BP	*Kobus ellipsiprymnus*	1.4	2.6	Grazer
369	Porc Epic	Porc Epic	100000 - 40000 BP	*Aepyceros melampus*	-3.0	-0.3	Mixed
370	Porc Epic	Porc Epic	100000 - 40000 BP	*Aepyceros melampus*	-1.9	1.5	Mixed
371	Porc Epic	Porc Epic	100000 - 40000 BP	*Aepyceros melampus*	-5.0	5.0	Mixed
372	Porc Epic	Porc Epic	100000 - 40000 BP	*Nanger granti*	-2.9	2.9	Mixed
373	Porc Epic	Porc Epic	100000 - 40000 BP	*Nanger* sp.	-4.6	3.5	Mixed
374	Porc Epic	Porc Epic	100000 - 40000 BP	*Madoqua guentheri*	-8.3	6.8	Browser
375	Porc Epic	Porc Epic	100000 - 40000 BP	*Damaliscus lunatus*	1.0	3.3	Grazer
376	Porc Epic	Porc Epic	100000 - 40000 BP	*Damaliscus lunatus*	-2.1	1.6	Grazer
377	Porc Epic	Porc Epic	100000 - 40000 BP	*Damaliscus lunatus*	1.0	0.1	Grazer
378	Porc Epic	Porc Epic	100000 - 40000 BP	*Syncerus* sp. *antiquus*	-4.6	4.0	Mixed
379	Porc Epic	Porc Epic	100000 - 40000 BP	*Syncerus* sp. *antiquus*	-7.4	7.0	Mixed
380	Porc Epic	Porc Epic	100000 - 40000 BP	*Syncerus* sp. *antiquus*	-6.3	4.6	Mixed
381	Porc Epic	Porc Epic	100000 - 40000 BP	*Syncerus* sp. *antiquus*	-6.4	3.9	Mixed
382	Porc Epic	Porc Epic	100000 - 40000 BP	*Syncerus* sp. *antiquus*	-7.6	-2.0	Mixed
383	Porc Epic	Porc Epic	100000 - 40000 BP	*Syncerus caffer*	-5.6	0.8	Grazer
384	Porc Epic	Porc Epic	100000 - 40000 BP	*Syncerus caffer*	-5.8	3.5	Grazer
385	Porc Epic	Porc Epic	100000 - 40000 BP	*Syncerus caffer*	0.5	1.6	Grazer
386	Porc Epic	Porc Epic	100000 - 40000 BP	*Syncerus caffer*	1.6	2.1	Grazer
387	Porc Epic	Porc Epic	100000 - 40000 BP	*Syncerus caffer*	2.0	-2.7	Grazer
388	Porc Epic	Porc Epic	100000 - 40000 BP	*Syncerus caffer*	-0.5	0.7	Grazer
389	Porc Epic	Porc Epic	100000 - 40000 BP	*Syncerus caffer*	1.5	-1.5	Grazer
390	Porc Epic	Porc Epic	100000 - 40000 BP	*Syncerus caffer*	-1.6	-0.2	Grazer

	Region	Site	Age	Taxon	$\delta^{13}C$	$\delta^{18}O$	Diet
391	Porc Epic	Porc Epic	100000 - 40000 BP	*Syncerus caffer*	1.4	2.4	Grazer
392	Porc Epic	Porc Epic	100000 - 40000 BP	*Oryx beisa*	-1.0	-0.9	Grazer
393	Porc Epic	Porc Epic	100000 - 40000 BP	*Neotragus* spp.	-10.0	4.6	Browser
394	Porc Epic	Porc Epic	100000 - 40000 BP	*Raphicerus* sp.	-10.1	7.4	Browser
395	Porc Epic	Porc Epic	100000 - 40000 BP	*Kobus ellipsiprymnus*	-3.0	2.4	Grazer
396	Porc Epic	Porc Epic	100000 - 40000 BP	*Kobus ellipsiprymnus*	0.1	-3.7	Grazer
397	Porc Epic	Porc Epic	100000 - 40000 BP	*Kobus* spp.	-2.3	2.8	Grazer
398	Porc Epic	Porc Epic	100000 - 40000 BP	*Redunca redunca*	-4.1	1.6	Grazer
399	Porc Epic	Porc Epic	100000 - 40000 BP	*Redunca redunca*	-0.9	-0.2	Grazer
400	Porc Epic	Porc Epic	100000 - 40000 BP	*Redunca* sp. *redunca*	-4.4	1.1	Grazer
401	Porc Epic	Porc Epic	100000 - 40000 BP	*Redunca* sp. *redunca*	0.0	-1.2	Grazer
402	Porc Epic	Porc Epic	100000 - 40000 BP	*Redunca* spp.	0.4	1.5	Grazer
403	Porc Epic	Porc Epic	100000 - 40000 BP	*Tragelaphus strepsiceros*	-5.7	2.3	Mixed
404	Porc Epic	Porc Epic	100000 - 40000 BP	*Tragelaphus strepsiceros*	-5.9	2.6	Mixed
405	Porc Epic	Porc Epic	100000 - 40000 BP	*Tragelaphus strepsiceros*	-8.5	4.6	Mixed
406	Porc Epic	Porc Epic	100000 - 40000 BP	*Tragelaphus strepsiceros*	-8.9	5.2	Mixed
407	Porc Epic	Porc Epic	100000 - 40000 BP	*Tragelaphus strepsiceros*	-6.8	3.5	Mixed
408	Porc Epic	Porc Epic	100000 - 40000 BP	*Tragelaphus* spp.	-8.7	-0.4	Browser
409	Porc Epic	Porc Epic	100000 - 40000 BP	*Tragelaphus* spp.	-1.1	0.6	Browser
410	Porc Epic	Porc Epic	100000 - 40000 BP	*Phacochoerus africanus*	-1.9	2.3	Grazer
411	Porc Epic	Porc Epic	100000 - 40000 BP	*Phacochoerus africanus*	-3.2	1.7	Grazer
412	Porc Epic	Porc Epic	100000 - 40000 BP	*Phacochoerus africanus*	-8.5	6.0	Grazer
413	Porc Epic	Porc Epic	100000 - 40000 BP	*Phacochoerus africanus*	-1.5	3.0	Grazer
414	Porc Epic	Porc Epic	100000 - 40000 BP	*Phacochoerus africanus*	-3.8	2.9	Grazer
415	Porc Epic	Porc Epic	100000 - 40000 BP	*Phacochoerus africanus*	-1.7	-1.6	Grazer
416	Porc Epic	Porc Epic	100000 - 40000 BP	*Phacochoerus africanus*	-1.3	4.1	Grazer
417	Porc Epic	Porc Epic	100000 - 40000 BP	*Phacochoerus africanus*	-11.2	0.4	Grazer
418	Porc Epic	Porc Epic	100000 - 40000 BP	*Phacochoerus africanus*	-3.2	-0.4	Grazer

	Region	Site	Age	Taxon	$\delta^{13}C$	$\delta^{18}O$	Diet
419	Porc Epic	Porc Epic	100000 - 40000 BP	*Phacochoerus africanus*	-3.6	0.3	Grazer
420	Porc Epic	Porc Epic	100000 - 40000 BP	*Phacochoerus africanus*	-4.1	0.8	Grazer
421	Porc Epic	Porc Epic	100000 - 40000 BP	*Phacochoerus africanus*	-1.9	0.5	Grazer
422	Porc Epic	Porc Epic	100000 - 40000 BP	*Phacochoerus africanus*	-1.2	-0.3	Grazer
423	Porc Epic	Porc Epic	100000 - 40000 BP	*Potamochoerus porcus*	-5.5	-1.8	Omnivore
424	Porc Epic	Porc Epic	100000 - 40000 BP	*Equus quagga*	-3.0	3.8	Grazer
425	Porc Epic	Porc Epic	100000 - 40000 BP	*Equus quagga*	-1.0	2.1	Grazer
426	Porc Epic	Porc Epic	100000 - 40000 BP	*Equus quagga*	-4.0	0.1	Grazer
427	Porc Epic	Porc Epic	100000 - 40000 BP	*Equus quagga*	-1.9	4.0	Grazer
428	Porc Epic	Porc Epic	100000 - 40000 BP	*Equus grevyi*	-0.9	1.6	Grazer
429	Kalemba	Kalemba RS	40000 - 8000 BP	*Eudorcas thomsonii*	-11.0	-0.8	Mixed
430	Kalemba	Kalemba RS	40000 - 8000 BP	*Connochaetes taurinus*	-4.8	-2.2	Grazer
431	Kalemba	Kalemba RS	40000 - 8000 BP	*Connochaetes taurinus*	1.0	-0.6	Grazer
432	Kalemba	Kalemba RS	40000 - 8000 BP	*Connochaetes taurinus*	-0.8	-3.5	Grazer
433	Kalemba	Kalemba RS	40000 - 8000 BP	*Connochaetes taurinus*	-0.2	-4.4	Grazer
434	Kalemba	Kalemba RS	40000 - 8000 BP	*Connochaetes taurinus*	0.8	-4.3	Grazer
435	Kalemba	Kalemba RS	40000 - 8000 BP	*Connochaetes taurinus*	-1.5	-3.4	Grazer
436	Kalemba	Kalemba RS	40000 - 8000 BP	*Connochaetes taurinus*	-0.8	-3.6	Grazer
437	Kalemba	Kalemba RS	40000 - 8000 BP	*Connochaetes taurinus*	0.5	-6.5	Grazer
438	Kalemba	Kalemba RS	40000 - 8000 BP	*Connochaetes taurinus*	-0.7	-4.6	Grazer
439	Kalemba	Kalemba RS	40000 - 8000 BP	*Sylvicapra grimmia*	-13.8	-6.1	Browser
440	Kalemba	Kalemba RS	40000 - 8000 BP	*Sylvicapra grimmia*	-11.1	-6.4	Browser
441	Kalemba	Kalemba RS	40000 - 8000 BP	*Sylvicapra grimmia*	-11.5	-2.4	Browser
442	Kalemba	Kalemba RS	40000 - 8000 BP	*Sylvicapra grimmia*	-14.9	-3.7	Browser
443	Kalemba	Kalemba RS	40000 - 8000 BP	*Sylvicapra grimmia*	-10.5	-3.5	Browser
444	Kalemba	Kalemba RS	40000 - 8000 BP	*Sylvicapra grimmia*	-5.6	-4.0	Browser
445	Kalemba	Kalemba RS	40000 - 8000 BP	*Hippotragus niger*	-0.6	-5.2	Grazer
446	Kalemba	Kalemba RS	40000 - 8000 BP	*Ourebia ourebi*	-10.3	-0.6	Mixed

	Region	Site	Age	Taxon	$\delta^{13}C$	$\delta^{18}O$	Diet
447	Kalemba	Kalemba RS	40000 - 8000 BP	*Kobus ellipsiprymnus*	-8.3	-5.1	Grazer
448	Kalemba	Kalemba RS	40000 - 8000 BP	*Kobus ellipsiprymnus*	0.5	-2.3	Grazer
449	Kalemba	Kalemba RS	40000 - 8000 BP	*Kobus ellipsiprymnus*	0.1	-3.4	Grazer
450	Kalemba	Kalemba RS	40000 - 8000 BP	*Kobus ellipsiprymnus*	1.1	-3.9	Grazer
451	Kalemba	Kalemba RS	40000 - 8000 BP	*Kobus ellipsiprymnus*	0.0	-5.8	Grazer
452	Kalemba	Kalemba RS	40000 - 8000 BP	*Kobus ellipsiprymnus*	0.2	-5.7	Grazer
453	Kalemba	Kalemba RS	40000 - 8000 BP	*Kobus ellipsiprymnus*	0.4	-5.7	Grazer
454	Kalemba	Kalemba RS	40000 - 8000 BP	*Kobus ellipsiprymnus*	-3.0	-5.1	Grazer
455	Kalemba	Kalemba RS	40000 - 8000 BP	*Kobus ellipsiprymnus*	-0.8	-5.4	Grazer
456	Kalemba	Kalemba RS	40000 - 8000 BP	*Kobus ellipsiprymnus*	0.3	-3.6	Grazer
457	Kalemba	Kalemba RS	40000 - 8000 BP	*Kobus ellipsiprymnus*	-0.6	-5.1	Grazer
458	Kalemba	Kalemba RS	40000 - 8000 BP	*Kobus ellipsiprymnus*	-0.4	-6.2	Grazer
459	Kalemba	Kalemba RS	40000 - 8000 BP	*Kobus ellipsiprymnus*	-0.5	-3.2	Grazer
460	Kalemba	Kalemba RS	40000 - 8000 BP	*Redunca arundinum*	1.8	-1.3	Grazer
461	Kalemba	Kalemba RS	40000 - 8000 BP	*Redunca arundinum*	0.4	-4.4	Grazer
462	Kalemba	Kalemba RS	40000 - 8000 BP	*Redunca arundinum*	-0.9	-1.2	Grazer
463	Kalemba	Kalemba RS	40000 - 8000 BP	*Redunca arundinum*	-10.1	-0.1	Grazer
464	Kalemba	Kalemba RS	40000 - 8000 BP	*Tragelaphus oryx*	-12.2	-5.8	Browser
465	Kalemba	Kalemba RS	40000 - 8000 BP	*Tragelaphus oryx*	-2.3	-1.2	Browser
466	Kalemba	Kalemba RS	40000 - 8000 BP	*Tragelaphus oryx*	-14.7	-7.4	Browser
467	Kalemba	Kalemba RS	40000 - 8000 BP	*Tragelaphus oryx*	-13.0	-4.0	Browser
468	Kalemba	Kalemba RS	40000 - 8000 BP	*Tragelaphus scriptus*	-10.9	-0.7	Browser
469	Kalemba	Kalemba RS	40000 - 8000 BP	*Phacochoerus africanus*	-5.6	-2.7	Grazer
470	Kalemba	Kalemba RS	40000 - 8000 BP	*Phacochoerus africanus*	-8.5	-5.1	Grazer
471	Kalemba	Kalemba RS	40000 - 8000 BP	*Phacochoerus africanus*	-1.9	-4.2	Grazer
472	Kalemba	Kalemba RS	40000 - 8000 BP	*Phacochoerus africanus*	-4.6	-5.9	Grazer
473	Kalemba	Kalemba RS	40000 - 8000 BP	*Phacochoerus africanus*	-2.5	-2.9	Grazer
474	Kalemba	Kalemba RS	40000 - 8000 BP	*Potamochoerus porcus*	-1.3	-1.0	Omnivore

	Region	Site	Age	Taxon	$\delta^{13}C$	$\delta^{18}O$	Diet
475	Kalemba	Kalemba RS	40000 - 8000 BP	*Potamochoerus porcus*	-11.4	-2.8	Omnivore
476	Kalemba	Kalemba RS	40000 - 8000 BP	*Potamochoerus porcus*	-9.9	-2.3	Omnivore
477	Kalemba	Kalemba RS	40000 - 8000 BP	*Potamochoerus porcus*	-2.5	-5.9	Omnivore
478	Kalemba	Kalemba RS	40000 - 8000 BP	*Potamochoerus porcus*	-13.0	-7.3	Omnivore
479	Kalemba	Kalemba RS	40000 - 8000 BP	*Potamochoerus porcus*	-0.1	-4.8	Omnivore
480	Kalemba	Kalemba RS	40000 - 8000 BP	*Potamochoerus porcus*	-13.1	-7.5	Omnivore
481	Kalemba	Kalemba RS	40000 - 8000 BP	*Potamochoerus porcus*	-7.7	-6.8	Omnivore
482	Kalemba	Kalemba RS	40000 - 8000 BP	*Potamochoerus porcus*	-10.9	-6.6	Omnivore
483	Kalemba	Kalemba RS	40000 - 8000 BP	*Equus quagga*	-1.8	-2.3	Grazer
484	Kalemba	Kalemba RS	40000 - 8000 BP	*Equus quagga*	-0.7	-2.1	Grazer
485	Kalemba	Kalemba RS	40000 - 8000 BP	*Equus quagga*	-2.3	-1.8	Grazer
486	Kalemba	Kalemba RS	40000 - 8000 BP	*Equus quagga*	-3.9	-2.9	Grazer
487	Kalemba	Kalemba RS	40000 - 8000 BP	*Equus quagga*	-1.3	-3.6	Grazer
488	Kalemba	Kalemba RS	40000 - 8000 BP	*Equus quagga*	-4.3	-4.2	Grazer
489	Kalemba	Kalemba RS	40000 - 8000 BP	*Equus quagga*	-2.1	-3.3	Grazer
490	Kalemba	Kalemba RS	40000 - 8000 BP	*Equus quagga*	0.0	-5.4	Grazer
491	Kalemba	Kalemba RS	40000 - 8000 BP	*Equus quagga*	-0.3	-4.9	Grazer
492	Kalemba	Kalemba RS	40000 - 8000 BP	*Equus quagga*	-11.2	-4.6	Grazer
493	Kalemba	Kalemba RS	40000 - 8000 BP	*Equus quagga*	-0.6	-4.8	Grazer
494	Kalemba	Kalemba RS	40000 - 8000 BP	*Equus quagga*	-0.7	-5.1	Grazer
495	Kalemba	Kalemba RS	40000 - 8000 BP	*Equus quagga*	-3.0	-4.7	Grazer
496	Kalemba	Kalemba RS	40000 - 8000 BP	*Equus quagga*	-2.5	-4.9	Grazer
497	Kalemba	Kalemba RS	40000 - 8000 BP	*Equus quagga*	-4.1	-4.3	Grazer
498	Kalemba	Kalemba RS	40000 - 8000 BP	*Equus quagga*	-5.9	-4.6	Grazer
499	Kalemba	Kalemba RS	40000 - 8000 BP	*Equus quagga*	-8.7	-4.6	Grazer
500	Kalemba	Kalemba RS	40000 - 8000 BP	*Equus quagga*	-1.9	-3.9	Grazer
501	Kalemba	Kalemba RS	40000 - 8000 BP	*Equus quagga*	-2.4	-5.7	Grazer
502	Kalemba	Kalemba RS	40000 - 8000 BP	*Equus quagga*	0.5	-5.0	Grazer

	Region	Site	Age	Taxon	$\delta^{13}C$	$\delta^{18}O$	Diet
503	Kalemba	Kalemba RS	40000 - 8000 BP	*Equus quagga*	-2.2	-5.7	Grazer
504	Kalemba	Kalemba RS	40000 - 8000 BP	*Equus quagga*	-7.4	-5.8	Grazer
505	Kalemba	Kalemba RS	40000 - 8000 BP	*Equus quagga*	-1.4	-5.6	Grazer
506	Kalemba	Kalemba RS	40000 - 8000 BP	*Equus quagga*	-1.3	-4.9	Grazer
507	Kalemba	Kalemba RS	40000 - 8000 BP	*Equus quagga*	0.3	-5.1	Grazer
508	Kalemba	Kalemba RS	40000 - 8000 BP	*Equus quagga*	-3.1	-6.1	Grazer
509	Kalemba	Kalemba RS	40000 - 8000 BP	*Equus quagga*	-4.9	-3.9	Grazer
510	Kalemba	Kalemba RS	40000 - 8000 BP	*Equus quagga*	-0.2	-2.1	Grazer
511	Kalemba	Kalemba RS	40000 - 8000 BP	*Equus quagga*	-4.9	-4.0	Grazer
512	Kalemba	Kalemba RS	40000 - 8000 BP	*Equus quagga*	-2.6	-2.0	Grazer
513	Kalemba	Kalemba RS	40000 - 8000 BP	*Equus quagga*	-1.0	-2.4	Grazer
514	Kalemba	Kalemba RS	40000 - 8000 BP	*Equus quagga*	-6.4	-2.9	Grazer
515	Kalemba	Kalemba RS	40000 - 8000 BP	*Equus quagga*	-9.7	-0.3	Grazer
516	Kalemba	Kalemba RS	40000 - 8000 BP	*Equus quagga*	-9.1	-0.8	Grazer
517	Lukenya	Lukenya	46000 - 15000 BP	*Eudorcas thomsonii*	-4.5	-0.4	Mixed
518	Lukenya	Lukenya	46000 - 26000 BP	*Eudorcas thomsonii*	-4.0	-2.8	Mixed
519	Lukenya	Lukenya	30000 - 25000 BP	*Eudorcas thomsonii*	-5.0	0.1	Mixed
520	Lukenya	Lukenya	38000 - 42000 BP	*Eudorcas thomsonii*	-0.1	-3.0	Mixed
521	Lukenya	Lukenya	46000 - 15000 BP	*Nanger granti*	-7.0	0.6	Mixed
522	Lukenya	Lukenya	12000 - 16000 BP	*Alcelaphus buselaphus*	-1.8	-2.4	Grazer
523	Lukenya	Lukenya	12000 - 16000 BP	*Alcelaphus buselaphus*	-0.8	-1.9	Grazer
524	Lukenya	Lukenya	12000 - 16000 BP	*Alcelaphus buselaphus*	-2.3	-4.0	Grazer
525	Lukenya	Lukenya	46000 - 15000 BP	*Alcelaphus buselaphus*	0.7	-3.5	Grazer
526	Lukenya	Lukenya	46000 - 15000 BP	*Alcelaphus buselaphus*	0.0	-1.3	Grazer
527	Lukenya	Lukenya	46000 - 15000 BP	*Alcelaphus buselaphus*	-2.1	-3.0	Grazer
528	Lukenya	Lukenya	46000 - 26000 BP	*Alcelaphus buselaphus*	-3.9	-3.6	Grazer
529	Lukenya	Lukenya	46000 - 26000 BP	*Alcelaphus buselaphus*	0.8	-3.3	Grazer
530	Lukenya	Lukenya	46000 - 26000 BP	*Alcelaphus buselaphus*	1.0	-4.6	Grazer

	Region	Site	Age	Taxon	$\delta^{13}C$	$\delta^{18}O$	Diet
531	Lukenya	Lukenya	46000 - 26000 BP	*Alcelaphus buselaphus*	0.8	-3.8	Grazer
532	Lukenya	Lukenya	30000 - 25000 BP	*Alcelaphus buselaphus*	1.3	-3.5	Grazer
533	Lukenya	Lukenya	30000 - 25000 BP	*Alcelaphus buselaphus*	1.4	-4.4	Grazer
534	Lukenya	Lukenya	30000 - 25000 BP	*Alcelaphus buselaphus*	-0.4	-5.2	Grazer
535	Lukenya	Lukenya	30000 - 25000 BP	*Alcelaphus buselaphus*	-1.8	-5.7	Grazer
536	Lukenya	Lukenya	12000 - 16000 BP	*Connochaetes taurinus*	-0.7	-3.2	Grazer
537	Lukenya	Lukenya	12000 - 16000 BP	*Connochaetes taurinus*	0.2	-3.2	Grazer
538	Lukenya	Lukenya	46000 - 15000 BP	*Connochaetes taurinus*	1.6	1.5	Grazer
539	Lukenya	Lukenya	46000 - 15000 BP	*Connochaetes taurinus*	0.3	-2.9	Grazer
540	Lukenya	Lukenya	46000 - 15000 BP	*Connochaetes taurinus*	-0.5	-2.3	Grazer
541	Lukenya	Lukenya	46000 - 26000 BP	*Connochaetes taurinus*	-0.2	-1.1	Grazer
542	Lukenya	Lukenya	30000 - 25000 BP	*Connochaetes taurinus*	-0.4	-0.1	Grazer
543	Lukenya	Lukenya	12000 - 16000 BP	*Damaliscus hypsodon*	-0.7	-2.0	Grazer
544	Lukenya	Lukenya	46000 - 15000 BP	*Damaliscus hypsodon*	0.2	-0.5	Grazer
545	Lukenya	Lukenya	46000 - 15000 BP	*Damaliscus hypsodon*	-0.2	0.2	Grazer
546	Lukenya	Lukenya	46000 - 15000 BP	*Damaliscus hypsodon*	0.1	-0.7	Grazer
547	Lukenya	Lukenya	46000 - 15000 BP	*Damaliscus hypsodon*	-1.8	-0.7	Grazer
548	Lukenya	Lukenya	46000 - 15000 BP	*Damaliscus hypsodon*	1.9	-2.3	Grazer
549	Lukenya	Lukenya	46000 - 15000 BP	*Damaliscus hypsodon*	-0.5	-0.3	Grazer
550	Lukenya	Lukenya	46000 - 15000 BP	*Damaliscus hypsodon*	1.1	-1.9	Grazer
551	Lukenya	Lukenya	46000 - 15000 BP	*Damaliscus hypsodon*	-1.0	-0.3	Grazer
552	Lukenya	Lukenya	46000 - 15000 BP	*Damaliscus hypsodon*	0.2	-2.1	Grazer
553	Lukenya	Lukenya	46000 - 15000 BP	*Damaliscus hypsodon*	-0.8	-1.7	Grazer
554	Lukenya	Lukenya	46000 - 15000 BP	*Damaliscus hypsodon*	-0.8	0.7	Grazer
555	Lukenya	Lukenya	46000 - 15000 BP	*Damaliscus hypsodon*	-0.8	-2.0	Grazer
556	Lukenya	Lukenya	46000 - 15000 BP	*Damaliscus hypsodon*	1.8	-2.4	Grazer
557	Lukenya	Lukenya	46000 - 26000 BP	*Damaliscus hypsodon*	2.0	-1.2	Grazer
558	Lukenya	Lukenya	46000 - 15000 BP	*Damaliscus hypsodon*	-0.4	-1.6	Grazer

	Region	Site	Age	Taxon	$\delta^{13}C$	$\delta^{18}O$	Diet
559	Lukenya	Lukenya	46000 - 26000 BP	*Damaliscus hypsodon*	1.2	-4.4	Grazer
560	Lukenya	Lukenya	46000 - 26000 BP	*Damaliscus hypsodon*	-1.5	-3.5	Grazer
561	Lukenya	Lukenya	46000 - 26000 BP	*Damaliscus hypsodon*	0.0	-3.2	Grazer
562	Lukenya	Lukenya	46000 - 26000 BP	*Damaliscus hypsodon*	-0.8	-3.9	Grazer
563	Lukenya	Lukenya	30000 - 25000 BP	*Damaliscus hypsodon*	1.0	-4.6	Grazer
564	Lukenya	Lukenya	30000 - 25000 BP	*Damaliscus hypsodon*	0.8	-4.1	Grazer
565	Lukenya	Lukenya	30000 - 25000 BP	*Damaliscus hypsodon*	0.0	-4.2	Grazer
566	Lukenya	Lukenya	30000 - 25000 BP	*Damaliscus hypsodon*	0.4	-4.6	Grazer
567	Lukenya	Lukenya	30000 - 25000 BP	*Damaliscus hypsodon*	0.6	-2.2	Grazer
568	Lukenya	Lukenya	38000 - 42000 BP	*Damaliscus hypsodon*	0.5	-3.2	Grazer
569	Lukenya	Lukenya	38000 - 42000 BP	*Damaliscus hypsodon*	1.3	-4.0	Grazer
570	Lukenya	Lukenya	38000 - 42000 BP	*Damaliscus hypsodon*	-1.7	-3.2	Grazer
571	Lukenya	Lukenya	38000 - 42000 BP	*Damaliscus hypsodon*	1.3	-4.4	Grazer
572	Lukenya	Lukenya	38000 - 42000 BP	*Damaliscus hypsodon*	-0.8	-3.4	Grazer
573	Lukenya	Lukenya	38000 - 42000 BP	*Damaliscus hypsodon*	1.1	-1.4	Grazer
574	Lukenya	Lukenya	38000 - 42000 BP	*Damaliscus hypsodon*	0.6	-5.9	Grazer
575	Lukenya	Lukenya	38000 - 42000 BP	*Damaliscus hypsodon*	1.1	-5.0	Grazer
576	Lukenya	Lukenya	38000 - 42000 BP	*Damaliscus hypsodon*	0.9	-3.7	Grazer
577	Lukenya	Lukenya	38000 - 42000 BP	*Damaliscus hypsodon*	1.3	-2.8	Grazer
578	Lukenya	Lukenya	38000 - 42000 BP	*Damaliscus hypsodon*	2.0	-2.5	Grazer
579	Lukenya	Lukenya	38000 - 42000 BP	*Damaliscus hypsodon*	1.3	-3.2	Grazer
580	Lukenya	Lukenya	38000 - 42000 BP	*Damaliscus hypsodon*	1.1	-3.9	Grazer
581	Lukenya	Lukenya	38000 - 42000 BP	*Damaliscus hypsodon*	1.3	-4.4	Grazer
582	Lukenya	Lukenya	38000 - 42000 BP	*Damaliscus hypsodon*	-0.2	-4.0	Grazer
583	Lukenya	Lukenya	12000 - 16000 BP	*Sylvicapra grimmia*	-9.5	-0.4	Browser
584	Lukenya	Lukenya	46000 - 26000 BP	*Oryx beisa*	-0.5	-1.0	Grazer
585	Lukenya	Lukenya	12000 - 16000 BP	*Ourebia ourebi*	-5.0	-3.4	Mixed
586	Lukenya	Lukenya	46000 - 26000 BP	*Ourebia ourebi*	-3.2	-0.8	Mixed

	Region	Site	Age	Taxon	$\delta^{13}C$	$\delta^{18}O$	Diet
587	Lukenya	Lukenya	12000 - 16000 BP	*Redunca fulvorufula*	-3.1	0.4	Grazer
588	Lukenya	Lukenya	46000 - 15000 BP	*Redunca fulvorufula*	-0.4	0.2	Grazer
589	Lukenya	Lukenya	46000 - 15000 BP	*Tragelaphus oryx*	-10.1	-1.4	Browser
590	Lukenya	Lukenya	46000 - 15000 BP	*Tragelaphus oryx*	-11.0	-2.2	Browser
591	Lukenya	Lukenya	46000 - 15000 BP	*Potamochoerus porcus*	-14.4	-7.5	Omnivore
592	Lukenya	Lukenya	12000 - 16000 BP	*Phacochoerus africanus*	-2.7	-0.9	Grazer
593	Lukenya	Lukenya	46000 - 15000 BP	*Phacochoerus africanus*	-1.5	0.6	Grazer
594	Lukenya	Lukenya	12000 - 16000 BP	*Equus quagga*	-2.7	-0.6	Grazer
595	Lukenya	Lukenya	46000 - 15000 BP	*Equus quagga*	-1.9	-5.0	Grazer
596	Lukenya	Lukenya	46000 - 15000 BP	*Equus quagga*	-0.5	-3.8	Grazer
597	Lukenya	Lukenya	46000 - 15000 BP	*Equus quagga*	-0.6	-2.6	Grazer
598	Lukenya	Lukenya	46000 - 26000 BP	*Equus quagga*	-3.4	-0.1	Grazer
599	Lukenya	Lukenya	46000 - 26000 BP	*Equus quagga*	-3.4	-1.8	Grazer
600	Lukenya	Lukenya	46000 - 26000 BP	*Equus quagga*	0.6	-1.5	Grazer
601	Lukenya	Lukenya	30000 - 25000 BP	*Equus quagga*	-2.4	-1.9	Grazer
602	Lukenya	Lukenya	30000 - 25000 BP	*Equus quagga*	-1.1	-3.4	Grazer
603	Lukenya	Lukenya	30000 - 25000 BP	*Equus quagga*	-2.6	-3.4	Grazer
604	Lukenya	Lukenya	30000 - 25000 BP	*Equus quagga*	-4.1	-2.0	Grazer
605	Lukenya	Lukenya	38000 - 42000 BP	*Equus quagga*	0.8	-0.9	Grazer
606	Lukenya	Lukenya	1100 - 2500 BP	*Alcelaphus buselaphus*	0.7	-2.7	Grazer
607	Lukenya	Lukenya	1100 - 2500 BP	*Alcelaphus buselaphus*	2.5	-1.4	Grazer
608	Lukenya	Lukenya	1100 - 2500 BP	*Alcelaphus buselaphus*	2.8	-2.6	Grazer
609	Lukenya	Lukenya	1100 - 2500 BP	*Connochaetes taurinus*	3.6	-1.7	Grazer
610	Lukenya	Lukenya	1100 - 2500 BP	*Connochaetes taurinus*	3.3	-2.7	Grazer
611	Lukenya	Lukenya	4000 - 8100 BP	*Alcelaphus buselaphus*	2.6	-1.9	Grazer
612	Lukenya	Lukenya	4000 - 8100 BP	*Alcelaphus buselaphus*	-1.2	-0.7	Grazer
613	Lukenya	Lukenya	4000 - 8100 BP	*Connochaetes taurinus*	0.8	-3.2	Grazer
614	Lukenya	Lukenya	4000 - 8100 BP	*Connochaetes taurinus*	1.7	1.7	Grazer

	Region	Site	Age	Taxon	$\delta^{13}C$	$\delta^{18}O$	Diet
615	Lukenya	Lukenya	4000 - 8100 BP	*Connochaetes taurinus*	2.4	-3.2	Grazer
616	Lukenya	Lukenya	4000 - 8100 BP	*Eudorcas thomsonii*	0.8	-4.7	Mixed
617	Lukenya	Lukenya	4000 - 8100 BP	*Eudorcas thomsonii*	-2.3	-0.1	Mixed
618	Lukenya	Lukenya	4000 - 8100 BP	*Oreotragus oreotragus*	-7.8	-0.3	Mixed
619	Lukenya	Lukenya	4000 - 8100 BP	*Sylvicapra grimmia*	-13.0	-3.6	Browser
620	Lukenya	Lukenya	4000 - 8100 BP	*Madoqua kirkii*	-8.7	0.9	Browser
621	Lukenya	Lukenya	4000 - 8100 BP	*Ourebia ourebi*	-0.3	-0.8	Mixed
622	Lukenya	Lukenya	4000 - 8100 BP	*Raphicerus campestris*	-11.4	-2.4	Browser
623	Lukenya	Lukenya	4000 - 8100 BP	*Redunca fulvorufula*	0.3	-3.2	Grazer
624	Lukenya	Lukenya	4000 - 8100 BP	*Redunca fulvorufula*	0.0	-3.2	Grazer
625	Lukenya	Lukenya	4000 - 8100 BP	*Equus quagga*	0.5	1.9	Grazer
626	Lukenya	Lukenya	4000 - 8100 BP	*Equus quagga*	-1.2	-1.0	Grazer
627	Lukenya	Lukenya	4000 - 8100 BP	*Potamochoerus porcus*	-8.9	-0.4	Omnivore
628	PYS	Panga ya Saidi	1000 - 500 BP	*Tragelaphus scriptus*	-11.4	-2.3	Browser
629	PYS	Panga ya Saidi	1000 - 500 BP	*Potamochoerus larvatus*	-6.8	-4.3	Browser
630	PYS	Panga ya Saidi	1000 - 500 BP	*Sylvicapra grimmia*	-11.6	-4.9	Browser
631	PYS	Panga ya Saidi	1000 - 500 BP	Bovid Size 1-2	-11.2	-3.5	Browser
632	PYS	Panga ya Saidi	1000 - 500 BP	Bovid Size 1-2	-12.4	-4	Browser
633	PYS	Panga ya Saidi	1000 - 500 BP	Bovid Size 3-4	3.2	-3.2	Grazer
634	PYS	Panga ya Saidi	1000 - 500 BP	*Sylvicapra grimmia*	-11.4	-3.4	Browser
635	PYS	Panga ya Saidi	1000 - 500 BP	*Sylvicapra grimmia*	-9.8	-4.1	Browser
636	PYS	Panga ya Saidi	1000 - 500 BP	*Potamochoerus larvatus*	-10	-3.5	Browser
637	PYS	Panga ya Saidi	1000 - 500 BP	*Phacochoerus* sp.	-0.2	-3.2	Grazer
638	PYS	Panga ya Saidi	1000 - 500 BP	Bovid Size 3	0.5	-2.4	Grazer
639	PYS	Panga ya Saidi	1000 - 500 BP	*Papio* sp.	-11.5	-0.8	Omnivore
640	PYS	Panga ya Saidi	1000 - 500 BP	Bovid Size 3	-9.8	-4	Browser
641	PYS	Panga ya Saidi	8500 -7500 BP	Bovid Size 3-4 cf. Bovini	0.6	-3.9	Grazer
642	PYS	Panga ya Saidi	8500 -7500 BP	Bovid Size 3-4 cf. Bovini	0.1	-4.2	Grazer

	Region	Site	Age	Taxon	$\delta^{13}C$	$\delta^{18}O$	Diet
643	PYS	Panga ya Saidi	8500 -7500 BP	*Sylvicapra grimmia*	-9.8	-4.2	Browser
644	PYS	Panga ya Saidi	8500 -7500 BP	Neotragini	-10.1	-3.8	Browser
645	PYS	Panga ya Saidi	8500 -7500 BP	*Phacochoerus* sp.	-2.8	-2.3	Grazer
646	PYS	Panga ya Saidi	8500 -7500 BP	Cercopithecinae	-9.9	-3.6	Omnivore
647	PYS	Panga ya Saidi	14000 - 15000 BP	*Potamochoerus larvatus*	-6.6	-4	Browser
648	PYS	Panga ya Saidi	14000 - 15000 BP	*Kobus ellipsiprymnus*	0.4	-3.1	Grazer
649	PYS	Panga ya Saidi	14000 - 15000 BP	*Ourebia ourebi*	-1	-1.6	Grazer
650	PYS	Panga ya Saidi	14000 - 15000 BP	*Sylvicapra grimmia*	-10.3	-3.1	Browser
651	PYS	Panga ya Saidi	14000 - 15000 BP	*Phacochoerus* sp.	-2.6	-2.3	Grazer
652	PYS	Panga ya Saidi	14000 - 15000 BP	*Phacochoerus* sp.	-2.7	-1.7	Grazer
653	PYS	Panga ya Saidi	14000 - 15000 BP	*Phacochoerus* sp.	-6.9	-8.7	Grazer
654	PYS	Panga ya Saidi	14000 - 15000 BP	Bovid Size 3	-0.4	-1.8	Grazer
655	PYS	Panga ya Saidi	14000 - 15000 BP	Bovid Size 1	-3.1	-2.2	Grazer
656	PYS	Panga ya Saidi	14000 - 15000 BP	*Potamochoerus larvatus*	-11	-5.1	Browser
657	PYS	Panga ya Saidi	14000 - 15000 BP	Neotragini	-11	-3.5	Browser
658	PYS	Panga ya Saidi	14000 - 15000 BP	Neotragini	-11.4	-3.1	Browser
659	PYS	Panga ya Saidi	14000 - 15000 BP	*Sylvicapra grimmia*	-11.5	-4.2	Browser
660	PYS	Panga ya Saidi	14000 - 15000 BP	*Potamochoerus larvatus*	-10.1	-4.6	Browser
661	PYS	Panga ya Saidi	14000 - 15000 BP	*Phacochoerus* sp.	-1.1	-3.6	Grazer
662	PYS	Panga ya Saidi	14000 - 15000 BP	*Phacochoerus* sp.	-0.7	-1.3	Grazer
663	PYS	Panga ya Saidi	14000 - 15000 BP	*Kobus ellipsiprymnus*	0.3	-1.6	Grazer
664	PYS	Panga ya Saidi	14000 - 15000 BP	*Phacochoerus* sp.	2.1	-0.4	Grazer
665	PYS	Panga ya Saidi	14000 - 15000 BP	*Phacochoerus* sp.	-2.9	-2.4	Grazer
666	PYS	Panga ya Saidi	14000 - 15000 BP	Colobus/cercopithecine	-11.6	-3.7	Browser
667	PYS	Panga ya Saidi	14000 - 15000 BP	Colobus/cercopithecine	-12	-2.2	Browser
668	PYS	Panga ya Saidi	14000 - 15000 BP	Bovid Size 3	-0.8	-2	Grazer
669	PYS	Panga ya Saidi	14000 - 15000 BP	Bovid Size 3	2.4	0.1	Grazer
670	PYS	Panga ya Saidi	14000 - 15000 BP	Bovid Size 3	-5.2	-2.7	Grazer

	Region	Site	Age	Taxon	$\delta^{13}C$	$\delta^{18}O$	Diet
671	PYS	Panga ya Saidi	25000-20000 BP	*Kobus ellipsiprymnus*	0.7	-1.9	Grazer
672	PYS	Panga ya Saidi	25000-20000 BP	Bovid Size 1	-2.1	-4.7	Grazer
673	PYS	Panga ya Saidi	25000-20000 BP	*Alcelaphus/Damaliscus*	0.2	-1	Grazer
674	PYS	Panga ya Saidi	25000-20000 BP	Bovid Size 2	-11.3	-2.9	Browser
675	PYS	Panga ya Saidi	325000 - 33500 BP	Bovid Size 3	0.5	-0.7	Grazer
676	PYS	Panga ya Saidi	325000 - 33500 BP	*Sylvicapra grimmia*	-10.6	-2.8	Browser
677	PYS	Panga ya Saidi	325000 - 33500 BP	*Phacochoerus* sp.	-2	-0.6	Grazer
678	PYS	Panga ya Saidi	325000 - 33500 BP	*Kobus ellipsiprymnus*	-0.3	-2.4	Grazer
679	PYS	Panga ya Saidi	325000 - 33500 BP	*Phacochoerus* sp.	0.9	-0.8	Grazer
680	PYS	Panga ya Saidi	325000 - 33500 BP	*Colobus* sp.	-11.2	-3.1	Browser
681	PYS	Panga ya Saidi	325000 - 33500 BP	*Phacochoerus* sp.	-1.8	-4.9	Grazer
682	PYS	Panga ya Saidi	325000 - 33500 BP	*Phacochoerus* sp.	0.4	-1.2	Grazer
683	PYS	Panga ya Saidi	325000 - 33500 BP	*Phacochoerus* sp.	1.5	-0.7	Grazer
684	PYS	Panga ya Saidi	48000 - 49000 BP	*Ourebia ourebi*	0.2	-1.6	Grazer
685	PYS	Panga ya Saidi	48000 - 49000 BP	*Ourebia ourebi*	-3.7	-2.4	Grazer
686	PYS	Panga ya Saidi	48000 - 49000 BP	Cephalophini, small	-10.2	-3.6	Browser
687	PYS	Panga ya Saidi	48000 - 49000 BP	*Phacochoerus* sp.	-2	-0.9	Grazer
688	PYS	Panga ya Saidi	48000 - 49000 BP	*Phacochoerus* sp.	-0.9	0.1	Grazer
689	PYS	Panga ya Saidi	48000 - 49000 BP	*Alcelaphus/Damaliscus*	-2.2	-1	Grazer
690	PYS	Panga ya Saidi	48000 - 49000 BP	*Kobus ellipsiprymnus*	2.6	0.1	Grazer
691	PYS	Panga ya Saidi	48000 - 49000 BP	*Alcelaphus/Damaliscus*	1.6	-0.5	Grazer
692	PYS	Panga ya Saidi	48000 - 49000 BP	*Papio* sp.	-9.2	0.1	Omnivore
693	PYS	Panga ya Saidi	48000 - 49000 BP	Bovid Size 1	-4.6	-3.2	Grazer
694	PYS	Panga ya Saidi	48000 - 49000 BP	*Papio* sp.	-9.3	-1.8	Omnivore
695	PYS	Panga ya Saidi	48000 - 49000 BP	*Ourebia ourebi*	-0.2	-2.4	Grazer
696	PYS	Panga ya Saidi	48000 - 49000 BP	Bovid Size 1	0.8	-2.3	Grazer
697	PYS	Panga ya Saidi	48000 - 49000 BP	Large tragelaphine	-7.1	-0.5	Browser
698	PYS	Panga ya Saidi	48000 - 49000 BP	Large tragelaphine	-6.8	0.3	Browser

	Region	Site	Age	Taxon	$\delta^{13}C$	$\delta^{18}O$	Diet
699	PYS	Panga ya Saidi	48000 - 49000 BP	Large tragelaphine	-6.3	0.1	Browser
700	PYS	Panga ya Saidi	48000 - 49000 BP	*Kobus ellipsiprymnus*	3.3	0.2	Grazer
701	PYS	Panga ya Saidi	48000 - 49000 BP	*Kobus ellipsiprymnus*	1.3	-0.6	Grazer
702	PYS	Panga ya Saidi	48000 - 49000 BP	*Phacochoerus* sp.	-2.3	-3	Grazer
703	PYS	Panga ya Saidi	48000 - 49000 BP	*Phacochoerus* sp.	-3.5	-0.7	Grazer
704	PYS	Panga ya Saidi	48000 - 49000 BP	*Alcelaphus/Damaliscus*	3.4	-0.7	Grazer
705	PYS	Panga ya Saidi	48000 - 49000 BP	*Syncerus caffer*	2.3	-2.2	Grazer
706	PYS	Panga ya Saidi	48000 - 49000 BP	Bovid Size 3 Alcelaphini	1.9	-0.6	Grazer
707	PYS	Panga ya Saidi	48000 - 49000 BP	*Alcelaphus/Damaliscus*	-4.2	-1.6	Grazer
708	PYS	Panga ya Saidi	48000 - 49000 BP	*Alcelaphus/Damaliscus*	-2.2	-1.3	Grazer
709	PYS	Panga ya Saidi	48000 - 49000 BP	*Alcelaphus/Damaliscus*	1.1	-1.9	Grazer
710	PYS	Panga ya Saidi	48000 - 49000 BP	*Alcelaphus/Damaliscus*	2.7	-1.7	Grazer
711	PYS	Panga ya Saidi	48000 - 49000 BP	Bovid Size 3	1.8	-0.6	Grazer
712	PYS	Panga ya Saidi	48000 - 49000 BP	Bovid Size 2	0.3	0.2	Grazer
713	PYS	Panga ya Saidi	48000 - 49000 BP	*Papio* sp.	-10.7	-3.3	Omnivore
714	PYS	Panga ya Saidi	48000 - 49000 BP	*Papio* sp.	-10.8	-2.4	Omnivore
715	PYS	Panga ya Saidi	48000 - 49000 BP	Bovid Size 2	-1.8	-1.2	N/A
716	PYS	Panga ya Saidi	48000 - 49000 BP	Bovid Size 3 Alcelaphini	-6.8	-3.6	Grazer
717	PYS	Panga ya Saidi	48000 - 49000 BP	*Phacochoerus* sp.	-0.2	-1.6	Grazer
718	PYS	Panga ya Saidi	48000 - 49000 BP	*Phacochoerus* sp.	0.4	-2.5	Grazer
719	PYS	Panga ya Saidi	48000 - 49000 BP	*Connochaetes taurinus*	-0.9	-1.2	Grazer
720	PYS	Panga ya Saidi	48000 - 49000 BP	Bovid Size 3	-1.3	-4.5	Grazer
721	PYS	Panga ya Saidi	68000 - 60000 BP	*Potamochoerus larvatus*	-3.7	-2.5	Grazer
722	PYS	Panga ya Saidi	68000 - 60000 BP	*Potamochoerus larvatus*	-4.4	-10.7	Browser
723	PYS	Panga ya Saidi	68000 - 60000 BP	*Kobus ellipsiprymnus*	1.1	0.8	Grazer
724	PYS	Panga ya Saidi	68000 - 60000 BP	*Phacochoerus* sp.	-2.7	-2.7	Grazer
725	PYS	Panga ya Saidi	68000 - 60000 BP	Suid	-5.6	-6.5	Browser
726	PYS	Panga ya Saidi	68000 - 60000 BP	Bovid Size 2	-0.3	-1.5	Grazer

	Region	Site	Age	Taxon	$\delta^{13}C$	$\delta^{18}O$	Diet
727	PYS	Panga ya Saidi	68000 - 60000 BP	Bovid Size 2	-3.7	-2.9	Grazer
728	PYS	Panga ya Saidi	68000 - 60000 BP	Bovid Size 2	-5.8	-3.4	Browser
729	PYS	Panga ya Saidi	68000 - 60000 BP	Bovid Size 1 Madoqua sp.	-7.5	-2.7	Browser
730	PYS	Panga ya Saidi	68000 - 60000 BP	*Redunca redunca*	0.4	-1.7	Grazer
731	PYS	Panga ya Saidi	68000 - 60000 BP	*Sylvicapra grimmia*	-12.5	-5.4	Browser
732	PYS	Panga ya Saidi	68000 - 60000 BP	*Potamochoerus larvatus*	-16.2	-5.8	Browser
733	PYS	Panga ya Saidi	68000 - 60000 BP	*Potamochoerus larvatus*	-2.9	-7.1	Browser
734	PYS	Panga ya Saidi	68000 - 60000 BP	*Syncerus caffer*	-2.9	-2.4	Grazer
735	PYS	Panga ya Saidi	68000 - 60000 BP	Reduncine Size 2	0.7	-5	Grazer
736	PYS	Panga ya Saidi	68000 - 60000 BP	Bovid Size 2-3	0.3	-1.9	Grazer
737	PYS	Panga ya Saidi	68000 - 60000 BP	Bovid Size 3	-1	-0.3	Grazer
738	PYS	Panga ya Saidi	68000 - 60000 BP	Bovid Size 1-2	-13.5	-5.4	Browser
739	PYS	Panga ya Saidi	68000 - 60000 BP	Bovid Size 3	-2	-0.5	Grazer
740	PYS	Panga ya Saidi	68000 - 60000 BP	*Sylvicapra grimmia*	-11.7	-3.7	Browser
741	PYS	Panga ya Saidi	68000 - 60000 BP	*Sylvicapra grimmia*	-12.5	-2.2	Browser
742	PYS	Panga ya Saidi	68000 - 60000 BP	*Potamochoerus larvatus*	-11.9	-7.2	Browser
743	PYS	Panga ya Saidi	68000 - 60000 BP	Suid	-9.8	-2.9	Browser
744	PYS	Panga ya Saidi	68000 - 60000 BP	Suid	-11.5	-0.9	Browser
745	PYS	Panga ya Saidi	68000 - 60000 BP	*Potamochoerus larvatus*	-16.6	-5.3	Browser
746	PYS	Panga ya Saidi	68000 - 60000 BP	Reduncine (*Kobus* sp.)	-1.5	-3.7	Grazer
747	PYS	Panga ya Saidi	68000 - 60000 BP	Reduncine (size 3)	-1.4	-1.4	Grazer
748	PYS	Panga ya Saidi	68000 - 60000 BP	Bovid size 3 *Kobus*	-0.5	-0.8	Grazer
749	PYS	Panga ya Saidi	68000 - 60000 BP	Bovid Size 2	-1.1	-2.1	Grazer
750	PYS	Panga ya Saidi	78000 - 73000 BP	*Tragelaphus scriptus*	-11.3	-3	Browser
751	PYS	Panga ya Saidi	78000 - 73000 BP	*Sylvicapra grimmia*	-9	-1.5	Browser
752	PYS	Panga ya Saidi	78000 - 73000 BP	*Sylvicapra grimmia*	-12.7	-3.4	Browser
753	PYS	Panga ya Saidi	78000 - 73000 BP	Suid	-14.4	-6.2	Browser
754	PYS	Panga ya Saidi	78000 - 73000 BP	Suid	-13.1	-3.1	Browser

	Region	Site	Age	Taxon	$\delta^{13}C$	$\delta^{18}O$	Diet
755	PYS	Panga ya Saidi	78000 - 73000 BP	Cercopithecinae	-13.5	-5.2	Omnivore
756	PYS	Panga ya Saidi	78000 - 73000 BP	Cercopithecinae	-14.5	-6.7	Omnivore

Statistical analysis

Two-way ANOVAs, Post-hoc Tests (Tukey's method), Levene's Test and Shapiro-Wilk Test were performed with two major objectives: (1) identify the effects of taxon (family) and phase on $\delta^{13}C$ and $\delta^{18}O$ values, and (2) identify the effect of dietary habit on stable isotope values.

$\delta^{13}C$ and $\delta^{18}O$ values, taxa and phases

- I grouped data from taxa at the family level given limited species-specific data. Some families still include limited data (Hystricidae n=1, Leporidae n=2, and Macroscelidea n=4), and these are excluded from analysis.
- Full details regarding ANOVA, Tukey Test, Levene's Test, and Shapiro-Wilk Test are given below

Results Summary:

Two-way ANOVAs

Existence of differences among groups: Two-way ANOVAs were performed to check the effect of phase and family on both $\delta^{13}C$ values (model 1) and $\delta^{18}O$ values (model 2). There is not a statistically significant interaction between the effects of phase and family on $\delta^{13}C$ values ($F(13,199) = 0.49$, $p = 0.93$), and the same is true for the effect of these variables on $\delta^{18}O$ values ($F(13,199) = 1.51$, $p = 0.11$). Simple main affects analysis showed that both phase and family have a significant effect on $\delta^{13}C$ values ($p < 0.0001$) and $\delta^{18}O$ values ($p < 0.0001$ and $p = 0.03$, respectively).

```
> d13C.ANOVA <- aov(d13C ~ Phase + Family + Phase:Family, data = data)
> summary(d13C.ANOVA)
             Df Sum Sq Mean Sq F value   Pr(>F)
Phase         3  273.1   91.03  19.469 4.14e-11 ***
Family        6  589.2   98.20  21.001  < 2e-16 ***
Phase:Family 13   29.9    2.30   0.492    0.927
Residuals   199  930.5    4.68
---
Signif. codes:  0 ‘***’ 0.001 ‘**’ 0.01 ‘*’ 0.05 ‘.’ 0.1 ‘ ’ 1
> d18O.ANOVA <- aov(d18O ~ Phase + Family + Phase:Family, data = data)
> summary(d18O.ANOVA)
             Df Sum Sq Mean Sq F value  Pr(>F)
Phase         3   91.6  30.529  13.386 5.4e-08 ***
Family        6   32.8   5.470   2.398  0.0293 *
Phase:Family 13   44.9   3.451   1.513  0.1149
Residuals   199  453.8   2.281
---
Signif. codes:  0 ‘***’ 0.001 ‘**’ 0.01 ‘*’ 0.05 ‘.’ 0.1 ‘ ’ 1
> d13C.ANOVA <- aov(d13C ~ Phase + Family, data = data)
> summary(d13C.ANOVA)
            Df Sum Sq Mean Sq F value   Pr(>F)
Phase        3  273.1   91.03   20.09 1.68e-11 ***
Family       6  589.2   98.20   21.68  < 2e-16 ***
Residuals  212  960.4    4.53
---
Signif. codes:  0 ‘***’ 0.001 ‘**’ 0.01 ‘*’ 0.05 ‘.’ 0.1 ‘ ’ 1
> d18O.ANOVA <- aov(d18O ~ Phase + Family, data = data)
> summary(d18O.ANOVA)
            Df Sum Sq Mean Sq F value   Pr(>F)
Phase        3   91.6  30.529  12.978 8.15e-08 ***
Family       6   32.8   5.470   2.325    0.034 *
Residuals  212  498.7   2.352
---
Signif. codes:  0 ‘***’ 0.001 ‘**’ 0.01 ‘*’ 0.05 ‘.’ 0.1 ‘ ’ 1
```

Levene's and Shapiro-Wilk Tests

Quality of models: Levene's Test suggests that groups have equal variance in $\delta^{13}C$ values ($F = 0.65$, $p = 0.88$) and $\delta^{18}O$ values ($F = 0.81$, $p = 0.71$). The Shapiro-Wilk Test suggests that residuals for $\delta^{13}C$ and $\delta^{18}O$ are not normally distributed ($W = 0.86$, $W = 0.91$, respectively, $p < 0.0001$), so results should be treated with caution even though F tests are pretty robust to violations of the normality assumption (Ito, 1980).

```
> leveneTest(d13C ~ Phase*Family, data=data)
Levene's Test for Homogeneity of Variance (center = median)
       Df F value Pr(>F)
group  22  0.6494 0.8836
      199
> leveneTest(d18O ~ Phase*Family, data=data)
Levene's Test for Homogeneity of Variance (center = median)
       Df F value Pr(>F)
group  22  0.8114 0.7096
      199
```

```
> aovd13C_residuals <- residuals(object = d13C.ANOVA)
> shapiro.test(x = aovd13C_residuals)

        Shapiro-Wilk normality test

data:  aovd13C_residuals
W = 0.85615, p-value = 1.411e-13

> aovd18O_residuals <- residuals(object = d18O.ANOVA)
> shapiro.test(x = aovd18O_residuals)

        Shapiro-Wilk normality test

data:  aovd18O_residuals
W = 0.90784, p-value = 1.774e-10
```

Tukey Tests

Model details: Post-hoc comparisons using Tukey's method suggest that Equidae samples are significantly enriched in ^{13}C relative to samples from all other taxa (model 1, $p < 0.0001$). Additionally, samples from phases III and IV tend to be significantly enriched in ^{13}C relative to samples from phases I and II ($p < 0.0004$). While post-hoc comparisons suggest no significant differences in $\delta^{18}O$ among taxa, they do suggest that samples from phase III are consistently enriched in ^{18}O relative to samples from phases I and II ($p \leq 0.01$).

```
> TukeyHSD(d13C.ANOVA, which = "Family")
  Tukey multiple comparisons of means
    95% family-wise confidence level

Fit: aov(formula = d13C ~ Phase + Family, data = data)

$Family
                                                       diff         lwr         upr     p adj
Cercopithecidae-Bovidae                          -0.38025076  -1.7226794  0.96217785 0.9800359
Equidae-Bovidae                                   7.61411420   5.4166102  9.81161824 0.0000000
Galagonidae-Bovidae                               1.03023871  -1.4402900  3.50076743 0.8770883
Nesomyidae - C. gambianus-Bovidae                 1.11087759  -0.6879870  2.90974218 0.5237310
Procaviidae - D. validus-Bovidae                 -0.74721008  -1.8528744  0.35845426 0.4103156
Suidae-Bovidae                                    1.04205929  -1.2788484  3.36296700 0.8339541
Equidae-Cercopithecidae                           7.99436496   5.5665042 10.42222571 0.0000000
Galagonidae-Cercopithecidae                       1.41048947  -1.2670086  4.08798756 0.7027244
Nesomyidae - C. gambianus-Cercopithecidae         1.49112836  -0.5828527  3.56510946 0.3330740
Procaviidae - D. validus-Cercopithecidae         -0.36695932  -1.8795655  1.14564686 0.9911200
Suidae-Cercopithecidae                            1.42231006  -1.1177877  3.96240777 0.6388472
Galagonidae-Equidae                              -6.58387549  -9.7769783 -3.39077270 0.0000001
Nesomyidae - C. gambianus-Equidae                -6.50323660  -9.2103212 -3.79615200 0.0000000
Procaviidae - D. validus-Equidae                 -8.36132428 -10.6667281 -6.05592044 0.0000000
Suidae-Equidae                                   -6.57205490  -9.6508543 -3.49325549 0.0000000
Nesomyidae - C. gambianus-Galagonidae             0.08063889  -2.8524133  3.01369109 1.0000000
Procaviidae - D. validus-Galagonidae             -1.77744879  -4.3444266  0.78952902 0.3796945
Suidae-Galagonidae                                0.01182059  -3.2674315  3.29107264 1.0000000
Procaviidae - D. validus-Nesomyidae - C. gambianus -1.85808768  -3.7872784  0.07110299 0.0673834
Suidae-Nesomyidae - C. gambianus                 -0.06881830  -2.8770020  2.73936538 1.0000000
Suidae-Procaviidae - D. validus                   1.78926938  -0.6340497  4.21258848 0.3010085

> TukeyHSD(d13C.ANOVA, which = "Phase")
  Tukey multiple comparisons of means
    95% family-wise confidence level

Fit: aov(formula = d13C ~ Phase + Family, data = data)

$Phase
                     diff        lwr       upr     p adj
Phase 2-Phase 1 -0.8080556 -1.8899496 0.2738385 0.2169608
Phase 3-Phase 1  1.8185833  0.9781192 2.6590475 0.0000004
Phase 4-Phase 1  2.5748718  0.9428634 4.2068802 0.0003611
Phase 3-Phase 2  2.6266389  1.5204855 3.7327923 0.0000000
Phase 4-Phase 2  3.3829274  1.5994905 5.1663642 0.0000107
Phase 4-Phase 3  0.7562885 -0.8919021 2.4044790 0.6349557
```

```
> TukeyHSD(d18O.ANOVA, which = "Family")
  Tukey multiple comparisons of means
    95% family-wise confidence level

Fit: aov(formula = d18O ~ Phase + Family, data = data)

$Family
                                                      diff        lwr       upr     p adj
Cercopithecidae-Bovidae                          0.909697790 -0.0576595 1.8770551 0.0804396
Equidae-Bovidae                                  1.324108359 -0.2594183 2.9076350 0.1684957
Galagonidae-Bovidae                              0.004322554 -1.7759464 1.7845915 1.0000000
Nesomyidae - C. gambianus-Bovidae                0.131057705 -1.1652084 1.4273238 0.9999385
Procaviidae - D. validus-Bovidae                 0.452341296 -0.3444031 1.2490857 0.6234395
Suidae-Bovidae                                   0.335978783 -1.3364729 2.0084305 0.9968208
Equidae-Cercopithecidae                          0.414410569 -1.3351117 2.1639329 0.9921864
Galagonidae-Cercopithecidae                     -0.905375236 -2.8347868 1.0240363 0.8030547
Nesomyidae - C. gambianus-Cercopithecidae       -0.778640085 -2.2731558 0.7158757 0.7135274
Procaviidae - D. validus-Cercopithecidae        -0.457356494 -1.5473441 0.6326311 0.8738680
Suidae-Cercopithecidae                          -0.573719007 -2.4041195 1.2566815 0.9668125
Galagonidae-Equidae                             -1.319785805 -3.6207433 0.9811717 0.6118216
Nesomyidae - C. gambianus-Equidae               -1.193050654 -3.1437823 0.7576810 0.5356457
Procaviidae - D. validus-Equidae                -0.871767063 -2.5330466 0.7895125 0.7065368
Suidae-Equidae                                  -0.988129576 -3.2067198 1.2304607 0.8391660
Nesomyidae - C. gambianus-Galagonidae            0.126735151 -1.9868293 2.2402996 0.9999972
Procaviidae - D. validus-Galagonidae             0.448018742 -1.4017516 2.2977891 0.9911976
Suidae-Galagonidae                               0.331656229 -2.0313807 2.6946931 0.9995837
Procaviidae - D. validus-Nesomyidae - C. gambianus  0.321283591 -1.0688958 1.7114630 0.9931562
Suidae-Nesomyidae - C. gambianus                 0.204921078 -1.8186628 2.2285050 0.9999380
Suidae-Procaviidae - D. validus                 -0.116362513 -1.8626121 1.6298870 0.9999948

> TukeyHSD(d18O.ANOVA, which = "Phase")
  Tukey multiple comparisons of means
    95% family-wise confidence level

Fit: aov(formula = d18O ~ Phase + Family, data = data)

$Phase
                      diff        lwr       upr     p adj
Phase 2-Phase 1  0.50732975 -0.2722857 1.2869452 0.3340824
Phase 3-Phase 1  1.45052419  0.8448837 2.0561647 0.0000000
Phase 4-Phase 1  0.48446650 -0.6915627 1.6604957 0.7101318
Phase 3-Phase 2  0.94319444  0.1460976 1.7402913 0.0130749
Phase 4-Phase 2 -0.02286325 -1.3080121 1.2622856 0.9999648
Phase 4-Phase 3 -0.96605769 -2.1537478 0.2216324 0.1544123
```

$\delta^{13}C$ and $\delta^{18}O$ values and dietary habit

Approach:

Same as above, but cut 5 data points from "NA" Diet category and 3 data points from "Mixed feeder" Diet category before analysis. This leaves grazers, browsers, and omnivores.

Two-way ANOVAs

Existence of differences among groups: Two-way ANOVAs were performed to check the effect of phase and diet on both $\delta^{13}C$ values (model 3) and $\delta^{18}O$ values (model 4). There is not a statistically significant interaction between the effects of phase and diet habit on $\delta^{13}C$ values ($F(4,213) = 0.35$, $p = 0.84$), and the same is true for the effect of these variables on $\delta^{18}O$ values ($F(4,213) = 0.62$, $p = 0.65$). Simple main affects analysis showed that both phase and diet habit have a significant effect on $\delta^{18}O$ values ($p < 0.0001$ and $p = 0.02$, respectively) and $\delta^{13}C$ values ($p < 0.0001$).

```
> d13C.ANOVA <- aov(d13C ~ Phase + DIET1 + Phase:DIET1, data = data)
> summary(d13C.ANOVA)
             Df Sum Sq Mean Sq F value Pr(>F)
Phase         3  240.7    80.2  34.865 <2e-16 ***
DIET1         2  967.4   483.7 210.203 <2e-16 ***
Phase:DIET1   4    3.2     0.8   0.353  0.842
Residuals   213  490.2     2.3
---
Signif. codes:  0 ‘***’ 0.001 ‘**’ 0.01 ‘*’ 0.05 ‘.’ 0.1 ‘ ’ 1
> d18O.ANOVA <- aov(d18O ~ Phase + DIET1 + Phase:DIET1, data = data)
> summary(d18O.ANOVA)
             Df Sum Sq Mean Sq F value   Pr(>F)
Phase         3   85.6  28.542  11.840 3.33e-07 ***
DIET1         2   18.1   9.071   3.763   0.0248 *
Phase:DIET1   4    6.0   1.498   0.621   0.6477
Residuals   213  513.4   2.411
---
Signif. codes:  0 ‘***’ 0.001 ‘**’ 0.01 ‘*’ 0.05 ‘.’ 0.1 ‘ ’ 1
> d13C.ANOVA <- aov(d13C ~ Phase + DIET1, data = data)
> summary(d13C.ANOVA)
             Df Sum Sq Mean Sq F value Pr(>F)
Phase         3  240.7    80.2   35.29 <2e-16 ***
DIET1         2  967.4   483.7  212.74 <2e-16 ***
Residuals   217  493.4     2.3
---
Signif. codes:  0 ‘***’ 0.001 ‘**’ 0.01 ‘*’ 0.05 ‘.’ 0.1 ‘ ’ 1
> d18O.ANOVA <- aov(d18O ~ Phase + DIET1, data = data)
> summary(d18O.ANOVA)
             Df Sum Sq Mean Sq F value   Pr(>F)
Phase         3   85.6  28.542   11.92 2.94e-07 ***
DIET1         2   18.1   9.071    3.79   0.0241 *
Residuals   217  519.4   2.394
---
Signif. codes:  0 ‘***’ 0.001 ‘**’ 0.01 ‘*’ 0.05 ‘.’ 0.1 ‘ ’ 1
```

Levene's and Shapiro-Wilk Tests

Quality of models: Levene's Test suggests that groups do not have equal variance in $\delta^{13}C$ values ($F = 2.19$, $p = 0.02$) but that they do have equal variance in $\delta^{18}O$ values ($F = 1.61$, $p = 0.11$). Model 3 may not be reliable. The Shapiro-Wilk Test suggests that residuals for $\delta^{13}C$ and $\delta^{18}O$ are not normally distributed ($W = 0.89$, $W = 0.90$, respectively, $p < 0.0001$), so results of model 4 should be treated with caution.

```
> leveneTest(d13C ~ Phase*DIET1, data=data)
Levene's Test for Homogeneity of Variance (center = median)
       Df F value  Pr(>F)
group   9  2.1946 0.02358 *
      213
---
Signif. codes:  0 ‘***’ 0.001 ‘**’ 0.01 ‘*’ 0.05 ‘.’ 0.1 ‘ ’ 1
> leveneTest(d18O ~ Phase*DIET1, data=data)

Levene's Test for Homogeneity of Variance (center = median)
       Df F value Pr(>F)
group   9  1.6115 0.1134
      213
> plot(d13C.ANOVA, 1)
> plot(d18O.ANOVA, 1)
> aovd13C_residuals <- residuals(object = d13C.ANOVA)
> shapiro.test(x = aovd13C_residuals)

        Shapiro-Wilk normality test

data:  aovd13C_residuals
W = 0.88777, p-value = 7.965e-12

> aovd18O_residuals <- residuals(object = d18O.ANOVA)
> shapiro.test(x = aovd18O_residuals)

        Shapiro-Wilk normality test

data:  aovd18O_residuals
W = 0.90455, p-value = 9.802e-11
```

Tukey Tests

Model details: Post-hoc comparisons using Tukey's method suggest that grazers, browsers, and omnivores tend to have significantly different $\delta^{13}C$ values, with grazers most enriched in ^{13}C, browsers most depleted in ^{13}C, and omnivores between the two (model 3, $p < 0.0001$). Additionally, samples from phases III and IV again tend to be significantly enriched in ^{13}C relative to samples from phases I and II ($p < 0.0001$), and samples from phase I may also be enriched in ^{13}C relative to those from phase II ($p = 0.008$). Post-hoc comparisons suggest that grazers are enriched in ^{18}O relative to browsers (model 4, $p = 0.03$), and they again suggest that samples from phase III are consistently enriched in ^{18}O relative to samples from phases I and II ($p \leq 0.02$).

```
> TukeyHSD(d13C.ANOVA, which = "DIET1")
  Tukey multiple comparisons of means
    95% family-wise confidence level

Fit: aov(formula = d13C ~ Phase + DIET1, data = data)

$DIET1
                     diff        lwr       upr p adj
Grazer-Browser    8.063473  7.1071584  9.019788 0e+00
Omnivore-Browser  1.652467  0.9295607  2.375373 5e-07
Omnivore-Grazer  -6.411006 -7.5496164 -5.272396 0e+00

> TukeyHSD(d13C.ANOVA, which = "Phase")
  Tukey multiple comparisons of means
    95% family-wise confidence level

Fit: aov(formula = d13C ~ Phase + DIET1, data = data)

$Phase
                     diff        lwr        upr     p adj
Phase 2-Phase 1 -0.9248345 -1.6719705 -0.1776986 0.0084014
Phase 3-Phase 1  1.6406918  1.0426373  2.2387464 0.0000000
Phase 4-Phase 1  2.3388058  1.1441380  3.5334737 0.0000051
Phase 3-Phase 2  2.5655263  1.7898791  3.3411735 0.0000000
Phase 4-Phase 2  3.2636404  1.9708950  4.5563857 0.0000000
Phase 4-Phase 3  0.6981140 -0.5145886  1.9108167 0.4450284

> TukeyHSD(d18O.ANOVA, which = "DIET1")
  Tukey multiple comparisons of means
    95% family-wise confidence level

Fit: aov(formula = d18O ~ Phase + DIET1, data = data)

$DIET1
                       diff         lwr        upr     p adj
Grazer-Browser    1.07910183  0.09788115 2.06032252 0.0271661
Omnivore-Browser -0.05464045 -0.79637356 0.68709267 0.9834781
Omnivore-Grazer  -1.13374228 -2.30200590 0.03452134 0.0593000

> TukeyHSD(d18O.ANOVA, which = "Phase")
  Tukey multiple comparisons of means
    95% family-wise confidence level

Fit: aov(formula = d18O ~ Phase + DIET1, data = data)

$Phase
                     diff        lwr       upr     p adj
Phase 2-Phase 1  0.5009794 -0.2656148 1.2675736 0.3303919
Phase 3-Phase 1  1.4113741  0.7977440 2.0250043 0.0000001
Phase 4-Phase 1  0.4359794 -0.7898021 1.6617609 0.7937293
Phase 3-Phase 2  0.9103947  0.1145467 1.7062427 0.0177570
Phase 4-Phase 2 -0.0650000 -1.3914133 1.2614133 0.9992684
Phase 4-Phase 3 -0.9753947 -2.2196807 0.2688913 0.1803479
```

General linear model and regression

Objective: Use GLM to identify the extent to which $\delta^{13}C$ values can predict $\delta^{18}O$ values when controlling for taxon and phase, and highlight examples of taxon-specific regression between $\delta^{13}C$ and $\delta^{18}O$ data.

General linear model (GLM)

Approach:

- As with the previous models, data was grouped at family level given limited species-specific data. Some families still include limited data (Hystricidae n=1, Leporidae n=2, and Macroscelidea n=4), and these are excluded from analysis.
- Full details regarding GLM selection and evaluation are given below

Results Summary:

GLM Key Detail: We used a general linear model to evaluate the extent to which $\delta^{13}C$ values can predict $\delta^{18}O$ values when controlling for phase and family. Using the R package *glmulti*, we found that the model that most parsimoniously predicts $\delta^{18}O$ values (AIC = 760.97, model 3) includes the three predictors and interactions among all terms. This model clarifies the strong positive association between $\delta^{18}O$ and $\delta^{13}C$ values ($p < 0.0001$), which is particularly visible through the strong regression between $\delta^{18}O$ and $\delta^{13}C$ values within both Bovidae and Procaviidae (Figure 5.3).

```
> output <- glmulti(d18O ~
+                     d13C + factor(Phase) + factor(Family), data=data, marginality=TRUE, crit=aic)
Initialization...
TASK: Exhaustive screening of candidate set.
Fitting...
Completed.
> summary(output)
$name
[1] "glmulti.analysis"

$method
[1] "h"

$fitting
[1] "glm"

$crit
[1] "aic"

$level
[1] 2

$marginality
[1] TRUE

$confsetsize
[1] 100

$bestic
[1] 760.9729

$icvalues
 [1] 760.9729 765.8977 776.4153 783.8208 789.1374 789.9634 792.0516 794.5066 796.4322 800.0669 811.8184
[12] 812.3505 817.6419 831.6861 833.8351 836.7574 863.1272 863.2247

$bestmodel
[1] "d18O ~ 1 + factor(Phase) + factor(Family) + d13C + factor(Family):factor(Phase) + "
[2] "    factor(Phase):d13C + factor(Family):d13C"

$modelweights
 [1] 9.210793e-01 7.850092e-02 4.083274e-04 1.006794e-05 7.054276e-07 4.667380e-07 1.643021e-07
 [8] 4.814440e-08 1.838249e-08 2.986270e-09 8.381652e-12 6.423530e-12 4.557889e-13 4.065406e-16
[15] 1.388226e-16 3.220325e-17 6.050127e-23 5.762325e-23




$includeobjects
[1] TRUE

> b <- glm(data$d18O ~ as.factor(data$Phase) + as.factor(data$Family) + data$d13C + data$d13C*as.factor(data$Phase) +
data$d13C*as.factor(data$Family) + as.factor(data$Phase)*as.factor(data$Family))
> summary(b)


Call:
glm(formula = data$d18O ~ as.factor(data$Phase) + as.factor(data$Family) +
    data$d13C + data$d13C * as.factor(data$Phase) + data$d13C *
    as.factor(data$Family) + as.factor(data$Phase) * as.factor(data$Family))

Deviance Residuals:
    Min       1Q   Median       3Q      Max
-3.9724  -0.5918   0.0420   0.6518   4.8097
```

```
Coefficients: (5 not defined because of singularities)
                                                                          Estimate Std. Error t value Pr(>|t|)
(Intercept)                                                               3.970624   1.467899   2.705 0.007455 **
as.factor(data$Phase)Phase 2                                             -0.454812   1.924070  -0.236 0.813394
as.factor(data$Phase)Phase 3                                             -5.225041   1.521113  -3.435 0.000728 ***
as.factor(data$Phase)Phase 4                                            -24.859144   7.110043  -3.496 0.000588 ***
as.factor(data$Family)Cercopithecidae                                   -10.218598   2.995651  -3.411 0.000791 ***
as.factor(data$Family)Equidae                                            13.530684   5.702014   2.373 0.018649 *
as.factor(data$Family)Galagonidae                                        -3.495312   6.580058  -0.531 0.595905
as.factor(data$Family)Nesomyidae - C. gambianus                          -3.866695   5.052343  -0.765 0.445031
as.factor(data$Family)Procaviidae - D. validus                            0.451900   1.407574   0.321 0.748528
as.factor(data$Family)Suidae                                              0.042327   2.548607   0.017 0.986767
data$d13C                                                                 0.684753   0.113998   6.007 9.53e-09 ***
as.factor(data$Phase)Phase 2:data$d13C                                   -0.067272   0.143492  -0.469 0.639737
as.factor(data$Phase)Phase 3:data$d13C                                   -0.503074   0.119890  -4.196 4.17e-05 ***
as.factor(data$Phase)Phase 4:data$d13C                                   -2.182902   0.608160  -3.589 0.000422 ***
as.factor(data$Family)Cercopithecidae:data$d13C                          -0.867679   0.230486  -3.765 0.000223 ***
as.factor(data$Family)Equidae:data$d13C                                   0.127448   0.373416   0.341 0.733255
as.factor(data$Family)Galagonidae:data$d13C                              -0.238060   0.552808  -0.431 0.667222
as.factor(data$Family)Nesomyidae - C. gambianus:data$d13C                -0.247357   0.434293  -0.570 0.569652
as.factor(data$Family)Procaviidae - D. validus:data$d13C                  0.005328   0.105765   0.050 0.959877
as.factor(data$Family)Suidae:data$d13C                                   -0.058151   0.198118  -0.294 0.769448
as.factor(data$Phase)Phase 2:as.factor(data$Family)Cercopithecidae        0.407110   0.727777   0.559 0.576559
as.factor(data$Phase)Phase 3:as.factor(data$Family)Cercopithecidae       -0.101292   0.989248  -0.102 0.918553
as.factor(data$Phase)Phase 4:as.factor(data$Family)Cercopithecidae       -6.737186   1.596905  -4.219 3.81e-05 ***
as.factor(data$Phase)Phase 2:as.factor(data$Family)Equidae               -16.020796   5.222328  -3.068 0.002473 **
as.factor(data$Phase)Phase 3:as.factor(data$Family)Equidae               -12.943352   5.308245  -2.438 0.015679 *
as.factor(data$Phase)Phase 4:as.factor(data$Family)Equidae                       NA         NA      NA       NA
as.factor(data$Phase)Phase 2:as.factor(data$Family)Galagonidae                   NA         NA      NA       NA
as.factor(data$Phase)Phase 3:as.factor(data$Family)Galagonidae                   NA         NA      NA       NA
as.factor(data$Phase)Phase 4:as.factor(data$Family)Galagonidae                   NA         NA      NA       NA
as.factor(data$Phase)Phase 2:as.factor(data$Family)Nesomyidae - C. gambianus  2.469574   1.075447   2.296 0.022754 *
as.factor(data$Phase)Phase 3:as.factor(data$Family)Nesomyidae - C. gambianus  0.531951   1.015516   0.524 0.601015
as.factor(data$Phase)Phase 4:as.factor(data$Family)Nesomyidae - C. gambianus       NA         NA      NA       NA
as.factor(data$Phase)Phase 2:as.factor(data$Family)Procaviidae - D. validus   1.821384   0.677466   2.689 0.007818 **
as.factor(data$Phase)Phase 3:as.factor(data$Family)Procaviidae - D. validus   0.261826   0.522930   0.501 0.617171
as.factor(data$Phase)Phase 4:as.factor(data$Family)Procaviidae - D. validus  -0.863867   0.923261  -0.936 0.350638
as.factor(data$Phase)Phase 2:as.factor(data$Family)Suidae                 -1.313990   1.587982  -0.827 0.409021
as.factor(data$Phase)Phase 3:as.factor(data$Family)Suidae                 -1.024576   1.157120  -0.885 0.377037
as.factor(data$Phase)Phase 4:as.factor(data$Family)Suidae                  4.945857   2.884260   1.715 0.088026 .
---
Signif. codes:  0 ‘***’ 0.001 ‘**’ 0.01 ‘*’ 0.05 ‘.’ 0.1 ‘ ’ 1

(Dispersion parameter for gaussian family taken to be 1.559792)

    Null deviance: 623.12  on 221  degrees of freedom
Residual deviance: 294.80  on 189  degrees of freedom
AIC: 760.97

Number of Fisher Scoring iterations: 2
```

Taxon-specific regression

Approach:

- Used data only from the three families that include the largest ranges of $\delta^{13}C$ values (Bovidae from –20.4 to –1.9 ‰, Equidae from –8.2 to 2.0 ‰, and Procaviidae from –18.4 to –2.5 ‰) (Figure 5.3).
- There is a significant regression between $\delta^{13}C$ and $\delta^{18}O$ data within each family.

```
> Bovidae<-subset(data,Family=='Bovidae')
> summary(lm(d18O ~ d13C, data=Bovidae))

Call:
lm(formula = d18O ~ d13C, data = Bovidae)

Residuals:
    Min      1Q  Median      3Q     Max
-4.0067 -0.7093  0.1663  0.7826  3.1755

Coefficients:
            Estimate Std. Error t value Pr(>|t|)
(Intercept)   0.6689     0.5648   1.184    0.239
d13C          0.3903     0.0459   8.504  1.2e-13 ***
---
Signif. codes:  0 ‘***’ 0.001 ‘**’ 0.01 ‘*’ 0.05 ‘.’ 0.1 ‘ ’ 1

Residual standard error: 1.264 on 107 degrees of freedom
Multiple R-squared:  0.4033,    Adjusted R-squared:  0.3977
F-statistic: 72.32 on 1 and 107 DF,  p-value: 1.204e-13


> Equidae<-subset(data,Family=='Equidae')
> summary(lm(d18O ~ d13C, data=Equidae))

Call:
lm(formula = d18O ~ d13C, data = Equidae)

Residuals:
    Min      1Q  Median      3Q     Max
-1.1784 -0.4407  0.0155  0.5365  0.9188

Coefficients:
            Estimate Std. Error t value Pr(>|t|)
(Intercept)  -1.0193     0.6714  -1.518   0.1727
d13C          0.3756     0.1590   2.362   0.0502 .
---
Signif. codes:  0 ‘***’ 0.001 ‘**’ 0.01 ‘*’ 0.05 ‘.’ 0.1 ‘ ’ 1

Residual standard error: 0.8383 on 7 degrees of freedom
Multiple R-squared:  0.4435,    Adjusted R-squared:  0.364
F-statistic: 5.578 on 1 and 7 DF,  p-value: 0.0502


> Procaviidae<-subset(data,Family=='Procav')
> summary(lm(d18O ~ d13C, data=Procaviidae))

Call:
lm(formula = d18O ~ d13C, data = Procaviidae)

Residuals:
    Min      1Q  Median      3Q     Max
-6.4558 -0.5050  0.2548  0.9151  3.9803

Coefficients:
            Estimate Std. Error t value Pr(>|t|)
(Intercept)   0.3360     1.6639   0.202   0.8409
d13C          0.3177     0.1272   2.498   0.0162 *
---
Signif. codes:  0 ‘***’ 0.001 ‘**’ 0.01 ‘*’ 0.05 ‘.’ 0.1 ‘ ’ 1

Residual standard error: 1.953 on 45 degrees of freedom
Multiple R-squared:  0.1217,    Adjusted R-squared:  0.1022
F-statistic: 6.238 on 1 and 45 DF,  p-value: 0.01623
```

Eastern Africa regional comparison

Objective and Data Overview

Objective: Explore the KC $\delta^{13}C$ data relative to regional datasets.
Approach:

- It would be useful to control at least for taxon when making regional comparison (as in Figure 5.5-6). However, with the exception of Equus, regional taxon-specific regional comparisons are probably too small for statistical tests. This is particularly true if we wish to consider time.
- We also analyze browsers from all sites except L. Turkana region which does not have a representative sample size (only 1 browser).

Equids statistical analysis

Equids are sufficiently well represented in six regional sites (KC, L. Victoria, L. Turkana, Kalemba, Lukenya, and Porc Epic) to permit statistical comparisons. A one-way analysis of variance suggests that there are significant differences in equid $\delta^{13}C$ values among these sites ($F(4,216) = 115.4$, $p < 0.0001$). The $\delta^{13}C$ model fails Levene's test for equal variance ($F = 7.75$, $p = 0.007$), but significant differences in $\delta^{13}C$ values among sites are still supported by a Kruskal-Wallis test ($H(4) = 180.14$, $p < 0.0001$). Post-hoc Wilcoxon rank sum tests suggest that KC equid $\delta^{13}C$ values are significantly different than those at all other sites ($p < 0.0001$ according to Bonferroni correction), that there are significant differences in median equid $\delta^{13}C$ values between L. Victoria and Lukenya and Kalemba ($p < 0.02$), and that there is a significant difference in median $\delta^{13}C$ values between Kalemba and L. Turkana ($p = 0.006$, see below).

```
> summary(aov(d13C ~ Region.Site, data = Equid.subset))
             Df Sum Sq Mean Sq F value Pr(>F)
Region.Site   5   6944    1389   115.4 <2e-16 ***
Residuals   266   3202      12
---
Signif. codes:  0 ‘***’ 0.001 ‘**’ 0.01 ‘*’ 0.05 ‘.’ 0.1 ‘ ’ 1
> leveneTest(d13C ~ as.factor(Region.Site), data=Equid.subset)
Levene's Test for Homogeneity of Variance (center = median)
       Df F value    Pr(>F)
group   5  7.7478 8.023e-07 ***
      266
---
Signif. codes:  0 ‘***’ 0.001 ‘**’ 0.01 ‘*’ 0.05 ‘.’ 0.1 ‘ ’ 1
> kruskal.test(d13C ~ Region.Site, data = Equid.subset)

        Kruskal-Wallis rank sum test

data:  d13C by Region.Site
Kruskal-Wallis chi-squared = 180.14, df = 5, p-value < 2.2e-16

> pairwise.wilcox.test(Equid.subset$d13C, Equid.subset$Region.Site,
+                      p.adjust.method = "bonferroni", exact=FALSE)

        Pairwise comparisons using Wilcoxon rank sum test with continuity correction

data:  Equid.subset$d13C and Equid.subset$Region.Site

            Kalemba Rockshelter KC      L. Turkana L. Victoria Lukenya
KC          < 2e-16             -       -          -           -
L. Turkana  0.00577             4.8e-15 -          -           -
L. Victoria 0.00016             3.5e-15 0.66325    -           -
Lukenya     1.00000             9.6e-09 0.12315    0.01591     -
Porc Epic   1.00000             1.3e-06 0.64512    0.14704     1.00000

P value adjustment method: bonferroni
```

Browser statistical analysis

Browsers are sufficiently well represented in all sites except Turkana region to permit statistical comparisons. A one-way analysis of variance suggests that there are significant differences in browser $\delta^{13}C$ values among these sites ($F(6,853) = 221.6$, $p < 0.0001$). The $\delta^{13}C$ model fails Levene's test for equal variance ($F = 28.24$, $p < 0.0001$), but significant differences in $\delta^{13}C$ values among sites are still supported by a Kruskal-Wallis test ($H(6) = 509.4$, $p < 0.0001$). Post-hoc Wilcoxon rank sum tests suggest that browser $\delta^{13}C$ values from KC, L. Victoria, and Lukenya are distinct from each other and from those of all other sites ($p < 0.03$ according to Bonferroni correction, see R output for full details). Post-hoc tests also suggest that the median Kalemba Rockshelter browser $\delta^{13}C$ value is distinct from those at KC, L. Victoria, and Lukenya.

```
> summary(aov(d13C ~ Region.Site, data = Browser.subset))
             Df Sum Sq Mean Sq F value Pr(>F)
Region.Site   6  18723  3120.5   221.6 <2e-16 ***
Residuals   853  12013    14.1
---
Signif. codes:  0 '***' 0.001 '**' 0.01 '*' 0.05 '.' 0.1 ' ' 1
> leveneTest(d13C ~ as.factor(Region.Site), data=Browser.subset)
Levene's Test for Homogeneity of Variance (center = median)
       Df F value    Pr(>F)
group   6  28.238 < 2.2e-16 ***
      853
---
Signif. codes:  0 '***' 0.001 '**' 0.01 '*' 0.05 '.' 0.1 ' ' 1
> kruskal.test(d13C ~ Region.Site, data = Browser.subset)

        Kruskal-Wallis rank sum test

data:  d13C by Region.Site
Kruskal-Wallis chi-squared = 509.4, df = 6, p-value < 2.2e-16

> pairwise.wilcox.test(Browser.subset$d13C, Browser.subset$Region.Site,
+                      p.adjust.method = "bonferroni", exact=FALSE)

        Pairwise comparisons using Wilcoxon rank sum test with continuity correction

data:  Browser.subset$d13C and Browser.subset$Region.Site

                    EBA     Kalemba Rockshelter KC      L. Victoria Lukenya Porc Epic
Kalemba Rockshelter 1.000   -                   -       -           -       -
KC                  < 2e-16 < 2e-16             -       -           -       -
L. Victoria         1.2e-07 < 2e-16             < 2e-16 -           -       -
Lukenya             0.028   1.0e-06             < 2e-16 2.3e-07     -       -
Porc Epic           1.000   1.000               < 2e-16 3.8e-15     1.4e-05 -
PYS                 1.000   1.000               < 2e-16 < 2e-16     2.2e-06 1.000

P value adjustment method: bonferroni
```

Appendix 2 – Tables associated with "Chapter 6: the Unguja Ukuu isotopic case study"

Table A2:1 *Isotopic dataset of caprine and wild fauna collagen $\delta^{13}C$ and $\delta^{15}N$ values from Unguja Ukuu and Fukuchani on Unguja Island and Panga ya Saidi on the coastal strip, mainland of eastern Africa. It also includes indicators of bone collagen preservation standards (C/N ratio, %C, and %N). All species identified via ZooMS (Culley et al., 2021a; Culley et al., 2021b).*

	ZooMS Sample #	Site	Taxon	Trench	Context	$\delta^{15}N$	$\delta^{13}C$	Phase	%N (5-17%)	%C (15-48%)	C/N ratio (2.9-3.6, %)
1	UU222	Unguja Ukuu	*Capra hircus*	14	1412	12.7	-8.4	Late Phase	14.6	40.9	3.3
2	UU238	Unguja Ukuu	*Capra hircus*	14	1414	10.7	-9.0	Late Phase	15.4	44.0	3.3
3	UU220	Unguja Ukuu	*Capra hircus*	14	1412	14.9	-13.1	Late Phase	15.1	42.4	3.3
4	UU218	Unguja Ukuu	*Philantomba monticola*	14	1412	4.5	-21.7	Late Phase	15.3	45.2	3.4
5	UU237	Unguja Ukuu	*Capra hircus*	14	1414	15.8	-14.3	Late Phase	15.8	44.4	3.3
6	UU221	Unguja Ukuu	*Capra hircus*	14	1412	11.5	-8.0	Late Phase	14.8	42.9	3.4
7	UU216	Unguja Ukuu	*Philantomba monticola*	14	1412	5.5	-21.0	Late Phase	15.9	44.8	3.3
8	UU219	Unguja Ukuu	*Neotragus moschatus*	14	1412	6.5	-21.2	Late Phase	15.6	44.4	3.3
9	UU223	Unguja Ukuu	*Capra hircus*	14	1412	12.6	-8.3	Late Phase	14.9	42.6	3.3
10	UU45A	Unguja Ukuu	*Capra hircus*	14	1404	6.8	-10.8	Late Phase	14.6	41.5	3.3
11	UU106	Unguja Ukuu	*Capra hircus*	14	1412	14.8	-8.2	Late Phase	12.8	36.7	3.3
12	UU84	Unguja Ukuu	*Capra hircus*	14	1408	13.3	-7.3	Late Phase	15.1	43.1	3.3
13	UU107	Unguja Ukuu	*Capra hircus*	14	1414	11.8	-10.3	Late Phase	13.0	36.9	3.3
14	UU108	Unguja Ukuu	*Ovis aries*	14	1414	7.2	-8.8	Late Phase	16.5	41.4	2.9
15	UU35A	Unguja Ukuu	*Ovis aries*	14	1404	12.9	-8.7	Late Phase	15.4	41.3	3.1
16	UU135	Unguja Ukuu	Alcelaphini	14	1423	10.3	-14.2	Early Phase	15.9	42.7	3.1
17	UU168	Unguja Ukuu	*Capra hircus*	14	1428	14.3	-10.0	Early Phase	13.2	36.9	3.3
18	UU154	Unguja Ukuu	*Ovis aries*	14	1423	9.2	-11.0	Early Phase	16.1	43.3	3.1

	ZooMS Sample #	Site	Taxon	Trench	Context	$\delta^{15}N$	$\delta^{13}C$	Phase	%N (5-17%)	%C (15-48%)	C/N ratio (2.9-3.6, %)
19	UU142	Unguja Ukuu	*Capra hircus*	14	1423	10.3	-10.3	Early Phase	9.6	26.1	3.2
20	UU120	Unguja Ukuu	*Capra hircus*	14	1420	5.8	-10.6	Early Phase	15.1	42.2	3.3
21	UU228	Unguja Ukuu	*Dendrohyrax*			6.6	-21.4		15.9	46.3	3.4
22	UU243	Unguja Ukuu	Cercopithecidae	11	001	5.6	-18.8		15.3	43.8	3.3
23	UU245	Unguja Ukuu	Cercopithecidae			3.4	-19.8		15.2	43.9	3.4
24	UU246	Unguja Ukuu	*Philantomba monticola*	11	002	7.7	-20.9		15.6	46.2	3.5
25	UU26	Unguja Ukuu	*Capra hircus*	11	010	11.9	-13.6		13.7	42.7	3.6
26	UU01	Unguja Ukuu	*Ovis aries*	11	003	10.3	-9.4		15.3	41.3	3.2
27	UU30	Unguja Ukuu	*Neotragus moschatus*	11	012	8.1	-22.8		16.1	42.2	3.1
28	FK 01	Fukuchani	*Capra hircus*	10	008	10.1	-13.8		15.4	43.0	3.2
29	FK13	Fukuchani	*Neotragus moschatus*	11	007	10.0	-20.8		15.2	44.9	3.5
30	FK03	Fukuchani	*Neotragus moschatus*	11	007	8.5	-20.8		15.1	45.4	3.5
31	FK04	Fukuchani	*Neotragus moschatus*	11	007	8.5	-20.9		14.6	44.4	3.5
32	FK14	Fukuchani	*Neotragus moschatus*	11	007	8.5	-21.2		15.7	48.2	3.6
33	FK02	Fukuchani	*Neotragus moschatus*	11	007	7.1	-20.2		14.3	42.1	3.4
34	FK05	Fukuchani	*Neotragus moschatus*	11	007	10.2	-20.4		15.7	46.4	3.5
35	PYS91	Panga ya Saidi	*Oreotragus oreotragus*			7.0	-21.4		13.9	39.9	3.3
36	PYS89	Panga ya Saidi	*Oreotragus oreotragus*			7.7	-21.9		13.9	39.9	3.3
37	PYS109	Panga ya Saidi	*Oreotragus oreotragus*			9.1	-21.3		16.3	47.2	3.4
38	PYS81	Panga ya Saidi	*Ovis aries*			13.4	-15.4		11.4	30.3	3.1
39	PYS80	Panga ya Saidi	*Oreotragus oreotragus*			5.9	-21.5		16.4	44.7	3.2
40	PYS79	Panga ya Saidi	*Sylvicapra grimmia*			11.8	-20.2		15.8	42.9	3.2
41	PYS110	Panga ya Saidi	Tragelaphini			7.1	-20.0		16.0	44.4	3.2

	ZooMS Sample #	Site	Taxon	Trench	Context	$\delta^{15}N$	$\delta^{13}C$	Phase	%N (5-17%)	%C (15-48%)	C/N ratio (2.9-3.6, %)
42	PYS114	Panga ya Saidi	*Sylvicapra grimmia*			4.7	-20.8		15.7	44.7	3.3
43	PYS86	Panga ya Saidi	*Sylvicapra grimmia*			4.6	-20.8		15.2	41.7	3.2
44	PYS102	Panga ya Saidi	*Oreotragus oreotragus*			10.0	-20.1		16.3	45.2	3.2
45	PYS113	Panga ya Saidi	Cercopithecidae			10.2	-19.2		15.7	43.8	3.3
46	PYS104	Panga ya Saidi	Tragelaphini			10.7	-15.2		15.4	43.5	3.3
47	PYS90	Panga ya Saidi	*Oreotragus oreotragus*			7.3	-20.8		15.7	44.3	3.3
48	PYS92	Panga ya Saidi	*Sylvicapra grimmia*			4.7	-21.1		15.6	43.7	3.3
49	PYS82	Panga ya Saidi	*Sylvicapra grimmia*			5.2	-21.5		14.6	41.1	3.3
50	PYS108	Panga ya Saidi	*Oreotragus oreotragus*			7.9	-20.7		13.2	36.4	3.2
51	PYS88	Panga ya Saidi	Cercopithecidae			8.6	-19.3		16.0	44.6	3.3
52	PYS85	Panga ya Saidi	*Oreotragus oreotragus*			6.8	-20.6		16.1	44.9	3.2

Table A2:2 *Caprine enamel $\delta^{13}C$, $\delta^{18}O$ and $^{87}Sr/^{86}Sr$ values from Unguja Ukuu, Unguja Island. All species identified via ZooMS (Culley et al., 2021a; Culley et al., 2021b). The caprine specimen (no. 10) with extreme outlier $\delta^{13}C$ and $\delta^{18}O$ values is highlighted with an asterisk (*).*

	Site	**Trench**	**Context**	**ZooMS Sample #**	**Taxa**	δ^{13}**C**	δ^{18}**O**	^{87}**Sr/**^{86}**Sr**	**Element**
1	Unguja Ukuu	15	1551	UU213	*Capra hircus*	-5.4	-0.8	0.71095	Upper molar
2	Unguja Ukuu	14	1408	UU87	*Capra hircus*	-4.5	-4.6	0.71052	Upper premolar
3	Unguja Ukuu	14	1438	UU204	*Capra hircus*	-4.9	0.4	0.71256	Lower molar
4	Unguja Ukuu	14	1443	UU206	*Capra hircus*	-6.5	0.4	0.71030	Upper premolar
5	Unguja Ukuu	11	017	UU32	*Capra hircus*	-4.8	-1.1	0.70973	Upper molar
6	Unguja Ukuu	10	005	UU16	*Capra hircus*	-4.9	4.4	0.70791	Lower molar
7	Unguja Ukuu	14	1423	UU127	*Capra hircus*	-6.5	-0.4	0.70994	Lower molar
8	Unguja Ukuu	14	1404	UU39A	*Ovis aries*	-4.4	-2.4	0.70911	Lower premolar deciduous
9	Unguja Ukuu	14	1412	UU100	*Capra hircus*	-2.2	0.1	0.71025	Lower molar
10	Unguja Ukuu	13	006	UU20	*Capra hircus*	-20.1*	-16.4*	0.71013	Upper molar

Table A2:3 *Human enamel $\delta^{13}C$ and $\delta^{18}O$ and $^{87}Sr/^{86}Sr$ values from Unguja Ukuu and Kuumbi Cave, Unguja Island and Panga ya Saidi on the coastal strip eastern Africa mainland. The four PYS 403 human teeth belong to the same individual and have similar $^{87}Sr/^{86}Sr$ values (unpublished). The published $\delta^{13}C_{enamel}$, and $\delta^{18}O$ values from these teeth are also nearly identical (Roberts et al., 2020). The Human enamel $\delta^{13}C$ and $\delta^{18}O$ from KC are also published (Iminjili et al., 2023).*

	Site	**Context**	**ZooMS Sample #**	**Taxon**	$\delta^{13}C$	$\delta^{18}O$	$^{87}Sr/^{86}Sr$	**Element**
1	Unguja Ukuu	UU 11-014 (743)	50586 D1	*Homo sapiens*	-2.7	-3.8	0.70962	Enamel
2	Kuumbi Cave	KC 10 1015 5976	50592 D.1	*Homo sapiens*	-12.1	-5.4	0.70915	Human
3	Kuumbi Cave	KC 10 1022 8835	50593 D.1	*Homo sapiens*	-10.4	-3.5	0.70930	Incisor/premolar
4	Panga ya Saidi	PYS 403	PYS 13	*Homo sapiens*	-11.1	-3.2	0.71126	2nd/3rd molar
5	Panga ya Saidi	PYS 403	PYS 13	*Homo sapiens*	-8.9	-3.4	0.71104	1st molar
6	Panga ya Saidi	PYS 403	PYS 13 403	*Homo sapiens*	-9.7	-3.1	0.71123	Incisor
7	Panga ya Saidi	PYS 403	PYS 13 403	*Homo sapiens*	-9.0	-4.5	0.71095	Premolar

Table A2:4 *Wild herbivore enamel $\delta^{13}C$ and $\delta^{18}O$ values from Kuumbi Cave, Unguja Island used for comparison with caprines from Unguja Ukuu (Iminjili et al., 2023).*

	Phase	**Context**	**Age**	**Taxon**	δ^{13}**C**	δ^{18}**O**	**Diet**
1	Phase 3	1024	Late Pleistocene (18,830-17,080 BP)	*Cephalophus adersi*	-12.6	-3.0	Browser
2	Phase 1	1002	Iron Age (2,000-500 BP)	*Philantomba monticola*	-11.4	-3.4	Browser
3	Phase 1	1002	Iron Age (2,000-500 BP)	*Philantomba monticola*	-11.1	-3.7	Browser
4	Phase 1	1002	Iron Age (2,000-500 BP)	*Philantomba monticola*	-11.2	-3.0	Browser
5	Phase 1	1002	Iron Age (2,000-500 BP)	*Philantomba monticola*	-11.3	-2.5	Browser
6	Phase 1	1003	Iron Age (2,000-500 BP)	*Philantomba monticola*	-10.6	-3.9	Browser
7	Phase 1	1003	Iron Age (2,000-500 BP)	*Philantomba monticola*	-11.3	-7.8	Browser
8	Phase 1	1003	Iron Age (2,000-500 BP)	*Philantomba monticola*	-11.7	-4.2	Browser
9	Phase 1	1003	Iron Age (2,000-500 BP)	*Philantomba monticola*	-12.4	-3.4	Browser
10	Phase 1	1003	Iron Age (2,000-500 BP)	*Philantomba monticola*	-15.5	-8.1	Browser
11	Phase 1	1004	Iron Age (2,000-500 BP)	*Philantomba monticola*	-12.7	-3.7	Browser
12	Phase 1	1004	Iron Age (2,000-500 BP)	*Philantomba monticola*	-11.7	-3.9	Browser
13	Phase 1	1004	Iron Age (2,000-500 BP)	*Philantomba monticola*	-11.8	-3.7	Browser
14	Phase 1	1004	Iron Age (2,000-500 BP)	*Philantomba monticola*	-11.9	-3.8	Browser
15	Phase 4	1025	Sterile (>20,000 BP)	*Philantomba monticola*	-11.0	-3.5	Browser
16	Phase 4	1025	Sterile (>20,000 BP)	*Philantomba monticola*	-11.2	-4.0	Browser
17	Phase 2	1017	Terminal Pleistocene (13,040-11,340 BP)	*Equus quagga*	-4.3	-3.1	Grazer
18	Phase 2	1017	Terminal Pleistocene (13,040-11,340 BP)	*Equus quagga*	-8.2	-4.2	Grazer
19	Phase 3	1018	Late Pleistocene (18,830-17,080 BP)	*Equus quagga*	-2.0	-1.8	Grazer
20	Phase 3	1018	Late Pleistocene (18,830-17,080 BP)	*Equus quagga*	-2.6	-1.2	Grazer
21	Phase 3	1018	Late Pleistocene (18,830-17,080 BP)	*Equus quagga*	-3.5	-1.4	Grazer
22	Phase 3	1019	Late Pleistocene (18,830-17,080 BP)	*Equus quagga*	-4.1	-2.0	Grazer
23	Phase 3	1019	Late Pleistocene (18,830-17,080 BP)	*Equus quagga*	-3.8	-1.9	Grazer
24	Phase 4	1025	Sterile (>20,000 BP)	*Equus quagga*	-4.0	-3.7	Grazer
25	Phase 4	1025	Sterile (>20,000 BP)	*Equus quagga*	-2.0	-2.9	Grazer

	Phase	Context	Age	Taxon	$\delta^{13}C$	$\delta^{18}O$	Diet
26	Phase 1	1002	Iron Age (2,000-500 BP)	*Neotragus moschatus*	-17.4	-10.0	Browser
27	Phase 1	1002	Iron Age (2,000-500 BP)	*Neotragus moschatus*	-11.0	-2.9	Browser
28	Phase 1	1003	Iron Age (2,000-500 BP)	*Neotragus moschatus*	-13.0	-5.1	Browser
29	Phase 1	1003	Iron Age (2,000-500 BP)	*Neotragus moschatus*	-15.3	-6.2	Browser
30	Phase 1	1007	Iron Age (2,000-500 BP)	*Neotragus moschatus*	-12.7	-4.2	Browser
31	Phase 1	1007	Iron Age (2,000-500 BP)	*Neotragus moschatus*	-12.4	-5.0	Browser
32	Phase 1	1011	Iron Age (2,000-500 BP)	*Neotragus moschatus*	-13.0	-3.5	Browser
33	Phase 1	1011	Iron Age (2,000-500 BP)	*Neotragus moschatus*	-13.1	-3.5	Browser
34	Phase 1	1011	Iron Age (2,000-500 BP)	*Neotragus moschatus*	-11.3	-4.6	Browser
35	Phase 1	1011	Iron Age (2,000-500 BP)	*Neotragus moschatus*	-14.1	-5.9	Browser
36	Phase 1	1011	Iron Age (2,000-500 BP)	*Neotragus moschatus*	-12.3	-3.7	Browser
37	Phase 2	1015	Terminal Pleistocene (13,040-11,340 BP)	*Neotragus moschatus*	-14.8	-3.3	Browser
38	Phase 2	1016	Terminal Pleistocene (13,040-11,340 BP)	*Neotragus moschatus*	-13.0	-4.0	Browser
39	Phase 2	1017	Terminal Pleistocene (13,040-11,340 BP)	*Neotragus moschatus*	-11.5	-3.0	Browser
40	Phase 3	1018	Late Pleistocene (18,830-17,080 BP)	*Neotragus moschatus*	-12.1	-0.9	Browser
41	Phase 3	1018	Late Pleistocene (18,830-17,080 BP)	*Neotragus moschatus*	-10.9	-3.7	Browser
42	Phase 3	1018	Late Pleistocene (18,830-17,080 BP)	*Neotragus moschatus*	-12.7	-5.8	Browser
43	Phase 3	1018	Late Pleistocene (18,830-17,080 BP)	*Neotragus moschatus*	-13.3	-6.0	Browser
44	Phase 3	1024	Late Pleistocene (18,830-17,080 BP)	*Neotragus moschatus*	-12.3	-3.7	Browser
45	Phase 3	1024	Late Pleistocene (18,830-17,080 BP)	*Neotragus moschatus*	-12.1	-3.8	Browser
46	Phase 3	1024	Late Pleistocene (18,830-17,080 BP)	*Neotragus moschatus*	-11.8	-4.6	Browser
47	Phase 3	1024	Late Pleistocene (18,830-17,080 BP)	*Neotragus moschatus*	-11.9	-3.8	Browser
48	Phase 3	1024	Late Pleistocene (18,830-17,080 BP)	*Neotragus moschatus*	-12.4	-3.1	Browser
49	Phase 3	1024	Late Pleistocene (18,830-17,080 BP)	*Neotragus moschatus*	-12.4	-3.5	Browser
50	Phase 4	1025	Sterile (>20,000 BP)	*Neotragus moschatus*	-12.3	-2.8	Browser
51	Phase 4	1025	Sterile (>20,000 BP)	*Neotragus moschatus*	-12.0	-3.7	Browser
52	Phase 3	1019	Late Pleistocene (18,830-17,080 BP)	*Redunca redunca*	-4.6	-2.1	Grazer

	Phase	Context	Age	Taxon	$\delta^{13}C$	$\delta^{18}O$	Diet
53	Phase 3	1019	Late Pleistocene (18,830-17,080 BP)	*Redunca redunca*	-5.5	-3.6	Grazer
54	Phase 3	1019	Late Pleistocene (18,830-17,080 BP)	*Redunca redunca*	-1.9	-1.9	Grazer
55	Phase 3	1019	Late Pleistocene (18,830-17,080 BP)	*Redunca redunca*	-3.5	-0.7	Grazer
56	Phase 3	1019	Late Pleistocene (18,830-17,080 BP)	*Redunca redunca*	-2.9	-2.4	Grazer
57	Phase 3	1022	Late Pleistocene (18,830-17,080 BP)	*Redunca redunca*	-4.8	-2.3	Grazer

Table A2:5 *Caprine (sheep) collagen* $\delta^{13}C$ *and* $\delta^{15}N$ *values from Enkapune Ya Muto. Samples were identified using morphology and isotope values (Ambrose and DeNiro, 1989; Marean, 1992a).*

	Site	**Taxon**	**$\delta^{15}N$**	**$\delta^{13}C$**
1	Enkapune ya Muto	*Ovis aries*	11	-7.1
2	Enkapune ya Muto	*Ovis aries*	10.3	-10.3
3	Enkapune ya Muto	*Ovis aries*	8.3	-5.6
4	Enkapune ya Muto	*Ovis aries*	10.1	-6.8
5	Enkapune ya Muto	*Ovis aries*	7.6	-6.4
6	Enkapune ya Muto	*Ovis aries*	5.8	-8.6

Table A2:6 *Caprine enamel $\delta^{13}C$ and $\delta^{18}O$ values from the Turkana Basin (Dongodien) and Victoria Basin (Gogo Falls and Wadh Lang'o. Note: Caprines not identified to species. Age, taxon and isotopes data are from Chritz et al (2019).*

	Site	**Age**	**Taxon**	$\delta^{13}C$	$\delta^{18}O$
1	Dongodien	3950 BP	Caprini	-4.5	6.0
2	Dongodien	3950 BP	Caprini	-1.4	1.8
3	Dongodien	3950 BP	Caprini	-7.9	3.2
4	Dongodien	3950 BP	Caprini	-7.5	1.5
5	Dongodien	3950 BP	Caprini	-6.8	5.2
6	Dongodien	3950 BP	Caprini	-5.5	4.7
7	Dongodien	3950 BP	Caprini	-5.3	4.8
8	Dongodien	3950 BP	Caprini	-4.8	5.1
9	Dongodien	3950 BP	Caprini	-4.5	6.0
10	Dongodien	3950 BP	Caprini	-3.7	2.1
11	Dongodien	3950 BP	Caprini	-3.4	4.9
12	Dongodien	3950 BP	Caprini	-3.1	4.4
13	Dongodien	3950 BP	Caprini	-2.9	6.7
14	Dongodien	3950 BP	Caprini	-2.3	4.6
15	Dongodien	3950 BP	Caprini	-2.1	5.1
16	Dongodien	3950 BP	Caprini	-1.6	4.6
17	Dongodien	3950 BP	Caprini	-1.5	5.8
18	Dongodien	3950 BP	Caprini	0.0	4.1
19	Dongodien	3950 BP	Caprini	0.1	3.6
20	Dongodien	3950 BP	Caprini	-5.9	4.4
21	Dongodien	3950 BP	Caprini	-5.4	2.4
22	Gogo Falls	1700 BP	Caprini	-2.1	-0.6
23	Gogo Falls	1700 BP	Caprini	-2.0	1.6
24	Gogo Falls	1700 BP	Caprini	-0.9	3.2
25	Gogo Falls	1700 BP	Caprini	-0.7	-2.8
26	Gogo Falls	1700 BP	Caprini	-0.4	2.0

	Site	Age	Taxon	$\delta^{13}C$	$\delta^{18}O$
27	Gogo Falls	1700 BP	Caprini	0.2	1.9
28	Gogo Falls	1700 BP	Caprini	0.4	3.3
29	Gogo Falls	1700 BP	Caprini	0.5	4.3
30	Gogo Falls	1700 BP	Caprini	0.5	3.8
31	Gogo Falls	1700 BP	Caprini	0.7	1.6
32	Gogo Falls	1700 BP	Caprini	0.9	0.7
33	Gogo Falls	1700 BP	Caprini	1.7	1.3
34	Gogo Falls	1700 BP	Caprini	2.2	3.0
35	Gogo Falls	1700 BP	Caprini	2.6	2.9
36	Wadh Lang'o	1300 BP	Caprini	1.6	4.1
37	Wadh Lang'o	1300 BP	Caprini	3.1	4.7
38	Wadh Lang'o	1300 BP	Caprini	-1.4	0.1
39	Wadh Lang'o	1300 BP	Caprini	-0.5	4.3
40	Wadh Lang'o	1300 BP	Caprini	-0.3	1.7
41	Wadh Lang'o	1300 BP	Caprini	-0.2	2.0
42	Wadh Lang'o	1300 BP	Caprini	1.1	2.6
43	Wadh Lang'o	1300 BP	Caprini	1.7	3.9
44	Wadh Lang'o	1300 BP	Caprini	2.1	4.1
45	Wadh Lang'o	1300 BP	Caprini	2.2	-2.4
46	Wadh Lang'o	1300 BP	Caprini	2.2	-0.3
47	Wadh Lang'o	1300 BP	Caprini	2.8	5.4
48	Wadh Lang'o	1300 BP	Caprini	4.0	5.0
49	Wadh Lang'o	1800 BP	Caprini	0.1	1.6
50	Wadh Lang'o	1800 BP	Caprini	2.7	1.1
51	Wadh Lang'o	1800 BP	Caprini	-0.7	2.1
52	Wadh Lang'o	1800 BP	Caprini	-0.1	0.1
53	Wadh Lang'o	1800 BP	Caprini	2.0	3.7
54	Wadh Lang'o	1800 BP	Caprini	-2.2	4.2

Table A2:7 *Published caprine enamel $\delta^{13}C$ values from Luxmanda include the minimum, mean, and maximum values from sequential samples. I use the mean values to represent bulk samples in my discussions. Note: $\delta^{18}O$ values are not included here as they are not published. Integrated caprine identifications combine isotopically informed, ZooMS, and morphological identifications (Prendergast et al., 2019a).*

Code Number	**$\delta^{13}C$ values**			**Taxon identifications**
	Min	**Mean**	**Max**	**Integrated (isotopic, ZooMS, and morphology)**
LUXoc1M3	0.7	1.7	3.0	*Ovis aries*
LUXoc2M3	0.9	1.8	2.8	*Ovis aries*
LUXoc3M3	1.6	2.1	3.8	*Ovis aries*
LUXoc4M3	0.3	1.3	2.3	*Ovis aries*
LUXoc5M3	-1.5	0.0	1.4	*Ovis aries*
LUXoc6M3	0.1	0.8	2.5	*Ovis aries*
LUXoc8M3	0.8	2.1	3.3	*Ovis aries*
LUXoc9M3	-0.7	0.4	3.1	*Ovis aries*
LUXoc10M3	-1.2	0.1	2.0	*Ovis aries*
LUXoc11M3	1.1	1.7	2.6	*Ovis aries*
LUXoc12M3	1.5	2.6	3.3	*Ovis aries*
LUXoc13M3	0.6	1.9	3.1	*Ovis aries*
LUXoc14M3	2.1	3.1	3.9	*Ovis aries*
LUXoc15M3	-0.2	1.3	2.4	*Ovis aries*
LUXoc16M3	-1.2	-0.2	0.8	*Ovis aries*
LUXoc7M3	-4.6	-2.8	-0.8	*Capra hircus*
LUXoc17M1	1.6	1.9	2.3	*Capra hircus*
LUXoc18M1	-6.0	-5.2	-3.8	*Capra hircus*
LUXoc19M3	-1.7	-1.3	-0.9	*Capra hircus*
LUXoc20M3	-5.0	-2.9	-0.7	*Capra hircus*

Appendix 3 – Tables associated with "Chapter 7 – The *Wanyika* scientific dates case study"

Table A3:1 Wanyika dataset of scientific dates from archaeological sites in eastern Africa (Abridged version) (Iminjili et al., 2025a; Iminjili et al., 2025b).

Entry ID	Site Name	Country	Latitude	Longitude	Date Type	Date BP	Date BP SD	Min Chronology (Calibrated BCE/CE)	Max Chronology (Calibrated BCE/CE)	Mean Chronology (Calibrated BCE/CE)	Min Chronology (Calibrated BP - 1950)	Max Chronology (Calibrated BP - 1950)	Mean Chronology (Calibrated BP - 1950)
1	Kabusanze	Rwanda	-2.7	29.6	c14	1610	26	417	543	480	1533	1407	1470
2	Kabusanze	Rwanda	-2.7	29.6	c14	1630	26	411	538	475	1539	1412	1476
3	Kabusanze	Rwanda	-2.7	29.6	c14	1694	37	251	524	388	1699	1426	1563
4	Masangano	Rwanda	-1.7	29.9	c14	1698	27	256	427	342	1694	1523	1609
5	Karama	Rwanda	-1.9	29.8	c14	1291	25	668	845	757	1282	1105	1194
6	Musanze 2	Rwanda	-1.5	29.7	c14	956	26	1031	1177	1104	919	773	846
7	Musanze 3	Rwanda	-1.6	29.8	c14	996	25	1020	1154	1087	930	796	863
8	Nguri Cave	Rwanda	-1.4	29.7	c14	956	26	1030	1177	1104	920	773	847
9	Mweru	Rwanda	-1.4	29.7	c14	951	25	1033	1177	1105	917	773	845
10	Mweru	Rwanda	-1.4	29.7	c14	940	26	1035	1205	1120	915	745	830
11	Kabuye I	Rwanda	-2.4	29.5	c14	1595	30	419	569	494	1531	1381	1456
12	Kabuye II	Rwanda	-2.4	29.5	c14	1406	36	595	770	683	1355	1180	1268
13	Kabuye III	Rwanda	-2.4	29.5	c14	1660	30	354	533	444	1596	1417	1507
14	Kabuye IV	Rwanda	-2.4	29.5	c14	1726	30	251	415	333	1699	1535	1617
15	Mutwarubona I	Rwanda	-2.4	29.5	c14	2020	330	-815	657	-79	2765	1293	2029
16	Mutwarubona II	Rwanda	-2.4	29.5	c14	1380	170	263	1024	644	1687	926	1307

Entry ID	Site Name	Country	Latitude	Longitude	Date Type	Date BP	Date BP SD	Min Chronology (Calibrated BCE/CE)	Max Chronology (Calibrated BCE/CE)	Mean Chronology (Calibrated BCE/CE)	Min Chronology (Calibrated BP - 1950)	Max Chronology (Calibrated BP - 1950)	Mean Chronology (Calibrated BP - 1950)
17	Mutara 1	Rwanda	-1.7	30.2	c14	2180	50	-366	-57	-212	2316	2007	2162
18	Mutara 2	Rwanda	-1.7	30.2	c14	1655	60	254	573	414	1696	1377	1537
19	Ndora	Rwanda	-2.3	29.5	c14	1700	100	133	588	361	1817	1362	1590
20	Cyamakuza	Rwanda	-2.3	29.5	c14	1650	80	248	590	419	1702	1360	1531
21	Chombo	Kenya	-4.1	39.3	c14	1180	60	692	1017	855	1258	933	1096
22	Early Mombasa	Kenya	-4.1	39.7	c14	1000	95	884	1265	1075	1066	685	876
23	Early Mombasa	Kenya	-4.1	39.7	c14	1040	90	775	1219	997	1175	731	953
24	Early Mombasa	Kenya	-4.1	39.7	c14	980	60	992	1214	1103	958	736	847
25	Early Mombasa	Kenya	-4.1	39.7	c14	1040	100	774	1221	998	1176	729	953
26	Early Mombasa	Kenya	-4.1	39.7	c14	895	90	995	1286	1141	955	664	810
27	Galu	Kenya	-4.4	39.6	c14	1400	240	130	1155	643	1820	795	1308
28	Galu	Kenya	-4.4	39.6	c14	740	70	1183	1400	1292	767	550	659
29	Galu	Kenya	-4.4	39.6	c14	1300	70	641	954	798	1309	996	1153
30	Kwale	Kenya	-4.2	39.5	c14	1680	110	131	635	383	1819	1315	1567
31	Kwale	Kenya	-4.2	39.5	c14	1690	110	128	601	365	1822	1349	1586
32	Kwale Forest	Kenya	-4.2	39.5	c14	1830	115	-49	526	239	1999	1424	1712
33	Kwale Ditch	Kenya	-4.2	39.5	c14	1790	115	-36	541	253	1986	1409	1698
34	Mteza	Kenya	-4.1	39.3	c14	1190	50	707	993	850	1243	957	1100
35	Ungwana	Kenya	-2.5	40.5	c14	870	100	994	1381	1188	956	569	763
36	Ungwana	Kenya	-2.5	40.5	c14	1210	140	601	1153	877	1349	797	1073
37	Ungwana	Kenya	-2.5	40.5	c14	530	90	1285	1627	1456	665	323	494

Entry ID	Site Name	Country	Latitude	Longitude	Date Type	Date BP	Date BP SD	Min Chronology (Calibrated BCE/CE)	Max Chronology (Calibrated BCE/CE)	Mean Chronology (Calibrated BCE/CE)	Min Chronology (Calibrated BP - 1950)	Max Chronology (Calibrated BP - 1950)	Mean Chronology (Calibrated BP - 1950)
38	Ungwana	Kenya	-2.5	40.5	c14	1360	650	-920	1811	446	2870	139	1505
39	Panga ya Saidi	Kenya	-3.7	39.7	c14	1212	23	771	955	863	1179	995	1087
40	Panga ya Saidi	Kenya	-3.7	39.7	c14	522	25	1403	1449	1426	547	501	524
41	Panga ya Saidi	Kenya	-3.7	39.7	c14	536	24	1396	1448	1422	554	502	528
42	Panga ya Saidi	Kenya	-3.7	39.7	c14	388	27	1452	1629	1541	498	321	410
43	Mgombani	Kenya	-3.8	39.7	c14	1184	26	773	975	874	1177	975	1076
44	Mgombani	Kenya	-3.8	39.7	c14	1179	25	773	984	879	1177	966	1072
45	Mgombani	Kenya	-3.8	39.7	c14	1217	29	708	960	834	1242	990	1116
46	Mgombani	Kenya	-3.8	39.7	c14	1300	50	659	876	768	1291	1074	1183
47	Mbuyuni	Kenya	-3.6	39.3	c14	350	50	1457	1649	1553	493	301	397
48	Mtsengo	Kenya	-3.4	39.4	c14	580	50	1300	1444	1372	650	506	578
49	Mtsengo	Kenya	-3.4	39.4	c14	448	20	1430	1495	1463	520	455	488
50	Shanga	Kenya	-2.1	41.1	c14	1175	30	773	988	881	1177	962	1070
51	Shanga	Kenya	-2.1	41.1	c14	980	30	1023	1158	1091	927	792	860
52	Shanga	Kenya	-2.1	41.1	c14	830	30	1181	1278	1230	769	672	721
53	Shanga	Kenya	-2.1	41.1	c14	1160	30	774	992	883	1176	958	1067
54	Shanga	Kenya	-2.1	41.1	c14	680	30	1280	1394	1337	670	556	613
55	Shanga	Kenya	-2.1	41.1	c14	1120	30	888	1018	953	1062	932	997
56	Shanga	Kenya	-2.1	41.1	c14	870	30	1055	1270	1163	895	680	788
57	Shanga	Kenya	-2.1	41.1	c14	1235	35	683	953	818	1267	997	1132
58	Shanga	Kenya	-2.1	41.1	c14	1180	40	774	986	880	1176	964	1070

Entry ID	Site Name	Country	Latitude	Longitude	Date Type	Date BP	Date BP SD	Min Chronology (Calibrated BCE/CE)	Max Chronology (Calibrated BCE/CE)	Mean Chronology (Calibrated BCE/CE)	Min Chronology (Calibrated BP - 1950)	Max Chronology (Calibrated BP - 1950)	Mean Chronology (Calibrated BP - 1950)
59	Shanga	Kenya	-2.1	41.1	c14	1170	45	774	992	883	1176	958	1067
60	Shanga	Kenya	-2.1	41.1	c14	1100	50	775	1109	942	1175	841	1008
61	Shanga	Kenya	-2.1	41.1	c14	1060	45	893	1148	1021	1057	802	930
62	Shanga	Kenya	-2.1	41.1	c14	985	35	997	1164	1081	953	786	870
63	Shanga	Kenya	-2.1	41.1	c14	1175	30	774	988	881	1176	962	1069
64	Shanga	Kenya	-2.1	41.1	c14	1160	30	774	992	883	1176	958	1067
65	Shanga	Kenya	-2.1	41.1	c14	1120	30	888	1018	953	1062	932	997
66	Manda	Kenya	-2.3	40.9	c14	1170	110	661	1142	902	1289	808	1049
67	Manda	Kenya	-2.3	40.9	c14	1480	110	359	836	598	1591	1114	1353
68	Manda	Kenya	-2.3	40.9	c14	1240	100	649	1017	833	1301	933	1117
69	Mtwapa	Kenya	-4.0	39.7	c14	610	70	1284	1440	1362	666	510	588
70	Mtwapa	Kenya	-4.0	39.7	c14	610	70	1284	1440	1362	666	510	588
71	Mtwapa	Kenya	-4.0	39.7	c14	630	70	1278	1434	1356	672	516	594
72	Mtwapa	Kenya	-4.0	39.7	c14	650	70	1270	1431	1351	680	519	600
73	Mtwapa	Kenya	-4.0	39.7	c14	2850	70	-1204	-829	-1017	3154	2779	2967
74	Mtwapa	Kenya	-4.0	39.7	c14	3740	70	-2394	-1901	-2148	4344	3851	4098
75	Mtwapa	Kenya	-4.0	39.7	c14	480	70	1322	1631	1477	628	319	474
76	Mtwapa	Kenya	-4.0	39.7	c14	480	70	1322	1631	1477	628	319	474
77	Mtwapa	Kenya	-4.0	39.7	c14	480	70	1321	1632	1477	629	318	474
78	Mtwapa	Kenya	-4.0	39.7	c14	480	70	1321	1632	1477	629	318	474
79	Mtwapa	Kenya	-4.0	39.7	c14	490	70	1316	1630	1473	634	320	477

Entry ID	Site Name	Country	Latitude	Longitude	Date Type	Date BP	Date BP SD	Min Chronology (Calibrated BCE/CE)	Max Chronology (Calibrated BCE/CE)	Mean Chronology (Calibrated BCE/CE)	Min Chronology (Calibrated BP - 1950)	Max Chronology (Calibrated BP - 1950)	Mean Chronology (Calibrated BP - 1950)
80	Mtwapa	Kenya	-4.0	39.7	c14	500	70	1305	1627	1466	645	323	484
81	Mtwapa	Kenya	-4.0	39.7	c14	510	70	1300	1624	1462	650	326	488
82	Mtwapa	Kenya	-4.0	39.7	c14	340	70	1440	1800	1620	510	150	330
83	Mtwapa	Kenya	-4.0	39.7	c14	340	70	1440	1800	1620	510	150	330
84	Mtwapa	Kenya	-4.0	39.7	c14	350	70	1436	1798	1617	514	152	333
85	Mtwapa	Kenya	-4.0	39.7	c14	360	70	1435	1795	1615	515	155	335
86	Mtwapa	Kenya	-4.0	39.7	c14	360	70	1433	1795	1614	517	155	336
87	Mtwapa	Kenya	-4.0	39.7	c14	370	70	1431	1665	1548	519	285	402
88	Gedi Ruins	Kenya	-3.3	40.0	c14	845	45	1053	1282	1168	897	668	783
89	Lothagam North	Kenya	2.9	36.1	c14	4280	15	-2911	-2877	-2894	4861	4827	4844
90	Lothagam North	Kenya	2.9	36.1	c14	4135	20	-2865	-2577	-2721	4815	4527	4671
91	Lothagam North	Kenya	2.9	36.1	c14	3845	20	-2404	-2149	-2277	4354	4099	4227
92	Lothagam North	Kenya	2.9	36.1	c14	4140	20	-2866	-2580	-2723	4816	4530	4673
93	Lothagam North	Kenya	2.9	36.1	c14	4265	15	-2908	-2782	-2845	4858	4732	4795
94	Lothagam North	Kenya	2.9	36.1	c14	4165	20	-2874	-2628	-2751	4824	4578	4701
95	Lothagam North	Kenya	2.9	36.1	c14	4385	15	-3075	-2911	-2993	5025	4861	4943
96	Lothagam North	Kenya	2.9	36.1	c14	4240	20	-2901	-2701	-2801	4851	4651	4751
97	Lothagam West	Kenya	2.8	36.0	c14	4290	20	-2916	-2878	-2897	4866	4828	4847
98	Jarigole	Kenya	3.6	36.3	c14	4275	15	-2911	-2874	-2893	4861	4824	4843
99	Jarigole	Kenya	3.6	36.3	c14	4215	15	-2890	-2696	-2793	4840	4646	4743
100	Jarigole	Kenya	3.6	36.3	c14	4185	15	-2880	-2639	-2760	4830	4589	4710

Entry ID	Site Name	Country	Latitude	Longitude	Date Type	Date BP	Date BP SD	Min Chronology (Calibrated BCE/CE)	Max Chronology (Calibrated BCE/CE)	Mean Chronology (Calibrated BCE/CE)	Min Chronology (Calibrated BP - 1950)	Max Chronology (Calibrated BP - 1950)	Mean Chronology (Calibrated BP - 1950)
101	Jarigole	Kenya	3.6	36.3	c14	4165	15	-2872	-2630	-2751	4822	4580	4701
102	Jarigole	Kenya	3.6	36.3	c14	4130	15	-2858	-2577	-2718	4808	4527	4668
103	Jarigole	Kenya	3.6	36.3	c14	4401	39	-3311	-2901	-3106	5261	4851	5056
104	Jarigole	Kenya	3.6	36.3	c14	4381	39	-3096	-2896	-2996	5046	4846	4946
105	Jarigole	Kenya	3.6	36.3	c14	4251	39	-2916	-2671	-2794	4866	4621	4744
106	Jarigole	Kenya	3.6	36.3	c14	4146	53	-2881	-2501	-2691	4831	4451	4641
107	Kalakol	Kenya	3.5	35.9	c14	3890	15	-2460	-2238	-2349	4410	4188	4299
108	Manemanya	Kenya	3.6	35.9	c14	4255	20	-2907	-2706	-2807	4857	4656	4757
109	Manemanya	Kenya	3.6	35.9	c14	3805	15	-2289	-2142	-2216	4239	4092	4166
110	Il Lokeridede	Kenya	3.9	36.3	c14	4180	60	-2891	-2577	-2734	4841	4527	4684
111	Aliel	Kenya	2.7	36.1	c14	4490	30	-3341	-3026	-3184	5291	4976	5134
112	Abalete Akoit A	Kenya	4.3	35.9	c14	3370	190	-2198	-1133	-1666	4148	3083	3616
113	Abalete Akoit A	Kenya	4.3	35.9	c14	3160	40	-1501	-1292	-1397	3451	3242	3347
114	Kaerdit	Kenya	4.3	35.9	c14	1365	25	645	774	710	1305	1176	1241
115	Enkapune ya Moto	Kenya	-0.5	36.1	c14	1295	140	440	1033	737	1510	917	1214
116	Enkapune ya Moto	Kenya	-0.5	36.1	c14	500	145	1226	1803	1515	724	147	436
117	Enkapune ya Moto	Kenya	-0.5	36.1	c14	2355	170	-815	15	-400	2765	1935	2350
118	Enkapune ya Moto	Kenya	-0.5	36.1	c14	2595	175	-1194	-206	-700	3144	2156	2650
119	Enkapune ya Moto	Kenya	-0.5	36.1	c14	2570	175	-1116	-201	-659	3066	2151	2609
120	Enkapune ya Moto	Kenya	-0.5	36.1	c14	2610	70	-906	-482	-694	2856	2432	2644
121	Enkapune ya Moto	Kenya	-0.5	36.1	c14	2820	70	-1191	-809	-1000	3141	2759	2950

Entry ID	Site Name	Country	Latitude	Longitude	Date Type	Date BP	Date BP SD	Min Chronology (Calibrated BCE/CE)	Max Chronology (Calibrated BCE/CE)	Mean Chronology (Calibrated BCE/CE)	Min Chronology (Calibrated BP - 1950)	Max Chronology (Calibrated BP - 1950)	Mean Chronology (Calibrated BP - 1950)
122	Enkapune ya Moto	Kenya	-0.5	36.1	c14	2330	235	-928	204	-362	2878	1746	2312
123	Enkapune ya Moto	Kenya	-0.5	36.1	c14	2560	70	-812	-418	-615	2762	2368	2565
124	Enkapune ya Moto	Kenya	-0.5	36.1	c14	2860	70	-1211	-834	-1023	3161	2784	2973
125	Enkapune ya Moto	Kenya	-0.5	36.1	c14	2710	80	-1077	-570	-824	3027	2520	2774
126	Enkapune ya Moto	Kenya	-0.5	36.1	c14	3280	190	-2033	-1046	-1540	3983	2996	3490
127	Enkapune ya Moto	Kenya	-0.5	36.1	c14	3390	70	-1879	-1501	-1690	3829	3451	3640
128	Enkapune ya Moto	Kenya	-0.5	36.1	c14	3125	185	-1873	-900	-1387	3823	2850	3337
129	Enkapune ya Moto	Kenya	-0.5	36.1	c14	3110	70	-1502	-1128	-1315	3452	3078	3265
130	Enkapune ya Moto	Kenya	-0.5	36.1	c14	3030	70	-1424	-1024	-1224	3374	2974	3174
131	Enkapune ya Moto	Kenya	-0.5	36.1	c14	3990	70	-2846	-2208	-2527	4796	4158	4477
132	Enkapune ya Moto	Kenya	-0.5	36.1	c14	4475	210	-3641	-2581	-3111	5591	4531	5061
133	Enkapune ya Moto	Kenya	-0.5	36.1	c14	4535	170	-3645	-2708	-3177	5595	4658	5127
134	Enkapune ya Moto	Kenya	-0.5	36.1	c14	4860	70	-3785	-3379	-3582	5735	5329	5532
135	Ele Bor	Kenya	3.3	37.7	c14	599	37	1301	1427	1364	649	523	586
136	Ele Bor	Kenya	3.3	37.7	c14	1351	46	607	833	720	1343	1117	1230
137	Ele Bor	Kenya	3.3	37.7	c14	1591	68	361	639	500	1589	1311	1450
138	Ele Bor	Kenya	3.3	37.7	c14	3758	168	-2625	-1687	-2156	4575	3637	4106
139	Ele Bor	Kenya	3.3	37.7	c14	4199	240	-3496	-2062	-2779	5446	4012	4729
140	Dongodien	Kenya	3.9	36.3	c14	4100	125	-2921	-2233	-2577	4871	4183	4527
141	Dongodien	Kenya	3.9	36.3	c14	3960	60	-2618	-2207	-2413	4568	4157	4363
142	Dongodien	Kenya	3.9	36.3	c14	3945	135	-2870	-2038	-2454	4820	3988	4404

Entry ID	Site Name	Country	Latitude	Longitude	Date Type	Date BP	Date BP SD	Min Chronology (Calibrated BCE/CE)	Max Chronology (Calibrated BCE/CE)	Mean Chronology (Calibrated BCE/CE)	Min Chronology (Calibrated BP - 1950)	Max Chronology (Calibrated BP - 1950)	Mean Chronology (Calibrated BP - 1950)
143	Dongodien	Kenya	3.9	36.3	c14	4180	40	-2886	-2586	-2736	4836	4536	4686
144	Dongodien	Kenya	3.9	36.3	c14	4180	53	-2888	-2581	-2735	4838	4531	4685
145	Dongodien	Kenya	3.9	36.3	c14	4240	40	-2912	-2637	-2775	4862	4587	4725
146	Dongodien	Kenya	3.9	36.3	c14	4180	40	-2886	-2585	-2736	4836	4535	4686
147	Dongodien	Kenya	3.9	36.3	c14	3970	60	-2623	-2210	-2417	4573	4160	4367
148	Dongodien	Kenya	3.9	36.3	c14	4160	110	-3014	-2455	-2735	4964	4405	4685
149	Dongodien	Kenya	3.9	36.3	OSL	2650	180	-999	-279	-639	2949	2229	2589
150	Dongodien	Kenya	3.9	36.3	OSL	4040	270	-2569	-1489	-2029	4519	3439	3979
151	Dongodien	Kenya	3.9	36.3	c14	4560	185	-3706	-2703	-3205	5656	4653	5155
152	Dongodien	Kenya	3.9	36.3	c14	3405	130	-2031	-1411	-1721	3981	3361	3671
153	Dongodien	Kenya	3.9	36.3	c14	4580	170	-3697	-2881	-3289	5647	4831	5239
154	Dongodien	Kenya	3.9	36.3	c14	3125	210	-1878	-835	-1357	3828	2785	3307
155	FwJj 25	Kenya	4.1	36.3	OSL	4200	280	-2749	-1629	-2189	4699	3579	4139
156	FwJj 25	Kenya	4.1	36.3	OSL	1340	300	71	1271	671	1879	679	1279
157	FwJj 5	Kenya	4.3	36.3	OSL	900	60	991	1231	1111	959	719	839
158	FwJj 27	Kenya	4.3	36.3	OSL	4300	270	-2829	-1749	-2289	4779	3699	4239
159	FwJj 27	Kenya	4.3	36.3	OSL	903	140	828	1388	1108	1122	562	842
160	FxJj 12-N	Kenya	4.1	36.3	c14	3245	155	-1897	-1056	-1477	3847	3006	3427
161	Ileret	Kenya	4.3	36.2	c14	4000	140	-2890	-2067	-2479	4840	4017	4429
162	Ileret	Kenya	4.3	36.2	c14	3405	130	-2031	-1410	-1721	3981	3360	3671
163	Ileret	Kenya	4.3	36.2	c14	4540	230	-3611	-2199	-2905	5561	4149	4855

Entry ID	Site Name	Country	Latitude	Longitude	Date Type	Date BP	Date BP SD	Min Chronology (Calibrated BCE/CE)	Max Chronology (Calibrated BCE/CE)	Mean Chronology (Calibrated BCE/CE)	Min Chronology (Calibrated BP - 1950)	Max Chronology (Calibrated BP - 1950)	Mean Chronology (Calibrated BP - 1950)
164	Ileret	Kenya	4.3	36.2	c14	4580	170	-3696	-2881	-3289	5646	4831	5239
165	Kangatotha	Kenya	3.1	35.9	c14	5020	220	-4339	-3356	-3848	6289	5306	5798
166	Baawa I	Kenya	1.0	36.7	c14	2700	40	-916	-791	-854	2866	2741	2804
167	Baawa II	Kenya	1.1	36.7	c14	607	30	1303	1416	1360	647	534	591
168	Maasai Plains	Kenya	0.6	36.6	c14	480	50	1328	1623	1476	622	327	475
169	Mili Sita	Kenya	0.3	36.9	c14	240	40	1517	1948	1733	433	2	218
170	Mili Sita	Kenya	0.3	36.9	c14	170	40	1666	1948	1807	284	2	143
171	Cattle Dip Lolldaiga	Kenya	0.3	36.8	c14	250	50	1502	1948	1725	448	2	225
172	Kulchurdo RS	Kenya	2.3	37.8	c14	1465	70	433	769	601	1517	1181	1349
173	Ololopoli	Kenya	-2.6	37.3	c14	373	29	1458	1632	1545	492	318	405
174	CB HdJn6	Kenya	-2.6	37.3	c14	171	29	1666	1948	1807	284	2	143
175	Nyarindi RS	Kenya	-0.3	34.3	c14	3253	23	-1537	-1432	-1485	3487	3382	3435
176	Molo Cave	Kenya	-0.3	36.1	c14	1532	21	532	637	585	1418	1313	1366
177	Molo Cave	Kenya	-0.3	36.1	c14	2101	22	-168	-46	-107	2118	1996	2057
178	Wadh Lang'o	Kenya	-0.4	34.8	c14	1420	30	592	679	636	1358	1271	1315
179	Wadh Lang'o	Kenya	-0.4	34.8	c14	1280	45	669	881	775	1281	1069	1175
180	Wadh Lang'o	Kenya	-0.4	34.8	c14	1449	28	583	660	622	1367	1290	1329
181	Wadh Lang'o	Kenya	-0.4	34.8	c14	1484	26	563	648	606	1387	1302	1345
182	Wadh Lang'o	Kenya	-0.4	34.8	c14	1741	28	250	406	328	1700	1544	1622
183	Wadh Lang'o	Kenya	-0.4	34.8	c14	1698	28	256	427	342	1694	1523	1609
184	Wadh Lang'o	Kenya	-0.4	34.8	c14	1746	28	248	403	326	1702	1547	1625

Entry ID	Site Name	Country	Latitude	Longitude	Date Type	Date BP	Date BP SD	Min Chronology (Calibrated BCE/CE)	Max Chronology (Calibrated BCE/CE)	Mean Chronology (Calibrated BCE/CE)	Min Chronology (Calibrated BP - 1950)	Max Chronology (Calibrated BP - 1950)	Mean Chronology (Calibrated BP - 1950)
185	Wadh Lang'o	Kenya	-0.4	34.8	c14	1742	27	250	406	328	1700	1544	1622
186	Wadh Lang'o	Kenya	-0.4	34.8	c14	1819	28	135	340	238	1815	1610	1713
187	Wadh Lang'o	Kenya	-0.4	34.8	c14	3850	30	-2454	-2149	-2302	4404	4099	4252
188	Wadh Lang'o	Kenya	-0.4	34.8	c14	3770	35	-2287	-2035	-2161	4237	3985	4111
189	Wadh Lang'o	Kenya	-0.4	34.8	c14	3740	35	-2277	-1981	-2129	4227	3931	4079
190	Wadh Lang'o	Kenya	-0.4	34.8	c14	1989	28	-44	117	37	1994	1833	1914
191	Wadh Lang'o	Kenya	-0.4	34.8	c14	1950	35	-36	204	84	1986	1746	1866
192	Usenge 3	Kenya	-0.1	34.7	c14	1560	40	422	603	513	1528	1347	1438
193	Usenge 3	Kenya	-0.1	34.7	c14	3310	40	-1680	-1451	-1566	3630	3401	3516
194	Usenge 3	Kenya	-0.1	34.7	c14	3240	70	-1683	-1302	-1493	3633	3252	3443
195	Usenge 3	Kenya	-0.1	34.7	c14	170	40	1666	1948	1807	284	2	143
196	Usenge 1	Kenya	-0.1	34.7	c14	160	40	1670	1948	1809	280	2	141
197	Siror	Kenya	0.1	34.2	c14	2905	37	-1209	-933	-1071	3159	2883	3021
198	Siror	Kenya	0.1	34.2	c14	2889	36	-1197	-923	-1060	3147	2873	3010
199	Usare	Kenya	-0.2	34.4	c14	295	30	1503	1794	1649	447	156	302
200	Usare	Kenya	-0.2	34.4	c14	300	30	1502	1791	1647	448	159	304
201	Usare	Kenya	-0.2	34.4	c14	3010	60	-1404	-1024	-1214	3354	2974	3164
202	Okiro	Kenya	-0.2	34.3	c14	289	24	1510	1794	1652	440	156	298
203	Gogo Falls	Kenya	-0.9	34.3	c14	3480	75	-2009	-1542	-1776	3959	3492	3726
204	Gogo Falls	Kenya	-0.9	34.3	OH	3613	115	-1893	-1433	-1663	3843	3383	3613
205	Gogo Falls	Kenya	-0.9	34.3	c14	1900	70	-44	335	146	1994	1615	1805

Entry ID	Site Name	Country	Latitude	Longitude	Date Type	Date BP	Date BP SD	Min Chronology (Calibrated BCE/CE)	Max Chronology (Calibrated BCE/CE)	Mean Chronology (Calibrated BCE/CE)	Min Chronology (Calibrated BP - 1950)	Max Chronology (Calibrated BP - 1950)	Mean Chronology (Calibrated BP - 1950)
206	Gogo Falls	Kenya	-0.9	34.3	c14	1710	70	219	540	380	1731	1410	1571
207	Gogo Falls	Kenya	-0.9	34.3	c14	1770	80	84	526	305	1866	1424	1645
208	Gogo Falls	Kenya	-0.9	34.3	c14	1990	80	-157	231	37	2107	1719	1913
209	Gogo Falls	Kenya	-0.9	34.3	c14	3020	100	-1490	-933	-1212	3440	2883	3162
210	Gogo Falls	Kenya	-0.9	34.3	c14	3170	70	-1602	-1223	-1413	3552	3173	3363
211	Gogo Falls	Kenya	-0.9	34.3	OH	2617	194	-1055	-279	-667	3005	2229	2617
212	Gogo Falls	Kenya	-0.9	34.3	c14	2000	70	-147	207	30	2097	1743	1920
213	Gogo Falls	Kenya	-0.9	34.3	OH	2474	65	-654	-394	-524	2604	2344	2474
214	Gogo Falls	Kenya	-0.9	34.3	OH	2096	93	-332	40	-146	2282	1910	2096
215	Gogo Falls	Kenya	-0.9	34.3	c14	2030	70	-186	202	8	2136	1748	1942
216	Gogo Falls	Kenya	-0.9	34.3	c14	2030	65	-181	201	10	2131	1749	1940
217	Kakapel RS	Kenya	0.7	34.4	c14	3584	28	-2023	-1776	-1900	3973	3726	3850
218	Kakapel RS	Kenya	0.7	34.4	c14	832	21	1185	1275	1230	765	675	720
219	Kakapel RS	Kenya	0.7	34.4	c14	845	21	1180	1270	1225	770	680	725
220	Kakapel RS	Kenya	0.7	34.4	c14	848	16	1180	1269	1225	770	681	726
221	Kakapel RS	Kenya	0.7	34.4	c14	864	21	1161	1266	1214	789	684	737
222	Kakapel RS	Kenya	0.7	34.4	c14	895	28	1046	1261	1154	904	689	797
223	Kakapel RS	Kenya	0.7	34.4	c14	813	15	1221	1274	1248	729	676	703
224	Kakapel RS	Kenya	0.7	34.4	c14	887	18	1155	1225	1190	795	725	760
225	Kakapel RS	Kenya	0.7	34.4	c14	962	18	1036	1156	1096	914	794	854
226	Kakapel RS	Kenya	0.7	34.4	c14	977	18	1029	1154	1092	921	796	859

Entry ID	Site Name	Country	Latitude	Longitude	Date Type	Date BP	Date BP SD	Min Chronology (Calibrated BCE/CE)	Max Chronology (Calibrated BCE/CE)	Mean Chronology (Calibrated BCE/CE)	Min Chronology (Calibrated BP - 1950)	Max Chronology (Calibrated BP - 1950)	Mean Chronology (Calibrated BP - 1950)
227	Kakapel RS	Kenya	0.7	34.4	c14	1713	15	261	413	337	1689	1537	1613
228	Kakapel RS	Kenya	0.7	34.4	c14	2236	18	-375	-190	-283	2325	2140	2233
229	Kakapel RS	Kenya	0.7	34.4	c14	940	18	1041	1181	1111	909	769	839
230	Kakapel RS	Kenya	0.7	34.4	c14	222	29	1643	1948	1796	307	2	155
231	Kakapel RS	Kenya	0.7	34.4	c14	210	15	1660	1805	1733	290	145	218
232	Kakapel RS	Kenya	0.7	34.4	c14	901	18	1052	1220	1136	898	730	814
233	Kakapel RS	Kenya	0.7	34.4	c14	920	20	1045	1216	1131	905	734	820
234	Kakapel RS	Kenya	0.7	34.4	c14	965	25	1029	1160	1095	921	790	856
235	Kakapel RS	Kenya	0.7	34.4	c14	975	15	1030	1154	1092	920	796	858
236	Kakapel RS	Kenya	0.7	34.4	c14	985	20	1025	1153	1089	925	797	861
237	Kakapel RS	Kenya	0.7	34.4	c14	985	15	1026	1153	1090	924	797	861
238	Kakapel RS	Kenya	0.7	34.4	c14	995	20	1021	1153	1087	929	797	863
239	Kakapel RS	Kenya	0.7	34.4	c14	1020	20	992	1144	1068	958	806	882
240	Kakapel RS	Kenya	0.7	34.4	c14	1020	20	992	1144	1068	958	806	882
241	Kakapel RS	Kenya	0.7	34.4	c14	1060	35	895	1137	1016	1055	813	934
242	Kakapel RS	Kenya	0.7	34.4	c14	2235	20	-375	-189	-282	2325	2139	2232
243	Kakapel RS	Kenya	0.7	34.4	c14	2266	29	-392	-195	-294	2342	2145	2244
244	Kakapel RS	Kenya	0.7	34.4	c14	2280	20	-393	-201	-297	2343	2151	2247
245	White Rock	Kenya	-0.5	34.4	c14	4015	260	-3336	-1824	-2580	5286	3774	4530
246	Lanet	Kenya	-0.3	36.1	c14	365	100	1400	1947	1674	550	3	277
247	Hyrax Hill	Kenya	-0.3	36.1	c14	830	100	1025	1390	1208	925	560	743

Entry ID	Site Name	Country	Latitude	Longitude	Date Type	Date BP	Date BP SD	Min Chronology (Calibrated BCE/CE)	Max Chronology (Calibrated BCE/CE)	Mean Chronology (Calibrated BCE/CE)	Min Chronology (Calibrated BP - 1950)	Max Chronology (Calibrated BP - 1950)	Mean Chronology (Calibrated BP - 1950)
248	Hyrax Hill	Kenya	-0.3	36.1	c14	1295	105	600	990	795	1350	960	1155
249	Hyrax Hill	Kenya	-0.3	36.1	c14	1955	125	-346	385	20	2296	1565	1931
250	Hyrax Hill	Kenya	-0.3	36.1	c14	530	120	1272	1646	1459	678	304	491
251	Hyrax Hill	Kenya	-0.3	36.1	c14	490	80	1310	1632	1471	640	318	479
252	Hyrax Hill	Kenya	-0.3	36.1	c14	430	105	1305	1798	1552	645	152	399
253	Hyrax Hill	Kenya	-0.3	36.1	c14	2354	23	-466	-206	-336	2416	2156	2286
254	Deloraine Farm I	Kenya	-0.2	35.8	c14	1070	110	710	1219	965	1240	731	986
255	Deloraine Farm II	Kenya	-0.2	35.8	c14	1150	135	654	1172	913	1296	778	1037
256	Deloraine Farm II	Kenya	-0.2	35.8	c14	1095	150	664	1225	945	1286	725	1006
257	Deloraine Farm II	Kenya	-0.2	35.8	c14	985	130	775	1283	1029	1175	667	921
258	Deloraine Farm II	Kenya	-0.2	35.8	c14	1110	120	678	1182	930	1272	768	1020
259	Deloraine Farm II	Kenya	-0.2	35.8	c14	1000	115	775	1275	1025	1175	675	925
260	Deloraine Farm II	Kenya	-0.2	35.8	c14	1300	140	440	1030	735	1510	920	1215
261	Deloraine Farm II	Kenya	-0.2	35.8	c14	1940	80	-101	328	114	2051	1622	1837
262	Deloraine Farm III	Kenya	-0.2	35.8	c14	350	60	1448	1663	1556	502	287	395
263	Deloraine Farm III	Kenya	-0.2	35.8	c14	1190	70	683	1017	850	1267	933	1100
264	Deloraine Farm III	Kenya	-0.2	35.8	c14	1230	60	676	975	826	1274	975	1125
265	Deloraine Farm IV	Kenya	-0.2	35.8	c14	650	60	1277	1418	1348	673	532	603
266	Deloraine Farm V	Kenya	-0.2	35.8	c14	1160	15	881	988	935	1069	962	1016
267	Ngenyn	Kenya	0.5	36.0	c14	2080	110	-376	202	-87	2326	1748	2037
268	Ngenyn	Kenya	0.5	36.0	c14	1970	150	-361	408	24	2311	1542	1927

Entry ID	Site Name	Country	Latitude	Longitude	Date Type	Date BP	Date BP SD	Min Chronology (Calibrated BCE/CE)	Max Chronology (Calibrated BCE/CE)	Mean Chronology (Calibrated BCE/CE)	Min Chronology (Calibrated BP - 1950)	Max Chronology (Calibrated BP - 1950)	Mean Chronology (Calibrated BP - 1950)
269	Ngenyn	Kenya	0.5	36.0	c14	2020	130	-369	325	-22	2319	1625	1972
270	Maringishu	Kenya	0.0	36.0	c14	1695	105	130	595	363	1820	1355	1588
271	Prolonged Drift	Kenya	-0.5	36.2	c14	2315	150	-787	-2	-395	2737	1952	2345
272	Prolonged Drift	Kenya	-0.5	36.2	c14	2530	160	-1007	-198	-603	2957	2148	2553
273	Prolonged Drift	Kenya	-0.5	36.2	c14	4040	140	-2903	-2146	-2525	4853	4096	4475
274	Prolonged Drift	Kenya	-0.5	36.2	c14	3540	120	-2197	-1536	-1867	4147	3486	3817
275	Prolonged Drift	Kenya	-0.5	36.2	c14	1370	140	425	986	706	1525	964	1245
276	Prolonged Drift	Kenya	-0.5	36.2	c14	1260	160	480	1155	818	1470	795	1133
277	Prolonged Drift	Kenya	-0.5	36.2	c14	2530	160	-1006	-197	-602	2956	2147	2552
278	Prolonged Drift	Kenya	-0.5	36.2	c14	2898	32	-1199	-931	-1065	3149	2881	3015
279	Naivasha C Island I	Kenya	-0.8	36.4	c14	2035	140	-387	324	-32	2337	1626	1982
280	Naivasha C Island I	Kenya	-0.8	36.4	c14	2660	120	-1103	-410	-757	3053	2360	2707
281	Naivasha C Island I	Kenya	-0.8	36.4	c14	2405	150	-820	-107	-464	2770	2057	2414
282	Naivasha C Island I	Kenya	-0.8	36.4	c14	2030	140	-384	328	-28	2334	1622	1978
283	Naivasha C Island I	Kenya	-0.8	36.4	c14	2660	160	-1208	-396	-802	3158	2346	2752
284	Naivasha C Island I	Kenya	-0.8	36.4	c14	2215	120	-731	72	-330	2681	1878	2280
285	Naivasha C Island I	Kenya	-0.8	36.4	c14	2535	140	-976	-208	-592	2926	2158	2542
286	Naivasha C Island I	Kenya	-0.8	36.4	c14	2795	155	-1402	-545	-974	3352	2495	2924
287	Naivasha C Island I	Kenya	-0.8	36.4	c14	1835	150	-146	554	204	2096	1396	1746
288	Naivasha C Island I	Kenya	-0.8	36.4	c14	1300	80	608	970	789	1342	980	1161
289	Naivasha C Island I	Kenya	-0.8	36.4	c14	1814	180	-175	636	231	2125	1314	1720

Entry ID	Site Name	Country	Latitude	Longitude	Date Type	Date BP	Date BP SD	Min Chronology (Calibrated BCE/CE)	Max Chronology (Calibrated BCE/CE)	Mean Chronology (Calibrated BCE/CE)	Min Chronology (Calibrated BP - 1950)	Max Chronology (Calibrated BP - 1950)	Mean Chronology (Calibrated BP - 1950)
290	Naivasha Causeway	Kenya	-0.8	36.4	c14	895	105	905	1381	1143	1045	569	807
291	Naivasha Causeway	Kenya	-0.8	36.4	c14	2045	125	-370	241	-65	2320	1709	2015
292	Naivasha Causeway	Kenya	-0.8	36.4	c14	2380	140	-803	-112	-458	2753	2062	2408
293	Naivasha Railway RS	Kenya	-0.8	36.4	c14	2000	135	-364	342	-11	2314	1608	1961
294	Naivasha Railway RS	Kenya	-0.8	36.4	c14	195	125	1491	1950	1721	459	0	230
295	Naivasha Burial	Kenya	-0.7	36.4	c14	2235	20	-375	-189	-282	2325	2139	2232
296	Naivasha Burial	Kenya	-0.7	36.4	c14	2400	20	-539	-393	-466	2489	2343	2416
297	Naivasha Burial	Kenya	-0.7	36.4	c14	2320	20	-405	-205	-305	2355	2155	2255
298	Naivasha Burial	Kenya	-0.7	36.4	c14	2255	20	-386	-194	-290	2336	2144	2240
299	Naivasha Burial	Kenya	-0.7	36.4	c14	2310	15	-401	-204	-303	2351	2154	2253
300	Ol Kalou	Kenya	-0.3	36.4	c14	1800	20	219	340	280	1731	1610	1671
301	Prettejohn's Gully	Kenya	-0.5	36.1	c14	3670	20	-2135	-1941	-2038	4085	3891	3988
302	Prettejohn's Gully	Kenya	-0.5	36.1	c14	3640	20	-2114	-1897	-2006	4064	3847	3956
303	Masai Gorge RS	Kenya	-0.7	36.3	c14	405	120	1303	1947	1625	647	3	325
304	Masai Gorge RS	Kenya	-0.7	36.3	c14	1025	130	771	1275	1023	1179	675	927
305	Masai Gorge RS	Kenya	-0.7	36.3	c14	1545	135	222	775	499	1728	1175	1452
306	Masai Gorge RS	Kenya	-0.7	36.3	c14	1560	135	223	773	498	1727	1177	1452
307	Masai Gorge RS	Kenya	-0.7	36.3	c14	2325	145	-781	-52	-417	2731	2002	2367
308	Masai Gorge RS	Kenya	-0.7	36.3	c14	2495	150	-924	-194	-559	2874	2144	2509
309	Masai Gorge RS	Kenya	-0.7	36.3	c14	2515	140	-921	-203	-562	2871	2153	2512
310	Masai Gorge RS	Kenya	-0.7	36.3	c14	2595	135	-1046	-387	-717	2996	2337	2667

Entry ID	Site Name	Country	Latitude	Longitude	Date Type	Date BP	Date BP SD	Min Chronology (Calibrated BCE/CE)	Max Chronology (Calibrated BCE/CE)	Mean Chronology (Calibrated BCE/CE)	Min Chronology (Calibrated BP - 1950)	Max Chronology (Calibrated BP - 1950)	Mean Chronology (Calibrated BP - 1950)
311	Masai Gorge RS	Kenya	-0.7	36.3	c14	2865	150	-1438	-771	-1105	3388	2721	3055
312	Kapsoo Hill RS	Kenya	0.9	35.3	c14	2477	24	-756	-416	-586	2706	2366	2536
313	Kapsoo Hill RS	Kenya	0.9	35.3	c14	2113	24	-174	-49	-112	2124	1999	2062
314	Kapsoo Hill RS	Kenya	0.9	35.3	c14	2200	20	-360	-151	-256	2310	2101	2206
315	Ndabibi	Kenya	-0.7	36.3	c14	1255	125	576	1037	807	1374	913	1144
316	Ndabibi	Kenya	-0.7	36.3	c14	1665	145	76	661	369	1874	1289	1582
317	Ndabibi	Kenya	-0.7	36.3	c14	1815	120	-44	530	243	1994	1420	1707
318	Ndabibi	Kenya	-0.7	36.3	c14	2225	155	-756	116	-320	2706	1834	2270
319	Ndabibi	Kenya	-0.7	36.3	c14	1415	150	363	987	675	1587	963	1275
320	Ndabibi	Kenya	-0.7	36.3	c14	410	110	1314	1806	1560	636	144	390
321	Akira	Kenya	-0.7	36.3	c14	445	120	1292	1800	1546	658	150	404
322	Akira	Kenya	-0.7	36.3	c14	485	135	1,269	1,802	1536	681	148	415
323	Akira	Kenya	-1.0	36.4	c14	1965	140	-356	407	26	2306	1543	1925
324	Akira	Kenya	-1.0	36.4	c14	1440	120	386	888	637	1564	1062	1313
325	Akira	Kenya	-1.0	36.4	c14	1255	140	548	1134	841	1402	816	1109
326	Akira	Kenya	-1.0	36.4	c14	1775	115	21	550	286	1929	1400	1665
327	Akira	Kenya	-1.0	36.4	c14	1090	150	665	1228	947	1285	722	1004
328	Salasun	Kenya	-1.1	36.4	c14	1185	140	608	1162	885	1342	788	1065
329	Salasun	Kenya	-1.1	36.4	c14	2680	150	-1200	-406	-803	3150	2356	2753
330	Salasun	Kenya	-1.1	36.4	c14	1315	135	440	1024	732	1510	926	1218
331	Salasun	Kenya	-1.1	36.4	c14	2990	170	-1599	-807	-1203	3549	2757	3153

Entry ID	Site Name	Country	Latitude	Longitude	Date Type	Date BP	Date BP SD	Min Chronology (Calibrated BCE/CE)	Max Chronology (Calibrated BCE/CE)	Mean Chronology (Calibrated BCE/CE)	Min Chronology (Calibrated BP - 1950)	Max Chronology (Calibrated BP - 1950)	Mean Chronology (Calibrated BP - 1950)
332	Salasun	Kenya	-1.1	36.4	c14	1110	115	680	1180	930	1270	770	1020
333	Narosura	Kenya	-1.8	36.1	c14	2640	115	-1013	-410	-712	2963	2360	2662
334	Narosura	Kenya	-1.8	36.1	c14	2660	115	-1049	-415	-732	2999	2365	2682
335	Narosura	Kenya	-1.8	36.1	c14	2360	110	-773	-172	-473	2723	2122	2423
336	Narosura	Kenya	-1.8	36.1	c14	2760	115	-1259	-563	-911	3209	2513	2861
337	Narosura	Kenya	-1.8	36.1	c14	2260	110	-747	17	-365	2697	1933	2315
338	Lukenya	Kenya	-1.4	37.0	c14	1840	140	-111	542	216	2061	1408	1735
339	Lukenya	Kenya	-1.4	37.0	c14	1930	175	-365	525	80	2315	1425	1870
340	Lukenya	Kenya	-1.4	37.0	c14	2115	130	-402	209	-97	2352	1741	2047
341	Lukenya	Kenya	-1.4	37.0	c14	1490	131	256	871	564	1694	1079	1387
342	Lukenya	Kenya	-1.4	37.0	c14	2311	127	-761	-59	-410	2711	2009	2360
343	Lukenya	Kenya	-1.4	37.0	c14	1307	122	546	1017	782	1404	933	1169
344	Lukenya	Kenya	-1.4	37.0	c14	4145	240	-3366	-2037	-2702	5316	3987	4652
345	Lukenya	Kenya	-1.4	37.0	c14	4200	155	-3330	-2342	-2836	5280	4292	4786
346	Lukenya	Kenya	-1.4	37.0	c14	4490	160	-3631	-2702	-3167	5581	4652	5117
347	Lukenya	Kenya	-1.4	37.0	c14	1250	115	604	1025	815	1346	925	1136
348	Lukenya	Kenya	-1.4	37.0	c14	1240	145	570	1152	861	1380	798	1089
349	Lukenya	Kenya	-1.4	37.0	c14	1804	119	-40	537	249	1990	1413	1702
350	Lukenya	Kenya	-1.4	37.0	c14	1501	170	206	961	584	1744	989	1367
351	Lukenya	Kenya	-1.4	37.0	c14	1891	133	-186	475	145	2136	1475	1806
352	Lukenya	Kenya	-1.4	37.0	c14	2085	135	-396	235	-81	2346	1715	2031

Entry ID	Site Name	Country	Latitude	Longitude	Date Type	Date BP	Date BP SD	Min Chronology (Calibrated BCE/CE)	Max Chronology (Calibrated BCE/CE)	Mean Chronology (Calibrated BCE/CE)	Min Chronology (Calibrated BP - 1950)	Max Chronology (Calibrated BP - 1950)	Mean Chronology (Calibrated BP - 1950)
353	Lukenya	Kenya	-1.4	37.0	c14	1710	135	68	638	353	1882	1312	1597
354	Lukenya	Kenya	-1.4	37.0	c14	2415	155	-832	-100	-466	2782	2050	2416
355	Lukenya	Kenya	-1.4	37.0	c14	2030	125	-373	250	-62	2323	1700	2012
356	Lukenya	Kenya	-1.4	37.0	c14	1775	150	-53	602	275	2003	1348	1676
357	Lukenya	Kenya	-1.4	37.0	c14	3290	145	-1941	-1206	-1574	3891	3156	3524
358	Lukenya	Kenya	-1.4	37.0	c14	1820	200	-349	645	148	2299	1305	1802
359	Lukenya	Kenya	-1.4	37.0	c14	2070	155	-411	341	-35	2361	1609	1985
360	Lukenya	Kenya	-1.4	37.0	c14	1340	145	430	1015	723	1520	935	1228
361	Lukenya	Kenya	-1.4	37.0	c14	970	130	775	1290	1033	1175	660	918
362	Lukenya	Kenya	-1.4	37.0	c14	1810	135	-55	569	257	2005	1381	1693
363	Lukenya	Kenya	-1.4	37.0	c14	1600	130	164	765	465	1786	1185	1486
364	Lukenya	Kenya	-1.4	37.0	c14	1855	180	-348	590	121	2298	1360	1829
365	Lukenya	Kenya	-1.4	37.0	c14	2050	115	-365	230	-68	2315	1720	2018
366	Lukenya	Kenya	-1.4	37.0	c14	2045	125	-368	241	-64	2318	1709	2014
367	Lukenya	Kenya	-1.4	37.0	c14	2295	135	-770	-46	-408	2720	1996	2358
368	Lukenya	Kenya	-1.4	37.0	c14	3340	23	-1677	-1508	-1593	3627	3458	3543
369	Lukenya	Kenya	-1.4	37.0	c14	3296	25	-1618	-1460	-1539	3568	3410	3489
370	Lukenya	Kenya	-1.4	37.0	c14	3359	23	-1730	-1536	-1633	3680	3486	3583
371	Lukenya	Kenya	-1.4	37.0	c14	2257	29	-389	-193	-291	2339	2143	2241
372	Lukenya	Kenya	-1.4	37.0	c14	2133	30	-341	-52	-197	2291	2002	2147
373	Lukenya	Kenya	-1.4	37.0	c14	2226	29	-376	-176	-276	2326	2126	2226

Entry ID	Site Name	Country	Latitude	Longitude	Date Type	Date BP	Date BP SD	Min Chronology (Calibrated BCE/CE)	Max Chronology (Calibrated BCE/CE)	Mean Chronology (Calibrated BCE/CE)	Min Chronology (Calibrated BP - 1950)	Max Chronology (Calibrated BP - 1950)	Mean Chronology (Calibrated BP - 1950)
374	Chyulu Hills	Kenya	-2.4	37.5	c14	985	75	898	1226	1062	1052	724	888
375	Chyulu Hills	Kenya	-2.4	37.5	c14	1520	75	413	664	539	1537	1286	1412
376	Chyulu Hills	Kenya	-2.4	37.5	c14	435	105	1303	1798	1551	647	152	400
377	Gatung'ang'a	Kenya	-0.2	37.0	c14	810	130	995	1408	1202	955	542	749
378	Gatung'ang'a	Kenya	-0.2	37.0	c14	820	130	993	1405	1199	957	545	751
379	Gatung'ang'a	Kenya	-0.2	37.0	c14	850	150	894	1410	1152	1056	540	798
380	Gatung'ang'a	Kenya	-0.2	37.0	c14	690	100	1169	1443	1306	781	507	644
381	Gatung'ang'a	Kenya	-0.2	37.0	c14	600	80	1276	1455	1366	674	495	585
382	Lemek North-East	Kenya	-1.7	35.6	c14	2225	140	-751	112	-320	2701	1838	2270
383	Lemek North-East	Kenya	-1.7	35.6	OH	2506	70	-696	-416	-556	2646	2366	2506
384	Lemek North-East	Kenya	-1.7	35.6	OH	2566	78	-772	-460	-616	2722	2410	2566
385	Lemek West	Kenya	-1.7	35.5	OH	2172	86	-394	-50	-222	2344	2000	2172
386	Lemek West	Kenya	-1.7	35.5	OH	1756	46	102	286	194	1848	1664	1756
387	Lemek North-West	Kenya	-1.7	35.5	OH	2636	56	-798	-574	-686	2748	2524	2636
388	Lemek North-West	Kenya	-1.7	35.5	OH	2653	71	-845	-561	-703	2795	2511	2653
389	Ngamuriak	Kenya	-1.6	35.5	c14	1940	140	-351	419	34	2301	1531	1916
390	Ngamuriak	Kenya	-1.6	35.5	c14	2135	140	-482	231	-126	2432	1719	2076
391	Ngamuriak	Kenya	-1.6	35.5	OH	2038	78	-244	68	-88	2194	1882	2038
392	Ngamuriak	Kenya	-1.6	35.5	OH	2076	81	-288	36	-126	2238	1914	2076
393	Ngamuriak	Kenya	-1.6	35.5	OH	1764	62	62	310	186	1888	1640	1764
394	Ngamuriak	Kenya	-1.6	35.5	OH	1661	141	7	571	289	1943	1379	1661

Entry ID	Site Name	Country	Latitude	Longitude	Date Type	Date BP	Date BP SD	Min Chronology (Calibrated BCE/CE)	Max Chronology (Calibrated BCE/CE)	Mean Chronology (Calibrated BCE/CE)	Min Chronology (Calibrated BP - 1950)	Max Chronology (Calibrated BP - 1950)	Mean Chronology (Calibrated BP - 1950)
395	Ngamuriak	Kenya	-1.6	35.5	OH	1540	51	308	512	410	1642	1438	1540
396	Ngamuriak	Kenya	-1.6	35.5	OH	1783	99	-31	365	167	1981	1585	1783
397	Ngamuriak	Kenya	-1.6	35.5	OH	1952	72	-146	142	-2	2096	1808	1952
398	Ngamuriak	Kenya	-1.6	35.5	OH	2927	74	-1125	-829	-977	3075	2779	2927
399	North Horr I	Kenya	3.3	37.1	c14	4405	130	-3494	-2635	-3065	5444	4585	5015
400	North Horr I	Kenya	3.3	37.1	c14	3330	130	-1938	-1290	-1614	3888	3240	3564
401	North Horr II	Kenya	3.3	37.1	c14	1525	155	219	881	550	1731	1069	1400
402	North Horr II	Kenya	3.3	37.1	c14	748	140	1025	1445	1235	925	505	715
403	Kokurmatakore	Kenya	3.1	37.4	c14	960	190	683	1394	1039	1267	556	912
404	Kokurmatakore	Kenya	3.1	37.4	c14	1110	155	654	1225	940	1296	725	1011
405	Kokurmatakore	Kenya	3.1	37.4	c14	3460	155	-2198	-1415	-1807	4148	3365	3757
406	Kokurmatakore	Kenya	3.1	37.4	c14	585	115	1,223	1,626	1425	727	324	526
407	Kokurmatakore	Kenya	3.1	37.4	c14	510	115	1,284	1,644	1464	666	306	486
408	Lopoy	Kenya	3.2	36.1	c14	870	80	1027	1286	1157	923	664	794
409	Lopoy	Kenya	3.2	36.1	c14	950	80	989	1269	1129	961	681	821
410	Lopoy	Kenya	3.2	36.1	c14	1100	80	772	1154	963	1178	796	987
411	Lopoy	Kenya	3.2	36.1	c14	1375	125	430	968	699	1520	982	1251
412	Apeget I	Kenya	3.4	35.9	c14	1800	300	-511	883	186	2461	1067	1764
413	Apeget II	Kenya	3.4	35.9	c14	2210	60	-390	-66	-228	2340	2016	2178
414	Aipa	Kenya	3.2	35.9	c14	5420	80	-4441	-3996	-4219	6391	5946	6169
415	Namoratunga	Kenya	3.5	35.9	c14	2285	165	-784	55	-365	2734	1895	2315

Entry ID	Site Name	Country	Latitude	Longitude	Date Type	Date BP	Date BP SD	Min Chronology (Calibrated BCE/CE)	Max Chronology (Calibrated BCE/CE)	Mean Chronology (Calibrated BCE/CE)	Min Chronology (Calibrated BP - 1950)	Max Chronology (Calibrated BP - 1950)	Mean Chronology (Calibrated BP - 1950)
416	Namoratunga	Kenya	3.5	35.9	c14	1200	100	656	1030	843	1294	920	1107
417	Turkwell Scheme	Kenya	3.1	36.1	c14	1500	100	366	772	569	1584	1178	1381
418	Muringa	Kenya	0.8	35.5	c14	300	80	1446	1948	1697	504	2	253
419	Muringa	Kenya	0.8	35.5	c14	300	80	1446	1948	1697	504	2	253
420	Prospect Farm	Kenya	-0.6	36.2	c14	2690	80	-1045	-549	-797	2995	2499	2747
421	Prospect Farm	Kenya	-0.6	36.2	c14	2910	110	-1387	-828	-1108	3337	2778	3058
422	Prospect Farm	Kenya	-0.6	36.2	OH	2840	161	-1212	-568	-890	3162	2518	2840
423	Prospect Farm	Kenya	-0.6	36.2	OH	3124	245	-1664	-684	-1174	3614	2634	3124
424	Prospect Farm	Kenya	-0.6	36.2	OH	3102	177	-1506	-798	-1152	3456	2748	3102
425	Prospect Farm	Kenya	-0.6	36.2	OH	3279	205	-1739	-919	-1329	3689	2869	3279
426	Prospect Farm	Kenya	-0.6	36.2	OH	2930	64	-1108	-852	-980	3058	2802	2930
427	Prospect Farm	Kenya	-0.6	36.2	OH	2994	86	-1216	-872	-1044	3166	2822	2994
428	Prospect Farm	Kenya	-0.6	36.2	OH	2951	107	-1215	-787	-1001	3165	2737	2951
429	Prospect Farm	Kenya	-0.6	36.2	OH	3257	250	-1807	-807	-1307	3757	2757	3257
430	Prospect Farm	Kenya	-0.6	36.2	OH	3059	154	-1417	-801	-1109	3367	2751	3059
431	Prospect Farm	Kenya	-0.6	36.2	OH	3080	177	-1484	-776	-1130	3434	2726	3080
432	Prospect Farm	Kenya	-0.6	36.2	OH	3168	133	-1484	-952	-1218	3434	2902	3168
433	Prospect Farm	Kenya	-0.6	36.2	OH	3015	175	-1415	-715	-1065	3365	2665	3015
434	Prospect Farm	Kenya	-0.6	36.2	OH	3168	133	-1484	-952	-1218	3434	2902	3168
435	Prospect Farm	Kenya	-0.6	36.2	OH	2815	204	-1273	-457	-865	3223	2407	2815
436	Prospect Farm	Kenya	-0.6	36.2	OH	3146	133	-1462	-930	-1196	3412	2880	3146

Entry ID	Site Name	Country	Latitude	Longitude	Date Type	Date BP	Date BP SD	Min Chronology (Calibrated BCE/CE)	Max Chronology (Calibrated BCE/CE)	Mean Chronology (Calibrated BCE/CE)	Min Chronology (Calibrated BP - 1950)	Max Chronology (Calibrated BP - 1950)	Mean Chronology (Calibrated BP - 1950)
437	Prospect Farm	Kenya	-0.6	36.2	OH	2578	80	-788	-468	-628	2738	2418	2578
438	Prospect Farm	Kenya	-0.6	36.2	OH	2562	129	-870	-354	-612	2820	2304	2562
439	Keringet Cave	Kenya	-0.6	35.4	c14	2910	115	-1389	-827	-1108	3339	2777	3058
440	Keringet Cave	Kenya	-0.6	35.4	c14	2430	110	-797	-204	-501	2747	2154	2451
441	Keringet Cave	Kenya	-0.6	35.4	c14	2050	110	-361	227	-67	2311	1723	2017
442	Keringet Cave	Kenya	-0.6	35.4	c14	1585	15	430	570	500	1520	1380	1450
443	Keringet Cave	Kenya	-0.6	35.4	c14	2465	20	-751	-411	-581	2701	2361	2531
444	Lion Hill	Kenya	-0.4	36.1	c14	1850	130	-101	530	215	2051	1420	1736
445	Shulumai RS	Kenya	0.5	37.2	c14	1100	90	709	1161	935	1241	789	1015
446	Eburu SLT Cave	Kenya	-0.6	36.2	c14	2090	70	-355	116	-120	2305	1834	2070
447	Eburu SLT Cave	Kenya	-0.6	36.2	c14	3570	70	-2132	-1691	-1912	4082	3641	3862
448	Eburu SLT Cave	Kenya	-0.6	36.2	c14	3000	70	-1406	-1012	-1209	3356	2962	3159
449	Ol Tepesi RS	Kenya	-0.7	36.2	c14	1390	70	547	842	695	1403	1108	1256
450	Ol Tepesi RS	Kenya	-0.7	36.2	c14	3120	70	-1506	-1130	-1318	3456	3080	3268
451	Ol Tepesi RS	Kenya	-0.7	36.2	c14	4560	80	-3517	-2935	-3226	5467	4885	5176
452	Enkapune ya Sauli	Kenya	-0.8	35.1	c14	595	130	1185	1635	1410	765	315	540
453	Enkapune ya Sauli	Kenya	-0.8	35.1	c14	1480	160	243	954	599	1707	996	1352
454	Enkapune ya Sauli	Kenya	-0.8	35.1	c14	2040	160	-399	361	-19	2349	1589	1969
455	Pickford's Site	Kenya	-1.1	36.5	c14	1770	190	-170	653	242	2120	1297	1709
456	Pickford's Site	Kenya	-1.1	36.5	c14	4430	165	-3526	-2629	-3078	5476	4579	5028
457	Pickford's Site	Kenya	-1.1	36.5	c14	2025	135	-374	326	-24	2324	1624	1974

Entry ID	Site Name	Country	Latitude	Longitude	Date Type	Date BP	Date BP SD	Min Chronology (Calibrated BCE/CE)	Max Chronology (Calibrated BCE/CE)	Mean Chronology (Calibrated BCE/CE)	Min Chronology (Calibrated BP - 1950)	Max Chronology (Calibrated BP - 1950)	Mean Chronology (Calibrated BP - 1950)
458	Pickford's Site	Kenya	-1.1	36.5	c14	1815	120	-45	529	242	1995	1421	1708
459	Kasiole 2 Burial	Kenya	-1.3	35.9	c14	1110	15	893	1018	956	1057	932	995
460	Laikipia Burial	Kenya	0.4	36.9	c14	635	15	1302	1399	1351	648	551	600
461	Naishi RS	Kenya	-0.5	36.1	c14	2470	15	-751	-414	-583	2701	2364	2533
462	Naishi RS	Kenya	-0.5	36.1	c14	2550	15	-790	-547	-669	2740	2497	2619
463	Oltioki	Kenya	0.5	36.1	c14	1536	31	437	638	538	1513	1312	1413
464	Oltioki	Kenya	0.5	36.1	c14	1609	27	416	545	481	1534	1405	1470
465	Sokotei 1	Kenya	0.5	36.1	c14	3120	29	-1435	-1270	-1353	3385	3220	3303
466	Sokotei 1	Kenya	0.5	36.1	c14	3107	29	-1428	-1262	-1345	3378	3212	3295
467	Wei wei Valley	Kenya	1.4	35.5	c14	188	23	1661	1948	1805	289	2	146
468	Wei wei Valley	Kenya	1.4	35.5	c14	240	24	1641	1803	1722	309	147	228
469	Wei wei Valley	Kenya	1.4	35.5	c14	386	24	1454	1628	1541	496	322	409
470	Wei wei Valley	Kenya	1.4	35.5	c14	4924	30	-3768	-3637	-3703	5718	5587	5653
471	Wei wei Valley	Kenya	1.4	35.5	c14	277	23	1515	1798	1657	435	152	294
472	Wei wei Valley	Kenya	1.4	35.5	c14	189	23	1661	1948	1805	289	2	146
473	Wei wei Valley	Kenya	1.4	35.5	c14	248	23	1638	1800	1719	312	150	231
474	Morpus	Kenya	1.4	35.3	c14	164	24	1670	1948	1809	280	2	141
475	Morpus	Kenya	1.4	35.3	c14	189	25	1660	1948	1804	290	2	146
476	Morpus	Kenya	1.4	35.3	c14	179	24	1665	1948	1807	285	2	144
477	Porr	Kenya	2.9	36.6	OSL	2555	175	-894	-194	-544	2844	2144	2494
478	Porr	Kenya	2.9	36.6	c14	2575	20	-802	-556	-679	2752	2506	2629

Entry ID	Site Name	Country	Latitude	Longitude	Date Type	Date BP	Date BP SD	Min Chronology (Calibrated BCE/CE)	Max Chronology (Calibrated BCE/CE)	Mean Chronology (Calibrated BCE/CE)	Min Chronology (Calibrated BP - 1950)	Max Chronology (Calibrated BP - 1950)	Mean Chronology (Calibrated BP - 1950)
479	Lowasera	Kenya	2.9	36.7	c14	2520	150	-975	-199	-587	2925	2149	2537
480	Lowasera	Kenya	2.9	36.7	c14	3070	135	-1613	-925	-1269	3563	2875	3219
481	Lowasera	Kenya	2.9	36.7	c14	3920	120	-2852	-2031	-2442	4802	3981	4392
482	Lowasera	Kenya	2.9	36.7	c14	4410	110	-3484	-2702	-3093	5434	4652	5043
483	Kahinju	Kenya	-3.0	38.6	IRSL	5960	480	-4919	-2999	-3959	6869	4949	5909
484	Kahinju	Kenya	-3.0	38.6	IRSL	5160	410	-3979	-2339	-3159	5929	4289	5109
485	Kahinju	Kenya	-3.0	38.6	IRSL	4970	400	-3769	-2169	-2969	5719	4119	4919
486	Kahinju	Kenya	-3.0	38.6	IRSL	3870	330	-2529	-1209	-1869	4479	3159	3819
487	Kahinju	Kenya	-3.0	38.6	c14	3423	55	-1879	-1539	-1709	3829	3489	3659
488	Kahinju	Kenya	-3.0	38.6	c14	2987	57	-1387	-1012	-1200	3337	2962	3150
489	Kahinju	Kenya	-3.0	38.6	c14	2973	52	-1380	-1008	-1194	3330	2958	3144
490	Kahinju	Kenya	-3.0	38.6	IRSL	3200	260	-1719	-679	-1199	3669	2629	3149
491	Kahinju	Kenya	-3.0	38.6	IRSL	3160	280	-1719	-599	-1159	3669	2549	3109
492	Kahinju	Kenya	-3.0	38.6	IRSL	3000	260	-1519	-479	-999	3469	2429	2949
493	Kahinju	Kenya	-3.0	38.6	c14	2527	84	-801	-411	-606	2751	2361	2556
494	Kahinju	Kenya	-3.0	38.6	IRSL	2960	280	-1519	-399	-959	3469	2349	2909
495	Kahinju	Kenya	-3.0	38.6	IRSL	940	70	921	1201	1061	1029	749	889
496	Kahinju	Kenya	-3.0	38.6	IRSL	4020	320	-2,659	#####	-2019	4609	3329	3969
497	Kahinju	Kenya	-3.0	38.6	IRSL	2300	180	-659	61	-299	2609	1889	2249
498	Kahinju	Kenya	-3.0	38.6	IRSL	2730	230	-1,189	-269	-729	3139	2219	2679
499	Kahinju	Kenya	-3.0	38.6	IRSL	2170	170	-509	171	-169	2459	1779	2119

Entry ID	Site Name	Country	Latitude	Longitude	Date Type	Date BP	Date BP SD	Min Chronology (Calibrated BCE/CE)	Max Chronology (Calibrated BCE/CE)	Mean Chronology (Calibrated BCE/CE)	Min Chronology (Calibrated BP - 1950)	Max Chronology (Calibrated BP - 1950)	Mean Chronology (Calibrated BP - 1950)
500	Kathuva	Kenya	-3.0	39.1	IRSL	4830	390	-3609	-2049	-2829	5559	3999	4779
501	Kathuva	Kenya	-3.0	39.1	IRSL	3450	290	-2029	-869	-1449	3979	2819	3399
502	Kathuva	Kenya	-3.0	39.1	IRSL	3600	320	-2239	-959	-1599	4189	2909	3549
503	Kathuva	Kenya	-3.0	39.1	IRSL	3120	270	-1659	-579	-1119	3609	2529	3069
504	Kathuva	Kenya	-3.0	39.1	c14	1671	49	254	540	397	1696	1410	1553
505	Kathuva	Kenya	-3.0	39.1	IRSL	1720	150	-19	581	281	1969	1369	1669
506	Kathuva	Kenya	-3.0	39.1	c14	1486	39	540	655	598	1410	1295	1353
507	Kathuva	Kenya	-3.0	39.1	c14	1526	61	428	647	538	1522	1303	1413
508	Mwiitu	Kenya	-3.0	38.6	IRSL	3020	270	-1556	-476	-1016	3506	2426	2966
509	Mwiitu	Kenya	-3.0	38.6	IRSL	1020	80	824	1144	984	1126	806	966
510	Kizingitini	Kenya	-4.0	39.7	c14	610	70	1284	1440	1362	666	510	588
511	Kizingitini	Kenya	-4.0	39.7	c14	790	70	1050	1392	1221	900	558	729
512	Kizingitini	Kenya	-4.0	39.7	c14	420	70	1416	1642	1529	534	308	421
513	Kizingitini	Kenya	-4.0	39.7	c14	420	70	1416	1641	1529	534	309	422
514	Kizingitini	Kenya	-4.0	39.7	c14	530	70	1296	1616	1456	654	334	494
515	Kizingitini	Kenya	-4.0	39.7	c14	430	70	1410	1639	1525	540	311	426
516	Kizingitini	Kenya	-4.0	39.7	c14	440	70	1405	1638	1522	545	312	429
517	Kasigau	Kenya	-3.8	38.7	c14	840	70	1040	1295	1168	910	655	783
518	Kasigau	Kenya	-3.8	38.7	c14	790	70	1050	1392	1221	900	558	729
519	Kasigau	Kenya	-3.8	38.7	c14	1560	70	390	648	519	1560	1302	1431
520	Kasigau	Kenya	-3.8	38.7	c14	1710	70	219	540	380	1731	1410	1571

Entry ID	Site Name	Country	Latitude	Longitude	Date Type	Date BP	Date BP SD	Min Chronology (Calibrated BCE/CE)	Max Chronology (Calibrated BCE/CE)	Mean Chronology (Calibrated BCE/CE)	Min Chronology (Calibrated BP - 1950)	Max Chronology (Calibrated BP - 1950)	Mean Chronology (Calibrated BP - 1950)
521	Kasigau	Kenya	-3.8	38.7	c14	2770	70	-1106	-795	-951	3056	2745	2901
522	Kasigau	Kenya	-3.8	38.7	c14	1150	70	690	1031	861	1260	919	1090
523	Kasigau	Kenya	-3.8	38.7	c14	380	70	1430	1660	1545	520	290	405
524	Kasigau	Kenya	-3.8	38.7	c14	2670	70	-997	-550	-774	2947	2500	2724
525	Kasigau	Kenya	-3.8	38.7	c14	3540	70	-2036	-1636	-1836	3986	3586	3786
526	Kasigau	Kenya	-3.8	38.7	c14	4410	51	-3329	-2899	-3114	5279	4849	5064
527	Kasigau	Kenya	-3.8	38.7	c14	4470	70	-3346	-2926	-3136	5296	4876	5086
528	Kasigau	Kenya	-3.8	38.7	c14	5330	70	-4327	-3985	-4156	6277	5935	6106
529	Kasigau	Kenya	-3.8	38.7	c14	840	70	1040	1295	1168	910	655	783
530	Kasigau	Kenya	-3.8	38.7	c14	910	70	1026	1269	1148	924	681	803
531	Kasigau	Kenya	-3.8	38.7	c14	990	70	901	1222	1062	1049	728	889
532	Kasigau	Kenya	-3.8	38.7	c14	1000	70	898	1218	1058	1052	732	892
533	Kasigau	Kenya	-3.8	38.7	c14	1140	70	690	1040	865	1260	910	1085
534	Kasigau	Kenya	-3.8	38.7	c14	1150	70	691	1031	861	1259	919	1089
535	Kasigau	Kenya	-3.8	38.7	c14	207	40	1643	1948	1796	307	2	155
536	Kasigau	Kenya	-3.8	38.7	c14	290	70	1453	1948	1701	497	2	250
537	Kasigau	Kenya	-3.8	38.7	c14	300	70	1450	1948	1699	500	2	251
538	Kasigau	Kenya	-3.8	38.7	c14	330	70	1445	1800	1623	505	150	328
539	Kasigau	Kenya	-3.8	38.7	c14	380	70	1430	1659	1545	520	291	406
540	Kasigau	Kenya	-3.8	38.7	c14	170	70	1650	1949	1800	300	1	151
541	Kasigau	Kenya	-3.8	38.7	c14	180	70	1639	1949	1794	311	1	156

Entry ID	Site Name	Country	Latitude	Longitude	Date Type	Date BP	Date BP SD	Min Chronology (Calibrated BCE/CE)	Max Chronology (Calibrated BCE/CE)	Mean Chronology (Calibrated BCE/CE)	Min Chronology (Calibrated BP - 1950)	Max Chronology (Calibrated BP - 1950)	Mean Chronology (Calibrated BP - 1950)
542	Kasigau	Kenya	-3.8	38.7	c14	180	70	1639	1949	1794	311	1	156
543	Kasigau	Kenya	-3.8	38.7	c14	240	70	1503	1949	1726	447	1	224
544	Kasigau	Kenya	-3.8	38.7	c14	320	70	1446	1805	1626	504	145	325
545	Kasigau	Kenya	-3.8	38.7	c14	350	70	1436	1798	1617	514	152	333
546	Kasigau	Kenya	-3.8	38.7	c14	180	70	1639	1949	1794	311	1	156
547	Kasigau	Kenya	-3.8	38.7	c14	260	70	1478	1948	1713	472	2	237
548	Kasigau	Kenya	-3.8	38.7	c14	360	70	1435	1795	1615	515	155	335
549	Kirinkai	Kenya	-2.7	37.3	c14	822	27	1183	1280	1232	767	670	719
550	Ilnyangusi	Kenya	-2.7	37.3	c14	1145	30	775	1015	895	1175	935	1055
551	Ilnyangusi Manyatta	Kenya	-2.7	37.3	c14	697	58	1230	1404	1317	720	546	633
552	Lemomo Hill	Kenya	-2.7	37.3	c14	620	28	1300	1409	1355	650	541	596
553	Lemomo Hill	Kenya	-2.7	37.3	c14	526	58	1303	1495	1399	647	455	551
554	Ilmaarba	Kenya	-2.7	37.3	c14	556	31	1322	1444	1383	628	506	567
555	Ololopoli	Kenya	-2.7	37.3	c14	476	27	1412	1476	1444	538	474	506
556	Irrpurai	Kenya	-2.7	37.3	c14	237	29	1638	1948	1793	312	2	157
557	Irrpurai	Kenya	-2.7	37.3	c14	201	27	1651	1948	1800	299	2	151
558	Kisii District	Kenya	-0.7	34.8	c14	2090	170	-538	344	-97	2488	1606	2047
559	Kisii District	Kenya	-0.7	34.8	c14	1190	75	680	1019	850	1270	931	1101
560	Kisii District	Kenya	-0.7	34.8	c14	1650	90	238	632	435	1712	1318	1515
561	Kisii District	Kenya	-0.7	34.8	c14	165	90	1521	1956	1739	429	-6	212
562	Kisima Farm A4	Kenya	0.2	36.5	c14	1900	90	-58	370	156	2008	1580	1794

Entry ID	Site Name	Country	Latitude	Longitude	Date Type	Date BP	Date BP SD	Min Chronology (Calibrated BCE/CE)	Max Chronology (Calibrated BCE/CE)	Mean Chronology (Calibrated BCE/CE)	Min Chronology (Calibrated BP - 1950)	Max Chronology (Calibrated BP - 1950)	Mean Chronology (Calibrated BP - 1950)
563	Kisima Farm A4	Kenya	0.2	36.5	c14	2100	110	-390	200	-95	2340	1750	2045
564	Kisima Farm A4	Kenya	0.2	36.5	c14	530	100	1284	1630	1457	666	320	493
565	Kisima Farm C4	Kenya	0.2	36.5	c14	760	90	1048	1410	1229	902	540	721
566	Kisima Farm C4	Kenya	0.2	36.5	c14	1110	15	893	1018	956	1057	932	995
567	Kisima Farm A5	Kenya	0.2	36.5	c14	2490	110	-827	-232	-530	2777	2182	2480
568	Kisima Farm A5	Kenya	0.2	36.5	c14	2830	120	-1376	-784	-1080	3326	2734	3030
569	Kisima Farm A5	Kenya	0.2	36.5	c14	2320	160	-796	13	-392	2746	1937	2342
570	Kisima Farm A5	Kenya	0.2	36.5	c14	2855	20	-1105	-911	-1008	3055	2861	2958
571	Kisima Farm A5	Kenya	0.2	36.5	c14	545	95	1279	1626	1453	671	324	498
572	Kisima Farm A5	Kenya	0.2	36.5	c14	2015	195	-516	483	-17	2466	1467	1967
573	Kisima Farm A5	Kenya	0.2	36.5	c14	2675	20	-896	-788	-842	2846	2738	2792
574	Kisima Farm A12	Kenya	0.3	36.5	c14	1100	120	682	1209	946	1268	741	1005
575	Kisima Farm A12	Kenya	0.3	36.5	c14	980	100	892	1269	1081	1058	681	870
576	Ol Ngoroi RS	Kenya	0.2	36.7	c14	4090	40	-2859	-2474	-2667	4809	4424	4617
577	Nderit Drift	Kenya	-0.9	36.1	c14	4040	140	-2903	-2145	-2524	4853	4095	4474
578	Nderit Drift	Kenya	-0.9	36.1	c14	3135	155	-1743	-936	-1340	3693	2886	3290
579	Nderit Drift	Kenya	-0.9	36.1	c14	1370	140	426	986	706	1524	964	1244
580	Nderit Drift	Kenya	-0.9	36.1	c14	1925	160	-358	526	84	2308	1424	1866
581	Nderit Drift	Kenya	-0.9	36.1	c14	2360	155	-800	-58	-429	2750	2008	2379
582	Nderit Drift	Kenya	-0.9	36.1	c14	260	120	1460	1947	1704	490	3	247
583	Nderit Drift	Kenya	-0.9	36.1	c14	260	105	1465	1948	1707	485	2	244

Entry ID	Site Name	Country	Latitude	Longitude	Date Type	Date BP	Date BP SD	Min Chronology (Calibrated BCE/CE)	Max Chronology (Calibrated BCE/CE)	Mean Chronology (Calibrated BCE/CE)	Min Chronology (Calibrated BP - 1950)	Max Chronology (Calibrated BP - 1950)	Mean Chronology (Calibrated BP - 1950)
584	Remnant	Kenya	-0.9	35.8	c14	1355	145	420	994	707	1530	956	1243
585	Remnant	Kenya	-0.9	35.8	c14	2315	150	-789	2	-394	2739	1948	2344
586	Rotian	Kenya	-0.9	35.5	c14	2155	140	-537	208	-165	2487	1742	2115
587	Rotian	Kenya	-0.9	35.5	c14	1965	150	-361	411	25	2311	1539	1925
588	Njoro River Cave	Kenya	-0.4	35.7	c14	2920	80	-1380	-856	-1118	3330	2806	3068
589	Njoro River Cave	Kenya	-0.4	35.7	c14	2900	75	-1281	-837	-1059	3231	2787	3009
590	Njoro River Cave	Kenya	-0.4	35.7	c14	3090	65	-1494	-1126	-1310	3444	3076	3260
591	Njoro River Cave	Kenya	-0.4	35.7	c14	3165	100	-1632	-1121	-1377	3582	3071	3327
592	Njoro River Cave II	Kenya	-0.4	35.9	c14	2070	15	-111	20	-46	2061	1930	1996
593	Rigo Cave	Kenya	-0.3	35.6	c14	2445	290	-1268	200	-534	3218	1750	2484
594	Rigo Cave	Kenya	-0.3	35.6	c14	2410	125	-800	-191	-496	2750	2141	2446
595	Rigo Cave	Kenya	-0.3	35.6	c14	2400	15	-517	-394	-456	2467	2344	2406
596	Rigo Cave	Kenya	-0.3	35.6	c14	2440	20	-741	-403	-572	2691	2353	2522
597	Rigo Cave	Kenya	-0.3	35.6	c14	2480	20	-757	-418	-588	2707	2368	2538
598	Rigo Cave	Kenya	-0.3	35.6	c14	2570	15	-798	-564	-681	2748	2514	2631
599	Tunnel Rock	Kenya	-0.6	36.1	c14	2050	60	-181	120	-31	2131	1830	1981
600	Tunnel Rock	Kenya	-0.6	36.1	c14	2730	60	-1005	-792	-899	2955	2742	2849
601	Yala Alego	Kenya	0.1	34.2	c14	1550	235	-41	992	476	1991	958	1475
602	Ulore II-Urewe	Kenya	0.2	34.2	c14	1680	270	-356	959	302	2306	991	1649
603	Ulore II-Urewe	Kenya	0.2	34.2	c14	1630	110	222	649	436	1728	1301	1515
604	Ulore II-Urewe	Kenya	0.2	34.2	c14	1560	95	259	666	463	1691	1284	1488

Entry ID	Site Name	Country	Latitude	Longitude	Date Type	Date BP	Date BP SD	Min Chronology (Calibrated BCE/CE)	Max Chronology (Calibrated BCE/CE)	Mean Chronology (Calibrated BCE/CE)	Min Chronology (Calibrated BP - 1950)	Max Chronology (Calibrated BP - 1950)	Mean Chronology (Calibrated BP - 1950)
605	Abindu RS	Kenya	-0.1	34.7	c14	1980	240	-727	585	-71	2677	1365	2021
606	Agoro RS	Kenya	-0.1	34.7	c14	2375	320	-1265	329	-468	3215	1621	2418
607	Jawuoyo RS	Kenya	-0.1	34.7	c14	2040	110	-360	239	-61	2310	1711	2011
608	Jawuoyo RS	Kenya	-0.1	34.7	c14	1895	15	118	211	165	1832	1739	1786
609	Nyaidha RS	Kenya	-0.2	34.5	c14	2230	320	-1050	526	-262	3000	1424	2212
610	Randhore RS	Kenya	-0.2	34.5	c14	1310	95	596	975	786	1354	975	1165
611	Rangong RS	Kenya	-0.2	34.5	c14	2315	185	-810	70	-370	2760	1880	2320
612	Lake Elmenteita	Kenya	-0.5	36.2	c14	1830	130	-89	540	226	2039	1410	1725
613	Cole's Burial	Kenya	-0.4	36.3	c14	2355	150	-795	-60	-428	2745	2010	2378
614	Cole's Burial	Kenya	-0.4	36.3	c14	2500	130	-898	-209	-554	2848	2159	2504
615	Cole's Burial	Kenya	-0.4	36.3	c14	3070	20	-1400	-1226	-1313	3350	3176	3263
616	Egerton Cave	Kenya	-0.4	35.9	c14	1880	15	125	218	172	1825	1732	1779
617	Emurula Ole P Cairns	Kenya	-1.4	36.0	c14	270	15	1532	1795	1664	418	155	287
618	Gil Gil	Kenya	-0.5	36.3	c14	2200	130	-732	119	-307	2682	1831	2257
619	Gil Gil	Kenya	-0.5	36.3	c14	2040	155	-397	342	-28	2347	1608	1978
620	Gil Gil	Kenya	-0.5	36.3	c14	1170	15	775	986	881	1175	964	1070
621	GuJe 20-Oldorotua	Kenya	-1.3	35.0	c14	790	25	1223	1282	1253	727	668	698
622	GuJe 66-Oldorotua	Kenya	-1.3	35.0	c14	875	25	1054	1266	1160	896	684	790
623	New Mara Bridge	Kenya	-1.3	35.0	c14	1390	150	386	992	689	1564	958	1261
624	New Mara Bridge	Kenya	-1.3	35.0	c14	1315	145	436	1025	731	1514	925	1220
625	Oldorotua 1	Kenya	-1.3	35.0	OH	1207	104	535	951	743	1415	999	1207

Entry ID	Site Name	Country	Latitude	Longitude	Date Type	Date BP	Date BP SD	Min Chronology (Calibrated BCE/CE)	Max Chronology (Calibrated BCE/CE)	Mean Chronology (Calibrated BCE/CE)	Min Chronology (Calibrated BP - 1950)	Max Chronology (Calibrated BP - 1950)	Mean Chronology (Calibrated BP - 1950)
626	Oldorotua 1	Kenya	-1.3	35.0	OH	2026	89	-254	102	-76	2204	1848	2026
627	Oldorotua 1	Kenya	-1.3	35.0	OH	1296	50	554	754	654	1396	1196	1296
628	Oldorotua 1	Kenya	-1.3	35.0	OH	1039	71	769	1053	911	1181	897	1039
629	Oldorotua 1	Kenya	-1.3	35.0	OH	1357	56	481	705	593	1469	1245	1357
630	Oldorotua 1	Kenya	-1.3	35.0	OH	1332	38	542	694	618	1408	1256	1332
631	Oldorotua 1	Kenya	-1.3	35.0	OH	1338	90	432	792	612	1518	1158	1338
632	Oldorotua 2	Kenya	-1.3	35.0	OH	1483	98	271	663	467	1679	1287	1483
633	Oldorotua 2	Kenya	-1.3	35.0	OH	1400	67	416	684	550	1534	1266	1400
634	Oldorotua 2	Kenya	-1.3	35.0	OH	1541	117	175	643	409	1775	1307	1541
635	Oldorotua 2	Kenya	-1.3	35.0	OH	1413	74	389	685	537	1561	1265	1413
636	Oldorotua 4	Kenya	-1.3	34.6	OH	1400	93	364	736	550	1586	1214	1400
637	Oldorotua 4	Kenya	-1.3	34.6	OH	1426	99	326	722	524	1624	1228	1426
638	Oldorotua 4	Kenya	-1.3	34.6	OH	1366	113	358	810	584	1592	1140	1366
639	Oldorotua 4	Kenya	-1.3	34.6	OH	1808	80	-18	302	142	1968	1648	1808
640	Oldorotua 3	Kenya	-1.3	35.0	OH	1983	51	-135	69	-33	2085	1881	1983
641	Oldorotua 3	Kenya	-1.3	35.0	OH	1808	142	-142	426	142	2092	1524	1808
642	Oldorotua 3	Kenya	-1.3	35.0	OH	2878	39	-1006	-850	-928	2956	2800	2878
643	Oldorotua 3	Kenya	-1.3	35.0	OH	872	35	1008	1148	1078	942	802	872
644	Oldorotua 3	Kenya	-1.3	35.0	OH	2904	38	-1030	-878	-954	2980	2828	2904
645	Oldorotua 3	Kenya	-1.3	35.0	OH	3033	45	-1173	-993	-1083	3123	2943	3033
646	Oldorotua 3	Kenya	-1.3	35.0	OH	2840	100	-1090	-690	-890	3040	2640	2840

Entry ID	Site Name	Country	Latitude	Longitude	Date Type	Date BP	Date BP SD	Min Chronology (Calibrated BCE/CE)	Max Chronology (Calibrated BCE/CE)	Mean Chronology (Calibrated BCE/CE)	Min Chronology (Calibrated BP - 1950)	Max Chronology (Calibrated BP - 1950)	Mean Chronology (Calibrated BP - 1950)
647	Oldorotua 5	Kenya	-1.2	34.6	OH	1985	43	-121	51	-35	2071	1899	1985
648	Oldorotua 5	Kenya	-1.2	34.6	OH	1901	165	-281	379	49	2231	1571	1901
649	Koyage I	Kenya	-1.4	35.2	OH	1664	79	128	444	286	1822	1506	1664
650	Koyage I	Kenya	-1.4	35.2	OH	1447	70	363	643	503	1587	1307	1447
651	Sambo Ngige	Kenya	-1.5	35.5	OH	1326	74	476	772	624	1474	1178	1326
652	Sambo Ngige	Kenya	-1.5	35.5	OH	1346	78	448	760	604	1502	1190	1346
653	Sambo Ngige	Kenya	-1.5	35.5	OH	1419	52	427	635	531	1523	1315	1419
654	Regero	Kenya	-1.3	35.2	OH	1934	79	-142	174	16	2092	1776	1934
655	Regero	Kenya	-1.3	35.2	OH	2042	81	-254	70	-92	2204	1880	2042
656	Sugenya	Kenya	-1.6	35.4	OH	1768	45	92	272	182	1858	1678	1768
657	Sugenya	Kenya	-1.6	35.4	OH	1776	74	26	322	174	1924	1628	1776
658	Sugenya	Kenya	-1.6	35.4	c14	2230	60	-395	-108	-252	2345	2058	2202
659	Sugenya	Kenya	-1.6	35.4	c14	2680	60	-991	-593	-792	2941	2543	2742
660	Mt. Suswa	Kenya	-1.1	36.2	c14	4730	250	-4151	-2787	-3469	6101	4737	5419
661	GuJe 17	Kenya	-1.3	34.9	OH	1529	78	265	577	421	1685	1373	1529
662	GuJe 17	Kenya	-1.3	34.9	OH	1554	91	214	578	396	1736	1372	1554
663	GuJe 18	Kenya	-1.3	34.9	OH	1684	58	150	382	266	1800	1568	1684
664	GuJe 18	Kenya	-1.3	34.9	OH	1643	99	109	505	307	1841	1445	1643
665	GuJf 22	Kenya	-1.2	35.2	OH	1921	78	-127	185	29	2077	1765	1921
666	GuJf 22	Kenya	-1.2	35.2	OH	2027	97	-271	117	-77	2221	1833	2027
667	GuJf 28	Kenya	-1.2	35.2	OH	1600	101	148	552	350	1802	1398	1600

Entry ID	Site Name	Country	Latitude	Longitude	Date Type	Date BP	Date BP SD	Min Chronology (Calibrated BCE/CE)	Max Chronology (Calibrated BCE/CE)	Mean Chronology (Calibrated BCE/CE)	Min Chronology (Calibrated BP - 1950)	Max Chronology (Calibrated BP - 1950)	Mean Chronology (Calibrated BP - 1950)
668	GuJf 28	Kenya	-1.2	35.2	OH	1607	73	197	489	343	1753	1461	1607
669	GuJf 38	Kenya	-1.3	35.1	OH	2228	84	-446	-110	-278	2396	2060	2228
670	GuJf 38	Kenya	-1.3	35.1	OH	1647	29	245	361	303	1705	1589	1647
671	GuJf 50	Kenya	-1.4	35.2	OH	1485	79	307	623	465	1643	1327	1485
672	GuJf 50	Kenya	-1.4	35.2	OH	1756	68	58	330	194	1892	1620	1756
673	GvJe 9	Kenya	-1.2	34.7	OH	1909	86	-131	213	41	2081	1737	1909
674	GvJe 9	Kenya	-1.2	34.7	OH	1714	56	124	348	236	1826	1602	1714
675	GvJe 9	Kenya	-1.2	34.7	OH	1770	68	44	316	180	1906	1634	1770
676	GvJe 10	Kenya	-1.3	34.7	OH	1399	64	423	679	551	1527	1271	1399
677	Olopilukunya	Kenya	-1.8	35.9	c14	2325	70	-742	-169	-456	2692	2119	2406
678	Elmeteitan Obsidian Q	Kenya	-0.7	36.2	c14	2150	25	-346	-59	-203	2296	2009	2153
679	Elmeteitan Obsidian Q	Kenya	-0.7	36.2	c14	2170	20	-352	-102	-227	2302	2052	2177
680	Elmeteitan Obsidian Q	Kenya	-0.7	36.2	c14	2110	25	-176	-46	-111	2126	1996	2061
681	Thimlich Ohingini	Kenya	-0.9	34.3	c14	200	80	1517	1949	1733	433	1	217
682	Marula RS	Kenya	-0.6	36.3	c14	865	220	680	1457	1069	1270	493	882
683	Kibwezi	Kenya	-2.4	38.0	c14	480	200	1216	1948	1582	734	2	368
684	Indapi dapo	Kenya	-1.0	35.9	c14	2420	20	-721	-398	-560	2671	2348	2510
685	Indapi dapo	Kenya	-1.0	35.9	c14	2330	15	-406	-208	-307	2356	2158	2257
686	Oloika 1	Kenya	-1.0	35.8	c14	2420	20	-721	-398	-560	2671	2348	2510
687	Oloika 2	Kenya	-1.1	35.8	c14	2095	15	-152	-47	-100	2102	1997	2050
688	Dilit 01	Kenya	3.5	35.8	c14	3315	25	-1623	-1502	-1563	3573	3452	3513

Entry ID	Site Name	Country	Latitude	Longitude	Date Type	Date BP	Date BP SD	Min Chronology (Calibrated BCE/CE)	Max Chronology (Calibrated BCE/CE)	Mean Chronology (Calibrated BCE/CE)	Min Chronology (Calibrated BP - 1950)	Max Chronology (Calibrated BP - 1950)	Mean Chronology (Calibrated BP - 1950)
689	Songo Mnara	Tanzania	-9.0	39.6	c14	498	25	1410	1455	1433	540	495	518
690	Songo Mnara	Tanzania	-9.0	39.6	c14	582	20	1321	1424	1373	629	526	578
691	Kimu	Tanzania	-5.3	38.6	c14	942	28	1033	1205	1119	917	745	831
692	Kimu	Tanzania	-5.3	38.6	c14	963	28	1027	1176	1102	923	774	849
693	Kimu	Tanzania	-5.3	38.6	c14	1025	30	990	1152	1071	960	798	879
694	Amboni Cave	Tanzania	-5.1	39.0	c14	1590	130	170	770	470	1780	1180	1480
695	Bandarikuu	Tanzania	-5.1	39.8	c14	1225	20	771	890	831	1179	1060	1120
696	Changwehela	Tanzania	-6.3	38.3	c14	870	50	1045	1277	1161	905	673	789
697	Changwehela	Tanzania	-6.3	38.3	c14	650	60	1277	1418	1348	673	532	603
698	Chwaka	Tanzania	-5.0	39.8	c14	1000	30	996	1155	1076	954	795	875
699	Chwaka	Tanzania	-5.0	39.8	c14	750	40	1222	1385	1304	728	565	647
700	Chwaka	Tanzania	-5.0	39.8	c14	750	30	1225	1383	1304	725	567	646
701	Chwaka	Tanzania	-5.0	39.8	c14	890	40	1045	1267	1156	905	683	794
702	Dakawa	Tanzania	-6.3	37.4	c14	1320	70	606	891	749	1344	1059	1202
703	Dakawa	Tanzania	-6.3	37.4	c14	1250	80	660	978	819	1290	972	1131
704	Dakawa	Tanzania	-6.3	37.4	c14	1260	80	655	975	815	1295	975	1135
705	Dakawa	Tanzania	-6.3	37.4	c14	1300	70	641	954	798	1309	996	1153
706	Dakawa	Tanzania	-6.3	37.4	c14	1270	80	650	975	813	1300	975	1138
707	Dakawa	Tanzania	-6.3	37.4	c14	1280	50	665	885	775	1285	1065	1175
708	Dakawa	Tanzania	-6.3	37.4	c14	2300	70	-716	-149	-433	2666	2099	2383
709	Dakawa	Tanzania	-6.3	37.4	c14	1130	70	709	1122	916	1241	828	1035

Entry ID	Site Name	Country	Latitude	Longitude	Date Type	Date BP	Date BP SD	Min Chronology (Calibrated BCE/CE)	Max Chronology (Calibrated BCE/CE)	Mean Chronology (Calibrated BCE/CE)	Min Chronology (Calibrated BP - 1950)	Max Chronology (Calibrated BP - 1950)	Mean Chronology (Calibrated BP - 1950)
710	Dakawa	Tanzania	-6.3	37.4	c14	840	70	1040	1294	1167	910	656	783
711	Gombe	Tanzania	-5.1	39.8	c14	1060	70	776	1179	978	1174	771	973
712	Kaliwa	Tanzania	-5.1	39.8	c14	540	50	1310	1458	1384	640	492	566
713	Kaole	Tanzania	-6.3	38.6	c14	1130	60	773	1029	901	1177	921	1049
714	Kaole	Tanzania	-6.3	38.6	c14	1270	60	658	954	806	1292	996	1144
715	Kaole	Tanzania	-6.3	38.6	c14	720	60	1225	1395	1310	725	555	640
716	Mkiu KI/MA6	Tanzania	-7.4	39.3	c14	1050	50	893	1154	1024	1057	796	927
717	Mkukutu-Kibiti	Tanzania	-7.7	38.9	c14	1670	60	250	547	399	1700	1403	1552
718	Mkukutu-Kibiti	Tanzania	-7.7	38.9	c14	1635	70	253	596	425	1697	1354	1526
719	Mkukutu-Kibiti	Tanzania	-7.7	38.9	c14	1635	70	254	596	425	1696	1354	1525
720	Kilwa Kisiwani	Tanzania	-8.6	39.3	c14	890	100	989	1379	1184	961	571	766
721	Kilwa Kisiwani	Tanzania	-8.6	39.3	c14	1320	110	567	990	779	1383	960	1172
722	Kilwa Kisiwani	Tanzania	-8.6	39.3	c14	1020	100	775	1262	1019	1175	688	932
723	Kilwa Kisiwani	Tanzania	-8.6	39.3	c14	1825	110	-46	525	240	1996	1425	1711
724	Kilwa Kisiwani	Tanzania	-8.6	39.3	c14	447	25	1428	1611	1520	522	339	431
725	Kilwa Kisiwani	Tanzania	-8.6	39.3	c14	686	25	1281	1391	1336	669	559	614
726	Kilwa Kisiwani	Tanzania	-8.6	39.3	c14	1072	27	896	1032	964	1054	918	986
727	Kilwa Kisiwani	Tanzania	-8.6	39.3	c14	964	25	1029	1160	1095	921	790	856
728	Kilwa Kisiwani	Tanzania	-8.6	39.3	c14	970	27	1028	1158	1093	922	792	857
729	Kilwa Kisiwani	Tanzania	-8.6	39.3	c14	949	24	1034	1178	1106	916	772	844
730	Kilwa Kisiwani	Tanzania	-8.6	39.3	c14	1084	28	895	1028	962	1055	922	989

Entry ID	Site Name	Country	Latitude	Longitude	Date Type	Date BP	Date BP SD	Min Chronology (Calibrated BCE/CE)	Max Chronology (Calibrated BCE/CE)	Mean Chronology (Calibrated BCE/CE)	Min Chronology (Calibrated BP - 1950)	Max Chronology (Calibrated BP - 1950)	Mean Chronology (Calibrated BP - 1950)
731	Kilwa Kisiwani	Tanzania	-8.6	39.3	c14	1014	26	992	1151	1072	958	799	879
732	Kilwa Kisiwani	Tanzania	-8.6	39.3	c14	1110	22	893	1019	956	1057	931	994
733	Kilwa Kisiwani	Tanzania	-8.6	39.3	c14	1151	26	774	994	884	1176	956	1066
734	Kilwa Kisiwani	Tanzania	-8.6	39.3	c14	1142	25	884	993	939	1066	957	1012
735	Kilwa Kisiwani	Tanzania	-8.6	39.3	c14	1235	27	692	891	792	1258	1059	1159
736	Kilwa Kisiwani	Tanzania	-8.6	39.3	c14	1134	23	890	993	942	1060	957	1009
737	Kilwa Kisiwani	Tanzania	-8.6	39.3	c14	1121	22	891	1012	952	1059	938	999
738	Kilwa Kisiwani	Tanzania	-8.6	39.3	c14	1096	28	893	1024	959	1057	926	992
739	Kilwa Kisiwani	Tanzania	-8.6	39.3	c14	965	22	1033	1157	1095	917	793	855
740	Kilwa Kisiwani	Tanzania	-8.6	39.3	c14	1078	24	898	1028	963	1052	922	987
741	Kilwa Kisiwani	Tanzania	-8.6	39.3	c14	693	28	1278	1391	1335	672	559	616
742	Kilwa Kisiwani	Tanzania	-8.6	39.3	c14	782	26	1223	1286	1255	727	664	696
743	Kilwa Kisiwani	Tanzania	-8.6	39.3	c14	398	26	1448	1625	1537	502	325	414
744	Kilwa Kisiwani	Tanzania	-8.6	39.3	c14	449	26	1426	1612	1519	524	338	431
745	Kimimba	Tanzania	-5.1	39.8	c14	1885	30	81	240	161	1869	1710	1790
746	Kimimba	Tanzania	-5.1	39.8	c14	1300	40	661	870	766	1289	1080	1185
747	Kinunda Cave	Tanzania	-8.0	39.8	c14	1330	60	640	880	760	1310	1070	1190
748	Kinunda Cave	Tanzania	-8.0	39.8	c14	490	60	1319	1625	1472	631	325	478
749	Kivinja	Tanzania	-7.6	39.2	c14	1515	65	425	655	540	1525	1295	1410
750	Kivinja	Tanzania	-7.6	39.2	c14	1395	70	544	838	691	1406	1112	1259

Entry ID	Site Name	Country	Latitude	Longitude	Date Type	Date BP	Date BP SD	Min Chronology (Calibrated BCE/CE)	Max Chronology (Calibrated BCE/CE)	Mean Chronology (Calibrated BCE/CE)	Min Chronology (Calibrated BP - 1950)	Max Chronology (Calibrated BP - 1950)	Mean Chronology (Calibrated BP - 1950)
751	Kivinja	Tanzania	-7.6	39.2	c14	1110	65	773	1130	952	1177	820	999
752	Kiwangwa	Tanzania	-6.2	38.3	c14	1405	55	576	773	675	1374	1177	1276
753	Kiwangwa	Tanzania	-6.2	38.3	c14	1275	45	671	883	777	1279	1067	1173
754	Kiwangwa	Tanzania	-6.2	38.3	c14	1440	60	532	773	653	1418	1177	1298
755	Kiwangwa	Tanzania	-6.2	38.3	c14	1250	60	665	967	816	1285	983	1134
756	Madola Kiwangwa	Tanzania	-6.3	38.7	c14	3767	33	-2285	-2035	-2160	4235	3985	4110
757	Kwale Island	Tanzania	-7.3	39.5	c14	1555	55	420	637	529	1530	1313	1422
758	Kwale Island	Tanzania	-7.3	39.5	c14	1710	60	238	530	384	1712	1420	1566
759	Kwale Island	Tanzania	-7.3	39.5	c14	710	65	1225	1400	1313	725	550	638
760	Kwelikwiji	Tanzania	-6.2	35.7	c14	3050	85	-1491	-1016	-1254	3441	2966	3204
761	Kwelikwiji	Tanzania	-6.2	35.7	c14	3210	85	-1681	-1230	-1456	3631	3180	3406
762	Limbo	Tanzania	-7.5	39.1	c14	1970	60	-91	223	66	2041	1727	1884
763	Limbo	Tanzania	-7.5	39.1	c14	1980	90	-181	308	64	2131	1642	1887
764	Limbo	Tanzania	-7.5	39.1	c14	1700	60	245	531	388	1705	1419	1562
765	Limbo	Tanzania	-7.5	39.1	c14	1610	60	345	602	474	1605	1348	1477
766	Machaga	Tanzania	-6.2	39.2	c14	2660	40	-902	-771	-837	2852	2721	2787
767	Machaga	Tanzania	-6.2	39.2	c14	4120	40	-2871	-2497	-2684	4821	4447	4634
768	Machaga	Tanzania	-6.2	39.2	c14	1955	75	-109	250	71	2059	1700	1880
769	Masuguru	Tanzania	-6.2	38.3	c14	1290	60	651	891	771	1299	1059	1179
770	Masuguru	Tanzania	-6.2	38.3	c14	1430	60	540	773	657	1410	1177	1294
771	Mduuni	Tanzania	-5.0	39.7	c14	790	30	1220	1286	1253	730	664	697

Entry ID	Site Name	Country	Latitude	Longitude	Date Type	Date BP	Date BP SD	Min Chronology (Calibrated BCE/CE)	Max Chronology (Calibrated BCE/CE)	Mean Chronology (Calibrated BCE/CE)	Min Chronology (Calibrated BP - 1950)	Max Chronology (Calibrated BP - 1950)	Mean Chronology (Calibrated BP - 1950)
772	Misasa	Tanzania	-7.5	39.2	c14	1975	50	-52	204	76	2002	1746	1874
773	Misasa	Tanzania	-7.3	39.1	c14	1725	45	240	428	334	1710	1522	1616
774	Misasa	Tanzania	-7.3	39.1	c14	1295	55	657	882	770	1293	1068	1181
775	Misasa	Tanzania	-7.3	39.1	c14	1485	50	439	667	553	1511	1283	1397
776	Misasa	Tanzania	-7.3	39.1	c14	2470	70	-771	-405	-588	2721	2355	2538
777	Misasa	Tanzania	-7.3	39.1	c14	2940	70	-1377	-922	-1150	3327	2872	3100
778	Misasa	Tanzania	-7.3	39.1	c14	1960	60	-54	227	87	2004	1723	1864
779	Mlongo	Tanzania	-7.9	39.6	c14	1740	60	204	526	365	1746	1424	1585
780	Mpiji	Tanzania	-6.9	38.9	c14	1340	60	609	876	743	1341	1074	1208
781	Mpiji	Tanzania	-6.9	38.9	c14	1420	60	547	773	660	1403	1177	1290
782	Mpiji	Tanzania	-6.9	38.9	c14	1390	80	543	876	710	1407	1074	1241
783	Tumbe	Tanzania	-5.0	39.8	c14	1370	40	609	774	692	1341	1176	1259
784	Tumbe	Tanzania	-5.0	39.8	c14	1310	30	658	836	747	1292	1114	1203
785	Tumbe	Tanzania	-5.0	39.8	c14	1280	40	670	880	775	1280	1070	1175
786	Tumbe	Tanzania	-5.0	39.8	c14	1180	40	774	987	881	1176	963	1070
787	Tumbe	Tanzania	-5.0	39.8	c14	230	30	1640	1948	1794	310	2	156
788	Tumbe	Tanzania	-5.0	39.8	c14	1150	40	774	1017	896	1176	933	1055
789	Tumbe	Tanzania	-5.0	39.8	c14	1160	40	773	994	884	1177	956	1067
790	Tumbe	Tanzania	-5.0	39.8	c14	1300	40	661	870	766	1289	1080	1185
791	Ukunju Cave	Tanzania	-8.0	39.8	c14	2880	60	-766	-344	-555	2716	2294	2505
792	Ukunju Cave	Tanzania	-8.0	39.8	c14	2810	60	-716	-225	-471	2666	2175	2421

Entry ID	Site Name	Country	Latitude	Longitude	Date Type	Date BP	Date BP SD	Min Chronology (Calibrated BCE/CE)	Max Chronology (Calibrated BCE/CE)	Mean Chronology (Calibrated BCE/CE)	Min Chronology (Calibrated BP - 1950)	Max Chronology (Calibrated BP - 1950)	Mean Chronology (Calibrated BP - 1950)
793	Kua	Tanzania	-7.9	39.8	c14	531	25	1399	1447	1423	551	503	527
794	Kua	Tanzania	-7.9	39.8	c14	470	25	1418	1479	1449	532	471	502
795	Kua	Tanzania	-7.9	39.8	c14	263	30	1519	1803	1661	431	147	289
796	Nkese	Tanzania	-4.8	38.4	c14	1780	70	85	428	257	1865	1522	1694
797	Nkese	Tanzania	-4.8	38.4	c14	2020	100	-352	244	-54	2302	1706	2004
798	Nkese	Tanzania	-4.8	38.4	c14	1800	30	208	360	284	1742	1590	1666
799	Mikindani Bay	Tanzania	-10.3	40.1	c14	2195	35	-366	-109	-238	2316	2059	2188
800	Pemba Village	Tanzania	-10.3	40.1	c14	1560	35	425	600	513	1525	1350	1438
801	Pemba Village	Tanzania	-10.3	40.1	c14	1480	35	550	650	600	1400	1300	1350
802	Mikindani Region	Tanzania	-10.3	40.1	c14	1070	35	892	1101	997	1058	849	954
803	Kwa Mgogo	Tanzania	-3.7	37.7	c14	1220	40	687	969	828	1263	981	1122
804	Kwa Mgogo	Tanzania	-3.7	37.7	c14	1060	50	890	1152	1021	1060	798	929
805	Gonja Maore	Tanzania	-3.7	37.7	c14	1080	115	692	1215	954	1258	735	997
806	Gonja Maore	Tanzania	-3.7	37.7	c14	380	40	1455	1632	1544	495	318	407
807	Jiko Chongweni Hill	Tanzania	-3.7	37.7	c14	880	50	1045	1273	1159	905	677	791
808	Bombo Kaburi	Tanzania	-3.7	37.7	c14	1730	115	75	590	333	1875	1360	1618
809	Makangale	Tanzania	-4.9	39.7	c14	1287	30	670	868	769	1280	1082	1181
810	Makangale	Tanzania	-4.9	39.7	c14	1253	30	683	886	785	1267	1064	1166
811	Makangale	Tanzania	-4.9	39.7	c14	1188	30	772	975	874	1178	975	1077
812	Makangale	Tanzania	-4.9	39.7	c14	2615	38	-831	-551	-691	2781	2501	2641
813	Makangale	Tanzania	-4.9	39.7	c14	1419	31	593	760	677	1357	1190	1274

Entry ID	Site Name	Country	Latitude	Longitude	Date Type	Date BP	Date BP SD	Min Chronology (Calibrated BCE/CE)	Max Chronology (Calibrated BCE/CE)	Mean Chronology (Calibrated BCE/CE)	Min Chronology (Calibrated BP - 1950)	Max Chronology (Calibrated BP - 1950)	Mean Chronology (Calibrated BP - 1950)
814	Makangale	Tanzania	-4.9	39.7	c14	994	20	1022	1153	1088	928	797	863
815	Makangale	Tanzania	-4.9	39.7	c14	998	20	1021	1153	1087	929	797	863
816	Makangale	Tanzania	-4.9	39.7	c14	1271	20	680	875	778	1270	1075	1173
817	Makangale	Tanzania	-4.9	39.7	c14	1281	20	675	851	763	1275	1099	1187
818	Makangale	Tanzania	-4.9	39.7	c14	1075	20	899	1029	964	1051	921	986
819	Makangale	Tanzania	-4.9	39.7	c14	623	20	1303	1404	1354	647	546	597
820	Makangale	Tanzania	-4.9	39.7	c14	1520	30	480	643	562	1470	1307	1389
821	Fukuchani	Tanzania	-5.8	39.3	c14	1325	23	665	773	719	1285	1177	1231
822	Fukuchani	Tanzania	-5.8	39.3	c14	1269	30	678	880	779	1272	1070	1171
823	Fukuchani	Tanzania	-5.8	39.3	c14	1428	30	591	674	633	1359	1276	1318
824	Unguja Ukuu	Tanzania	-6.3	39.4	c14	1210	150	586	1160	873	1364	790	1077
825	Unguja Ukuu	Tanzania	-6.3	39.4	c14	1380	110	435	953	694	1515	997	1256
826	Unguja Ukuu	Tanzania	-6.3	39.4	c14	950	100	896	1279	1088	1054	671	863
827	Unguja Ukuu	Tanzania	-6.3	39.4	c14	1670	100	204	637	421	1746	1313	1530
828	Unguja Ukuu	Tanzania	-6.3	39.4	c14	1520	110	258	772	515	1692	1178	1435
829	Unguja Ukuu	Tanzania	-6.3	39.4	c14	1290	100	605	988	797	1345	962	1154
830	Unguja Ukuu	Tanzania	-6.3	39.4	c14	1200	100	655	1030	843	1295	920	1108
831	Unguja Ukuu	Tanzania	-6.3	39.4	c14	1350	100	541	968	755	1409	982	1196
832	Unguja Ukuu	Tanzania	-6.3	39.4	c14	1300	60	651	886	769	1299	1064	1182
833	Unguja Ukuu	Tanzania	-6.3	39.4	c14	1460	60	439	769	604	1511	1181	1346
834	Unguja Ukuu	Tanzania	-6.3	39.4	c14	1066	23	899	1034	967	1051	916	984

Entry ID	Site Name	Country	Latitude	Longitude	Date Type	Date BP	Date BP SD	Min Chronology (Calibrated BCE/CE)	Max Chronology (Calibrated BCE/CE)	Mean Chronology (Calibrated BCE/CE)	Min Chronology (Calibrated BP - 1950)	Max Chronology (Calibrated BP - 1950)	Mean Chronology (Calibrated BP - 1950)
835	Unguja Ukuu	Tanzania	-6.3	39.4	c14	1178	25	773	986	880	1177	964	1071
836	Unguja Ukuu	Tanzania	-6.3	39.4	c14	1266	35	679	882	781	1271	1068	1170
837	Unguja Ukuu	Tanzania	-6.3	39.4	c14	1310	31	658	837	748	1292	1113	1203
838	Unguja Ukuu	Tanzania	-6.3	39.4	c14	1403	28	603	766	685	1347	1184	1266
839	Unguja Ukuu	Tanzania	-6.3	39.4	c14	1318	23	666	773	720	1284	1177	1231
840	Unguja Ukuu	Tanzania	-6.3	39.4	c14	1305	28	661	838	750	1289	1112	1201
841	Unguja Ukuu	Tanzania	-6.3	39.4	c14	1372	25	641	774	708	1309	1176	1243
842	Unguja Ukuu	Tanzania	-6.3	39.4	c14	1390	25	608	770	689	1342	1180	1261
843	Unguja Ukuu	Tanzania	-6.3	39.4	c14	1342	24	655	774	715	1295	1176	1236
844	Unguja Ukuu	Tanzania	-6.3	39.4	c14	1280	26	675	870	773	1275	1080	1178
845	Unguja Ukuu	Tanzania	-6.3	39.4	c14	1367	26	643	774	709	1307	1176	1242
846	Unguja Ukuu	Tanzania	-6.3	39.4	c14	1151	26	775	994	885	1175	956	1066
847	Unguja Ukuu	Tanzania	-6.3	39.4	c14	1244	27	690	887	789	1260	1063	1162
848	Unguja Ukuu	Tanzania	-6.3	39.4	c14	1287	25	670	852	761	1280	1098	1189
849	Unguja Ukuu	Tanzania	-6.3	39.4	c14	1226	25	707	894	801	1243	1056	1150
850	Unguja Ukuu	Tanzania	-6.3	39.4	c14	1317	24	664	774	719	1286	1176	1231
851	Unguja Ukuu	Tanzania	-6.3	39.4	c14	1265	23	681	880	781	1269	1070	1170
852	Unguja Ukuu	Tanzania	-6.3	39.4	c14	1232	26	703	892	798	1247	1058	1153
853	Unguja Ukuu	Tanzania	-6.3	39.4	c14	1305	24	663	830	747	1287	1120	1204
854	Unguja Ukuu	Tanzania	-6.3	39.4	c14	1314	26	660	775	718	1290	1175	1233
855	Unguja Ukuu	Tanzania	-6.3	39.4	c14	1245	22	693	885	789	1257	1065	1161

Entry ID	Site Name	Country	Latitude	Longitude	Date Type	Date BP	Date BP SD	Min Chronology (Calibrated BCE/CE)	Max Chronology (Calibrated BCE/CE)	Mean Chronology (Calibrated BCE/CE)	Min Chronology (Calibrated BP - 1950)	Max Chronology (Calibrated BP - 1950)	Mean Chronology (Calibrated BP - 1950)
856	Unguja Ukuu	Tanzania	-6.3	39.4	c14	1282	24	674	861	768	1276	1089	1183
857	Unguja Ukuu	Tanzania	-6.3	39.4	c14	1301	24	664	835	750	1286	1115	1201
858	Unguja Ukuu	Tanzania	-6.3	39.4	c14	1265	45	672	887	780	1278	1063	1171
859	Unguja Ukuu	Tanzania	-6.3	39.4	c14	1611	20	421	537	479	1529	1413	1471
860	Unguja Ukuu	Tanzania	-6.3	39.4	c14	1482	20	572	645	609	1378	1305	1342
861	Unguja Ukuu	Tanzania	-6.3	39.4	c14	1413	20	605	673	639	1345	1277	1311
862	Unguja Ukuu	Tanzania	-6.3	39.4	c14	350	100	1406	1948	1677	544	2	273
863	Unguja Ukuu	Tanzania	-6.3	39.4	c14	400	100	1325	1802	1564	625	148	387
864	Unguja Ukuu	Tanzania	-6.3	39.4	c14	1610	26	418	541	480	1532	1409	1471
865	Unguja Ukuu	Tanzania	-6.3	39.4	c14	2084	26	272	626	449	1678	1324	1501
866	Unguja Ukuu	Tanzania	-6.3	39.4	c14	2056	32	316	665	491	1634	1285	1460
867	Unguja Ukuu	Tanzania	-6.3	39.4	c14	1233	26	705	891	798	1245	1059	1152
868	Unguja Ukuu	Tanzania	-6.3	39.4	c14	1925	26	453	784	619	1497	1166	1332
869	Unguja Ukuu	Tanzania	-6.3	39.4	c14	1799	25	597	918	758	1353	1032	1193
870	Unguja Ukuu	Tanzania	-6.3	39.4	c14	1659	27	363	530	447	1587	1420	1504
871	Unguja Ukuu	Tanzania	-6.3	39.4	c14	1245	33	682	891	787	1268	1059	1164
872	Unguja Ukuu	Tanzania	-6.3	39.4	c14	1240	22	708	886	797	1242	1064	1153
873	Unguja Ukuu	Tanzania	-6.3	39.4	c14	1616	22	419	535	477	1531	1415	1473
874	Unguja Ukuu	Tanzania	-6.3	39.4	c14	2856	26	-1109	-913	-1011	3059	2863	2961
875	Unguja Ukuu	Tanzania	-6.3	39.4	c14	1283	27	674	868	771	1276	1082	1179

Entry ID	Site Name	Country	Latitude	Longitude	Date Type	Date BP	Date BP SD	Min Chronology (Calibrated BCE/CE)	Max Chronology (Calibrated BCE/CE)	Mean Chronology (Calibrated BCE/CE)	Min Chronology (Calibrated BP - 1950)	Max Chronology (Calibrated BP - 1950)	Mean Chronology (Calibrated BP - 1950)
876	Unguja Ukuu	Tanzania	-6.3	39.4	c14	1257	36	680	886	783	1270	1064	1167
877	Unguja Ukuu	Tanzania	-6.3	39.4	c14	4362	35	-3086	-2892	-2989	5036	4842	4939
878	Unguja Ukuu	Tanzania	-6.3	39.4	c14	4687	32	-3524	-3367	-3446	5474	5317	5396
879	Kuumbi Cave	Tanzania	-6.4	39.6	c14	1980	45	-53	202	75	2003	1748	1876
880	Kuumbi Cave	Tanzania	-6.4	39.6	c14	1815	40	129	358	244	1821	1592	1707
881	Kuumbi Cave	Tanzania	-6.4	39.6	c14	4005	40	-2623	-2347	-2485	4573	4297	4435
882	Kuumbi Cave	Tanzania	-6.4	39.6	c14	5330	45	-4319	-3994	-4157	6269	5944	6107
883	Kuumbi Cave	Tanzania	-6.4	39.6	c14	1535	30	438	638	538	1512	1312	1412
884	Kuumbi Cave	Tanzania	-6.4	39.6	c14	1525	40	437	644	541	1513	1306	1410
885	Kuumbi Cave	Tanzania	-6.4	39.6	c14	1590	30	422	571	497	1528	1379	1454
886	Kuumbi Cave	Tanzania	-6.4	39.6	c14	5110	35	-3972	-3792	-3882	5922	5742	5832
887	Kuumbi Cave	Tanzania	-6.4	39.6	c14	2110	30	-190	10	-90	2140	1940	2040
888	Kuumbi Cave	Tanzania	-6.4	39.6	c14	1245	55	670	964	817	1280	986	1133
889	Kuumbi Cave	Tanzania	-6.4	39.6	c14	1899	20	82	215	149	1868	1735	1802
890	Kuumbi Cave	Tanzania	-6.4	39.6	c14	5332	20	-4241	-4050	-4146	6191	6000	6096
891	Kuumbi Cave	Tanzania	-6.4	39.6	OSL	590	50	1326	1526	1426	624	424	524
892	Kuumbi Cave	Tanzania	-6.4	39.6	c14	4467	21	-3334	-2938	-3136	5284	4888	5086
893	Kuumbi Cave	Tanzania	-6.4	39.6	c14	1622	21	417	534	476	1533	1416	1475
894	Kuumbi Cave	Tanzania	-6.4	39.6	c14	4459	20	-3330	-2932	-3131	5280	4882	5081
895	Kuumbi Cave	Tanzania	-6.4	39.6	OSL	1360	125	406	906	656	1544	1044	1294
896	Kuumbi Cave	Tanzania	-6.4	39.6	OSL	685	85	1161	1501	1331	789	449	619

Entry ID	Site Name	Country	Latitude	Longitude	Date Type	Date BP	Date BP SD	Min Chronology (Calibrated BCE/CE)	Max Chronology (Calibrated BCE/CE)	Mean Chronology (Calibrated BCE/CE)	Min Chronology (Calibrated BP - 1950)	Max Chronology (Calibrated BP - 1950)	Mean Chronology (Calibrated BP - 1950)
897	Kuumbi Cave	Tanzania	-6.4	39.6	c14	3100	22	-1418	-1268	-1343	3368	3218	3293
898	Kuumbi Cave	Tanzania	-6.4	39.6	c14	4887	20	-3707	-3537	-3622	5657	5487	5572
899	Kuumbi Cave	Tanzania	-6.4	39.6	OSL	960	80	896	1216	1056	1054	734	894
900	Kuumbi Cave	Tanzania	-6.4	39.6	c14	1479	23	573	647	610	1377	1303	1340
901	Kuumbi Cave	Tanzania	-6.4	39.6	c14	5082	23	-3955	-3790	-3873	5905	5740	5823
902	Juani Primary School	Tanzania	-8.0	39.8	c14	1153	25	775	994	885	1175	956	1066
903	Juani Primary School	Tanzania	-8.0	39.8	c14	1612	21	420	537	479	1530	1413	1472
904	Juani Primary School	Tanzania	-8.0	39.8	c14	1604	20	423	540	482	1527	1410	1469
905	Juani Primary School	Tanzania	-8.0	39.8	c14	1173	20	774	985	880	1176	965	1071
906	Juani Primary School	Tanzania	-8.0	39.8	c14	1184	21	772	975	874	1178	975	1077
907	Juani Primary School	Tanzania	-8.0	39.8	c14	1181	20	772	975	874	1178	975	1077
908	Juani Primary School	Tanzania	-8.0	39.8	c14	1646	23	390	531	461	1560	1419	1490
909	Juani Primary School	Tanzania	-8.0	39.8	c14	1002	21	999	1153	1076	951	797	874
910	Juani Primary School	Tanzania	-8.0	39.8	c14	930	24	1043	1209	1126	907	741	824
911	Kirando 11	Tanzania	-7.0	30.6	c14	595	55	1296	1438	1367	654	512	583
912	Kirando 58	Tanzania	-7.0	30.6	c14	1040	80	778	1216	997	1172	734	953
913	Mbinga 4	Tanzania	-10.9	35.0	c14	1235	55	676	970	823	1274	980	1127
914	Mbinga 4	Tanzania	-10.9	35.0	c14	1090	110	690	1210	950	1260	740	1000
915	Ludewa 15	Tanzania	-10.1	34.7	c14	1180	90	671	1029	850	1279	921	1100
916	Ngorongoro Burial	Tanzania	-2.7	35.6	c14	2260	180	-787	115	-336	2737	1835	2286
917	Serengeti	Tanzania	-2.0	34.7	c14	755	135	1028	1435	1232	922	515	719

Entry ID	Site Name	Country	Latitude	Longitude	Date Type	Date BP	Date BP SD	Min Chronology (Calibrated BCE/CE)	Max Chronology (Calibrated BCE/CE)	Mean Chronology (Calibrated BCE/CE)	Min Chronology (Calibrated BP - 1950)	Max Chronology (Calibrated BP - 1950)	Mean Chronology (Calibrated BP - 1950)
918	Serengeti	Tanzania	-2.0	34.7	c14	260	100	1465	1948	1707	485	2	244
919	Serengeti	Tanzania	-2.0	34.7	c14	225	105	1494	1949	1722	456	1	229
920	Serengeti	Tanzania	-2.0	34.7	c14	205	120	1492	1949	1721	458	1	230
921	Serengeti	Tanzania	-2.5	34.8	c14	3000	140	-1504	-839	-1172	3454	2789	3122
922	Seronera	Tanzania	-2.4	34.8	c14	2020	115	-361	315	-23	2311	1635	1973
923	Seronera	Tanzania	-2.4	34.8	c14	265	100	1460	1948	1704	490	2	246
924	Seronera	Tanzania	-2.4	34.8	c14	280	95	1454	1948	1701	496	2	249
925	Chabula-Nguru Hills	Tanzania	-6.2	37.7	c14	3025	85	-1441	-1005	-1223	3391	2955	3173
926	Mumba RS	Tanzania	-2.2	35.7	c14	920	30	1043	1217	1130	907	733	820
927	Mumba RS	Tanzania	-2.2	35.7	c14	302	38	1486	1795	1641	464	155	310
928	Mumba RS	Tanzania	-2.2	35.7	c14	345	30	1480	1642	1561	470	308	389
929	Mumba RS	Tanzania	-2.2	35.7	c14	4860	100	-3933	-3372	-3653	5883	5322	5603
930	Mumba RS	Tanzania	-2.2	35.7	c14	4890	70	-3910	-3384	-3647	5860	5334	5597
931	Mumba RS	Tanzania	-2.2	35.7	c14	4190	20	-2883	-2636	-2760	4833	4586	4710
932	Mumba RS	Tanzania	-2.2	35.7	c14	1843	60	68	364	216	1882	1586	1734
933	Mumba RS	Tanzania	-2.2	35.7	c14	1780	80	75	523	299	1875	1427	1651
934	Mumba RS	Tanzania	-2.2	35.7	c14	1710	25	256	418	337	1694	1532	1613
935	Ufana Valley	Tanzania	-4.3	35.3	c14	2855	20	-1106	-911	-1009	3056	2861	2959
936	Daumboy RS	Tanzania	-4.3	35.3	c14	1120	70	771	1141	956	1179	809	994
937	Daumboy RS	Tanzania	-4.3	35.3	c14	4060	70	-2874	-2352	-2613	4824	4302	4563
938	Baura 1	Tanzania	-4.9	35.9	c14	2500	40	-774	-420	-597	2724	2370	2547

Entry ID	Site Name	Country	Latitude	Longitude	Date Type	Date BP	Date BP SD	Min Chronology (Calibrated BCE/CE)	Max Chronology (Calibrated BCE/CE)	Mean Chronology (Calibrated BCE/CE)	Min Chronology (Calibrated BP - 1950)	Max Chronology (Calibrated BP - 1950)	Mean Chronology (Calibrated BP - 1950)
939	Baura 1	Tanzania	-4.9	35.9	c14	460	40	1407	1620	1514	543	330	437
940	Lusangi 1	Tanzania	-4.8	35.7	c14	1660	100	214	637	426	1736	1313	1525
941	Markasi Lusangi 1	Tanzania	-4.8	35.7	c14	1030	40	907	1156	1032	1043	794	919
942	Markasi Lusangi 2	Tanzania	-4.8	35.7	c14	4510	70	-3369	-2929	-3149	5319	4879	5099
943	Markasi Lusangi 2	Tanzania	-4.8	35.7	c14	760	60	1178	1393	1286	772	557	665
944	Luxmanda	Tanzania	-4.3	35.3	c14	2145	25	-343	-58	-201	2293	2008	2151
945	Luxmanda	Tanzania	-4.3	35.3	c14	2395	25	-542	-389	-466	2492	2339	2416
946	Luxmanda	Tanzania	-4.3	35.3	c14	2515	25	-778	-514	-646	2728	2464	2596
947	Luxmanda	Tanzania	-4.3	35.3	c14	2580	25	-805	-551	-678	2755	2501	2628
948	Luxmanda	Tanzania	-4.3	35.3	c14	2880	20	-1118	-931	-1025	3068	2881	2975
949	Luxmanda	Tanzania	-4.3	35.3	c14	2900	20	-1192	-936	-1064	3142	2886	3014
950	Luxmanda	Tanzania	-4.3	35.3	c14	2905	20	-1196	-940	-1068	3146	2890	3018
951	Luxmanda	Tanzania	-4.3	35.3	c14	2905	20	-1196	-940	-1068	3146	2890	3018
952	Luxmanda	Tanzania	-4.3	35.3	c14	2925	20	-1203	-1012	-1108	3153	2962	3058
953	Luxmanda	Tanzania	-4.3	35.3	c14	2960	25	-1258	-1021	-1140	3208	2971	3090
954	Sonai RS	Tanzania	-3.4	35.4	c14	465	30	1415	1495	1455	535	455	495
955	Sonai RS	Tanzania	-3.4	35.4	c14	1220	30	706	959	833	1244	991	1118
956	Sonai RS	Tanzania	-3.4	35.4	c14	1254	30	683	886	785	1267	1064	1166
957	Gileodabeshta 2	Tanzania	-3.6	35.2	c14	2910	20	-1199	-991	-1095	3149	2941	3045
958	Gileodabeshta 2	Tanzania	-3.6	35.2	c14	310	30	1499	1662	1581	451	288	370
959	Gol Kopjes	Tanzania	-2.7	35.0	c14	3300	300	-2439	-837	-1638	4389	2787	3588

Entry ID	Site Name	Country	Latitude	Longitude	Date Type	Date BP	Date BP SD	Min Chronology (Calibrated BCE/CE)	Max Chronology (Calibrated BCE/CE)	Mean Chronology (Calibrated BCE/CE)	Min Chronology (Calibrated BP - 1950)	Max Chronology (Calibrated BP - 1950)	Mean Chronology (Calibrated BP - 1950)
960	Gol Kopjes	Tanzania	-2.7	35.0	c14	4895	260	-4317	-2974	-3646	6267	4924	5596
961	Gol Kopjes	Tanzania	-2.7	35.0	c14	280	120	1452	1948	1700	498	2	250
962	Nasera RS	Tanzania	-2.6	35.2	c14	2060	100	-360	209	-76	2310	1741	2026
963	Nasera RS	Tanzania	-2.6	35.2	c14	2180	200	-766	235	-266	2716	1715	2216
964	Nasera RS	Tanzania	-2.6	35.2	c14	4720	105	-3703	-3103	-3403	5653	5053	5353
965	Lululampembele	Tanzania	-3.9	34.7	c14	3830	180	-2864	-1768	-2316	4814	3718	4266
966	Kandaga RS	Tanzania	-4.3	35.5	c14	3375	180	-2192	-1222	-1707	4142	3172	3657
967	Kwa Mwango-Isanzu	Tanzania	-4.6	34.5	c14	3270	110	-1874	-1262	-1568	3824	3212	3518
968	Kirumi Isumbirira	Tanzania	-4.6	34.4	c14	3665	140	-2460	-1681	-2071	4410	3631	4021
969	Engaruka	Tanzania	-3.0	36.0	c14	3554	30	-1954	-1750	-1852	3904	3700	3802
970	Engaruka	Tanzania	-3.0	36.0	c14	1015	30	992	1153	1073	958	797	878
971	Engaruka	Tanzania	-3.0	36.0	c14	1085	30	894	1028	961	1056	922	989
972	Engaruka	Tanzania	-3.0	36.0	c14	490	90	1303	1636	1470	647	314	481
973	Engaruka	Tanzania	-3.0	36.0	c14	1230	120	599	1045	822	1351	905	1128
974	Engaruka	Tanzania	-3.0	36.0	c14	1620	90	251	639	445	1699	1311	1505
975	Engaruka	Tanzania	-3.0	36.0	c14	280	90	1454	1948	1701	496	2	249
976	Engaruka	Tanzania	-3.0	36.0	c14	220	80	1509	1949	1729	441	1	221
977	Engaruka	Tanzania	-3.0	36.0	c14	320	60	1453	1799	1626	497	151	324
978	Engaruka	Tanzania	-3.0	36.0	c14	250	60	1497	1949	1723	453	1	227
979	Engaruka	Tanzania	-3.0	36.0	c14	470	110	1295	1661	1478	655	289	472
980	Engaruka	Tanzania	-3.0	36.0	c14	300	100	1443	1948	1696	507	2	255

Entry ID	Site Name	Country	Latitude	Longitude	Date Type	Date BP	Date BP SD	Min Chronology (Calibrated BCE/CE)	Max Chronology (Calibrated BCE/CE)	Mean Chronology (Calibrated BCE/CE)	Min Chronology (Calibrated BP - 1950)	Max Chronology (Calibrated BP - 1950)	Mean Chronology (Calibrated BP - 1950)
981	Engaruka	Tanzania	-3.0	36.0	c14	200	100	1502	1950	1726	448	0	224
982	Engaruka	Tanzania	-3.0	36.0	c14	415	50	1432	1632	1532	518	318	418
983	Engaruka	Tanzania	-3.0	36.0	c14	225	40	1533	1948	1741	417	2	210
984	Engaruka	Tanzania	-3.0	36.0	c14	315	40	1477	1665	1571	473	285	379
985	Engaruka	Tanzania	-3.0	36.0	c14	365	40	1459	1635	1547	491	315	403
986	Engaruka	Tanzania	-3.0	36.0	c14	220	90	1503	1949	1726	447	1	224
987	Engaruka	Tanzania	-3.0	36.0	c14	240	60	1506	1949	1728	444	1	223
988	Engaruka	Tanzania	-3.0	36.0	c14	450	30	1423	1615	1519	527	335	431
989	Engaruka	Tanzania	-3.0	36.0	c14	235	30	1637	1948	1793	313	2	158
990	Engaruka	Tanzania	-3.0	36.0	c14	175	40	1664	1948	1806	286	2	144
991	Engaruka	Tanzania	-3.0	36.0	c14	185	40	1658	1948	1803	292	2	147
992	Engaruka	Tanzania	-3.0	36.0	c14	190	80	1517	1950	1734	433	0	217
993	Kemondo 2	Tanzania	-1.5	31.7	c14	1590	60	377	635	506	1573	1315	1444
994	Kemondo 2	Tanzania	-1.5	31.7	c14	1820	110	-44	526	241	1994	1424	1709
995	Kemondo 2	Tanzania	-1.5	31.7	c14	1450	60	440	772	606	1510	1178	1344
996	Kemondo 2	Tanzania	-1.5	31.7	c14	1870	120	-145	434	145	2095	1516	1806
997	Kemondo 2	Tanzania	-1.5	31.7	c14	1826	42	123	343	233	1827	1607	1717
998	Kemondo 2	Tanzania	-1.5	31.7	c14	1860	50	67	338	203	1883	1612	1748
999	Kemondo 2	Tanzania	-1.5	31.7	c14	1930	120	-177	405	114	2127	1545	1836
1000	Kemondo 2	Tanzania	-1.5	31.7	c14	2120	120	-399	201	-99	2349	1749	2049
1001	Kemondo 2	Tanzania	-1.5	31.7	c14	1410	60	553	774	664	1397	1176	1287

Entry ID	Site Name	Country	Latitude	Longitude	Date Type	Date BP	Date BP SD	Min Chronology (Calibrated BCE/CE)	Max Chronology (Calibrated BCE/CE)	Mean Chronology (Calibrated BCE/CE)	Min Chronology (Calibrated BP - 1950)	Max Chronology (Calibrated BP - 1950)	Mean Chronology (Calibrated BP - 1950)
1002	Kemondo 2	Tanzania	-1.5	31.7	c14	1480	60	436	673	555	1514	1277	1396
1003	Kemondo 2	Tanzania	-1.5	31.7	c14	1620	60	263	596	430	1687	1354	1521
1004	Kemondo 2	Tanzania	-1.5	31.7	c14	1440	110	415	878	647	1535	1072	1304
1005	Kemondo 2	Tanzania	-1.5	31.7	c14	1580	60	392	638	515	1558	1312	1435
1006	Kemondo 2	Tanzania	-1.5	31.7	c14	1670	120	132	640	386	1818	1310	1564
1007	Kemondo 3	Tanzania	-1.5	31.7	c14	1660	70	250	575	413	1700	1375	1538
1008	Kemondo 3	Tanzania	-1.5	31.7	c14	1717	37	250	420	335	1700	1530	1615
1009	Kemondo 3	Tanzania	-1.5	31.7	c14	1560	80	364	654	509	1586	1296	1441
1010	Kemondo 3	Tanzania	-1.5	31.7	c14	1620	70	256	632	444	1694	1318	1506
1011	Kemondo 3	Tanzania	-1.5	31.7	c14	1830	100	-44	430	193	1994	1520	1757
1012	Kemondo 3	Tanzania	-1.5	31.7	c14	2520	100	-824	-393	-609	2774	2343	2559
1013	Kemondo 3	Tanzania	-1.5	31.7	c14	1920	120	-166	406	120	2116	1544	1830
1014	Kemondo 3	Tanzania	-1.5	31.7	c14	1500	60	435	659	547	1515	1291	1403
1015	Kemondo 3	Tanzania	-1.5	31.7	c14	1684	55	250	537	394	1700	1413	1557
1016	Kemondo 3	Tanzania	-1.5	31.7	c14	1740	70	139	529	334	1811	1421	1616
1017	Machame Kisiki	Tanzania	-3.2	37.2	c14	1828	29	130	336	233	1820	1614	1717
1018	Machame Kisiki	Tanzania	-3.2	37.2	c14	1531	29	438	640	539	1512	1310	1411
1019	Rugamora Mahe	Tanzania	-1.7	31.7	c14	2470	110	-811	-211	-511	2761	2161	2461
1020	Rugamora Mahe	Tanzania	-1.7	31.7	c14	1830	110	-49	524	238	1999	1426	1713
1021	Rugamora Mahe	Tanzania	-1.7	31.7	c14	1780	150	-56	601	273	2006	1349	1678
1022	Rugamora Mahe	Tanzania	-1.7	31.7	c14	2560	100	-896	-401	-649	2846	2351	2599

Entry ID	Site Name	Country	Latitude	Longitude	Date Type	Date BP	Date BP SD	Min Chronology (Calibrated BCE/CE)	Max Chronology (Calibrated BCE/CE)	Mean Chronology (Calibrated BCE/CE)	Min Chronology (Calibrated BP - 1950)	Max Chronology (Calibrated BP - 1950)	Mean Chronology (Calibrated BP - 1950)
1023	Rugamora Mahe	Tanzania	-1.7	31.7	c14	2500	115	-894	-230	-562	2844	2180	2512
1024	Rugamora Mahe	Tanzania	-1.7	31.7	c14	2400	115	-791	-194	-493	2741	2144	2443
1025	Rugamora Mahe	Tanzania	-1.7	31.7	c14	1890	115	-137	416	140	2087	1534	1811
1026	Makongo	Tanzania	-1.6	31.5	c14	965	100	894	1274	1084	1056	676	866
1027	Makongo	Tanzania	-1.6	31.5	c14	1910	100	-106	380	137	2056	1570	1813
1028	Makongo	Tanzania	-1.6	31.5	c14	1040	100	774	1221	998	1176	729	953
1029	Mwanga A	Tanzania	-3.7	37.6	c14	862	40	1051	1277	1164	899	673	786
1030	Mwanga C	Tanzania	-3.7	37.6	c14	560	50	1305	1451	1378	645	499	572
1031	Mwanga G	Tanzania	-3.7	37.6	c14	366	45	1456	1640	1548	494	310	402
1032	Mwanga G	Tanzania	-3.7	37.6	c14	873	36	1050	1273	1162	900	677	789
1033	Campi ya Simba	Tanzania	-3.6	37.7	c14	900	36	1042	1257	1150	908	693	801
1034	Campi ya Simba	Tanzania	-3.6	37.7	c14	927	36	1040	1215	1128	910	735	823
1035	Campi ya Simba	Tanzania	-3.6	37.7	c14	945	36	1030	1208	1119	920	742	831
1036	Campi ya Simba	Tanzania	-3.6	37.7	c14	900	36	1042	1257	1150	908	693	801
1037	Ngalanga	Tanzania	-3.6	37.7	c14	194	45	1650	1948	1799	300	2	151
1038	Ngalanga	Tanzania	-3.6	37.7	c14	236	41	1520	1948	1734	430	2	216
1039	Ngalanga	Tanzania	-3.6	37.7	c14	278	42	1499	1804	1652	451	146	299
1040	Ngalanga	Tanzania	-3.6	37.7	c14	261	41	1506	1948	1727	444	2	223
1041	Ngalanga	Tanzania	-3.6	37.7	c14	245	41	1512	1948	1730	438	2	220
1042	Maua Farm	Tanzania	-2.9	37.2	c14	4140	200	-3335	-2145	-2740	5285	4095	4690
1043	Maua Farm	Tanzania	-2.9	37.2	c14	2160	190	-756	245	-256	2706	1705	2206

Entry ID	Site Name	Country	Latitude	Longitude	Date Type	Date BP	Date BP SD	Min Chronology (Calibrated BCE/CE)	Max Chronology (Calibrated BCE/CE)	Mean Chronology (Calibrated BCE/CE)	Min Chronology (Calibrated BP - 1950)	Max Chronology (Calibrated BP - 1950)	Mean Chronology (Calibrated BP - 1950)
1044	Maua Farm	Tanzania	-2.9	37.2	c14	1545	140	210	829	520	1740	1121	1431
1045	Wasendo Madukani I	Tanzania	-3.0	37.2	c14	1885	120	-147	420	137	2097	1530	1814
1046	Wasendo Madukani I	Tanzania	-3.0	37.2	c14	1895	120	-148	416	134	2098	1534	1816
1047	Wasendo Madukani I	Tanzania	-3.0	37.2	c14	3225	140	-1878	-1117	-1498	3828	3067	3448
1048	Wasendo Madukani I	Tanzania	-3.0	37.2	c14	3145	160	-1750	-932	-1341	3700	2882	3291
1049	Wasendo Madukani I	Tanzania	-3.0	37.2	c14	1420	135	371	966	669	1579	984	1282
1050	Wasendo Madukani I	Tanzania	-3.0	37.2	c14	2170	165	-748	224	-262	2698	1726	2212
1051	Wasendo Madukani I	Tanzania	-3.0	37.2	c14	3200	180	-1900	-941	-1421	3850	2891	3371
1052	Simba 1	Tanzania	-3.0	37.1	c14	4930	180	-4230	-3191	-3711	6180	5141	5661
1053	Simba 1	Tanzania	-3.0	37.1	c14	5020	165	-4235	-3380	-3808	6185	5330	5758
1054	Mwika	Tanzania	-3.2	37.3	c14	1740	350	-739	1017	139	2689	933	1811
1055	Old Moshi II	Tanzania	-3.2	37.2	c14	2260	450	-1426	647	-390	3376	1303	2340
1056	Matunda	Tanzania	-3.2	37.2	c14	525	200	1051	1947	1499	899	3	451
1057	Marangu TTC	Tanzania	-3.2	37.3	c14	745	190	891	1625	1258	1059	325	692
1058	Usangi Hospital	Tanzania	-3.4	37.4	c14	1060	135	685	1262	974	1265	688	977
1059	Usangi Hospital	Tanzania	-3.4	37.4	c14	5330	140	-4446	-3801	-4124	6396	5751	6074
1060	Usangi Hospital	Tanzania	-3.4	37.4	c14	1470	280	-41	1157	558	1991	793	1392
1061	Bombo	Tanzania	-4.2	38.0	c14	1060	110	711	1223	967	1239	727	983
1062	Mwanga IIIA	Tanzania	-3.4	37.4	c14	1020	110	775	1265	1020	1175	685	930
1063	Kisese II	Tanzania	-4.0	35.3	c14	3870	30	-2458	-2204	-2331	4408	4154	4281
1064	Kisese II	Tanzania	-4.0	35.3	c14	3770	20	-2281	-2038	-2160	4231	3988	4110

Entry ID	Site Name	Country	Latitude	Longitude	Date Type	Date BP	Date BP SD	Min Chronology (Calibrated BCE/CE)	Max Chronology (Calibrated BCE/CE)	Mean Chronology (Calibrated BCE/CE)	Min Chronology (Calibrated BP - 1950)	Max Chronology (Calibrated BP - 1950)	Mean Chronology (Calibrated BP - 1950)
1065	Kisese II	Tanzania	-4.0	35.3	c14	3840	30	-2451	-2143	-2297	4401	4093	4247
1066	Gishimangeda Cave	Tanzania	-3.5	35.3	c14	2120	20	-172	-53	-113	2122	2003	2063
1067	Gishimangeda Cave	Tanzania	-3.5	35.3	c14	2005	20	-46	73	14	1996	1877	1937
1068	Gishimangeda Cave	Tanzania	-3.5	35.3	c14	1870	20	125	235	180	1825	1715	1770
1069	Gishimangeda Cave	Tanzania	-3.5	35.3	c14	2410	20	-542	-396	-469	2492	2346	2419
1070	Gishimangeda Cave	Tanzania	-3.5	35.3	c14	2530	15	-778	-543	-661	2728	2493	2611
1071	Gishimangeda Cave	Tanzania	-3.5	35.3	c14	2140	15	-336	-61	-199	2286	2011	2149
1072	Gishimangeda Cave	Tanzania	-3.5	35.3	c14	2005	20	-46	72	13	1996	1878	1937
1073	Gishimangeda Cave	Tanzania	-3.5	35.3	c14	2355	20	-459	-209	-334	2409	2159	2284
1074	Gishimangeda Cave	Tanzania	-3.5	35.3	c14	2030	20	-53	58	3	2003	1892	1948
1075	Gishimangeda Cave	Tanzania	-3.5	35.3	c14	2510	20	-775	-517	-646	2725	2467	2596
1076	Gishimangeda Cave	Tanzania	-3.5	35.3	c14	1780	25	236	361	299	1714	1589	1652
1077	Ngombezi	Tanzania	-5.2	38.5	c14	238	30	1635	1948	1792	315	2	159
1078	Maurui	Tanzania	-5.1	38.4	c14	525	30	1396	1454	1425	554	496	525
1079	Maurui	Tanzania	-5.1	38.4	c14	630	30	1299	1404	1352	651	546	599
1080	Nyangoma RS	Tanzania	-2.4	33.6	c14	2640	120	-1043	-407	-725	2993	2357	2675
1081	Ivuna	Tanzania	-8.3	32.2	c14	540	110	1276	1633	1455	674	317	496
1082	Ivuna	Tanzania	-8.3	32.2	c14	590	115	1221	1627	1424	729	323	526
1083	Ivuna	Tanzania	-8.3	32.2	c14	715	110	1049	1445	1247	901	505	703
1084	Ivuna	Tanzania	-8.3	32.2	c14	735	110	1047	1435	1241	903	515	709
1085	Pwaga-Uvinza	Tanzania	-5.0	30.4	c14	210	110	1496	1949	1723	454	1	228

Entry ID	Site Name	Country	Latitude	Longitude	Date Type	Date BP	Date BP SD	Min Chronology (Calibrated BCE/CE)	Max Chronology (Calibrated BCE/CE)	Mean Chronology (Calibrated BCE/CE)	Min Chronology (Calibrated BP - 1950)	Max Chronology (Calibrated BP - 1950)	Mean Chronology (Calibrated BP - 1950)
1086	Pwaga-Uvinza	Tanzania	-5.0	30.4	c14	765	105	1044	1410	1227	906	540	723
1087	Pwaga-Uvinza	Tanzania	-5.0	30.4	c14	1530	160	204	883	544	1746	1067	1407
1088	Nyamsunga-Uvinza	Tanzania	-5.0	30.2	c14	260	110	1463	1948	1706	487	2	245
1089	Nyamsunga-Uvinza	Tanzania	-5.0	30.2	c14	1360	200	252	1139	696	1698	811	1255
1090	Dembeni	Comoros	-12.8	45.2	c14	390	190	1300	1948	1624	650	2	326
1091	Dembeni	Comoros	-12.8	45.2	c14	920	240	650	1450	1050	1300	500	900
1092	Sima	Comoros	-12.2	44.3	c14	1230	24	707	891	799	1243	1059	1151
1093	Sima	Comoros	-12.2	44.3	c14	1232	23	707	890	799	1243	1060	1152
1094	Sima	Comoros	-12.2	44.3	c14	1163	23	775	990	883	1175	960	1068
1095	Sima	Comoros	-12.2	44.3	c14	1276	24	677	873	775	1273	1077	1175
1096	Sima	Comoros	-12.2	44.3	c14	1204	24	772	959	866	1178	991	1085
1097	Sima	Comoros	-12.2	44.3	c14	1242	23	703	887	795	1247	1063	1155
1098	Sima	Comoros	-12.2	44.3	c14	1262	23	682	881	782	1268	1069	1169
1099	Sima	Comoros	-12.2	44.3	c14	1960	70	-97	244	74	2047	1706	1877
1100	Sima	Comoros	-12.2	44.3	c14	525	40	1325	1457	1391	625	493	559
1101	Domoni	Comoros	-12.3	44.5	c14	920	50	1027	1228	1128	923	722	823
1102	Domoni	Comoros	-12.3	44.5	TL	1210	55	671	891	781	1279	1059	1169
1103	Bagamoyo	Comoros	-12.2	44.4	c14	820	11	1221	1271	1246	729	679	704
1104	M'Bachile	Comoros	-11.8	43.2	c14	1440	60	532	773	653	1418	1177	1298
1105	Koungou	Comoros	-12.2	44.4	c14	1180	60	692	1017	855	1258	933	1096

Entry ID	Site Name	Country	Latitude	Longitude	Date Type	Date BP	Date BP SD	Min Chronology (Calibrated BCE/CE)	Max Chronology (Calibrated BCE/CE)	Mean Chronology (Calibrated BCE/CE)	Min Chronology (Calibrated BP - 1950)	Max Chronology (Calibrated BP - 1950)	Mean Chronology (Calibrated BP - 1950)
1106	Koungou	Comoros	-12.2	44.4	c14	1200	60	686	992	839	1264	958	1111
1107	Koungou	Comoros	-12.2	44.4	c14	1950	70	371	791	581	1579	1159	1369
1108	Koungou	Comoros	-12.2	44.4	c14	990	290	430	1476	953	1520	474	997
1109	Koungou	Comoros	-12.2	44.4	c14	1950	90	335	833	584	1615	1117	1366
1110	Koungou	Comoros	-12.2	44.4	c14	1820	110	442	996	719	1508	954	1231
1111	Koungou	Comoros	-12.2	44.4	c14	1980	130	225	869	547	1725	1081	1403
1112	Mwali Mdjini	Comoros	-12.3	43.7	c14	1190	140	607	1160	884	1343	790	1067
1113	Nyamawi	Comoros	-11.4	43.4	c14	1120	30	889	1017	953	1061	933	997
1114	Nyamawi	Comoros	-11.4	43.4	c14	1070	30	893	1038	966	1057	912	985
1115	Lakaria	Comoros	-11.4	43.3	c14	540	30	1327	1449	1388	623	501	562
1116	Vohemar Necropolis	Madagascar	-13.4	50.0	c14	760	60	1178	1393	1286	772	557	665
1117	Tony-Velondriake	Madagascar	-22.1	43.2	c14	2012	37	-55	117	31	2005	1833	1919
1118	Tony-Velondriake	Madagascar	-22.1	43.2	c14	2004	37	-51	118	34	2001	1832	1917
1119	Tony-Velondriake	Madagascar	-22.1	43.2	c14	1677	27	362	524	443	1588	1426	1507
1120	Tony-Velondriake	Madagascar	-22.1	43.2	c14	2010	25	-50	113	32	2000	1837	1919
1121	Tony-Velondriake	Madagascar	-22.1	43.2	c14	1179	21	885	988	937	1065	962	1014
1122	Tony-Velondriake	Madagascar	-22.1	43.2	c14	3086	32	-952	-580	-766	2902	2530	2716
1123	Kingany	Madagascar	-15.8	45.9	c14	1050	80	776	1211	994	1174	739	957
1124	Andakatomena	Madagascar	-23.5	43.8	c14	1855	12	137	248	193	1813	1702	1758
1125	Andakatomena	Madagascar	-23.5	43.8	c14	1785	15	247	360	304	1703	1590	1647

Entry ID	Site Name	Country	Latitude	Longitude	Date Type	Date BP	Date BP SD	Min Chronology (Calibrated BCE/CE)	Max Chronology (Calibrated BCE/CE)	Mean Chronology (Calibrated BCE/CE)	Min Chronology (Calibrated BP - 1950)	Max Chronology (Calibrated BP - 1950)	Mean Chronology (Calibrated BP - 1950)
1126	Ankarafantsika	Madagascar	-16.4	46.9	c14	605	50	1295	1430	1363	655	520	588
1127	Benavony	Madagascar	-14.4	50.2	c14	1197	21	772	960	866	1178	990	1084
1128	Benavony	Madagascar	-14.4	50.2	c14	1250	21	690	883	787	1260	1067	1164
1129	Benavony	Madagascar	-14.4	50.2	c14	617	21	1305	1406	1356	645	544	595
1130	Benavony	Madagascar	-14.4	50.2	c14	1200	21	772	957	865	1178	993	1086
1131	Benavony	Madagascar	-14.4	50.2	c14	701	21	1278	1387	1333	672	563	618
1132	Benavony	Madagascar	-14.4	50.2	c14	697	21	1280	1388	1334	670	562	616
1133	Benavony	Madagascar	-14.4	50.2	c14	970	21	1031	1155	1093	919	795	857
1134	Benavony	Madagascar	-14.4	50.2	c14	1281	21	675	859	767	1275	1091	1183
1135	Benavony	Madagascar	-14.4	50.2	c14	1211	21	771	951	861	1179	999	1089
1136	Benavony	Madagascar	-14.4	50.2	c14	710	110	1050	1447	1249	900	503	702
1137	Benavony	Madagascar	-14.4	50.2	c14	2980	50	-1379	-1013	-1196	3329	2963	3146
1138	Benavony	Madagascar	-14.4	50.2	c14	3790	50	-2437	-2028	-2233	4387	3978	4183
1139	Matavy	Madagascar	-14.3	50.2	c14	883	21	1054	1228	1141	896	722	809
1140	Matavy	Madagascar	-14.3	50.2	c14	663	21	1289	1395	1342	661	555	608
1141	Matavy	Madagascar	-14.3	50.2	c14	821	21	1216	1276	1246	734	674	704
1142	Matavy	Madagascar	-14.3	50.2	c14	842	21	1180	1272	1226	770	678	724
1143	Matavy	Madagascar	-14.3	50.2	c14	784	21	1225	1285	1255	725	665	695
1144	Trañovato	Madagascar	-25.0	46.9	c14	794	29	1220	1295	1258	730	655	693
1145	Trañovato	Madagascar	-25.0	46.9	c14	873	31	1159	1272	1216	791	678	735
1146	Ampahijolike	Madagascar	-24.8	45.6	c14	821	29	1215	1285	1250	735	665	700

Entry ID	Site Name	Country	Latitude	Longitude	Date Type	Date BP	Date BP SD	Min Chronology (Calibrated BCE/CE)	Max Chronology (Calibrated BCE/CE)	Mean Chronology (Calibrated BCE/CE)	Min Chronology (Calibrated BP - 1950)	Max Chronology (Calibrated BP - 1950)	Mean Chronology (Calibrated BP - 1950)
1147	Ampahijolike	Madagascar	-24.8	45.6	c14	603	29	1319	1431	1375	631	519	575
1148	Ampahijolike	Madagascar	-24.8	45.6	c14	629	29	1305	1417	1361	645	533	589
1149	Ampahijolike	Madagascar	-24.8	45.6	c14	862	30	1163	1276	1220	787	674	731
1150	Andaro	Madagascar	-24.6	45.4	c14	1140	27	892	1017	955	1058	933	996
1151	Andaro	Madagascar	-24.6	45.4	c14	1320	190	385	1156	771	1565	794	1180
1152	Andaro	Madagascar	-24.6	45.4	c14	929	26	1046	1222	1134	904	728	816
1153	Andaro	Madagascar	-24.6	45.4	c14	1042	29	991	1150	1071	959	800	880
1154	Andaro	Madagascar	-24.6	45.4	c14	1060	38	905	1150	1028	1045	800	923
1155	Andaro	Madagascar	-24.6	45.4	c14	1190	24	773	989	881	1177	961	1069
1156	Andaro	Madagascar	-24.6	45.4	c14	972	26	1030	1180	1105	920	770	845
1157	Andaro	Madagascar	-24.6	45.4	OSL	670	120	1100	1580	1340	850	370	610
1158	Andaro	Madagascar	-24.6	45.4	OSL	685	85	1155	1495	1325	795	455	625
1159	Andaro	Madagascar	-24.6	45.4	OSL	530	55	1370	1590	1480	580	360	470
1160	Bevala	Madagascar	-25.6	45.2	c14	535	30	1404	1451	1428	546	499	523
1161	Bevala	Madagascar	-25.6	45.2	c14	1360	35	651	774	713	1299	1176	1238
1162	Enijo	Madagascar	-25.3	44.5	c14	654	30	1297	1404	1351	653	546	600
1163	Maroaloke	Madagascar	-25.2	46.2	c14	915	45	1042	1268	1155	908	682	795
1164	Maroaloke	Madagascar	-25.2	46.2	c14	2025	40	-65	118	27	2015	1832	1924
1165	Maroaloke	Madagascar	-25.2	46.2	c14	1940	45	-41	227	93	1991	1723	1857
1166	Maroaloke	Madagascar	-25.2	46.2	c14	1415	45	594	773	684	1356	1177	1267
1167	Maroaloke	Madagascar	-25.2	46.2	c14	2285	40	-394	-189	-292	2344	2139	2242

Entry ID	Site Name	Country	Latitude	Longitude	Date Type	Date BP	Date BP SD	Min Chronology (Calibrated BCE/CE)	Max Chronology (Calibrated BCE/CE)	Mean Chronology (Calibrated BCE/CE)	Min Chronology (Calibrated BP - 1950)	Max Chronology (Calibrated BP - 1950)	Mean Chronology (Calibrated BP - 1950)
1168	Reampeko II	Madagascar	-25.3	44.6	c14	956	29	1034	1208	1121	916	742	829
1169	Reampeko II	Madagascar	-25.3	44.6	c14	902	26	1054	1265	1160	896	685	791
1170	Reampeko II	Madagascar	-25.3	44.6	c14	1442	29	594	677	636	1356	1273	1315
1171	Talaky	Madagascar	-25.5	45.7	c14	1080	35	898	1140	1019	1052	810	931
1172	Talaky	Madagascar	-25.5	45.7	c14	1025	35	993	1153	1073	957	797	877
1173	Talaky	Madagascar	-25.5	45.7	c14	900	30	1052	1268	1160	898	682	790
1174	Talaky	Madagascar	-25.5	45.7	c14	560	25	1397	1445	1421	553	505	529
1175	Talaky	Madagascar	-25.5	45.7	c14	915	40	1044	1267	1156	906	683	795
1176	Talaky	Madagascar	-25.5	45.7	c14	1035	40	991	1153	1072	959	797	878
1177	Talaky	Madagascar	-25.5	45.7	c14	1010	40	994	1176	1085	956	774	865
1178	Talaky	Madagascar	-25.5	45.7	c14	840	80	1044	1384	1214	906	566	736
1179	Talaky	Madagascar	-25.5	45.7	c14	1735	35	251	418	335	1699	1532	1616
1180	Talaky	Madagascar	-25.5	45.7	c14	1240	35	690	965	828	1260	985	1123
1181	Talaky	Madagascar	-25.5	45.7	c14	1270	40	681	951	816	1269	999	1134
1182	Talaky	Madagascar	-25.5	45.7	c14	1835	30	129	340	235	1821	1610	1716
1183	Talaky	Madagascar	-25.5	45.7	c14	5480	35	-4434	-4168	-4301	6384	6118	6251
1184	Talaky	Madagascar	-25.5	45.7	c14	2285	35	-393	-190	-292	2343	2140	2242
1185	Talaky	Madagascar	-25.5	45.7	c14	4030	40	-2662	-2344	-2503	4612	4294	4453
1186	Talaky	Madagascar	-25.5	45.7	c14	1825	30	136	342	239	1814	1608	1711
1187	Talaky	Madagascar	-25.5	45.7	c14	530	35	1400	1456	1428	550	494	522
1188	Talaky	Madagascar	-25.5	45.7	c14	1780	35	225	387	306	1725	1563	1644

Entry ID	Site Name	Country	Latitude	Longitude	Date Type	Date BP	Date BP SD	Min Chronology (Calibrated BCE/CE)	Max Chronology (Calibrated BCE/CE)	Mean Chronology (Calibrated BCE/CE)	Min Chronology (Calibrated BP - 1950)	Max Chronology (Calibrated BP - 1950)	Mean Chronology (Calibrated BP - 1950)
1189	Talaky	Madagascar	-25.5	45.7	c14	402	29	1453	1628	1541	497	322	410
1190	Talaky	Madagascar	-25.5	45.7	OSL	685	60	1205	1445	1325	745	505	625
1191	Anjohibe	Madagascar	-15.5	46.9	c14	1555	30	431	600	516	1519	1350	1435
1192	Anjohibe	Madagascar	-15.5	46.9	c14	3810	35	-2400	-2047	-2224	4350	3997	4174
1193	Anjohibe	Madagascar	-15.5	46.9	c14	3275	35	-1615	-1442	-1529	3565	3392	3479
1194	Anjohibe	Madagascar	-15.5	46.9	c14	360	25	1471	1635	1553	479	315	397
1195	Anjohibe	Madagascar	-15.5	46.9	c14	3730	70	-2340	-1897	-2119	4290	3847	4069
1196	Anjohibe	Madagascar	-15.5	46.9	c14	830	60	1046	1299	1173	904	651	778
1197	Anjohibe	Madagascar	-15.5	46.9	c14	2060	70	-347	125	-111	2297	1825	2061
1198	Anjohibe	Madagascar	-15.5	46.9	c14	2635	40	-899	-572	-736	2849	2522	2686
1199	Anjohibe	Madagascar	-15.5	46.9	c14	2890	40	-1200	-923	-1062	3150	2873	3012
1200	Anjohibe	Madagascar	-15.5	46.9	c14	3095	30	-1422	-1232	-1327	3372	3182	3277
1201	Anjohibe	Madagascar	-15.5	46.9	c14	3455	25	-1878	-1635	-1757	3828	3585	3707
1202	Anjohibe	Madagascar	-15.5	46.9	c14	4055	40	-2846	-2463	-2655	4796	4413	4605
1203	Anjohibe	Madagascar	-15.5	46.9	c14	4815	40	-3650	-3384	-3517	5600	5334	5467
1204	Anjohibe	Madagascar	-15.5	46.9	c14	1700	35	250	472	361	1700	1478	1589
1205	Anjohibe	Madagascar	-15.5	46.9	c14	2820	35	-1050	-834	-942	3000	2784	2892
1206	Anjohibe	Madagascar	-15.5	46.9	c14	4500	130	-3526	-2884	-3205	5476	4834	5155
1207	Andrahomana	Madagascar	-25.2	46.6	c14	3975	53	-2578	-2210	-2394	4528	4160	4344
1208	Andrahomana	Madagascar	-25.2	46.6	c14	1940	30	29	205	117	1921	1745	1833
1209	Andrahomana	Madagascar	-25.2	46.6	c14	2300	25	-394	-196	-295	2344	2146	2245

Entry ID	Site Name	Country	Latitude	Longitude	Date Type	Date BP	Date BP SD	Min Chronology (Calibrated BCE/CE)	Max Chronology (Calibrated BCE/CE)	Mean Chronology (Calibrated BCE/CE)	Min Chronology (Calibrated BP - 1950)	Max Chronology (Calibrated BP - 1950)	Mean Chronology (Calibrated BP - 1950)
1210	Andrahomana	Madagascar	-25.2	46.6	c14	1755	25	250	407	329	1700	1543	1622
1211	Andrahomana	Madagascar	-25.2	46.6	c14	1000	150	692	1380	1036	1258	570	914
1212	Andrahomana	Madagascar	-25.2	46.6	c14	2845	35	-1106	-834	-970	3056	2784	2920
1213	Ambinanaimbe	Madagascar	-25.1	47.0	c14	565	15	1400	1436	1418	550	514	532
1214	Ambinanaimbe	Madagascar	-25.1	47.0	c14	625	20	1318	1410	1364	632	540	586
1215	Andavadoaka	Madagascar	-22.1	43.2	c14	850	15	1211	1274	1243	739	676	708
1216	Andavadoaka	Madagascar	-22.1	43.2	c14	935	20	1047	1217	1132	903	733	818
1217	Andavadoaka	Madagascar	-22.1	43.2	c14	900	20	1154	1225	1190	796	725	761
1218	Asambalahy	Madagascar	-22.3	44.7	c14	830	20	1219	1277	1248	731	673	702
1219	Nosy-Ve	Madagascar	-23.6	43.8	c14	900	15	1159	1221	1190	791	729	760
1220	Nosy-Ve	Madagascar	-23.6	43.8	c14	900	15	1159	1220	1190	791	730	761
1221	Nosy-Ve	Madagascar	-23.6	43.8	c14	910	20	1072	1224	1148	878	726	802
1222	Nosy-Ve	Madagascar	-23.6	43.8	c14	1025	20	1018	1150	1084	932	800	866
1223	Nosy-Ve	Madagascar	-23.6	43.8	c14	2155	20	-340	-62	-201	2290	2012	2151
1224	Nosy-Ve	Madagascar	-23.6	43.8	c14	2055	20	-63	54	-5	2013	1896	1955
1225	Nosy-Ve	Madagascar	-23.6	43.8	c14	2340	15	-404	-204	-304	2354	2154	2254
1226	Nosy-Ve	Madagascar	-23.6	43.8	c14	2970	20	-1226	-1016	-1121	3176	2966	3071
1227	Nosy-Ve	Madagascar	-23.6	43.8	c14	4125	25	-2864	-2493	-2679	4814	4443	4629
1228	Nosy-Ve	Madagascar	-23.6	43.8	c14	1250	50	682	972	827	1268	978	1123
1229	Andranosoa	Madagascar	-24.8	45.3	c14	1150	15	894	993	944	1056	957	1007
1230	Andranosoa	Madagascar	-24.8	45.3	c14	730	90	1180	1427	1304	770	523	647

Entry ID	Site Name	Country	Latitude	Longitude	Date Type	Date BP	Date BP SD	Min Chronology (Calibrated BCE/CE)	Max Chronology (Calibrated BCE/CE)	Mean Chronology (Calibrated BCE/CE)	Min Chronology (Calibrated BP - 1950)	Max Chronology (Calibrated BP - 1950)	Mean Chronology (Calibrated BP - 1950)
1231	Andranosoa	Madagascar	-24.8	45.3	c14	920	90	993	1287	1140	957	663	810
1232	Andranosoa	Madagascar	-24.8	45.3	TL	950	210	634	1474	1054	1316	476	896
1233	Andranosoa	Madagascar	-24.8	45.3	c14	985	15	1035	1152	1094	915	798	857
1234	Andranosoa	Madagascar	-24.8	45.3	c14	980	15	1035	1155	1095	915	795	855
1235	Andranosoa	Madagascar	-24.8	45.3	c14	1000	20	1027	1151	1089	923	799	861
1236	Andranosoa	Madagascar	-24.8	45.3	c14	1000	15	1027	1150	1089	923	800	862
1237	Andranosoa	Madagascar	-24.8	45.3	c14	980	15	1035	1155	1095	915	795	855
1238	Andranosoa	Madagascar	-24.8	45.3	c14	970	15	1037	1160	1099	913	790	852
1239	Andranosoa	Madagascar	-24.8	45.3	c14	1165	25	889	990	940	1061	960	1011
1240	Andranosoa	Madagascar	-24.8	45.3	c14	970	15	1037	1160	1099	913	790	852
1241	Andranosoa	Madagascar	-24.8	45.3	c14	220	70	1513	1949	1731	437	1	219
1242	Andranosoa	Madagascar	-24.8	45.3	c14	1260	25	691	889	790	1259	1061	1160
1243	Andranosoa	Madagascar	-24.8	45.3	c14	1270	20	691	883	787	1259	1067	1163
1244	Andranosoa	Madagascar	-24.8	45.3	c14	1275	20	690	881	786	1260	1069	1165
1245	Andranosoa	Madagascar	-24.8	45.3	c14	925	20	1052	1219	1136	898	731	815
1246	Andranosoa	Madagascar	-24.8	45.3	c14	1010	15	1023	1150	1087	927	800	864
1247	Rezoky	Madagascar	-22.1	44.6	c14	675	15	1297	1394	1346	653	556	605
1248	Rezoky	Madagascar	-22.1	44.6	c14	720	15	1283	1385	1334	667	565	616
1249	Rezoky	Madagascar	-22.1	44.6	c14	695	20	1288	1392	1340	662	558	610
1250	Rezoky	Madagascar	-22.1	44.6	c14	760	15	1270	1380	1325	680	570	625
1251	Rezoky	Madagascar	-22.1	44.6	c14	495	20	1424	1459	1442	526	491	509

Entry ID	Site Name	Country	Latitude	Longitude	Date Type	Date BP	Date BP SD	Min Chronology (Calibrated BCE/CE)	Max Chronology (Calibrated BCE/CE)	Mean Chronology (Calibrated BCE/CE)	Min Chronology (Calibrated BP - 1950)	Max Chronology (Calibrated BP - 1950)	Mean Chronology (Calibrated BP - 1950)
1252	Rezoky	Madagascar	-22.1	44.6	c14	690	20	1290	1393	1342	660	557	609
1253	Rezoky	Madagascar	-22.1	44.6	c14	815	20	1223	1281	1252	727	669	698
1254	Rezoky	Madagascar	-22.1	44.6	c14	820	25	1220	1281	1251	730	669	700
1255	Rezoky	Madagascar	-22.1	44.6	c14	795	20	1226	1289	1258	724	661	693
1256	Rezoky	Madagascar	-22.1	44.6	c14	700	20	1287	1390	1339	663	560	612
1257	Rezoky	Madagascar	-22.1	44.6	c14	680	15	1295	1394	1345	655	556	606
1258	Rezoky	Madagascar	-22.1	44.6	c14	790	20	1226	1291	1259	724	659	692
1259	Lakatoni Anja	Madagascar	-12.5	49.5	c14	1300	80	608	967	788	1342	983	1163
1260	Lakatoni Anja	Madagascar	-12.5	49.5	c14	1680	65	246	546	396	1704	1404	1554
1261	Lakatoni Anja	Madagascar	-12.5	49.5	OSL	3470	370	-2197	-717	-1457	4147	2667	3407
1262	Lakatoni Anja	Madagascar	-12.5	49.5	OSL	4380	400	-3167	-1567	-2367	5117	3517	4317
1263	Lakatoni Anja	Madagascar	-12.5	49.5	OSL	930	90	903	1263	1083	1047	687	867
1264	Lakatoni Anja	Madagascar	-12.5	49.5	OSL	2700	230	-1147	-227	-687	3097	2177	2637
1265	Lakatoni Anja	Madagascar	-12.5	49.5	OSL	1330	130	423	943	683	1527	1007	1267
1266	Lakatoni Anja	Madagascar	-12.5	49.5	OSL	2210	190	-577	183	-197	2527	1767	2147
1267	Lakatoni Anja	Madagascar	-12.5	49.5	c14	1460	40	552	663	608	1398	1287	1343
1268	Lakatoni Anja	Madagascar	-12.5	49.5	c14	1070	40	891	1130	1011	1059	820	940
1269	Lakatoni Anja	Madagascar	-12.5	49.5	c14	930	30	1042	1211	1127	908	739	824
1270	Lakatoni Anja	Madagascar	-12.5	49.5	c14	920	30	1043	1217	1130	907	733	820
1271	Lakatoni Anja	Madagascar	-12.5	49.5	c14	690	30	1277	1393	1335	673	557	615
1272	Lakatoni Anja	Madagascar	-12.5	49.5	c14	1490	30	550	645	598	1400	1305	1353

Entry ID	Site Name	Country	Latitude	Longitude	Date Type	Date BP	Date BP SD	Min Chronology (Calibrated BCE/CE)	Max Chronology (Calibrated BCE/CE)	Mean Chronology (Calibrated BCE/CE)	Min Chronology (Calibrated BP - 1950)	Max Chronology (Calibrated BP - 1950)	Mean Chronology (Calibrated BP - 1950)
1273	Lakatoni Anja	Madagascar	-12.5	49.5	c14	1480	30	554	650	602	1396	1300	1348
1274	Lakatoni Anja	Madagascar	-12.5	49.5	c14	1590	30	422	571	497	1528	1379	1454
1275	Mahilaka	Madagascar	-13.8	48.3	c14	825	70	1044	1380	1212	906	570	738
1276	Mahilaka	Madagascar	-13.8	48.3	c14	890	45	1044	1267	1156	906	683	795
1277	Mahilaka	Madagascar	-13.8	48.3	c14	910	75	1023	1272	1148	927	678	803
1278	Mahilaka	Madagascar	-13.8	48.3	c14	930	90	986	1281	1134	964	669	817
1279	Mahilaka	Madagascar	-13.8	48.3	c14	1030	65	893	1180	1037	1057	770	914
1280	Mahilaka	Madagascar	-13.8	48.3	c14	1120	160	647	1227	937	1303	723	1013
1281	Mahilaka	Madagascar	-13.8	48.3	c14	1175	70	689	1021	855	1261	929	1095
1282	Mahilaka	Madagascar	-13.8	48.3	c14	879	24	1054	1264	1159	896	686	791
1283	Mahilaka	Madagascar	-13.8	48.3	c14	1023	26	991	1150	1071	959	800	880
1284	Mahilaka	Madagascar	-13.8	48.3	c14	960	24	1030	1162	1096	920	788	854
1285	Mahilaka	Madagascar	-13.8	48.3	c14	966	24	1030	1159	1095	920	791	856
1286	Ambohiposa	Madagascar	-13.4	50.0	c14	1110	40	881	1027	954	1069	923	996
1287	Ambohiposa	Madagascar	-13.4	50.0	c14	760	40	1219	1383	1301	731	567	649
1288	Ampasimahavelona	Madagascar	-13.4	50.0	c14	1130	40	775	1023	899	1175	927	1051
1289	Ampasimahavelona	Madagascar	-13.4	50.0	c14	1180	40	774	986	880	1176	964	1070
1290	Amboatany	Madagascar	-21.7	46.8	TL	1670	65	192	452	322	1758	1498	1628
1291	Amboatany	Madagascar	-21.7	46.8	TL	1480	100	312	712	512	1638	1238	1438
1292	Ambohidahy	Madagascar	-18.9	47.5	c14	560	30	1393	1449	1421	557	501	529
1293	Ambohidahy	Madagascar	-18.9	47.5	c14	590	30	1322	1438	1380	628	512	570

Entry ID	Site Name	Country	Latitude	Longitude	Date Type	Date BP	Date BP SD	Min Chronology (Calibrated BCE/CE)	Max Chronology (Calibrated BCE/CE)	Mean Chronology (Calibrated BCE/CE)	Min Chronology (Calibrated BP - 1950)	Max Chronology (Calibrated BP - 1950)	Mean Chronology (Calibrated BP - 1950)
1294	Ambohidahy	Madagascar	-18.9	47.5	c14	570	30	1327	1445	1386	623	505	564
1295	Ambohidahy	Madagascar	-18.9	47.5	c14	553	20	1403	1442	1423	547	508	528
1296	Ambohidahy	Madagascar	-18.9	47.5	c14	566	21	1397	1440	1419	553	510	532
1297	Ambohidahy	Madagascar	-18.9	47.5	TL	1520	100	272	672	472	1678	1278	1478
1298	Ambohidahy	Madagascar	-18.9	47.5	TL	1500	100	292	692	492	1658	1258	1458
1299	Ambohidahy	Madagascar	-18.9	47.5	TL	1420	110	352	792	572	1598	1158	1378
1300	Ambohidahy	Madagascar	-18.9	47.5	TL	1100	190	512	1272	892	1438	678	1058
1301	Ambohidahy	Madagascar	-18.9	47.5	c14	430	30	1445	1624	1535	505	326	416
1302	Ambohidahy	Madagascar	-18.9	47.5	c14	420	30	1448	1625	1537	502	325	414
1303	Ambohinanjakana	Madagascar	-18.7	47.6	TL	1780	50	112	312	212	1838	1638	1738
1304	Ambohinanjakana	Madagascar	-18.7	47.6	TL	1720	50	172	372	272	1778	1578	1678
1305	Ambohinanjakana	Madagascar	-18.7	47.6	TL	1650	70	202	482	342	1748	1468	1608
1306	Ambohinanjakana	Madagascar	-18.7	47.6	c14	221	61	1519	1949	1734	431	1	216
1307	Ankadivory	Madagascar	-18.8	47.6	c14	810	100	1045	1396	1221	905	554	730
1308	Ankadivory	Madagascar	-18.8	47.6	c14	880	50	1046	1283	1165	904	667	786
1309	Ankadivory	Madagascar	-18.8	47.6	TL	1295	140	417	977	697	1533	973	1253
1310	Ankadivory	Madagascar	-18.8	47.6	c14	523	80	1302	1627	1465	648	323	486
1311	Ankadivory	Madagascar	-18.8	47.6	c14	810	185	778	1604	1191	1172	346	759
1312	Beropitika	Madagascar	-24.6	45.6	c14	750	90	1156	1418	1287	794	532	663
1313	Antanimenabe-Irodo	Madagascar	-12.6	49.5	c14	980	100	892	1269	1081	1058	681	870

Entry ID	Site Name	Country	Latitude	Longitude	Date Type	Date BP	Date BP SD	Min Chronology (Calibrated BCE/CE)	Max Chronology (Calibrated BCE/CE)	Mean Chronology (Calibrated BCE/CE)	Min Chronology (Calibrated BP - 1950)	Max Chronology (Calibrated BP - 1950)	Mean Chronology (Calibrated BP - 1950)
1314	Antanimenabe-Irodo	Madagascar	-12.6	49.5	c14	1200	40	710	987	849	1240	963	1102
1315	Antanimenabe-Irodo	Madagascar	-12.7	49.5	c14	980	100	892	1269	1081	1058	681	870
1316	Tafiantsirbeka-Irodo	Madagascar	-12.6	49.5	c14	1090	90	1240	1647	1444	710	303	507
1317	Tafiampatsa-Irodo	Madagascar	-12.7	49.5	c14	1150	90	678	1124	901	1272	826	1049
1318	Maliavola	Madagascar	-24.1	46.3	c14	1144	29	890	1017	954	1060	933	997
1319	Maliavola	Madagascar	-24.1	46.3	TL	1475	100	318	718	518	1632	1232	1432
1320	Nosy Mangabe	Madagascar	-15.5	49.8	TL	950	100	843	1243	1043	1107	707	907
1321	Nosy Mangabe	Madagascar	-15.5	49.8	c14	1250	60	665	967	816	1285	983	1134
1322	Sandrakatsy East	Madagascar	-16.3	49.6	c14	1140	60	772	1026	899	1178	924	1051
1323	Sandrakatsy East	Madagascar	-16.3	49.6	c14	1240	50	675	962	819	1275	988	1132
1324	Sandrakatsy West	Madagascar	-16.2	49.4	c14	970	60	994	1215	1105	956	735	846
1325	Sarodrano	Madagascar	-23.5	43.7	c14	1460	90	418	841	630	1532	1109	1321
1326	Sarodrano	Madagascar	-23.5	43.7	c14	535	80	1296	1624	1460	654	326	490
1327	Sarodrano	Madagascar	-23.5	43.7	c14	210	80	1512	1949	1731	438	1	220
1328	Tsiandrora	Madagascar	-25.1	46.9	c14	950	80	994	1271	1133	956	679	818
1329	Vohimasina	Madagascar	-20.1	47.0	c14	710	60	1229	1405	1317	721	545	633
1330	Vohimasina	Madagascar	-20.1	47.0	TL	1410	115	352	812	582	1598	1138	1368
1331	Vohimasina	Madagascar	-20.1	47.0	TL	1515	95	287	667	477	1663	1283	1473
1332	Vohimasina	Madagascar	-20.1	47.0	c14	480	50	1401	1624	1513	549	326	438
1333	Ambatary	Madagascar	-13.5	50.0	c14	620	40	1296	1416	1356	654	534	594
1334	Ambinanibe	Madagascar	-25.1	47.0	c14	700	100	1185	1446	1316	765	504	635

Entry ID	Site Name	Country	Latitude	Longitude	Date Type	Date BP	Date BP SD	Min Chronology (Calibrated BCE/CE)	Max Chronology (Calibrated BCE/CE)	Mean Chronology (Calibrated BCE/CE)	Min Chronology (Calibrated BP - 1950)	Max Chronology (Calibrated BP - 1950)	Mean Chronology (Calibrated BP - 1950)
1335	Lamboharana	Madagascar	-22.2	43.2	c14	935	15	1051	1213	1132	899	737	818
1336	Lamboharana	Madagascar	-22.2	43.2	c14	990	20	1030	1153	1092	920	797	859
1337	Lamboharana	Madagascar	-22.2	43.2	c14	1010	15	1023	1150	1087	927	800	864
1338	Lamboharana	Madagascar	-22.2	43.2	c14	1740	50	222	517	370	1728	1433	1581
1339	Lamboharana	Madagascar	-22.2	43.2	c14	2020	300	-770	631	-70	2720	1319	2020
1340	Lamboharana	Madagascar	-22.2	43.2	c14	3495	55	-1934	-1621	-1778	3884	3571	3728
1341	Lamboharana	Madagascar	-22.2	43.2	c14	1220	80	679	1018	849	1271	932	1102
1342	Lamboharana	Madagascar	-22.2	43.2	c14	2350	120	-770	-108	-439	2720	2058	2389
1343	Lamboharana	Madagascar	-22.2	43.2	c14	1300	20	681	863	772	1269	1087	1178
1344	Lamboharana	Madagascar	-22.2	43.2	c14	1450	20	598	666	632	1352	1284	1318
1345	Lamboharana	Madagascar	-22.2	43.2	c14	1100	15	974	1025	1000	976	925	951
1346	Lamboharana	Madagascar	-22.2	43.2	c14	3300	20	-1614	-1449	-1532	3564	3399	3482
1347	Lamboharana	Madagascar	-22.2	43.2	c14	1715	15	341	418	380	1609	1532	1571
1348	Lamboharana	Madagascar	-22.2	43.2	c14	2830	20	-1016	-835	-926	2966	2785	2876
1349	Lamboharana	Madagascar	-22.2	43.2	c14	1220	25	771	965	868	1179	985	1082
1350	Lamboharana	Madagascar	-22.2	43.2	c14	2925	20	-1203	-938	-1071	3153	2888	3021
1351	Lamboharana	Madagascar	-22.2	43.2	c14	1755	20	251	387	319	1699	1563	1631
1352	Lamboharana	Madagascar	-22.2	43.2	c14	1515	20	546	641	594	1404	1309	1357
1353	Lamboharana	Madagascar	-22.2	43.2	c14	725	20	1281	1385	1333	669	565	617
1354	Taolambiby	Madagascar	-23.7	44.6	c14	2325	43	-411	-191	-301	2361	2141	2251
1355	Taolambiby	Madagascar	-23.7	44.6	c14	1231	27	771	960	866	1179	990	1085

Entry ID	Site Name	Country	Latitude	Longitude	Date Type	Date BP	Date BP SD	Min Chronology (Calibrated BCE/CE)	Max Chronology (Calibrated BCE/CE)	Mean Chronology (Calibrated BCE/CE)	Min Chronology (Calibrated BP - 1950)	Max Chronology (Calibrated BP - 1950)	Mean Chronology (Calibrated BP - 1950)
1356	Taolambiby	Madagascar	-23.7	44.6	c14	1150	28	889	994	942	1061	956	1009
1357	Taolambiby	Madagascar	-23.7	44.6	c14	1142	27	891	1016	954	1059	934	997
1358	Taolambiby	Madagascar	-23.7	44.6	c14	1193	27	773	989	881	1177	961	1069
1359	Taolambiby	Madagascar	-23.7	44.6	c14	1175	26	881	992	937	1069	958	1014
1360	Taolambiby	Madagascar	-23.7	44.6	c14	2713	44	-929	-777	-853	2879	2727	2803
1361	Taolambiby	Madagascar	-23.7	44.6	c14	2290	90	-723	-59	-391	2673	2009	2341
1362	Taolambiby	Madagascar	-23.7	44.6	c14	1540	45	437	645	541	1513	1305	1409
1363	Taolambiby	Madagascar	-23.7	44.6	c14	2535	30	-783	-426	-605	2733	2376	2555
1364	Taolambiby	Madagascar	-23.7	44.6	c14	2605	30	-811	-546	-679	2761	2496	2629
1365	Taolambiby	Madagascar	-23.7	44.6	c14	3025	35	-1384	-1055	-1220	3334	3005	3170
1366	Taolambiby	Madagascar	-23.7	44.6	c14	2500	25	-760	-416	-588	2710	2366	2538
1367	Taolambiby	Madagascar	-23.7	44.6	c14	2535	30	-783	-425	-604	2733	2375	2554
1368	Taolambiby	Madagascar	-23.7	44.6	c14	1260	15	773	881	827	1177	1069	1123
1369	Taolambiby	Madagascar	-23.7	44.6	c14	1745	30	251	413	332	1699	1537	1618
1370	Taolambiby	Madagascar	-23.7	44.6	c14	2300	50	-403	-186	-295	2353	2136	2245
1371	Taolambiby	Madagascar	-23.7	44.6	c14	2855	35	-1112	-842	-977	3062	2792	2927
1372	Taolambiby	Madagascar	-23.7	44.6	c14	2550	30	-793	-489	-641	2743	2439	2591
1373	Taolambiby	Madagascar	-23.7	44.6	c14	2905	40	-1203	-917	-1060	3153	2867	3010
1374	Taolambiby	Madagascar	-23.7	44.6	c14	2470	25	-752	-403	-578	2702	2353	2528
1375	Taolambiby	Madagascar	-23.7	44.6	c14	1440	30	593	764	679	1357	1186	1272
1376	Taolambiby	Madagascar	-23.7	44.6	c14	2540	30	-788	-481	-635	2738	2431	2585

Entry ID	Site Name	Country	Latitude	Longitude	Date Type	Date BP	Date BP SD	Min Chronology (Calibrated BCE/CE)	Max Chronology (Calibrated BCE/CE)	Mean Chronology (Calibrated BCE/CE)	Min Chronology (Calibrated BP - 1950)	Max Chronology (Calibrated BP - 1950)	Mean Chronology (Calibrated BP - 1950)
1377	Taolambiby	Madagascar	-23.7	44.6	c14	2745	40	-976	-796	-886	2926	2746	2836
1378	Taolambiby	Madagascar	-23.7	44.6	c14	1257	29	690	891	791	1260	1059	1160
1379	Taolambiby	Madagascar	-23.7	44.6	c14	1749	29	250	412	331	1700	1538	1619
1380	Taolambiby	Madagascar	-23.7	44.6	c14	1242	24	771	951	861	1179	999	1089
1381	Taolambiby	Madagascar	-23.7	44.6	c14	1245	20	773	887	830	1177	1063	1120
1382	Taolambiby	Madagascar	-23.7	44.6	c14	1260	15	773	881	827	1177	1069	1123
1383	Taolambiby	Madagascar	-23.7	44.6	c14	1255	15	775	881	828	1175	1069	1122
1384	Taolambiby	Madagascar	-23.7	44.6	c14	1945	15	61	199	130	1889	1751	1820
1385	Taolambiby	Madagascar	-23.7	44.6	c14	1160	20	892	990	941	1058	960	1009
1386	Taolambiby	Madagascar	-23.7	44.6	c14	2400	15	-543	-382	-463	2493	2332	2413
1387	Taolambiby	Madagascar	-23.7	44.6	c14	2565	40	-803	-484	-644	2753	2434	2594
1388	Taolambiby	Madagascar	-23.7	44.6	c14	1385	25	645	773	709	1305	1177	1241
1389	Taolambiby	Madagascar	-23.7	44.6	c14	1618	25	417	571	494	1533	1379	1456
1390	Taolambiby	Madagascar	-23.7	44.6	c14	1218	27	772	968	870	1178	982	1080
1391	Taolambiby	Madagascar	-23.7	44.6	c14	1283	24	687	878	783	1263	1072	1168
1392	Taolambiby	Madagascar	-23.7	44.6	c14	1234	27	771	960	866	1179	990	1085
1393	Taolambiby	Madagascar	-23.7	44.6	c14	2685	30	-900	-777	-839	2850	2727	2789
1394	Taolambiby	Madagascar	-23.7	44.6	c14	2185	30	-355	-65	-210	2305	2015	2160
1395	Taolambiby	Madagascar	-23.7	44.6	c14	2915	30	-1200	-930	-1065	3150	2880	3015
1396	Taolambiby	Madagascar	-23.7	44.6	c14	2215	30	-372	-111	-242	2322	2061	2192
1397	Taolambiby	Madagascar	-23.7	44.6	c14	1265	30	689	888	789	1261	1062	1162

Entry ID	Site Name	Country	Latitude	Longitude	Date Type	Date BP	Date BP SD	Min Chronology (Calibrated BCE/CE)	Max Chronology (Calibrated BCE/CE)	Mean Chronology (Calibrated BCE/CE)	Min Chronology (Calibrated BP - 1950)	Max Chronology (Calibrated BP - 1950)	Mean Chronology (Calibrated BP - 1950)
1398	Taolambiby	Madagascar	-23.7	44.6	c14	1251	28	691	894	793	1259	1056	1158
1399	Taolambiby	Madagascar	-23.7	44.6	c14	810	100	1046	1397	1222	904	553	729
1400	Taolambiby	Madagascar	-23.7	44.6	c14	1121	26	895	1023	959	1055	927	991
1401	Taolambiby	Madagascar	-23.7	44.6	c14	1036	27	992	1149	1071	958	801	880
1402	Taolambiby	Madagascar	-23.7	44.6	c14	1133	28	893	1019	956	1057	931	994
1403	Taolambiby	Madagascar	-23.7	44.6	c14	1990	25	-45	119	37	1995	1831	1913
1404	Taolambiby	Madagascar	-23.7	44.6	c14	2120	30	-179	17	-81	2129	1933	2031
1405	Taolambiby	Madagascar	-23.7	44.6	c14	2150	30	-341	-56	-199	2291	2006	2149
1406	Taolambiby	Madagascar	-23.7	44.6	c14	2510	30	-769	-418	-594	2719	2368	2544
1407	Taolambiby	Madagascar	-23.7	44.6	c14	2615	30	-815	-549	-682	2765	2499	2632
1408	Taolambiby	Madagascar	-23.7	44.6	c14	2720	35	-919	-792	-856	2869	2742	2806
1409	Taolambiby	Madagascar	-23.7	44.6	c14	2995	30	-1286	-1019	-1153	3236	2969	3103
1410	Taolambiby	Madagascar	-23.7	44.6	c14	2290	25	-392	-194	-293	2342	2144	2243
1411	Taolambiby	Madagascar	-23.7	44.6	c14	2945	30	-1223	-985	-1104	3173	2935	3054
1412	Taolambiby	Madagascar	-23.7	44.6	c14	2600	30	-810	-545	-678	2760	2495	2628
1413	Taolambiby	Madagascar	-23.7	44.6	c14	2645	30	-895	-588	-742	2845	2538	2692
1414	Taolambiby	Madagascar	-23.7	44.6	c14	3025	40	-1386	-1053	-1220	3336	3003	3170
1415	Taolambiby	Madagascar	-23.7	44.6	c14	2165	30	-346	-60	-203	2296	2010	2153
1416	Taolambiby	Madagascar	-23.7	44.6	c14	3005	30	-1371	-1049	-1210	3321	2999	3160
1417	Taolambiby	Madagascar	-23.7	44.6	c14	2005	30	-50	116	33	2000	1834	1917
1418	Taolambiby	Madagascar	-23.7	44.6	c14	3115	30	-1425	-1227	-1326	3375	3177	3276

Entry ID	Site Name	Country	Latitude	Longitude	Date Type	Date BP	Date BP SD	Min Chronology (Calibrated BCE/CE)	Max Chronology (Calibrated BCE/CE)	Mean Chronology (Calibrated BCE/CE)	Min Chronology (Calibrated BP - 1950)	Max Chronology (Calibrated BP - 1950)	Mean Chronology (Calibrated BP - 1950)
1419	Taolambiby	Madagascar	-23.7	44.6	c14	2871	27	-1114	-905	-1010	3064	2855	2960
1420	Taolambiby	Madagascar	-23.7	44.6	c14	2080	26	-137	25	-56	2087	1925	2006
1421	Taolambiby	Madagascar	-23.7	44.6	c14	2069	26	-107	54	-27	2057	1896	1977
1422	Taolambiby	Madagascar	-23.7	44.6	c14	2452	26	-750	-397	-574	2700	2347	2524
1423	Taolambiby	Madagascar	-23.7	44.6	c14	2431	28	-745	-391	-568	2695	2341	2518
1424	Taolambiby	Madagascar	-23.7	44.6	c14	2506	27	-766	-418	-592	2716	2368	2542
1425	Taolambiby	Madagascar	-23.7	44.6	c14	2445	27	-749	-395	-572	2699	2345	2522
1426	Taolambiby	Madagascar	-23.7	44.6	c14	2112	26	-156	18	-69	2106	1932	2019
1427	Taolambiby	Madagascar	-23.7	44.6	c14	1940	120	-171	410	120	2121	1540	1831
1428	Tsirave	Madagascar	-21.3	45.7	c14	1990	25	-45	120	38	1995	1830	1913
1429	Tsirave	Madagascar	-21.3	45.7	c14	2350	30	-456	-198	-327	2406	2148	2277
1430	Tsirave	Madagascar	-21.3	45.7	c14	1305	35	678	873	776	1272	1077	1175
1431	Tsirave	Madagascar	-21.3	45.7	c14	2440	30	-750	-392	-571	2700	2342	2521
1432	Tsirave	Madagascar	-21.3	45.7	c14	1150	15	894	993	944	1056	957	1007
1433	Tsirave	Madagascar	-21.3	45.7	c14	1215	20	771	966	869	1179	984	1082
1434	Tsirave	Madagascar	-21.3	45.7	c14	1230	25	772	957	865	1178	993	1086
1435	Tsirave	Madagascar	-21.3	45.7	c14	1245	20	773	887	830	1177	1063	1120
1436	Tsirave	Madagascar	-21.3	45.7	c14	1240	15	773	888	831	1177	1062	1120
1437	Tsirave	Madagascar	-21.3	45.7	c14	1255	15	775	881	828	1175	1069	1122
1438	Tsirave	Madagascar	-21.3	45.7	c14	1265	20	692	885	789	1258	1065	1162
1439	Tsirave	Madagascar	-21.3	45.7	c14	1250	15	774	884	829	1176	1066	1121

Entry ID	Site Name	Country	Latitude	Longitude	Date Type	Date BP	Date BP SD	Min Chronology (Calibrated BCE/CE)	Max Chronology (Calibrated BCE/CE)	Mean Chronology (Calibrated BCE/CE)	Min Chronology (Calibrated BP - 1950)	Max Chronology (Calibrated BP - 1950)	Mean Chronology (Calibrated BP - 1950)
1440	Tsirave	Madagascar	-21.3	45.7	c14	2194	70	-388	-49	-219	2338	1999	2169
1441	Tsirave	Madagascar	-21.3	45.7	c14	1290	30	682	881	782	1268	1069	1169
1442	Tsirave	Madagascar	-21.3	45.7	c14	1390	30	641	773	707	1309	1177	1243
1443	Tsirave	Madagascar	-21.3	45.7	c14	1050	20	991	1137	1064	959	813	886
1444	Tsirave	Madagascar	-21.3	45.7	c14	1275	20	690	881	786	1260	1069	1165
1445	Tsirave	Madagascar	-21.3	45.7	c14	1260	15	773	881	827	1177	1069	1123
1446	Tsirave	Madagascar	-21.3	45.7	c14	2350	35	-471	-196	-334	2421	2146	2284
1447	Tsirave	Madagascar	-21.3	45.7	c14	1670	30	365	526	446	1585	1424	1505
1448	Tsirave	Madagascar	-21.3	45.7	c14	1950	25	25	203	114	1925	1747	1836
1449	Tsirave	Madagascar	-21.3	45.7	c14	3585	35	-2020	-1751	-1886	3970	3701	3836
1450	Tsirave	Madagascar	-21.3	45.7	c14	1280	15	690	875	783	1260	1075	1168
1451	Tsirave	Madagascar	-21.3	45.7	c14	1270	15	693	881	787	1257	1069	1163
1452	Tsirave	Madagascar	-21.3	45.7	c14	1165	20	891	989	940	1059	961	1010
1453	Tsirave	Madagascar	-21.3	45.7	c14	1245	20	774	886	830	1176	1064	1120
1454	Tsirave	Madagascar	-21.3	45.7	c14	1410	20	641	767	704	1309	1183	1246
1455	Tsirave	Madagascar	-21.3	45.7	c14	1525	20	542	639	591	1408	1311	1360
1456	Tsirave	Madagascar	-21.3	45.7	c14	1220	20	771	962	867	1179	988	1084
1457	Tsirave	Madagascar	-21.3	45.7	c14	1735	20	255	414	335	1695	1536	1616
1458	Tsirave	Madagascar	-21.3	45.7	c14	1115	20	900	1023	962	1050	927	989
1459	Tsirave	Madagascar	-21.3	45.7	c14	1325	20	675	775	725	1275	1175	1225
1460	Tsirave	Madagascar	-21.3	45.7	c14	1695	20	341	463	402	1609	1487	1548

Entry ID	Site Name	Country	Latitude	Longitude	Date Type	Date BP	Date BP SD	Min Chronology (Calibrated BCE/CE)	Max Chronology (Calibrated BCE/CE)	Mean Chronology (Calibrated BCE/CE)	Min Chronology (Calibrated BP - 1950)	Max Chronology (Calibrated BP - 1950)	Mean Chronology (Calibrated BP - 1950)
1461	Tsirave	Madagascar	-21.3	45.7	c14	1310	20	678	844	761	1272	1106	1189
1462	Tsirave	Madagascar	-21.3	45.7	c14	940	20	1046	1216	1131	904	734	819
1463	Tsirave	Madagascar	-21.3	45.7	c14	1310	20	678	844	761	1272	1106	1189
1464	Tsirave	Madagascar	-21.3	45.7	c14	1185	20	881	988	935	1069	962	1016
1465	Tsirave	Madagascar	-21.3	45.7	c14	1230	20	771	952	862	1179	998	1089
1466	Tsirave	Madagascar	-21.3	45.7	c14	1225	20	772	957	865	1178	993	1086
1467	Tsirave	Madagascar	-21.3	45.7	c14	1120	20	897	1022	960	1053	928	991
1468	Tsirave	Madagascar	-21.3	45.7	c14	1935	20	62	203	133	1888	1747	1818
1469	Tsirave	Madagascar	-21.3	45.7	c14	1175	20	888	986	937	1062	964	1013
1470	Tsirave	Madagascar	-21.3	45.7	c14	1245	20	773	887	830	1177	1063	1120
1471	Tsirave	Madagascar	-21.3	45.7	c14	1235	20	772	892	832	1178	1058	1118
1472	Tsirave	Madagascar	-21.3	45.7	c14	1700	20	340	430	385	1610	1520	1565
1473	Tsirave	Madagascar	-21.3	45.7	c14	1240	20	772	889	831	1178	1061	1120
1474	Tsirave	Madagascar	-21.3	45.7	c14	860	30	1164	1276	1220	786	674	730
1475	Tsirave	Madagascar	-21.3	45.7	c14	2425	30	-746	-387	-567	2696	2337	2517
1476	Tsirave	Madagascar	-21.3	45.7	c14	2560	30	-797	-518	-658	2747	2468	2608
1477	Tsirave	Madagascar	-21.3	45.7	c14	2155	35	-347	-53	-200	2297	2003	2150
1478	Tsirave	Madagascar	-21.3	45.7	c14	2235	30	-378	-153	-266	2328	2103	2216
1479	Itampolo	Madagascar	-24.7	43.9	c14	1627	26	414	543	479	1536	1407	1472
1480	Itampolo	Madagascar	-24.7	43.9	c14	1880	70	24	363	194	1926	1587	1757
1481	Itampolo	Madagascar	-24.7	43.9	c14	980	200	682	1395	1039	1268	555	912

Entry ID	Site Name	Country	Latitude	Longitude	Date Type	Date BP	Date BP SD	Min Chronology (Calibrated BCE/CE)	Max Chronology (Calibrated BCE/CE)	Mean Chronology (Calibrated BCE/CE)	Min Chronology (Calibrated BP - 1950)	Max Chronology (Calibrated BP - 1950)	Mean Chronology (Calibrated BP - 1950)
1482	Itampolo	Madagascar	-24.7	43.9	c14	2290	90	-722	-58	-390	2672	2008	2340
1483	Itampolo	Madagascar	-24.7	43.9	c14	1835	38	125	342	234	1825	1608	1717
1484	Itampolo	Madagascar	-24.7	43.9	c14	1883	25	118	244	181	1832	1706	1769
1485	Itampolo	Madagascar	-24.7	43.9	c14	1271	24	690	884	787	1260	1066	1163
1486	Itampolo	Madagascar	-24.7	43.9	c14	1376	24	650	774	712	1300	1176	1238
1487	Itampolo	Madagascar	-24.7	43.9	c14	1576	25	435	592	514	1515	1358	1437
1488	Itampolo	Madagascar	-24.7	43.9	c14	1305	23	679	860	770	1271	1090	1181
1489	Itampolo	Madagascar	-24.7	43.9	c14	1311	26	676	860	768	1274	1090	1182
1490	Itampolo	Madagascar	-24.7	43.9	c14	1708	24	258	428	343	1692	1522	1607
1491	Amb/Andolonomby	Madagascar	-23.1	43.6	c14	1297	24	682	872	777	1268	1078	1173
1492	Amb/Andolonomby	Madagascar	-23.1	43.6	c14	930	15	1053	1214	1134	897	736	817
1493	Amb/Andolonomby	Madagascar	-23.1	43.6	c14	960	15	1044	1182	1113	906	768	837
1494	Amb/Andolonomby	Madagascar	-23.1	43.6	c14	985	15	1035	1152	1094	915	798	857
1495	Amb/Andolonomby	Madagascar	-23.1	43.6	c14	985	15	1035	1152	1094	915	798	857
1496	Amb/Andolonomby	Madagascar	-23.1	43.6	c14	1010	15	1023	1150	1087	927	800	864
1497	Amb/Andolonomby	Madagascar	-23.1	43.6	c14	1970	50	-50	205	78	2000	1745	1873
1498	Amb/Andolonomby	Madagascar	-23.1	43.6	c14	1296	32	680	880	780	1270	1070	1170
1499	Amb/Andolonomby	Madagascar	-23.1	43.6	c14	2125	20	-154	-52	-103	2104	2002	2053
1500	Amb/Andolonomby	Madagascar	-23.1	43.6	c14	1245	15	773	886	830	1177	1064	1121
1501	Amb/Andolonomby	Madagascar	-23.1	43.6	c14	1780	20	248	361	305	1702	1589	1646

Entry ID	Site Name	Country	Latitude	Longitude	Date Type	Date BP	Date BP SD	Min Chronology (Calibrated BCE/CE)	Max Chronology (Calibrated BCE/CE)	Mean Chronology (Calibrated BCE/CE)	Min Chronology (Calibrated BP - 1950)	Max Chronology (Calibrated BP - 1950)	Mean Chronology (Calibrated BP - 1950)
1502	Amb/Andolonomby	Madagascar	-23.1	43.6	c14	2035	15	-51	57	3	2001	1893	1947
1503	Amb/Andolonomby	Madagascar	-23.1	43.6	c14	1230	15	771	893	832	1179	1057	1118
1504	Amb/Andolonomby	Madagascar	-23.1	43.6	c14	2480	20	-753	-408	-581	2703	2358	2531
1505	Amb/Andolonomby	Madagascar	-23.1	43.6	c14	1675	20	365	522	444	1585	1428	1507
1506	Amb/Andolonomby	Madagascar	-23.1	43.6	c14	1220	24	771	965	868	1179	985	1082
1507	Amb/Andolonomby	Madagascar	-23.1	43.6	c14	1417	23	637	767	702	1313	1183	1248
1508	Amb/Andolonomby	Madagascar	-23.1	43.6	c14	1720	40	248	470	359	1702	1480	1591
1509	Amb/Andolonomby	Madagascar	-23.1	43.6	c14	1890	90	-50	374	162	2000	1576	1788
1510	Amb/Andolonomby	Madagascar	-23.1	43.6	c14	2915	170	-1506	-596	-1051	3456	2546	3001
1511	Amb/Andolonomby	Madagascar	-23.1	43.6	c14	4920	90	-3945	-3382	-3664	5895	5332	5614
1512	Amb/Andolonomby	Madagascar	-23.1	43.6	c14	4965	70	-3947	-3534	-3741	5897	5484	5691
1513	Amb/Andolonomby	Madagascar	-23.1	43.6	c14	750	370	640	1948	1294	1310	2	656
1514	Amb/Andolonomby	Madagascar	-23.1	43.6	c14	1214	24	772	969	871	1178	981	1080
1515	Amb/Andolonomby	Madagascar	-23.1	43.6	c14	1239	23	771	948	860	1179	1002	1091
1516	Amb/Andolonomby	Madagascar	-23.1	43.6	c14	555	15	1404	1439	1422	546	511	529
1517	Amb/Andolonomby	Madagascar	-23.1	43.6	c14	230	15	1664	1802	1733	286	148	217
1518	Amb/Andolonomby	Madagascar	-23.1	43.6	c14	645	15	1316	1401	1359	634	549	592
1519	Amb/Andolonomby	Madagascar	-23.1	43.6	c14	220	15	1666	1805	1736	284	145	215
1520	Amb/Andolonomby	Madagascar	-23.1	43.6	c14	1338	26	664	775	720	1286	1175	1231
1521	Amb/Andolonomby	Madagascar	-23.1	43.6	c14	1360	25	660	773	717	1290	1177	1234
1522	Amb/Andolonomby	Madagascar	-23.1	43.6	c14	850	20	1188	1275	1232	762	675	719

Entry ID	Site Name	Country	Latitude	Longitude	Date Type	Date BP	Date BP SD	Min Chronology (Calibrated BCE/CE)	Max Chronology (Calibrated BCE/CE)	Mean Chronology (Calibrated BCE/CE)	Min Chronology (Calibrated BP - 1950)	Max Chronology (Calibrated BP - 1950)	Mean Chronology (Calibrated BP - 1950)
1523	Andolonomby	Madagascar	-23.1	43.8	c14	1345	25	669	773	721	1281	1177	1229
1524	Andolonomby	Madagascar	-23.1	43.8	c14	1395	30	640	773	707	1310	1177	1244
1525	Andolonomby	Madagascar	-23.1	43.8	c14	1475	30	579	661	620	1371	1289	1330
1526	Andolonomby	Madagascar	-23.1	43.8	c14	1560	25	439	635	537	1511	1315	1413
1527	Andolonomby	Madagascar	-23.1	43.8	c14	1650	25	388	532	460	1562	1418	1490
1528	Andolonomby	Madagascar	-23.1	43.8	c14	1650	25	387	532	460	1563	1418	1491
1529	Andolonomby	Madagascar	-23.1	43.8	c14	1670	30	365	526	446	1585	1424	1505
1530	Andolonomby	Madagascar	-23.1	43.8	c14	1695	25	262	519	391	1688	1431	1560
1531	Andolonomby	Madagascar	-23.1	43.8	c14	1785	25	242	366	304	1708	1584	1646
1532	Andolonomby	Madagascar	-23.1	43.8	c14	1800	25	225	361	293	1725	1589	1657
1533	Andolonomby	Madagascar	-23.1	43.8	c14	1810	30	203	364	284	1747	1586	1667
1534	Andolonomby	Madagascar	-23.1	43.8	c14	1895	25	82	233	158	1868	1717	1793
1535	Andolonomby	Madagascar	-23.1	43.8	c14	2465	25	-751	-402	-577	2701	2352	2527
1536	Andolonomby	Madagascar	-23.1	43.8	c14	2545	35	-791	-479	-635	2741	2429	2585
1537	Andolonomby	Madagascar	-23.1	43.8	c14	1620	25	417	569	493	1533	1381	1457
1538	Andolonomby	Madagascar	-23.1	43.8	c14	1625	30	412	574	493	1538	1376	1457
1539	Andolonomby	Madagascar	-23.1	43.8	c14	1810	30	145	364	255	1805	1586	1696
1540	Andolonomby	Madagascar	-23.1	43.8	c14	1815	25	203	360	282	1747	1590	1669
1541	Andolonomby	Madagascar	-23.1	43.8	c14	5420	30	-4338	-4058	-4198	6288	6008	6148
1542	Andolonomby	Madagascar	-23.1	43.8	c14	1520	25	542	640	591	1408	1310	1359
1543	Andolonomby	Madagascar	-23.1	43.8	c14	1610	30	418	576	497	1532	1374	1453

Entry ID	Site Name	Country	Latitude	Longitude	Date Type	Date BP	Date BP SD	Min Chronology (Calibrated BCE/CE)	Max Chronology (Calibrated BCE/CE)	Mean Chronology (Calibrated BCE/CE)	Min Chronology (Calibrated BP - 1950)	Max Chronology (Calibrated BP - 1950)	Mean Chronology (Calibrated BP - 1950)
1544	Andolonomby	Madagascar	-23.1	43.8	c14	1905	30	71	230	151	1879	1720	1800
1545	Andolonomby	Madagascar	-23.1	43.8	c14	1630	25	414	540	477	1536	1410	1473
1546	Andolonomby	Madagascar	-23.1	43.8	c14	2675	40	-913	-599	-756	2863	2549	2706
1547	Manombo-Tulear	Madagascar	-23.0	43.5	c14	1295	25	683	874	779	1267	1076	1172
1548	Antsaragnasoa-Velo	Madagascar	-22.1	43.2	c14	1954	27	427	731	579	1523	1219	1371
1549	Antsaragnasoa-Velo	Madagascar	-22.1	43.2	c14	915	25	1050	1225	1138	900	725	813
1550	Antsaragnasoa-Velo	Madagascar	-22.1	43.2	c14	279	22	1516	1799	1658	434	151	293
1551	Ankilibehandry-Belo	Madagascar	-20.7	44.0	c14	1990	50	-59	203	72	2009	1747	1878
1552	Ankilibehandry-Belo	Madagascar	-20.7	44.0	c14	1830	60	81	386	234	1869	1564	1717
1553	Ankilibehandry-Belo	Madagascar	-20.7	44.0	c14	2050	60	-161	124	-19	2111	1826	1969
1554	Ankilibehandry-Belo	Madagascar	-20.7	44.0	c14	1370	40	641	775	708	1309	1175	1242
1555	Ankilibehandry-Belo	Madagascar	-20.7	44.0	c14	1220	50	690	990	840	1260	960	1110
1556	Ankilibehandry-Belo	Madagascar	-20.7	44.0	c14	2140	50	-353	22	-166	2303	1928	2116
1557	Ankilibehandry-Belo	Madagascar	-20.7	44.0	c14	2000	60	-98	205	54	2048	1745	1897
1558	Ankilibehandry-Belo	Madagascar	-20.7	44.0	c14	1650	30	384	536	460	1566	1414	1490
1559	Ankilibehandry-Belo	Madagascar	-20.7	44.0	c14	190	80	1518	1950	1734	432	0	216
1560	Ankilibehandry-Belo	Madagascar	-20.7	44.0	c14	1280	60	667	964	816	1283	986	1135
1561	Ankilibehandry-Belo	Madagascar	-20.7	44.0	c14	1413	80	533	877	705	1417	1073	1245
1562	Ankilibehandry-Belo	Madagascar	-20.7	44.0	c14	1550	50	434	641	538	1516	1309	1413
1563	Ankilibehandry-Belo	Madagascar	-20.7	44.0	c14	1650	50	341	580	461	1609	1370	1490
1564	Ankilibehandry-Belo	Madagascar	-20.7	44.0	c14	1866	45	73	339	206	1877	1611	1744

Entry ID	Site Name	Country	Latitude	Longitude	Date Type	Date BP	Date BP SD	Min Chronology (Calibrated BCE/CE)	Max Chronology (Calibrated BCE/CE)	Mean Chronology (Calibrated BCE/CE)	Min Chronology (Calibrated BP - 1950)	Max Chronology (Calibrated BP - 1950)	Mean Chronology (Calibrated BP - 1950)
1565	Ankilibehandry-Belo	Madagascar	-20.7	44.0	c14	2000	50	-66	203	69	2016	1747	1882
1566	Ankilibehandry-Belo	Madagascar	-20.7	44.0	c14	2008	90	-178	245	34	2128	1705	1917
1567	Ankilibehandry-Belo	Madagascar	-20.7	44.0	c14	2275	35	-389	-189	-289	2339	2139	2239
1568	Ankilibehandry-Belo	Madagascar	-20.7	44.0	c14	2005	30	-50	116	33	2000	1834	1917
1569	Ankilibehandry-Belo	Madagascar	-20.7	44.0	c14	2195	30	-362	-66	-214	2312	2016	2164
1570	Beloha-Anavoha	Madagascar	-25.2	45.1	c14	1320	30	669	854	762	1281	1096	1189
1571	Beloha-Anavoha	Madagascar	-25.2	45.1	c14	1265	25	690	887	789	1260	1063	1162
1572	Beloha-Anavoha	Madagascar	-25.2	45.1	c14	2060	30	-101	60	-21	2051	1890	1971
1573	Beloha-Anavoha	Madagascar	-25.2	45.1	c14	1375	30	649	773	711	1301	1177	1239
1574	Ranobe Pond	Madagascar	-23.4	43.9	c14	1300	80	645	971	808	1305	979	1142
1575	Ranobe Pond	Madagascar	-23.4	43.9	c14	1360	80	583	893	738	1367	1057	1212
1576	Ranobe Pond	Madagascar	-23.4	43.9	c14	600	70	1292	1453	1373	658	497	578
1577	Tsiroanomandidy Wet	Madagascar	-18.5	46.4	c14	1160	110	680	1152	916	1270	798	1034
1578	Tsiandroina	Madagascar	-18.8	46.7	c14	1980	60	-61	220	80	2011	1730	1871
1579	Tsiandroina	Madagascar	-18.8	46.7	c14	1694	40	255	525	390	1695	1425	1560
1580	Tritrivakely Crater Lake	Madagascar	-19.3	47.0	c14	3810	70	-2457	-1982	-2220	4407	3932	4170
1581	Tritrivakely Crater Lake	Madagascar	-19.3	47.0	c14	4340	90	-3331	-2630	-2981	5281	4580	4931
1582	Tritrivakely Crater Lake	Madagascar	-19.3	47.0	c14	2840	60	-1126	-812	-969	3076	2762	2919
1583	Tritrivakely Crater Lake	Madagascar	-19.3	47.0	c14	1240	100	659	1020	840	1291	930	1111
1584	Mitsinjo Flood Plain	Madagascar	-16.2	46.0	c14	3420	120	-2022	-1436	-1729	3972	3386	3679
1585	Mitsinjo Flood Plain	Madagascar	-16.2	46.0	c14	3160	210	-1910	-851	-1381	3860	2801	3331

Entry ID	Site Name	Country	Latitude	Longitude	Date Type	Date BP	Date BP SD	Min Chronology (Calibrated BCE/CE)	Max Chronology (Calibrated BCE/CE)	Mean Chronology (Calibrated BCE/CE)	Min Chronology (Calibrated BP - 1950)	Max Chronology (Calibrated BP - 1950)	Mean Chronology (Calibrated BP - 1950)
1586	Mitsinjo Flood Plain	Madagascar	-16.2	46.0	c14	2400	90	-774	-204	-489	2724	2154	2439
1587	Mitsinjo Flood Plain	Madagascar	-16.2	46.0	c14	890	80	1025	1280	1153	925	670	798
1588	Mitsinjo Flood Plain	Madagascar	-16.2	46.0	c14	530	80	1287	1624	1456	663	326	495
1589	Mitsinjo Flood Plain	Madagascar	-16.2	46.0	c14	470	90	1314	1644	1479	636	306	471
1590	Mitoho Cave	Madagascar	-23.7	43.7	c14	4030	70	-2860	-2287	-2574	4810	4237	4524
1591	Ambohitratoandro Wet	Madagascar	-19.0	47.1	c14	3720	50	-2273	-1901	-2087	4223	3851	4037
1592	Ampanihy	Madagascar	-22.8	43.8	c14	2430	100	-782	-200	-491	2732	2150	2441
1593	Amparihibe Deep	Madagascar	-13.4	48.3	c14	1130	50	774	1026	900	1176	924	1050
1594	Amparihibe Deep	Madagascar	-13.4	48.3	c14	1660	90	226	603	415	1724	1347	1536
1595	Amparihibe Deep	Madagascar	-13.4	48.3	c14	1780	70	86	430	258	1864	1520	1692
1596	Amparihibe Deep	Madagascar	-13.4	48.3	c14	1820	60	83	389	236	1867	1561	1714
1597	Ampasambazimba	Madagascar	-18.9	47.3	c14	2291	55	-404	-165	-285	2354	2115	2235
1598	Ampasambazimba	Madagascar	-18.9	47.3	c14	1035	50	974	1180	1077	976	770	873
1599	Ampasambazimba	Madagascar	-18.9	47.3	c14	1410	40	599	773	686	1351	1177	1264
1600	Ampasambazimba	Madagascar	-18.9	47.3	c14	2402	45	-750	-204	-477	2700	2154	2427
1601	Ampasambazimba	Madagascar	-18.9	47.3	c14	4725	180	-3904	-2919	-3412	5854	4869	5362
1602	Ampasambazimba	Madagascar	-18.9	46.7	c14	2885	30	-1127	-904	-1016	3077	2854	2966
1603	Ampasambazimba	Madagascar	-18.9	46.7	c14	4730	45	-3628	-3367	-3498	5578	5317	5448
1604	Ampasambazimba	Madagascar	-18.9	46.7	c14	2835	30	-1048	-834	-941	2998	2784	2891
1605	Ampasambazimba	Madagascar	-18.9	46.7	c14	1450	25	596	670	633	1354	1280	1317
1606	Ampasambazimba	Madagascar	-18.9	46.7	c14	4610	45	-3508	-3098	-3303	5458	5048	5253

Entry ID	Site Name	Country	Latitude	Longitude	Date Type	Date BP	Date BP SD	Min Chronology (Calibrated BCE/CE)	Max Chronology (Calibrated BCE/CE)	Mean Chronology (Calibrated BCE/CE)	Min Chronology (Calibrated BP - 1950)	Max Chronology (Calibrated BP - 1950)	Mean Chronology (Calibrated BP - 1950)
1607	Ampasambazimba	Madagascar	-18.9	46.7	c14	1300	30	680	876	778	1270	1074	1172
1608	Ampasambazimba	Madagascar	-18.9	46.7	c14	2175	30	-352	-61	-207	2302	2011	2157
1609	Ampasambazimba	Madagascar	-18.9	46.7	c14	4540	35	-3361	-3034	-3198	5311	4984	5148
1610	Ampasambazimba	Madagascar	-18.9	46.7	c14	4610	40	-3504	-3099	-3302	5454	5049	5252
1611	Ampasambazimba	Madagascar	-18.9	46.7	c14	4750	40	-3631	-3372	-3502	5581	5322	5452
1612	Ampasambazimba	Madagascar	-18.9	46.7	c14	3905	35	-2466	-2204	-2335	4416	4154	4285
1613	Ampasambazimba	Madagascar	-18.9	46.7	c14	4890	40	-3761	-3524	-3643	5711	5474	5593
1614	Anavoha	Madagascar	-25.3	44.5	c14	1954	110	-156	364	104	2106	1586	1846
1615	Anavoha	Madagascar	-25.2	45.1	c14	1486	76	422	771	597	1528	1179	1354
1616	Anavoha	Madagascar	-25.2	45.1	c14	1330	25	669	830	750	1281	1120	1201
1617	Anavoha	Madagascar	-25.2	45.1	c14	1725	35	250	425	338	1700	1525	1613
1618	Anavoha	Madagascar	-25.2	45.1	c14	3430	30	-1872	-1544	-1708	3822	3494	3658
1619	Anavoha	Madagascar	-25.2	45.1	c14	2245	35	-382	-163	-273	2332	2113	2223
1620	Anavoha	Madagascar	-25.2	45.1	c14	2300	30	-396	-194	-295	2346	2144	2245
1621	Anavoha	Madagascar	-25.2	45.1	c14	1308	34	676	873	775	1274	1077	1176
1622	Anavoha	Madagascar	-25.2	45.1	c14	1640	30	387	542	465	1563	1408	1486
1623	Andavambatobe Cave	Madagascar	-15.9	46.0	c14	580	100	1230	1622	1426	720	328	524
1624	Andrahomana Cave	Madagascar	-25.0	46.8	c14	4440	60	-3334	-2903	-3119	5284	4853	5069
1625	Andrahomana Cave	Madagascar	-25.0	46.8	c14	1536	35	474	645	560	1476	1305	1391
1626	Andrahomana	Madagascar	-25.2	46.6	c14	4566	35	-3370	-3093	-3232	5320	5043	5182

Entry ID	Site Name	Country	Latitude	Longitude	Date Type	Date BP	Date BP SD	Min Chronology (Calibrated BCE/CE)	Max Chronology (Calibrated BCE/CE)	Mean Chronology (Calibrated BCE/CE)	Min Chronology (Calibrated BP - 1950)	Max Chronology (Calibrated BP - 1950)	Mean Chronology (Calibrated BP - 1950)
1627	Andraikiba	Madagascar	-19.1	47.0	c14	1200	70	688	1020	854	1262	930	1096
1628	Andraikiba	Madagascar	-19.1	47.0	c14	2310	100	-749	-61	-405	2699	2011	2355
1629	Andraikiba	Madagascar	-19.1	47.0	c14	2320	70	-718	-147	-433	2668	2097	2383
1630	Ankazoabo Grotte	Madagascar	-23.8	43.9	c14	1269	80	666	985	826	1284	965	1125
1631	Ankazoabo Grotte	Madagascar	-23.8	43.9	c14	2148	35	-346	-51	-199	2296	2001	2149
1632	Ankazoabo Grotte	Madagascar	-23.8	43.9	c14	1865	35	85	332	209	1865	1618	1742
1633	Ankazoabo Grotte	Madagascar	-23.8	43.9	c14	1555	30	440	637	539	1510	1313	1412
1634	Ankazoabo Grotte	Madagascar	-23.8	43.9	c14	1450	30	589	674	632	1361	1276	1319
1635	Ankazoabo Grotte	Madagascar	-23.8	43.9	c14	1148	162	640	1259	950	1310	691	1001
1636	Ampandramandratsy	Madagascar	-22.3	44.7	c14	825	20	1220	1279	1250	730	671	701
1637	Ankilitelo	Madagascar	-22.9	43.9	c14	290	30	1508	1799	1654	442	151	297
1638	Antsetsindrano	Madagascar	-20.1	47.0	c14	250	60	1507	1948	1728	443	2	223
1639	Antsetsindrano	Madagascar	-20.1	47.0	c14	430	60	1430	1635	1533	520	315	418
1640	Antsetsindrano	Madagascar	-20.1	47.0	c14	360	60	1450	1668	1559	500	282	391
1641	Antsiroandoha	Madagascar	-12.4	49.2	c14	1020	50	900	1177	1039	1050	773	912
1642	Antsiroandoha	Madagascar	-12.4	49.2	c14	4400	60	-3331	-2891	-3111	5281	4841	5061
1643	Baie des Galions	Madagascar	-25.0	47.0	c14	2250	420	-819	1125	153	2769	825	1797
1644	Behavoha	Madagascar	-25.0	44.4	c14	2160	110	-400	116	-142	2350	1834	2092
1645	Beloha-Anavoha	Madagascar	-25.2	45.1	c14	1065	40	901	1150	1026	1049	800	925
1646	Beloha	Madagascar	-25.3	44.9	c14	1380	90	539	950	745	1411	1000	1206

Entry ID	Site Name	Country	Latitude	Longitude	Date Type	Date BP	Date BP SD	Min Chronology (Calibrated BCE/CE)	Max Chronology (Calibrated BCE/CE)	Mean Chronology (Calibrated BCE/CE)	Min Chronology (Calibrated BP - 1950)	Max Chronology (Calibrated BP - 1950)	Mean Chronology (Calibrated BP - 1950)
1647	Beloha-Anavoha	Madagascar	-25.2	45.1	c14	1277	35	684	887	786	1266	1063	1165
1648	Bemafandry	Madagascar	-24.9	44.1	c14	1980	90	-154	325	86	2104	1625	1865
1649	Bemafandry	Madagascar	-24.9	44.1	c14	2060	150	-395	337	-29	2345	1613	1979
1650	Bevoha	Madagascar	-23.1	43.8	c14	1815	60	119	410	265	1831	1540	1686
1651	Bevoha	Madagascar	-23.1	43.8	c14	1930	63	-49	313	132	1999	1637	1818
1652	Bevoha	Madagascar	-23.1	43.8	c14	1730	192	-136	769	317	2086	1181	1634
1653	Itasy	Madagascar	-19.2	46.9	c14	2260	60	-400	-112	-256	2350	2062	2206
1654	Kavitaha	Madagascar	-19.3	47.0	c14	670	80	1230	1441	1336	720	509	615
1655	Kavitaha	Madagascar	-19.3	47.0	c14	710	100	1180	1445	1313	770	505	638
1656	Kavitaha	Madagascar	-19.3	47.0	c14	960	90	909	1280	1095	1041	670	856
1657	Kavitaha	Madagascar	-19.3	47.0	c14	1400	80	543	881	712	1407	1069	1238
1658	Kavitaha	Madagascar	-19.3	47.0	c14	1490	60	439	766	603	1511	1184	1348
1659	Komango	Madagascar	-19.3	44.8	c14	1750	60	143	522	333	1807	1428	1618
1660	Komango	Madagascar	-19.3	44.8	c14	3390	50	-1866	-1503	-1685	3816	3453	3635
1661	Lavakasaka	Madagascar	-19.6	47.3	c14	2380	70	-753	-192	-473	2703	2142	2423
1662	Lohavohitra	Madagascar	-19.6	47.3	c14	230	60	1515	1949	1732	435	1	218
1663	Lohavohitra	Madagascar	-19.6	47.3	c14	260	60	1503	1948	1726	447	2	225
1664	Lohavohitra	Madagascar	-19.6	47.3	c14	270	45	1503	1936	1720	447	14	231
1665	Mahery	Madagascar	-12.8	49.3	c14	2950	70	-1380	-927	-1154	3330	2877	3104
1666	Mahery	Madagascar	-12.8	49.3	c14	3680	70	-2283	-1783	-2033	4233	3733	3983
1667	Mahery	Madagascar	-12.8	49.3	c14	4620	90	-3628	-3031	-3330	5578	4981	5280

Entry ID	Site Name	Country	Latitude	Longitude	Date Type	Date BP	Date BP SD	Min Chronology (Calibrated BCE/CE)	Max Chronology (Calibrated BCE/CE)	Mean Chronology (Calibrated BCE/CE)	Min Chronology (Calibrated BP - 1950)	Max Chronology (Calibrated BP - 1950)	Mean Chronology (Calibrated BP - 1950)
1668	Mananjary	Madagascar	-20.6	48.5	c14	213	40	1650	1948	1799	300	2	151
1669	Mananjary	Madagascar	-20.6	48.5	c14	2327	40	-409	-193	-301	2359	2143	2251
1670	Marais d'Ifanja	Madagascar	-19.3	46.9	c14	4200	80	-2912	-2492	-2702	4862	4442	4652
1671	Masinandriana	Madagascar	-19.0	47.6	c14	2154	40	-352	11	-171	2302	1939	2121
1672	Masinandriana	Madagascar	-19.0	47.6	c14	4496	40	-3346	-2935	-3141	5296	4885	5091
1673	Andavadoaka	Madagascar	-22.1	43.2	c14	1585	20	435	581	508	1515	1369	1442
1674	Andavadoaka	Madagascar	-22.1	43.2	c14	1530	20	542	637	590	1408	1313	1361
1675	Andavadoaka	Madagascar	-22.1	43.2	c14	2185	20	-353	-71	-212	2303	2021	2162
1676	Andavadoaka	Madagascar	-22.1	43.2	c14	2055	20	-63	54	-5	2013	1896	1955
1677	Andavadoaka	Madagascar	-22.1	43.2	c14	2160	20	-341	-64	-203	2291	2014	2153
1678	Ankilivalo	Madagascar	-23.5	45.0	c14	200	15	1667	1842	1755	283	108	196
1679	Ankilivalo	Madagascar	-23.5	45.0	c14	195	15	1669	1948	1809	281	2	142
1680	Andaboy	Madagascar	-21.9	43.4	c14	975	15	1038	1158	1098	912	792	852
1681	Beanka	Madagascar	-20.9	44.1	c14	290	15	1518	1669	1594	432	281	357
1682	Ampisorogna	Madagascar	-22.1	43.4	c14	2125	20	-154	-52	-103	2104	2002	2053
1683	Itampolove	Madagascar	-22.2	43.3	c14	935	20	1047	1217	1132	903	733	818
1684	Itampolove	Madagascar	-22.2	43.3	c14	1310	20	678	844	761	1272	1106	1189
1685	Itampolove	Madagascar	-22.2	43.3	c14	1895	20	85	226	156	1865	1724	1795
1686	Itampolove	Madagascar	-22.2	43.3	c14	4025	20	-2581	-2409	-2495	4531	4359	4445
1687	Ampoza	Madagascar	-22.3	44.3	c14	1705	55	250	526	388	1700	1424	1562
1688	Ampoza	Madagascar	-22.3	44.3	c14	1810	60	122	410	266	1828	1540	1684

Entry ID	Site Name	Country	Latitude	Longitude	Date Type	Date BP	Date BP SD	Min Chronology (Calibrated BCE/CE)	Max Chronology (Calibrated BCE/CE)	Mean Chronology (Calibrated BCE/CE)	Min Chronology (Calibrated BP - 1950)	Max Chronology (Calibrated BP - 1950)	Mean Chronology (Calibrated BP - 1950)
1689	Ampoza	Madagascar	-22.3	44.3	c14	1850	55	78	362	220	1872	1588	1730
1690	Ampoza	Madagascar	-22.3	44.3	c14	1910	120	-141	415	137	2091	1535	1813
1691	Ampoza	Madagascar	-22.3	44.3	c14	2035	35	-89	113	12	2039	1837	1938
1692	Ampoza	Madagascar	-22.3	44.3	c14	2285	40	-394	-189	-292	2344	2139	2242
1693	Ampoza	Madagascar	-22.3	44.3	c14	2370	50	-732	-196	-464	2682	2146	2414
1694	Ampoza	Madagascar	-22.3	44.3	c14	2517	40	-774	-417	-596	2724	2367	2546
1695	Ampoza	Madagascar	-22.3	44.3	c14	2760	60	-1016	-789	-903	2966	2739	2853
1696	Ampoza	Madagascar	-22.3	44.3	c14	1230	20	772	952	862	1178	998	1088
1697	Ampoza	Madagascar	-22.3	44.3	c14	1225	20	772	957	865	1178	993	1086
1698	Ampoza	Madagascar	-22.3	44.3	c14	1165	20	891	988	940	1059	962	1011
1699	Ampoza	Madagascar	-22.3	44.3	c14	1215	20	771	966	869	1179	984	1082
1700	Ampoza	Madagascar	-22.3	44.3	c14	1155	15	893	991	942	1057	959	1008
1701	Ampoza	Madagascar	-22.3	44.3	c14	1200	20	772	985	879	1178	965	1072
1702	Ampoza	Madagascar	-22.3	44.3	c14	2675	25	-898	-773	-836	2848	2723	2786
1703	Ampoza	Madagascar	-22.3	44.3	c14	2660	40	-905	-587	-746	2855	2537	2696
1704	Ampoza	Madagascar	-22.3	44.3	c14	2470	15	-750	-404	-577	2700	2354	2527
1705	Ampoza	Madagascar	-22.3	44.3	c14	2795	20	-989	-824	-907	2939	2774	2857
1706	Ampoza	Madagascar	-22.3	44.3	c14	2670	20	-894	-773	-834	2844	2723	2784
1707	Ampoza	Madagascar	-22.3	44.3	c14	2735	20	-907	-804	-856	2857	2754	2806
1708	Ampoza	Madagascar	-22.3	44.3	c14	2730	20	-906	-802	-854	2856	2752	2804
1709	Ampoza	Madagascar	-22.3	44.3	c14	2485	20	-754	-410	-582	2704	2360	2532

Entry ID	Site Name	Country	Latitude	Longitude	Date Type	Date BP	Date BP SD	Min Chronology (Calibrated BCE/CE)	Max Chronology (Calibrated BCE/CE)	Mean Chronology (Calibrated BCE/CE)	Min Chronology (Calibrated BP - 1950)	Max Chronology (Calibrated BP - 1950)	Mean Chronology (Calibrated BP - 1950)
1710	Ampoza	Madagascar	-22.3	44.3	c14	2710	20	-900	-796	-848	2850	2746	2798
1711	Ampoza	Madagascar	-22.3	44.3	c14	2455	20	-748	-399	-574	2698	2349	2524
1712	Ampoza	Madagascar	-22.3	44.3	c14	2475	20	-752	-406	-579	2702	2356	2529
1713	Ampoza	Madagascar	-22.3	44.3	c14	2735	20	-907	-804	-856	2857	2754	2806
1714	Tulear	Madagascar	-23.4	43.8	c14	1195	15	772	974	873	1178	976	1077
1715	Androka	Madagascar	-25.0	44.1	c14	1540	20	535	635	585	1415	1315	1365
1716	Androka	Madagascar	-25.0	44.1	c14	1545	20	530	635	583	1420	1315	1368
1717	Anakao	Madagascar	-23.7	43.7	c14	2775	95	-1213	-762	-988	3163	2712	2938
1718	Anakao	Madagascar	-23.7	43.7	c14	2375	100	-763	-184	-474	2713	2134	2424
1719	Anakao	Madagascar	-23.7	43.7	c14	3960	150	-2876	-2030	-2453	4826	3980	4403
1720	Faux Cap	Madagascar	-25.6	45.5	c14	1610	40	411	588	500	1539	1362	1451
1721	Faux Cap	Madagascar	-25.6	45.5	c14	3260	50	-1621	-1327	-1474	3571	3277	3424
1722	Faux Cap	Madagascar	-25.6	45.5	c14	4060	50	-2857	-2350	-2604	4807	4300	4554
1723	Faux Cap	Madagascar	-25.6	45.5	c14	4140	50	-2876	-2493	-2685	4826	4443	4635
1724	Manombo-Tulear	Madagascar	-23.0	43.5	c14	1525	25	540	640	590	1410	1310	1360
1725	Manombo-Tulear	Madagascar	-23.0	43.5	c14	1605	30	420	577	499	1530	1373	1452
1726	Manombo-Tulear	Madagascar	-23.0	43.5	c14	1465	25	591	661	626	1359	1289	1324
1727	Manombo-Tulear	Madagascar	-23.0	43.5	c14	2325	30	-402	-199	-301	2352	2149	2251
1728	Manombo-Tulear	Madagascar	-23.0	43.5	c14	1685	25	343	522	433	1607	1428	1518
1729	Manombo-Tulear	Madagascar	-23.0	43.5	c14	1795	25	230	362	296	1720	1588	1654
1730	Manombo-Tulear	Madagascar	-23.0	43.5	c14	1420	25	606	769	688	1344	1181	1263

Entry ID	Site Name	Country	Latitude	Longitude	Date Type	Date BP	Date BP SD	Min Chronology (Calibrated BCE/CE)	Max Chronology (Calibrated BCE/CE)	Mean Chronology (Calibrated BCE/CE)	Min Chronology (Calibrated BP - 1950)	Max Chronology (Calibrated BP - 1950)	Mean Chronology (Calibrated BP - 1950)
1731	Manombo-Tulear	Madagascar	-23.0	43.5	c14	1730	30	252	419	336	1698	1531	1615
1732	Manombo	Madagascar	-23.0	43.5	c14	860	20	1186	1272	1229	764	678	721
1733	Tsimanampesotse	Madagascar	-24.1	43.8	c14	905	25	1054	1260	1157	896	690	793
1734	Tsimanampesotse	Madagascar	-24.1	43.8	c14	295	25	1508	1796	1652	442	154	298
1735	Mikoboka P Cave #13	Madagascar	-22.9	43.9	c14	1380	30	646	773	710	1304	1177	1241
1736	Mandrare Rivermouth	Madagascar	-25.0	46.7	c14	1416	26	608	770	689	1342	1180	1261
1737	Cap Ste Marie	Madagascar	-25.6	45.2	c14	3004	29	-1370	-1049	-1210	3320	2999	3160
1738	Kotoala	Madagascar	-25.5	45.6	c14	4572	29	-3368	-3099	-3234	5318	5049	5184
1739	Montefeno	Madagascar	-25.0	45.8	c14	401	25	1455	1627	1541	495	323	409
1740	Montefeno	Madagascar	-25.0	45.8	c14	355	24	1496	1644	1570	454	306	380
1741	Montefeno	Madagascar	-25.3	45.8	OSL	1960	240	-430	530	50	2380	1420	1900
1742	Montefeno	Madagascar	-25.3	45.8	OSL	690	60	1200	1440	1320	750	510	630
1743	Anjankitike	Madagascar	-25.0	46.4	OSL	545	40	1385	1545	1465	565	405	485
1744	Anjankitike	Madagascar	-25.0	46.4	OSL	250	115	1530	1990	1760	420	-40	190
1745	Anjankitike	Madagascar	-25.0	46.4	OSL	235	90	1595	1955	1775	355	-5	175
1746	Anjankitike	Madagascar	-25.0	46.4	OSL	490	50	1420	1620	1520	530	330	430
1747	Anjankitike	Madagascar	-25.0	46.4	OSL	405	55	1495	1715	1605	455	235	345
1748	Mionjona	Madagascar	-25.0	46.4	OSL	290	45	1630	1810	1720	320	140	230
1749	Mionjona	Madagascar	-25.0	46.4	OSL	310	45	1610	1790	1700	340	160	250
1750	Ambohitrikanjaka	Madagascar	-18.9	48.6	c14	380	90	1415	1803	1609	535	147	341
1751	Angavobe	Madagascar	-18.9	47.7	c14	330	80	1443	1936	1690	507	14	261

Entry ID	Site Name	Country	Latitude	Longitude	Date Type	Date BP	Date BP SD	Min Chronology (Calibrated BCE/CE)	Max Chronology (Calibrated BCE/CE)	Mean Chronology (Calibrated BCE/CE)	Min Chronology (Calibrated BP - 1950)	Max Chronology (Calibrated BP - 1950)	Mean Chronology (Calibrated BP - 1950)
1752	Fanongoavana	Madagascar	-19.1	47.9	c14	410	100	1393	1805	1599	557	145	351
1753	Fanongoavana	Madagascar	-19.1	47.9	c14	450	120	1298	1804	1551	652	146	399
1754	Fanongoavana	Madagascar	-19.1	47.9	c14	450	100	1318	1796	1557	632	154	393
1755	Vohitrarivo	Madagascar	-20.1	47.3	c14	290	80	1459	1946	1703	491	4	248
1756	Lakato'ni Gavin	Madagascar	-12.3	49.4	c14	1035	15	991	1130	1061	959	820	890
1757	Antsirafaly	Madagascar	-23.6	43.7	c14	1550	20	525	635	580	1425	1315	1370
1758	Ampehabe Cave	Madagascar	-23.4	44.3	c14	1405	25	639	770	705	1311	1180	1246
1759	Antsirabe	Madagascar	-19.9	47.0	c14	1260	25	691	889	790	1259	1061	1160
1760	Antsirabe	Madagascar	-19.9	47.0	c14	1800	35	145	373	259	1805	1577	1691
1761	Antsirabe	Madagascar	-19.9	47.0	c14	1215	25	771	969	870	1179	981	1080
1762	Amborolana	Madagascar	-14.5	50.2	c14	838	22	1180	1274	1227	770	676	723
1763	Amborolana	Madagascar	-14.5	50.2	c14	699	21	1279	1387	1333	671	563	617
1764	Amborolana	Madagascar	-14.5	50.2	c14	900	21	1051	1221	1136	899	729	814
1765	Amborolana	Madagascar	-14.5	50.2	c14	918	22	1046	1218	1132	904	732	818
1766	Amborolana	Madagascar	-14.5	50.2	c14	988	21	1024	1153	1089	926	797	862
1767	Amborolana	Madagascar	-14.5	50.2	c14	957	21	1033	1160	1097	917	790	854
1768	Amborolana	Madagascar	-14.5	50.2	c14	995	21	1021	1153	1087	929	797	863
1769	Amborolana	Madagascar	-14.5	50.2	c14	885	22	1053	1226	1140	897	724	811
1770	Amborolana	Madagascar	-14.5	50.2	c14	736	22	1266	1383	1325	684	567	626
1771	Amborolana	Madagascar	-14.5	50.2	c14	689	22	1281	1390	1336	669	560	615
1772	Amborolana	Madagascar	-14.5	50.2	c14	791	22	1225	1280	1253	725	670	698

Entry ID	Site Name	Country	Latitude	Longitude	Date Type	Date BP	Date BP SD	Min Chronology (Calibrated BCE/CE)	Max Chronology (Calibrated BCE/CE)	Mean Chronology (Calibrated BCE/CE)	Min Chronology (Calibrated BP - 1950)	Max Chronology (Calibrated BP - 1950)	Mean Chronology (Calibrated BP - 1950)
1773	Amborolana	Madagascar	-14.5	50.2	c14	866	22	1160	1265	1213	790	685	738
1774	Ambodimadiro	Madagascar	-14.5	50.2	c14	865	22	1160	1266	1213	790	684	737
1775	Ambodimadiro	Madagascar	-14.5	50.2	c14	957	22	1032	1161	1097	918	789	854
1776	Bemanevika	Madagascar	-14.2	50.1	c14	779	21	1226	1286	1256	724	664	694
1777	Bemanevika	Madagascar	-14.2	50.1	c14	862	21	1162	1266	1214	788	684	736
1778	Bemanevika	Madagascar	-14.2	50.1	c14	662	21	1290	1394	1342	660	556	608
1779	Benavony	Madagascar	-14.4	50.2	c14	594	21	1314	1420	1367	636	530	583
1780	Benavony	Madagascar	-14.4	50.2	c14	1049	21	978	1094	1036	972	856	914
1781	Andrangana	Madagascar	-12.9	49.8	c14	647	21	1298	1396	1347	652	554	603
1782	Andrangana	Madagascar	-12.9	49.8	c14	642	21	1299	1398	1349	651	552	602
1783	Andrangana	Madagascar	-12.9	49.8	c14	589	15	1321	1415	1368	629	535	582
1784	Andrangana	Madagascar	-12.9	49.8	c14	517	21	1407	1448	1428	543	502	523
1785	Andrangana	Madagascar	-12.9	49.8	c14	684	21	1282	1390	1336	668	560	614
1786	Lake Sahaka	Madagascar	-13.2	49.9	c14	238	21	1644	1800	1722	306	150	228
1787	Bobalila	Madagascar	-12.9	49.7	c14	851	21	1170	1270	1220	780	680	730
1788	Bobalila	Madagascar	-12.9	49.7	c14	617	21	1304	1406	1355	646	544	595
1789	Bobalila	Madagascar	-12.9	49.7	c14	661	21	1290	1395	1343	660	555	608
1790	Bobalila	Madagascar	-12.9	49.7	c14	688	21	1281	1389	1335	669	561	615
1791	Bobalila	Madagascar	-12.9	49.7	c14	659	21	1291	1395	1343	659	555	607
1792	Antravy Émeraude	Madagascar	-12.1	49.3	c14	736	21	1266	1383	1325	684	567	626